

https://dspace.org/

A bioactive association platform delivery system for enhanced efficacy of pharmaceutical products

Braithwaite, Miles Charles

2015
http://hdl.handle.net/10539/18434

Downloaded from a DSpace repository. https://dspace.org/

A BIOACTIVE ASSOCIATION PLATFORM DELIVERY SYSTEM FOR ENHANCED EFFICACY OF PHARMACEUTICAL PRODUCTS

by

MILES CHARLES BRAITHWAITE

A Thesis submitted to the Faculty of Health Sciences, University of the Witwatersrand, in fulfilment of the requirements for the degree of Doctor of Philosophy

Supervisor:

Professor Viness Pillay

Wits Advanced Drug Delivery Platform Research Unit

Department of Pharmacy and Pharmacology, Faculty of Health Sciences,

University of the Witwatersrand, Johannesburg, South Africa

Co-Supervisor:

Professor Yahya E. Choonara

Wits Advanced Drug Delivery Platform Research Unit

Department of Pharmacy and Pharmacology, Faculty of Health Sciences,

University of the Witwatersrand, Johannesburg, South Africa

Johannesburg, 2015

DECLARATION

I, Miles Charles Braithwaite, declare that this thesis is my own work. It has been submitted for the degree of Doctor of Philosophy in the Faculty of Health Sciences at the University of the Witwatersrand, Johannesburg. It has not been submitted before for any other degree or examination at this or any other University.

…….

This ……..day of …….. 2015

RESEARCH OUTPUTS

Research Publications related to Doctoral Research

1. Braithwaite MC, Kumar P, Tyagi C, Tomar LK, Choonara YE, Pillay V. 2013. Vitamin D therapy and related metabolomics: Is the calciferol dose and form the only requirements for successful clinical therapeutics. *Medical Hypotheses* 81: 656-663 *[Medical hypothesis]*.

2. Braithwaite MC, Tyagi C, Tomar LK, Kumar P, Choonara YE, Pillay V. 2014. Nutraceutical-based therapeutics and formulation strategies augmenting their efficiency to complement modern medicine: An overview. *Journal of Functional Foods* 6: 82-99 *[Review].*

3. Braithwaite MC, Choonara YE, Kumar P, Tyagi C, Tomar LK, Pillay V. A novel multi-tiered experimental approach unfolding the mechanisms behind cyclodextrin-vitamin inclusion complexes for enhanced vitamin solubility and stability. Submitted: 11/2014 *[Research Article].*

4. Braithwaite MC, Kumar P, Tomar LK, Du Toit LC, Choonara YE, Pillay V. A bioactive association platform oral drug delivery system for enhanced efficacy of cholecalciferol: Synthesis, characterization, and *in vitro* and *in vivo* analysis. Submitted: 12/2014 *[Research Article].*

Patents Filed

1. A Bioactive Association Platform Delivery System. Braithwaite MC, Pillay V, Choonara YE, Kumar P. Provisional SA Patent Application Number: SA 2014/01769. 18 February 2014.

ABSTRACT

Oral delivery of drugs is inundated by formulation challenges predominantly due to poor physicochemical properties of chemical entities resulting in anomalies in serum levels and inconsistent pharmacokinetics and pharmacodynamics. Similar challenges exist for nutraceutical products however, there has been a recent shift in research paradigms towards novel formulation strategies to render these agents invaluable complementary treatments. In this view, vitamin D has gained interest, however it's effective therapeutic use is limited by low aqueous solubility, erratic inter-patient response, and inadequate formulation design. Cholecalciferol (D_3), being a potent form of the vitamin, is widely supplemented and prescribed and was selected as the model agent for proof of concept in the design of a novel oral Drug Delivery System (DDS) in the current research. An ideal physiological milieu is often essential for intended performance of even advanced DDS's. GIT topology may have an even greater impact on modified dosage forms compared to conventional dosage forms. The use of absorption and solubility enhancers is a tried and tested formulation strategy to improve bioavailability and efficacy of drugs with unfavourable physicochemical characteristics. Despite being an integral part of modern formulation design, these bioenhancers may prove only marginally effective in oral delivery unless the physiological state is considered during formulation. It was therefore imperative that the DDS designed in this investigation included measures to mitigate this effect and achieve robust efficacy regardless of the dynamic GIT condition. In addition, most nutraceuticals typically occur as multicomponent products, yet different combined BCS class vitamins may encounter erratic absorption due to differences in solubility and flocculation effects that impede dispersion in aqueous media. It is therefore imperative to formulate and evaluate a DDS containing more than one nutraceutical agent for greater "real-world" relevance instead of a single vitamin DDS formulation that has been pursued in past studies. The current work therefore set out to develop a DDS capable of orally delivering multiple nutraceutical actives and biological constituents from a single formulation framework with modifiable release kinetics and a unified release of synergistic vitamins, with D_3 as the focus agent for enhanced oral bioavailability. Few researchers have investigated the use of multiple biological enhancers combined with synthetic carriers in a dosage form to aid nutraceutical delivery.

The design process began with the conceptualization of a molecule termed a "Bioactive Booster" (defined as a unique combination of a specific bioactive and carrier molecule/ polymer) intended to form a sequential constituent of the novel DDS. Each BB would play an integral role in the DDS functionality by providing: (i) enhanced membrane absorption and aqueous solubility of cholecalciferol; (ii) surfactant effects for micellization of cholecalciferol and other vitamins; (iii) improved physicochemical stability; and (iv) aligned vitamin release profiles. The DDS, coined a "Bioactive Association Platform" (BAP), was intended to deliver D_3 in a more efficient manner by harnessing the value of naturally occurring GIT biological molecules and synthetic carriers within a convenient capsule capable of providing a tailored microenvironment conducive to enhanced oral bioavailability. Synergistic selected bioactives included, bile acids, bile salts, pancreatic lipase and synergistic vitamins (ascorbic acid and α-tocopherol). Preformulation work involved preliminary *in silico* testing, physicochemical analysis and release testing with these bioactives to ascertain the most appropriate BAP component candidates/ BB's. Extensive characterization, solubility studies and inclusion efficiency results explicated "βD_3-8" to be an ideal and unique Inclusion Complex (IC) to deliver cholecalciferol. Alginate and chitosan were also explored during preformulation as polymeric hydrogels capable of binding and releasing enzyme and bile constituents from pH-responsive polymeric beads, scaffolds, or film candidates. Ultimately preformulation identified the most attractive BB candidates for final inclusion in the BAP, namely: (i) a novel "3-vitamin" minitablet containing ascorbic acid, α-tocopherol in the form of TPGS (d-α-Tocopheryl polyethylene glycol 1000 succinate), and cholecalciferol in the form of a βD_3-8 IC and; (ii) an optimized film containing two bile salts and pancreatic lipase. *Ex vivo* permeability studies demonstrated the minitablets' superior D_3 membrane diffusion properties. Likewise the optimized pH-responsive bioactive-film selection and composition was based on studies investigating: film influence on model drug release from the minitablets; physicochemical and physicomechanical analysis; and enzyme activity profiles. The optimized film and novel minitablets were validated by physicochemical and mechanical analysis prior to insertion into two gelatin capsules to form the final BAP. The BAP also embodied a dual pH responsive mechanism for targeted duodenal release and protection of gastric sensitive vitamin and enzyme constituents due to the presence of an alginate film component and a pH responsive capsule coating. Two final BAP DDS's were formulated: (i) "high dose" formulation (4000IU D_3) and (ii) "low dose" formulation (1000IU D_3).

In vitro dissolution studies demonstrated a superior biphasic dissolution profile for the BAP compared to a market comparator vitamin D_3 product. The BAP produced an Area Under the dissolution Curve (AUC) for cholecalciferol release that was 10%-28% greater than that of conventional comparator products (1000IU BAP: 12334.55 vs. 11206.55; 4000IU BAP: 12436.41 vs. 9700.76), attesting to the enhancement in dissolution and solubility parameters imparted by the DDS mechanism. Therefore the total amount of cholecalciferol released *in vitro* was greater for the BAP than the comparator, with a higher incremental area under the curve (1000IU: D_{AUC}=1128; 4000IU: D_{AUC}=2735.65). Enhanced total dissolution was confirmed for the BAP compared to the comparator with a higher fraction of D_3 released during dissolution studies (1000IU BAP: 80.15% vs. 67.12%; 4000IU BAP: 84.01% vs. 59%). Dissolution Efficiency (DE) was also higher for D_3 released from the BAP compared to conventional D_3 tablets (11%-28% increase in DE). The improved BAP D_3 release properties were due to: (i) TPGS acting as a rapid emulsifier and surfactant to the fat-soluble vitamins; (ii) cyclodextrin phase solubility enhancements; and (iii) bio-surfactant effects of the bile salts released from the films enhancing the wettability and aqueous dispersion of the model drug (a unique triple phenomenon).The dissolution profiles also demonstrated a successful unified "in-concert" release profile for all three vitamins.

In vivo performance of the BAP revealed similar improvements to those found in the *in vitro* release testing. The BAP was successful at achieving a greater mean change from baseline D_3 to peak plasma level (C_{max}) for the 1000IU BAP compared to a reference product (38.24ng/mL vs. 26.18ng/mL). The mean change from baseline D_3 to C_{max} for the 4000IU BAP was 55.66ng/mL vs. 46.05ng/mL for the market comparator. Cholecalciferol bioavailability was greatly improved *in vivo* for the 4000IU BAP with an $AUC_{0\text{-}inf}$ 3.2x greater than that of the conventional product. Both BAP formulations were superior at improving and maintaining *in vivo* serum levels of 25-hydroxyvitamin D_3, considered the universal indicator of vitamin D status. Histopathological assessments illustrated an absence of adverse tissue reactions to the BAP and all animals in the dosing study tolerated the system well. A level A *in vitro-in vivo* correlation (IVIVC) analysis provided convincing correlations between the *in vitro* release data and *in vivo* absorption data for both BAP formulations.

ACKNOWLEDGEMENTS

I would like to extend my sincere thanks to my supervisor and mentor, Professor Viness Pillay, without whom none of this would have been possible. His expertise, guidance, insights, support and dedication during this research were unwavering. His encouragement often provided the impetus to push on during trying times. He was always available for discussion and a source of inspiration and wisdom throughout the course of this research.

I would also like to extend my thanks to my co-supervisor, Professor Yahya E. Choonara for his knowledge, direction, expertise and optimism and for always steering me in the right direction.

A special thank you to my colleague Mr. Pradeep Kumar for your invaluable after-hours support with aspects of the experimental work, and your expertise and assistance with the molecular modeling components of this study.

Thank you to post-doctoral researchers of the Wits Advanced Drug Delivery Platform (WADDP) who assisted with essential aspects of this research: Dr. Lomas K. Tomar and Dr. Charu Tyagi for their hard work and dedication involved with the editing process of the publications related to this research. To Dr. Tomar, thank you also for your expertise relating to the HPLC analysis. To Dr. Lisa C. Du Toit, thank you for your time and efforts involved in assisting with the *in vitro-in vivo* correlations and pharmacokinetic analysis.

Thank you to Mr. Felix Mashingaidze and Ms. Karen Machoba for your assistance with the preclinical animal studies in the pig-model. Your commitment and unconditional kindness will be forever remembered.

This research would also have not been possible without the financial assistance of the National Research Foundation (NRF) of South Africa, their support is sincerely appreciated.

Lastly, I would like to thank my family and friends for their moral support, especially for times when my research took precedence at the cost of sacrificing family time. A sincere thank you to my fiancé, Mischke Coetzee who has been steadfast in her support and providing me with the strength to persevere at every obstacle. Thank you Mischke for allowing this research to take priority at this time in our lives and for being so patient.

DEDICATION

This research is dedicated to those people in my life who have always been there for me through the peaks and troughs and motivated me to look beyond the present to what the future may hold. I dedicate this work to Science and to all those who have so strongly believed in my academic potential and pushed me to excel beyond what I had assumed possible.

TABLE OF CONTENTS

DECLARATION ii

RESEARCH OUTPUTS iii

Research Publications related to Doctoral Research iii

Patents Filed iii

ABSTRACT iv

ACKNOWLEDGEMENTS v

DEDICATION vi

TABLE OF CONTENTS vii

LIST OF FIGURES xviii

LIST OF TABLES xxvi

LIST OF ABBREVIATIONS xxviii

CHAPTER 1 1

DESIGN CONCEPT OF A 'BIOACTIVE ASSOCIATION PLATFORM' (BAP) ORAL DELIVERY SYSTEM FOR ENHANCED EFFICACY OF CHOLECALCIFEROL 1

1.1. Introduction 1

1.2. Rationale and Conceptualization of the BAP Delivery System Archetype 5

1.2.1. Rationale behind the BAP concept 5

1.2.2. The BAP design 7

1.2.3. An optimal cholecalciferol dose for inclusion in the BAP 11

1.3. Aim and Objectives of the Research 12

1.4. References 14

CHAPTER 2 17

NUTRACEUTICAL-BASED THERAPEUTICS AND CURRENT FORMULATION STRATEGIES 17

2.1. Introduction 17

2.2. The Nutraceutical Value Proposition 18

2.2.1. Nutraceuticals impacting the incidence and progression of disease 18

2.2.2. Vitamin D correlated to chronic disease 19
2.2.3. Causes of vitamin D insufficiency 21
2.2.4. The controversy and validity of nutraceutical study design 21
2.2.5. Nutraceuticals and future medical research 22
2.3. Routes of Nutraceutical Delivery to the Body 24
2.3.1. Oral delivery 24
2.3.2. Dermal delivery 25
2.3.3. Ophthalmic delivery 26
2.4. Nutraceutical Formulation Strategies 26
2.4.1. Liposomal carrier systems 27
2.4.2. Electrospun fiber mats 28
2.4.3. Cyclodextrin complexation 30
2.4.4. Biodegradable hydrogels 32
2.4.5. Nanotechnology-based applications for nutraceutical delivery 35
2.4.5.1. Nanosuspensions and nanoemulsions 35
2.4.5.2. Nanostructured lipid carriers (NLC) 37
2.4.5.3. Nanomicelles 38
2.4.5.4. Nanoparticles, nanocapsules and nano-encapsulation 38
2.4.5.5. Nanosponges and microsponges 40
2.4.6. Microparticulate systems: microparticles, microspheres and microcapsules 41
2.4.7. Solid dispersions 42
2.4.8. Self-emulsifying drug delivery systems (SEDDS) 43
2.4.9. Particle coatings for protection, site-specific delivery and enhanced efficacy 44
2.5. Concluding Remarks 52
2.6. References 54
CHAPTER 3 66

VITAMIN D THERAPY AND RELATED METABOLOMICS: IS THE CALCIFEROL DOSE AND FORM THE ONLY REQUIREMENTS FOR SUCCESSFUL CLINICAL THERAPEUTICS? 66

3.1. Introduction 66

3.2. Hypothesis 68

3.3. Evaluation of the Hypothesis 69

3.3.1. The metabolome is a unique set of molecular circumstances that influences therapeutic response to vitamin D 69

3.3.2. Synergistic mechanisms influence treatment success more than single drug protocols 69

3.3.3. The endocrine system and physiological feedback mechanisms influence serum levels and response to dose 70

3.3.4. Complexity or extent of underlying disease will determine timing and strategy behind vitamin D prescribing and monitoring 72

3.3.5. Genetic differences govern a patient's response to vitamin D 73

3.3.6. Drug and supplement interactions reduce absorption, retention or activation of vitamin D 74

3.3.7. Mild to moderate organ insufficiency and chronic disease influences vitamin D status 77

3.3.8. Lifestyle and dietary patterns affect bioavailability and action of vitamin D 79

3.3.9. Product quality, regulatory affairs and vitamin D success 81

3.3.10. Smart delivery systems introduce more variables that need to be considered and understood 82

3.4. Concluding Remarks 83

3.5. References 84

CHAPTER 4 90

DESIGN, SYNTHESIS & EVALUATION OF THE BAP DRUG DELIVERY SYSTEM COMPONENTS 90

4.1. Introduction 90

4.2. Materials and Methods 91

4.2.1. Materials 91

4.2.2. BAP candidate A: Cyclodextrin-vitamin complexes 92

4.2.2.1. Synthesis of cyclodextrin-vitamin complexes and inclusion efficiency determinations 92

4.2.2.2. Preparation of cyclodextrin-vitamin physical mixtures (blends) for comparison with complexes 93

4.2.2.3. Preliminary molecular mechanic simulations/ computations of CD-vitamin complexes 94

4.2.2.4. Visual examination of aqueous solutions to confirm the presence of vitamins in complexes 95

4.2.2.5. UV absorption spectra of aqueous solutions to confirm vitamin-cyclodextrin complexation 95

4.2.2.6. Thermodynamic Analysis of Inclusion Complexes by Differential Scanning Calorimetry (DSC) 96

4.2.2.7. Chemical structure stability mapping of vitamin inclusion complexes by Fourier Transform Infrared Spectroscopy (FTIR) to confirm complexation 96

4.2.2.8. Determination of crystallinity transitions of the vitamin complexes by X-ray Powder Diffraction (XRPD) 96

4.2.2.9. Vitamin inclusion efficiency (IE) determinations of CD-vitamin complexes by Ultra-Violet Spectroscopy 97

4.2.2.10. Phase solubility studies 98

4.2.2.10.1. Effect of βCD concentration on cholecalciferol and ascorbic acid solubility 98

4.2.2.10.2. Effect of blending time on cholecalciferol solubility 98

4.2.3. BAP candidate B: Polyelectrolyte microbead complexes 99

4.2.3.1. Synthesis of chitosan-bioactive microbeads 99

4.2.3.2. Synthesis of alginate-bioactive microbeads 100

4.2.3.3. Complexation efficiency (CE) and entrapment efficiency (EE) of polymer-bioactive complex microbeads 101

4.2.3.4. Chemical structure analysis of polyelectrolyte microbeads by Fourier Transform Infrared Spectroscopy (FTIR) 102

4.2.3.5. Thermodynamic analysis of microbead complexes by Differential Scanning Calorimetry (DSC) 102

4.2.4. BAP candidate C: Bioactive-polymer scaffolds 103

4.2.4.1. Bile salt and lipase scaffolds rationalized as attractive BAP candidates 103

4.2.4.2. Synthesis of bile salt scaffolds or pancreatic lipase scaffolds and combination lipase/ bile salt scaffolds 104

4.2.4.3. In vitro release testing of bile-salt scaffolds and pancreatic lipase scaffolds 104

4.2.5. BAP candidate D: Alginate hydrogel films containing pancreatic lipase and/ or bile Salts 106

4.2.5.1. Rheological properties of film-forming solutions 106

4.2.5.2. Synthesis of polymer films as carriers of bile salts and pancreatic lipase 107

4.2.5.3. Karl Fischer moisture content analysis of films 108

4.2.5.4. Investigation of the physico-mechanical behaviour of films 108

4.2.5.5. Morphological analysis of films using Scanning Electron Microscopy (SEM) 109

4.3. Results and Discussion 109

4.3.1. Preliminary molecular mechanic simulations/ computations of bioactive-CD complexes to test the feasibility of CD-vitamin complexes 109

4.3.2. Visual observations tests to confirm the presence of vitamins in inclusion complexes 111

4.3.3. UV absorption spectra of aqueous complex solutions to confirm vitamin-cyclodextrin complexation 114

4.3.4. Thermodynamic analysis of CD-vitamin complexes by Differential Scanning Calorimetry (DSC) 117

4.3.4.1. Thermograms of αCD cholecalciferol inclusion complexes 119

4.3.4.2. Thermograms of βCD cholecalciferol inclusion complexes 119

4.3.4.3. Thermograms of γCD cholecalciferol inclusion complexes 123

4.3.4.4. Thermograms of 2HPβCD-cholecalciferol inclusion complexes 123

4.3.4.5. Thermal characteristics of other vitamin inclusion complexes 124

4.3.4.6. Summary discussion: Thermal analysis of vitamin IC's 127

4.3.5. Chemical structure stability mapping of CD-vitamin complexes by Fourier Transform Infrared Spectroscopy (FTIR) to confirm complexation 128

4.3.5.1. FTIR spectra of αCD, βCD, γCD and 2HPβCD cholecalciferol IC's 128

4.3.5.2. FTIR spectra of βCD vitamin inclusion complexes 129

4.3.5.3. Intensity shifts in FTIR spectra of vitamin inclusion complexes ..130

4.3.5.4. Summary discussion: FTIR of vitamin IC's.....133

4.3.6. Determination of crystallinity transitions of the vitamin-CD complexes by X-ray Powder Diffraction (XRPD) 134

4.3.6.1. XRD crystalline structure of cholecalciferol inclusion complexes134

4.3.6.2. XRD crystalline structure of ascorbic acid inclusion complexes .135

4.3.6.3. Crystallinity discussion and implications 136

4.3.7. Inclusion efficiency (IE) determinations of CD-vitamin complexes 138

4.3.8. Phase solubility studies of vitamin complexes 142

4.3.8.1. Cholecalciferol phase solubility-study 1 142

4.3.8.2. Cholecalciferol phase solubility-study 2 143

4.3.8.3. Ascorbic acid phase solubility 144

4.3.8.4. Vitamin phase solubility implications for BAP formulation development.....146

4.3.9. Microbead bioactive complexes: Entrapment efficiency (EE).....147

4.3.9.1. Chitosan bioactive microbeads: Entrapment efficiency 147

4.3.9.2. Alginate bioactive microbeads: Entrapment efficiency 147

4.3.10. Chemical structure analysis of polyelectrolyte microbead complexes by Fourier Transform Infrared Spectroscopy (FTIR) 149

4.3.11. Thermodynamic analysis of microbead complexes by Differential Scanning Calorimetry (DSC) 152

4.3.12. Microbeads as suitable BAP candidates.....155

4.3.13. Bile salt-alginate scaffolds release studies 156

4.3.13.1. Preliminary bile salt scaffold release studies.....156

4.3.13.2. Final bile salt-alginate scaffold release studies: USP method ..158

4.3.14. Pancreatic lipase-alginate scaffolds dissolution studies.....160

4.3.15. An artificial milieu environment using bile and lipase scaffolds 161

4.3.16. Rheological properties of film forming solutions.....163

4.3.16.1. Rheology: General observations.....163

4.3.16.2. Rheology: Bioactive combination pregels (NaD, NaC, and Lip) 164

4.3.16.3. Rheology: Bile salt pregels 165

4.3.16.4. Pregel rheological parameters and their implications 165

4.3.17. Karl Fischer moisture content analysis of 66B/33L films 168

4.3.18. Investigation of the physico-mechanical behaviour of films 170

4.3.19. Morphological analysis of 66B/33L films using Scanning Electron Microscopy (SEM) 172

4.4. Concluding Remarks 173

4.5. References 175

CHAPTER 5 185

IN VITRO FORMULATION, CHARACTERIZATION, AND TESTING OF THE FINAL BAP DRUG DELIVERY SYSTEM 185

5.1. Introduction 185

5.2. Materials and Methods 186

5.2.1. Materials 186

5.2.2. BAP component A: “3-vitamin” minitablets as final vitamin carriers 186

5.2.2.1. A novel minitablet formulation: A rational approach for multivitamin inclusion in the BAP 186

5.2.2.2. Comprehensive molecular mechanics simulations of cholecalciferol complexes to confirm optimized IC for inclusion in minitablet 187

5.2.2.3. Formulation of “3-vitamin” minitablets 189

5.2.2.4. Karl Fischer moisture content analysis of “3-vitamin” minitablets 193

5.2.2.5. Texture Analysis (TA) of minitablets to determine hardness, resilience and compressibility 193

5.2.2.6. Magnetic Resonance Imaging (MRI) to illustrate minitablet dissolution 194

5.2.2.7. Comparative *ex vivo* permeability of cholecalciferol from “3-vitamin” minitablets vs. a conventional comparator tablet 194

5.2.2.8. Thermodynamic analysis of minitablets by Differential Scanning Calorimetry (DSC) 196

5.2.2.9. Chemical structure stability mapping of minitablets by Fourier Transform Infrared Spectroscopy (FTIR) 196

5.2.3. BAP component B: Optimized bile salt-lipase film for inclusion in BAP 196

5.2.3.1. Synthesis of bile salt-lipase alginate films 196

5.2.3.2. Influence of bile salt-lipase films on cholecalciferol release from minitablets: Selection of an optimized film 197

5.2.3.3. Enzyme activity profiles of 66B/33L(0%; 0.25%, 0.5%, 1%) films following hydration in SIF: Selection of an optimized film.....199

5.2.3.4. Thermodynamic analysis of optimized 66B/33L(0.5%) BAP films by Differential Scanning Calorimetry (DSC).....200

5.2.3.5. Chemical structure analysis of optimized 66B/33L(0.5%) BAP films 201

by Fourier Transform Infrared Spectroscopy (FTIR) 201

5.2.4. Final BAP DDS capsule: Combined technologies for improved release 201

5.2.4.1. Final BAP: Assembling each BAP DDS capsule 201

5.2.4.2. Comparative *in vitro* dissolution testing of BAP DDS 203

5.3. Results and Discussion.....205

5.3.1. Evaluation of comprehensive modeling simulations to confirm β-CD||VitD IC superiority 205

5.3.1.1. Energetic stabilization of CD||VitD inclusion complexes 205

5.3.1.2. The inclusion mode of VitD with respective cyclodextrin 207

5.3.1.3. Space-filling model for determination of best-fit geometrical conformation.....208

5.3.2. Karl Fischer moisture content of minitablets 210

5.3.3. Texture analysis profiles of minitablets to determine hardness, resilience and compressibility.....210

5.3.4. Magnetic Resonance Imaging (MRI) depicting minitablet dissolution 212

5.3.5. *Ex vivo* permeability studies: Franz Diffusion (FD) of minitablets and market comparator 213

5.3.6. Thermodynamic analysis of minitablets by Differential Scanning Calorimetry (DSC).....215

5.3.7. Chemical structure stability mapping of minitablet and constituents by Fourier Transform Infrared Spectroscopy (FTIR) 217

5.3.8. Bile salt/lipase influence on cholecalciferol release study: Selection of an optimized film 218

5.3.9. Lipase enzyme activity profiles of combined lipase-bile salt films-Selection of an optimized film based on enzyme activity 224

5.3.10. Thermodynamic analysis of optimized 66B/33L(0.5%) BAP films by 228

Differential Scanning Calorimetry (DSC) 228

5.3.11. Chemical structure analysis of optimized 66B/33L(0.5%) films by Fourier Transform Infrared Spectroscopy (FTIR) 229

5.3.12. Comparative *in vitro* drug release studies of the final BAP DDS 231

5.3.12.1. A superior BAP cholecalciferol dissolution profile 233

5.3.12.2. Dissolution calculations and cholecalciferol model selection 235

5.3.12.3. A unified vitamin release phenomenon 237

5.3.12.4. A unique BAP vitamin delivery mechanism 239

5.4. Concluding Remarks 241

5.5. References 242

CHAPTER 6 249

COMPARATIVE *IN VIVO* PRECLINICAL EVALUATION OF THE BAP DRUG DELIVERY SYSTEM IN THE LARGE WHITE PIG MODEL 249

6.1. Introduction 249

6.1.1. The pertinence of *in vivo* analysis of novel drug delivery systems and applicability of the pig model 249

6.1.2. Study objectives*: In vivo* parameters under evaluation 250

6.1.3. Safety evaluation of the cholecalciferol study dose and delivery mechanism 251

6.1.3.1. Safety assessment in humans 251

6.1.3.2. Safety assessment in pigs 251

6.2. Materials and Methods 252

6.2.1. Materials and preparative work 252

6.2.2. Surgical and invasive procedures and *in vivo* animal study design 254

6.2.2.1. Preparative procedures: Insertion of jugular catheter 254

6.2.2.2. *In vivo* design: Dosing study – A comparative *in vivo* relative bioavailability study.....255

6.2.3. X-ray studies for gastrointestinal tracking of the BAP 257

6.2.4. Histological analysis of intestinal tissue samples.....258

6.2.5. Quantification of *in vivo* cholecalciferol and 25-hydroxyvitamin D_3 concentrations released from the BAP and comparator products.....259

6.2.5.1. Quantification of *in vivo* cholecalciferol concentrations in plasma 259

6.2.5.2. Quantification of *in vivo* 25-hydroxyvitamin D_3 concentrations in serum 260

6.2.6. Pharmacokinetic modelling of drug release data employing noncompartmental and compartmental algorithms.....261

6.2.7. Establishment of an *in vitro-in vivo* correlation for cholecalciferol release from the BAP DDS.....261

6.3. Results and Discussion.....262

6.3.1. Surgical procedures and post-surgical assessment of the pig model following catheter surgery and dosing study.....262

6.3.2. X-ray studies for gastrointestinal tracking of the BAP 264

6.3.3. Histological analysis of intestinal tissue following 5 day dosing study 265

6.3.3.1. Placebo tissue samples 265

6.3.3.2. BAP DDS tissue samples 265

6.3.4. Quantification of *in vivo* cholecalciferol and 25-hydroxyvitamin D_3 concentrations released from the BAP DDS and comparator products 267

6.3.5. Pharmacokinetic analysis: Comparative *in vivo* evaluation of the BAP DDS and comparator products.....268

6.3.5.1. BAP DDS and comparator 4000IU cholecalciferol noncompartmental and compartmental analyses.....268

6.3.5.2. BAP DDS and comparator 1000IU cholecalciferol noncompartmental and compartmental analyses.....275

6.3.6. Comparative *in vivo* evaluation of 25-hydroxyvitamin D_3 serum levels in response to BAP DDS and comparator product dosing.....280

6.3.6.1. Rise in 25-hydroxyvitamin D metabolite as an essential biomarker of an effective cholecalciferol formulation 280

6.3.6.2. Evaluation of 25-hydroxyvitamin D_3 response to BAP and comparator products 280

6.3.7. Establishment of an *in vitro-in vivo* correlation for cholecalciferol release from the BAP DDS 284

6.4. Concluding Remarks 287

6.5. References 289

CHAPTER 7 296

CONCLUSION AND RECOMMENDATIONS 296

7.1. Conclusion 296

7.1.1. BAP component achievements 296

7.1.2. Final BAP DDS capsule(s) achievements 297

7.2. Recommendations 299

7.3. References 300

8. APPENDICES 301

8.1. Animal Ethics Clearance Certificate 301

8.2. Modifications & Extension Approvals to Animal Study 303

8.3. Doctoral Research Publications (2011-2014) 307

8.3.1. Paper 1: Medical hypothesis 307

8.3.2. Paper 2: Review 308

8.3.3. Additional papers to be submitted (2014) 309

8.3.3.1. Paper 3: Research paper I 309

8.3.3.2. Paper 4: Research paper II 310

LIST OF FIGURES

Figure 1.1: Detailed schematic representing an example of 2 possible Bioactive Booster molecules that may be designed for inclusion in the novel BAP DDS. 10

Figure 1.2: Multiple Bioactive Boosters (BB1 and BB2) complex together to form the BAP which is then encased within a capsule to be delivered as an oral drug delivery system 11

Figure 2.1: Research articles dealing with nutraceutical or functional foods published in the period 1989-2009 (ISI Web of Knowledge) (Bernal *et al*., 2011) [Reproduced with permission from Elsevier Science BV Ltd. © 2011] ..... ….. 18

Figure 2.2: Vitamin D modulates the function of macrophages, monocytes, and dendritic cells (DC). IKK: IkB kinase; IkB: inhibitor of NF-kB; LPS: lipopolysaccharides; TLR: Toll-like receptors; VDR: vitamin D nuclear receptor (Borges *et al*., 2011) [Reproduced with permission from Elsevier Science BV Ltd. © 2011]. ….. 20

Figure 2.3: (A) SEM micrograph of PCL/AP with AP concentration 9 and 16% respectively, magnification: 2500x. PCL concentration: 10%$^{w}/_{v}$ and (B) Log of viable S. aureus cells versus the time of exposure to PCL, PCL/AP (9%) and PCL/AP(30%) fibrous materials (Paneva *et al*., 2011) [Reproduced with permission from Elsevier Science BV Ltd. © 2011]. 30

Figure 2.4: Scanning electron micrographs of 9%($^{w}/_{w)}$ soy protein cold-set gels made with (A) 10mM CaCl2 (filamentous gel) and (B) 20mM CaCl2 (particulate gel) (Maltais *et al*., 2009) [Reproduced with permission from Elsevier Science BV Ltd. © 2009]. 34

Figure 2.5: Illustrations of several functionalities of milk proteins useful for nutraceutical delivery (Livney, 2010) [Reproduced with permission from Elsevier Science BV Ltd. © 2010]..... 35

Figure 2.6: (A) *In vitro* penetration profiles of lutein from nanosuspension loaded pellets and from coarse lutein powder pellets, both filled into hard gelatine capsule (Mitri *et al*., 2011) [Reproduced with permission from Elsevier Science BV Ltd. © 2011] and (B) Influence of carrier oil type on the bioaccessibility of β-carotene initially encapsulated within oil-in-water nanoemulsions. Measurements were made before and after filtration (0.45μm pore size) of the middle phase (Qian *et al*., 2012) [Reproduced with permission from Elsevier Science BV Ltd. © 2012]..... 37

Figure 2.7: Pre-corneal drainage of 99mTc-DTPA in preparations (Zhang and Wang, 2009) [Reproduced with permission from Elsevier Science BV Ltd. © 2009]..... 46

Figure 3.1: Schematic depicting and summarizing multiple factors that influence vitamin D treatment success. 68

Figure 3.2: Schematic diagram illustrating the synthesis of active vitamin D 1,25-$(OH)_2$ D, by sequential hydroxylation in liver, kidneys and local tissues. Cutaneous photosynthesis is the main source of vitamin D with minor contribution from the contemporary western diet. Target tissues obtain 1,25-$(OH)_2$ D from either

circulating pool formed in the kidneys or locally from tissue 1α-hydroxylation [Reproduced with permission from Lee, 2011 © Elsevier BV Ltd.]. 71

Figure 3.3: The role of vitamin D in health relative to degree of sufficiency and tissue requirement: (a) vitamin D sufficiency enhances metabolic, immune and organ functions, (b) parathyroid hormone (PTH) activation generates sufficient 1,25-$(OH)_2$ D in states of moderate vitamin D deficiency and tissue requirement, (c) severe deficiency and critical tissue requirement in face of insufficient PTH axis leading to break down of various tissue homeostatic mechanisms resulting in morbidity and mortality [Reproduced with permission from Lee, 2011 © Elsevier B.V. Ltd.]. 77

Figure 4.1: UV Spectra of solutions of (a) βD3-8 inclusion complex (aqueous solution); (b) βC-8 inclusion complex (aqueous solution); (c) HPβD_3-4 inclusion complex (aqueous solution); (d) γD3-4 inclusion complex (aqueous solution); (e) cholecalciferol (ethanol solution); (f) ascorbic acid (aqueous solution)..... 117

Figure 4.2: DSC Pilot run 10°C-250°C showing three water loss peaks for αCD and clearly defined melting point for Vitamin D_3 at 84.5°C in congruence with literature values..... 121

Figure 4.3: DSC profiles of (a) αCD, αD_3-4 and cholecalciferol; (b) αCD, α*D3*-4 complex, and physical mixture of αCD and cholecalciferol; (c) βCD, βD_3-8 and cholecalciferol; (d) water loss run from 10°C-250°C for two βD_3 complexes, cholecalciferol and βCD..... 122

Figure 4.4: DSC profile of βCD and βD_3-4 complex. 123

Figure 4.5: DSC profiles of (a) γCD, γD_3-4 complex and cholecalciferol; (b) 2-hydoxypropylβCD, 2-hydoxypropylβCD-D_3-4 complex and cholecalciferol; (c) βCD to βE-4 complex; (d) DSC profile of physical blend of βCD and vitamin C, βC-8 complex, βCD, and vitamin C. 126

Figure 4.6: DSC profiles of 2-hydoxypropylβCD and 2-hydoxypropylβCD-D_3-4 complex..... 127

Figure 4.7: FTIR spectra of (a) αCD, cholecalciferol, and αD_3-4 complex; (b) βCD, cholecalciferol, and βD_3 complex; (c) βCD, cholecalciferol, and physical blend of βCD and cholecalciferol; (d) cholecalciferol, γCD and γD_3-4 complex..... 132

Figure 4.8: FTIR "split" spectra of HPβD_3-4 complex, HPβCD, and vitamin D_3 132

Figure 4.9: FTIR spectra of (a) HPβD_3-4 complex, HPβCD, and cholecalciferol; (b) βE-4 complex, βCD, and α-tocopherol; (c) βC-8 complex, vitamin C, and βCD. 133

Figure 4.10: X-ray powder diffractograms of (a) βCD, βD_3-8, cholecalciferol, and βCD and cholecalciferol physical mixture; (b) βCD, βC-4, cholecalciferol, and βCD and vitamin C physical mixture. 137

Figure 4.11: UV Standard Calibration Curve generated on UV-spectrophotometer for cholecalciferol aqueous solutions at 265nm used for IE% determinations of vitamin-CD complexes. 139

Figure 4.12: UV Standard Calibration Curves generated on UV-spectrophotometer for (a) Ascorbic acid aqueous solutions at 265nm and (b) α-Tocopherol aqueous solutions at 295nm used for IE% determinations of vitamin-CD complexes. 139

Figure 4.13: Effect of βCD concentrations on the aqueous solubility of vitamin D_3 after 72 hours of blending (βCD 0-11mM). 145

Figure 4.14: Effect of βCD concentrations on the aqueous solubility of vitamin D_3 after 24 hours and then after 72 hours of blending (βCD 0.25-1.75mM). 145

Figure 4.15: Effect of βCD concentrations on the aqueous solubility of ascorbic acid after 72 hours of blending (βCD 0-10mM) 146

Figure 4.16: Bar chart illustrating the EE values obtained for all polymer-bioactive microbead complexes 149

Figure 4.17: FTIR spectra of (a) chitosan (CHI), cholic acid (CA), and CA-CHI complex microbeads; (b) chitosan (CHI), deoxycholic acid (DA), and DA-CHI complex microbeads; (c) chitosan, lecithin, and lecithin-chitosan complex (LT-CHI). 151

Figure 4.18: FTIR spectra of (a) alginate (Alg), cholic acid (CA), and CA-Alg complex microbeads; (b) alginate (Alg), deoxycholic acid (DA), and DA-Alg complex microbeads. 151

Figure 4.19: DSC profiles of (a) chitosan (CHI), cholic acid (CA) and CA-CHI complex microbeads; (b) chitosan (CHI), deoxycholic acid (DA) and DA-CHI complex microbeads; (c) chitosan (CHI), lecithin (LT) and LT-CHI complex microbeads; (d) chitosan, CA-CHI microbeads, DA-CHI microbeads, LT-CHI microbeads. 154

Figure 4.20: DSC profiles of (a) alginate (Alg), cholic acid (CA), CA-Alg complex microbeads; (b) alginate (Alg), deoxycholic acid (DA), DA-Alg complex microbeads; (c) alginate (Alg), cholic acid (CA), deoxycholic acid (DA), CA-Alg complex microbeads, DA-Alg complex microbeads. 155

Figure 4.21: Preliminary release testing of Na dexoycholate- 4%$^{w}/_{v}$ alginate scaffold (0.5%$^{w}/_{v}$ CL) at (a) 30 minutes and (b) 3 hour time points. It was evident that at 30 minutes the scaffold had hydrated, expanded and was fully submerged but was still an intact single mass. By 3 hours the scaffold integrity was lost with separation into fragmented parts allowing the majority of the bile salt to be released into solution. 157

Figure 4.22: Preliminary bile salt release profiles of Sodium dexoycholate (4% alginate) scaffolds containing crosslinker at varying concentrations (0%, 0.5%, 1%) in 200mL phosphate buffer (pH 6.8). 158

Figure 4.23: Release profile of bile salt alginate (4%$^{w}/_{v}$) scaffolds crosslinked with 0.5%$^{w}/_{v}$ calcium gluconate containing the bile salts: sodium deoxycholate or sodium cholate hydrate in phosphate buffer (SIF pH 6.8) (USP method: USP 2 Apparatus). 160

Figure 4.24: (a) *In vitro* release profile of different pancreatic lipase-alginate scaffold formulations in phosphate buffer (SIF pH 6.8) (USP 2 Apparatus) (b) Photographic image of a typical Lipase-4% Alginate scaffold (0.5%CL). 161

Figure 4.25: Overlaid scaffold release curves showing the release profiles of two bile salts (NaD, NaC) and pancreatic lipase from customizable polymeric scaffolds..... 163

Figure 4.26: Oscillatory frequency sweep showing the viscous (G") moduli (----) and the elastic moduli (G') (-----) of two different alginate pregel solutions as a function of frequency: (a) 4%A vs. (b) 4%A Comb100 166

Figure 4.27: Oscillatory frequency sweep showing the viscous (G") moduli (----) and the elastic moduli (G') (-----) of three different alginate pregel solutions as a function of frequency: (a) 4%A2%G vs. (b) 4%A2%G Comb50 vs. (c) 4%A2%G Comb200……166

Figure 4.28: Oscillatory frequency sweep showing the viscous (G") moduli (----) and the elastic moduli (G') (-----) of two different alginate pregel solutions as a function of frequency: (a) 4%A4%G vs. (b) 4%A4%G Comb100..... 167

Figure 4.29: Oscillatory frequency sweep showing the viscous (G") moduli (----) and the elastic moduli (G') (-----) of three different bile salt alginate pregel solutions as a function of frequency: (a) 4%AC100 vs. (b) 4%A2%C100 vs. 4%A2%D100 167

Figure 4.30: Bar-chart illustrating the relationship between crosslinker concentration and moisture content of five different bioactive films: Comparison of five bioactive film formulations: 66B/33L(0%); 66B/33L(0.2%); 66B/33L(0.3%); 66B/33L(0.5%); 66B/33L(0.7%)..... 169

Figure 4.31: Graphical representation of texture analysis results obtained for five bioactive films including: 66B/33L(0%); 66B/33L(0.2%); 66B/33L(0.3%); 66B/33L(0.5%); 66B/33L(0.7%) showing (a) Maximum break force vs. CL %; (b) Water content and Tensile strength vs. CL %; (c) CL % vs. Tensile strength; (d) A 3D-Mesh plot correlating Tensile Strength with Crosslinker concentration and moisture content..... 172

Figure 4.32: Scanning Electron micrographs of the surface morphology of bioactive-alginate film formulation 66B/33L(0.5%) at (a) 2220x magnification and (b) 2240x magnification 173

Figure 4.33: Photographic images depicting the four BAP component candidates that were formulated and tested during the preformulation studies: (a) BAP candidate A: CD-vitamin complexes; (b) BAP candidate B: Bioactive microbeads (alginate); (c) BAP candidate C: polymeric-bioactive scaffolds (alginate); (d): BAP candidate D: Bioactive-polymer films..... 174

Figure 5.1: Models depicting the molecules used in the study showing (a) chemical structure of vitamin D; (b) stereographic view of the α-cyclodextrin bucket; (c) stereographic view of the β-cyclodextrin bucket; and (d) stereographic view of the γ-cyclodextrin bucket. The upper wider ring in cyclodextrin bucket represents the secondary hydroxyl groups and the lower narrower ring represents the primary hydroxyl groups. Colour codes for elements are: Carbon (cyan), Oxygen (red) and Nitrogen (blue). Hydrogen atoms are not shown for clarity..... 188

Figure 5.2: Punch and die mechanism: A: Stainless steel funnel; B: Stainless steel base plate; C: Stainless steel bottom sheath; D: Stainless steel top sheath; E:

Stainless steel die; F: Stainless steel bottom punch; G: Stainless steel top punch. 191

Figure 5.3: Schematic of the stepwise method used to manufacture the “3-vitamin” minitablet component..... 192

Figure 5.4: “3-vitamin” minitablets formed after compression using a modified die and punch: (a) top-view; (b) side-view. 192

Figure 5.5: Schematic showing the components making up a single Franz Diffusion cell used for the *ex vivo* cholecalciferol permeability studies (Vertical Franz Cell: www.permegear.com)..... 195

Figure 5.6: Illustrative schematic showing the assembling of the two BAP capsules containing all formulation components.. 202

Figure 5.7: Final BAP components used in the formulation design and to assemble the BAP DDS capsule: Component A: Novel “3-vitamin” minitablets consisting of ascorbic acid, TPGS and βD_3-8 IC; Component B: Bile salt-lipase bioactive film 202

Figure 5.8: BAP DDS capsule: (a) prior to coating; (b) coated with modified kollicoat® pH responsive coating containing the six bioactives: cholecalciferol (model drug), ascorbic acid, α-tocopherol, pancreatic lipase, sodium deoxycholate, sodium cholate hydrate and various polymers and carrier mechanisms. 202

Figure 5.9: Molecular models depicting minimum energy inclusion complexes of VitD with (a) α-CD; (b) β-CD; (c) γ-CD; and (d) HP-β-CD. The 3D models were slightly rotated in order to clearly visualize the H-bonds formed between the molecules. Cyclodextrins are depicted in tube rendering and VitD stick rendering. Template showing the respective configurations are also shown for easy understanding and depiction. 208

Figure 5.10: 3D overlapping sphere space-filled models for (a) α-CD||VitD; (b) β-CD||VitD; (c) γ-CD||VitD and d) HP-β-CD||VitD. Colour codes for molecules are: Cyclodextrin (red) and VitD (yellow). 209

Figure 5.11: Matrix resilience values calculated during TA studies of novel “3-vitamin” minitablets (n=5) represented in a 3-dimensional bar chart format 211

Figure 5.12: Magnetic resonance images of the erosion and dissolution of the “3-vitamin” minitablet in phosphate buffer (pH 6.8) simulating the condition in the duodenum. Images captured at (a) 5 minutes; (b) 10 minutes; (c) 15 minutes; (d) 20 minutes; (e) 25 minutes; (f) 30 minutes. 212

Figure 5.13: Overlaid cumulative cholecalciferol permeation profiles from a novel 4000IU “3-vitamin” minitablet and a conventional 4000IU cholecalciferol comparator tablet. 214

Figure 5.14: DSC thermograms of: (a) overlaid “3-vitamin” minitablet, TPGS and cholecalciferol (vitamin D_3); (b) ascorbic acid..... 216

Figure 5.15: FTIR spectra of: (a) minitablet and individual constituents; (b) Dissolved minitablet and individual constituents..... 217

Figure 5.16: *In vitro* dissolution profiles showing comparative cholecalciferol release from (a) “3-vitamin” minitablets vs. “3-vitamin” minitablets wrapped with 66B/33L film; and (b) “3-vitamin” minitablets vs. “3-vitamin” minitablets wrapped with 33B/66L film..... 222

Figure 5.17: *In vitro* dissolution profiles showing comparative cholecalciferol release from “3-vitamin” minitablets vs. “3-vitamin” minitablets wrapped with 100B High film vs. “3-vitamin” minitablets wrapped with 100B Low film 223

Figure 5.18: *In vitro* dissolution profiles showing comparative cholecalciferol release from (a) “3-vitamin” minitablets vs. “3-vitamin” minitablets wrapped with 80B/20L film; and (b) “3-vitamin” minitablets vs. “3-vitamin” minitablets wrapped with 100L film..... 224

Figure 5.19: Lipase activity profiles of 66B/33L (0%-1%$^{w}/_{v}$ CL) films (200mg) containing: 20mg NaC, 20mg NaD, 20mg lipase 227

Figure 5.20: Photographic image of 66B/33L(0.5%) film containing: pancreatic lipase (100mg), sodium deoxycholate (100mg) and sodium cholate (100mg) 228

Figure 5.21: DSC thermograms of: (a) overlaid NaD, NaC, pancreatic lipase and 66B/33L(0.5%) film; (b) overlaid NaD, pancreatic lipase, sodium alginate, 66B/33L(0.5%) film. 229

Figure 5.22: FTIR spectra of bioactive alginate/ glycerin film containing bile salts and lipase and individual constituents..... 230

Figure 5.23: *In vitro* dissolution study of BAP DDS using a USP 4 apparatus (Flow-through cell dissolution tester, Type DFZ60, Erweka). (a) Seven cells containing BAP DDS components at different stages of the dissolution study; (b) Exposed minitablets in one cell after dissolution of capsules; (c) Manifold, pump and HLB Oasis cartridges used for the solid phase extraction of fat-soluble vitamins from dissolution samples prior to HPLC analysis.. 232

Figure 5.24: HPLC chromatograms of standard vitamin peaks: (a) Cholecalciferol peak at 7.279 minutes; (b) α-tocopherol peak at 9.853 minutes; (c) Ascorbic acid peak at 3.041 minutes. 232

Figure 5.25: Calibration curve generated for cholecalciferol standards (UV detection at 265nm) for HPLC quantification of dissolution samples during vitamin release studies..... 233

Figure 5.26: Calibration curve generated for: (a) α-tocopherol standards (UV detection at 295nm) and (b) ascorbic acid standards (UV detection at 265nm) for HPLC quantification of dissolution samples during vitamin release studies..... 233

Figure 5.27: Dissolution profiles of (a) Cholecalciferol release from 1000IU BAP DDS and 1000IU comparator product; (b) Cholecalciferol release from 4000IU BAP DDS and 4000IU comparator product in SIF (USP4 apparatus). 235

Figure 5.28: Dissolution profiles of vitamin release from 1000IU BAP DDS (a) Vitamin C release; (b) Vitamin E release; (c) Vitamin D_3 release; (d) Profiles of all vitamins released from 1000IU BAP (vitamin D_3, ascorbic acid and α-tocopherol) in SIF (USP4 apparatus) 238

Figure 5.29: Dissolution profiles of vitamin release from 4000IU BAP DDS: (a) Vitamin C release; (b) Vitamin E release; (c) Vitamin D_3 release; (d) Profiles of all vitamins released from 4000IU BAP (vitamin D_3, ascorbic acid and α-tocopherol) in SIF (USP4 apparatus) 239

Figure 5.30: Dissolution profiles showing the release/ activity level of all bioactives from the BAP including (a) all vitamins released and lipase enzyme activity provided by the 1000IU BAP; (b) all vitamins released and lipase enzyme activity provided by the 4000IU BAP 240

Figure 6.1: Schematic of the experimental design and *in vivo* testing employed in animal species (Pigs underwent surgical insertion of jugular catheter 10 days after arrival at CAS followed by a 10 day recovery period; The dosing study occurred 10 days following jugular catheter surgery with daily dosing from day 0 to day 5)..... 256

Figure 6.2: Time-line of a single pig throughout the entire study where two phases of anaesthesia will occur, during implantation of the intrajugular catheter (once off) and once daily for a period of 5 continuous days during the dosing study. X-ray studies were performed additionally on 1 pig and histopathology on 1 pig following humane euthanasia. 258

Figure 6.3: Sequential images depicting the intrajugular catheter surgery in one study animal during the *in vivo* evaluation of the BAP DDS: (a) and (b) Surgical incision to expose the jugular vein; (c) Insertion of the jugular catheter into the lumen of the jugular vein and fastening to the wall of the vein; (d) Sutured left lateral aspect of the neck of a pig after completion of jugular catheter surgery; (e) External injection ports of the catheter positioned on the dorsal aspect of the scapula. 262

Figure 6.4: Photographic evidence of (a) Housing of the pigs at CAS; (b) Pig under general anaesthetic during dosing study; (c) Sterile blood sampling from jugular catheter ports during dosing study. 263

Figure 6.5: X-ray images of one study animal dosed a test product containing barium showing the outline of the capsule at 30 minutes post dosing: (a) lateral X-ray image of stomach; (b) medial X-ray image of stomach..... 264

Figure 6.6: Microscopic slide images demonstrating the condition of each tissue sample harvested from two study animals 265

Figure 6.7: Calibration curves generated for (a) cholecalciferol and (b) 25-hydroxyvitamin D_3 from the ELISA Kits used to quantify the levels of actives in plasma and serum respectively. 267

Figure 6.8: Graphical results for (a) noncompartmental and (b) compartmental PK analysis of cholecalciferol release from BAP DDS 4000IU. 273

Figure 6.9: Graphical results for (a) noncompartmental and (b) compartmental PK analysis of cholecalciferol release from Comparator 4000IU..... 273

Figure 6.10: Overlaid mean plasma concentration-time profiles of cholecalciferol following single oral administration of BAP DDS 4000IU and comparator 4000IU. 274

Figure 6.11: Graphical results for (a) noncompartmental and (b) compartmental PK analysis of cholecalciferol release from BAP DDS 1000IU. 278

Figure 6.12: Graphical results for (a) noncompartmental and (b) compartmental PK analysis of cholecalciferol release from Comparator 1000IU. 278

Figure 6.13: Overlaid mean plasma concentration-time profiles of cholecalciferol following single oral administration of BAP DDS 1000IU and Comparator 1000IU. 279

Figure 6.14: Time course of the rise in serum 25(OH)D_3 levels following daily doses of BAP DDS (4000IU cholecalciferol), Comparator (4000IU cholecalciferol), and a placebo DDS 282

Figure 6.15: Time course of the rise in serum 25(OH)D_3 levels following daily doses of BAP DDS (1000IU cholecalciferol), and Comparator (1000IU cholecalciferol) 282

Figure 6.16: (a) Levy Regression Plot showing the relationship between the % of cholecalciferol absorbed *in vivo* and the % released *in vitro* from the 4000IU DDS; (b) Drug release profiles of the *in vitro* cholecalciferol release and the observed mean *in vivo* release profile extracted using deconvolution analysis for a single dose cholecalciferol released from the 4000IU BAP. 285

Figure 6.17: Levy Regression Plot showing the relationship between the % of cholecalciferol absorbed *in vivo* and the % released *in vitro* from the 1000IU DDS. 286

LIST OF TABLES

Table 1.1: Enhancing bioactive candidates and their possible functions in the cholecalciferol BAP 8

Table 2.1: Summary of recent formulation approaches for improved nutraceutical delivery 47

Table 4.1**:** Summary of the molar ratios of CD's and vitamins that were combined during the synthesis of vitamin-CD complexes 92

Table 4.2: Chitosan and alginate bioactive microbead formulations 101

Table 4.3: Alginate ($4\%^{w}/_{v}$) bioactive scaffold formulations 104

Table 4.4: Alginate-glycerin bioactive pregel formulations 107

Table 4.5: Alginate-glycerin bioactive film formulations 108

Table 4.6: Textural parameters for determination of tensile strength and maximum break force 109

Table 4.7: Calculated energy parameters (kcal/mol) of the complex molecular assemblies from molecular modelling pilot study 110

Table 4.8: Summary table illustrating visual observations of aqueous solutions containing: Cyclodextrin; Vitamin-CD complexes; and Vitamins 112

Table 4.9: List of cyclodextrin and vitamin melting points as derived from Material Safety Data Sheets (MSDS) for each native compound 118

Table 4.10: Summary of the % crystallinity of inclusion complex samples 137

Table 4.11: IE% calculations for CD-vitamin inclusion (n=3) 142

Table 4.12: Mean EE values obtained for polymer microbead formulations 148

Table 4.13: Moisture content of 66B/33L film formulations with different crosslinker concentrations subjected to Karl Fischer hydration testing 169

Table 4.14: Mechanical properties of five 66B/33L bioactive films containing different amounts of crosslinker 171

Table 5.1: Composition of the directly compressed "3-vitamin" minitablets (low dose cholecalciferol minitablets) 190

Table 5.2: Textural parameters employed for physicomechanical evaluation of "3-vitamin" minitablet formulations 193

Table 5.3: Bile salt-lipase alginate film formulations 197

Table 5.4: Inherent energy attributes representing the molecular assemblies modeled using static lattice atomistic simulations in vacuum 207

Table 5.5: Mechanical properties of five “3-vitamin” minitablets (1:3 ascorbic acid: TPGS and βCDD$_3$-8 IC) tested during the TA studies 211

Table 5.6: Dissolution data obtained following cholecalciferol release from a 4000IU minitablet with/ without polymer bioactive films of varied composition..... 221

Table 5.7: 1000IU BAP dissolution parameters calculated for the *in vitro* dissolution study using DDSolver add-in software. 237

Table 5.8: 4000IU BAP vitamin dissolution parameters calculated for the *in vitro* dissolution study using DDSolver add-in software……..... 238

Table 6.1: Medication and recommended dosages administered to pigs during the *in vivo* study 251

Table 6.2: Results of noncompartmental analysis of BAP 4000IU cholecalciferol release 270

Table 6.3: Results of noncompartmental analysis of comparator 4000IU cholecalciferol release 270

Table 6.4: Results of compartmental analysis of BAP 4000IU cholecalciferol release 271

Table 6.5: Results of compartmental analysis of comparator 4000IU cholecalciferol release 272

Table 6.6: Results of noncompartmental analysis of BAP 1000IU cholecalciferol release 275

Table 6.7: Results of noncompartmental analysis of comparator 1000IU cholecalciferol release 275

Table 6.8: Results of compartmental analysis of BAP 1000IU cholecalciferol release 276

Table 6.9: Results of compartmental analysis of comparator 1000IU cholecalciferol release 277

Table 6.10: 25-hydroxyvitamin D$_3$ levels over a 6 day period 281

LIST OF ABBREVIATIONS

Alg - Alginate

BAP - Bioactive Association Platform

BB - Bioactive Booster

CA - Cholic acid

CD - Cyclodextrin

CD||VitD - Cyclodextrin vitamin D_3 complex

CHI - Chitosan

DA - Deoxycholic acid

ELISA - Enzyme-linked immunosorbent assay

HPLC - High performance liquid chromatography

IC - Inclusion complex

IE - Inclusion efficiency

IU - Cholecalciferol International Units (1IU=0.025ug)

LT - Lecithin

MRI - Magnetic resonance imaging

NaC - Sodium cholate hydrate

NaD - Sodium deoxycholate

SEM - Scanning electron microscopy

SIF - Simulated intestinal fluid

TPGS - d-α-Tocopheryl polyethylene glycol 1000 succinate/ vitamin E TPGS

UV-Spec - UV-visible spectrophotometry

VitD - Vitamin D_3/ Cholecalciferol/ VD3

XRD - X-ray powder diffraction

α-CD - Alpha cyclodextrin

α-CD||VitD/ αCD-D_3 - Alpha cyclodextrin vitamin D_3 complex

β-CD - Beta cyclodextrin

β-CD||VitD/ βCD-D_3 - Beta cyclodextrin vitamin D_3 complex

γ-CD - Gamma cyclodextrin

γ-CD||VitD/ γCD-D_3 - Gamma cyclodextrin vitamin D_3 complex

2-HPβ-CD - 2-hydroxypropyl-β-cyclodextrin

HP-β-CD||VitD - 2-hydroxypropyl-β-cyclodextrin vitamin D_3 complex

βE - Beta cyclodextrin vitamin E complex

βCD-C - Beta cyclodextrin vitamin C complex

CHAPTER 1

DESIGN CONCEPT OF A 'BIOACTIVE ASSOCIATION PLATFORM' (BAP) ORAL DELIVERY SYSTEM FOR ENHANCED EFFICACY OF CHOLECALCIFEROL

1.1. Introduction

The rate and extent of drug absorption from the gastro-intestinal tract (GIT) depends on an intricate interplay between various physiological factors including, blood flow, intestinal transit time, gastric emptying rate, pH and absorption processes (Dahan *et al*., 2009). Ultimately it is said that the aforementioned variables within a patient and the physicochemical properties of a drug influence oral drug bioavailability on two levels: (i) the drugs permeability through GIT membranes and (ii) the drugs solubility/ dissolution within the GIT environment. The GIT milieu provides challenges for oral delivery of many drugs due to presystemic metabolism, variable pH, ever changing motility and differences in biological and chemical composition. These characteristics may lead to inadequate absorption of drugs delivered via the oral route, especially relevant to those compounds with physicochemical barriers to bioavailability. Many Drug Delivery System's (DDS's) are formulated using polymers that are "environmentally-responsive", being able to control the release of drug in response to a specific pH, temperature, hydration or other stimuli within the GIT of a patient as a means of enhancing a drug's therapeutic index (Bajpai *et al*., 2008; Hoare and Kohane, 2008). These are mechanisms that have been designed to solve formulation challenges whilst taking advantage of the physiological condition. Advances in polymer release science have enabled pharmaceutical scientists to use modified release vehicles to formulate drug delivery systems that are "intelligent" rather than using the conventional approach to randomly combine components within a delivery system. However, even advanced DDS's formulated to solve inherent limitations in the physicochemical characteristics of bioactives may fail to facilitate optimal absorption when the normal physiology is disturbed (van Hasselt *et al*., 2009). These same challenges hamper oral delivery of allopathic, complementary and nutraceutical treatment modalities.

An intuitive problem with many DDS's is their reliance on a specific consistent physiological climate within a patient for the intended performance of the delivery device to allow for optimal absorption, dissolution or bioactivation of the drug. As discussed, unforeseen disturbances inter-patient and intra-patient factors may make

the GIT milieu less conducive to an orally administered product. Even sophisticated drug delivery systems may not always achieve a predictable and improved treatment outcome. This may be as a result of a number of factors one of which is a deficiency of intra-luminal constituents known to be essential to the absorption of certain compounds through the human GIT. Unfortunately, no products are conceptualized with an abnormal physiology or compromised GIT function as an innate element, which is evident in that no two patients are the same due to genetics, disease, lifestyle, and concomitant drug intake. These predisposing factors and dynamic molecular variables influence the efficacy of pharmaceutical and nutraceutical products and need to be accounted for during formulation design.

Most patients demonstrate differences in enzyme concentration, hormonal levels and organ function which may affect the product at the time of dosing and thus interfere with the utilization and absorption of drugs and micronutrients' from the GIT (Basu and Donaldson, 2003). Such factors and associated nutrient or drug interactions that occur in a patient at the time of dosing can severely influence the efficacy of a drug. This may result in lower, higher or variable levels of the active in the blood stream and possible therapeutic failure or intoxication. Furthermore, these patient factors become more critical when a bioactive relies on multiple steps of bioconversion by the patient's biochemistry and physiology prior to pharmacological activation. Cholecalciferol (vitamin D_3) is one such nutraceutical that is subject to various steps of bioconversion into metabolites in the skin, GIT and kidney until final conversion into the active form for biological action. This nutraceutical also poses physicochemical barriers to optimal oral bioavailability as it exists as a lipophillic vitamin with high membrane solubility but poor aqueous solubility and high susceptibility to degradation. As such cholecalciferol is a secosteroid nutraceutical that would benefit greatly from advanced formulation design to enhance oral bioavailability.

Despite the utility and acceptance of cholecalciferol as a fundamental macronutrient, there is currently a widespread deficiency in the global population. An estimated 1 billion people worldwide, across all age groups and ethnicities, manifest a vitamin D deficiency (Holick, 2007). Approximately 36% of the healthy US adult population and 57% of US in-patients show signs of vitamin D deficiency (Zhang and Naughton, 2010). Despite the widespread availability in "Over the Counter" (OTC) supplements and existence of potent prescription metabolites, the global insufficiency predominates. Prescribed vitamin D_3 metabolites are used to treat conditions such

as chronic malabsorption, liver disease, renal osteodystrophy, osteoporosis and osteomalacia (Gibbon, 2007). Even though oral products are widely available they do not seem to adequately address the prevalence of deficiency and this may be due to inter- and intra-patient variability, interactions at the time of dosing, and resultant reduced bioavailability of actives (Braithwaite *et al*., 2013). The result is formulations that fail to adequately compensate for malnutrient uptake. Recently researchers have started to design novel formulations for improved bioavailability of vitamin D_3 to alleviate the burden of deficiency in the population (Diarrassouba *et al*., 2015; Guttoff *et al*., 2015). Further emphasis needs to be focussed on this important area of research through smart formulation design of not only single vitamin cholecalciferol DDS's but through multivitamin formulations containing numerous essential vitamins in addition to the model agent. Complementary and alternative medicines have long since assumed a lower priority in terms of scientific development and are not subject to the same stringent regulations to which allopathic medicines are governed in many countries – a fact that often results in poorer quality finished products.

Limitations with current vitamin D supplements and prescribed formulations include:

- Small incremental response in a patient to administered doses as seen by delayed improvements in blood levels (Moyad, 2010);

- Reliance on the administration of fat-soluble vitamins such as vitamin D with food to ensure enhanced absorption in a patient following activation of the GIT response;

- Susceptibility to interactions with concomitant medications and the physiological milieu, resulting in impeded absorption and activity loss of vitamin D (NIH Office of Dietary Supplements, 2010; Gibbon, 2003);

- Poor aqueous solubility of fat-soluble hydrophobic drugs and vitamins poses formulation challenges that results in reduced dissolution in the GIT media (Gursoy and Benita, 2004);

- Delayed and erratic bioavailability of hydrophobic vitamins compared to hydrophilic vitamins from multivitamin formulations;

- Sub-optimal quantity of vitamin D in many current products (400IU) based on out-dated traditional recommendations. Many vitamin formulations are based on Recommended Dietary Allowances (RDA) that advise vitamin levels that are sufficient to prevent deficiency but ineffective in the treatment or prevention of vitamin D related diseases (Schwalfenberg, 2010);

- Erratic response and poor success in elderly patients or patients with altered gastro-intestinal tract (GIT) and metabolic capacity (Bolin *et al*., 2010);

- Paucity of scientifically formulated and rate modulated nutraceuticals on the market for efficient and reliable treatment outcomes;

- Most novel DDS vitamin formulations have been restricted to the synthesis and testing of formulations containing a single vitamin agent and not dosage forms containing multiple synergistic vitamins (Diarrassouba *et al*., 2015; Guttoff *et al*., 2015).

- Vitamin D_3 formulations influenced by disturbances in the GIT milieu and inter- and intra- patient variability in digestive organ physiology.

  Research therefore necessitates the development of a cholecalciferol DDS that utilizes latest advances in polymer and drug delivery science to achieve targeted drug release, optimal absorption and enhanced stability in the *in vivo* environment of the GIT, whilst also circumventing inter-patient variations in physiology and organ function. The inclusion of one or more co-vitamin bioactives in addition to cholecalciferol would also position the cholecalciferol DDS to be even more relevant to the needs of clinicians. Such a novel DDS will facilitate more predictable and efficacious responses to pharmaceutical or supplemental products and ensure better treatment outcomes in healthy and ill patients.

  In the current research vitamin D_3 (cholecalciferol) will be used as the model drug to demonstrate proof of concept of a novel DDS designed specifically to fulfil the aforementioned goal. Since a significant amount of research has been directed towards the importance of vitamin D in the global population, vitamin D_3 (cholecalciferol) was selected as a clinically relevant nutraceutical bioactive for proof of concept studies. Studies have demonstrated that vitamin D has a significant

influence on the progression and occurrence of many chronic diseases (Ebeling, 2005; Schwalfenberg, 2010; Zhang and Naughton, 2010). Vitamin D acts as a steroid hormone in the body that is an essential precursor compound to various biologically active compounds and is regarded as being vital to many physiologic processes. Research has also demonstrated that vitamin D is necessary for innate immune-functioning and has played a role as a complementary treatment in chronic disease protocols for Tuberculosis (Schwalfenberg, 2010).

The current clinical approach is to administer high dose physiologically inert vitamin D precursors (vitamin D_2 or vitamin D_3) found higher up in the vitamin D synthesis cascade or to prescribe the activated forms (alfacalcidiol and calcitriol). The active forms available, namely, Rocaltrol® (Roche Diagnostics, Indianapolis, Indiana, USA) and One-Alpha® (Adcock Ingram Critical Care, Midrand, Gauteng, South Africa) are in limited access as they are restricted to prescription use and are reserved exclusively for a small group of patients especially those with renal impairment. The development of a cholecalciferol DDS that will overcome formulation and current product limitations, as well as inter-patient physiological variations, has utility for nutraceutical therapy. Such a DDS may also be utilized as a generic platform to be harnessed to deliver other life-saving hydrophobic drugs and nutraceuticals more efficaciously and predictably.

1.2. Rationale and Conceptualization of the BAP Delivery System Archetype

1.2.1. Rationale behind the BAP concept

As discussed already, modifying a drugs physicochemical properties is only half of the way to achieving the goal of enhanced efficacy of a pharmaceutical product. The next step in the drug development evolution involves an ability to alter the physiological condition in favour of superior drug response. If one is able to modify a drugs physicochemical factors including solubility, diffusivity, lipophilicity, stability, particle size, surface area, and crystal form, as well as the physiology within a patient, one may further enhance delivery via the oral route. Physiological parameters include factors such as, GIT endocrine secretions, absorption mechanisms, digestive and metabolic processes. Previous studies and current formulation approaches involve the inclusion of polymers that are stimuli-responsive enabling the targeted release of drug in a bodily organ in response to endogenous physiological stimuli in order to improve drug release (Wei *et al*., 2009). However, a patient may be deficient in one or more physiological factors (hormones, enzymes,

co-enzymes, carrier molecules, and emulsifiers) required by the body for its normal metabolic processes. Even in a patient with no known deficiencies, the physiological process can be variable in efficiency due to external influences or dynamic states and compartmental interactions at the time of dosing.

A deficiency or interference with of one or more natural substances found in a patient will alter the physiological condition and affect the way the body is able to process a product. It may be difficult to ensure that all intended multivitamin constituents are optimally absorbed in cases of disturbed GIT function. Each co-included vitamin has independent challenges to bioavailability due to differences in stability, aqueous diffusion and solubility, and an increased propensity for interactions that may occur *in situ*. Therefore fixed-dose combination formulations offer even greater challenges to test the optimal functioning of the physiological process. This is even more pertinent for drugs and nutraceuticals that are lipophilic and already face challenges in terms of bioavailability due to low aqueous solubility. Patients with chronic debilitating disease are prone to abnormal physiological responses and would not be able to achieve complete assimilation that is required. A stimulus that is expected to elicit a response from a DDS may or may not be present and in turn will intrinsically affect the intended pharmacokinetic profile of a dosage form unless the abnormality is nullified. A patient with compromised or sub-optimal organ functioning, such as pancreatitis for example, may experience considerable malabsorption of fat and associated vitamins and nutrients (Dipiro *et al*., 2002). Circadian rhythms are present for a reason and if the physiological process is disturbed even on a sub-clinical level then there is room for inefficient product utilization and compromised therapeutics. Research has delved into exploiting existing physiological organ systems to enhance uptake of a drug to a particular site within the body and to achieve a more prolonged level of an active in the blood stream (Samstein *et al.*, 2008). It has been noted further how the intrinsic qualities of a naturally secreted physiological substance has immense value in drug delivery and may even enhance stability and prevent premature degradation of a DDS (Samstein *et al.*, 2008). To ensure maximal therapeutic efficacy an “intelligent” delivery mechanism should provide modified physicochemical parameters to model agent(s) whilst taking into consideration disturbances in the dynamic physiological milieu that may influence bioavailability.

1.2.2. The BAP design

This study involved the design of a DDS consisting of a novel arrangement of polymers, carrier molecules, fat and water soluble vitamins, and physiological co-factors (e.g. enzymes, bile, hormones) to deliver cholecalciferol more effectively via the GIT. The formulation of the novel system resulted in the development of a DDS coined a “Bioactive Association Platform” (BAP). The BAP harnessed the value of naturally occurring biological substances incorporated within the product as co-factors (bile acids, enzymes and hormones). The biological molecules were included in the DDS to facilitate the mimicry of GIT action on the DDS for enhanced, independent and predictable vitamin utilization irrespective of the state of the patients GIT. The BAP DDS also included selected synthetic carriers, polymers and synergistic vitamins within a unique and stable interactive framework. Both the carrier molecules and polymers and the physiological/ biological co-factors were intended to improve dissolution, diffusibility and permeation of the model drug, cholecalciferol. The result was to create a DDS mechanism that provided the body with: (i) the intended bioactives; (ii) carrier molecules and (iii) a conducive artificial microenvironment, all within a convenient oral capsule. The necessary biological molecules would be released in a predetermined manner or with a modifiable activity level or would be optimized to enhance the dissolution and permeation parameters of the model drug. The final BAP would assist in the creation of a micro-environment containing a physiological milieu, advantageous to the rapid uptake of vitamin D_3 and two synergistic vitamins (ascorbic acid and α-tocopherol). The BAP was also intended to achieve a unified release of both hydrophobic and hydrophilic vitamins. A harmonized “in-concert” vitamin release phenomena would ensure rapid and complete bioavailability of all nutraceutical constituents regardless of the individual vitamins BCS class categorisation or its inherent bioavailability.

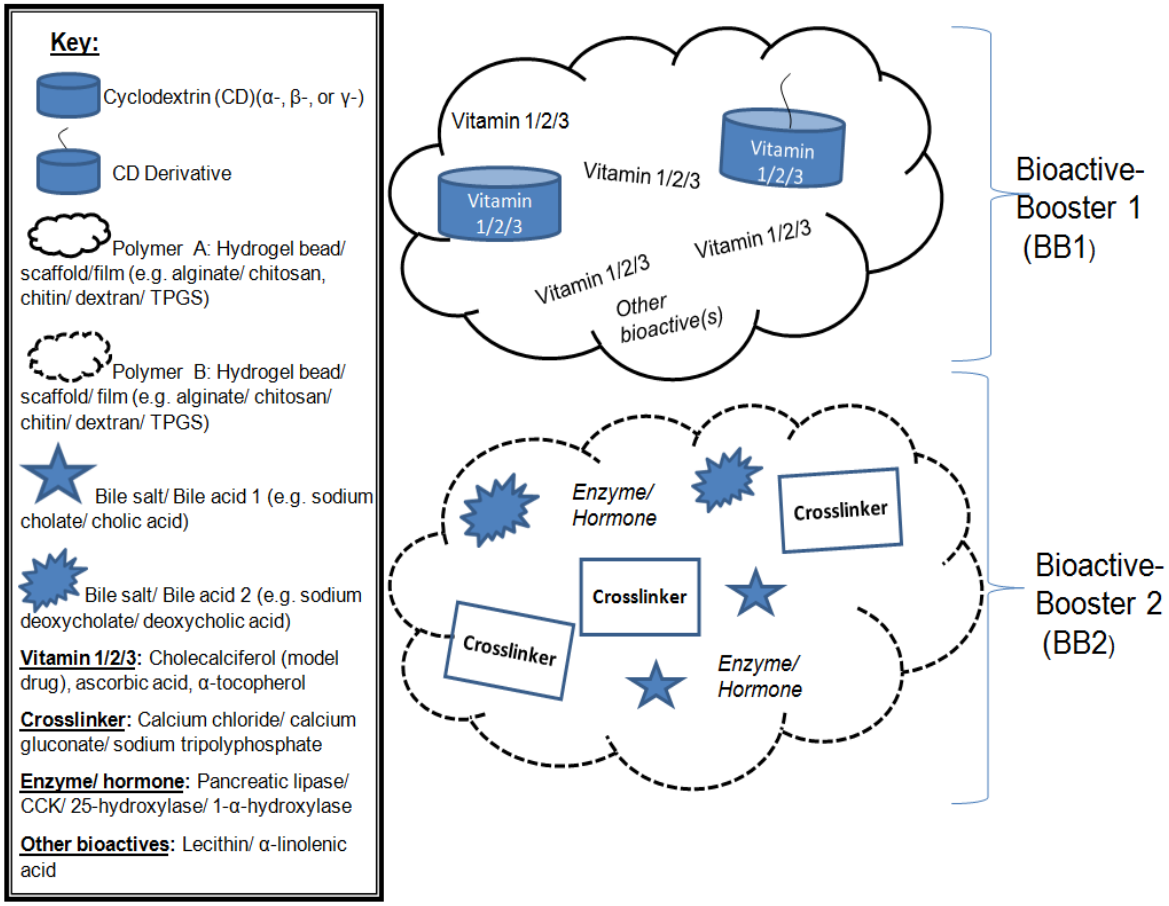
The design process of the DDS initially began with the conceptualization of a molecule termed a “Bioactive Booster” (BB) (Figure 1.1). A Bioactive Booster (BB) was defined as a unique combination of a selected bioactive and carrier molecule/ polymer, to form a sequential constituent of the BAP DDS. A BB may consist of polymers, carrier molecules, model drugs (cholecalciferol) or other bioactives termed ‘enhancing co-factors’ linked to one another. Multiple bioactives were identified as candidates for inclusion within uniquely designed BBs. Each BB played an integral role in the BAP including: (i) to enhance the absorption of cholecalciferol; (ii) to improve cholecalciferol permeation through membranes, (iii) to act as surfactants or emulsifiers or facilitate micellization of cholecalciferol; (iv) to stabilize

actives; (v) to accelerate/ improve model drug solubility; or (vi) to align all vitamins' release profiles. A BB may consist of a bioactive dispersed within a polymeric matrix or even a carrier molecule bound to a selected bioactive or model drug. Each BB was intended to be a specific BAP component. Multiple enhancing bioactives were identified during the study, each of which held relevance to improving the delivery of cholecalciferol and some of which were to be tested to form BB's by binding to carriers/ polymers. These bioactive candidates were selected for binding polymers or carriers in pre-defined arrangements to form BB's as vital constituents of the BAP DDS. Table 1.1 lists multiple identified enhancing bioactive candidates and their proposed functions in the creation of the BAP:

Table 1.1: Enhancing bioactive candidates and their possible functions in the cholecalciferol BAP

Enhancing bioactive candidate	**Function**
Lecithin	To aid in emulsification of fat soluble vitamins including cholecalciferol for enhanced absorption
α-linolenic acid	Essential fatty acid intended as a lipid substrate stimulus for GIT digestive secretions to enhance cholecalciferol absorption
Bile acids (Cholic acid; Deoxycholic acid)	GIT bile agent: Emulsification, increased solubility and transport of fat and lipid soluble vitamins including cholecalciferol
Bile salts (Sodium cholate; Sodium deoxycholate)	GIT bile agent: Emulsification, increased solubility and transport of fat and lipid soluble vitamins including cholecalciferol
Vitamin C (Ascorbic acid)	Clinically synergistic vitamin
Vitamin E (α-tocopherol)	Clinically synergistic vitamin
Calcium	Synergistic mineral and hydrogel crosslinker
Cholecystokinin	GIT hormone for enhanced stimulation and release of pancreatic enzymes and bile
Pancreatic lipase	Enzyme to aid breakdown of lipids and fat soluble vitamins
25-hydroxylase	Enzyme for liver bioactivation of vitamin D_3 to 25-hydroxyvitamin D_3 metabolite
1-α-hydroxylase	Enzyme for kidney bioactivation to 1,25-dihydroxyvitamin D_3 metabolite

Cyclodextrins (CD) were selected as specific integral carrier molecules to complex with some of the bioactives for improved stability, protection, solubility and activity retention. Cyclodextrins enhance permeation of bioactives and allow for modified release. Careful polymer selection, modification and carrier binding would facilitate the design of BB's containing actives that may be customized to release from the DDS in a pre-determined sequence to assist optimal GIT functioning and major organ (liver, kidney and pancreas) assimilation of the model vitamin. Individual bioactives may be dispersed, dissolved, embedded or cross-linked independently or collectively within polymers, waxes, solutions or emulsions. Hormones and enzymes may be adsorbed onto surfaces or embedded within polymer matrices. Polymers may be cross linked to varying extents then frozen and lyophilized to form spongy scaffolds. Alternatively plasticisers may be added to polymeric hydrogels and dried to facilitate the formation of bioactive booster films with unique release properties. Figure 1.1 depicts the proposed arrangement of the BAP design concept and includes various proposed polymers (alginate, chitosan, dextran, chitin or D-α-tocopheryl polyethylene glycol 1000 succinate). Each BB molecule forms a vital component of the BAP that may be combined or connected to other BB's in a customized configuration and inserted into a capsule to achieve the desired BAP DDS (Figure 1.2). The advantage of synthesizing separate BB's that are later combined into one final BAP is that individual bioactives will be restricted from interacting with each other and may be protected from the physiological extremes of the GIT. Additionally, certain bioactives are more suited to interact with specific polymers or carriers than others due to differences in physico-chemical properties. Bioactive-CD complexes or individual bioactives and biological co-factors may be either immersed within cationic, anionic, or non-ionic polymers or within polymeric waxes to form a macro-molecular framework of the DDS for inclusion in a capsule (Figure 1.2).



CD: Cyclodextrin; TPGS: D-α-Tocopheryl polyethylene glycol 1000 succinate; CCK: Cholecystokinin

Figure 1.1: Detailed schematic representing an example of 2 possible Bioactive Booster molecules that may be designed for inclusion in the novel BAP DDS.

The ultimate design of the BB network involved the concept of combining technologies and carrier mechanisms and the controlled provision of biological co-factors (enzymes, bile salts/ bile acids) to form a unique 'Bioactive Association Platform' (BAP) DDS customized for the optimal delivery of cholecalciferol. The DDS will precipitate pre-programmed release and activity of certain essential physiological co-factors and synergistic constituents.

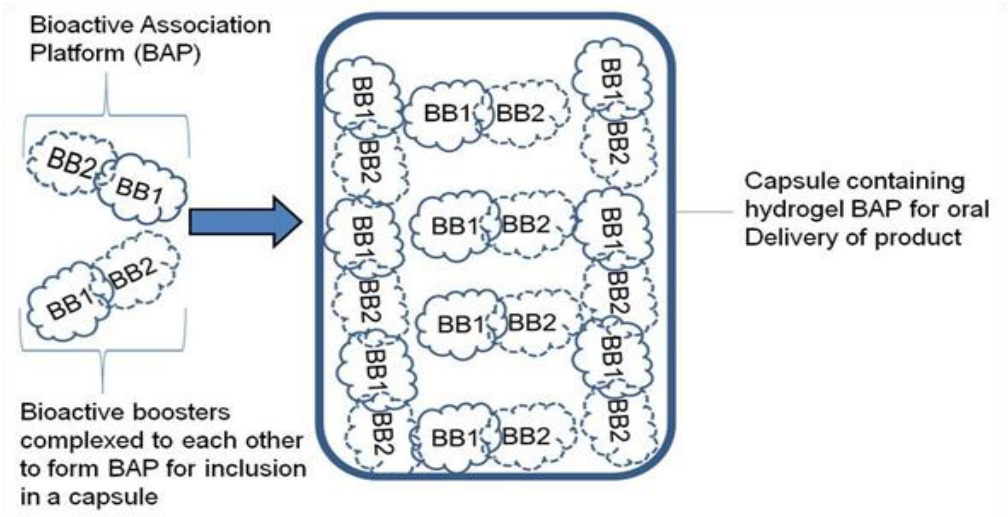


Figure 1.2: Multiple Bioactive Boosters (BB1 and BB2) included together to form the BAP encased within a capsule for oral delivery.

1.2.3. An optimal cholecalciferol dose for inclusion in the BAP

Various studies have reported the administration of vitamin D_3 at different doses and frequencies, with no expert consensus regarding an optimal dosage. It has been noted that the traditional recommendation of 400IU/ day may be inadequate to achieve optimal serum levels or positive health benefits (Vieth, 2004). Recommendations have started to promote daily oral intakes of at least 1000IU-2000IU (25-50ug) in order to reach the required blood levels for sufficiency and disease prevention (Vieth, 2004; Schwalfenberg *et al*., 2010). Certain populations at higher deficiency risks due to chronic disease, concomitant drug therapy or lifestyle factors, require doses greater than 2000IU/ day. Since past recommendations have underestimated the true requirements resulting in inadequate to no clinical benefits, physicians are increasingly advocating higher doses (Vieth, 2004; Binkley *et al*., 2012). Despite a trend towards increased doses, the chance of vitamin D toxicity is considered low with studies reporting adverse effects in patients only after cumulative daily doses in excess of 50000IU (Zhang and Naughton, 2010). An upper limit of safety may be a dose as high as 10000IU/ day over successive months (Schwalfenberg *et al*., 2010). Recently it has been noted that to reach meaningful plasma levels, adults require 1600IU to 4000IU cholecalciferol/ day (Jetter *et al*., 2014). For the reasons discussed it was decided that the quantity of cholecalciferol to be included in the BAP would be 1000IU and 4000IU in two separate test dosage forms. These two amounts of model drug would facilitate the evaluation of two independent test formulations (a low dose and a high dose

product) that are aligned with the most recent dosing recommendations and would enable a meaningful *in vivo* evaluation of the BAP delivery system.

1.3. Aim and Objectives of the Research

The aim of this investigation was the design and development of an oral BAP DDS consisting of BB's containing cholecalciferol and enhancing co-factors formulated to achieve passive pre-programmed release kinetics based on the modified provision of three or more of the following agents: cholecalciferol (model drug), vitamin E, vitamin C, calcium, fatty acids, cholecystokinin, lecithin, bile acids, bile salts, pancreatic lipase, 25-hydroxylase, 1-α-hydroxylase. The BAP was intended to overcome cholecalciferol product challenges with improved bioavailability, predictability and efficacy of the model drug and a merging of the release profiles of three vitamin bioactives from the same oral device. The above aim was to be achieved through the following objectives:

1. Preformulation to determine appropriate carriers for all bioactives: Preliminary molecular modelling simulations, binding of bioactives to prospective carriers and/ or polymers, and analysis of the physicomechanical and physicochemical characteristics of BAP component candidates: rheology, textural profiling, thermal behaviour, structural analysis, crystallinity, morphological analysis, phase-solubility, hydration. Performance of preliminary *in vitro* bioactive release studies of different BAP component candidates.
2. Determination of an ideal biological composition (enzymes, bile, or hormones) of BAP components to enable (i) milieu-like activity and (ii) improved *in vitro* cholecalciferol release i.e. Selection of an optimized biological co-factor matrix.
3. Determination of enzyme activity retention within polymer matrices/ carrier framework: Selection of an optimized carrier for enzyme delivery.
4. Selection of the most appropriate BAP components (BB's) for inclusion in final BAP to achieve desired sequence of unified controlled vitamin release, modified enzyme activity profile, and improved cholecalciferol dissolution/ aqueous release behaviour.
5. Building final BAP by combining individual optimized BB components and encasing within capsules for oral delivery.
6. Comparative *in vitro* diffusion studies of cholecalciferol from BAP BB component(s) to determine the rate and extent of tissue permeation through biological membranes of the GIT.

7. Analysis of the physicomechanical and physicochemical characteristics of final BAP components: rheology, textural profiling, thermal behaviour, crystallinity, structural analysis, scanning electron microscopy, magnetic resonance imaging**.**
8. Comparative *in vitro* drug release studies of the BAP DDS capsules to elucidate release kinetics of cholecalciferol and other synergistic vitamins from the BAP.
9. Execution of *ex vivo* and *in vivo* animal studies to determine preclinical performance and safety of the BAP: release behaviour, pharmacokinetics, bio-imaging and x-rays, tissue toxicity, and plasma blood levels.
10. *In vitro-in vivo* correlations to assess the relationship between *in vitro* dissolution parameters of cholecalciferol to *in vivo* bioavailability results of preclinical animal studies.

1.4. References

Bajpai AK, Shukla SK, Bhanu S, Kankane S. 2008. Responsive polymers in controlled drug delivery. *Progress in Polymer Science* 33: 1088-1118.

Basu TK, Donaldson D. 2003. Intestinal absorption in health and disease: micronutrients. *Best Practice & Research Clinical Gastroenterology* 17: 957–979.

Binkley N, Ramamurthy R, Krueger D. 2012. Low vitamin D status: Definition, prevalence, consequences, an correction. *Rheumatic Disease Clinics of North America* 38: 45-59.

Bolin T, Bare M, Caplan G, Daniells S, Holyday M. 2010. Malabsorption may contribute to malnutrition in the elderly. *Nutrition* 26 (7-8): 852-853.

Braithwaite MC, Kumar P, Tyagi C, Tomar LK, Choonara YE, Pillay V. 2013. Vitamin D therapy and related metabolomics: Is the calciferol dose and form the only requirements for successful clinical therapeutics? *Medical Hypotheses* 81: 656-663.

Dahan A, Miller J.M., Amidon GL. 2009. Prediction of solubility and permeability class membership: provisional BCS classification of the world's top oral drugs. *American Association of Pharmaceutical Scientists Journal* 11: 740-746.

Diarrassouba F, Garrait G, Remondetto G, Alvarez P, Beyssac E, Subirade M. 2015. Improved bioavailability of vitamin D_3 using a β-lactoglobulin-based coagulum. *Food Chemistry* 172: 361-367.

Dipiro JT, Talpert RL, Yee GC, Matzke GR, Wells BG, Posey LM. 2002. Pharmacotherapy, a Pathophysiologic Approach 5th edition. McGraw-Hill. New York. 707-709.

Ebeling PR. 2005. Megadose therapy for vitamin D deficiency. *Medical Journal of Australia* 183(1): 4-5.

Gibbon CJ. South African Medicine Formulary (SAMF) 6th Edition. 2003. Health and Medical Publishing Group of the South African Medical Association, Cape Town: 84.

Gursoy RN, Benita S. 2004. Self-emulsifying drug delivery systems (SEDDS) for improved oral delivery of lipophilic drugs. *Biomedicine & Pharmacotherapy* 58: 173–182.

Guttoff M, Saberi AH, McClements DJ. 2015. Formation of vitamin D nanoemulsion-based delivery systems by spontaneous emulsification: factors affecting particle size and stability. *Food chemistry* 171: 117-122.

Hoare TR, Kohane DS. 2008. Hydrogels in drug delivery: Progress and challenges. *Polymer* 49: 1993-2007.

Holick MF. 2007. Vitamin D deficiency. *New England Journal of Medicine* 357: 266–281.

Moyad MA. 2010. Vitamin D: a rapid review: dosage of vitamin D needed to achieve 35 to 40ng/mL (90–100nmol/L). Retrieved from URL: www.medscape.com. [Accessed July 2010].

Jetter A, Egli A, Dawson-Hughes B, Staehelin HB, Stoecklin E, Goessl R, Henschkowski J, Bischoff-Ferrari HA. 2014. Pharmacokinetics of oral vitamin D_3 and calcifediol. *Bone* 59: 14-19.

NIH Office of Dietary Supplements. Dietary supplement fact sheet: vitamin D. Retrieved from URL: http://ods.od.nih.gov/factsheets/vitamind.asp. [Accessed November 2010].

Samstein R, Perica K, Balderrama F, Look M, Fahmy TM. 2008. The use of deoxycholic acid to enhance the oral bioavailability of biodegradable nanoparticles. *Biomaterials* 29: 703-708.

Schwalfenberg GK, Genuis SJ, Hiltz MN. 2010. Addressing vitamin D deficiency in Canada: A public health innovation whose time has come. *Public Health* 24: 350–359.

Van Hasselt PM, Janssens GEPJ, Slot TK, van der Ham M, Minderhoud TC, Talelli M, Akkermans LM, Rijcken CJF, van Nostrum CF. 2009. The influence of bile acids

on the oral bioavailability of vitamin K encapsulated in polymeric micelles. *Journal of Controlled Release* 133: 161–168.

Vieth R. 2004. Why the optimal requirement for vitamin D_3 is probably much higher than what is officially recommended for adults. *Journal of Steroid Biochemistry and Molecular Biology* 89-90: 575-579.

Wei L, Cai C, Lin J, Chen T. 2009. Dual-drug delivery system based on hydrogel/micelle composites. *Biomaterials* 30(13): 2606-2613.

Zhang R, Naughton DP. 2010. Vitamin D in health and disease: Current perspectives. *Nutrition Journal* 9: 65. Retrieved from URL: http://www.nutritionj.com/content/9/1/65. [Accessed 12 March 2012].

CHAPTER 2

NUTRACEUTICAL-BASED THERAPEUTICS AND CURRENT FORMULATION STRATEGIES

2.1. Introduction

The word Nutraceutical originates from the marriage of two words ‘nutrition’ and ‘pharmaceutical’ and relates to a “food or food-based product, vitamin, mineral, or herb that offers various health benefits in the treatment and prevention of disease” (Henrotin *et al*., 2011; Camfield *et al*., 2011). Not only are nutraceuticals used in preventative medicine but, frequently prescribed and recommended as complementary or alternative treatments to chronic disease. Many clinicians strongly believe in a holistic approach to disease and prescribe nutraceuticals in combination with conventional drug regimens to treat primary disease, recurrent disease and to assist in symptom amelioration (Schwartz, 2009). According to nutraceutical proponents, populations who consume generous amounts of vegetables, grains, plant based fibre, and seafood have a lower prevalence of cardiovascular disease and cancers. Basic supplementation, holistic prescribing, and awareness of healthy nutritional practices may reduce the burden of chronic disease in the global population through innovative treatment and preventative strategies.

Research into functional foods and nutraceuticals has increased dramatically over recent years with more scientists publishing journal articles relating to this topical and popular subject than ever before (Figure 2.1).

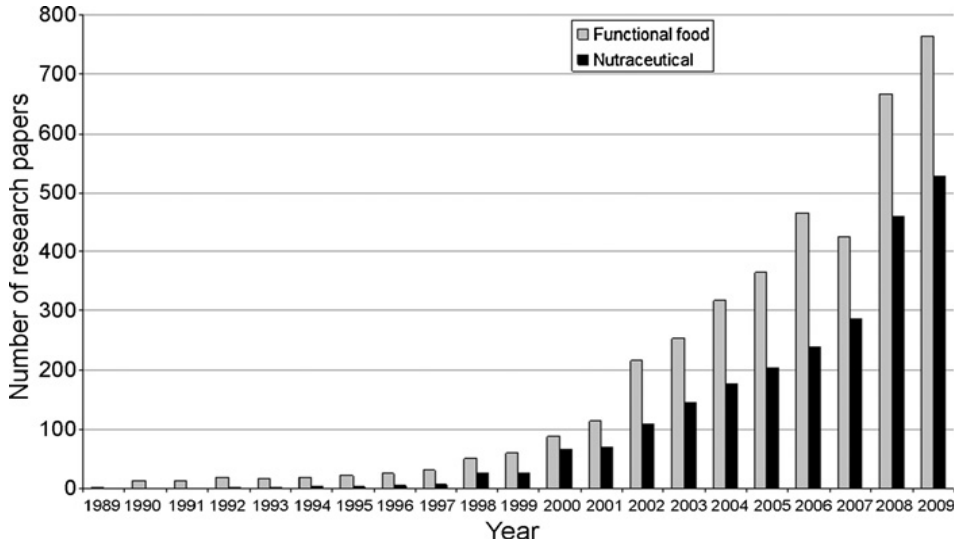


Figure 2.1: Research articles dealing with nutraceutical or functional foods published in the period 1989-2009 (ISI Web of Knowledge) (Bernal *et al*., 2011) [Reproduced with permission from Elsevier Science BV Ltd. © 2011]

A plethora of evidence supports the health benefits and value of nutraceuticals in the treatment and prevention of disease and the important role these compounds play in physiological functions (Bernal *et al*., 2011; Blaylock and Maroon, 2012; Gholse and Yadav, 2012; Telrandhe *et al*., 2012). Evidence substantiates the use of natural compounds due to their unique ability to promote the body's own natural healing process (Blaylock and Maroon, 2012; Gholse and Yadav, 2012). Not only are nutraceuticals used in preventative medicine but, they are frequently prescribed and recommended as complementary or alternative treatments to chronic disease. Some researchers have identified promising preliminary data supporting the view that nutraceuticals should be included in the clinical arsenal as they are potent adjuvants (Gianfrilli *et al*., 2011; Henroitin *et al*., 2011; Nair *et al*., 2010; Zlotogorski *et al*., 2013).

2.2. The Nutraceutical Value Proposition

2.2.1. Nutraceuticals impacting the incidence and progression of disease

Supplementation of key nutrients is an invaluable treatment approach in that these substances may exert a protective effect on the body by altering the course of many diseases and preventing conditions before they surface (Gupta *et al*., 2010; Kelsey *et al*., 2010). Simple dietary modification has been said to thwart the development of 35% of all cancers and the consumption of antioxidants has been linked to neuroprotective effects in both *in vitro* and *in vivo* studies (Gupta *et al*., 2010; Kelsey

et al., 2010). Supplementation of selected vitamins at certain life stages has reduced mortality and morbidity in many patients in both infancy and advanced age (Mayo-Wilson *et al*., 2011; Fernandes de Abreu *et al*., 2011). Vigilance at an early age has led to positive consequences later on in life reducing the risk for disease. This is evidenced for example in data derived from case-control studies that suggest that the consumption of vitamin D during infancy is associated with a reduction in type 1 diabetes mellitus incidence later on in life (Borges *et al*., 2011).

Various types of nutritional strategies have been investigated as a means to lower a patient's disease risk profile by supplementing with key nutrients. Dietary proteins such as soy, previously considered to have no biological properties in humans, have gained interest as agents to potentially lower serum cholesterol, blood pressure, and body weight. In addition, peptides found in milk and vegetable proteins have even brought a novel strategy to the treatment of hypertension with an efficacy that parallels that of Angiotensin I converting enzyme (ACE) inhibitors, without the adverse effects (Sirtori *et al*., 2009). Eating diets rich in fish oil, a source of vitamin D and omega 3, has lowered the incidence of Multiple Sclerosis (Fernandes de Abreu *et al*., 2011). Procyanidins derived from grape seed extract have been beneficial in the reduction of cholesterol, pancreatitis, vomiting and pain (Espin *et al*., 2007). Extracts of bitter melon and cinnamon have proven effective in the treatment of diabetes (Andlauer and Furst, 2002).

2.2.2. Vitamin D correlated to chronic disease

The levels of Vitamin D in the body are believed to affect the incidence of autoimmune disease, type 2 diabetes mellitus, HIV, osteoporosis, tuberculosis and cardiovascular disease (Borges *et al*., 2011; Szep *et al.*, 2011; Zhang and Naughton, 2010; Ebeling, 2005). Not only can this vitamin influence various disease states but it is a potent immune system modulator with an ability to affect the proliferation and expression of various immune system cells responsible for the innate immune response (Figure 2.2). A study by Zhang and Naughton (2010), demonstrated the vitamin's propensity to reduce the risk of cancer, hypertension and multiple sclerosis. A research study found that almost two-thirds of HIV-positive patients had inadequate levels of vitamin D and this deficiency was positively correlated to an increased prevalence of type 2 diabetes in the same patients (Szep *et al*., 2011).

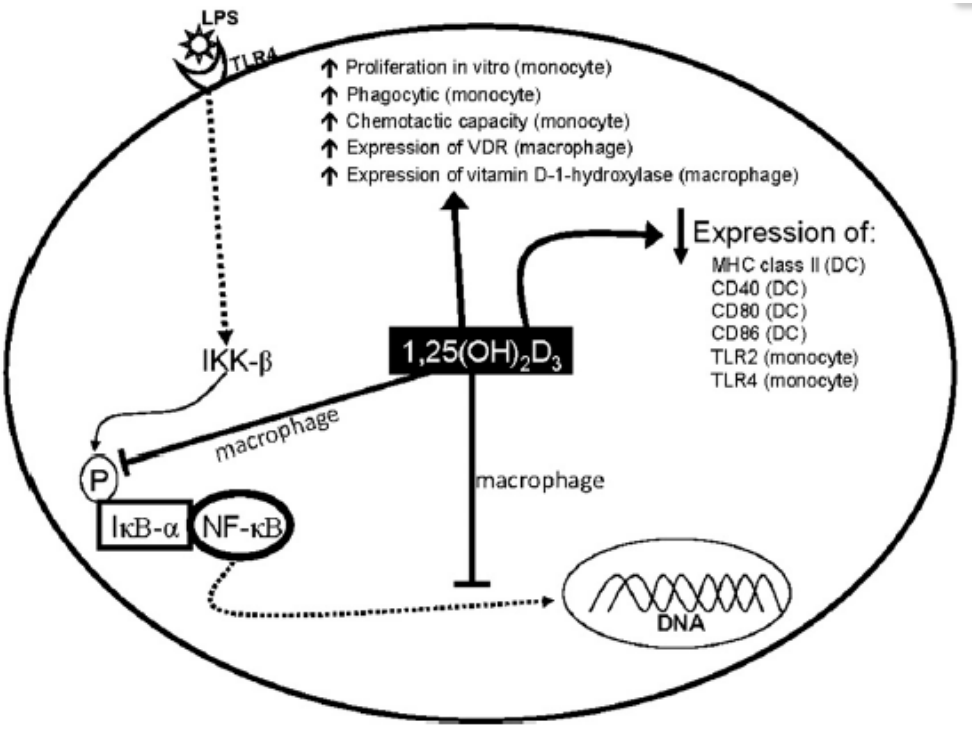


Figure 2.2: Vitamin D modulates the function of macrophages, monocytes, and dendritic cells (DC). IKK: IkB kinase; IkB: inhibitor of NF-kB; LPS: lipopolysaccharides; TLR: Toll-like receptors; VDR: vitamin D nuclear receptor (Borges *et al*., 2011) [Reproduced with permission from Elsevier Science BV Ltd. © 2011].

It is well recognized that a deficiency of a particular vitamin, mineral or co-factor may manifest in a specific vitamin related deficiency disease such as scurvy, beriberi or anaemia in an individual. For years the mainstream medical community was less cognisant of the fact that milder deficiency states and suboptimal levels of nutrients may actually manifest in, pre-empt or accelerate the progression of chronic disease. Increasingly there are now databases and repositories of studies that document a relationship between blood levels of nutraceuticals such as vitamin D and disease. Many studies show links between low levels of natural compounds and clinical disease progression and poor prognosis in patients with depleted vitamin levels (Lee *et al*., 2008; Fernandes de Abreu *et al*., 2011; Viard *et al*., 2011). The EuroSIDA study authors concluded that 25-hydroxyvitamin D deficiency in HIV positive patients on antiretroviral (ARV) treatment was independently associated with a higher risk of mortality and AIDS events (Viard *et al*., 2011). According to Lee and co-workers (2008), sub-optimal levels of plasma 25-hydroxyvitamin D may adversely affect cardiovascular health by predisposing patients to hypertension and left ventricular hypertrophy, as well as insulin resistance syndrome.

Similarly, early studies concluded that higher blood levels of another lipophillic vitamin - vitamin E due to regular supplementation were associated with a reduced risk of progression to full blown AIDS in HIV positive patients (Tang *et al*., 1997). Thus it follows that supplementation strategies with essential micronutrients is critical to the maintenance of optimal physiological functioning of the body and should not be underestimated.

2.2.3. Causes of vitamin D insufficiency

A nutrient deficiency may have various origins related to lifestyle, diet, genetics, patient history, climatic and geographical variation, and concomitant medications and many scientists have attempted to quantify these associations. Certain diseases and drug protocols may predispose a patient to a severe nutrient deficiency as has been confirmed in many laboratory investigations (Conesa-Botella *et al*., 2010). This is evident in numerous studies where HIV drug use has been correlated with lower levels of Vitamin D (Mueller *et al*., 2010; Viard *et al*., 2011; Conesa-Botella *et al*., 2010). The non-nucleoside reverse transcriptase inhibitor drug regimens (containing nevirapine or efavirenz) have been shown to decrease 25-hydroxyvitamin D levels in research conducted by Conesa-Botella and co-workers (2010). A high prevalence of a vitamin D deficiency in HIV positive patients on antiretroviral (ARV) treatment suggests that the HIV disease process, drug treatment in addition to geographic location or lifestyle play a combined role in micronutrient deficiency. As such it has become imperative to screen for specific nutraceutical deficiencies in patients on Highly Active Antiretroviral Therapy (HAART) and to prescribe nutraceuticals to complement their treatment protocols (Mueller *et al*., 2010). As a result routine blood test panels have been broadened to screen for vitamin D deficiency in HIV positive patients on treatment which has led to greater vigilance with regards to the impact of all drugs, not only ARV's, on a patients micronutrient status. It is not uncommon to find HIV patients on treatment becoming anaemic as a result of Zidovudine (AZT) therapy and practitioners are then compelled to prescribe other high potency micronutrients cocktails that may include iron, B12, B6 vitamin C and folic acid in an attempt to treat low haemoglobin counts.

2.2.4. The controversy and validity of nutraceutical study design

Despite evidence supporting the role of nutraceuticals as effective therapeutic agents, it is still debatable as to their exact contribution in combination therapies with allopathic drugs. Similarly a major challenge is how scientists will optimize this role using careful pharmaceutical formulation design. Contrasting opinions on the

interpretation of study findings have led many researchers to split into two schools of thought, those who are advocates for the use of nutraceuticals and those who are critics. Discrepancies in study findings and disparity in interpretations may be explained by the differences in doses administered in studies (Michos and Blumenthal, 2007). Secondly, it is extremely difficult to limit the intake of nutraceutical compounds that are present in subjects' daily diets so that confounding variables may be excluded at baseline and during the study. It is even more challenging to ascertain the extent to which dietary sources influence primary and secondary end-points above the effects attributable to the study 'drugs'. Studies have called for further research comparing different vitamin dosages, frequency of administration and means of delivery to the body to optimize treatment outcomes and disease prevention (Mayo-Wilson *et al*., 2011). Some researchers have noted the scarcity and inconclusiveness of human clinical trials and the poor *in vitro-in vivo* correlation of final marketed nutraceutical products (Espin *et al*., 2007). Numerous bioactive nutraceuticals and their associated formulation problems have been identified and in turn modified to improve the pharmacokinetic and therapeutic parameters when dosed in patients. Such strategies will further magnify the benefits and improve the argument for the use of 'natural' substances and strengthen *in vitro-in vivo* correlation.

2.2.5. Nutraceuticals and future medical research

When treating chronic disease it has become clear that conventional pharmacotherapeutic approaches often fall short. Research needs to delve into the identification of alternative nutraceutical agents that are more efficacious and safer whilst being flexible in their ability to treat a broader patient base. Supporting this view, research has noted how conventional antidepressants are associated with numerous side-effects, have a delayed onset, need to be dosed at high levels for efficacy, and are still successful in treating only 40%-60% of patients with Obsessive Compulsive Disorder (Camfield *et al*., 2011). In comparison, many nutraceuticals function in a pattern similar to antidepressants providing potential as alternative monotherapies or as augmentative treatments that are more tolerable and have similar or improved efficacy.

In cancer patients, tumorigenesis is a complex process and the use of multiple agents is globally accepted even though this strategy poses a risk of toxicity to the patient. The question to ponder is, should medical research accept such a risk or further explore the hidden benefits that molecules of nutraceutical origin have to

offer? Various identified vitamin analogues, metabolites and tailored nutritives have been tested and found to be beneficial in the treatment of life-threatening diseases such as breast cancer and prostate cancer (Gupta *et al*., 2010; Schwartz, 2009; Marotta *et al*., 2009). Calcitriol, the most active form of vitamin D_3, is an example of a potent vitamin metabolite that has antineoplastic efficacy and is able to enhance the effect of chemotherapeutic agents when prescribed as an additive in the treatment of tumours. However, preclinical data indicate that the antineoplastic effects of calcitriol are directly related to the dose administered, and only a highly concentrated specifically designed formulation is able to achieve Area Under the Curve (AUC) and maximum plasma concentrations in a linear fashion suitable for effective and sustained cancer treatment (Rassnick *et al*., 2011).

Medical research needs to further explore the hidden benefits that molecules of nutraceutical origin have to offer. Studies have underlined how individual nutraceuticals, in contrast to standard chemotherapeutic drugs, actually have a multitargeted action on the cell cycle with the added benefit of being less expensive, and thus more accessible to patients (Gupta *et al*., 2010). Nanochemoprevention is a new and exciting frontier that needs to be harnessed as the focus is the exploitation of the favourable properties of an array of nutraceuticals in an attempt to prevent and treat cancer (Nair *et al*., 2010). Hence more research needs to be directed towards natural agents and actives for the treatment of life-threatening conditions (Gupta *et al*., 2010).

Over the last few years one of the prominent focus areas has been, the methods to optimize dosage forms and formulations for improved bioavailability of promising natural candidates (Acosta, 2009; Ankola *et al*., 2007; Bernal *et al*., 2011; Telrandhe *et al*., 2012). According to many forward thinkers, future research should focus on the design of co-drugs consisting of nutraceuticals linked to drugs for enhanced efficacy, reduced dosage and substantial amelioration of side-effects. Most proponents tend to agree that the use of multiple synergistic nutrients provides a useful multi-tiered approach in the armoury of the clinician. Some have recommended the use of soy derivatives in combination with high doses of the vitamin D_3 metabolite, 1.25 dihydroxyvitamin D (calcitriol), as they are able to inhibit the metabolic breakdown of calcitriol (Schwartz, 2009). These tactics even broaden the spectrum of treatment from primary prevention; to treatment of recurrent disease

and also advanced stage disease (Schwartz, 2009). Similarly a major challenge is the formulation strategies to optimize treatment outcomes and disease prevention.

Despite the widespread increase in the use of nutraceuticals and supplements there are only a few commercial products that are scientifically formulated and validated. Only a few researchers have elucidated compatibility between ingredients contained in a product or put nutraceuticals through microbial enumeration tests. However one study did research the stability of vitamin D_3 and identified new degradation products resulting from an interaction between components within a formulation (Ballard *et al.*, 2007). Such studies highlight the degree of instability and interactions that may exist latent within nutraceutical products. The formulation design aspect thus becomes imperative as this will determine whether or not a nutraceutical product lives up to its intended expectation in achieving therapeutic outcomes. More attention needs to be focused on the potential interactions between vitamins, minerals, herbals and excipients when designing formulations in food and nutraceutical applications.

Insight into novel delivery vehicles and blends of technologies can offer advanced formulations. Numerous bioactive nutraceuticals and their associated formulation problems have been identified and in turn modified to improve the pharmacokinetic and therapeutic parameters when dosed in patients.

2.3. Routes of Nutraceutical Delivery to the Body

2.3.1. Oral delivery

Nutraceutical delivery through oral route is considered to be the most acceptable and preferred route as it follows the same natural process of food and nutrient consumption in the body, is non-invasive, and involves neither special technique nor complex instructions. But this route is often influenced by dietary factors that may either enhance or impede nutraceutical bioavailability. For example, lutein shows a dramatically increased absorption profile when consumed with a high fat meal, and lycopene absorption improves with concomitant intake of β-carotene (Alves-Rodrigues and Shao, 2004; Khachik *et al*., 2002). Fat-soluble vitamins are preferentially absorbed with a meal yet fibre interferes with the oral absorption of some antioxidants. Nutraceuticals delivered via the oral route include, glucosamine, chondroitin, lycopene, resveratrol, co-enzyme-Q10, creatine, melatonin, green tea

extract, acetyl-L-carnitine, S-adenosyl methionine (SAME), lipoic acid, and dehydroepiandrosterone (DHEA) and water and fat soluble vitamins to name but a few. Despite the purported benefits of nutraceuticals many have reportedly low oral bioavailability and studies have shown wide variations in serum levels and inconsistent pharmacokinetics following oral dosing. These anomalies are the result of extreme GIT conditions the bioactive is exposed to: low stomach pH, degradative and metabolic enzymes, and alkaline pH in the intestine, etc. Resveratrol, a polyphenol derived from grapes and peanuts, having a wide range of biological activities is rapidly metabolized in the liver and intestine resulting in an extremely low oral bioavailability (Walle *et al*., 2004). Despite the low inherent oral bioavailability of many nutraceuticals, the consumer has a strong preference for this route which has led scientists to focus their efforts and emphasize on improving the delivery mechanism. Novel technologies and formulation strategies therefore play a vital role in the success of orally administered nutraceuticals agents by protecting them from rapid elimination and degradation and enhancing solubility and permeation through GIT membranes.

2.3.2. Dermal delivery

Consumers are more concerned about rapid results and expect skin products to be as “natural” and “organic” as possible whilst still providing an all-in-one innovative solution to their health and beauty requirements (Patravale and Mandawgade, 2008). Nutraceutical derived antioxidant effects may be enhanced by the concomitant oral and dermal application of bioactives, such is the case with lutein (Palombo *et al*., 2007). Although oral dosing more often achieves higher more consistent plasma levels, dermal application may result in an accumulation of nutraceuticals in the skin. This often superior reservoir effect observed after dermal application is advantageous for long-term storage and repeated provision of nutraceuticals to the body even after cessation of treatment due to the unique buffering effect of the skin (Meinke *et al*., 2010). The chronic topical use of dermal products containing nutraceuticals such as Co-enzyme Q10 (CoQ10) and vitamin C may result in noticeable clinical results including reductions in wrinkle depth in elderly aged skin (Rabe *et al*., 2006). It is therefore not surprising that more patients are searching for treatments to impede and reverse the age-associated changes in the skin, and more demands have been placed on industry to develop natural dermal products. Nutraceuticals used topically with positive cosmetic benefits include co-enzyme Q10, genistein, curcumin, N-acetylcysteine, gluconolactone and fucose-rich sulfated polysaccharides (Rabe *et al*., 2006; Schwarz *et al*., 2013;

Wijesinghe and Jeon, 2012). Many nutraceuticals are suited for delivery via the trans-dermal route due to their ability to locally treat skin diseases. Curcumin is one such nutraceutical suited for transdermal application due to its potential for chemoprevention and treatment of skin based diseases such as dermatitis, psoriasis and skin cancer (Kunnamakkara *et al*., 2008). The dermal route is a favoured alternative to the oral route, as it by-passes the GIT milieu and reduces hepatic and renal inactivation (Walle *et al*., 2004). However, some nutraceuticals, when applied topically to the skin, may become unstable on exposure to light or heat due to photo degradation. In addition to modified carrier systems available for nutraceutical formulations, a number of delivery aid mechanisms exist - like chemical penetration enhancers, iontophoresis, sonophoresis, etc - that can be applied locally to assist in the transport of actives to the skin and underlying tissues.

2.3.3. Ophthalmic delivery

As per consumer's expectancy and acceptability, nutraceuticals are generally administered orally. However the optimal route of nutraceutical delivery in ocular therapy still remains topical instillation into the ocular cavity. Many nutraceuticals (e.g. co-enzyme Q10, vitamin E, lutein) when administered ophthalmically have disease modifying effects on pathologies of the eye due to their antioxidant, anti-inflammatory and anti-cataract properties. Intraocular treatment success is however largely dependent on the residence time and permeability of the topically administered drop or ointment. Further, this success is often thwarted by the body's defence mechanisms which make it difficult to sustain an effective concentration of drug at the site of action and thus the bioavailability of an instilled active is often low (de la Fuente *et al*., 2010). Advanced delivery devices have therefore been developed for prolonged rate-controlled intraocular delivery of drugs (Choonara *et al*., 2011). Simple inclusion of selected nutraceutical agents dosed locally and concurrently with allopathic agents may extend intraocular retention time, provide synergistic clinical benefits, and prove to be safer alternatives for long term ophthalmic therapy (Martinez-Sancho *et al*., 2006; Peng *et al*., 2010; Zhang and Wang, 2009).

2.4. Nutraceutical Formulation Strategies

Emphasis on formulation design will assist in improving the physicochemical characteristics of nutraceutical compounds and aid in the design of products that are more efficacious in the treatment and prevention of disease. With this viewpoint the

following discussion delves into the details and descriptions of current formulation strategies that have been employed to improve dosage form design and delivery of nutraceutical compounds to the body:

2.4.1. Liposomal carrier systems

Liposomes are spherical microscopic lipid vesicles most often formed from phospholipids that hold a small amount of the solvent in which they exist. These small particles have been harnessed to alter the pharmacokinetics of many nutraceuticals including vitamins, enzymes, herbals and minerals. The key variables influencing the delivery using these carriers include vesicle size, surface charge, lipid concentration and composition of nutraceuticals within the liposome. Liposomes have proved ideal as a cosmetic delivery system and in the treatment and prevention of skin conditions. The phospholipid membrane of liposomes is actually instrumental in transporting active agents across the stratum corneum and has successfully improved dermal delivery and deposition of vitamins to the skin (Padamwar and Pokharkar, 2006). Such systems owe their drug delivery advantages to the similarity of liposomal membranes to biological membranes. This property enables formulations to circumvent the barrier of the skin and assists in protecting sensitive nutraceuticals from UV exposure. It was found that the lipid: drug ratio, quantity of phospholipid, and amount of stabilizer employed influenced the vesicle size and deposition of vitamin E acetate in the rat skin (Padamwar and Pokharkar, 2006). Superior drug deposition (up to seven-fold increase) in comparison to control dermal formulations confirmed the benefits of liposomal dermal formulations for the delivery of nutraceuticals to the skin in this study. Other investigators developed a surfactant-free liposomal formulation to encapsulate coenzyme Q10 (CoQ10) (Lee and Tsai, 2010). They used solvent injection method to prepare liposomal vesicles smaller than 200nm that were found to improve CoQ10 penetration through the stratum corneum.

Apart from dermal formulations liposomal technology has been adopted for oral and parenteral administration. The nutraceutical that has benefitted greatly from delivery via liposomes is resveratrol - the polyphenol that has anti-inflammatory effects, antioxidant properties, cardioprotective benefits, and cancer prevention potential but, low inherent bioavailability and stability. The incorporation of resveratrol into liposomal carrier systems has conferred improvements in stability, biological activity and efficacy with an improved side-effect profile, making possible oral and intravenous dosage formulations of the compound (Amri *et al*., 2012). Liposomal

systems have also been employed in oromucosal sprays for sublingual absorption of some nutraceuticals like melatonin that showed improvements in bioavailability when compared to the conventional tablet formulations (Keller, 2001). Other nutraceuticals formulated within liposome delivery systems include, echinacea, glucosamine, kava kava, milk thistle, St John's wort and DHEA (Keller, 2001). Zinc gluconate and zinc sulfate formulated using liposomes resulted in improved area under the curve (AUC) and liposomal grape seed extract formulations showed benefits such as superior solubility and a faster onset of action according to Keller (2001).

2.4.2. Electrospun fiber mats

Researchers have formulated mats of electrospun fibers for the delivery of various nutraceuticals. Cellulose acetate (CA) nanofibre mats have been electrospun as carriers for dermal delivery of vitamins to the skin (Taepaiboon *et al*., 2007). Vitamin E in the form of α-tocopherol and vitamin A in the form of all-trans-retinoic acid loaded in as-spun fiber mats showed a gradual increase in the cumulative release of vitamins over the test periods. Another group synthesized ultra-fine electrospun fibrous mats of the same biopolymer (CA) for the delivery of popular nutraceutical, curcumin (Suwantong *et al*., 2007). Their study revealed that the system was non-toxic and was able to deliver curcumin to the skin as a possible topical/transdermal dressing with antioxidant, anti-inflammatory and anti-tumor potential. The same research group synthesized CA fiber mats containing asiaticoside - the most active compound contained in the plant *Centella asiatica L,* which has known wound healing properties (Suwantong *et al*., 2008). These 'herb-loaded' CA fiber mats, tested for dermal release achieved a maximum release of 26% of asiaticoside through different pigskin methods. Cytotoxicity evaluations of mat revealed no harmful substance being released to the skin thereby potentiating such formulations as transdermal wound dressing patches.

A novel carrier which was able to inhibit vitamin C from oxidative degradation has been reported (Paneva *et al*., 2011). Vitamin C derivative, ascorbyl palmitate (AP), was incorporated into nanofibrous mats of poly (ε-caprolactone) (PCL) and further coated with a second nutraceutical, namely silver, in the form of a nanoparticle solution onto these PCL/AP mats. The study findings confirmed the stability enhancement of vitamin C after storage over a 4 month period attesting to the success of this Drug Delivery System (DDS). The presence of AP actually facilitated the deposition of silver ions onto the mats after emersion in aqueous solutions of

silver nitrate, to further enhance the nutraceutical composition of the delivery system. Figure 2.3a shows the scanning electron micrographs of the PCL/AP mats obtained at a PCL concentration of 10%($^{w}/_{v}$). As the AP content increased, there was a resultant decrease in the diameter of the mat fibres as seen in Figure 2.3. This research also highlighted the antibacterial properties of AP and evaluated the antibacterial properties of the PCL/AP mats against the skin pathogen *S. aureus.* Figure 2.3b indicates how plain PCL samples failed to inhibit pathogenic growth yet the PCL/AP mats substantially reduced the number of viable pathogenic cells. The resultant PCL/AP nanofibrous delivery system was reported to have strong antibacterial and antioxidant properties and a high surface area, proving ideal for treatment applications via the dermal route. These researchers also noted that the PCL/AP mats demonstrated antibacterial and antioxidant activity similar to the silver nanoparticle coated PCL/AP mats. Despite reporting differences in microbial inhibition between mats containing differing concentrations of AP, the antimicrobial efficacy of PCL/AP mats containing silver nanoparticles was not reported. It would be interesting to compare the antibacterial efficacy of silver coated vs. uncoated PCL/AP mats since silver is documented to have antimicrobial activity (Paneva *et al*., 2011).

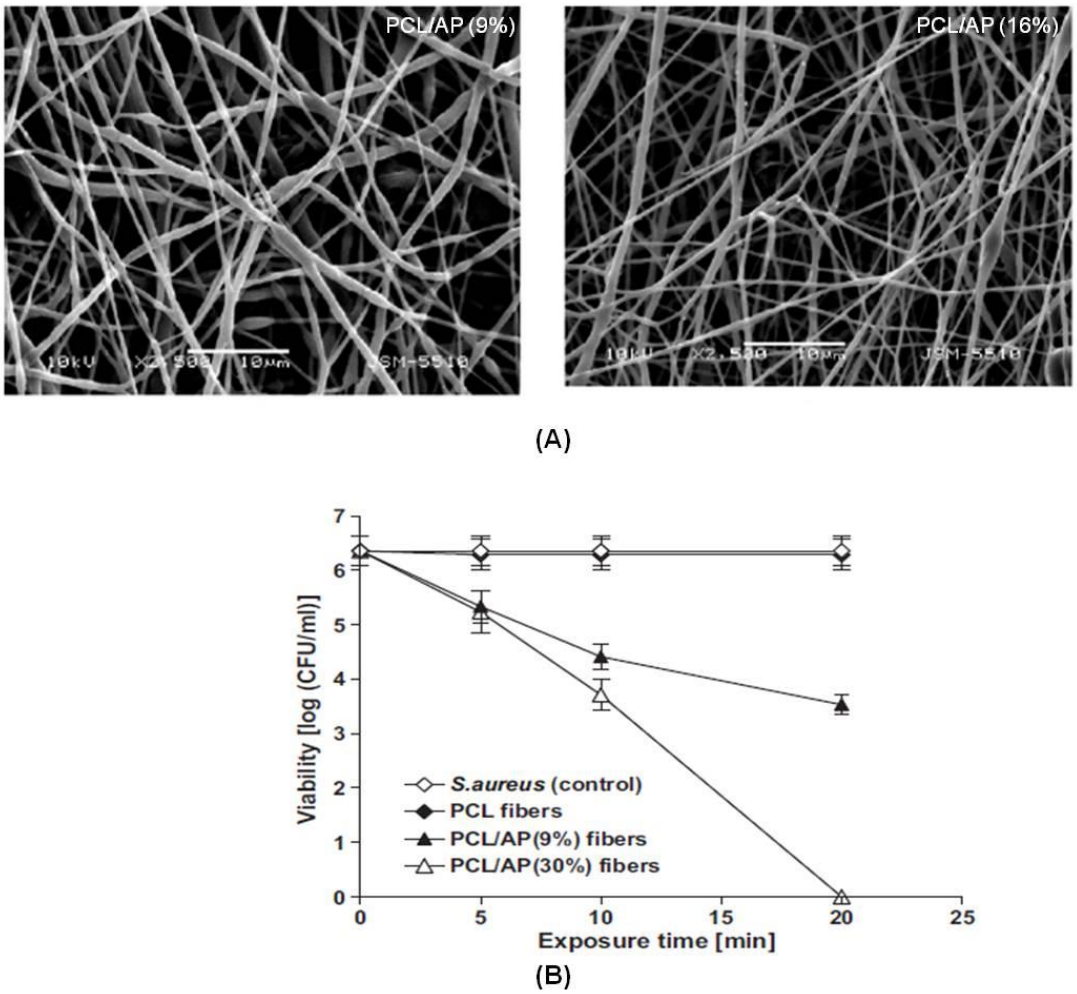


Figure 2.3: (A) SEM micrograph of PCL/AP with AP concentration 9 and 16% respectively, magnification: 2500x. PCL concentration: 10%$^{w}/_{v}$ and (B) Log of viable S. *aureus* cells versus the time of exposure to PCL, PCL/AP (9%) and PCL/AP(30%) fibrous materials (Paneva *et al*., 2011) [Reproduced with permission from Elsevier Science BV Ltd. © 2011].

2.4.3. Cyclodextrin complexation

Cyclodextrins (CD) and their derivatives have been widely utilized as carrier compounds to improve the inherent solubility, stability, permeation and bioavailability of nutraceuticals to the body (Tonnesen *et al*., 2002; Yuan *et al*., 2008; Gonnet *et al*., 2010; Yuan *et al*., 2012). Many vitamins are able to complex with these “cage-like” molecules with a resultant improvement in physicochemical properties when in contact with biological membranes. β-CD is the most commonly used CD due to its suitable cavity size. 7-dehydrocholesterol (7-DHC) which is a precursor vitamin used extensively in cosmetic and pharmaceutical products is almost insoluble in water and thus proves to be difficult to manipulate and include in dermal products. Researchers confirmed the formation of an inclusion complex

between hydroxypropyl-β-CD and 7-DHC that had enhanced solubility when compared to uncomplexed 7-DHC (Kim *et al*., 2010).

The liver protective nutraceutical, silymarin has particularly low water solubility and bioavailability and also requires novel formulation approaches for effective oral delivery. Silymarin-β-CD complexes formed by a co-precipitation method resulted in increased dissolution rates compared to the nutraceutical alone and a more sustained-release profile (Ghosh *et al*., 2011). Other investigators also utilized β-CD, in the formation of a nutraceutical inclusion complex with Garlic oil (GO) (Wang *et al*., 2011). GO has powerful antioxidant and antimicrobial properties but is limited as a food functional ingredient by its inherent volatility and poor physicochemical stability. Differential scanning calorimetry (DSC) studies established that the nutraceutical was successfully incorporated inside the CD cavity and protected from oxidation with a resultant improvement in stability of the complex. The GO/β-CD complex imparted improved aqueous solubility on GO and a controlled release rate was also achieved, demonstrated by *in vitro* dissolution studies. Investigations with vitamin A loaded hydroxypropyl-β-CD (HPCD) have demonstrated that CD's have the propensity to increase the solubility of a vitamin by almost 35000 times (Gonnet *et al*., 2010). Such an improvement would go a long way in improving the oral delivery of fat soluble vitamins (A, D, E, and K). HPCD's and their resultant inclusion complexes formed between herbal molecules such as astaxanthin have also proved successful in not only improving solubility but also hold merit as a strategy to control the release of nutraceuticals (Yuan *et al*., 2012).

Curcumin is another promising anticancer and antiviral nutraceutical agent but is limited by the fact that it is almost insoluble in water at neutral and acid pH and exhibits high decomposition at alkaline pH. Some have achieved a marked improvement in the stability of curcumin under basic conditions and a greater than expected solubility improvement after forming inclusion complexes with CD (Tonnesen *et al*., 2002). Other researchers utilized 2-hydroxypropyl-β-CD complexation to improve the oral bioavailability and permeation parameters of the *kaempferia parviflora* (KP) plant extract (Mekjaruskul *et al*., 2013). The KP extract contains methoxyflavones with biological properties that include antimicrobial effects, anti-inflammatory effects, and anti-allergic effects to name but a few. The formed KP-2-HP-β-CD formulation had 3.5 times greater permeation ability and approximately 21 to 34 times greater bioavailability when compared to a standard extracted formulation. Results obtained by researchers are continually contributing

towards the development of oral nutraceutical agents containing CD for improved GIT delivery and improved integrity within the harsh GIT milieu.

2.4.4. Biodegradable hydrogels

Biodegradable hydrogels have been widely researched to carry, protect and modify the delivery of a wide variety of pharmaceutical compounds including nutraceuticals. Many pharmaceutical polymers are stimuli-responsive and degrade or swell to varying extents depending on the physiological environment and changing thermal, pH, and hydration stimuli. For most nutritive molecules, preferential absorption occurs in the small intestine, and hydrogels may be used to facilitate this process by protecting nutraceuticals from degradation or denaturation and facilitating their controlled release.

Vitamins are ideal candidates for inclusion in gels as they are thermo-labile and would benefit greatly from the protection and transport characteristics of hydrogels to aid in the targeted absorption within the intestine. In another study, riboflavin was included in soy protein cold-set hydrogels which proved ideal in protecting the vitamin for at least 6 hours from gastric conditions and underwent pH dependant release in the intestine (Maltais *et al*., 2009) (Figure 2.4). Soy gel carriers provided additional benefits of additive nutritional value, provided by the soya carrier, a reduced need for inorganic solvents that may otherwise be incompatible with food based supplements, and the fact that the bioactive is not subjected to heating during the gelation procedure which would have denatured sensitive bioactives. The benefits of these hydrogel matrices may be extended for the delivery of other nutraceutical products.

Milk proteins have also proven to be very successful nutrition based hydrogel protein carriers as they are said to have ideal structural and physicochemical characteristics for the transport of bioactives via the GIT (Livney, 2010). Milk proteins, being inexpensive, readily available, and non-toxic have already been utilized as delivery vehicles to transport a multitude of drugs via the GIT. Such proteins make an extremely versatile delivery option in terms of the types and number of associations, functionalities and bonds that these proteins may form with various different bioactives as shown in Figure 2.5. Such a plethora of associations makes many nutraceutical compounds ideal candidates for complexation with milk proteins. Like soy proteins, milk proteins also exhibit favourable gelation properties that confer protective effects on bioactives and have favourable swelling behaviour.

In addition these proteins are found to possess superior buffering capacity for enhanced protection of sensitive nutraceutical bioactives from acid environments (Livney, 2010).

Milk protein gels are adept at pH-triggered release with various bioactives. An enzyme microbial transglutaminase (MTgase) induced complex casein (milk protein) hydrogel matrix has been successfully produced and said to be suitable for nutraceutical entrapment. By virtue of enzyme-induced crosslinking, vitamin B12 has been included in the casein hydrogel matrix to facilitate the controlled release of the vitamin in the body (Song *et al*., 2010; Elzoghby *et al*., 2011). Since the body is accustomed to the uptake of foods for its basic functioning it is logical that further pharmaceutical developments will explore other means of modifying food-based carriers like the milk and soy protein to form hydrogels for enhanced nutraceutical delivery.

Another interesting system consisted of a polyglycidyl methacrylate grafted sodium alginate (PGMA-*g*-SA) hydrogel that was pH sensitive and used as a delivery matrix for riboflavin (RF) (Abd El-Ghaffar *et al*., 2012). The swelling behaviour of pure sodium alginate in acidic pH is known to be slower than in basic pH and therefore sodium alginate provides a pH sensitive swelling behaviour that may afford a targeted release in intestinal media. The reported system achieved a more delayed or prolonged release of riboflavin from the polymer matrix compared to plain SA. PGMA grafted onto SA accounts for this observation as with increased grafting level the vitamin release impeded further. Investigators reported that ultimately the PGMA-*g*-SA polymer resulted in a slow and controlled release of 30% RF in simulated intestinal fluid (SIF) over 24 hours, and only 18% of RF in simulated gastric fluid (SGF), due to the pH responsive nature of the polymer. The PGMA grafting onto SA improved the entrapment of riboflavin on the hydrogel matrix, slowed swelling and degradation of the carrier, and controlled the release of the vitamin in a superior fashion compared to conventional pure SA beads crosslinked with calcium.

Many researchers utilize the common polysaccharide, alginate, to form gels due to its ability to react easily with polyvalent cations to undergo gelation (Norajit *et al*., 2010; Pereira *et al*., 2013). Recent research harnessed hydrogel technology to form hydrogel films consisting of alginate and *Aloe vera* for application as novel herbal biomedical wound dressings (Pereira *et al*., 2013). The synthesized hydrogel system

by a solvent-casting method, harnessed the therapeutic and delivery potential of alginate and the antimicrobial and anti-inflammatory effects of *Aloe vera* and was potentially proved to be effective in wound healing.

Another novel hydrogel formulation synthesized has used natural marine diatom-derived poly N-acetyl glucosamine nanofibers (pGlcNAc). The marine derived biomaterial was deacetylated and had the ability to form a hydrogel formulation with therapeutic properties as a treatment in degenerative disc disease (Gorapalli *et al*., 2012). Other researchers formulated a hydrogel containing the cationic polymer chitosan complexed with chondroitin sulfate that has long since been used to treat arthritis and joint conditions (Piai *et al*., 2010). The study noted that the hydrogel was able to release the nutraceutical, chondroitin sulfate, in a controlled manner and in response to variations in pH with a preferential release occurring at a basic pH.

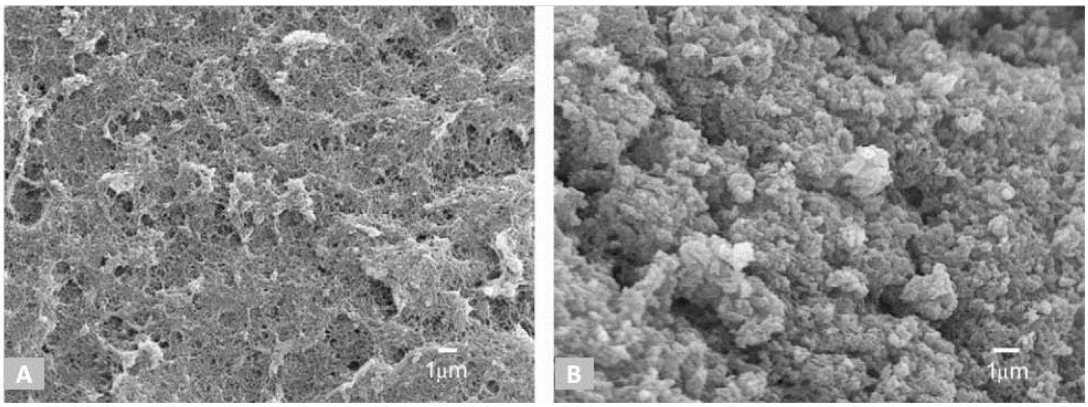


Figure 2.4: Scanning electron micrographs of 9%($^{w}/_{w}$) soy protein cold-set gels made with (A) 10mM CaCl2 (filamentous gel) and (B) 20mM CaCl2 (particulate gel) (Maltais *et al*., 2009) [Reproduced with permission from Elsevier Science BV Ltd. © 2009].

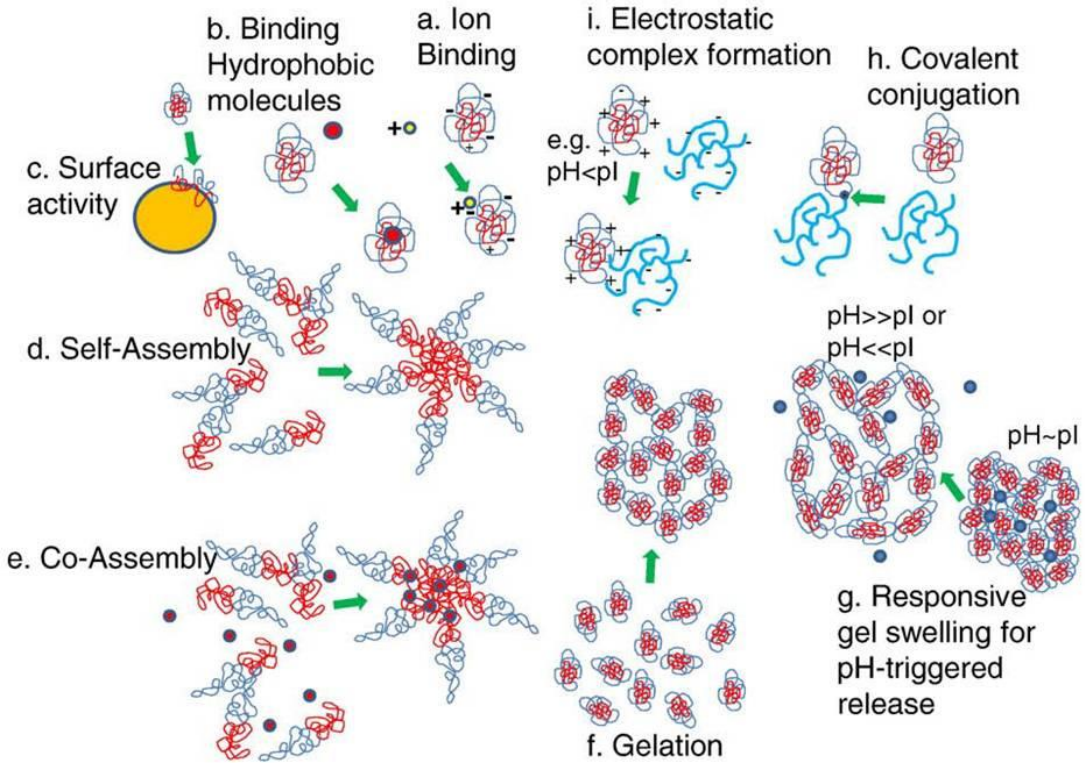


Figure 2.5: Illustrations of several functionalities of milk proteins useful for nutraceutical delivery (Livney, 2010) [Reproduced with permission from Elsevier Science BV Ltd. © 2010].

2.4.5. Nanotechnology-based applications for nutraceutical delivery

Nanotechnology has often been used to enhance the solubility of poorly soluble nutraceuticals for administration within a variety of dosage forms and is also stated to achieve good bioavailability and targeted delivery of the bioactives. The use of nanoparticle technology is suggested to increase the commercial potential of a multitude of nutraceuticals.

2.4.5.1. Nanosuspensions and nanoemulsions

The key factors dissolution velocity and saturation solubility determine the bioavailability and penetration of a nutraceutical in oral and dermal delivery respectively. Preparing nanosuspensions and nanoemulsions of hydrophobic nutraceuticals, with poor solubility, improves and enhances both these factors (Gonnet *et al*., 2010; Mitri *et al*., 2011; Li *et al*., 2012). A group of researchers prepared lutein – widely used antioxidant – by high pressure homogenization to produce ~400nm sized particles within a nano-suspension (Mitri *et al*., 2011). The nanosuspension was lyophilized and incorporated in creams and gels for dermal application and modified into pellets to fill into hard gelatine capsules for oral dosing. The nanoformulation provided enhanced penetration due to improved solubility and

larger surface area. The permeation of the lutein nanocrystal formulation across a 0.1µm synthetic cellulose nitrate membrane was reported to be 14 times greater compared to a coarse lutein powder. In the case of the oral formulation, the dissolution profiles demonstrated a clear advantage in terms of enhanced dissolution and bioavailability (Figure 2.6a).

In the recent study, the hydrophobic phytochemical 5-hydroxy-6,7,8,4-tetramethoxyflavone (PMF) isolated from sweet orange peels was incorporated in various oil-in-water nanoemulsions to efficiently deliver the compounds in dietary supplements (Li *et al*., 2012). PMF has anti-carcinogenic, anti-inflammatory, anti-oxidant, anti-viral and anti-thrombogenic effects which makes it attractive health additive for foods and nutritional supplement. However, due to low inherent bioavailability, high melting point and low solubility of this herbal nutraceutical it otherwise could not be utilized without a successful nano-enabled formulation.

Nanoemulsions have also been used to effectively deliver micronutrients such as carotenoids and fat soluble vitamins (A, D, E, and K) within liposomes via the oral route (Gonnet *et al*., 2010). Researchers investigated the influence of the carrier oil composition of a nanoemulsion-based delivery system on β-carotene bioaccessibility using an *in vitro* model to simulate the GIT (Qian *et al*., 2012). The investigators reported the β-carotene nanoemulsion formulation to possess good physical stability with resistance against chemical degradation in neutral and acidic gastric environments. Additionally, the bioaccessibility of β-carotene was observed to be higher when formulated in Long Chain Triglyceride (Corn oil) nanoemulsions than in Medium Chain Triglyceride (MCT) nanoemulsions or orange oil (Figure 2.6b). An oil/ water nanoemulsion of Hyaluronic acid (HA) has further been formulated and investigated as a carrier of lipophillic bioactives for transdermal delivery (Kong *et al*., 2011). An optimized HA formulation resulted in desirable stratum corneum permeability of vitamin E – used as model bioactive with an efficient partitioning and diffusion into the deeper dermal skin layers compared to the control.

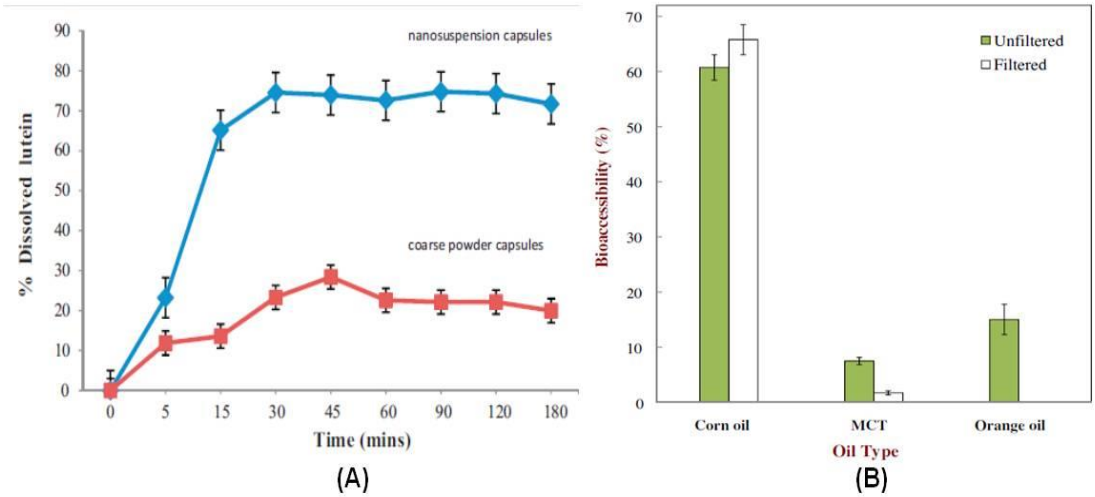


Figure 2.6: (A) *In vitro* penetration profiles of lutein from nanosuspension loaded pellets and from coarse lutein powder pellets, both filled into hard gelatine capsule (Mitri *et al*., 2011) [Reproduced with permission from Elsevier Science BV Ltd. © 2011] and (B) Influence of carrier oil type on the bioaccessibility of β-carotene initially encapsulated within oil-in-water nanoemulsions. Measurements were made before and after filtration (0.45μm pore size) of the middle phase (Qian *et al*., 2012) [Reproduced with permission from Elsevier Science BV Ltd. © 2012].

2.4.5.2. Nanostructured lipid carriers (NLC)

This new generation of lipid "nano-sized" structures comprising of a lipid matrix with special nanostructures hold potential for optimum nutraceutical delivery via the dermal, oral and topical routes. NLC's composed of cetyl palmitate and caprylic/ capric triacylglycerols were prepared to deliver the nutraceutical CoQ10 to the skin more efficiently (Teeranachaideekul *et al*., 2007). The prepared NLC's provided good physical stability, high entrapment efficiency, and a biphasic release pattern to the incorporated CoQ10. The biphasic release pattern of the NLC formulation proved ideal due to an initial rapid CoQ10 saturation of the skin followed by a controlled and extended maintenance phase ensuring continued supply of the vitamin. Scanning electron microscopy (SEM) analysis revealed particles with an anisometric shape and a size of approximately 200nm. It was similarly proved that CoQ10 loaded NLC dispersions had good long term physical and chemical stability (Junyaprasert *et al*., 2009). After storage at various temperatures (4°C, 25°C, 40°C) the entrapped CoQ10 remained above 90% and within the nanosize range in the NLC carrier system for 12 months at all three temperature ranges. This further demonstrates the stability enhancement and robustness of NLC's as a successful dermal delivery system for nutraceuticals.

Other researchers developed optimized NLC's of lutein for oral delivery that protected the entrapped nutraceutical from simulated gastric fluid and achieved a sustained release (Liu and Wu, 2010). Similarly, other groups developed fish oil based NLC's for the delivery of lutein in the view of synthesizing a DDS with dual benefits: an enhanced delivery mechanism that also provides other biological benefits due to its omega 3 fatty acid content (Lacatusu *et al*., 2013).

NLC's have also been used for the intravenous delivery of the antihepatotoxic herbal nutraceutical, silybin, as an improved application to treat liver disease (Jia *et al*., 2010). These researchers developed a silybin-NLC that had superior pharmaco-kinetic properties that included a higher AUC and a biphasic drug release. The novel silybin-NLC formulation achieved a prolonged residence time in the serum and targeted delivery to the liver for improved action (Jia *et al*., 2010).

2.4.5.3. Nanomicelles

Researchers have recognized the advantages of nanovehicles as a means to deliver nutraceuticals. Quercetin, a phytochemical, has attractive properties that lend to its potential use in the treatment of neurological disease, cardiovascular disease and cancer therapy and has further advanced to clinical trial evaluation, however the poor water solubility of these agents have limited their further commercialization. Researchers have succeeded in formulating a self-assembled nanomicellar delivery system made from the diblock copolymer polyethylene glycol (PEG)-derivatized phosphatidylethanolamine (PE) that was loaded with quercetin (Tan *et al*., 2012). These quercetin nanomicelles were found to be stable at a GIT pH range from 1.2 to 7.0, were relatively nontoxic, and were well tolerated in their *in vivo* preclinical studies. The enhanced solubility provided by the nanomicelles translated into a profound improvement and dramatic increase in the anticancer activity of quercetin at a dose of 30mg/kg in their formulation studies in mice compared to control ethanol suspension of quercetin. Similarly, other scientists have used casein micelles to nanoencapsulate vitamin D_2 with resultant protection against UV degradation (Semo *et al*., 2007). Such micellar systems can be identified as agents with great potential to deliver sensitive nutraceuticals with barriers to commercialization.

2.4.5.4. Nanoparticles, nanocapsules and nano-encapsulation

Many phytonutrients although documented to impart major health benefits have a limitation as nutraceutical additives because of high susceptibility to degradation or

low aqueous solubility. This is due to phytonutrient instability when subjected to temperature, pH and oxygen changes. One such popular antioxidant is epigallocatechin-3-gallate (EGCG) found in green tea that has long been documented to provide an array of health benefits including neuroprotection, anti-tumour effects and cardiovascular protection. But, the rapid degradation of EGCG observed in soft drinks leaves behind deterioration/ degradation products that discolour the drink and limit the health potential of the remaining compound as most of the activity is lost after long storage times. Co-assembled nanovehicles have been synthesized for the protection and enhanced delivery of EGCG and other antioxidant polyphenols (Shpigelman *et al*., 2010). These researchers used thermally modified β-lactoglobulin (βlg) to which EGCG complexed optimally resulting in nano-sized co-assembles of βlg-EGCG particles that conferred strong protection to EGCG against oxidation In addition, the nano βlg-EGCG particles were in a size range less than 50nm providing ideal transparency and suitability of the nano-system for inclusion in clear beverages. As natural self-assemblers and co-assemblers milk-proteins such as casein are being exploited to nanoencapsulate nutraceuticals. Milk proteins have been used to nanoencapsulate β-carotene and to deliver other nutraceuticals such as fatty acids and vitamin D (Livney *et al*., 2010). In another study the highly insoluble vitamin, β-carotene was modified for delivery by using both casein and dextran to form spherical nanoparticles consisting of a casein and β-carotene core and dextran shell (Pan *et al*., 2007). Other researchers encapsulated thymol and carvacrol essential oils (EO), with positive antimicrobial, antifungal and insecticidal properties, in zein nanoparticles (Wu *et al*., 2012). The EO-zein nanoparticles achieved an improvement in solubility up to 14 times whilst still maintaining antioxidant and antimicrobial effects.

Research has also delved into improving the stability and delivery of water soluble vitamins by creating minute advanced delivery vehicles. Studies have involved the preparation of sodium tripolyphosphate (STPP)-chitosan/vitamin C nanoparticles to achieve an enhanced shelf-life and delivery of vitamin C (Alishahi *et al*., 2011). *In vivo* studies showed that the mucoadhesive nature of chitosan also improved the release time of vitamin C to 12 hours compared to the 3-4 hours in the control. The release of the vitamin C was also shown to be pH dependant where a more rapid release was reported in PBS compared with that in a lower pH media.

Another interesting area of research is the preparation of solid lipid nanoparticles (SLN) in presence of a surfactant. The technology was initially developed for

parenteral delivery but the application has evolved for use in dermal formulations as well. Melatonin transdermal delivery has been noted to result in sustained plasma levels when SLN were used (Kandimalla *et al*., 2009). Resveratrol SLN's developed by researchers had a sustained release profile that allowed rapid permeation of the nutraceutical through the skin and gave resveratrol an enhanced cytotoxic effect suitable for the treatment of skin cancer (Teskac and Kristl, 2010). Studies have reported the formulation of vitamin E-loaded nanocapsules in the size range of 185nm (laboratory scale) to 253nm (pilot scale) and subjected these to an accelerated stability study (temperature: 40±2°C; relative humidity: 75±5%) (Khayata *et al*., 2012). Results obtained after 3 and 6 months of storage at the study conditions revealed good chemical and physical stability of the nanocapsules confirming that such a dosage form was highly suitable for the preservation of the integrity of nutraceuticals like vitamins with known susceptibility to heat and UV degradation (Cassano *et al*., 2009; Khayata *et al*., 2012). Thus encapsulating or complexing the nutrient bioactives in nanoparticles/nanocapsules not only improves their solubility but, also preserves their activity whilst shielding them from degradation and providing stability.

2.4.5.5. Nanosponges and microsponges

Nano and micro sponges are "non-collapsible" delivery systems that contain porous micro- and nanospheres and provide immense benefits in terms of their high internal surface area and bioactive loading capacity. These porous polymeric systems have been used by researchers to create a "melanosponge-α" containing a genetically engineered melanin. This formulation was able to distribute melanin over the skin surface and afford UV-A and UV-B sun protection. Microsponges have also proved useful in reducing allergic reactions when including cinnamic aldehydes in such systems (Patravale *et al*., 2008). Other researchers developed cyclodextrin-based nanosponges for enhanced solubility and stability of resveratrol (Ansari *et al*., 2011). These nanosponges were hyper-cross-linked cyclodextrin polymers that form three-dimensional networks. The nanosponge complexes improved the *in vitro* release, permeation, efficacy and stability of resveratrol and were proposed as suitable formulations for topical as well as buccal delivery of the nutraceutical (Ansari *et al*., 2011).

A research group recently synthesized acemannan sponges and investigated their clinical effect and scaffold forming ability in periodontal disease (Chantarwaratit *et al*., 2013). Acemannan is a biodegradable polysaccharide containing acetylated

polymannose and is extracted from *Aloe vera* gel. Periodontal ligament cells were treated with acemannan sponges in an *in vivo* study in dogs with induced premolar class II furcation defects. The nutraceutical delivery system resulted in increased periodontal cell proliferation, mineral deposition, new alveolar bone formation and cementum and periodontal ligament formation. The researchers proposed the acemannan DDS to be a successful candidate for delivery of the herbal derived polysaccharide biomolecule for the effective regeneration of periodontal tissue.

2.4.6. Microparticulate systems: microparticles, microspheres and microcapsules

Many herbal nutraceuticals have favourable anti-oxidant and antimicrobial properties. *Fadogia ancylantha* (Makoni tea), *Melissa officinalis* (lemon-balm) and *Tussilago farfara* (coltsfoot) are few such herbals that are attractive to the nutraceutical market and have been used in traditional drinks because of their high antioxidant polyphenol content. However they exist in the form of poorly-water-soluble sticky extracts with unpleasant smells and have a high propensity to degrade during storage. In addition to nanoparticulate complexation and encapsulation of the polyphenols, researchers have explored other means to deliver these sensitive polyphenol-rich extracts to the body. A novel maltodextrin/pectin (M/P) matrix microparticle powder was developed using a spray-drying method (Sansone *et al*., 2011). This strategy led to the encapsulation of these extracts forming stable powders, consisting of uniform micronized particles, with retention of activity and an improved shelf-life when subjected to stability tests. The M/P matrix also proved successful in masking the unpleasant odour of the extracts and greatly enhanced their water solubility (Sansone *et al*., 2011). Thermal analysis recorded the melting points for unprocessed Fadogia raw extracts between 130°C-250°C and a right shifted endotherm for the novel Fadogia-MP microparticle demonstrating high entrapment in the polymer matrix and a more stable nutraceutical product. Other nutraceutical researchers also used a microencapsulation technique to improve the stability of the antioxidant and pigment, lycopene, for inclusion in food based applications (Rocha *et al*., 2012). The researchers formed microcapsules of lycopene using a spray drying method and a modified starch (Capsul®). The resultant microcapsules were subjected to stability testing and were found to provide greater protection to the nutraceutical when compared to its free form.Such systems may be useful in the manufacture of functional foods and nutraceutical supplements with troublesome physicochemical and taste parameters.

Microspheres are frequently used in cosmetics in order to avoid incompatibility between formulation components and to protect an active from the invasive effects of the environment. Chemical inertia of nylon microspheres for example makes them highly suitable for holding both lipophillic and hydrophilic actives such as vitamin E and ascorbic acid (Patravale *et al*., 2008). Such delivery systems have achieved improved skin concentrations and a prolonged release, along with protection of vitamin constituents.

Another study involved the successful formulation of bio-degradable microspheres containing vitamin A palmitate and acyclovir for the intra-ocular treatment of herpes simplex and Epstein-Barr virus' (Martinez-Sancho *et al*., 2006). The inclusion of vitamin A improved the loading efficiency of acyclovir in the poly (D, L-lactic-co-glycolic) acid microspheres and improved the release profile of acyclovir during the first days of the *in vitro* assay. The inclusion of vitamin A in the ophthalmic formulation was rationalized in terms of the vitamins' antiviral activity and its ability to prevent the inherent risks of intravitreal injections due to vitamin A's ability to treat vitreoretinal diseases. The microspheres showed a constant release profile of acyclovir and vitamin A palmitate over a 49 day period. Such an approach demonstrates an ideal synergistic effect between a nutraceutical agent and a synthetic drug for the safe and effective treatment of disease and an improvement over current treatment options.

2.4.7. Solid dispersions

Solid dispersions (SD) are another method or means that have been used to enhance the bioavailability of oral nutraceuticals. Amorphous solid dispersions are systems where a bioactive is molecularly dispersed in a hydrophilic polymer matrix which results in an increase in solubility and rate of dissolution of the active. Poorly water-soluble nutraceuticals have slow dissolution rates and less than desirable bioavailability when dosed via the GIT. Research has involved the formation of various stable solid dispersions of CoQ10 with the carrier polymer, poloxamer 407 and an adsorbent and recrystallization inhibitor Aerosil® 200, all taken in different ratios, using the melting method, with an optimized formulation having a 1:5:6 weight ratio (Nepal *et al*., 2010). Dissolution profiles showed that pure CoQ10 was virtually insoluble, a physical mixture of CoQ10 and poloxamer 407 had only 5% dissolution, and the optimized SD formulation of the same ratio (1:5) achieved approximately 85% dissolution. In addition, the solubility of CoQ10 was evaluated and found to improve with an increase in the amount of poloxamer 407. The

optimized SD formulation achieved solubility four times greater than that of the same physical mixture. Interestingly, the SD dissolved maximally within 15 minutes and their aqueous solubilities were remarkably higher than that of the same physical mixtures.

In an interesting study the phytochemical, resveratrol, was mixed with different grades of polymers to form solid dispersions having varying types and strengths of association between polymer and active (Weigel *et al*., 2013). It was noted that amorphous dispersions of resveratrol were unstable unless the correct polymer blend was selected to have sufficient intermolecular forces between polymer and active to inhibit recrystallization. The group found that resveratrol blended with eudragit 100 and poly (vinylpyrrolidine) K29/32 had the greatest stability as solid dispersions. Progressive research in this area proves solid dispersions to be a competent formulation strategy to enhance oral bioavailability of some important nutraceuticals, but at the same time the rational selection of the correct polymer combination is an important criterion for the successful synthesis of stable solid dispersions.

2.4.8. Self-emulsifying drug delivery systems (SEDDS)

Novel Self-Emulsifying DDS (SEDDSs) have been developed and documented by different research groups as a means to enhance the oral bioavailability of the nutraceuticals. The reported development of a solid-SEDDS of CoQ10 was noted to result in a five-fold improvement in oral bioavailability (Onoue *et al*., 2012). This was achieved due to the fast self-emulsification and dispersion of the system in aqueous medium that led to an extremely rapid improvement in dissolution.

Tocotrienols, part of the family of vitamin E compounds, have been documented to possess various health related benefits and are therefore a focus area for improved formulation. Appropriateness of SEDDS of vitamin E to enhance bioavailability of the vitamin after oral dosing has been investigated (Yap and Yuen, 2004). The researchers found that vitamin E delivered as SEDDS resulted in a 2.5-4.5 times higher C_{max}, a higher AUC and a reduced lag time to absorption when compared to the non-SEDDS formulation. Recent research also supported the use of SEDDS and high-fat meals as methods to enhance the bioavailability of tocotrienols (Frank *et al*., 2012). Similarly, others developed self-emulsifying pellets of the milk thistle extract, silymarin, using extrusion/ spheronization technology. Results demonstrated SEDDS releasing 99% of silymarin in seven minutes compared to only 13.9%

release in the comparator milk thistle dry herbal extract (Losio *et al*., 2011). In addition the novel system showed preferential absorption into the lymphatic system which did not occur with the dry extract.

In addition to nanoemulsions already mentioned in earlier section, some researchers have taken the technology of SEDDS a step further by synthesizing these systems at a nanomolecular level (Li *et al*., 2011). A Self-nanoemulsifying DDS (SNEDDS) containing the herbal extract of persimmon leaf extract was formulated. The results of the study indicated improved oral bioavailability in that the AUC of two major flavonoid compounds (quercetin and kaempferol) was 1.5 times and 1.6 times higher for the SNEDDS formulation compared to the commercial control (tablet formulation). Further, another group recently developed a self-microemulsifying DDS (SMEDDS) to improve the low aqueous solubility and poor oral bioavailability of plant extracts of *Kaempferia parviflora* (Mekjaruskul *et al*., 2013). The researchers formulated a SMEDDS that achieved marked improvements in permeation through Caco-2 cells and bioavailability of the principle methoxyflavone compounds found in the plant known for its antimicrobial, aphrodisiac and anti-inflammatory properties. SEDDS therefore, not only proved to enhance the nutraceutical bioavailability but has also achieved targeted delivery to the liver which is advantageous for herbal extracts due to the avoidance of first pass effects and resultant higher plasma levels.

2.4.9. Particle coatings for protection, site-specific delivery and enhanced efficacy

Some delivery systems require combined technologies to ensure or potentiate their success. An interesting strategy to carry and deliver the gastric sensitive nutraceuticals orally was development of Chitosan/β-lactoglobulin (CS-βlg) core–shell nanoparticles (Chen and Subirade, 2005). Chitosan, despite having ideal properties as a nutraceutical carrier - biodegradable, biocompatible, muco-adhesiveness, versatility of use in health applications - is not stable at low pH and undergoes rapid degradation which can predispose bioactives to premature destruction. To protect chitosan and entrapped nutraceuticals from low gastric pH and pepsin, the chitosan nanoparticles were coated with β-lactoglobulin, a protein known to be highly resistant to pepsin degradation in the stomach. The carrier system passed through the stomach to reach the intestine unscathed where pancreatin then degraded the outer β-lactoglobulin shell to release chitosan nanoparticles that were able to enhance mucoadhesiveness and absorption

properties of the entrapped nutraceutical. This carrier system simultaneously harnessed the advantages of two carriers, the polymer chitosan and the milk protein β-lactoglobulin.

Researchers developed a novel technology to deliver CoQ10 effectively to the eye as a therapeutic agent to treat cataracts (Zhang and Wang, 2009). Their delivery system consisted of CoQ10-loaded soy phospatidylcholine (SPC) liposomes coated with the polymer trimethyl chitosan (TMC) of variable molecular weights. Liposomes are ideal in ophthalmic formulations as they do not interfere with vision and are excellent drug reservoirs. However, further modification by TMC coating imparted an added absorption enhancing effect to the liposomal formulation and improved their stability. The overall system dramatically improved corneal retention time when compared with a standard 99mTc-DTPA solution. This was explained by an electrostatic interaction between the cationic TMC layer around the CoQ10 liposomes and the negatively charged mucous layer of the cornea. It was observed that there was a direct relation between the molecular weight of the TMC coating and the precorneal retention time of the formulation and AUC values highlighting the advantages of the coating step. A curve of the remaining activity of the various liposomal CoQ10 formulations vs. time derived from gamma scintigraphy is shown in Figure 2.7. Their research further proved that CoQ10 as a nutraceutical active is an effective prophylactic agent to mitigate the onset and progression of cataracts as confirmed in their *in vivo* animal study. However, without a successful delivery system such as that developed in this research, CoQ10 would fail to be an effective treatment due to its inherent instability to light and lipophilicity that otherwise impedes bioavailability.

In other ophthalmic DDS's, nutraceuticals have been used as the coating material themselves (Peng *et al*., 2010). The nutraceutical confers beneficial clinical effects to the eye, like retardation of cataract development as done by antioxidants CoQ10 and vitamin E, in addition to providing a modified release of the principle allopathic agent. This group has effectively used vitamin E as a natural diffusion barrier coated onto commercial silicone contact lenses that significantly improved the duration of release of the hydrophilic drugs timolol, dexamethasone and fluconazole (Peng *et al*., 2010). Researchers are therefore utilizing the beneficial inherent physicochemical characteristics of nutraceuticals as "active" excipients to enhance and extend the delivery of drugs to the eye.

Another study improved bioflavonoid delivery through the combining of technologies by synthesizing hesperetin loaded NLC's coated with different biopolymers (Fathi and Varshosaz, 2013). The researchers achieved better hesperetin release profiles and improvements in stability, due to nutraceutical inclusion in NLC's coated with either, methoxypectin, alginate or chitosan.

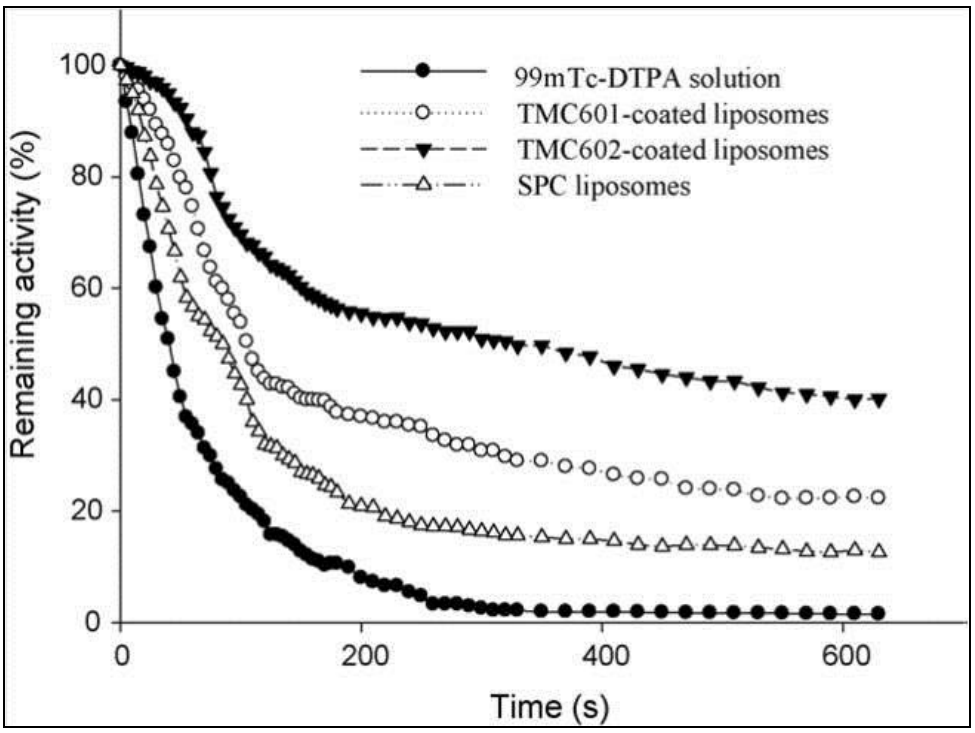


Figure 2.7: Pre-corneal drainage of 99mTc-DTPA in preparations (Zhang and Wang, 2009) [Reproduced with permission from Elsevier Science BV Ltd. © 2009]

Table 2.1 below summarizes the various formulation strategies used to enhance nutraceutical value, benefits and efficiency.

Table 2.1: Summary of recent formulation approaches for improved nutraceutical delivery

Formulation strategy	Nutraceutical	Salient features/ benefits	Reference
Liposomal carrier systems	Vitamin E acetate	Superior deposition in skin	Padamwar and Pokharkar (2006)
	Grape seed extract	Superior solubility and onset of action	Keller (2001)
	CoenzymeQ10	Improved skin penetration	Lee and Tsai (2010)
	Melatonin	Improved oral bioavailability	Keller (2001)
	Resveratrol	Improved stability and sustained release formulations	Amri *et al*. (2012)
	Zinc gluconate	Improved AUC of oral formulations	Keller (2001)
Electrospun fiber mats	α-tocopherol/vitamin A	CA nanofibres for gradual release	Taepaiboon *et al*. (2007)
	Curcumin	Ultra-fine fibrous mats for skin delivery	Suwantong *et al*. (2007)
	Asiaticoside	Herb loaded CA mats as a wound dressing	Suwantong *et al*. (2008)
	Ascorbyl palmitate	PCL nanofibrous mats for improved stability and antibacterial properties	Paneva *et al*. (2011)
Microsponges and nanosponges	Melanin	Melanosponge-α for skin application and protection from UV-A and UV-B	Patravale and Mandawgade, (2008)
	Resveratrol	Cyclodextrin-based nanosponges for improved solubility, stability, permeation for topical and buccal delivery	Ansari *et al*. (2011)
	Acemannan	Sponges for regeneration of periodontal tissues	Chantarawaratit *et al*. (2013)
Cyclodextrin complexation	7-dehydrocholesterol	Hydroxypropyl-β-CD complex with improved solubility	Kim *et al*. (2010)
	Silymarin	β-CD complexes with sustained release	Ghosh *et al*. (2011)

Formulation strategy	Nutraceutical	Salient features/ benefits	Reference
Cyclodextrin complexation	Garlic oil	β-CD complexes with solubility and controlled release	Wang *et al*. (2011)
	Vitamin A	Hydroxypropyl-β-CD complex with improved solubility	Gonnet *et al*. (2010)
	Astaxanthan	Controlled release and improved solubility	Yuan *et al*. (2012)
	Kaempferia parviflora	2-HP-β-CD complexes with permeation and oral bioavailability	Mekjaruskul *et al*. (2013)
	Curcumin	Complexes with improved stability and solubility	Tonnesen *et al*. (2002)
Biodegradable hydrogels	Riboflavin	Soy protein hydrogel for gastric protection and pH controlled release	Maltais *et al*. (2009)
	Ginseng	Alginate films with white ginseng as antioxidant	Norajit *et al*. (2010)
	Vitamin B12	Casein hydrogel for controlled release	Song *et al*. (2010) Elzoghby *et al*. (2011)
	Aloe vera	Alginate hydrogel as a wound healing dressing	Pereira *et al*. (2013)
	Riboflavin	PGMA-g-SA hydrogel for pH sensitive delayed release and improved vitamin entrapment	Abd El-Ghaffar *et al*. (2012)
	Chondroitin sulfate	Chitosan hydrogel for controlled release of Chondroitin	Piai *et al*. (2010)
	Poly N-acetyl glucosamine	Hydrogel treatment for degenerative disc disease	Gorapalli *et al*. (2012)
Nanotechnology	Lutein	Nanocrystal suspensions: increased oral bioavailability	Mitri *et al*. (2011)
	5-hydroxy-6,7,8,4-tetramethoxyflavone (PMF)	Nanoemulsions for efficient delivery	Li *et al*. (2012)
	Vitamins A, D, E , K	Nanoemulsions with improved absorption	Gonnet *et al*. (2010)

Formulation strategy	Nutraceutical	Salient features/ benefits	Reference
Nanotechnology	β-carotene	Nanoemulsions with stability and higher bioaccessibility	Qian *et al*. (2012)
	Vitamin E	Hyaluronic acid nanoemulsion with superior partitioning and diffusion into stratum corneum	Kong *et al*. (2011)
	CoenzymeQ10	NLC's with stability, high loading, biphasic release	Teeranachaideekul *et al*. (2007)
	Lutein	NLC's with sustained release and gastric protection	Liu and Wu (2010)
	Silybin	NLC's with High AUC and biphasic release	Jia *et al*. (2010)
	Melatonin	SLN's achieving sustained plasma levels	Kandimalla *et al*. (2009)
	Resveratrol	SLN's for rapid skin permeation and enhanced efficacy	Teskac and Kristi (2010)
	Quercetin	Nanomicelles with improved solubility and stability	Tan *et al*. (2012)
	Vitamin D_2	Nanomicelles providing UV protection	Semo *et al*. (2007)
	Vitamin E	Nanocapsules with stability and thermal integrity	Khayata *et al*. (2012)
	Epigallocatechin-3-gallate (ECGC)	Co-assembled nanovehicles for protection and delivery in food applications	Shpigelman *et al*. (2010)
	β-carotene	Casein/dextran nanoparticles for solubility and activity	Pan *et al*. (2007)
	Vitamin C	Chitosan nanoparticles with enhanced shelf-life and release time.	Alishahi *et al*. (2011)
	Thymol	Zein nanoparticles for improved solubility	Wu *et al*. (2012)
	Carvacrol	Zein nanoparticles for improved solubility	Wu *et al*. (2012)

Formulation strategy	Nutraceutical	Salient features/ benefits	Reference
Solid dispersions	Vitamin A palmitate	Liquid crystals for timed release	Patravale and Mandawgade (2008)
	CoenzymeQ10	Solid dispersion with solubility, stability and dissolution	Nepal *et al*. (2010)
	Resveratrol	Solid dispersion for improved stability	Weigiel *et al*. (2013)
Self-emulsifying drug delivery system	CoenzymeQ10	SEDDS with 5-fold increase in bioavailability and rapid dissolution	Onoue *et al*. (2012)
	Vitamin E	SEDDS with 2.5-4.5 times higher C_{max} and reduced lag time to absorption	Yap and Yuen (2004)
	Milk thistle	SEDDS with targeted delivery to lymphatic system	Losio *et al*. (2011)
	Persimmon leaf	SNEDDS with AUC 1.5-1.6 times higher than control	Li *et al*. (2011)
	Kaempferia parviflora	SMEDDS with high permeation through Caco-2 cells	Mekjaruskul *et al*. (2013)
Microparticulate systems	Fadogia ancylantha (Makoni tea) Melissa officinalis (lemon-balm) Tussilago farfara (coltsfoot)	Maltodextrin-pectin matrix micronized particles with improved solubility, shelf-life, stability and masking effects on unpleasant odours	Sansone *et al*. (2011)
	Vitamin A palmitate	Microspheres containing vitamin A palmitate and acyclovir with improved loading efficiency and release profile of co-administered acyclovir	Martinez *et al*. (2006)
	Lycopene	Microcapsules with improved stability	Rocha *et al*. (2012)
	Vitamin E	Nylon microspheres with prolonged	Patravale and Mandawgade

Formulation strategy	Nutraceutical	Salient features/ benefits	Reference
	Ascorbic acid	release and protection of the vitamins	(2008)
Particle coatings	CoenzymeQ10	TMC-coated liposomes containing coenzymeQ10 with improved corneal retention time and stability	Zang and Wang (2009)
	Vitamin E	Vitamin E coated contact lenses for prolonged release of bioactives	Peng *et al*. (2010)
	Gastric-sensitive nutraceuticals	Chitosan/ β-lactoglobulin core-shell nanoparticles for protection from gastric pH and pepsin and enhanced absorption	Chen and Subirade (2005)
		Hesperetin loaded NLC's coated with chitosan, alginate and methoxypectin enhanced release and stability	Fathi and Varshosaz (2013)

AUC:Area under curve; **CA**: Cellulose acetate; **β-CD**: Beta cyclodextrin; **PGMA**: Polyglycidyl methacrylate; **SA**:Sodium alginate ; **NLC**:Nanostructured lipid carrier; **SLN**: Solid lipid nanoparticle; **SEDDS**: Self emulsifying drug delivery system; **SNEDDS**: Self-nanoemulsifying DDS; **SMEDDS**: Self-microemulsifying DDS.

2.5. Concluding Remarks

Due to the increased incidence of lifestyle diseases and the numerous side-effects associated with allopathic medicines there has been considerable interest in developing effective nutrient-based complementary medicines, vitamin and herbal products. These products are also increasingly being formulated out of the growing acceptance that nutraceuticals have definitive merit in the treatment and prevention of disease. However, as is recognized with all new clinical entities, it is not only the pharmacological activity of the compound that influences its commercialization success but rather its physicochemical characteristics (Kawakami, 2012). These inherent properties of a compound affect pharmacokinetics and may significantly impede or enhance the assimilation and utilization of the bioactive by the body. There are therefore a multitude of delivery systems intended to improve the bioavailability of nutraceutical molecules at various organs sites through the use of novel formulation technologies.

Many nutraceutical compounds function optimally when combined into a multicomponent product resulting in an assumed synergistic output. Researchers have recognized the benefits of such carefully designed formulas that treat optimally because of an ability to treat a condition via multiple mechanisms. Such products are generally more affordable and accessible and may even provide less risk of resistance due to the existence of bioactives that act via diverse pharmacological actions (Friel and Lederman, 2006). However such formulations need to be scientifically designed and validated to ensure stability amongst constituents. In the quest for effective nutraceutical formulations it is important to create robust products that are adaptable to the harsh and unpredictable physiological condition, are protected from interactions, remain intact during storage, and control each bioactives release. Future approaches may involve formulations that allow every nutraceutical bioactive to be individually protected, packaged and combined with others, that themselves are also individually carried, released and protected. The merging of technologies will enable the harnessing of the individual strengths of each, which will in turn provide advances in the efficacy of multicomponent nutraceutical products. The use of a combination strategy would provide an independent individualized release, a reduced risk of inter-component interactions, predictable response, and enable the product to adjust to the physiological milieu. The popularity of fixed-dose combination products, whether natural or allopathic in

content, would encourage such a design and ensure enhanced pharmacological efficacy and patient safety within a convenient dosing mechanism.

2.6. References

Abd El-Ghaffar MA, Hashem MS, El-Awady MK, Rabie AM. 2012. pH-Sensitive Alginate Hydrogels for Riboflavin Controlled Release. *Carbohydrate Polymers* 89: 667-675.

Acosta E. 2009. Bioavailability of nanoparticles in nutrient and nutraceutical delivery. 2009. *Current Opinion in Colloid and Interface Science* 14: 3-15.

Alishahi A, Mirvaghefi A, Tehrani MR, Farahmand H, Shojaosadati S A, Dorkoosh FA, Elsabee MZ. 2011. Shelf life and delivery enhancement of vitamin C using chitosan nanoparticles. *Food Chemistry* 126: 935-940.

Alves-Rodrigues A, Shao A. 2004. The science behind lutein. *Toxicology Letters* 150: 57-83.

Amri A, Chaumeil JC, Sfar S, Charrueau C. 2012. Administration of resveratrol: What formulation solutions to bioavailability limitations? *Journal of Controlled Release* 158: 182-193.

Andlauer W, Furst P. 2002. Nutraceuticals: A piece of history, present status and outlook. *Food Research International* 35: 171-176.

Ankola DD, Viswanad B, Bhardwaj V, Ramarao P, Kumar MNVR. 2007. Development of potent oral nanoparticulate formulation of coenzyme Q10 for treatment of hypertension: Can the simple nutritional supplements be used as first line therapeutic agents for prophylaxis/ therapy? *European Journal of Pharmaceutics and Biopharmaceutics* 67: 361-369.

Ansari KA, Vavia PR, Trotta F, Cavalli R. 2011. Cyclodextrin-based nanosponges for delivery of resveratrol: *In vitro* characterisation, stability, cytotoxicity and permeation study. *American Association of Pharmaceutical Scientists* 12: 279-286.

Ballard JM, Zhu L, Nelson ED, Seburg RA. 2007. Degradation of vitamin D_3 in a stressed formulation: The identification of esters of vitamin D_3 formed by a transesterification with triglycerides. *Journal of Pharmaceutical and Biomedical Analysis* 43: 142-150.

Bernal J, Mendiola JA, Ibanez E, Cifuentes A. 2011. Advanced analysis of nutraceuticals. *Journal of Pharmaceutical and Biomedical Analysis* 55: 758-774.

Blaylock RL, Maroon J. 2012. Natural plant products and extracts that reduce immunoexcitotoxicity-associated neurodegeneration and promote repair within the central nervous system. *Surgical Neurology International* 3: 19. Retrieved from URL: http://www.surgicalneurologyint.com. [Accessed 21 February 2012].

Borges MC, Martini LA, Rogero MM. 2011. Current perspectives on vitamin D, immune system, and chronic diseases. *Nutrition* 27: 399-404.

Camfield DA, Sarris J, Berk M. 2011. Nutraceuticals in the treatment of Obsessive Compulsive Disorder (OCD): A review of mechanistic and clinical evidence, *Progress in Neuropsychopharmacology & Biological Psychiatry* 35: 887-895.

Cassano R, Trombino S, Muzzalupo R, Tavano L, Picci N. 2009. A novel dextran hydrogel linking trans-ferulic acid for the stabilization and transdermal delivery of vitamin E. *European Journal of Pharmaceutics and Biopharmaceutics* 72: 232-238.

Chantarwaratit P, Sangvanich P, Banlunara W, Soontornvipart K, Thunyakitpisal P. 2014. Acemannan sponges stimulate alveolar bone, cementum and periodontal ligament regeneration in a canine class II furcation defect model. *Journal of Periodontal Research* 49(2): 164-178.

Chen L, Subirade M. 2005. Chitosan/ β-lactoglobulin core-shell nanoparticles as nutraceutical carriers. *Biomaterials* 26: 6041–6053.

Choonara YE, Pillay V, Carmichael TR, Meyer LCR, Du Toit LC, Naylor S, Wanblad C. 2011. *In vivo* evaluation of a biodegradable donut-shaped minitablet for prolonged posterior segment drug delivery in the rabbit eye model. *Journal of Pharmaceutical Sciences* 100: 1819-1832.

Conesa-Botella A, Florence E, Lynen L, Colebunders R, Menten J, Moreno-Reyes R. 2010. Decrease of vitamin D concentration in patients with HIV infection on a non-nucleoside reverse transcriptase inhibitor-containing regimen. *AIDS Research and Therapy* 40: 1-6.

de la Fuente M, Ravina M, Paolicelli P, Sanchez A, Seijo B, Alonse MJ. 2010. Chitosan-based nanostructures: A delivery platform for ocular therapeutics. *Advanced Drug Delivery Reviews* 62: 100-117.

Ebeling PR. 2005. Megadose therapy for vitamin D deficiency. *Medical Journal of Australia* 183 (1): 4-5.

Elzoghby AO, El-Fotoh WSA, Elgindy NA. 2011. Casein-based formulations as promising controlled release drug delivery systems. *Journal of Controlled Release* 153: 206-216.

Espin JC, Garcia-Conesa MT, Tomas-Barberan FA. 2007. Nutraceuticals: facts and fiction. *Phytochemistry* 68: 2986-3008.

Fathi M, Varshosaz J. 2013. Novel hesperetin loaded nanocarriers for food fortification: production and characterization. *Journal of Functional Foods* 5: 1382-1391.

Fernandes de Abreu, DA, Landel V, Feron F. 2011. Seasonal, gestation and postnatal influences on multiple sclerosis: the beneficial role of vitamin D. supplementation during early life. *Journal of Neurological Sciences* 311: 64-68.

Frank J, Chin XWD, Schrader C, Eckert GP, Rimbach G. 2012. Do tocotrienols have potential as neuroprotective dietary factors? *Ageing Research Reviews* 11: 163-180.

Friel H, Lederman HA. 2006. Nutritional supplement for influenza A (H5N1) infection in humans. *Medical Hypotheses* 67: 578-587.

Gholse YN, Yadav SR. 2012. Developments in Nutraceuticals for Chemoprevention: A review, *International Journal of Pharmacy and Technology* 4: 1950-1973.

Ghosh A, Biswas S, Ghosh T. 2011. Preparation and evaluation of silymarin β-cyclodextrin molecular inclusion complexes. *Journal of Young Pharmacists* 3: 205-210.

Gianfrilli D, Lauretta R, Di dato C, Graziadio C, Pozza C, De Larichaudy J, Giannetta E, Isidori AM, Lenzi A. 2011. Propionyl-L-carnitine, L-arginine and niacin in sexual medicine: a nutraceutical approach to erectile dysfunction. *Andrologia* 1: 1-5.

Gonnet M, Lethuaut L, Boury F. 2010. New trends in encapsulation of liposoluble vitamins. *Journal of Controlled Release* 146: 276-290.

Gorapalli D, Seth A, Vournakis J, Whyne C, Akens M, Zhang A, Demcheva M, Qamirani E, Yee A. 2012. Evaluation of a novel poly N-acetyl glucosamine hydrogel for treatment of the degenerating intervertebral disc. *Life Sciences* 91: 1328-1335.

Gupta SC, Kim JH, Prasad S, Aggarwal BB. 2010. Regulation of survival, proliferation, invasion, angiogenesis, and metastasis of tumor cells through modulation of inflammatory pathways by nutraceuticals. *Cancer Metastasis Reviews* 29: 405-434.

Henrotin Y, Lambert C, Couchourel D, Ripoll C, Chiotelli E. 2011. Nutraceuticals: do they represent a new era in the management of arthritis? –a narrative review from the lessons taken with five products. *Osteoarthritis and Cartilage* 19: 1-21.

Jia L, Zhang D, Li Z, Duan C, Wang Y, Feng F, Wang F, Liu Y, Zhang Q. 2010. Nanostructured lipid carriers for parenteral delivery of silybin: biodistribution and pharmacokinetic studies. *Colloids and Surfaces B: Biointerfaces* 80: 213-218.

Junyaprasert VB, Teeranachaideekul V, Souto EB, Boonme P, Muller RH. 2009. Q10-loaded NLC versus nanoemulsions: Stability rheology and *in vitro* skin permeation. *International Journal of Pharmaceutics* 377: 207-214.

Kandimalla KK, Babu RJ, Singh M. 2009. Biphasic flux profiles of melatonin: The yin-yang of transdermal permeation enhancement mediated by fatty alcohol enhancers. *Journal of Pharmaceutical Sciences* 99: 209-218.

Kawakami K. 2012. Modification of physicochemical characteristics of active pharmaceutical ingredients and application of supersaturable dosage forms for improving bioavailability of poorly absorbed drugs. *Advanced Drug Delivery Reviews* 64: 480-495.

Keller BC. 2001. Liposomes in nutrition. *Trends in Food Science and Technology* 12: 25-31.

Kelsey NA, Wilkins HM, Linseman DA. 2010. Nutraceutical Antioxidants as Novel Neuroprotective Agents. *Molecules* 15: 7792-7813.

Khachik F, Carvalho L, Bernstein PS. 2002. Chemistry, distribution, and metabolism of tomato carotenoids and their impact on human health. *Experimental Biology and Medicine* 227: 845-851.

Khayata N, Abdelwahed W, Chehna MF, Charcosset C, Fessi H. 2012. Stability study and lyophilization of vitamin E-loaded nanocapsules prepared by membrane contactor. *International Journal of Pharmaceutics* 439: 254-259.

Kim SO, Youn JY, Kim KM, Kang KC, Pyo HB, Lee SJ. 2010. Characterization of an inclusion complex of 7-dehydrocholesterol and cyclodextrin. *Journal of Industrial and Engineering Chemistry* 16: 119-121.

Kong M, Chen XG, Kweon DK, Park HJ. 2011. Investigations on skin permeation of hyaluronic acid based nanoemulsion as transdermal carrier. *Carbohydrate Polymers* 86: 837-843.

Kunnamakkara A B, Anand P, Aggarwal BB. 2008. Curcumin inhibits proliferation, invasion, angiogenesis and metastasis of different cancers through interaction with multiple cell signaling proteins. *Cancer Letters* 269: 199-225.

Lacatusu I, Mitrea E, Badea N, Stan R, Oprea O, Maghea A. 2013. Lipid nanoparticles based omega-3 fatty acids as effective carriers for lutein delivery. Preparation and *in vitro* characterization studies. *Journal of Functional Foods* 5: 1260-1269.

Lee JH, O'Keefe JH, Bell D, Hensrud DD, Holick MF. 2008. Vitamin D Deficiency An Important, Common, and Easily Treatable Cardiovascular Risk Factor? *Journal of the American College of Cardiology* 52: 1949-1956.

Lee W, Tsai T. 2010. Preparation and characterization of liposomal coenzyme Q10 for *in vivo* topical application. *International Journal of Pharmaceutics* 395: 78-83.

Li W, Yi S, Wang Z, Chen S, Xin S, Xie J, Zhao C. 2011. Self-nanoemulsifying drug delivery system of persimmon leaf extract: optimization and bioavailability studies. *International Journal of Pharmaceutics* 420: 161-171.

Li Y, Zheng J, Xiao H, McClements DJ. 2012. Nanoemulsion-based delivery systems for poorly water-soluble bioactive compounds: Influence of formulation parameters on Polymethoxyflavone crystallization. *Food Hydrocolloids* 27: 517-528.

Liu C, Wu C. 2010. Optimization of nanostructured lipid carriers for lutein delivery. *Colloids and Surfaces A: Physicochemical and Engineering Aspects* 353: 149-156.

Livney YD. 2010. Milk proteins as vehicles for bioactives. *Current Opinion in Colloid & Interface Science* 15: 73-83.

Losio T, Voinovich D, Perissutti B, Serdoz F, Hasa D, Grabhar I, Dall'Acqua S, Zara, GP, Muntoni E, Pinto JF. 2011. Oral bioavailability of silymarin phytocomplex formulated as self-emulsifying pellets. *Phytomedicine* 18: 505-512.

Maltais A, Remondetto GE, Subirade M. 2009. Soy protein cold-set hydrogels as controlled delivery devices for nutraceutical compounds. *Food Hydrocolloids* 23: 1647-1653.

Marotta F, Yadav H, Pathak S, Minelli E, Signorelli P, Lorenzetti A, Marandola P. 2009. Inhibition of human breast cancer cell growth and enzymatic activity by a fermented nutraceutical: An *in vitro* and *in vivo* study. *Annals of the New York Academy of Sciences* 1155: 273-277.

Martınez-Sancho C, Herrero-Vanrell R, Negro S. 2006. Vitamin A palmitate and aciclovir biodegradable microspheres for intraocular sustained release. *International Journal of Pharmaceutics* 326: 100-106.

Mayo-Wilson E, Imdad A, Herzer K, Yakoob MY, Noormahomed Sheriff ZABN. 2011. Vitamin A supplements for preventing mortality, illness and blindness in

children aged under 5: systematic review and meta-analysis. *British Medical Journal* 343: d5094: 1-19.

Meinke MC, Darvin ME, Vollert H, Lademann J. 2010. Bioavailability of natural carotenoids in human skin compared to blood. *European Journal of Pharmaceutics and Biopharmaceutics* 76: 269-274.

Mekjaruskul C, Yang Y, Leed MGD, Sadgrove MP, Jay M, Sripanidkulchai B. 2013. Novel formulation strategies for enhancing oral delivery of methoxyflavones in kaempferia parvoflora by SMEDDS or complexation with 2-hydroxypropyl-β-cyclodextrin. *International Journal of Pharmaceutics* 445: 1-11.

Michos ED, Blumenthal RS. 2007. Vitamin D supplementation and cardiovascular disease risk. *Circulation* 115: 827-828.

Mitri K, Shegokar R, Gohla S, Anselmi C, Muller RH. 2011. Lutein nanocrystals as antioxidant formulation for oral and dermal delivery. *International Journal of Pharmaceutics* 420: 141-146.

Mueller NJ, Fux CA, Ledergerber B, Elzi L, Schmid P, Dang T, Magenta L, Calmy A, Vergopoulos A, Bischoff-Ferrari HA. 2010. High prevalence of severe vitamin D deficiency in combined antiretroviral therapy-naïve and successfully treated Swiss HIV patients. *AIDS* 24: 1127-1134.

Nair, HB, Sung B, Yadav VR, Kannappan R, Chaturvedi MM, Aggarwal BB. 2010. Delivery of anti-inflammatory nutraceuticals by nanoparticles for the prevention and treatment of cancer. *Biochemical Pharmacology* 80: 1833-1843.

Nepal PR, Han H, Choi H. 2010. Enhancement of solubility and dissolution of Coenzyme Q10 using solid dispersion formulation. *International Journal of Pharmaceutics* 383: 147-153.

Norajit K, Kim KM, Ryu GH. 2010. Comparative studies on the characterization and antioxidant properties of biodegradable alginate films containing ginseng extract. *Journal of Food Engineering* 98: 377-384.

Onoue S, Uchida A, Kuriyama K, Nakamura T, Set Y, Kato M, Hatanaka J, Tanaka T, Miyoshi H, Yamada S. 2012. Novel solid self-emulsifying drug delivery system of coenzyme Q10 with improved photochemical and pharmacokinetic behaviours. *European Journal of Pharmaceutical Sciences* 46: 492-499.

Padamwar M, Pokharkar VB. 2006. Development of vitamin loaded topical liposomal formulation using factorial design approach: Drug deposition and stability. *International Journal of Pharmaceutics* 320: 37-44.

Palombo P, Fabrizi G, Ruocco V, Ruocco E Fluhr J, Roberts R, Morganti P. 2007. Beneficial long-term effects of combined oral/ topical antioxidant treatment with the carotenoids lutein and zeaxanthin on human skin: a double-blind, placebo-controlled study. *Skin Pharmacology and Physiology* 20: 199-210.

Pan X, Yao P, Jiang M. 2007. Simultaneous nanoparticles formation and encapsulation driven by hydrophobic interaction of casein-graft-dextran and β-carotene. *Journal of Colloid and Interface Science* 315: 456-463.

Paneva D, Manolova N, Argirova M, Rashkov I. 2011. Antibacterial electrospun poly (ε-caprolactone)/ ascorbyl palmitate nanofibrous materials. *International Journal of Pharmaceutics* 416: 346-355.

Patravale VB, Mandawgade SD. 2008. Novel cosmetic delivery systems: an application update. *International Journal of Cosmetic Science* 30: 19-33.

Peng C, Kim J, Chauhan A. 2010. Extended delivery of hydrophilic drugs from silicone-hydrogel contact lenses containing Vitamin E diffusion barriers. *Biomaterials* 31: 4032-4047.

Pereira R, Mendes A, Bartolo P. 2013. Alginate/Aloe vera hydrogel films for biomedical applications. *Procedia CIRP* 5: 210-215.

Piai JF, Lopes LC, Fajardo AR, Rubira AF, Muniz E C. 2010. Kinetic study of chondroitin sulphate release from chondroitin sulphate/ chitosan complex hydrogel. *Journal of Molecular Liquids* 156: 28-32.

Qian C, Decker EA, Xiao H, McClements DJ. 2012. Nanoemulsion delivery systems. Influence of carrier oil on β-carotene bioaccessibility. *Food Chemistry* 135:1440-1447.

Rabe JH, Mamelak AJ, McElgunn PJS, Morison W, Sauder DN. 2006. Photoaging: Mechanism and repair. *Journal of American Academy of Dermatology* 55: 1-19.

Rocha GA, Favaro-Trindade CS, Grosso CRF. 2012. Microencapsulation of lycopene by spray drying: Characterization, stability and application of microcapsules. *Food and Bioproducts Processing* 90: 37-42.

Sansone F, Mencherini T, Picerno P, d'Amore M, Aquino RP, Lauro MR. 2011. Maltodextrin/pectin microparticles by spray drying as carrier for nutraceutical extracts. *Journal of Food Engineering* 105: 468-476.

Rassnick KM, Muindi JR, Johnson CS, Bailey DB, Trump DL. Oral bioavailability of DN101, a concentrated formulation of calcitriol, in tumor-bearing dogs. 2011. *Cancer Chemotherapy and Pharmacol*ogy 67: 165-171.

Schwartz GG. 2009. Vitamin D and Intervention Trials in Prostate Cancer: From Theory to Therapy. *Annals of Epidemiology* 19: 96-102.

Schwarz JC, Baisaeng N, Hoppel M, Low M, Keck CM, Valenta C. 2013. Ultra-small NLC for improved dermal delivery of co-enzyme Q10. *International Journal of Pharmaceutics* 447: 2013-2017.

Semo E, Kesselman E, Danino D, Livney YD. 2007. Casein micelle as a natural nanocapsular vehicle for nutraceuticals. *Food Hydrocolloids* 21: 936-942.

Shpigelman A, Israeli G, Livney YD. 2010. Thermally-induced-protein-polyphenol co-assemblies: beta-lactoglobulin based nanocomplexes as protective nanovehicles for EGCG. *Food Hydrocolloids* 24: 735-743.

Sirtori CR, Galli C, Anderson JW, Arnoldi A. 2009. Nutritional and nutraceutical approaches to dyslipidemia and atherosclerosis prevention: Focus on dietary proteins. *Atherosclerosis* 203: 8-17.

Song F, Zhang LM, Shi JF, Li NN. 2010. Novel casein hydrogels: formation, structure and controlled drug release. *Colloids and Surfaces B: Biointerfaces* 79: 142–148.

Suwantong O, Opanasopit P, Ruktanonchai U, Supaphol P. 2007. Electrospun cellulose acetate fiber mats containing curcumin and release characteristic of the herbal substance. *Polymer* 48: 7546-7557.

Suwantong O, Ruktanonchai U, Supaphol P. 2008. Electrospun cellulose acetate fiber mats containing asiaticoside or *Centella asiatica* crude extract and the release characteristics of asiaticoside. *Polymer* 49: 4239-4247.

Szep Z, Guaraldi G, Samir SS, Lore V, Ratcliffe SJ, Orlando G, Carli F, Rossi R, Rochira V, Tebras P. 2011. Vitamin D deficiency is associated with type 2 diabetes mellitus in HIV infection. *AIDS* 25: 525–529.

Taepaiboon P, Rungsardthong U, Supaphol P. 2007. Vitamin-loaded cellulose acetate nanofiber mats as transdermal and dermal therapeutic agents of vitamin A acid and vitamin E. *European Journal of Pharmaceutics and Biopharmaceutics* 67: 387-397.

Tan B, Liu Y, Chang K, Lim BKW, Chiu GNC. 2012. Perorally active nanomicellar formulation of quercetin in the treatment of lung cancer. *International Journal of Nanomedicine* 7: 651-661.

Tang AM, Graham NMH, Semba RD, Saah AJ. 1997. Association between serum vitamin A and E levels and HIV-1 disease progression. *AIDS* 11: 613-620.

Teeranachaideekul V, Souto EB, Junyaprasert VB, Muller RH. 2007. Cetyl-palmitate based NLC for topical delivery of Coenzyme Q10- Development, physicochemical characterization and *in vitro* release studies. *European Journal of Pharmaceutics and Biopharmaceutics* 67: 141-148.

Telrandhe UB, Kurmi R, Uplanchiwar V, Mansoori MH, Jain V, Jain RK, Jain SK. 2012. Nutraceuticals- A Phenomenal Resource in Modern Medicine. *International Journal of Universal Pharmacy and Life Sciences* 2: 179-195.

Teskac K, Kristl J. 2010. Evidence for solid lipid nanoparticles mediated cell uptake of resveratrol. *International Journal of Pharmaceutics* 390: 61-69.

Tonnesen HH, Masson M, Loftsson T. 2002. Studies of curcumin and curcuminoids. XXVII. Cyclodextrin complexation: solubility, chemical and photochemical stability. *International Journal of Pharmaceutics* 244: 127-135.

Viard J, Souberbielle J, Kirk O, Reekie J, Knysz B, Losso M, Gatell J, Pedersen C, Bogner JR, Lundgren JD, Mocroft A. 2011. Vitamin D and clinical disease progression in HIV infection: results from the EuroSIDA study. *AIDS* 25: 1305-1315.

Walle T, Hsieh F, DeLegge MH, Oatis JE, Walle UK. 2004. High absorption but very low bioavailability of oral resveratrol in humans. *Drug Metabolism and Distribution* 32: 1377-1382.

Wang J, Cao Y, Sun B, Wang C. 2011. Physicochemical and release characterization of garlic oil-β-cyclodextrin inclusion complexes. *Food Chemistry* 127: 1680-1685.

Weigel LA, Mauer LJ, Edgar KJ, Taylor LS. 2013. Crystallization of amorphous solid dispersions of resveratrol during preparation and storage-Impact of different polymers. *Journal of Pharmaceutical Sciences* 102: 171-184.

Wijesinghe WAJP and Jeon Y. 2012. Biological activities and potential industrial applications of fucose rich sulfated polysaccharides and fucoidans from brown seaweeds: A review. *Carbohydrate Polymers* 88: 13-20.

Wu Y, Luo Y, Wang Q. 2012. Antioxidant and antimicrobial properties of essential oils encapsulated in zein nanoparticles prepared by liquid-liquid dispersion method. *LWT – Food Science and Technology* 48: 283-290.

Yap SP, Yuen KH. 2004. Influence of lipolysis and droplet size on tocotrienol absorption from self-emulsifying formulations. *International Journal of Pharmaceutics* 281: 67-78.

Yuan C, Jin Z, Xu X, Zhuang H, Shen W. 2008. Preparation and stability of the inclusion complex of astaxanthin with hydroxypropyl-β-cyclodextrin. *Food Chemistry* 109: 264-268.

Yuan C, Jin Z, Xu X. 2012. Inclusion complex of astaxanthin with hydroxypropyl-β-cyclodextrin: UV, FTIR, HNMR and molecular modeling studies. *Carbohydrate Polymers* 89: 492-496.

Zhang R, Naughton DP. 2010. Vitamin D in health and disease: Current perspectives. *Nutrition Journal* 9: 65.

Zhang J, Wang S. 2009. Topical use of Coenzyme-Q10-loaded liposomes coated with trimethyl chitosan: Tolerance, precorneal retention and anti-cataract effect. *International Journal of Pharmaceutics* 372: 66-75.

Zlotogorski A, Dayan A, Dayan D, Chaushu G, Salo T, Vered M. 2013. Nutraceuticals as new treatment approaches for oral cancer: II. Green tea extracts and resveratrol. *Oral Oncology* 49: 502-506.

CHAPTER 3

VITAMIN D THERAPY AND RELATED METABOLOMICS: IS THE CALCIFEROL DOSE AND FORM THE ONLY REQUIREMENTS FOR SUCCESSFUL CLINICAL THERAPEUTICS?

3.1. Introduction

Many researchers have investigated the use of vitamin D in the treatment and prevention of multiple diseases (Borges *et al*., 2011; Zhang and Naughton, 2010). Despite much interest in this field, many clinical plans often fail to achieve the intended therapeutic outcomes and deficiency remains in the global population (Gilaberte *et al*., 2011; Gonzalez, 2010). In addition, there is little consensus over the ideal dose or formulation required to successfully achieve treatment goals in all patients and all indications. Controversy exists regarding the optimal prescribed dose, the most effective vitamin D form and regimen, ideal daily amount, and the safest serum levels to be monitored (Masterjohn, 2007). Many researchers have made claims and recommendations regarding safe upper limits, toxicity levels and optimal doses, but few are fully cognoscente of the power that physiological factors and interactions have on the ultimate fate and activity of the vitamin as a determinant of treatment success.

Early researchers questioned the efficacy and usefulness of oral vitamin D supplements in patients with disorders in underlying intestinal malabsorption syndromes, making a case for considering the physiological state rather than just the dose (Lo *et al.*, 1985). Some studies have recommended the use of vitamin D in conjunction with vitamin A and vitamin K as a means to achieve a greater treatment impact than relying solely on a single prescribed dose or molecular form of vitamin D (Masterjohn, 2007). Some researchers have confirmed that the potency of the two main supplemental forms of vitamin D namely vitamin D_3 (cholecalciferol) and vitamin D_2 (ergocalciferol) is not equivalent. Studies have noted that cholecalciferol may be two to three times more potent than ergocalciferol at increasing plasma levels of vitamin D (Romagnoli *et al*., 2008; Armas *et al*., 2004). However, other compounds in the immediate microenvironment need to be considered in conjunction with the form prescribed. For example, a strong relationship exists between vitamin D_2 and magnesium in terms of bone health; however the exact mechanism that occurs when the two interact within the biological system has yet to

be fully elucidated (Toyran and Severcan, 2007). Such a large number of variables that exist unnoticed at a biological level make it very challenging to predict an elicited biochemical response in each and every patient and with every dose. Without comprehensively evaluating the biological processes, underlying host factors, or pharmacodynamic and kinetic effects, the reasons for under- or over-shooting sought after treatment goals will continue to elude physician and patient alike.

Although vitamin D is generated within the body from sun exposure, recent research has sparked debate over the risk between too little and too much sun exposure and the best approach to achieve healthy serum levels (Gilaberte *et al*., 2011). Focus has thus shifted to adequate use of supplements and the diet instead of sun-exposure to achieve ideal levels. Therefore it is important to know how such products will perform in an ever changing environment. Many patients are prescribed various molecular forms, metabolites and doses of vitamin D but still show slower than expected rise in levels and poor clinical improvements in the targeted disease. Titrating up dosages or varying the form prescribed to a more active molecule in the vitamin D pathway may still fail to result in an associated improvement in a patient within the required time frame. It has been estimated that for every 100IU of vitamin D taken daily, its blood level increases by only a fraction (1ng/mL over a period of 2-3 months) (Gonzalez, 2010; Moyad, 2010). In this chapter, we explore, discuss, and hypothesise the influence that various physiological and metabolic milieu interactions and host/patient factors have on the therapeutic efficacy of a prescribed dose of vitamin D or its metabolites (Figure 3.1). Ultimately an argument is provided in support of such complex processes having a more profound effect than just the dosage or molecule that is administered.

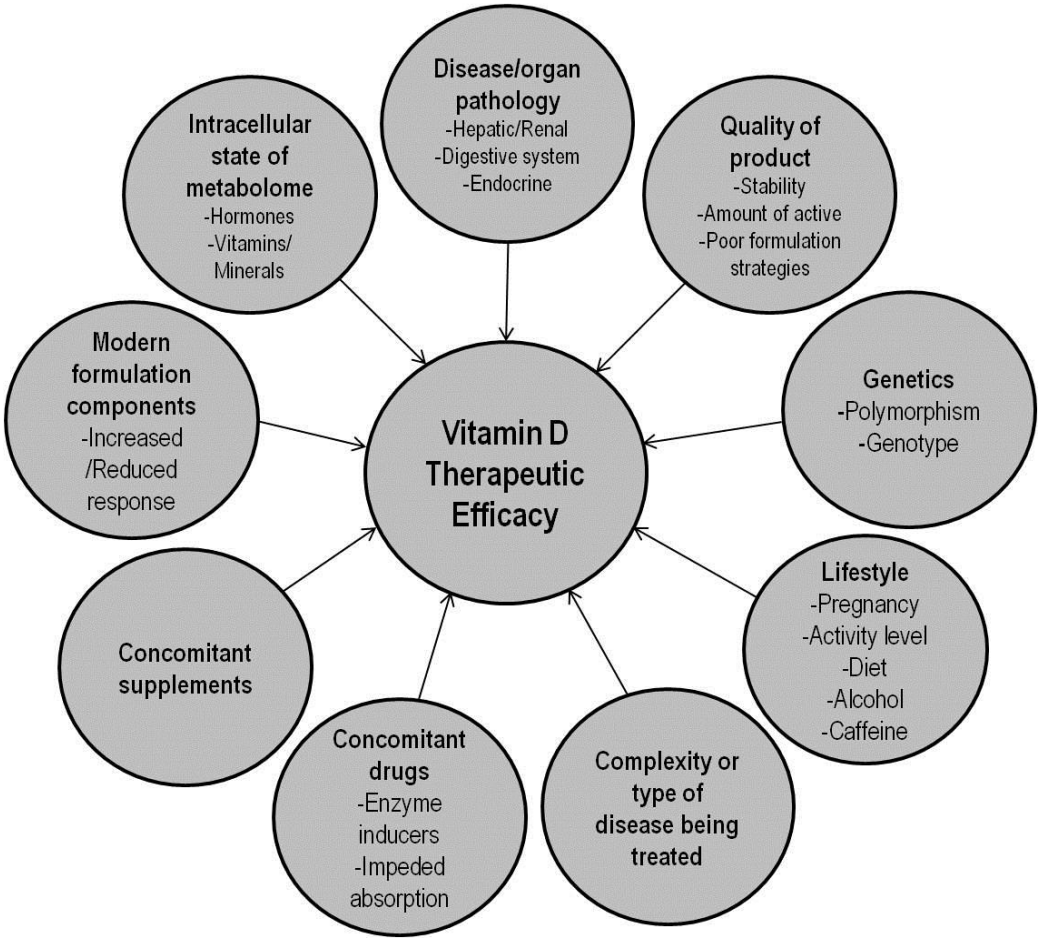


Figure 3.1: Schematic depicting and summarizing multiple factors that influence vitamin D treatment success.

3.2. Hypothesis

The interaction that occurs between vitamin D and the metabolome is more critical in determining the extent of treatment success in the wider patient population than merely the dose or the form consumed. Host factors including organ function, intracellular dynamics, genetics, disease prognosis, and the influence of lifestyle choices impact the efficacy of supplemental or prescribed products. Other variables including inconsistent product quality validation, formulation components, and the occurrence of co-administered agents are also factors affecting whether treatment objectives are achieved. Since vitamin D serum levels fluctuate based on multiple processes, and defined increases or decreases can only be correlated to an end point after a sufficient treatment period, all influences need to be carefully evaluated.

3.3. Evaluation of the Hypothesis

3.3.1. The metabolome is a unique set of molecular circumstances that influences therapeutic response to vitamin D

The metabolome is defined as a complete complement of all the molecules and metabolites available and participating in metabolic reactions within a biological cell, organ or organism due to cellular processing. Activated Vitamin D is known to have far reaching effects on various organ systems so much so that the vitamin has often been described and classified as a hormone; more specifically: the secosteroid hormone. Therefore it is logical to assume that the metabolome will be dynamically influenced by the presence of such a powerful bioactive and its metabolites whose levels and activity are also inextricably influenced by the micro-environment into which they are introduced. By considering the influence of current or past metabolite concentrations, genetic differences, the complexity of compartmental interactions, metabolic pathways and degradation kinetics, one may better understand how a dose of vitamin D may behave in a particular micro-environment. The traditional approach to pharmacology has been to study the effects of each single molecule on a single biological system, hormones, enzymes and genes and then to collect these individual parts into a larger picture. Such an approach would fail to accurately capture the complex pharmacokinetic and pharmacodynamic interplay that occurs in each patient in which multiple compounds are available for interaction with multiple targets with interdependent activities. One can therefore comprehend the possibility that each and every dose may elicit a different response at every administration resulting in an optimal or sub-optimal effect between patients or within the same individual. Therefore it is logical to understand why a particular dose or form of vitamin D may have result in inter- and intra-patient variability in even over chronic treatment periods.

3.3.2. Synergistic mechanisms influence treatment success more than single drug protocols

As discussed already, when a bioactive comes into contact with other biological molecules present either in the physiological milieu or introduced concomitantly by a formulation, the result is either a positive or a negative one on the pharmacokinetics and pharmacodynamics of the drug. Synergism is defined as the working together of two compounds to produce an effect greater than the sum of the individual components and is a concept that has been harnessed by many nutraceutical proponents. Researchers have since long employed the use of two or more selected

vitamins and minerals to achieve specific therapeutic effects in patients. Tarnopolsky discussed the theoretical rationale behind combining nutraceutical compounds that share a common pharmacological pathway to treat certain conditions (Tarnopolsky, 2008). Such a strategy is routinely used to potentiate the effects of vitamin D on specific diseases such as osteoporosis. Administration of vitamin D with calcium and vitamin C is a treatment protocol accepted to be superior to the use of the individual components for the maintenance of good bone health. Thus high dose vitamin D alone would fail to sufficiently achieve the therapeutic end point of reduced vertebral fractures in an osteoporotic or osteopenic patient.

Similarly, choosing one particular form of the vitamin over another (e.g. vitamin D_3 vs. vitamin D_2) will not achieve a holistic improvement without considering co-factors in the physiological process of bone development. A constant and adequate supply of complimentary nutrients including calcium, magnesium, vitamin K2, zinc, boron, silica, protein, fluoride, potassium, B vitamins, and iron to name a few, are required in addition to the correct dose and form of vitamin D for optimal bone homeostasis. Other vitamin and mineral constituents contribute additionally to bone health and repair by unique mechanisms that complement the action of vitamin D and assist in the amelioration of the disease state by targeting at various levels. Only if the correct balance of a plethora of constituents is present can the body affect optimal metabolic processes resulting in an ideal response. Vitamin D serum levels have also been inversely correlated to its antihypertensive effect. However, the vitamin D mediated reduction in blood pressure following supplementation is more pronounced when vitamin D and calcium are administered together. This is another example of two bioactives that together achieve more than the individual component. Previous research has also investigated combinations of allopathic agents with vitamin D to treat conditions such as cancer. As an example early research found promise utilizing ketoconazole and vitamin D to decrease serum testosterone levels which again supports the theory of synergism. The use of multi-tiered strategies prescribing numerous complementary compounds proves far superior to dosing with a single agent.

3.3.3. The endocrine system and physiological feedback mechanisms influence serum levels and response to dose

After ingestion, vitamin D is transported to the liver for the initial conversion step in its activation where it is hydroxylated to form calcidiol or 25-hydroxyvitamin D (25 (OH)D). Calcidiol is the metabolic storage form of the vitamin that circulates in the

serum and is measured by physicians in order to determine a patient's vitamin D status. Calcidiol then undergoes a second hydroxylation step that occurs mainly in the kidneys but also in local tissues (bone, cartilage and skin) to form 1,25-dihydroxycholecalciferol (1,25 $(OH)_2$) or Calcitriol (Reid, 2004; Wolpowitz and Gilchrist, 2006). Calcitriol is the activated hormonal form of vitamin D that has various biological functions in the body.

Metabolic processes that occur in the human body are influenced by various co-factor molecules and the existence of hormone or enzyme activated feedback mechanisms that control levels of cellular macromolecules. Certain conditions, pathologies, and cellular states may increase or decrease the levels of vitamins and minerals in relation to one another. Vitamin D utilization, synthesis and activity are dynamically influenced by the amount of other biological substances that are already present in the body and by the enzymatic system (Figure 3.2).

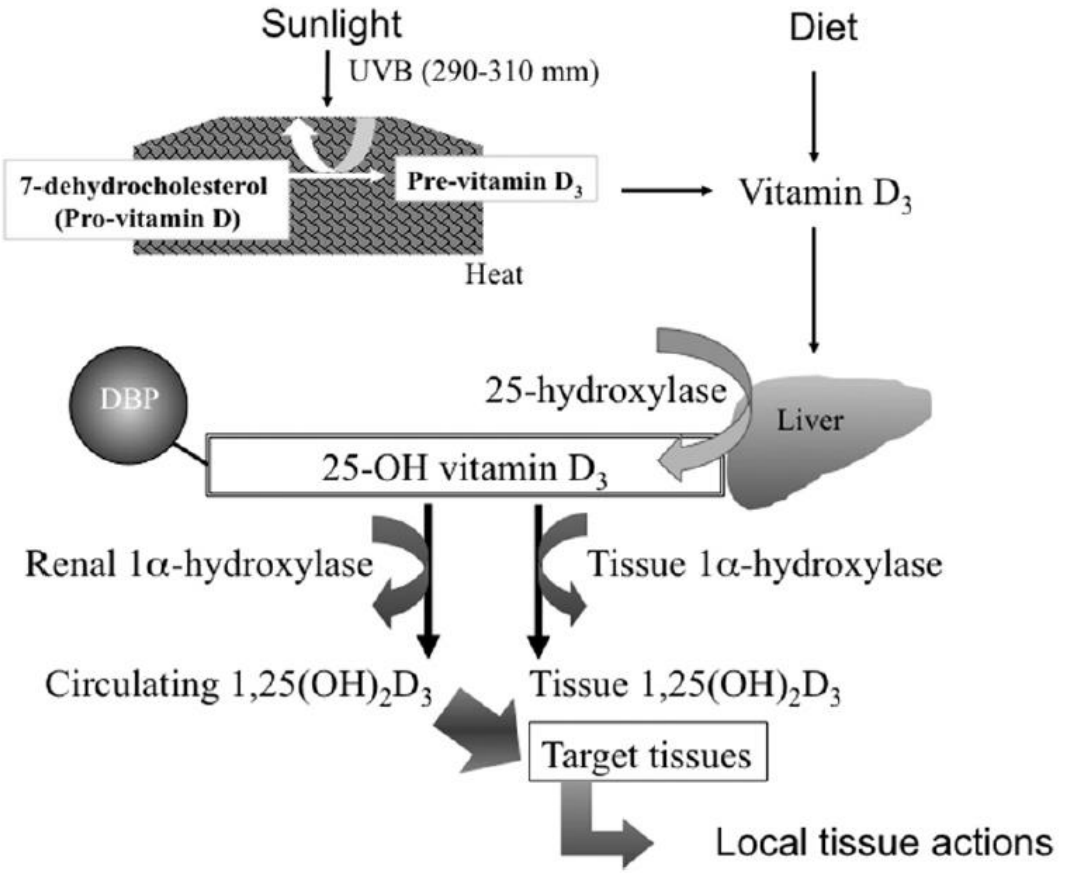


Figure 3.2: Schematic diagram illustrating the synthesis of active vitamin D,1,25-$(OH)_2$ D, by sequential hydroxylation in liver, kidneys and local tissues. Cutaneous photosynthesis is the main source of vitamin D with minor contribution from the contemporary western diet. Target tissues obtain 1,25-$(OH)_2$ D from either circulating pool formed in the kidneys or locally from tissue 1α-hydroxylation [Reproduced with permission from Lee, 2011 © Elsevier BV Ltd.].

The pathways of metabolism, transport and action of vitamin D in the body are well documented (Wolpowitz and Gilchrest, 2006; Reid 2004). Despite this, unexplainable mechanisms occur during pregnancy that leads to alterations in the metabolism of the vitamin and an unexpected increase in serum levels (Brannon and Picciano, 2011). Magnesium, a mineral that activate enzymes responsible for metabolizing vitamin D, is important for the function of the parathyroid gland and influences the sensitivity of tissues to vitamin D metabolites (Toyran and Severcan, 2007). Thus magnesium deficiency may result in a hypoparathyroid state, a resistance to vitamin D, and reduced synthesis of the active vitamin D_3 metabolite. Therefore vitamin D bioavailability and activation is directly influenced by the magnesium level within the individual. A magnesium deficiency or excess will therefore influence the effectiveness of vitamin D even in cases where a large dose or highly active form (e.g. synthetic 1,25 dihydroxyvitamin D_3) of the vitamin has been administered over a chronic time period (Zofkova and Kancheva, 1995). In a similar way, phosphate concentration may also influence the action of vitamin D. Phosphate is a regulator of the enzymatic conversion of vitamin D_3 to it most active metabolite: 1,25 dihydroxyvitamin D_3. By influencing the activity of the enzyme 1-α-hydroxylase, elevated levels of phosphate inversely influences or suppresses the conversion of vitamin D into its biologically active form (Reid, 2004).

3.3.4. Complexity or extent of underlying disease will determine timing and strategy behind vitamin D prescribing and monitoring

It is well accepted that disease states differ in terms of staging, severity and overall risk factors. Many diseases are known to have pre-defined risks and patient symptoms that need to be considered in addition to treating the underlying condition. For instance, menopause requires treatment for reduced physiological oestrogen secretion by using hormone replacement but may lead to an increased incidence of osteopenia and osteoporosis. As such these groups of patients are concomitantly treated with agents to prevent and treat bone degeneration. In such cases it is important to consider the complexity and staging of a condition and when to prescribe vitamin D supplements and at what stage. It is more prudent to prescribe vitamin D to these patients than younger female patients with a lower chance of osteoporosis due to an intact hormonal response. Such strategies would differ in patients with higher risk factors than those with no underlying condition. It is therefore important to consider disease stage and subsequent risk factors before deciding on when and how to initiate the prescription of vitamin D products.

Previous or current medication history due to a chronic condition may alter the way a physician should approach vitamin D treatment options. For example, there is known to be a higher incidence of osteopenia and osteoporosis in patients on antiepileptic treatments and therefore vitamin D protocols should start at an earlier life stage than in patients not taking antiepileptic drugs. Patients taking immunosuppressive agents such as cyclosporine and tacrolimus also experience a long term accelerated side-effect of osteoporosis and thus the physician needs to evaluate such risks and should prescribe vitamin D sooner rather than later.

It is therefore likely that the underlying condition or chronic medications may prevent the patient from achieving adequate vitamin D exposure as a result of supplementation or prescription. Such considerations will provide a large amount of valuable input on ideal timing and individualized serum monitoring that will improve the accepted treatment protocol in the general population.

3.3.5. Genetic differences govern a patient's response to vitamin D

The metabolism of vitamin D in the human body occurs via complex pathways and enzymatic actions in the liver and then in the kidneys and tissues to form the active form, 1,25-dihydroxyvitamin D_3 as shown in Figure 2.2 (Omdahl *et al*., 2002; Reid, 2004). This active form of vitamin D is required for biological activity; however interpatient variability in vitamin D metabolism and response as a result of genetic factors can reduce the effect of this metabolite. The established association between low blood levels of the major circulating form of vitamin D_3, i.e. 25-hydroxyvitamin D, and risk of disease may vary due to common genetic differences in the vitamin D receptor between patients. Thus major health outcomes and disease risk factors become less predictable in relation to serum levels due to genetic variances (Levin *et al*., 2012). Fu and co-workers supported the argument that genetics is a strong factor governing a patient's response to an administered dose of vitamin D. It was concluded that study subjects with different vitamin D binding protein (DBP) genotypes had different responses when administered the same vitamin D form and dose over a chronic time period (Fu *et al*., 2009). Therefore it is quite clear that the prescribed product may or may not translate into a serum level of activated form which is highly dependent on a patient's genetic make-up. Kohlmeier recently mentioned that "The response to vitamin D supplementation depends on the common rs4588 polymorphism of the *GC* gene" (Kohlmeier, 2013). It was also noted that serum vitamin D levels, in response to supplementation, are

found to be higher in patients with a 1307AA (A/A) genotype than in patients with a CC (C/C) genotype (Kohlmeier, 2013).

Hiraki and co-workers discussed the fact that genetic studies have estimated circulating levels of 25-hydroxyvitamin D to be 43%-80% heritable (Hiraki *et al*., 2013). Thus the form and dose prescribed may make only minor contributions to the levels of the vitamin D metabolite in cases where genetics are a strong contributor. Despite genome-wide association studies, that have identified differences in the encoding of proteins and genes involved in the vitamin D metabolic pathway, single nucleotide polymorphisms (SNP) account for only about 5% of the observed variance in the circulating metabolite (Hiraki *et al*., 2013). The study by Hiraki and co-workers (2013) utilized a number of novel methods in an attempt to elucidate further underlying genetic factors associated with variations in 25-hydroxyvitamin D. It was concluded that the major genetic effect on the circulating metabolite may actually be due to rare genetic variants other than the commonly identified SNPs in addition to the influence of the "gene-environmental" interaction. This is an interesting point to ponder in that one's genetic predisposition to high or low serum levels of the metabolite may be magnified by the environment. The physician needs to carefully evaluate genetics in tandem with lifestyle risks prior to prescribing and whilst monitoring a patients treatment plan. The study by Hiraki and co-workers emphasizes the need for further research to be done to explain how genetics may control this complex vitamin pathway.

3.3.6. Drug and supplement interactions reduce absorption, retention or activation of vitamin D

Extensive awareness of the potential medical benefits of vitamin D supplementation has resulted in a boom of prescribing the product without due consideration of the possible drug-vitamin or vitamin-vitamin interactions that may occur.

Due to the fact that Vitamin D activity and serum levels are largely affected by hepatic and renal metabolism, many drugs that induce or inhibit these metabolic pathways will influence the amount of 1,25 dihydroxyvitamin D_3 in circulation and available for bioactivity. Vitamin D therefore has a high propensity for interactions with other drugs that are hepatic enzyme inducers or inhibitors. Multiple classes of drugs inhibit or induce the liver cytochrome enzyme 25-hydroxylase CYP384 which itself is required for the conversion of vitamin D_3 (cholecalciferol) to 25-hydroxyvitamin D. Patients on long term treatment with oxidative enzyme inducing

drugs such as the antiepileptic agents, phenobarbital and phenytoin, will have reduced vitamin D activation despite judicious supplementation. Barbiturates are very effective at the catabolic hydroxylation of 1,25 dihydoxyvitaminD_3 and 25-hydroxyvitamin D into their inactive metabolites. Phenobarbital and phenytoin may even result in increased clearance of vitamin D metabolites and lower blood levels of vitamin D. Rifampicin and isoniazid are also potent CYP384 inducers and thus have the potential to alter the metabolism of vitamin D that is prescribed in Tuberculosis patients on anti-tuberculosis regimens. Some anti-retrovirals (Efavirenz) may be associated with significant decrease in 25-hydroxyvitamin D and an increased risk of hypovitaminosis due to a drug related abnormal vitamin D metabolism. Additionally, the antiretroviral Tenofovir may cause renal tubular dysfunction and subsequent decreased renal synthesis of 1,25 dihydroxyvitaminD_3 (Yin and Overton, 2011). Thus the efficacy of the prescribed vitamin D product will be diluted under such circumstances.

In addition to drugs that interfere with the normal metabolism of vitamin D and its metabolites, many drugs may alter the absorption or elimination of the vitamin. Agents such as mineral oils, antacids, laxatives, orlistat, glucocorticosteroids, antibacterials, colestipol and cholestyramine interfere with lipid and nutrient absorption from the gastro-intestinal tract (GIT) and will therefore minimize the absorption of consumed vitamin D and its metabolites (Gibbon, 2007). Recent research using innovative methods to inhibit intestinal cholesterol absorption through the use of nanostructured aluminium silicates (NSAS) also reported a reduction in the absorption of vitamin D_3 as an adverse effect (Ibrahim *et al*., 2013). In contrast to reducing the absorption of the vitamin, most studies conducted to date demonstrate that HMG-CoA reductase inhibitors increase 25-hydroxyvitamin D levels (Yavuz *et al*., 2009; Liberopoulos *et al*., 2013). An increase in blood levels will again lead to an erratic patient response and loss of prescriber control if not considered at the outset of treatment. Many patients take supplements and do not inform their doctors or self-prescribe and as such healthcare providers are unaware of deleterious interactions that are occurring beneath the surface.

Researchers have identified the potential for interactions that occur between the constituents of supplements (Lowe *et al*., 2002). Such supplement interactions need to be considered especially in a population that is increasingly self-prescribing over the counter products. The armoury of supplemental enhancers dosed by the general population and professional sportsmen may provide incalculable avenues for

untoward effects. Many healthcare providers are not experienced in the field of nutrition and nutraceuticals and thus have limited knowledge of the best vitamin combinations to take together and those that should not be combined. For example, calcium supplements may inhibit the simultaneous absorption of zinc and reduce the retention of copper (Lowe *et al.,* 2002). Even the natural product, resveratrol, is said to have important potential interactions with vitamin D due to overlapping metabolic process' that needs to be evaluated (Hayes, 2011). The use of one vitamin or mineral may antagonize the levels of another vitamin or mineral and hence result in an unexpected or impaired clinical response leaving the physician none the wiser to the reason for lack of product efficacy. This phenomenon can occur when there is an excessive consumption of a vitamin resulting in an increase in the demand for other vitamins. An example that applies to the current topic is the relationship that exists between vitamin D and Vitamin A. Vitamin D and vitamin A are mutually antagonistic and as such each may minimize the toxic effects of one another (Watts, 1990). Various forms of vitamin A (retinyl acetate and retinoic acid) will antagonize the action of vitamin D and its active metabolite (Rohde *et al*., 1999]. This may be because while vitamin D and vitamin A signal through common cofactors, they may compete for each other's function (Rohde *et al*., 2005). Human studies have shown that even the amount of vitamin A contained in a single serving of liver may impair the body's intestinal and serum calcium response to vitamin D (Johansson and Melhus, 2001).Vitamin-vitamin interactions are most often explained as an indirect effect in which a vitamin effects the level of a particular mineral which then has an effect on the original vitamin in question (Watts, 1990).

The extent of population exposure to over the counter and self-treatment products is high and is increasing every day as convenience buying lends to consumers making their own treatment decisions. Such decisions are very often made without the physician's knowledge especially when critical treatment decisions are made. As such the already large incidence of product interactions that exist to polypharmacy has the potential to rise even further. Drug-vitamin D interactions cannot be excluded from such important drug-related problems as these will directly or indirectly influence treatment outcomes. Due to the increasing prevalence of vitamin D supplementation, further evaluation of potential drug-vitamin D interactions is required.

3.3.7. Mild to moderate organ insufficiency and chronic disease influences vitamin D status

A deficiency of hormones, enzymes and digestive components may also have a significant effect on the absorption of vitamin D. Sub-optimal interactions that occur between vitamin D and the physiological environment most often occurs due to hepato-gastrointestinal diseases where mechanisms that predominate involve the disturbance in vitamin D absorption and metabolism. These types of diseases are becoming more and more prevalent yet are difficult to detect and diagnose in medical spheres. Normal organ function is necessary for efficient digestion and absorption of nutrients, drugs and also vitamins. The role of vitamin D in health relative to degree of sufficiency and tissue requirement is depicted in Figure 3.3.

Pancreatic exocrine deficiency is known to lead to malabsorption syndromes that manifest in severe lipid-soluble vitamin deficiencies (Fieker *et al*., 2011). In such cases, a consideration of only the dose and form of the deficient vitamin has very little impact if concomitant treatment with enzyme substitution therapy with pancreatic lipase is not initiated (Dominguez-Munoz, 2011).

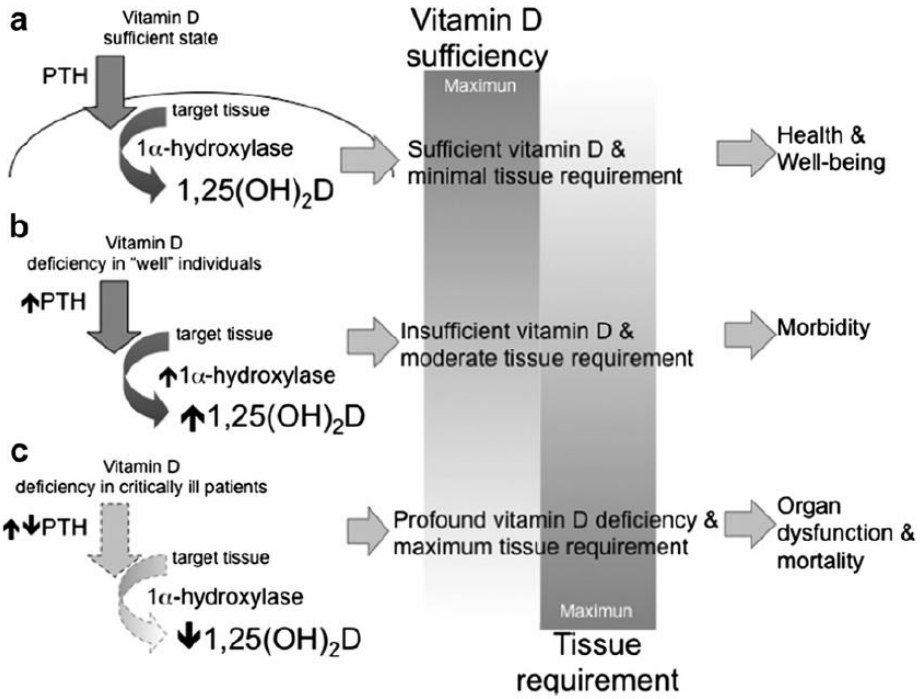


Figure 3.3: The role of vitamin D in health relative to degree of sufficiency and tissue requirement: (a) vitamin D sufficiency enhances metabolic, immune and organ functions, (b) parathyroid hormone (PTH) activation generates sufficient 1,25-$(OH)_2$ D in states of moderate vitamin D deficiency and tissue requirement, (c) severe deficiency and critical tissue requirement in face of insufficient PTH axis leading to break down of various tissue homeostatic mechanisms resulting in morbidity and mortality [Reproduced with permission from Lee, 2011 © Elsevier B.V. Ltd.].

The absorption of lipophillic substances such as fat-soluble vitamins and cholesterol is almost entirely dependent on the presence of another gastro-intestinal substance, namely, bile. A deficiency of bile will severely impact the absorption of lipophilic vitamins such as vitamin D because the bile constituent interaction is pivotal to the assimilation of the vitamin (van Hassalt *et al*., 2009). Bile is secreted by the liver and concentrated in the gall bladder and is an essential factor in the uptake of lipid-soluble vitamins, including vitamin D. Bile consists of various surface-active agents that emulsify fats, assist the action of lipase, and improve partitioning through intestinal mucosa thereby aiding the absorption of fat-soluble vitamins (Abrahamse *et al*., 2012). Some researchers have even noted the benefit bile acid constituents, such as deoxycholic acid, have on improving the transport, protection and targeted delivery of certain drugs to the liver (Samstein *et al*., 2008). The positive interaction that occurs between certain lipholphilic bioactives and the enterohepatic circulation may increase their transport from the GIT to the liver where final conversion into active metabolites occurs for action within the body. Such process' support vitamin D treatment success as the vitamin strongly relies on hepatic bio-transformation for its activity in the body. Samstein and co-workers actually went as far as including deoxycholic acid in an emulsion form to protect a drug-delivery system from harsh gastric conditions, to improve GIT permeability, and to enable targeted delivery to the liver (Samstein *et al*., 2008). Ultimately a higher concentration of the activated bioactive would reach the site of action. In these patients, evaluating the interactions between the intestinal milieu and the fat-soluble drug or vitamin of choice, will provide considerations that will greatly impact the disease state and assist practitioners with effective treatment strategies. Such a treatment approach holds merit for the wider patient population where high dose vitamin treatment often fails to achieve optimal plasma levels, evidenced by the increasing prevalence of vitamin D insufficiency in routine blood tests.

The general health of the gastro-intestinal tract, liver and kidneys affect the absorption and biotransformation of vitamin D to its active form. Thus misdiagnosis or poor treatment of gut, liver and kidney disease will negate all the positive effects that a prescribed dose and form of vitamin would have in a patient. Renal and hepatic disease, Crohn's disease, Wipple's disease and cystic fibrosis can lead to vitamin D malabsorption and reduced bioactivation. In such cases the treatment of the underlying disease state will have a far greater effect than merely increasing the dose supplemented or changing the form of the product that is prescribed. Early studies by Lo and group investigated the utility of an oral vitamin D absorption test

before initiating treatment and found that such a test may be useful in the screening of patients with a deficiency due to a suspected pathology (Lo *et al*., 1985).

Certain chronic diseases such as HIV are known to affect various organ systems. As such it may be argued that vitamin D supplementation in HIV positive individuals may not produce the same increase in the levels of the vitamin as seen in HIV negative patients. As already mentioned some anti-retrovirals reduce levels of vitamin D metabolites and thus the cause of a poor response to vitamin D supplementation in this patient population may be due to the ARV protocol or the disease or both.

3.3.8. Lifestyle and dietary patterns affect bioavailability and action of vitamin D

Lifestyle and dietary patterns may influence the bioavailability of many nutritional substances. As an example, it is known that dietary fibre interferes with adequate absorption of antioxidants. It is further well-known that fat-soluble vitamins are preferentially absorbed with fat. Since there is shown to be a 50% increase in the absorption of vitamin D when taken with a meal, a patient should be advised to eat before taking a vitamin D product to ensure maximal absorption (Mulligan and Licata, 2010). In general food needs to be eaten when taking vitamins to enhance absorption and minimize adverse effects. Restricted diets that reduce fat or meat intake may have the potential to reduce vitamin D absorption due to the lack of fat substrate to facilitate vitamin uptake. On the other side of the coin, individuals who partake in a lifestyle of excessive consumption and become obese are reported to have low serum 25-hydroxyvitamin D levels. Levels of serum 25-hydroxyvitamin D have been inversely correlated with body weight and body fat (Drinic *et al*., 2012). The resultant higher volumetric dilution of supplemented vitamin D in individuals of greater body size needs to be adjusted for by physicians. A particular dose and form will fail to achieve the same plasma elevations in all patients unless ‘tailor-made’ treatment strategies accurately address body composition. In addition, busy modern lifestyle and a sedentary existence may influence dietary patterns, gastric motility and the quality of meals that will all affect the ability of the host to absorb sufficient vitamin D.

Many patients may skip meals or experience lengthy periods without food that will ultimately affect the way the body is able to assimilate a vitamin product. It is therefore important to study and establish ideal times between meals in relation to

the time to dose a product, including vitamin D, so that patients are ensured of the best response from their prescribed products. Work patterns that encourage inactivity due to long seated meetings or chronic word-processing in front of computers may result in variations in gastric emptying and imbalances in normal digestive and elimination processes. It is established that vitamins are preferentially absorbed in the small intestine and many become instable when excessively exposed to gastric conditions. A sedentary lifestyle and small meals may reduce the amount of vitamin that ultimately reaches the site in the intestine for maximal absorption. Exercise is also becoming less easy to accommodate in a busy lifestyle due to work demands and social pressures. Intensity and duration of exercise or the lack thereof is known to affect GIT physiology which influences the rate and extent of absorption, distribution, metabolism and elimination of drugs (Khazenia and Ramsay, 2000). A lack of exercise slows metabolic rates and digestive processes. Similarly excessive exercise may delay gastric emptying due to a reduction in gastric contractions and that may reduce the amount of vitamin reaching the intestine (Khazenia and Ramsay, 2000). Alternatively chronic routine exercise may actually increase parasympathetic activities of the GIT causing more rapid transit through the stomach and intestine (Khazenia and Ramsay, 2000). Ultimately gastric emptying time and intestinal transit time is influenced by exercise routine and intensity and will affect the rate and extent of assimilation of gastric labile vitamin products.

Alcohol is another important factor to consider in the global population as it is a substance that has harmful effect on various physiological processes. Alcohol use varies from individual to individual and this will impact on vitamin D status and the success of an administered dose. Alcohol is known to interfere with the absorption mechanism of multiple nutrients from the diet by damaging mucous membranes of the gastro-intestinal tract, reducing pancreatic enzyme secretion and fat absorption which is essential to the bioaccessibility of fat-soluble vitamins.

Caffeine is also said to influence the effect that vitamin D has on vitamin D receptors in bone. Despite the fact that studies have shown average caffeine intake in the general population to fall within a safe range of approximately 106-170 mg/day (Knight *et al*., 2004), it has been suggested that caffeine levels greater than 300 mg/ day (>3 cups of coffee) may have deleterious effects on bone health (Rapuri *et al*., 2001). Individuals with the *tt* genetic variant of the Vitamin D Receptor (VDR) that are exposed to such levels of caffeine are said to be more susceptible to

accelerated bone loss (Rapuri *et al*., 2001). Another study by Rapuri and co-workers found that the dose of caffeine that is administered dependently decreased 1,25-dihydroxy vitamin D_3 induced vitamin D receptor expression by 50%-70% (Rapuri *et al*., 2007). Since caffeine intake may be high in certain age groups (35-49 year olds) with some people consuming 382mg/ day, the potential exists for a measurable reduction in vitamin D action following daily excessive amounts of caffeine. As caffeine is the most widely available and consumed psychoactive compound the association between caffeine levels and vitamin D expression needs to be considered. It was also found that certain subpopulations such as psychiatric patients have a higher prevalence of caffeine intoxication and dependence (Ciapparelli *et al*., 2010), and thus may be more likely to suffer from caffeine related side-effects. Also psychiatric patients with eating disorders tend to consume more caffeine as a means to suppress their appetite (Ciapparelli *et al*., 2010). It is logical therefore that caffeine intake in this group of patients is likely to perpetuate bad dietary habits that will indirectly reduce the absorption of dietary vitamin D. Therefore it is possible that excessive regular caffeine intake may reduce the pharmacological benefits of vitamin D in patients who require supplementation to prevent osteoporosis. Physiological homeostasis is also influenced by an individual's dietary habits and the consumption of caffeine is known to affect other hormonal and metabolic substances such as insulin and cortisol. Such endocrine changes in response to a dietary choice will in turn affect the way the body may respond to a drug or vitamin such as vitamin D when administered concomitantly. Thus one cannot exclude the influence that caffeine will have on prescribed dose of vitamin D.

3.3.9. Product quality, regulatory affairs and vitamin D success

The quality of the product consumed or the diet followed will influence the treatment success and levels of vitamin D in all patients. The quality and composition of supplemental and medicinal products varies, as does the dietary quality and consumption of vitamin D rich foods. In regions where complementary and alternative medicines are less regulated by health authorities, it may be difficult to ensure that patients receive good quality efficacious products. Some regulatory agencies do not require supplement manufacturers to perform rigorous analysis of their products for quality, purity and composition. Certain products contain excessive amounts of excipients, poor quality active ingredients, and poor quality protective packaging. Many nutraceuticals have not been subject to stability studies nor have they been involved in studies to elucidate the compatibility of formulation

components. As identified by Ballard and co-workers, there have been very few reports detailing the stability of vitamin D in commercial formulations (Ballard *et al*., 2007). Even so called inert combinations of excipients and vitamin actives that result in only minor interactions can still have significant long-term effects on the stability and efficacy of even the simplest commercial products.

3.3.10. Smart delivery systems introduce more variables that need to be considered and understood

Modern advances in pharmaceutics have led to the development of novel Drug Delivery Systems (DDS) and vehicles. Despite the advantages of these devices in drug delivery, the introduction of “foreign” carriers into the body has the potential to alter the way the digestive processes function. There is still much work to be done to elucidate the exact biological mechanisms and substances responsible for the breakdown of novel agents to enable the release of model drugs. Overuse or shifting of the balance to other metabolic processes that influence uptake and assimilation may have a long term effect on the way the body responds to administered doses of drugs. Fernandez and co-workers (2007) set out to identify which lipases are responsible for the lipolysis of “Labrasol” (a common lipid based self-emulsifying excipient used in the formulation of lipophilic drugs). These investigators found that the body employs different lipolytic mechanisms than were expected to metabolize the lipid-based carrier (Fernandez *et al*., 2007). Such unforeseen interactions with DDS’s containing a hydrophobic vitamin such as vitamin D may result in unpredictable absorption by virtue of the specificity and extent of action that each biological has on the formulation components. Unforeseen methods of breakdown and metabolism and “intelligent” DDS’s may ultimately result in a more rapid or even an unforeseen accumulation due to dose response curves that are no longer linear. Many practitioners do not consider the effect of modified release products on the patient and may underestimate or overestimate the effectiveness of such formulations. Although only a few vitamin supplements are formulated as smart delivery systems, technology advances will see the advent of more companies considering such options to optimize formulation design. Thus clinical response no longer depends on dose and molecular form alone but rather the interaction of the formulation components, including novel devices, with the active and the physiological environment.

3.4. Concluding Remarks

It is clear that the day to day impact of patient factors, physiological parameters, product composition and integrity, as well as the dose and molecular form, influence the therapeutic effectiveness of vitamin D products. It may be argued that *in vitro* and *in vivo* studies, no matter how scientifically validated, often fail to provide conclusive evidence for the results that are seen when a product is dosed in a real-time (uncontrolled) scenario in the general population. As such, further research needs to be done to more closely simulate how a patient will respond to a given dose under abnormal, stressed, or pathological states. Some lab-based studies have, for example, attempted to create an intestinal medium that more closely mimics the human GIT fluid, by mixing a bile salt system with different concentrations of lecithin, in order to recreate a more bio-similar condition for dissolution studies (Zughaid *et al*., 2012). Such lateral thinking and investigations would greatly assist in providing much needed information on milieu interactions when bioactives and biological macromolecules react. Such data will hopefully help to further explain how inter- and intra- patient interactions influence the amount and activity of drug that is available at receptor sites, and will assist practitioners in prescribing more effectively and predictably. Diagnostic tests and careful individualized patient analysis and monitoring should play a more pivotal role in the physicians approach prior to deciding on a particular product and dose recommendation. Another solution may be the conceptualization of novel formulations able to provide more robust efficacy regardless of the presence of underlying patient factors that may favour poor *in vivo* responses.

3.5. References

Abrahamse E, Minekus M, van Aken GA, van de Heijning B, Knol J, Bartke N, Oozer R, van der Beek EM, Ludwig T. 2012. Development of the digestive system-Experimental challenges and approaches of infant lipid digestion. *Food Digestion* 3: 63-77.

Armas LAG, Hollis BW, Heaney R. 2004. Vitamin D_2 is much less effective than vitamin D_3 in humans. *The Journal of Clinical Endocrinology and Metabolism* 89: 5387-5391.

Ballard JM, Zhu L, Nelson ED, Seburg RA. 2007. Degradation of vitamin D_3 in a stressed formulation: The identification of esters of vitamin D_3 formed by a transesterification with triglycerides. *Journal of Pharmaceutical and Biomedical Analysis* 43: 142-50.

Borges MC, Martini LA, Rogero MM. 2011. Current perspectives on vitamin D, immune system, and chronic diseases. *Nutrition* 27: 399-404.

Brannon PM, Picciano MF. 2011. Vitamin D in pregnancy and lactation in humans. *Annual Review of Nutrition* 31: 89-115.

Ciapparelli A, Paggini R, Carmassi C, Taponecco C, Consoli G, Ciampa G, Ramacciotti CE, Marazziti D, Del'Osso L. 2010. Patterns of caffeine consumption in psychiatric patients. An Italian study. *European Psychiatry* 25: 230-235.

Dominguez-Munoz JE. 2011. Pancreatic exocrine insufficiency: Diagnosis and treatment. *Journal of Gastroenterology and Hepatology* 26: 12-16.

Drincic AT, Armas LA, Van Diest EE, Heaney RP. 2012. Volumetric dilution, rather than sequestration best explains the low vitamin D status of obesity. *Obesity* 20: 1444-1448.

Fernandez S, Jannin V, Rodier J, Ritter N, Mahler B, Carriere F. 2007. Comparative study on digestive lipase activities on the self emulsifying excipients Labrasol, medium chain triglycerides and PEG esters. *Biochimica et Biophysica Acta* 1771: 663-640.

Fieker A, Philpott J, Armand M. 2011. Enzyme replacement therapy for pancreatic insufficiency: present and future. Journal of *Clinical and Experimental Gastroenterology* 4: 55-73.

Fu L, Yun F, Oczak M, Wong BYL, Vieth R, Cole DEC. 2009. Common genetic variants of the vitamin D binding protein (DBP) predict differences in response of serum 25-hydroxyvitamin D [25(OH)D] to vitamin D supplementation. *Clinical Biochemistry* 42: 1174-1177.

Gibbon CJ. South African Medicine Formulary (SAMF) 7th Edition. 2005. Health and Medical Publishing Group of the South African Medical Association, Cape Town. 78.

Gilaberte Y, Aguilera J, Carrascosa JM, Figueroa FL, Romani de Gabriel J, Nagore E. 2011. Vitamin D: Evidence and controversies. *Actas Dermo-sifiliograficas* 102: 572-88.

Gonzalez C. Vitamin D Supplementation: An Update. 2010. U.S. Pharmacist, Jobson Publishing. Posted: 11/11/2010.

Hayes DP. 2011. Resveratrol and vitamin D: significant potential interpretative problems arising from their mutual processes, interactions and effects. *Medical Hypotheses* 77: 765-772.

Hiraki LT, Major JM, Chen C, Cornelis MC, Hunter DJ, Rimm EB, Simon KC, Weinstein SJ, Purdue MP, Yu K, Albanes D, Kraft P. 2013. Exploring the genetic architecture of circulating 25-hydroxyvitamin D. *Genetic Epidemiology* 37 (1): 92-98.

Ibrahim F, Sivak O, Wong C, Hopkins P, Midha A, Gordon J, Darlington JW, Wasan KM. 2013. Impact of co-administration of protonated nanostructured aluminium silicate (cholesterol absorption inhibitor) on the absorption of lipid soluble vitamins D_3 and K1: An assessment of pharmacokinetic and *in vitro* intraluminal processing. *European Journal of Pharmaceutical Sciences* 49: 125-132.

Johansson S, Melhus H. 2001. Vitamin A antagonizes calcium response to vitamin D in man. *Journal of Bone and Mineral Research* 16:1899-1905.

Khazaeinia T, Ramsey AE. 2000. The effects of exercise on the pharmacokinetics of drugs. *Journal of Pharmaceutical Science* 3: 292-302.

Knight CA, Knight I, Mitchell DC, Zepp JE. 2004. Beverage caffeine intake in US consumers and subpopulations of interest: estimates from the Share of Intake Panel survey. *Food and Chemical Toxicology* 42: 1923-1930.

Kohlmeier M. 2013. How nutrients are affected by genetics. In: Nutrigenetics applying the science of personal nutrition.1st Edition. Science and Technology Books of Elsevier: 103.

Lee P. 2011. Vitamin D metabolism and deficiency in critical illness. *Best Practice and Research: Clinical Endocrinology and Metabolism* 25: 769–781.

Levin GP, Robinson-Cohen C, de Boer IH, Houston DK, Lohman K, Liu Y, Ktitchevsky SB, Cauley JA, Tanaka T, Ferrucci L, Bandinelli S, Patel KV, Hagstrom E, Michaelsson K, Melhus H, Wang T, Wolf M, Psaty BM, Siscovick D, Kestenbaum B. 2012. Genetic variants and associations of 25-hydroxyvitamin D concentrations with major clinical outcomes. *The Journal of the American Medical Association* 308: 1898-1905.

Liberopoulos EN, Makariou SE, Moutzouri E, Kostapanos MS, Challa A, Elisaf M. 2013. Effect of simvastatin/ezetimibe 10/10 mg versus simvastatin 40 mg on serum vitamin D Levels. *Journal of Cardiovascular Pharmacology and Therapeutics* 18(3): 229-233.

Lo CW, Paris PW, Clemens TL, Nolan J, Holick MF. Vitamin D absorption in healthy subjects and in patients with intestinal malabsorption syndromes. 1985. *American Journal of Clinical Nutrition* 42: 644-649.

Lowe NM, Fraser WD, Jackson MJ. 2002. Is there a potential therapeutic value of copper and zinc for osteoporosis? *Proceedings of the Nutrition Society* 61: 181-185.

Masterjohn C. 2007. Vitamin D toxicity redefined: Vitamin K and the molecular mechanism. *Medical Hypotheses* 68: 1026-1034.

Moyad MA. Vitamin D: a rapid review: dosage of vitamin D needed to achieve 35 to 40ng/mL (90–100 nmol/L). Retrieved from URL: www.medscape.com. [Accessed August 4, 2010].

Mulligan GB, Licata A. 2010. Taking vitamin D with the largest meal improves absorption and results in higher serum levels of 25-hydroxyvitamin D. *Journal of Bone and Mineral Research* 25: 928-930.

Omdahl JL, Morris HA, May BK. 2002. Hydroxylase enzymes of the vitamin D pathway: Expression, function, and regulation. *Annual Review of Nutrition* 22: 139-166.

Rapuri PB, Gallagher JC, Kinyamu HK, Ryschon KL. 2001. Caffeine intake increases the rate of bone loss in elderly women and interacts with vitamin D receptor genotypes. *The American Journal of Clinical Nutrition* 74: 694-700.

Rapuri PB, Gallagher JC, Nawaz Z. 2007. Caffeine decreases vitamin D receptor protein expression and 1,25 $(OH)_2D_3$ stimulated alkaline phosphatise activity in human osteoblast cells. *The Journal of Steroid Biochemistry and Molecular Biology* 103: 368-71.

Reid IR. Vitamin D. 2004. *Encyclopedia of endocrine diseases* 4: 657- 665.

Rohde CM, Manatt M, Clagett-Dame M, DeLuca HF. 1999. Vitamin A antagonizes the action of vitamin D in rats. *The Journal of Nutrition* 129: 2246-2250.

Rohde CM, DeLuca HF. 2005. All-trans retinoic acid antagonizes the action of calciferol and its active metabolite, 1,25-dihydroxycholecalciferol, in rats. *The Journal of Nutrition* 135: 1647-1652.

Romagnoli E, Mascia ML, Cipriani C. Fassino V, Mazzei F, D'Erasmo E, Carnevale V, Scillitani A, Minisola S. 2008. Short and long-term variations in serum calciotropic hormones after a single very large dose of ergocalciferol (vitamin D_2) or cholecalciferol (vitamin D_3) in the elderly. *The Journal of Clinical Endocrinology and Metabolism* 93: 3015-3020.

Samstein RM, Perica K, Balderrama F, Look M, Fahmy TM. 2008. The use of deoxycholic acid to enhance the oral bioavailability of biodegradable nanoparticles. *Biomaterials* 29:703-708.

Tarnopolsky MA. 2008. The mitochondrial cocktail: Rationale for combined nutraceutical therapy in mitochondrial cytopathies. *Advanced Drug Delivery Reviews* 60: 1561-1567.

Toyran N, Severcan F. 2007. Interaction between vitamin D_2 and magnesium in liposomes: differential scanning calorimetry and FTIR spectroscopy studies. *Journal of Molecular Structure* 839:19-27.

Van Hasselt PM, Janssens GEPJ. Slot TK, van der Ham M, Minderhoud TC, Talelli M, Akkermans LM, Rijcken CJ, van Nostrum CF. 2009. The influence of bile acids on the oral bioavailability of vitamin K encapsulated in polymeric micelles. *Journal of Controlled Release* 133:161–168.

Watts DL. 1990. Nutrient interrelationships Minerals-Vitamins-Endocrines. *Journal of Orthomolecular Medicine* 511-519.

Wolpowitz D, Gilchrest BA. 2006. The vitamin D questions: How much do you need and how should you get it? *Journal of American Academy of Dermatology* 54: 301-317.

Yavuz B, Ertugrul DT, Cil H, Ata N, Akin KO, Yalcin AA, Kucukazman M, Dal K, Hokkaomeroglu MS, Yavuz BB, Tutal E. 2009. Increased levels of 25 hydroxyvitamin D and 1.25-dihydroxyvitamin D after rosuvastatin treatment: a novel pleiotropic effect of statins? *Cardiovascular Drugs and Therapy* 23: 295-299.

Yin MT, Overton ET. 2011. Increasing clarity on bone loss associated with antiretroviral initiation. *The Journal of Infectious Diseases* (Editorial Commentary) 203: 1705-1707.

Zhang R, Naughton DP. 2010. Vitamin D in health and disease: Current perspectives. *Nutrition Journal* 9: 65. Retrieved from URL: http://www.nutritionj.com/content/9/1/65. [Accessed 12 March 2012].

Zofkova I, Kancheva RL. 1995. The relationship between magnesium and calciotropic hormones. *Magnesium Research* 8: 77-84.

Zughaid H, Forbes B, Martin GP, Patel N. 2012. Bile salt composition secondary to bile salt concentration in determining hydrocortisone and progesterone solubility in intestinal mimetic fluids. *International Journal of Pharmaceutics* 422: 295-301.

CHAPTER 4

DESIGN, SYNTHESIS & EVALUATION OF THE BAP DRUG DELIVERY SYSTEM COMPONENTS

4.1. Introduction

Pharmaceutical scientists have identified various methods to modify the delivery of bioactives to the body and many formulation approaches hold merit. Of these methodologies, carrier molecules and polymers are the two main categories of agents that have been harnessed to suit the needs of multiple medical applications in the realm of drug delivery.

Many natural compounds have far-reaching pharmacological effects including anti-inflammatory effects, anti-oxidant effects, antibacterial efficacy and anti-carcinogenic effects. However, many of these nutraceuticals have limited potential for use due to their low aqueous solubility and stability (Nguyen *et al*., 2013). Such is the case with cholecalciferol and other synergistic vitamins to be included in the BAP DDS. Problematic physicochemical properties may result in variable human bioavailability of these essential vitamins. As discussed already, cyclodextrins are valuable functional excipients that impart an enhancement in physicochemical characteristics to many bioactives. Since CD's continue to be investigated as carriers adept at formulation enhancement, in pharmaceutical and nutraceutical realms alike, these oligosaccharide carriers were pursued as potential carriers in the BAP DDS (Sangpheak *et al*., 2014; Garnero *et al*., 2014).

In terms of suitable polymer candidates, the long-since discovered polysaccharides, still remain at the forefront as useful constituents of stimuli-responsive drug delivery mechanisms. These polymers have been researched as controlled release vehicles, tissue regenerative supports, and taste masking agents. Not only are the common cationic and anionic polysaccharides, chitosan and alginate, readily available and biocompatible, but their ionic nature makes them ideal for ion- and pH- mediated effects within physiological environments. Additionally, these pH responsive polymers are ideal for further modification to widen their scope of sensitiveness to stimuli beyond just pH, including electrical, temperature and light (Alvarez-Lorenzo *et al*., 2013). The flexibility of use of alginate and chitosan offers many advantages for DDS component fabrication in the form of microbeads, scaffolds or even films.

These polymers are generally compatible with most bioactives and their ease of modification and synthesis make them invaluable contributors. Polyelectrolyte complexes of chitosan and alginate have been successfully investigated to take the form of microbeads delivering various biological bioactives, including important GIT enzymes (Won *et al*., 2005; Sankalia *et al*., 2007). Porous polymeric scaffolds are another modality that have been used with dual functionality, to deliver embedded drugs as well as acting as physical templates for the provision of cells and growth factors in tissue engineering applications (Lin and Yeh, 2004; Prabaharan *et al*., 2006; Shanmugasundaram *et al*., 2006). In addition to wound healing potential in biomedical medicine, scaffolds have a documented ability to offer controlled and sustained delivery of bioactives (Kim *et al*., 2005). Polymeric films containing blends of these polysaccharides, different plasticizers and bioactives have also been synthesized as a strategy to deliver nutraceutical bioactives successfully (Norajit *et al*., 2010; Benavides *et al*., 2012).

The properties discussed position CD's, polymeric beads, films and scaffolds as versatile and attractive options to pursue as Bioactive Booster (BB) components of the BAP DDS. The chapter that follows therefore explores and evaluates 4 different BAP formulation candidates:

(i) **BAP candidate A:** CD-complexes;
(ii) **BAP candidate B:** Bioactive-microbeads;
(iii) **BAP candidate C:** Polymeric-bioactive-scaffolds;
(iv) **BAP candidate D:** bioactive-polymer films.

4.2. Materials and Methods

4.2.1. Materials

Cholecalciferol, cyclodextrins (α-, β-, hydroxypropyl-β- and γ- cyclodextrins), lecithin (L-α-phosphatidylcholine), bile acids (deoxycholic acid and cholic acid), bile salts (sodium deoxycholate and sodium cholate hydrate), ascorbic acid, α-tocopherol, pancreatic lipase, chitosan (D-acetylated chitin), phosphate buffered saline tablets, sodium alginate, calcium carbonate, calcium gluconate, and sodium tripolyphosphate (NaTPP) were purchased from Sigma Aldrich® Inc. (St. Louis, MO, USA). Miscellaneous solvents included methanol, ethanol, acetone, dimethylsulfoxide (DMSO), and glycerin solution obtained from Merck Chemicals (Pty) Ltd (Wadeville, Gauteng, South Africa).

4.2.2. BAP candidate A: Cyclodextrin-vitamin complexes

4.2.2.1. Synthesis of cyclodextrin-vitamin complexes and inclusion efficiency determinations

Cyclodextrins have different molecular weights, cavity sizes, number of glucopyranose units, and solubilities and were therefore selected as ideal carriers to complex with 3 vitamins bioactives in order to modify their release characteristics from the BAP. CD's are known to provide major improvements in aqueous solubility and thus effectiveness of hydrophobic drugs (Yang *et al*., 2008) and thus would be ideal agents to improve the dissolution properties of fat soluble vitamins such as vitamin D_3 and vitamin E. Some research suggests that drug-cyclodextrin complexation not only has the ability to improve bioavailability of model drug but may greatly reduce the amount of bioactive required to render the desired therapeutic effect (Yang *et al.*, 2008). The 3 vitamin bioactives namely, vitamin D_3, vitamin E (α-tocopherol) and vitamin C were successfully bound to α-cyclodextrin, β-cyclodextrin, γ-cyclodextrin, and 2-hydroxy-propyl-β-cyclodextrin in multiple studies according to similar experimental conditions. Cyclodextrin (CD) was added to the bioactive vitamins (V) in varying molar ratios as per a modified co-precipitation method similar to that used by Mercê and co-workers (2009). The following CD: vitamin ratios were investigated where molar ratios of CD: vitamin varied from 10:1; 5:1 and 2.5:1 (Table 4.1).

Table 4.1: Summary of the molar ratios of CD's and vitamins that were combined during the synthesis of vitamin-CD complexes:

Cyclodextrin molar quantity (mmol)	Vitamin molar quantity (mmol)	Designated Inclusion Complex (IC) Nomenclature	CD-vitamin Ratio
0.2	0.02	CD-vitamin-2	10:1
0.2	0.04	CD-vitamin-4	5:1
0.2	0.08	CD-vitamin-8	2.5:1

Calculated quantities of dry CD and vitamins were weighed accurately and combined in one small beaker or placed in separate beakers awaiting the addition of solvent. Solvents were necessary to drive the process of complexation between each vitamin and the respective α-, β-, γ- or derivative cyclodextrin. Literature

revealed ideal solvents to assist in the solubilization of each vitamin and CD. Stock solutions of either ethanol (50%$^{v}/_{v}$) for vitamin D_3, acetone (100%) for vitamin E or distilled water for vitamin C were prepared. Each solvent (20mL) was added to the respective vitamin and cyclodextrin followed by constant stirring. In certain instances the vitamin was dissolved initially in the organic solvent separately whilst the CD was dissolved in the aqueous phase prior to combining the two solutions (vitamin E). Each of the CD-vitamin solutions were stirred over night at room temperature for pre-determined time periods (16 hours, 18 hours, 20 hours, or 40 hours) to ascertain whether mixing time had an influence on complexation. The use of different organic solvents during the preparation phase and the varying of mixing times was performed to determine whether a change in the experimental conditions would influence the Inclusion Efficiency (IE). After mixing for a set time period, the CD-vitamin mixtures were poured onto petri dishes to allow for solvent evaporation at room temperature for 48 hours.

The resultant solid precipitate was then collected for analysis. The precipitate contained the respective CD-vitamin complexes as well as a proportion of uncomplexed 'free' vitamin. A suitable organic solvent was pre-selected to wash and remove free vitamin, based on its ability to dissolve only the free vitamin and not the cyclodextrins containing complexed bioactive. The precipitate was washed with the 20mL suitable organic solvent to remove excess free vitamin and left to dry prior to UV Spectroscopy to determine Inclusion Efficiency values. Ethanol (20mL) was used as the solvent to remove free vitamin from the following complexes: α-CD-vitamin D_3, β-CD-vitamin D_3, γ-CD-vitamin D_3 and β-CD-vitamin C. Acetone (20mL) was used to remove 'free' (uncomplexed) vitamin E from β-CD-vitamin E complexes. Ethyl acetate (20mL) was used to remove uncomplexed vitamin D_3 from 2-hydroxy-propyl-β-cyclodextrin-vitamin D_3 complexes. The CD-vitamin synthesis and IE calculations were performed in triplicate (n=3) for each complex.

4.2.2.2. Preparation of cyclodextrin-vitamin physical mixtures (blends) for comparison with complexes

Each vitamin powder (vitamin D_3, vitamin E, or vitamin C) was physically mixed with the respective cyclodextrin powder in the same molar ratio as that used during the co-precipitation method to prepare inclusion-complexes. Dry native cyclodextrin (α-, β-, or γ-) (0.2mmol) was added to a petri dish containing 0.02mmol, 0.04mmol, or 0.08mmol of the respective vitamin. A spatula was used to mechanically blend the two components by dry mixing (without the addition of solvent) for 5-10 minutes to

ensure the formation of a homogenous powder blend. Physical mixtures were compared to complexes to elucidate the differences in binding through characterization tests (DSC, FTIR, and XRD).

4.2.2.3. Preliminary molecular mechanic simulations/ computations of CD-vitamin complexes

Molecular modelling software was utilized to determine the best binding arrangements of individual bioactives to one another to form these BBs: The following was determined: (i) which vitamin bioactive will preferentially bind to which carrier molecule (CDs), and (ii) relative bonding affinities, bond strength, and stability of bioactive-CD complexes. These results may provide insight into which vitamins will be released sooner and which later from the BAP due to preferential binding capacities. Additionally this preliminary *in silico* work provides insights into the entrapment efficiency of specific vitamin/ CD complexes.

Molecular Mechanic Computations were done in vacuum, which included model building of the energy-minimized structures of complexes, using the HyperChem^{TM} 8.0.8 Molecular Modeling System (Hypercube Inc., Gainesville, Florida, USA) and ChemBio3D Ultra 11.0 (CambridgeSoft Corporation, Cambridge, UK) on an HP Pavilion dv5 Pentium Dual CPU T3200 workstation. The cyclic-oligosacchrides such as α-CD, β-CD and γ-CD were generated as 3D models using a sugar builder module on HyperChem 8.0.8. The structures of bioactives were built up with natural bond angles as defined in the Hyperchem software. The generation of overall steric energy associated with the geometrically optimized structures was initially executed via energy-minimization using MM+ force field and the resulting structures were again energy-minimized using the AMBER 3 (Assisted Model Building and Energy Refinements) force field. The conformer having the lowest energy was used to create the complex.

A complex of one molecule with another was assembled by disposing them in a parallel way, and the same procedure of energy-minimization was repeated to generate the final models. Full geometry optimizations were carried out in vacuum employing the Polak–Ribiere conjugate gradient method until a root-mean-square (RMS) gradient of 0.001kcal/mol was reached. Force field options in the AMBER (with all hydrogen atoms explicitly included) and MM+ (extended to incorporate non-bonded cut-offs and restraints) methods was included in the HyperChem 8.0.8 as defaults. For calculations of energy attributes, the force fields were utilized with a

distance-dependent dielectric constant scaled by a factor of 1. The 1-4 scale factors are the following: electrostatic 0.5 and van der Waals 0.5.

4.2.2.4. Visual examination of aqueous solutions to confirm the presence of vitamins in complexes

In order to confirm the presence of vitamins within the inclusion complexes, by an alternative method to traditional characterization using UV, DSC or FTIR, a visual examination procedure was undertaken. Separate vessels containing aqueous solutions of complex, vitamin, and CD were examined. Addition of sample compounds to distilled water and stirring on magnetic stirrer for 30 minutes was performed to create aqueous solutions for comparison. Comparisons were drawn in terms of observed differences in aqueous solubility between samples and to confirm the presence of the vitamin. Each sample, either, vitamin, cyclodextrin or vitamin-complex (mean weight=25,94mg) was placed in individual vessels containing distilled water (20mL) and left to mix. Stirring for 30 minutes was done to mimic the physical mixing that occurs in the gastrointestinal milieu. Solutions were then examined for visual differences and similarities after the said time period.

4.2.2.5. UV absorption spectra of aqueous solutions to confirm vitamin-cyclodextrin complexation

UV-visible spectrophotometry is a commonly used method to detect the presence of cyclodextrin inclusion complexes (Kim *et al*., 2010). It is known that α-, β-, γ- and hydroxypropyl-β- cyclodextrins do not absorb in the UV visible spectrum (Al-Rawashdeh *et al*., 2013). This was initially confirmed by UV scanning of prepared aqueous solutions of the pure cyclodextrins to confirm the absence of peaks in the UV spectrum. Subsequent UV Scans of aqueous solutions containing the inclusion complexes vs. scans of the respective pure CDs and pure vitamins in solution were performed to confirm the presence of the vitamin within each complex. Each vitamin-CD complex (25.00mg) was added to vessels containing distilled water (20mL) and mixed for 30 minutes to dissolve prior to scanning on a UV-spectrophotometer (Specord 40 Spectrophotometer, Jena Analytik, Germany) to generate UV spectra. Cholecalciferol (25.00mg) and ascorbic acid (25.00mg) were dissolved in ethanol (20mL) and distilled water (20mL) respectively to obtain a comparative spectra.

4.2.2.6. Thermodynamic Analysis of Inclusion Complexes by Differential Scanning Calorimetry (DSC)

DSC analysis was performed on all inclusion complexes, selected physical mixtures, native vitamins (except vitamin E), and native cyclodextrins using a Differential Scanning Calorimeter (Mettler Toledo) fitted with $Star_e$ software (Mettler Toledo, Switzerland). Samples were carefully weighed and prepared. Samples weights ranged between 7mg-10mg and were placed in closed aluminium crucibles covered by a lid with a pinhole. The scan rate was set at 10°C/min between a temperature range of 10°C and 300°C initially. Re-analyses was done by running samples twice consecutively (run 1=10°C-125°C; run 2=10°C-300°C) to reduce water evaporation isotherms and to generate results indicative of the thermal properties of the samples under analysis without interference from water loss. For each run and temperature range, samples were subjected to DSC analysis under nitrogen. Reproducibility was assured by examining results obtained from multiple runs in at least triplicate. DSC was performed to confirm inclusion complex formation.

4.2.2.7. Chemical structure stability mapping of vitamin inclusion complexes by Fourier Transform Infrared Spectroscopy (FTIR) to confirm complexation

Fourier Transform Infrared (FTIR) Spectra were recorded between 650cm^{-1} and 4000cm^{-1} for the inclusion complexes, selected physical mixtures, pure vitamins, and native cyclodextrins using a PerkinElmer Spectrum 100 Series FTIR spectrometer coupled with Spectrum FTIR research grade software (Perkin Elmer Life and Analytical Sciences Inc., Massachusetts, USA). The vibration characteristics of chemical functional groups were detected in response to infrared light interactions. The procedure involved the placement of samples in powder form onto the sampling cup, smoothing sample powder into a thin bed, and compressing the sample into the holder using a compression gauge. The samples were placed in the infrared light path and a spectrum was obtained. FTIR was used to compare functional groups/ molecular vibrations in all samples with respect to CD, free vitamin and CD complexes as a means to confirm complexation.

4.2.2.8. Determination of crystallinity transitions of the vitamin complexes by X-ray Powder Diffraction (XRPD)

X-ray powder diffraction patterns were obtained with a 5th generation MiniFlex 600 benchtop X-ray diffractometer (Rigaku, Tokyo, Japan). XRPD was used to characterize the individual CD's, vitamin D_3, vitamin C, physical powder mixtures and the resultant inclusion complexes. The X-ray tube was set-up at a voltage of

40kV and a current of 15mA. The region $0^o \leq 2\Theta \leq 90^o$ (start degree: 0 and stop degree: 90) was evaluated. Data was analyzed using PDXL software to determine % crystallinity and to evaluate peak differences between complexes and individual constituents. Despite the formation of solid α-tocopherol-CD complexes, native vitamin E is present in a liquid phase at room temperature and thus XRPD was not a suitable analytical method to compare these complexes to the uncomplexed vitamin.

4.2.2.9. Vitamin inclusion efficiency (IE) determinations of CD-vitamin complexes by Ultra-Violet Spectroscopy

UV spectroscopy (Specord 40 Spectrophotometer, Jena Analytik, Germany) was used to generate calibration curves with known concentrations of each vitamin (1µg-5µg/mL) in varying organic and aqueous solvents and plotted against UV absorbance. This was utilized for the quantitative determination of vitamin contained in a known concentration of dissolved Inclusion Complex (IC). In order to remove free vitamin residue from the outside of each IC, a suitable organic 'washing' solvent was chosen for each IC in which only the respective vitamin was soluble and not the CD complex. The solvent was filtered through each IC powder to remove "free" uncomplexed vitamin leaving behind IC powder containing only the complexed vitamin. The inclusion efficiency (IE) or percentage of vitamin included within each complex was calculated using method 1 and method 2 as detailed below. UV absorbance values were taken at the UV_{max} wavelength for each vitamin: vitamin D_3: 265nm; vitamin C: 265nm; and vitamin E: 295nm. The two methods used to determine IE were:

Inclusion efficiency method 1: An indirect/ filtrate method for determining the inclusion efficiency was utilized initially by collecting and measuring only the organic solvent after washing the complex precipitate. For each complex an organic solvent was selected that the free vitamin was soluble in and the IC was not. The solvent filtrate was collected and assumed to contain only the free uncomplexed vitamin fraction which was then measured via UV spectroscopy after blanking with the same organic solvent. Indirect IE values were calculated for the amount of vitamin contained in the complexes using Equation 4.1.

$$IE\% = \frac{\text{Initial amount of vitamin (Ci) (mg)} - \text{Free vitamin in filtrate (Cf) (mg)}}{\text{Initial amount of vitamin (Ci) (mg)}} \times 100 \quad \text{[Equation 4.1]}$$

Inclusion efficiency method 2: A direct method was also developed to determine IE by addition of an accurately weighed amount (20-40mg) of pre-washed and filtered vitamin IC to 20mL millipore water. Magnetic stirring of the aqueous complex solution for 15-30 minutes facilitated the solubilization and release of vitamin from each IC and into the aqueous phase for accurate UV measurements. The UV absorbance of the aqueous complex solutions was measured on the UV-spectrophotometer to quantify IE. IE studies were performed in triplicate for each complex.

4.2.2.10. Phase solubility studies

4.2.2.10.1. Effect of βCD concentration on cholecalciferol and ascorbic acid solubility

Following high IE values for βD_3 complexes, phase solubility studies were conducted to determine the influence of βCD complexation on the solubility of vitamin D_3. An excess quantity of cholecalciferol (100mg) was added to separate vessels containing de-ionized water: ethanol ($9:1^{v}/_{v}$) (25mL) each with increasing quantities of βCD in the range of 0-11mM. Similarly a standard quantity of ascorbic acid (100mg) was added to separate vessels containing 25mL deionized water and increasing quantities of βCD. All solutions were placed in an orbital shaker at 50rpm at 37^{o}C and blended for 72 hours. The mixtures were then filtered with 0.22μm PVDF Millipore filters and centrifuged at 3000rpm for 5 minutes to remove solid particles. Cholecalciferol concentration was determined for each solution from the UV absorbance values recorded at 265nm using a UV spectrophotometer (SPECORD 40, Jena, Germany) after generating standard calibration curves (10-60μg/mL) (n=3). Likewise, ascorbic acid concentration was determined for each ascorbic acid solution from standard calibration curves (1-5μg/mL) (n=3). The phase solubility curves of the two vitamins were then constructed for the respective cholecalciferol and ascorbic acid solutions. The method was similar to procedures conducted by other researchers (Yang *et al.,* 2008; Zaibunnisa *et al*., 2011; Ruz *et al*., 2012).

4.2.2.10.2. Effect of blending time on cholecalciferol solubility

In a second study, the same procedure was followed as described already, except that the increasing quantities of βCD in each vessel were in the range of 0.25-1.75mM. The solutions were blended for 24 hours and then cholecalciferol concentration was determined. The solutions were subsequently returned to the

orbital shaker for an additional 48 hours of blending and thereafter analyzed for a second time on the UV spectrophotometer at the 72 hour time-point to once again quantify cholecalciferol concentration in each solution. Phase solubility curves were the plotted for the 24 hour time-point and for the final 72 hour time-point and compared to determine the influence of mixing time.

4.2.3. BAP candidate B: Polyelectrolyte microbead complexes

4.2.3.1. Synthesis of chitosan-bioactive microbeads

Chitosan (CT), a cationic polymer was selected to bind and modify the release of three anionic GIT milieu bioactives, namely deoxycholic acid, cholic acid, and lecithin from polymer microbeads.

Synthesis of cationic polymer solution: Stock solution of chitosan (3%$^{w}/_{v}$) was prepared by similar method to other researchers (Nagahama *et al*., 2009; Piai *et al*., 2010; Alishahi *et al*., 2011). CT (3g) was added to an aqueous solution of 1%$^{v}/_{v}$ acetic acid under constant magnetic stirring. Additional dilution resulted in a 1.5%$^{w}/_{v}$ chitosan solution. This was done in triplicate.

Synthesis of bioactive-polymer solutions: Ethanol (5mL) was added to each of three separate beakers and used as the organic co-solvent to dissolve deoxycholic acid (DA) (75.8mg), cholic acid (CA) (75.1mg), and lecithin (LT) (75.4mg), respectively. Each solution formed was an anionic bioactive solution.

Each anionic bioactive solution was then slowly poured into three separate previously prepared vessels containing 30mL 1.5% chitosan solution under constant stirring. The resultant three solutions were then placed on a magnetic stirrer for an additional 48 hours to assist in the complexation reaction between chitosan and the respective bioactive (cholic acid, deoxycholic acid, or lecithin). The following three microbead complexes were formed: Cholic acid-Chitosan (CA-CHI); Deoxycholic acid-Chitosan (DA-CHI); Lecithin-Chitosan (LT-CHI).

Synthesis of microbeads: A 2%$^{w}/_{v}$ stock solution of sodium tripolyphosphate (STPP) was prepared as a cross-linking agent. CA-CHI, DA-CHI, and LT-CHI were drawn up in separate syringes and added drop-wise via a hypodermic needle (23G, 0.6mm X 25mm) into separate beakers containing 2%$^{w}/_{v}$ Sodium Tripolyphosphate. The stepwise addition of each complex solution to 2%$^{w}/_{v}$ STPP via syringe and needle

facilitated the formation of microbeads of CA-CHI, DA-CHI, and LT-CHI. Beads were left for 24 hours to cure in STPP prior to removal from solution and subsequent drying at room temperature for the next 48 hours. Kindly refer to Table 4.2 for chitosan-bioactive formulations.

4.2.3.2. Synthesis of alginate-bioactive microbeads

Sodium alginate (low viscosity grade) was selected as an alternative polymer to chitosan as a carrier of the three bioactives deoxycholic acid (DA), cholic acid (CA), and lecithin (LT). Alginate is an anionic polymer used for the entrapment of the anionic bioactives DA, CA, and LT within polymer microbeads.

Synthesis of alginate polymer solution: 1.5%$^{w}/_{v}$ alginate was prepared by slowly adding alginate to distilled water followed by stirring. Once the alginate powder was completely dissolved, 30mL alginate (1.5%$^{w}/_{v}$) solution was measured and placed in a beaker (n=3).

Synthesis of bioactive-polymer solutions: 3mL ethanol was added to each of three separate beakers and used as the organic co-solvent to dissolve deoxycholic acid (75.4mg), cholic acid (75.1mg), and lecithin (75.8mg) respectively. An extra 2mL ethanol was added to CA to assist in solubilization.

Each bioactive ethanol solution was added to the separate beakers containing 30mL previously prepared 1.5%$^{w}/_{v}$ alginate solution. The resultant three solutions were then placed on a magnetic stirrer for 48 hours to assist in the mixing and entrapment of the respective bioactive (cholic acid, deoxycholic acid, or lecithin) within the alginate. The following three complexes were formed: Cholic acid-Alginate (CA-Alg); Deoxycholic acid-Alginate (DA-Alg); Lecithin-Alg (LT-Alg).

Synthesis of microbeads: A 2%$^{w}/_{v}$ stock solution of calcium gluconate (Ca^{+} gluc) was prepared as a cross-linking solution. CA-Alg, DA-Alg, and LT-Alg were drawn up in three separate syringes and added drop-wise via a hypodermic needle (23G, 0.6mm X 25mm) into individual petri dishes containing 2%$^{w}/_{v}$ calcium gluconate. The stepwise addition of each complex solution to calcium gluconate via syringe and needle facilitated the formation of beads of CA-Alg, DA-Alg, and LT-Alg. Beads were left for 24 hours to cure in separate petri dishes of calcium gluconate solution. Microbeads were then removed from solution and left to dry at room temperature for 48 hours. Kindly refer to Table 4.2 for alginate-bioactive formulations.

Table 4.2: Chitosan and alginate bioactive microbead formulations

Microbead Formulation	Polymer ($1.5\%^{w}/_{v}$)	Bioactive	Crosslinker (CL) ($2\%^{w}/_{v}$)
CA-CHI	Chitosan	Cholic acid (75.1mg)	STPP
DA-CHI	Chitosan	Deoxycholic acid (75.8mg)	STPP
LT-CHI	Chitosan	Lecithin (75.4mg)	STPP
CA-Alg	Sodium alginate	Cholic acid (75.1mg)	Ca^{+} gluc
DA-Alg	Sodium alginate	Deoxycholic acid (75.4mg)	Ca^{+} gluc
LT-Alg	Sodium alginate	Lecithin (75.8mg)	Ca^{+} gluc

STPP: sodium tripolyphosphate; Ca^{+} gluc: calcium gluconate; CA-CHI: cholic acid-chitosan; DA-CHI: deoxycholic acid-chitosan; LT-CHI: lecithin-chitosan: CA-Alg: cholic acid-alginate; DA-Alg: deoxycholic acid-alginate; LT-Alg: lecithin-alginate.

4.2.3.3. Complexation efficiency (CE) and entrapment efficiency (EE) of polymer-bioactive complex microbeads

Standard UV Calibration curves facilitated the calculation of the quantity of bioactive entrapped within or complexed to the respective polymer matrix (chitosan or alginate).

Chitosan-bioactive microbeads (100mg) was weighed and placed in three separate beakers. Acetic acid ($2\%^{v}/_{v}$) was made as a stock solution and 25mLs was added to each separate beaker containing 100mg of DA-CHI, 100mg CA-CHI and 100mg LT-CHI respectively. Each beaker was left overnight on magnetic stirrers to induce chitosan swelling, dissolution, and release of active from the beads into solution. A similar procedure was performed to determine the entrapment efficiency of the alginate-bioactive microbeads (DA-Alg, CA-Alg, and LT-Alg). An exception to the procedure was that acetic acid was not required to break the alginate-bioactive bond for release of bioactives. The addition of 25mLs of water instead was used to induce polymer swelling and release of DA, CA and LT from alginate microbeads into solution for quantification.

After swelling, each bead solution was then crushed using a pestle and mortar to ensure all bioactive was released from the respective polymer matrices. Crushed solution was drawn up in a syringe and passed through a millipore filter to remove excess polymer so only a solution containing active was the result.

Each filtered solution was then scanned on a UV spectrophotometer at specific UV_{max} wavelengths: DA at 205nm, CA at 198nm and LT at 215nm. A blank/ reference reading obtained at each new wavelength using either acetic acid ($2\%^{v}/_{v}$) or water and then a measurement was taken for each solution. If an absorbance value above 1 was observed then the solution was further diluted by the addition of millipore water and rescanned, noting the new dilution factor for each sample. An absorbance value was obtained for each 100mg bead solution of DA-CHI, CA-CHI, LT-CHI, DA-Alg, CA-Alg and LT-Alg polymer-bioactive microbead solutions. Using the absorbance values and the respective bioactive standard curves, calculations revealed the quantity of active that had been entrapped/ bound to the chitosan or alginate microbeads in a releasable form (Entrapment Efficiency).

4.2.3.4. Chemical structure analysis of polyelectrolyte microbeads by Fourier Transform Infrared Spectroscopy (FTIR)

A similar procedure was performed for the alginate and chitosan complexes as for the cyclodextrin complexes. The procedure included the placing of crushed microbead samples onto the sampling cup, smoothing powder into a thin bed, and compressing the sample into the holder using a compression gauge. Samples were placed in the light path and the spectrum was obtained. FTIR was used to elucidate and compare the molecular structure of chitosan and free bioactives, cholic acid, deoxycholic acid, and lecithin, to their resultant polyelectrolyte alginate/ chitosan microbead complexes.

4.2.3.5. Thermodynamic analysis of microbead complexes by Differential Scanning Calorimetry (DSC)

DSC was performed using a Differential Scanning Calorimeter (Mettler Toledo) fitted with $Star_e$ software (Mettler Toledo, Switzerland). Samples were carefully weighed and prepared over a number of hours. The samples had a mean weight of 16.6mg and were placed in closed aluminium crucibles covered by a lid with a pinhole. DSC curves were obtained for free bioactives, chitosan, lecithin and bile acids and the resultant alginate/ chitosan microbead complexes for comparison. Multiple samples were placed inside the DSC apparatus to run simultaneously. The scan rate was

10°C/min between a temperature range of 10°C and 250°C. For each run and temperature range, samples were subject to DSC analysis under nitrogen. Reproducibility was assured by examining results obtained from multiple runs in at least triplicate.

4.2.4. BAP candidate C: Bioactive-polymer scaffolds

4.2.4.1. Bile salt and lipase scaffolds rationalized as attractive BAP candidates

Bioactive loss from microbeads during preparation is a known phenomenon and many researchers have cited such limitations and delved into strategies to solve this challenge (Hua *et al*., 2010; George and Abraham, 2006). Due to low EE values with the microbeads and the inherent low solubility of the bile acids and lecithin, the beads were abandoned from further formulation development. Due to the observed leaching effect and low success of microbeads, another strategy was explored for incorporation of bioactive into polymer carriers. This approach involved the synthesis of polymeric scaffolds, prepared by inclusion of the bioactive dose within an alginate matrix and drying the solution to form a solid scaffold. This tactic mitigated the possibility of each bioactive leaching out into crosslinker solution during synthesis, as all constituents (including crosslinker) were homogenously blended and dried within self-contained vessels to form solid scaffold hydrogel structures. The formation of scaffolds was therefore considered an alternative approach to improve bioactive EE values with no risk of bioactive losses during preparation.

In addition, the use of bile salts was pursued as an alternative bile additive for scaffolds, with improved aqueous solubility over bile acids. The use of salt forms of most bioactives is an established methodology to improve bioavailability through improved dispersion and solubility within biological environments. The solubility limits and also toxicity concerns of bile acids prompted the formulation design to shift focus to include bile salts instead of bile acids as constituents of the scaffold devices (Sharma *et al*., 2010; Kawakami, 2012). Lecithin had demonstrated the lowest mean EE value of all formulations during microbead studies, therefore this bioactive was also excluded from scaffold studies and replaced with an enzyme bioactive, namely pancreatic lipase. Since the two bile salts already provided formulation emulsifying properties, a third emulsifier in the form of lecithin was considered illogical, and thus an enzyme was considered more attractive for investigation during further studies.

4.2.4.2. Synthesis of bile salt scaffolds or pancreatic lipase scaffolds and combination lipase/ bile salt scaffolds

A scaffold synthesis method was developed to ensure porous alginate scaffolds were formed using a modified technique from Archana and co-workers (2013), albeit at higher alginate concentrations and using calcium gluconate as a crosslinker. A 6%$^{w}/_{v}$ stock solution of sodium alginate was prepared from sodium alginate powder (low viscosity) and millipore water and 20mL was dispensed into multiple individual polytops awaiting addition of bioactive and crosslinker. Bioactive (pancreatic lipase, and bile salt: sodium cholate hydrate or sodium dexoycholate) (mean wt of 50mg) was added to the individual vessels containing 20mL of the previously prepared viscous sodium alginate solution. Calcium gluconate (10mL) was added in varying concentrations (0%$^{w}/_{v}$-1.25%$^{w}/_{v}$) to each vessel containing bioactive and alginate. Each vessel was mixed until a homogenous distribution of the bioactive, alginate and crosslinker was ensured. The resultant mixtures after dilution with crosslinker were alginate (4%$^{w}/_{v}$) hydrogels containing bioactive and crosslinker. Resultant bioactive-alginate gels were transferred to separate petri dishes and frozen at -80^{o}C overnight (24 hours) prior to lyophilizing to form dry spongy scaffolds. A summary of scaffold formulations is presented in Table 4.3.

Table 4.3: Alginate (4%$^{w}/_{v}$) bioactive scaffold formulations

Scaffold Formulation	Bioactive (mg)	Calcium gluconate Crosslinker (%$^{w}/_{v}$)
NaD-Alg (0%)	NaD: 50	0
NaD-Alg (0.5%)	NaD: 50	0.5
NaD-Alg (1%)	NaD: 50	1
NaC-Alg (0.5%)	NaC: 50	0.5
Lip-Alg (0%)	Lip: 50	0
Lip-Alg (0.5%)	Lip: 50	0.5
Lip-Alg (1.25%)	Lip: 50	1.25

NaD: sodium deoxycholate; NaC: sodium cholate hydrate; Lip: pancreatic lipase; Alg: alginate

4.2.4.3. In vitro release testing of bile-salt scaffolds and pancreatic lipase scaffolds

i) Preliminary bile salt release: A preliminary bioactive release study was conducted with scaffolds containing the bile salt sodium dexoycholate (NaD) (50mg). Different NaD scaffolds (mean weight of 406.21mg) containing 0%, 0.5% and 1% crosslinker

were placed in separate vessels containing 200mL phosphate buffer (pH 6.8). Scaffolds were left to dissolve and expand to release NaD into solution and 2mL aliquots were withdrawn and assayed for bile salt content spectrophotometrically (SPECORD 40 Jena, Germany) at appropriate time intervals: 15min, 30min, 60min, 120min, and 180min.

ii) Comparative final bile salt scaffold dissolution testing (0.5% cross-linked scaffolds): Following favourable release profiles with a 0.5%$^{w}/_{v}$ crosslinked NaD scaffold, a comparative release study was conducted with NaD and NaC scaffold crosslinked to the same extent. A standard USP 2 paddle apparatus (Caleva model 7ST, UK) fixed at 20rpm was used for a comparative dissolution study of sodium dexoycholate (NaD) (50mg) scaffold 0.5% (CL) (401.2mg) vs. sodium cholate hydrate (NaC) (50mg) scaffold 0.5% (CL). The dissolution media consisted of 900mL phosphate buffer solution adjusted to pH 6.8 (simulated intestinal fluid) and maintained at 37°C. Each scaffold was placed into its respective dissolution vessel and weighted down with weights to ensure complete submergence of each sample. A 3mL aliquot was withdrawn at appropriate time intervals (15mins, 30mins, 60mins, 2 hours, 3 hours), and replaced with 3mL of fresh dissolution media to maintain sink conditions. The amount of bile salt released at each specified sampling point was determined spectrophotometrically (SPECORD 40, Jena, Germany).

iii) Comparative dissolution testing of lipase-alginate scaffolds: Separate lipase-alginate scaffolds containing 50mg pancreatic lipase and varying crosslinker concentrations (0%$^{w}/_{v}$, 0.5%$^{w}/_{v}$ and 1.25%$^{w}/_{v}$ Ca gluconate) were subjected to dissolution testing to compare the release of lipase from each formulation. A standard USP 2 paddle apparatus (Caleva model 7ST, UK) fixed at 20rpm. The dissolution media consisted of 900mL phosphate buffer solution adjusted to pH 6.8 (simulated intestinal fluid) and maintained at 37°C. Each lipase scaffold was placed into separate demarcated vessel and weighted down to ensure complete submergence. A 3mL aliquot was withdrawn at appropriate time intervals (15min, 30min, 60min, 120min, 180min), and replaced with 3mL of fresh dissolution media to maintain sink conditions. The amount of pancreatic lipase released at each specified time point was determined spectrophotometrically (SPECORD 40, Jena, Germany).

4.2.5. BAP candidate D: Alginate hydrogel films containing pancreatic lipase and/ or bile Salts

4.2.5.1. Rheological properties of film-forming solutions

Polymeric films containing alginate were synthesized as an alternative carrier matrix for bile salt and enzyme components. As a preliminary step to film formation, various pregel solutions were formulated and assessed for rheological parameters prior to crosslinking. A stock solution of sodium alginate ($4\%^{w}/_{v}$) was prepared from low viscosity grade alginic acid sodium salt powder. Glycerin ($2\%^{v}/_{v}$) was added as a plasticizer to specific alginate solutions. Dry bioactive powder containing bile salts (sodium cholate hydrate and/ or sodium dexoycholate) and/ or pancreatic lipase were accurately weighed (in a range of 50-200mg) and placed in separate glass vessels. All three bioactives were added separately in various weight ranges to labelled vessels and then in combination to specific vessels. Aliquots of the alginate ($4\%^{w}/_{v}$)/ glycerin ($2\%^{v}/_{v}$) polymer solution (10mL) were added to each vessel containing previous weighed bioactive powders. Subsequent physical mixing and controlled sonication was performed to ensure dissolution and homogenous distribution of bioactives within the pregel solutions. The pregels were then subjected to rheological assessments whilst in the pregel phase prior to the addition of crosslinker and the drying step that would result in film formation. Visco-elastic parameters assessed included: viscosity (η), storage modulus (G') and loss modulus (G"). Comparative rheology testing was performed on a total of 10 pregel solutions each of a different composition, using a Modular Advanced Rheometer (ThermoHaake MARS Modular Advanced Rheometer, Thermo Electron, Karlsruhe, Germany) equipped with a $C35/1^{o}$ Ti sensor. Rheological analysis of the gel-phase, prior to crosslinking and drying, was performed as a preliminary method to assist in the selection of an optimized film formulation for inclusion in the BAP DDS. Table 4.4 lists the composition of the pre-gel formulations that underwent rheology.

Table 4.4: Alginate-glycerin bioactive pregel formulations

Pregel Formulation	Alginate ($\%^{w}/_{v}$)/ glycerin ($\%^{v}/_{v}$)	Bioactive (mg)
4%A	4/ 0	N/A
4%A Comb100	4/ 0	NaC: 100 NaD: 100 Lip: 100
4%A2%G	4/ 2	N/A
4%A2%G Comb 50	4/ 2	NaC: 50 NaD: 50 Lip: 50
4%A2%G Comb 200	4/ 2	NaC: 200 NaD: 200 Lip: 200
4%A/4%G	4/ 4	N/A
4%A4%G Comb 100	4/ 4	NaC: 100 NaD: 100 Lip: 100
4%AC100	4/ 0	NaC: 100
4%A2%C100	4/ 2	NaC: 100
4%2%D100	4/ 2	NaD: 100

NaD: sodium deoxycholate; NaC: sodium cholate hydrate; Lip: pancreatic lipase

4.2.5.2. Synthesis of polymer films as carriers of bile salts and pancreatic lipase

As an alternative to scaffolds, films were synthesized to provide a more malleable dosage form to carry bile and enzyme components. Film synthesis followed a similar procedure as already described for the synthesis of pre-gels with the exception that an initial polymer stock solution consisted of sodium alginate ($6\%^{w}/_{v}$) that was subsequently diluted down to $4\%^{w}/_{v}$ after addition of calcium gluconate crosslinker ($0\%^{w}/_{v}$-$0.7\%^{w}/_{v}$). In addition, all film formulations contained glycerin ($2\%^{v}/_{v}$) as a plasticizer to reduce brittleness and increase flexibility of the dry films. Glycerin is a commonly used plasticizer known to decrease the intermolecular forces between polymer chains for improved polymer chain mobility (da Silva *et al*., 2009). Controlled sonication was also performed for homogenous distribution of actives within the gels. The resultant gels were poured onto separate petri dishes and placed under a fumehood for 24 hours to dry. Dry polymer-bioactive films were collected by peeling off the petri dish surfaces and weighed in preparation for further

testing. Table 4.5 lists all bioactive film formulations that were synthesized during the study.

Table 4.5: Alginate-glycerin bioactive film formulations

Film Formulation	Mean weight of film (mg)	Alginate ($\%^{w}/_{v}$)/ glycerin ($\%^{v}/_{v}$)	Bioactive (mg)	Bile salt: lipase ratio	Calcium gluconate crosslinker ($\%^{w}/_{v}$)
66B/33L(0%)	1001.32	4%/ 2%	NaC: 100 NaD: 100 Lip: 100	2:1	0
66B/33L(0.2%)	1003.02	4%/ 2%	NaC: 100 NaD: 100 Lip: 100	2:1	0.2
66B/33L(0.3%)	1004.22	4%/ 2%	NaC: 100 NaD: 100 Lip: 100	2:1	0.3
66B/33L(0.5%)	1005.32	4%/ 2%	NaC: 100 NaD: 100 Lip: 100	2:1	0.5
66B/33L(0.7%)	1008.48	4%/ 2%	NaC: 100 NaD: 100 Lip: 100	2:1	0.7

NaD: sodium deoxycholate; NaC: sodium cholate hydrate; Lip: pancreatic lipase

4.2.5.3. Karl Fischer moisture content analysis of films

A Karl Fischer volumetric titrator (C30) (Mettler Toledo) was used to determine the moisture content within the different film formulations using a coulometric method. Various film formulations of standard weight (100mg) were added to the titration cell containing the reagent and solvent. The following film formulations were tested: 66B/33L(0%); 66B/33L(0.2%); 66B/33L(0.3%); 66B/33L(0.5%); 66B/33L(0.7%) (Table 4.5). The quantity of current required to convert the water contained in each film sample was used to determine the quantity of moisture locked within each film formulation.

4.2.5.4. Investigation of the physico-mechanical behaviour of films

The following film formulations were subjected to texture profiling: 66B/33L(0%); 66B/33L(0.2%); 66B/33L(0.3%); 66B/33L(0.5%); 66B/33L(0.7%) (Table 4.5). Texture analysis was conducted in order to assess the Tensile Strength (TS) and Maximum Break Force of the bile salt and lipase alginate films. A Texture analyzer (TA.XT.*plus Texture Analyser* Stable Microsystems®, Surrey, UK) was used to determine the physicochemical properties of each film formulation when subjected to a stretching force. The films were cut into 55mm x 10mm strips and evaluated

according to tensile strength at break. A calliper was attached at one end to the probe and the other end to the top of each film sample. The film sample was attached on one end to the calliper and on its bottom end to a vice. The stress-strain curve provided the tensile strength defined as the maximum stress each film was able to ensure prior to breaking. The experiment was conducted with at least four replications. Tensile strength (TS) was calculated by dividing the maximum force/ load at break by the initial cross-sectional area of the film. The parameters used for analysis of the films are highlighted in Table 4.6.

Table 4.6: Textural parameters for determination of tensile strength and maximum break force

Parameter	Tensile strength settings	Maximum break force settings
Pre-test speed	1mm/s	1mm/s
Test speed	1mm/s	1mm/s
Post-test speed	10mm/s	10mm/s
Test mode	Tension	Tension
Target mode	Force	Force
Trigger type	Auto (Force)	Auto (Force)
Trigger force	0.05N	0.05N
Test distance	15mm	15mm

4.2.5.5. Morphological analysis of films using Scanning Electron Microscopy (SEM)

Bile salt-alginate films and lipase-alginate films were morphologically analyzed using a scanning electron microscopy (SEM). To ensure that samples were electrically conducive to visualization, films samples were first sputter coated with gold (SPI Module^{TM} Sputter Coater, SPI Supplies, PA, USA). Samples were then mounted on a stub with silicon tape and observed under a scanning electron microscope (Phenom Microscope, FEI Company, Hillsboro, Oregon, USA). Surface images of the films were recorded at 2220–2240x magnification.

4.3. Results and Discussion

4.3.1. Preliminary molecular mechanic simulations/ computations of bioactive-CD complexes to test the feasibility of CD-vitamin complexes

Numerous non-covalent forces are involved in the formation of a stable CD inclusion complex. Non-covalent forces such as van der Waals forces and hydrophobic

interactions pre-dominate to form a stable inclusion complex between a bioactive compound (e.g. vitamin/ drug) and a cyclodextrin molecule. (Del Valle, 2004).

The 'complex' combinations and calculations in Table 4.7 have shown that the formation of the bioactive-CD complexes proposed as components of the BAP DDS are thermodynamically highly probable (indicated by complexes with bold *ΔE* values). These simulations provide insight into the most appropriate inclusion complexes to pursue instead of embarking on lengthy *in vitro* experiments with failed attempts at complexation. With favourable inclusion complex formation water molecules are displaced by more hydrophobic guest molecules (vitamin D, vitamin E, or vitamin C) present in solution to attain an apolar-apolar association and a decrease in cyclodextrin ring strain. Inclusion complex formation results in a more stable lower energy state. Molecular mechanics simulations therefore clearly demonstrated that it is not only the steric considerations that determine the ideal fit of a guest molecule within a CD ring but favourable net energetic driving forces are critical factors in the inclusion complex mechanism.

Table 4.7 shows results obtained for pilot molecular mechanic simulations performed for 3 bioactives (vitamin C, vitamin D, and vitamin E) and three cyclodextrins, namely α-CD, β-CD and γ-CD. Complexes with the largest ΔE value in Table 4.7 are the most stable and favourable bioactive-CD complexes. The high ΔE values of 54.85kcal/mol for the γCD-D_3 complex and 45.60kcal/mol for the γCD-E complex. Similarly respective energy transitions were obtained when the vitamins were combined with β and α CD's.

Table 4.7: Calculated energy parameters (kcal/mol) of the complex molecular assemblies from molecular modelling pilot study

Structure	**Energy (kcal/mol)**							
	Total[a]	**ΔE[b]**	**Bond[c]**	**Angle[d]**	**Dihedral[e]**	**VDW[f]**	**H bond[g]**	**Elec[h]**
Vit. C	13.195017	-	0.217101	10.844	2.98287	-0.848979	0	0
Vit. D	23.848542	-	1.18749	9.99989	9.11229	3.54887	0	0
Vit. E	22.267665	-	1.22039	6.929	4.83912	9.27919	-3.01731e-005	0
αCD	5.632474	-	4.63932	35.5586	69.5552	21.3145	-3.66162	-121.774
βCD	6.48255	-	5.1506	30.2803	83.1519	32.024	-3.53359	-

Structure	Energy (kcal/mol)							
	Total[a]	ΔE[b]	Bond[c]	Angle[d]	Dihedral[e]	VDW[f]	H bond[g]	Elec[h]
	7							140.591
γCD	21.718944	-	5.77269	44.248	90.7005	31.4266	-4.45081	-145.978
αCD Vit. C	-3.043616	21.871107	4.93447	46.1491	69.9174	7.71953	-3.35967	-128.404
αCD Vit. D	-4.045266	33.526282	5.68806	42.6169	78.4317	2.60214	-2.55052	-130.834
αCD Vit. E	16.115145	11.784994	7.04725	46.9448	74.8673	17.0575	-2.87665	-126.925
βCD Vit. C	4.905668	14.771906	5.23681	44.4992	89.5088	14.1009	-4.86614	-143.574
βCD Vit. D	7.335235	22.995864	5.85117	42.7115	95.3647	10.207	-4.5748	-142.224.
βCD Vit. E	-2.558448	31.308667	6.40447	43.6702	88.6477	22.5866	-4.477	-159.39
γCD Vit. C	19.062167	15.851794	5.85139	57.7285	94.1387	16.6856	-4.35506	-150.987
γCD Vit. D	-9.287180	54.854666	7.01544	51.8313	103.555	11.9464	-6.17025	-177.465
γCD Vit. E	-1.617937	45.604546	6.92705	49.0881	100.127	20.5947	-7.23649	-171.118

[a] *Total steric energy for an optimized structure*
[b] *$\Delta E_{interaction}$ = E(Host:Guest) - E(Host) - E(Guest);* ***Bold*** *indicates favourable complexes*
[c] *Bond stretching contributions, reference values were assigned to all of a structure's bond lengths*
[d] *Bond angle contributions, reference values were assigned to all of a structure's bond angles*
[e] *Torsional contribution arising from deviations from optimum dihedral angles*
[f] *van der Waals interactions due to non-bonded interatomic distances*
[g] *Hydrogen-bond energy function*
[h] *Electrostatic energy*

In summary, the 'complex' combinations and calculations in Table 4.7 showed that the formation of certain CD-vitamin complexes as constituents of the BAP DDS are thermodynamically highly probable and warrant further investigation and experimental validation.

4.3.2. Visual observations tests to confirm the presence of vitamins in inclusion complexes

Powder CD-vitamin IC's, individual CD's and uncomplexed vitamins were added to water to observe differences in the resultant solutions after mixing. This qualitative

visual observation method was explored to characterize the composition of vitamin, CD and complex aqueous solutions. These experiments were conducted to confirm complex formation, solubility behaviour and to illicit useful information to correlate with IE results. Noted was the amount of particulate matter present, degree of sedimentation, colour of solution and the observed aqueous solubility behaviour of complexes vs. uncomplexed vitamin or CD following mixing of each solution in millipore water. Table 4.8 below provides summarized observations and conclusions drawn when examining the aqueous sample solutions:

Table 4.8: Summary table illustrating visual observations of aqueous solutions containing: Cyclodextrin; Vitamin-CD complexes; and Vitamins

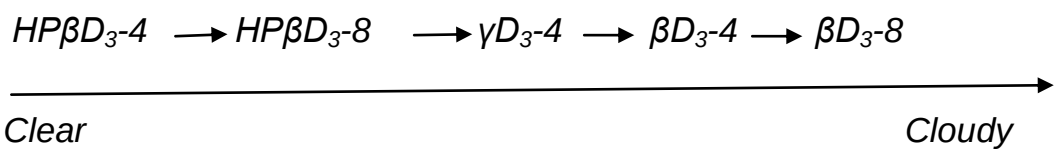
Compound	Amount of sample (mg)/ 20mL H_20	Observation	Conclusion
α-CD	25.97	Crystal clear/ completely clear solution	Excellent aqueous solubility: All sample dissolved
γ- CD	25.95	Clear solution	Good aqueous solubility: All sample dissolved.
β - CD	25.94	Clear solution	Good aqueous solubility: All sample dissolved.
HPβCD	26.01	Very clear solution	Excellent aqueous solubility: All sample dissolved.
Vitamin D_3	25.98	Opaque to white solution containing large amount of powdery residue on surface of solution.	Very poor aqueous solubility. Little to no vitamin in solution.
βD_3-4	26.01	Milky white to clear solution	Improved aqueous solubility of Vitamin D_3. Presence of vitamin.
βD_3-8	26.02	Milky white to very cloudy solution. No powdery appearance.	Improved aqueous solubility of vitamin D_3. More miscible in aqueous solution. Presence of vitamin.
αD_3-4	25.99	Clear solution with some tiny residue suspended.	Good aqueous solubility/ little to no vitamin present.
γ-D_3-4	26.00	Slightly cloudy solution	Improved solubility of vitamin D_3. Presence of vitamin.
HPβ-D_3-4	25.98	Cloudy to milky solution, some residue.	Improved solubility of vitamin D_3. Presence of vitamin.
HPβ-D_3-8	26.03	Cloudy to milky solution, some residue.	Improved solubility of vitamin D_3. Presence of vitamin.

Compound	Amount of sample (mg)/ 20mL H_20	Observation	Conclusion
Vitamin E	25.01	Oil droplet did not dissolve. Not miscible despite mixing.	Very poor aqueous solubility. Little to no vitamin in solution.
β-E-4	26.04	Opaque to clear solution.	Improved solubility of vitamin E. Presence of vitamin.
β-E-8	26.05	Opaque to clear solution	Improved solubility of vitamin E. Presence of vitamin.
Vitamin C	25.99	Clear solution	Good aqueous solubility. Vitamin in solution.
βC-8	26.00	Milky to clear solution	Good aqueous solubility. Presence of vitamin.

From visual observations it was clear that all resultant aqueous complex solutions had a cloudy/ milky appearance that was distinctly different to solutions of the plain cyclodextrins (Table 4.8). Plain cyclodextrin solutions were clear, indicative of their inherent aqueous solubility. The cloudy solutions that formed on addition and mixing of the complexes in water confirmed the presence of each respective vitamin and thus provided evidence for the presence of each vitamin and complexation. This is particularly evident for all Vitamin D_3 complexes (βD_3-4, βD_3-8, γ-D_3-4, HPβ-D_3-4 and HPβ-D_3-8) where aqueous solutions were all milkier than their respective plain CD solutions. It was interesting to note how the βD_3-8 complex solution had a more cloudy appearance than the βD_3-4 solution due to a higher concentration of vitamin D_3 present in the former complex. This is logical in that the βD_3-8 complex was synthesized with double the molar concentration of vitamin D_3, and also consistently achieved a higher mean IE% (78%) than the βD_3-4 complex (mean IE% of 54%). Thus the βD_3-8 solution contained more vitamin D_3. The only complex solution that was similar in appearance to its respective cyclodextrin solution was that of αD_3-4. In this case it was found that the resultant aqueous solution was almost as clear as the solution of α-CD which was consistent with IE experimental data, later discussed that shows that very little vitamin D_3 was incorporated into the α-cyclodextrin cyclic ring. Mean IE calculations for the α- complexes were consistently low (2% and 13% for αD_3-2 and αD_3-4 respectively) and may be explained by the fact that the α-ring, being the smallest CD ring, is not large enough to accommodate sufficient vitamin (see IE determinations under section 4.3.7). Vitamin E and Vitamin C complex solutions were also milkier than their respective cyclodextrin solutions confirming the

presence of the vitamin in solution. The milky appearance of the ascorbic acid IC solutions may indicate a reduction in the solubility power of ascorbic acid, resulting in a 'less clear' solution due to the presence of insoluble IC precipitates. Alternatively, this observation may indicate a visual diffraction phenomena since it was unexpected that an aqueous soluble vitamin would provide a milky solution, despite alterations in solubility in the presence of CD.

A comparison of the vitamin D_3 complex solutions revealed that the order of clear to cloudy (more opaque) aqueous solutions was found to be in the following sequence:



The above sequence correlated well with the inclusion efficiency values obtained in the IE studies discussed under section 4.3.7. Additionally, the clearest solutions also correlated well with the inherent aqueous solubility of the respective CD contained in each complex. HPβCD is the most aqueous soluble of the cyclodextrins (50g/ 100mL), γ-CD is the second most aqueous soluble (23g/ 100mL) and β-CD (1.85g/ 100mL) is the least aqueous soluble of the three. Thus the relative power of solubilization afforded by the particular cyclodextrin in the IC was evident with HPβ-D_3 complexes achieving the greatest solubility. The aqueous solubility of a cyclodextrin carrier is an important factor to consider when selecting an ideal complex as a constituent of a formulation, because a high IE value needs to be weighed up against the carrier molecules solubilisation power.

In summary, the visual observation experiments provide some preliminary confirmation of complexation and the presence of the respective vitamins in each synthesized complex. Phase solubility studies may provide further insights into the phenomena that occurs when specific vitamins IC's are dispersed in aqueous solutions.

4.3.3. UV absorption spectra of aqueous complex solutions to confirm vitamin-cyclodextrin complexation

Many researchers have noted changes in UV absorption spectra in a solution, as evidence for complex formation between bioactives and cyclodextrins (Kim *et al*., 2010; Iacovino *et al*., 2012; Sambasevam *et al*., 2013; Mura, 2014). It is well known

that cyclodextrins do not absorb in the UV spectrum (Al-Rawashdeh *et al*., 2013). However the vitamins, vitamin D_3, vitamin E and vitamin C do absorb in the UV-visible region due to the presence of chromophores (Murakami *et al*., 2003; Vaid *et al*., 2005). The UV spectra of the cyclodextrins, vitamins and resultant complexes confirmed complexation. Aqueous solutions of the resultant complexes showed UV peaks that were comparable to the UV spectrum of the respective vitamins confirming the presence of vitamin in each complex solutions (Figure 4.1a vs. e and Figure 4.1b vs. f).

The UV spectrum of βD_3-8 was similar to that of vitamin D_3 (in ethanol) with a similar UV_{max} indicating the presence of the vitamin in an aqueous solution (Figure 4.1a vs. e). Additionally, the cholecalciferol peak that resulted, illustrated the ability of the complex to solubilize the vitamin in aqueous medium which is otherwise a rate limiting step to bioavailability of the native vitamin. UV spectroscopy studies confirmed the absence of a UV peak for the βCD molecule in the UV range tested. In contrast, plain ethanol solutions of vitamin D_3 revealed a clearly defined UV peak with a UV_{max} at 265nm (Figure 4.1e). An almost identical absorption spectrum to vitamin D_3 was demonstrated for the resultant βD_3-8 complex, albeit at a higher frequency (275nm) (Figure 4.1a). Such shifts of a bioactive's absorption maximum to a different frequency have been noted as consequences of IC formation (Mura, 2014).

Despite stirring of the IC aqueous solution for 30 minutes prior to scanning, the γD_3-4 complex depicted a UV spectrum similar to that of γCD with little to no absorption in the UV range and no presence of cholecalciferol (Figure 4.1d). This exception may be explained by the fact that γCD has the largest CD ring and was therefore able to include a large proportion of the cholecalciferol molecule within its cavity leaving no exposed chromophore for UV detection. A similar observation was documented by Hu and co-workers (2012) where an inclusion complex of vitamin C was fully included within the β-CD cavity and did not show a characteristic UV peak for the included vitamin.

In contrast to the study conducted by Hu and co-workers (2012) the current results depicted a UV spectrum for a solution of the βC-8 complex with a distinctive peak indicative of the UV_{max} for vitamin C at 265nm (Figure 4.1b). This observation may be explained by the formation of inclusion and non-inclusion based complexes where a proportion of ascorbic acid is bound to the outside of the CD ring and is

visible during UV analysis (Loftsson *et al*., 2007). The relative formation of inclusion and non-inclusion based complexes may depend on variations in synthesis conditions and quantity of bioactive and CD that come into contact during complexation.

The UV spectra of HPβD_3 complexes also illustrated noticeable UV peaks and an absorbance that was not initially seen in a solution of pure HPβ-cyclodextrin. Aqueous solutions of HPβCD revealed no absorption in the 200-300nm UV range yet, the HPβD_3-4 IC had two absorption bands in the UV visible spectrum indicative of the presence of cholecalciferol (Figure 4.1c). UV-spectroscopy revealed that the solution of the complex had one vitamin D_3 peak at a higher absorption maximum (288nm) and a second peak at a low frequency (220nm) (Figure 4.1c). Modifications of the UV spectrum of a drug in the presence of a CD have been cited as evidence for IC formation by way of shifts in frequency of characteristic drug peaks (Mura, 2014). Such observations again confirm complexation.

For cholecalciferol IC's, a greater peak intensity was observed for all aqueous complex solutions compared to cholecalciferol aqueous solutions which is indicative of an enhanced aqueous solubility afforded by the CD carrier. Similar observations were noted when the HPβ-cyclodextrin was complexed with bioactives by other researchers (Misiuk and Zalewska, 2009). In contrast to cholecalciferol, plain ascorbic acid solutions had a high absorption intensity that became markedly reduced when complexed to βCD in the form of the βC-8. This may be evidence for the βC-8 IC reducing the solubility of the highly soluble vitamin C molecule and as further evidence to verify complexation. A reduction in ascorbic acid solubility upon complexation is correlated by discussions under section 4.3.2 (visual observation tests) and section 4.3.8 (phase-solubility results). Similar noticeable increases or decreases in maximum absorption intensities were noted by other researchers as confirmation of interactions between CD's and bioactives during the formation of complexes (Singh *et al*., 2010; Sambasevam *et al*., 2013; Mura, 2014).

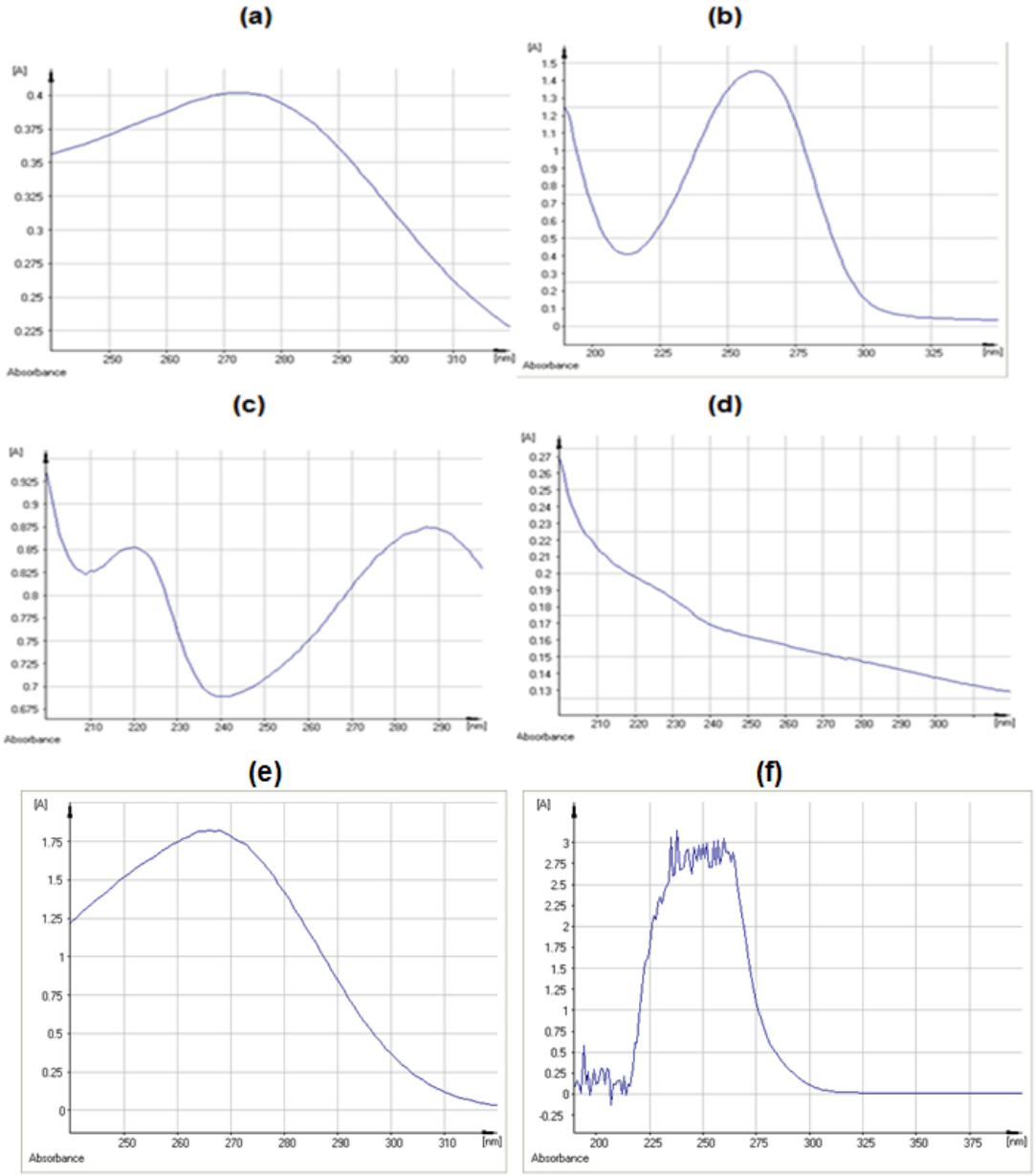


Figure 4.1: UV Spectra of solutions of (a) βD_3-8 inclusion complex (aqueous solution); (b) βC-8 inclusion complex (aqueous solution); (c) $HP\beta D_3$-4 inclusion complex (aqueous solution); (d) γD_3-4 inclusion complex (aqueous solution); (e) cholecalciferol (ethanol solution); (f) ascorbic acid (aqueous solution).

4.3.4. Thermodynamic analysis of CD-vitamin complexes by Differential Scanning Calorimetry (DSC)

Thermal analysis is a useful method for the study and recognition of inclusion complex formation (Wang *et al*., 2011). It is documented that when a bioactive is included in a CD its melting point, boiling point and sublimation point moves to a different temperature or may disappear entirely (Yap *et al*., 2005; Yang *et al*., 2008). Many vitamins have low melting points [cholecalciferol (84.5°C); α-tocopherol (3°C)] (Table 4.9) and thus are susceptible to structural instability and degradation as

temperature increases on exposure to volatile environments (Guttoff *et al*., 2015). Carrier molecules that bind vitamins and improve their thermal properties are therefore attractive options for formulation scientists. Differences between the individual vitamins, the cyclodextrins (CD), and the resultant IC's can elucidate important information when comparing thermal profiles and confirm complexation. Every compound has a characteristic melting point, distinctive crystallization temperature and degradation profile evident in DSC thermograms. Changes or shifts in these predefined thermal characteristics, confirms the existence or absence of a new compound or interactions indicative of an inclusion complex or bonds between the bioactive and the carrier.

Multiple DSC experiments were conducted at varied temperature dynamics to confirm and elaborate on the endothermic and exothermic peak transitions that appear for all compounds. Initial studies were conducted with samples being run between 10°C-250°C as depicted for Figure 4.2. Further DSC analysis involved samples being run twice consecutively at two different temperature dynamics (Run 1: 10°C-125°C; Run 2: 10°C-300°C) to assist with intermolecular water loss from CD's, vitamins and complexes to ensure an accurate reflection of the thermal properties of compounds with less interference from water endotherms. Therefore DSC profiles depicted in Figures (4.3-4.6) show the thermal behaviour of compounds from Run 2 (10°C -300°C) after an initial water loss run.

Table 4.9: List of cyclodextrin and vitamin melting points as derived from Material Safety Data Sheets (MSDS) for each native compound

Compound	Melting point
Cyclodextrins:	
α -cyclodextrin	278°C
β-cyclodextrin	260°C
Ɣ-cyclodextrin	267°C
2-hydroxypropyl –β-cyclodextrin	>260°C
Vitamins:	
Vitamin D_3 (cholecalciferol)	84.5°C
Vitamin A (Retinol palmitate)	28.5°C
Vitamin E (α-tocopherol)	3°C-4°C (liquid at room temperature)
Vitamin C (ascorbic acid)	>190°C

4.3.4.1. Thermograms of αCD cholecalciferol inclusion complexes

α-cyclodextrins have 3 characteristic regions of endothermic peaks that represent water loss from the molecule between 70°C-85°C, between 110°C-125°C, and between 130°C-170°C (Ho *et al*., 2011). In the current research, definitive endothermic water loss peaks were noted at similar temperatures for the αCD samples, namely at 85°C, 120°C and 155°C, in agreement with the observations by Ho and co-workers (2011) (Figure 4.2). For the αD_3 complexes, there were no sharp endothermic peaks or melting points observed (Figures 4.2 and Figure 4.3a). The change in the endothermic peak size of the α-cyclodextrin from a large peak at 135°C to a wider, flattened inflection for the αD_3 complex was evidence of an IC in which vitamin D_3 had replaced the water molecules in the cavity of the αCD molecule (Figure 4.3a). The broadened or reduced profile for the α-D_3 complex depicts non-existent melting points for the complex in Figure 4.3a. A similar observation was seen by Ho and co-workers (2011) in studies with other bioactives where complexes had reduced or even flattened endothermic peaks. The characteristic vitamin D_3 melting point in agreement with literature values at 84.5°C (Luo *et al*., 2012) (Table 4.3) and as seen in Figure 4.2, disappeared for the α-complex (Figure 4.3a). The complete disappearance of a bioactives endothermic peak in the DSC profile of an cyclodextrin IC is evidence for IC formation with an active or is indicative of the presence of a more amorphous compound (Hashem *et al*., 2013). A re-run of the αD_3 complexes at a higher and accelerated heating rate may reveal a signature melting point somewhere in the gradual endothermic hump region observed somewhere between 90°C-160°C that is suspected to be right shifted.

An interesting observation is seen in Figure 4.3b when the physical mixture, the IC, and αCD are compared. The αD_3 complex has a broad endotherm at a similar temperature to the physical mixture and αCD. Two clear glass transition temperatures (tg) are evident in both the physical mixture and αCD that are not present in the profile of the complex (Figure 4.3b). This is further evidence for a unique thermal profile and complex formation.

4.3.4.2. Thermograms of βCD cholecalciferol inclusion complexes

The DSC thermograms of βCD (Figure 4.3c and d) showed a broad endothermic peak between 80°C and 140°C similar to Racz and co-workers (2012) who found a peak for βCD between 71°C and 120°C. This was noted to be a loss of water by evaporation from the CD cavity. The shallower and broader endotherms for the βD_3

complexes (Figure 4.3c and d) correspond to reduced water loss and hence a reduction in the dehydration endothermic peaks when compared to the native βCD and cholecalciferol. These observed differences in the dehydration endotherms of CD complexes indicate a different solid state structure when a bioactive is bound to an IC (Racz *et al*., 2012). The melting point/ fusion of vitamin D_3 that normally occurs at 84.5°C disappeared for the βD_3-8 IC (Figure 4.3c) which may be due to the interaction between βCD and the vitamin, due to the formation of an IC as shown to be highly probable in preliminary molecular modeling. A similar observation was noted in a study by Dua and co-workers with βCD and the drug, aceclofenac (2011). Such observations are evidence of intermolecular interactions between cholecalciferol and the CD confirming inclusion complex formation. Confirmation of encapsulation of a bioactive is demonstrated in DSC profiles when the resultant complex no longer has the melting peak of the bioactive. When interpreting DSC data of a DDS containing vitamin D_3, the absence of the vitamin's endothermic peak may be regarded as conclusive evidence of encapsulation or dispersion in the carrier, as was confirmed in a study by Luo and co-workers (2012). Furthermore, the crystallization or oxidation exotherm that occurs at approximately 220°C for vitamin D_3 was not present in the IC (Figure 4.3c).The exothermic peak for cholecalciferol represents either an oxidation or a crystallization of cholecalciferol. This peak was not present in the DSC scan of the vitamin D_3 IC's which may indicate that the vitamin is protected from oxidation by being included or attached to the CD ring. This provides indirect evidence of vitamin D_3's inclusion in βCD. Similar results were observed in a study by Wang and co-workers with other nutraceutical compounds (Wang *et al*., 2011). Thus the vitamin D_3 complexes would be more stable to heat energy than vitamin D_3 which has a melting point between 85°C-95°C shown as an early sharp peak in Figure 4.3c at 84.5°C. Figure 4.3d depicts the DSC profiles for a water loss run from 10°C-250°C for 2 different βD_3 complexes, vitamin D_3 and the respective β-cyclodextrin. It was again confirmed that the complexes have decreased and shallower endothermic peaks compared to the thermal profile of βCD and thus provide evidence for different structures.

Figure 4.3d also highlights an interesting observation when comparing βD_3-2 and βD_3-4 complexes in that the βD_3-4 complex which contains a larger molar amount of bioactive has a smaller dehydration endothermic peak because more vitamin has replaced the intermolecular water molecules in the cyclodextrin ring compared to the βD_3-2 complex (Ho *et al*., 2011). A gradual progression from a large dehydration endotherm between 100°C-150°C for the pure cyclodextrin to a smaller endothermic

peak for the βD_3-2 complex to a further reduced peak for βD_3-4 in Figure 4.3d to an almost non-existent peak for the βD_3-8 complex in Figure 4.3c is confirmation that intermolecular water is displaced progressively more increasing quantities of vitamin guest is complexed during synthesis due to inclusion complex formation. A similar process was observed in the study by Ho and co-workers (2011) who varied the molar concentrations of ethylene to β-CD and compared the resultant DSC scans. A smaller water loss endotherm enthalpy peak also indicates a greater interaction between the bioactive and the βCD, confirming a better interaction between cholecalciferol and the CD in the βD_3-8 complex (Martins Mendes Gomes *et al*., 2014). The DSC data correlate well with IE results discussed later in section 4.3.7 and shown in Table 4.11, where the βD_3-8 IC was the most successful incorporating the largest quantity of vitamin with the highest IE value, followed by βD_3-4 and then βD_3-2.

Figure 4.4 again confirms the presence of an inclusion complex between vitamin D_3 and βCD in the βD_3-4 complex with a right shifted and shallower endothermic peak at 128°C compared to the endothermic peak between 115°C-120°C for the uncomplexed cyclodextrin. Once again the vitamin endotherm is absent, providing evidence to indicate complexation.

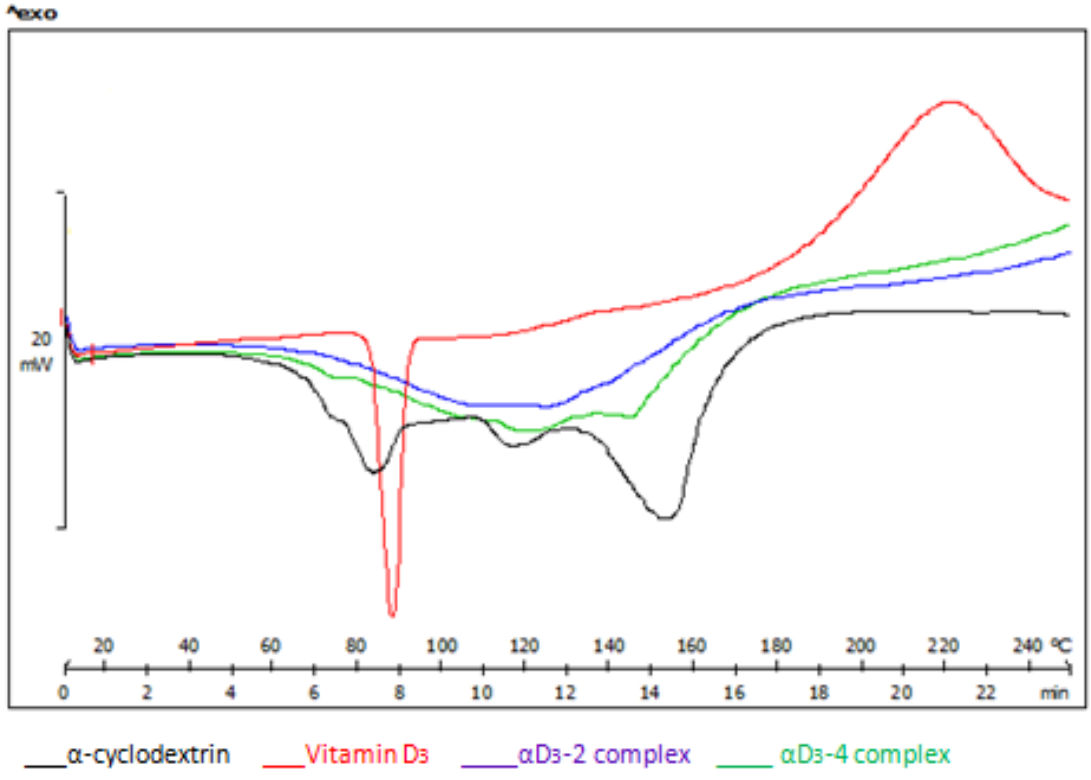


Figure 4.2: DSC Pilot run 10°C-250°C showing three water loss peaks for αCD and clearly defined melting point for vitamin D_3 at 84.5°C in congruence with literature

values.

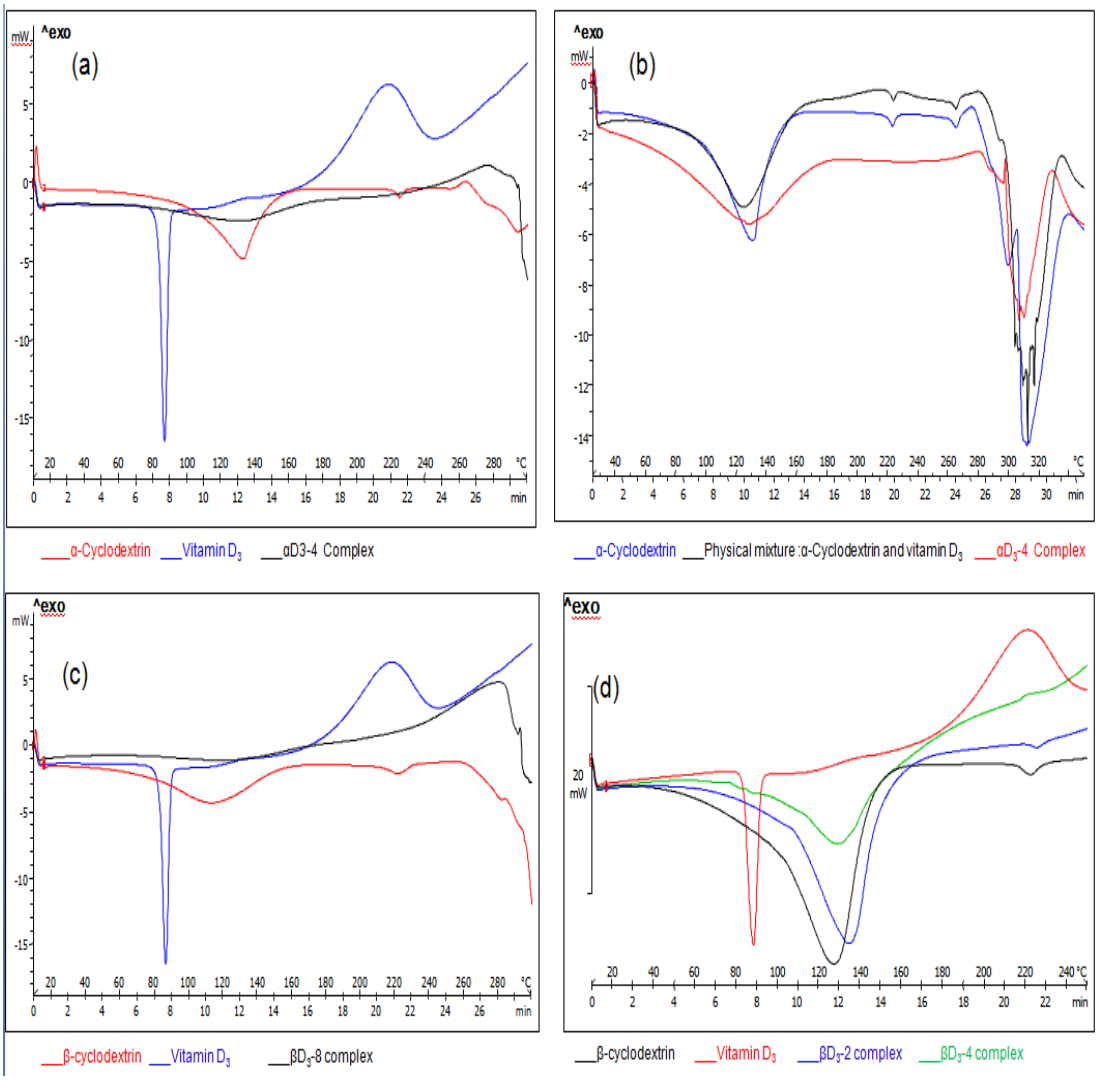


Figure 4.3: DSC profiles of (a) αCD, αD_3-4 and cholecalciferol; (b) αCD, αD_3-4 complex, and physical mixture of αCD and cholecalciferol; (c) βCD, βD_3-8 and cholecalciferol; (d) water loss run from 10°C-250°C for two βD_3 complexes, cholecalciferol and βCD.

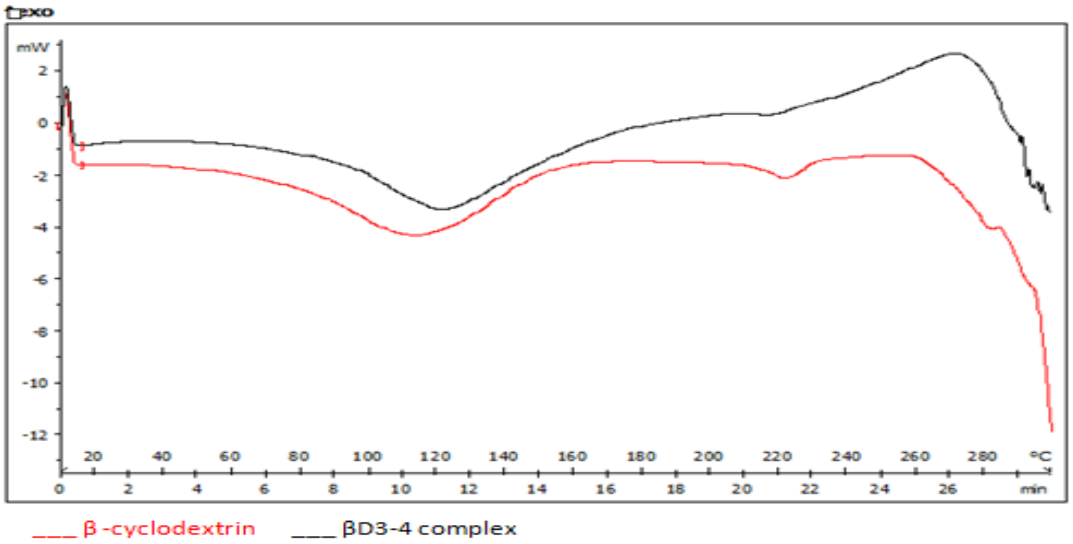


Figure 4.4: DSC profile of βCD and βD_3-4 complex.

4.3.4.3. Thermograms of γCD cholecalciferol inclusion complexes

The γD_3 complexes produced DSC thermograms that mimicked that of the native cyclodextrin molecule with no evidence of the melting point of the vitamin D_3 molecule (Figure 4.5a). Giordano and co-workers (2001) confirmed that a DSC profile of an inclusion complex created by complexation normally produces a flat curve similar to the respective CD which is evident in the current study with the γD_3-4 complex (Figure 4.5a) and as already discussed with the βD_3-8 complex (Figure 4.3c). IE results reported in section 4.3.7, also confirmed the presence of a high proportion of vitamin in the complex that is successfully protected from melting and degradation by the carrier molecule.

4.3.4.4. Thermograms of 2HPβCD-cholecalciferol inclusion complexes

Since initial molecular mechanics simulations revealed favourable energetic transitions for vitamin-βCD IC's the chemically modified βCD derivative, HPβCD, was investigated as a potential vitamin carrier. HPβCD is a commonly used chemically-modified cyclodextrin derivative that has a higher solubility and lower toxicity profile than the natural CD's (α-, β-, γ- CD's). Despite the fact that cyclodextrin derivatives may have superior solubility characteristics, the binding affinity and long term toxicity require consideration when selecting a CD to complex a bioactive. All cyclodextrins and their derivatives have varying binding capacities with bioactives that warrants investigation during the preformulation stages (Carrier *et al*., 2007).

A study with avobenzone and HPβCD conducted by Yang and co-workers (2008),

saw no bioactive endothermic transition evident in the DSC thermograms of the HPβCD-drug complex, due to the formation of an IC. Similarly, the inclusion complex that formed in a recent study between HPβCD and Rifampicin lacked the characteristic rifampicin peak due to "shielding" by the CD. The absence of the characteristic bioactive endotherm suggests that the active is contained within the carrier cavity (He *et al*., 2013). The present study saw the same observed results with cholecalciferol HPβCD IC's, which again support the formation of an IC this time with the more soluble HPβCD derivative (Figure 4.5b). The complete disappearance of the melting peak for vitamin D_3 in the HPβD_3 complex (Figure 4.5b) suggests what Yap and colleagues (2005) called "a strong interaction" between a bioactive and a CD and confirmation of an IC. Other researchers have also confirmed the disappearance of the melting point of 7-dehydrocholesterol (vitamin D_3 precursor) in complexes with HPβCD (Kim *et al*., 2010). The same observation is thus not unexpected with IC's of cholecalciferol and HPβCD in the current study. Furthermore, when the DSC profiles in Figure 4.5b were examined in conjunction with Figure 4.6 it was confirmed that the complex and pure HPβCD are indeed different compounds with unique and clearly different isotherms and thermal attributes.

4.3.4.5. Thermal characteristics of other vitamin inclusion complexes

As observed for other vitamin IC's formulated, the vitamin E complexes would be more stable than the native α-tocopherol molecule (Figure 4.5c). However, definitive confirmation could not be validated because α-tocopherol occurs in a liquid oil phase and thus could not undergo DSC analysis. However, thermal differences observed between the carrier molecule (βCD) and the βE-4 complex may be attributable to the inclusion of α-tocopherol within the CD ring.

Vitamin C has a very high melting point yet seems to crystallize and then rapidly degrade in close succession after reaching this critical temperature (Figures 4.5d). Inclusion complex formation resulted in a vitamin C complex with greater heat resilience and less chance of rapid degradation. From DSC analysis and as shown in Figure 4.5d it was apparent that the decomposition of the vitamin C complex occurred above the decomposition/ oxidation exothermic peak of pure vitamin C and therefore complex formation was thermodynamically favourable. Due to ascorbic acid's vulnerability to environmental degradation it is essential to protect the amount of bioactive that is available for activity (Alishahi *et al*., 2011). All other vitamin IC's revealed a flattened endotherm with respect to the CD. However, βC-8 was an

exception, showing a more prominent endotherm than βCD that was right shifted. The βCD endotherm occurred at 110^{o}C and was shifted to a more prominent peak at 132^{o}C for βC-8 (Figure 4.5d). This may be explained by the formation of a compound that is more crystalline in structure to βCD. Thermal transitions due to complexation may result in an ascorbic acid complex with a modified solubility profile. Complexation of the already highly soluble vitamin with the less soluble βCD carrier may impede the dissolution profile of ascorbic acid. Such physicochemical alterations evident in thermal analysis may be utilized to protect vitamin C from thermal degradation whilst slowing the molecules dispersion into aqueous media.

Most cyclodextrin studies have discussed the differences between physical mixtures and inclusion complexes. Important observations and conclusions can indeed be drawn from the present research when physical mixtures and inclusion complexes were compared. In Figure 4.5d it is noticeable that the DSC curve of vitamin C (ascorbic acid) showed an endothermic melting peak at approximately 195°C in agreement with material safety data sheets and literature values stated for vitamin C and in a study by Hu and co-workers (2012) who found a melting point at 197°C. The profile of the physical mixture showed two distinct endothermic peaks indicative of both the β-cyclodextrin and the vitamin C molecule. However the DSC profile of the βC-8 complex mimicked that of the CD and not of the vitamin where it was found that the prominent endothermic melting peak of vitamin C had disappeared. As published by other researchers (Giordano *et al*., 2001; Hu *et al*., 2012) a bioactive-CD physical mixture normally shows endothermic peaks at temperatures corresponding to the melting point of the bioactive and also the dehydration endotherm of the CD. Therefore a physical mixture typically shows a profile that looks like a superimposition of the curves of the two individual components (Dua *et al*., 2011). Carrier and co-workers (2007) noted that although it is widely accepted that the physical mixing of a bioactive and a cyclodextrin can result in some complex formation, it is apparent from DSC analysis that most of the mixed CD and bioactive is still present in its individual parts and not as one complex. As the thermogram of physical mixtures is similar to that of the individual pure compounds this may signify a lack of interaction between the individual components compared to what is present in true inclusion complexes (Yap *et al*., 2005). Similarly, Yang and co-workers (2008) noted how a simple physical blend of avobenzone and HPβCD demonstrated a lack of interaction between the active and HPβCD. This is an important difference to note between physical mixtures and complexes of cyclodextrins which supports the wide acceptance that it is the CD-bioactive complexes and not their physical

mixtures that improve the oral bioavailability of a drug (Carrier *et al*., 2007). Therefore it is imperative that complex formation is confirmed prior to final product formulation. Unlike other studies, that have reported a reduction of the endotherm following complexation, the βC-8 demonstrated a more distinct and right shifted endothermic peak. A larger endotherm for the complex may be indicative of an inclusion and a non-inclusion based complexation showing the presence of some "free" vitamin bound to the outside of the CD and a more crystalline compound.

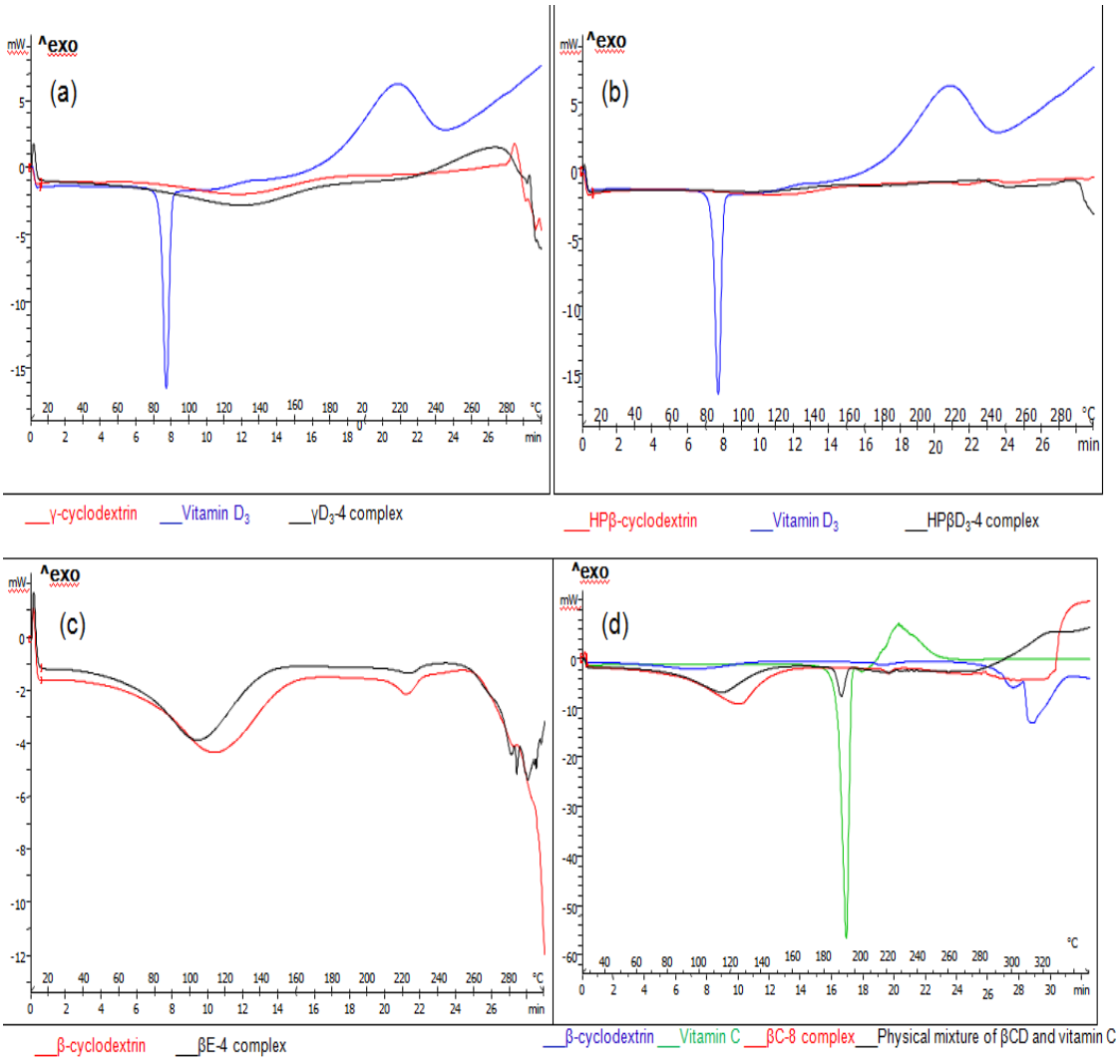


Figure 4.5: DSC profiles of (a) γCD, γD_3-4 complex and cholecalciferol; (b) 2-hydoxypropylβCD, 2-hydoxypropylβCD-D_3-4 complex and cholecalciferol; (c) βCD to βE-4 complex; (d) DSC profile of physical blend of βCD and vitamin C, βC-8 complex, βCD, and vitamin C.

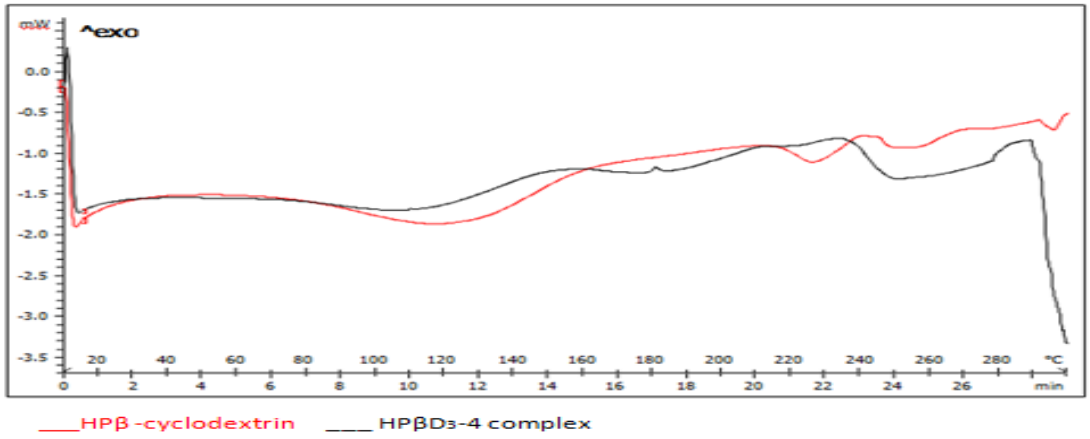


Figure 4.6: DSC profiles of 2-hydoxypropylβCD and 2-hydoxypropylβCD-D_3-4 complex.

4.3.4.6. Summary discussion: Thermal analysis of vitamin IC's

DSC thermograms of inclusion complexes normally exhibit a flat curve similar to the native CD with no evidence of an individual vitamins endotherm/ fusion, which was observed in most DSC figures and corroborated by other researchers (Giordano *et al*., 2001). The same observation was noted in a study by Wen and co-workers with 2HPβ-CD and the herbal bioactive, naringenin (2010). This group noted that these observations were due to the nutraceutical being entirely dispersed within the CD with resultant non-covalent forces between the host and guest bioactive causing marked differences in DSC data indicative of complexation. A similar observation was noted in the present research, except with ascorbic acid which had an exception with the resultant IC having a more distinct endotherm at a higher temperature than the parent CD. An interaction occurred between vitamin C and βCD, vitamin D_3 and βCD, HPβCD and γCD confirmed by thermal analysis. Vitamin endotherms were absent in resultant vitamin IC's and thermal profiles demonstrated endotherms that occurred at higher temperatures and were generally reduced with respect to the CD due to vitamin inclusion and water displacement. One can conclude that a vitamin is included or attached to the CD with a right-shifted endotherm, indicative of a compound with a higher melting point and more stable thermal properties. A right shifted endotherm of an inclusion complex is said to melt at a higher temperature and is able to absorb more heat energy before undergoing a structural transition. Such properties are attractive formulation characteristics making the resultant vitamin IC's less vulnerable to degradation during storage or upon exposure to temperature fluctuations during manufacture and during physiological transitions in the GIT.

4.3.5. Chemical structure stability mapping of CD-vitamin complexes by Fourier Transform Infrared Spectroscopy (FTIR) to confirm complexation

FTIR has been used extensively by scientists to identify and describe the existence of inclusion complexes (Zaibunnisa *et al*., 2011). An FTIR spectrum is a highly characteristic property of a compound and may be used to reveal the "fingerprint" structure of a new or different compound when compared to the spectra of known existing compounds. An FTIR spectrum provides information regarding the presence or absence of specific chemical groups in a molecule depicted by characteristic bands. Interaction between components is indicated in FTIR profiles by either additional bands/ peaks or the absence of characteristic peaks of the bioactive or the carrier. The formation of new peaks confirms the presence of specific molecular groups and the possible presence of a new compound. Comparison of the shape, intensity and position of bands in a vitamin, cyclodextrin, physical mixtures and inclusion complexes revealed pertinent information about molecular bonds that have formed especially when noticeable shifts and changes occur. As with UV-Spectroscopy and DSC analysis, complexes were initially washed with suitable organic solvent to remove free vitamin prior to performing FTIR analysis so that the spectra obtained were an accurate reflection of the IC structures. The FTIR spectra of all cyclodextrins, vitamins and resultant IC's, showed that all complexes had similar absorption bands to that of the pure cyclodextrins or cyclodextrin derivative. The FTIR profiles are depicted in Figures 4.7-4.9.

4.3.5.1. FTIR spectra of αCD, βCD, γCD and 2HPβCD cholecalciferol IC's

αD_3 complexes looked almost identical to α-cyclodextrin with the marked exception of a shift of the O-H stretching bands to a higher frequency in the complex compared to αCD (3253cm^{-1} vs. 3290cm^{-1}) (Figure 4.7a). An interesting comparison was that the βD_3 complex resulted in a shift to lower frequencies and the αD_3 complex resulted in a shift to higher frequencies with respect to O-H stretching bands of their respective parent CD molecules. This difference in hydroxyl stretching peak transitions may reflect differences in inclusion efficiency as reported under section 4.3.7 where βD_3 complexes entrapped more vitamin then αD_3 complexes and illustrated differences in intra-molecular interactions.

β-cyclodextrin had prominent absorption bands at 3301cm^{-1} representing O-H stretching and at 2924cm^{-1} for C-H stretching and at 1639cm^{-1} for H-O-H bending (Figure 4.7b and c). Other studies support the existence of these same characteristic peaks for the parent β-CD compound (Wang *et al*., 2011). The

absorption bands at 3301cm^{-1} and 2924cm^{-1} of β-CD were shifted towards lower frequencies at 3291cm^{-1} and 2923cm^{-1} for all the βD_3 complexes (Figure 4.7b). These changes have been said to be related to the formation of intra-molecular hydrogen bonds between the vitamin and CD ring in studies with other nutraceuticals (Wang *et al.*, 2011). As per a recent study by Teng and co-workers (2013), the characteristic vitamin D_3 O-H stretching occurs at 3292cm^{-1} and two alkyl C-H stretches are found at 2935cm^{-1} and 2874cm^{-1} (Figures 4.7b and c). The disappearance of the characteristic vitamin D_3 peaks indicates successful encapsulation in polymer matrices according to Teng and co-workers (2013). This same conclusion may be drawn in the current research where the characteristic vitamin D_3 O-H and C-H peaks are no longer evident in the IC's. Successful inclusion is demonstrated by the disappearance of these characteristic vitamin D_3 peaks in the IC's profiles observed in Figures 4.7-4.9

All γ-cyclodextrin complexes also showed FTIR changes that confirmed complex formation. The γ-D_3 complexes O-H stretching band shift to a higher frequency (3298cm^{-1}) compared to the native γ-cyclodextrin (3238cm^{-1}). In addition the C-H aliphatic band moved to a lower wavelength at 2923cm^{-1} for the γD3 complex vs. 2927cm^{-1} for γ-CD (Figure 4.7d).

Wen and co-workers (2010) found that the FTIR spectra of 2HPβ-CD and the 2HPβD_3 IC's with naringenin were remarkably similar and the same finding is correlated in Figure 4.8 of the present study albeit with cholecalciferol. The only exception was that the O-H stretching bands at 3339cm^{-1} for 2HPβ-CD were altered and shifted to a lower frequency at 3337cm^{-1} in the cholecalciferol complex. Also noticeable was the shift to a lower wavenumber for the characteristic C-O stretching band, previously found at 1019cm^{-1} for HPβ-CD and shifted to 1008cm^{-1} for the resultant HPβD_3 complex (Figure 4.9a).

4.3.5.2. FTIR spectra of βCD vitamin inclusion complexes

When comparing the βCD complexes of cholecalciferol, ascorbic acid and α-tocopherol to βCD the C-H aliphatic band that occurs around 2926cm^{-1} for β-CD was shifted to lower wavelengths for all resultant complexes (Figures 4.7 and 4.9). This confirms complex formation. Zaibunnisa and co-workers (2011) also reported a change and shift of the C-H band to a different (higher) wavenumber for a complex that formed between γ-cyclodextrin and β-carotene using a co-precipitation method similar to that used in the current study. In general the physical blends were similar

to the single components looking like a combination of the spectra of each constituent (Figure 4.7c). The same was confirmed by Liu and co-workers (2013) who commented on physical mixtures and inclusion complexes formed during a study that investigated inclusion complexes with luteolin. These researchers also noted that FTIR spectra of IC's were similar to the cyclodextrin carrier but with higher intensities indicating an increase in hydroxyl groups due to inclusion of the active in the CD ring (Liu *et al*., 2013). The same is observed in the current study (Figure 4.7b and c). Two characteristic vitamin C bands were seen in the FTIR spectrum of vitamin C at 1637cm^{-1} and 1850cm^{-1}. The resultant βC-8 complex had a similar peak in close proximity to these peaks at 1875cm^{-1} which was absent in the native βCD. This was proof of the ascorbic acid band of 1850cm^{-1} in the IC that has shifted to a higher frequency in the βC-8 complex due to a molecular interaction between the vitamin and the carrier (Figure 4.9c).

4.3.5.3. Intensity shifts in FTIR spectra of vitamin inclusion complexes

Comparisons between β-, γ-, and HPβ- CD's and their resultant vitamin D_3 complexes in all spectrums (Figures 4.7b and d and Figure 4.9a) revealed substantial changes in characteristic intensity of peaks at 3300cm^{-1}, 2924cm^{-1}, 1640cm^{-1}, and in the fingerprint region between 1500cm^{-1}-650cm^{-1} due to inclusion complex (IC) formation. The same peak intensity increases were noted for the βE-4 IC's when compared to the βCD (Figure 4.9b). Adsorption of the guest vitamins onto the CD molecule was confirmed by changes in intensity of characteristic bands in a study by Ho and co-workers with other bioactives (2011). Compounds with a small molecular size and present in low concentrations in complexes will only cause minimal vibrational changes in the intensity of peaks (Ho *et al*., 2011). However the current research has shown large intensity changes between the native CD and subsequent β-, γ-, and HPβ- complexes. This is indicative of the presence of a high concentration of vitamin in the complexes or due to the existence of a high molecular weight guest. Symmetric and antisymmetric O-H stretching is normally attributable to peaks between 4000cm^{-1} and 3000cm^{-1}.

In contrast, the spectrum of the αD_3 complex only showed a small change in intensity of the O-H peaks (Figure 4.7a) which is evidence for a lower amount of vitamin being bound and thus less interaction evident. Such observations correlate well with inclusion efficiency calculations discussed later in section 4.3.7 where the αD_3 complexes had the lowest values and proved to be the least successful at binding vitamin D. All cholecalciferol IC's and the βE-4 IC had large changes in the

intensity of the O-H stretching peaks compared to the respective CD evidenced by enlarged bands with a higher intensity of transmittance between 3200cm^{-1} and 3300cm^{-1}. Teng and co-workers (2013) also noted that an increase in intensity of O-H stretching peaks in other vitamin D_3-loaded systems suggests an increased involvement of hydrogen bonding with vitamin D_3 and nanoparticle carriers and confirms encapsulation. Similarly other studies with vitamin D_3 and zein nanoparticles have suggested hydrogen bonding that occurs between carriers and the vitamin in the 3300cm^{-1} region (Luo *et al*., 2012).

The intensity changes demonstrated in the O-H stretching region in the current study indicate complexation between the CD's and the respective vitamins. In addition, according to Ho and co-workers (2011) these intensity changes are clear evidence for guest adsorption onto the surface of a CD molecule. Thus it can be confirmed that vitamins were adsorbed onto the outside of the CD ring as well as inclusion within the ring of the carrier molecule.

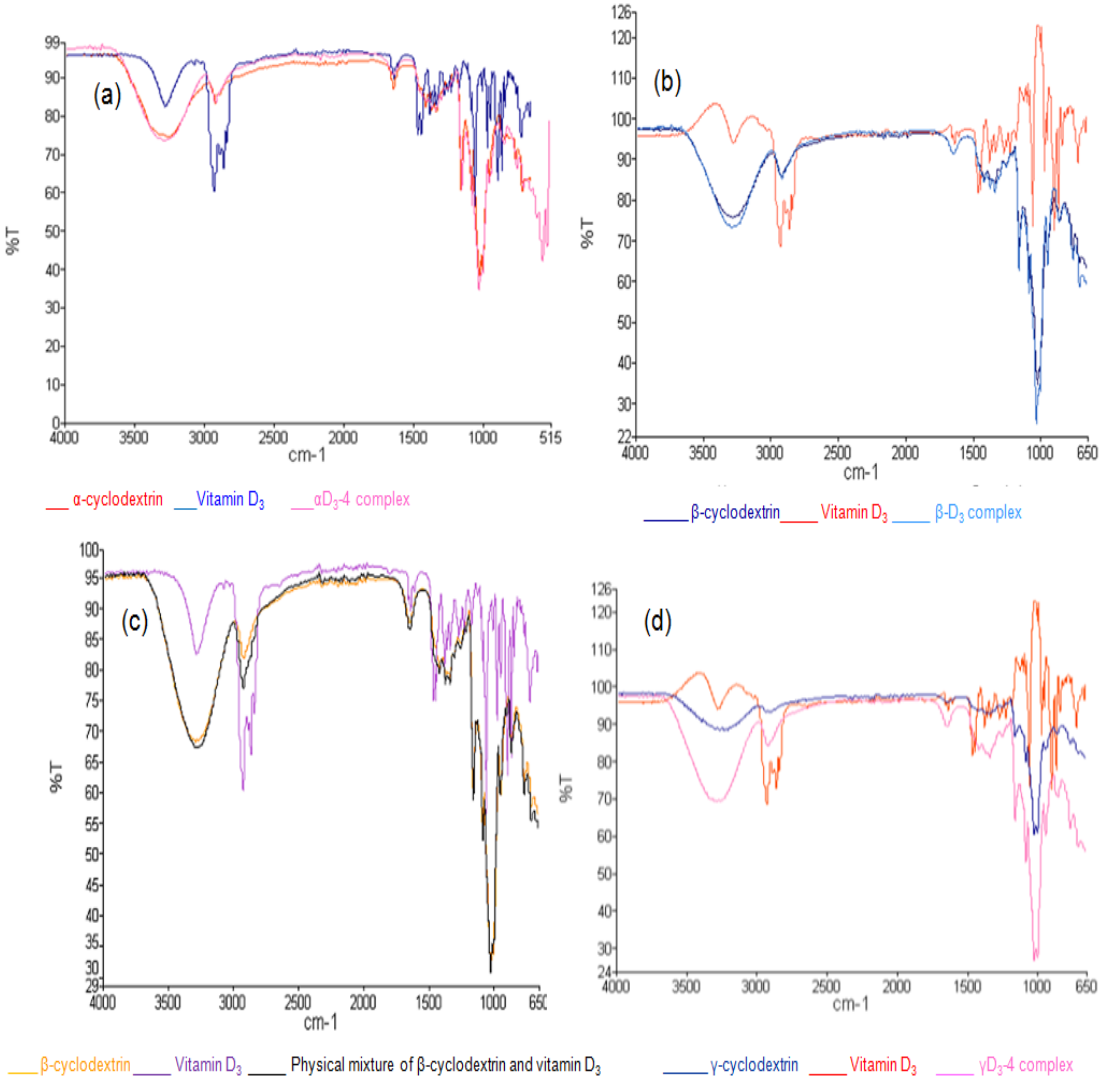


Figure 4.7: FTIR spectra of (a) αCD, cholecalciferol, and αD_3-4 complex; (b) βCD, cholecalciferol, and βD_3 complex; (c) βCD, cholecalciferol, and physical blend of βCD and cholecalciferol; (d) cholecalciferol, γCD and γD_3-4 complex.

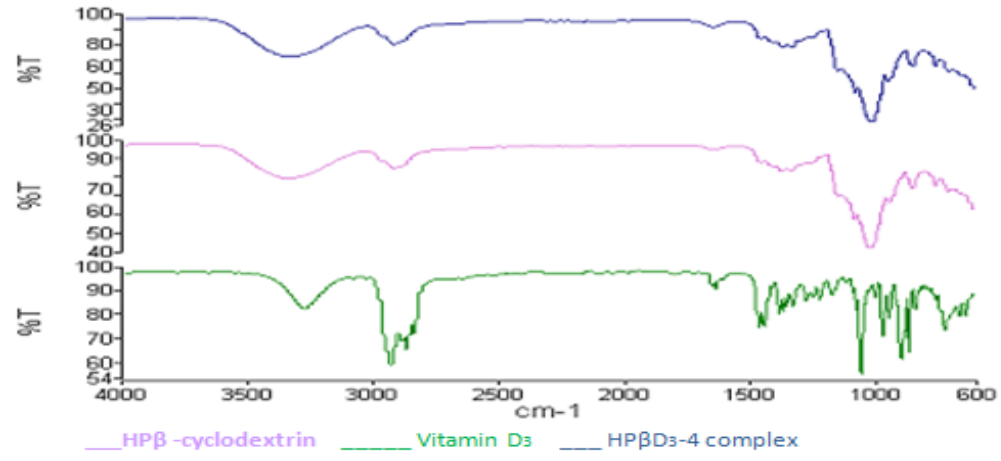


Figure 4.8: FTIR "split" spectra of $HP\beta D_3$-4 complex, HPβCD, and vitamin D_3.

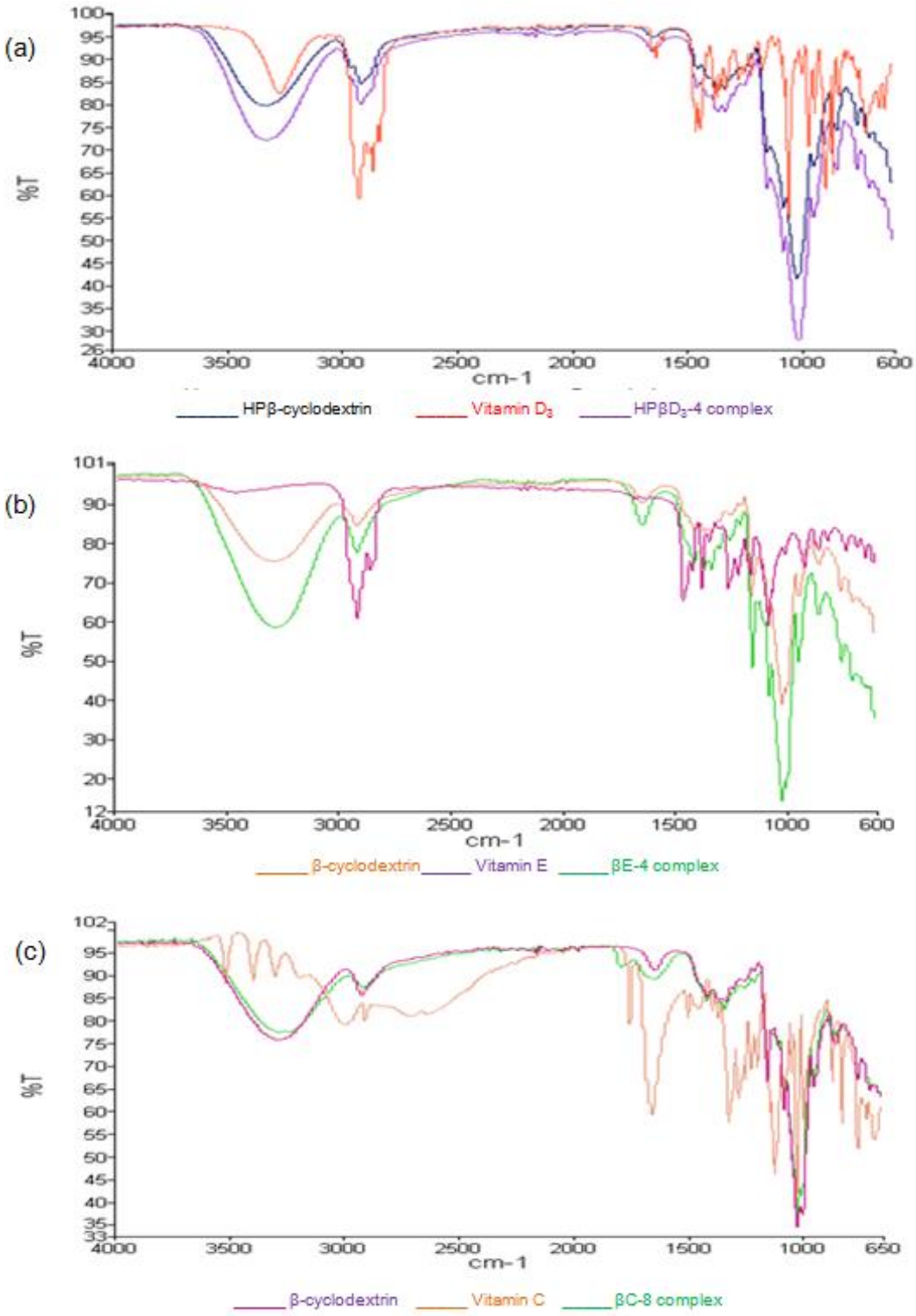


Figure 4.9: FTIR spectra of (a) HPβD_3-4 complex, HPβCD, and cholecalciferol; (b) βE-4 complex, βCD, and α-tocopherol; (c) βC-8 complex, vitamin C, and βCD.

4.3.5.4. Summary discussion: FTIR of vitamin IC's

Evidence for the existence of the vitamin guests in the resultant complexes is difficult to conclude if analyzing FTIR spectra in isolation. In the present research, it was prudent to search for a few transmittance bands in the complex that are also

attributable to the individual vitamin (this was seen in the ascorbic acid spectra) (Figure 4.9c). Since FTIR data has the benefit of being interpreted in conjunction with the other physico-chemical tests performed (DSC, UV-Spectroscopy and visual examination tests), it was confirmed that the complexes represented new compounds. Figure 4.7b shows an FTIR spectrum for a βD_3 complex that is almost identical to that of βCD, however when viewed alongside DSC thermograms (Figures 4.3c and d) it is clear that the resultant IC's had higher melting points and are were new and different compounds. When interpreting Figures 4.7b and d and Figure 4.9a it is clear that the vitamin D_3 IC's have spectra with similar absorbance bands to their respective native CD's but with differing intensities meaning that there was a different quantity of specific chemical groups present in the complexes due to molecular interactions occurring between the vitamin and the respective CD carrier.

The FTIR spectra of all complexes showed little to no features of the pure vitamins in any of the studies regardless of variations in solvents and mixing times in the methods. Such disappearance of nutraceutical FTIR bands was also noted and discussed in a study by Wang and co-workers (2011) where a GO/ β-CD IC had no characteristic peaks originally evident in the pure garlic oil prior to complexation. In summary, the FTIR spectra of the vitamin-CD complexes in the current study resulted in a disappearance of characteristic peaks of the individual vitamins, changes in intensity of specific peaks initially found in the native CD, and shifts in frequencies of specific molecular bands to lower or higher wavelengths. In all cases it is evidenced that the IC's structures differ to that of the native CD or vitamins due to vitamin inclusion within CD cavities or the existence of non-inclusion based hydrogen bonding interactions between the vitamin and the carrier.

4.3.6. Determination of crystallinity transitions of the vitamin-CD complexes by X-ray Powder Diffraction (XRPD)

X-ray powder diffraction is a powerful analytical tool used to determine whether a compound is crystalline or amorphous. Peak position is an indication of the amorphous or crystalline nature of a sample and may also be used to characterize and identify different compounds.

4.3.6.1. XRD crystalline structure of cholecalciferol inclusion complexes

The inclusion complex of cholecalciferol prepared with each CD using the co-precipitation method was characterized by XRPD. Diffractograms and crystallinity computation revealed that vitamin D_3 is highly crystalline as characterized by

numerous definitive and sharp peaks (Figure 4.10a). The diffractogram of cholecalciferol demonstrated strong peaks indicative of high crystallinity that was in agreement with previous studies (Ignjatovic *et al*., 2013). Non-complexed CD molecules tested (with the exception of βCD) were less crystalline in nature than cholecalciferol. The cyclodextrins 2-HPβCD and γCD, had more disperse diffraction peaks and scattered patterns, revealing a more amorphous structure than cholecalciferol. The complexes formed after complexation of cholecalciferol with each CD showed profiles with amorphous aspects attributable to the CD and crystalline aspects attributable to the presence of the vitamin. The profiles of the complexes vs. the physical mixtures differed in the peaks that were present and their relative intensities showing that complexes and physical mixtures have different crystalline structures. The characteristic vitamin D_3 peaks were present in all complexes and physical mixtures but in different intensities and at different 2θ values to the original cholecalciferol profile. All complexes were less crystalline than the uncomplexed cholecalciferol. The decrease in crystallinity of vitamin D_3 when a complex was formed provides evidence that all complexes are more amorphous in nature than the native vitamin. In general amorphous bioactives (despite being less ordered in structure), are more soluble and hence XRPD confirmed that the IC's physicochemical structure may support an improvement in solubility of the cholecalciferol IC's. Shifted peaks and a reduction in crystallinity of the complexes in comparison to the native vitamins further confirmed inclusion complexation (Ghosh *et al*., 2011).

4.3.6.2. XRD crystalline structure of ascorbic acid inclusion complexes

Analysis of βCD physical blends of ascorbic acid and native βCD as well as each individual constituent was undertaken (Figure 4.10b). Unlike the D_3 inclusion complexes that became more amorphous following complexation, the βC-4 inclusion complex was more crystalline than the original uncomplexed vitamin C. Such a transition may reduce the solubility of the already highly aqueous soluble antioxidant vitamin (vitamin C solubility=1g/ 3mL H_20). Despite an increase in crystallinity and possible reduction in solubility, following complexation, the ascorbic acid IC was found to be more thermodynamically stable which is important to ensure vitamin efficacy. Additionally, the resultant complex (with higher crystallinity) may be utilized to modify and slow vitamin C release, whilst simultaneously providing protection from degradation. A lower aqueous solubility may slow the dissolution profile of ascorbic acid from a less aqueous soluble IC.

4.3.6.3. Crystallinity discussion and implications

Table 4.10 shows the % crystallinity of IC's, native CD's and native vitamins. The resultant vitamin complexes had noted differences in their crystalline structures and % crystallinity when compared to their respective physical mixtures. Crystallinity evaluations therefore again confirmed that a simple physical blend does not result in a substantial interaction between the bioactive and the CD (Yang *et al*., 2008). This fact supports the wide acceptance that CD-bioactive complexes and not physical blends result in unique physicochemical enhancements (Carrier *et al*., 2007). Ruz and co-workers (2012) noted how physical mixtures had XRPD peaks attributable to the bioactive but at lower intensities. Similar observations occurred with the physical mixtures in the current study as illustrated in Figures 4.10a and b. Despite other researchers (Ruz *et al*., 2012) noting the disappearance of distinct drug peaks in XRPD patterns of complexes, the current study revealed that complexes still retained the original vitamin peaks albeit at differing 2Θ values and at dissimilar intensities to the original vitamin which may be due to the presence of the vitamin on the outside of the CD and also within the CD ring. Modified solubility phenomena resulting from changes in crystalline structure, may have useful applications including the harmonization of oral release profiles of co-formulated vitamin constituents that have different inherent solubilities.

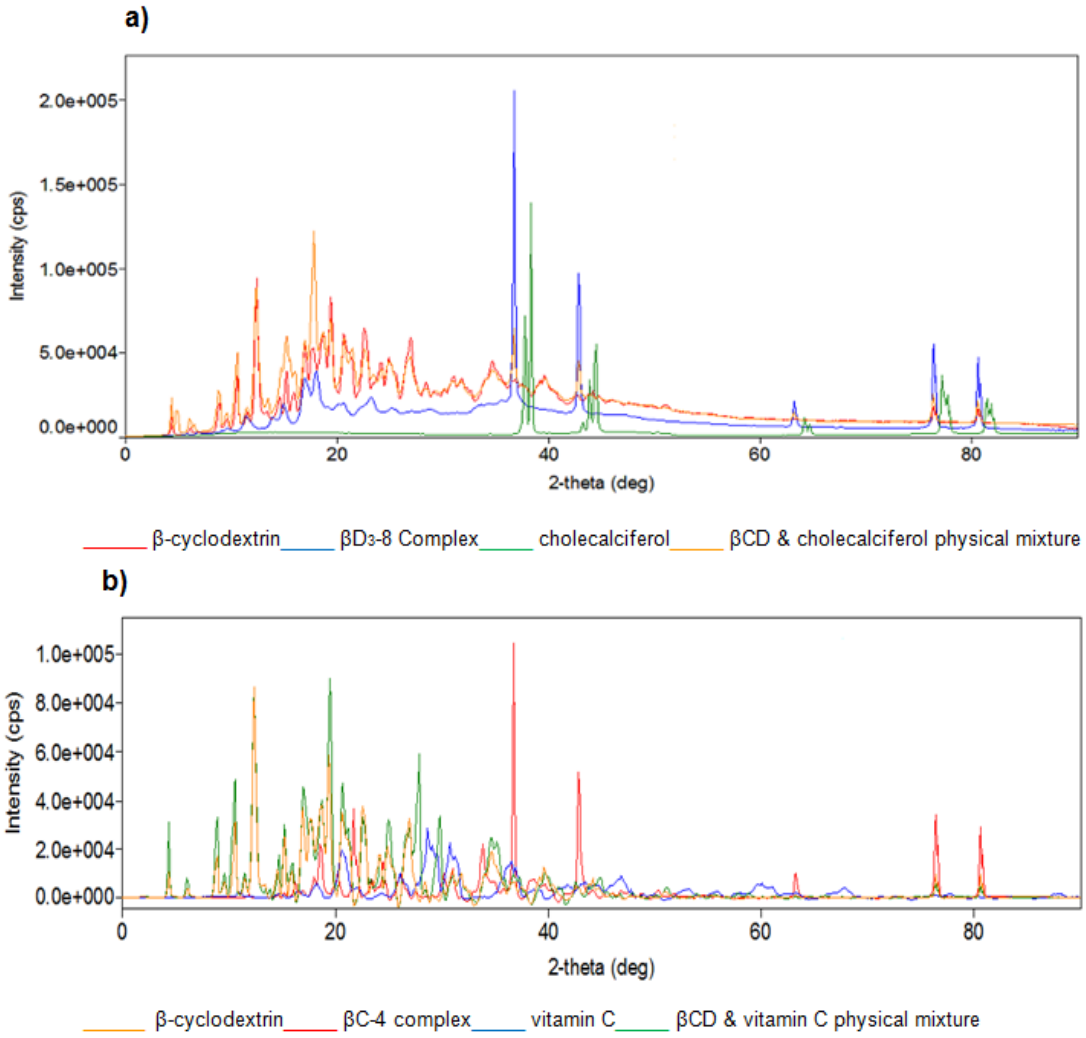


Figure 4.10: X-ray powder diffractograms of (a) βCD, βD_3-8, cholecalciferol, and βCD and cholecalciferol physical mixture; (b) βCD, βC-4, cholecalciferol, and βCD and vitamin C physical mixture.

Table 4.10: Summary of the % crystallinity of inclusion complex samples

Sample No.	Compound/ Complex	Crystallinity (%)	Observation
1.	βCD	100	Highly crystalline
2.	cholecalciferol	99	High crystallinity
3.	βCD and cholecalciferol physical blend	98	Similar crystallinity to individual components
4.	βCD-cholecalciferol-8 complex	91	Reduction in cholecalciferol crystallinity
5.	Ascorbic acid	85	Contains amorphous aspects
6.	βCD and ascorbic acid physical blend	100	Increase in ascorbic acid crystallinity

Sample No.	Compound/ Complex	Crystallinity (%)	Observation
7.	βCD-ascorbic acid-4 complex	98	Increase in ascorbic acid crystallinity
8.	γCD	92	High crystallinity
9.	γCD and cholecalciferol physical blend	100	High crystallinity
10.	γCD-cholecalciferol-4 complex	93	Reduction in cholecalciferol crystallinity
11.	2HPβCD	59	Highly amorphous
12.	HPβCD and cholecalciferol physical blend	99	High crystallinity
13.	2HPβCD-cholecalciferol-4 complex	73	Complex with largest reduction in cholecalciferol crystallinity

4.3.7. Inclusion efficiency (IE) determinations of CD-vitamin complexes

The entrapment efficiency of encapsulation systems is rarely measured by researchers (Loveday and Singh, 2008). This value is however an essential indicator as it determines the quantity of bioactive guest that is carried by the cyclodextrin carrier. This assists with accurate dosage calculations when using such carrier molecules to transport bioactives within drug delivery systems. The amount of vitamin entrapped, bound to, or included within the cyclodextrin is determined using IE calculations. In the current research various experimental conditions were manipulated to gather information regarding the inclusion efficiency that is achieved when a particular cyclodextrin and a vitamin are complexed via co-precipitation at different molar ratios. IE calculations for each complex are listed in Table 4.11.

Since all three vitamins used during the study absorb at characteristic UV_{max} wavelengths in the ultra-violet visible spectrum, UV-spectroscopy was used for IE determinations of synthesized complexes. Standard calibration curves were plotted for each vitamin for concentration (ug/mL) vs. Absorbance and used in the IE calculations to determine the extent of included vitamin within each complex (Figure 4.11 and Figure 4.12).

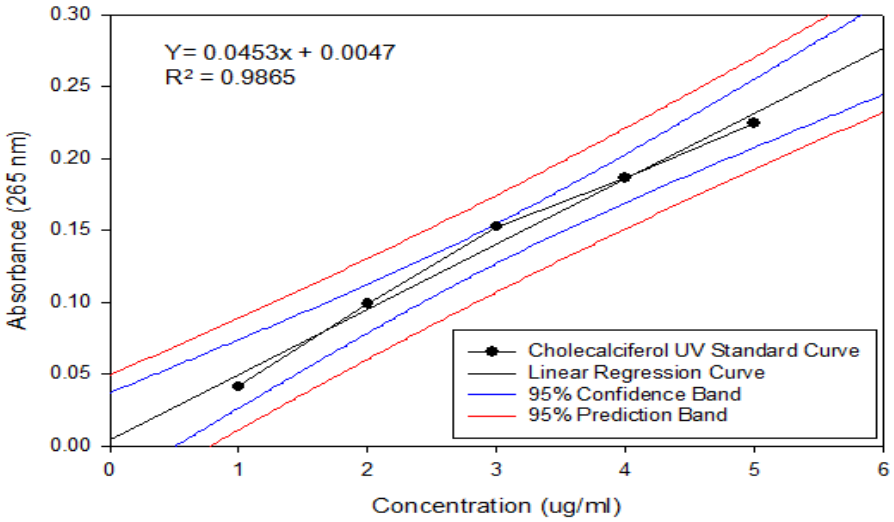


Figure 4.11: UV Standard Calibration Curve generated on UV-spectrophotometer for cholecalciferol aqueous solutions at 265nm used for IE% determinations of vitamin-CD complexes.

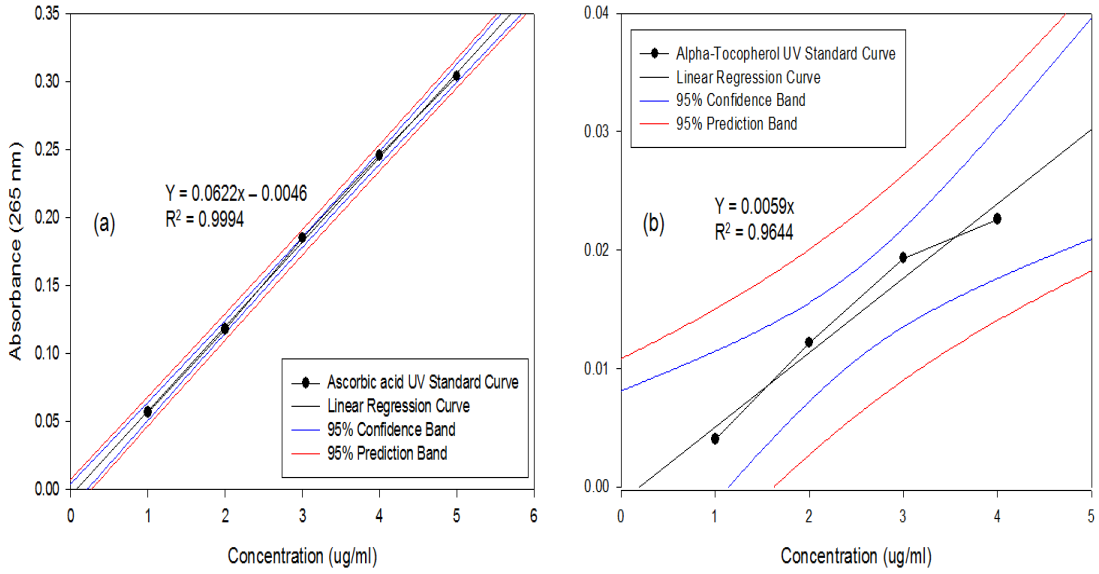


Figure 4.12: UV Standard Calibration Curves generated on UV-spectrophotometer for (a) Ascorbic acid aqueous solutions at 265nm and (b) α-Tocopherol aqueous solutions at 295nm used for IE% determinations of vitamin-CD complexes.

Table 4.11 summarizes the results obtained for mean IE calculations for triplicate IE studies that were conducted. βCD IC's consistently achieved the highest Inclusion Efficiency (IE%) of all the vitamin-CD inclusion complexes (Table 4.11). The ease of miscibility of ascorbic acid and β-cyclodextrin in the aqueous phase during preparation accounted for the high IE% of ascorbic acid complexes. The βC-8 complex achieved the highest mean IE of all vitamin-CD complexes (82%) (Table 4.11). The high IE% of βC-8 IC's revealed that this combination resulted in a successful complexation reaction correlating well with the results of other

researchers (Hu *et al*., 2012). The formation of vitamin complexes with the fat-soluble vitamins cholecalciferol and α-tocopherol required the use of two different solvents to assist in solubilizing each respective cyclodextrin and the vitamin separately and thus potential existed for each phase not to mix adequately. Overall results for these vitamins indicated that βCD-cholecalciferol achieved consistently higher IE% values than the other fat-soluble vitamin complexes regardless of experimental conditions. The βD_3-8 complex had the third highest mean IE% of 78% after the vitamin C complexes. γD_3-4 complexes also achieved a reasonably high mean IE% of 72%, and βD_3-4 was the next highest at 54%. The βD_3-2 complexes followed with an IE of 25%. $HP\beta D_3$ complexes followed with an IE% means of 19% for $HP\beta D_3$-8 and 26% for $HP\beta D_3$-4. The α-tocopherol and βCD complexes resulted in low IE values (8.9%-20.44%). However, the lowest mean IE% obtained for all vitamins and CD complexes occurred with αD_3 complexes revealing that this αCD is considered a less favourable option to complex with cholecalciferol, possibly due to a small cavity size of the cyclodextrin. In fact αD_3-2 had an IE% of as low as only 2% and αD_3-4 of 13% in the IE studies. The FTIR spectrum of αCD-cholecalciferol IC's only showed small change in intensity of peaks at 3300cm^{-1}, 2924cm^{-1} and 1640cm^{-1} (Figure 4.7a) which was evident of a lower quantity of vitamin complexed in the α-cavity.

There was a noted difference in the inclusion efficiency of βCD-cholecalciferol complexes and 2-HPβCD-cholecalciferol complexes. Low IE values for $HP\beta D_3$ was unexpected although this may be interpreted as less significant in light of the fact that HPβCD may still prove an attractive option due to the carrier's superior aqueous solubility in comparison to other CD molecules. This characteristic will aid solubilization of an entrapped bioactive at a faster rate than the native CD carriers. All CD molecules and their derivatives have varying binding capacities with bioactives and these characteristics need to be investigated during formulation planning when utilizing carrier molecules (Carrier *et al*., 2007). Thus the low IE% for the 2- HPβCD-cholecalciferol complexes needs to be considered against the known high solubility profile of 2-HPβCD and the relative binding capacities with each vitamin. If a carrier molecule does not bind efficiently to a bioactive of interest then the positive physiochemical characteristics of the carrier cannot be imparted upon the drug. It should be noted that he excessive use of chemically modified CD molecules may cause side-effects, including local irritation to membranes. Although chemically modified CD's are often favoured for rapid aqueous solubility, these molecules are considered less safe than the natural α-, β-, and γ-CD molecules in

nutraceutical applications as such products are consumed on a chronic basis (Uekaji *et al*., 2012). Therefore HPβCD IC's were deemed unsuitable for BAP inclusion due to the need to dose on a daily basis.

In the vitamin E studies, βCD-α-tocpherol complexes had low IE values, some as low as 7.6%, with a mean IE% of 8.9% for βE-8 indicating that certain highly hydrophobic guests such as vitamin E may require a high molar excess of CD in relation to the amount of vitamin in order to facilitate a meaningful inclusion complex reaction. It was indeed noted with this vitamin that a higher molar ratio of cyclodextrin to vitamin to achieved larger IE values and drove the inclusion complex reaction. This was evidenced by an IE value that approximately doubled to 20.44% for βE-4 compared to 7.6%-10.22% for βE-8 complexes. The CD: vitamin synthesis ratio was optimized at a molar ratio of 5:1 (CD: α-tocopherol). Koontz and co-workers (2009) reported similar values, after optimizing molar reactant ratios at 8:1 (CD: α-tocopherol) where complexes were produced with an α-tocopherol content of 18.1% compared to 20.44% in the current study.

The highest IE% value for βCD-cholecalciferol IC's occurred with CD: cholecalciferol molar ratio of 2.5:1 for the most successful cholecalciferol complex, namely 'βCDD_3-8'. The high IE for the βCDD_3-8 IC was also corroborated by the results of thermal analysis in section 4.3.4, where the water loss endotherm was the lowest for this IC compared to other cholecalciferol βCD complexes. A lower endothermic transition indicates the greatest interaction between a bioactive and a CD (Martins Mendes Gomes *et al*., 2014). Despite other researchers noting that CD: cholecalciferol synthesis ratios of 10:1 and 5:1 were ideal (Mercê *et al*., 2009), the lower molar quantity of βCD and higher mixing time in the current study revealed a uniquely successful candidate with an unexpectedly high mean IE value of 78% for βCDD_3-8. Similarly, ascorbic acid IC's achieved highest IE% with a CD: vitamin molar synthesis ratio of 2.5:1. The Other cholecalciferol IC's achieved highest IE% with a CD: vitamin molar synthesis ratio of 5:1 (2HPβCD-cholecalciferol, γCD-cholecalciferol). The following represents the quantum of highest to lowest IE% values obtained for the various vitamin inclusion complexes:

βCDC-8 > βCDC-4 > βCDD_3-8 > γCDD_3-4 > βCDD_3-4 >2HPβCDD_3-4> βCDD_3-2 > βCDE-4 > 2HPβCDD_3-8 > αCDD_3-4 > βCDE-8 > αCDD_3-2.

Table 4.11: IE% calculations for CD-vitamin inclusion (n=3)

Inclusion Complex	CD mass (mg)	Vitamin Mass (mg)	Mean IE (%)	SD
αCDD_3-2	196.6	7.8	2	1.41
αCDD_3-4	197.4	15.7	13	1.18
βCDD_3-2	227.8	7.6	25	2.51
βCDD_3-4	228	15.5	54	4.84
βCDD_3-8	227.4	30.8	78	6.08
γCDD_3-4	259.1	15.5	72	3.39
2-HPβCDD_3-4	228.4	15.7	26	6.43
2-HPβCDD_3-8	227.6	30.9	19	4.94
βCDC-4	228.1	7.8	80	3.25
βCDC-8	228.9	15.4	82	5.49
βCDE-4	227.7	18.4	20.44	2.85
βCDE-8	227.5	41.9	8.9	1.82

Cyclodextrins: αCD: α-cyclodextrin; βCD: β-cyclodextrin; γCD: γ-cyclodextrin; 2-HPβCD: 2-hydroxypropyl-β-cyclodextrin; Vitamins: D_3: vitamin D_3/ cholecalciferol; C: vitamin C/ ascorbic acid; E: vitamin E/ α-tocopherol; Inclusion Complexes: αCDD_3: α-cyclodextrin-cholecalciferol complex; βCDD_3: β-cyclodextrin-cholecalciferol complex; γCDD_3:γ-cyclodextrin-cholecalciferol complex; 2-HPβCDD_3:2-hydroxypropyl-β-cyclodextrin-cholecalciferol complex; βCDC: β-cyclodextrin-ascorbic acid complex; βCDE: β-cyclodextrin-α-tocopherol complex; Other: IE%=inclusion efficiency; SD: standard deviation.

4.3.8. Phase solubility studies of vitamin complexes

The intensity and of the vitamin D_3 UV_{max} peak at 265nm and the Absorbance (A) value was found to increase as the concentration of βCD in solution increased proving that the addition of CD will increase solubility of cholecalciferol. The change in the A value of an active in the presence of increasing concentrations of CD confirms complexation. Such an observation was also used to confirm inclusion complex formation between other actives and cyclodextrins by other researchers (Yang *et al*., 2008).

4.3.8.1. Cholecalciferol phase solubility-study 1

The change in the UV absorbance value of the vitamin in the presence of increasing concentrations of CD (βCD: 0-11mM; 72 hour mixing) confirmed complexation and

solubility transitions. It was noted that the solubility of vitamin D_3 increased linearly with an increase in the concentration of βCD until reaching a CD concentration of 3mM over 72 hours (Figure 4.13). However, as the concentration of βCD increased further (4-11mM), the solubility of cholecalciferol dropped suggesting the formation of an insoluble complex at higher βCD concentrations with a B-type solubility curve (Figure 4.13). A similar behaviour was noted by other researchers where it was suggested that βCD may lead to B-type curves due to this CD having the lowest aqueous solubility of the CD's (Zaibunnisa *et al*., 2011; Ruz *et al*., 2012). Other researchers noted this observation where self-aggregation was found to be dependent on concentration (Loftsson *et al*., 2007; Zaibunnisa *et al*., 2011; Ruz *et al*., 2012). Due to the fact that the solubility limit was reached at 3mM it is important to consider the volume of solvent used for complexation reactions via co-precipitation as well as the nature of the solvent to prevent insoluble aggregate formation. Although the solubility limit was reached at 3mM concentration of βCD followed by a decline, it was evident that a gradual rise in solubility occurred again in the latter part of the study (from 7-11mM βCD) as is observed in Figure 4.13.

4.3.8.2. Cholecalciferol phase solubility-study 2

The second part of the phase solubility study conducted with cholecalciferol confirmed a linear phase solubility curve at lower βCD concentrations (βCD range of 0.25-1.75mM). Cholecalciferol concentrations increased linearly with increasing concentrations of the βCD. The observations elucidated the effect of blending time (βCD 0.25-1.75mM; 24hr then 72hr mixing). Analysis at 24 hours and subsequent additional blending and re-analysis of the same samples at 72 hours revealed a further solubility enhancement due to extended mixing times (Figure 4.14). The phase solubility diagram in this study were classified as an A_L type with the synthesis of 1:1 complexes, according to the method described by Higuchi and Connors (Higuchi and Connors, 1965), showing the synthesis of a soluble vitamin inclusion complex at lower CD concentrations (Ruz *et al*., 2012). The linear host-guest correlation coefficient R^2 was 0.9729.

The apparent solubility constant (K_a) was calculated for the cholecalciferol system in study 2 at 72 hours using the phase solubility profile and Equation 4.2 (Loftsson *et al*., 2007; Ruz *et al*., 2012):

$$K_a = \frac{Slope}{S_0(1-Slope)}$$ [Equation 4.2]

-where S_0 is the solubility of cholecalciferol when no CD is present and the slope is derived from the phase solubility plot after 72 hours in Figure 4.14.

The apparent stability constant $K_{1:1}$ of the complexes obtained from the solubility plot at 72 hours was -58.45M^{-1} (Figure 4.14). The S_0 value for cholecalciferol was computed to be 0.019mg/mL. The difference in the slopes obtained for samples mixed for 24 hours and 72 hours in Study 2 (Figure 4.14) reveal the variable nature of Ka that was highly dependent on experimental conditions, solvent, and intrinsic solubility of the bioactive (Loftsson *et al*., 2007). The difference between the two curves in Figure 4.14 illustrated the importance of the blending process. Blending the vitamins for 72 hours with βCD at varying concentrations (0.25-1.75mM) resulted in a 5-8 times higher solubility enhancement of cholecalciferol vs. a 24 hour blending period at the same CD concentrations.

Overall, the water-insoluble bioactive, cholecalciferol was successfully solubilized to varying extents after complexation with βCD to a maximum of value of 36.84ug/mL or 1474IU/mL in a predominantly aqueous medium (water: ethanol (9:1$^{v}/_{v}$)). Phase solubility data has suggested that both inclusion and non-inclusion complexes are formed between CD's and vitamins due to IC's and aggregates of different types that co-exist as in aqueous media and each have individual true stability constants (Loftsson *et al*., 2007). As done so in the current study, phase solubility may be used to:(i) quantify the power of solubilization that is afforded to a bioactive following complexation, (ii) to detect the molar limit of CD to be added during synthesis, or (iii) during the screening stages to confirm or deny the ability of a specific bioactive to bind with a selected cyclodextrin molecule prior to formulation design.

4.3.8.3. Ascorbic acid phase solubility

The phase solubility curve for the ascorbic acid solutions at increasing concentrations of βCD (βCD 0-10mM; 72 hour mixing) revealed a strikingly similar phenomena for ascorbic acid as observed for cholecalciferol (Figure 4.15). Even though the physicochemical properties of ascorbic acid differ to that of cholecalciferol, the hydrophilic vitamin actually demonstrated a similar B-type curve which was unexpected (Figure 4.15). As with cholecalciferol, phase solubility demonstrated that ascorbic acid solubility was enhanced up to 3mM concentrations of βCD followed by a subsequent reduction in solubility. Other researchers have

noted similar phase-solubility profiles with other drugs complexed to βCD where the ascending part of the curve is followed by a descending portion due to precipitation of complexes past a specific CD concentration (Hashem *et al*., 2013). However, the solubility of the vitamin increased again from 5-10mM concentrations of the CD. A similar rise, although less pronounced, was also observed for cholecalciferol solutions from 7-11mM as depicted in Figure 4.13.

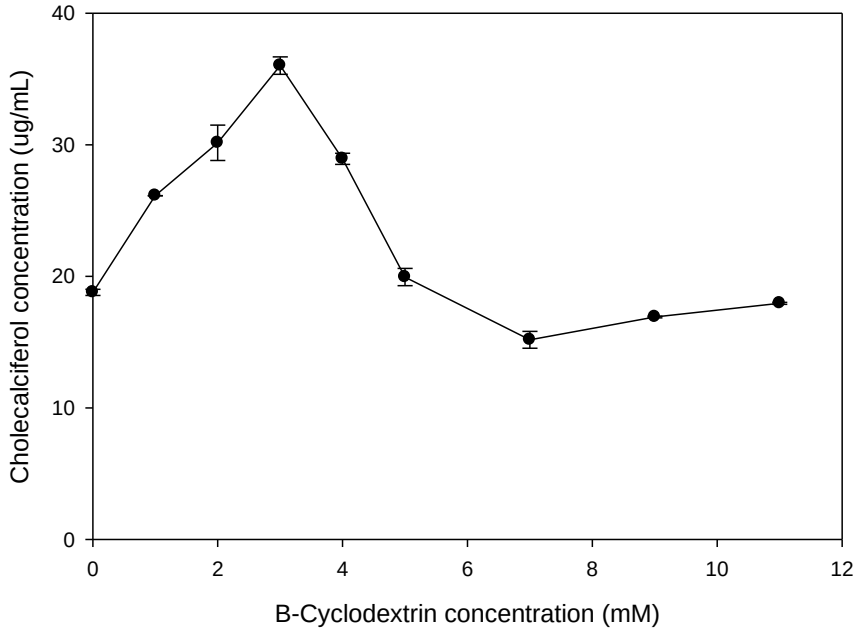


Figure 4.13: Effect of βCD concentrations on the aqueous solubility of vitamin D_3 after 72 hours of blending (βCD 0-11mM).

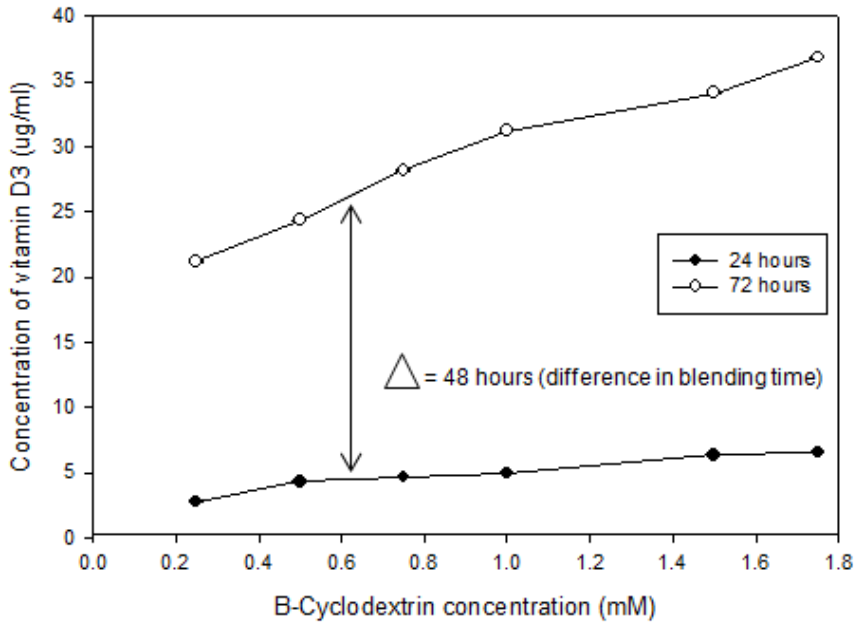


Figure 4.14: Effect of mixing time on the aqueous solubility of cholecalciferol after 24 hours and then after 72 hours of blending (βCD 0.25-1.75mM).

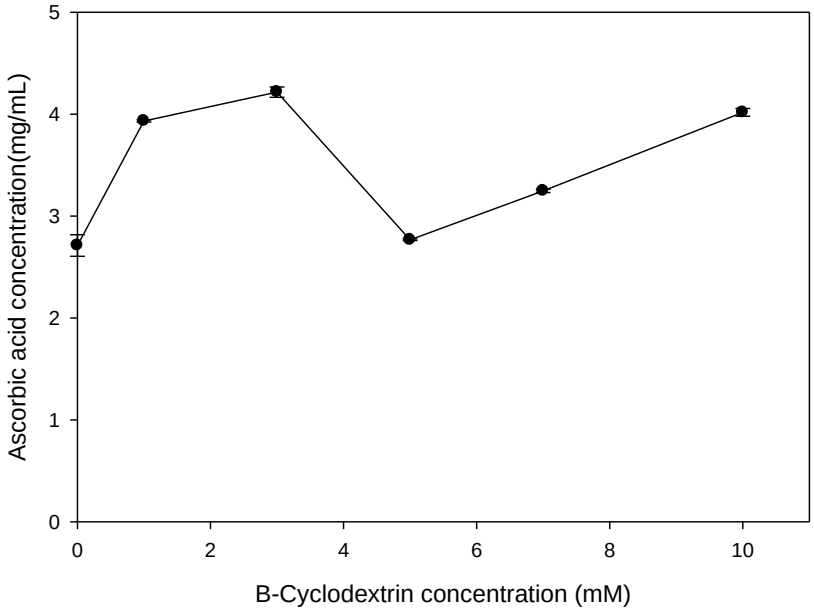


Figure 4.15: Effect of βCD concentrations on the aqueous solubility of ascorbic acid after 72 hours of blending (βCD 0-10mM).

4.3.8.4. Vitamin phase solubility implications for BAP formulation development

Phase solubility studies with the two vitamins, cholecalciferol and ascorbic acid, highlighted an interesting phenomenon that has the potential to be harnessed to adjust solubility parameters of two vastly different BCS class vitamins. Data suggested that complexation with βCD may assist in a strategy to release both vitamins in concert by virtue of a cyclodextrin-mediated modifiable aqueous solubility phenomena. This may be facilitated by varying the synthesis conditions, CD types and CD concentrations to achieve specific complexes with aligned or modified solubility for inclusion in the BAP. By manipulating synthesis conditions it may be possible to increase the solubility of one agent and slow the aqueous solubility of another to harmonize release. The B-type curve for ascorbic acid IC's demonstrate an area of reduced solubility, which correlates with the visual observation tests under section 4.3.2 that noted slightly milky solutions of the ascorbic acid complexes. Other studies have suggested how drug release may be intentionally mediated by "fine-tuning" ratios of CD's (Jansook *et al.*, 2010). Instead, the preliminary findings of the current study suggested an ability to align solubility and hence the release behaviour of two vitamins to be included in the BAP. The phase solubility results therefore form the basis of a concept to administer two or more

vitamins with varied physical properties in one formulation to obtain a unified release profile for a “maximal optimal synergistic nutrotherapeutic paradigm” with vitamin D_3 being the primary therapeutic agent in the BAP.

It is hypothesized that, through the continuum of phase solubility and careful control of experimental parameters, different types of vitamin IC’s are possible with enhancing or impeding effects on the parent vitamins inherent solubility. Phase-solubility data therefore provided useful insights into the design of a BAP formulation containing different vitamin IC’s to achieve analogous oral release even when hydrophobic and hydrophilic actives are co-incorporated.

4.3.9. Microbead bioactive complexes: Entrapment efficiency (EE)

4.3.9.1. Chitosan bioactive microbeads: Entrapment efficiency

It is evident from the EE results (Table 4.12) that complexing anionic bioactives (DA, CA and LT) with the cationic polymer, chitosan, resulted in a polyelectrolyte complex that did not swell substantially enough to release sufficient bioactive. Chitosan complexed tightly with anionic bioactives DA, CA and LT irreversibly. Thus a very low concentration of bioactive was detected and low EE values were reported for all three bioactives (mean EE: 3.81%). It was concluded that chitosan is not an ideal polymeric carrier for DA, CA, and LT due to low entrapment efficiency (Table 4.12). It is important to note that the values listed in Table 4.12 for Chitosan may be an underestimate of the amount of drug entrapped as, in addition to leaching out during preparation, some drug may be irreversibly bound to the polymer and not released into solution for quantification.

4.3.9.2. Alginate bioactive microbeads: Entrapment efficiency

In comparison, the use of alginate as a bead carrier provided moderately improved concentrations of bioactive when the DA-Alg, Ca-Alg and LT-Alg were placed in solution and allowed to swell to release the bile acids and lecithin (Table 4.12). The mean entrapment efficiency values were higher for the alginate complexes compared to their respective chitosan counterparts (Table 4.12). These results indicated that alginate was a more suitable polymer for entrapment and release of cholic acid, deoxycholic acid and lecithin from alginate microbead bioactive boosters. The mean EE for all three alginate microbeads was 16.82% vs. 3.81% of the chitosan microbeads. Despite a notable increase in mean EE when using alginate instead of chitosan as the microbead matrix, the entrapment value for

lecithin remained consistently low with only a marginal improvement (5% vs. 3.65%). Loading beads with higher amounts of bioactive was investigated to determine whether the addition of more bioactive would result in a higher loading efficiency. Three-fold the amount of bioactive was added during experimental synthesis (225mg instead of 75mg of DA, CA and LT). Experimental addition of more bioactive to alginate resulted in even lower EE values indicating that EE reached a saturation point and further bioactive addition did not translate into improved EE without pursuing further modifications of experimental procedures. Figure 4.16 illustrates the EE% calculated for the amount of bioactive released from chitosan and alginate microbeads.

Table 4.12: Mean EE values obtained for polymer microbead formulations

Formulation	Entrapment Efficiency (EE) (%)
Chitosan-bioactive microbeads:	
Deoxycholic acid-chitosan beads (DA-CHI)	4.19 (SD: 0.25)
Cholic acid-chitosan beads (CA-CHI)	3.59 (SD: 0.30)
Lecithin-Chitosan beads (LT-CHI)	3.65 (SD: 0.26)
Mean EE of all 3 bioactives entrapped in Chitosan beads	**3.81%**
Alginate-bioactive microbeads:	
Deoxycholic acid-alginate beads (DA-Alg)	22.83 (SD:1.95)
Cholic acid-alginate beads (CA-Alg)	22.63 (SD: 2.07)
Lecithin-alginate beads (LT-Alg)	5 (SD: 0.41)
Mean EE of all 3 bioactives entrapped in Alg beads	**16.82%**

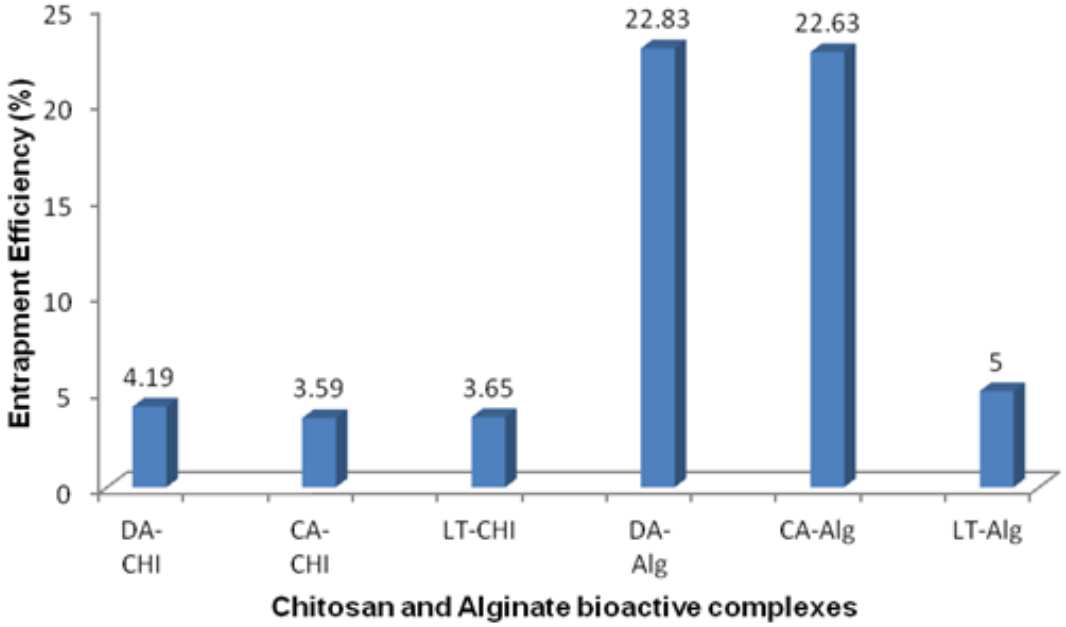


Figure 4.16: Bar chart illustrating the EE values obtained for all polymer-bioactive microbead complexes.

4.3.10. Chemical structure analysis of polyelectrolyte microbead complexes by Fourier Transform Infrared Spectroscopy (FTIR)

The bile acid FTIR spectra were in accordance with previously reported observations for CA and DA (Yang *et al*., 2005; Mooranian *et al*., 2014). The spectra of CA-CHI and DA-CHI microbeads showed weaker band intensities compared to the spectra of the individual compounds with less bond-peak activity being evident in the complexes (Figure 4.17a and b). A similar reduction in the FTIR spectra activity was observed by other researchers when alginate was combined with cholic acid (Mooranian *et al*., 2014). For both alginate and chitosan bile acid microbeads, the narrow peaks of CA and DA in the OH stretching region ($3600cm^{-1}$-$3000cm^{-1}$) disappeared in the microbeads to become one broad band that occurred at a lower frequency ($3295cm^{-1}$). The broad OH stretching band was flattened for the chitosan microbeads but was larger and distinctly prominent for the alginate microbeads (Figure 18a and b). The difference in the intensity of the shifted OH stretching band between the chitosan and the alginate beads may reflect differences in entrapment efficiency of the bile acids in each polymer. As discussed in section 4.39 alginate microbeads had a larger EE and thus a high hydroxyl peak intensity may be indicative of a larger quantity of bile acid entrapped within this microbead. Also noticeable was that the CH vibrations - characteristic for CA and DA at $2966cm^{-1}$ and $2927cm^{-1}$ (Yang *et al*., 2005) respectively, became greatly reduced in intensity

in the microbead complexes (Figure 4.17 and Figure 4.18). The carbonyl group of the COOH stretching bands are represented by sharp peaks in cholic acid and deoxycholic acid at 1712cm^{-1} which subsequently disappeared in the spectra of the polymeric microbeads (Figure 4.17 and 4.18).

LT-CHI beads also revealed a reduced intensity to the spectra of the individual constituents. Peaks at 1750cm^{-1}, 1650cm^{-1} and 1560cm^{-1} are due to the presence of both chitosan and lecithin in the LT-CHI microbeads, in agreement with data reported by other researchers (Chadha *et al*., 2012). The lecithin C=O peak at 1750cm^{-1} became greatly reduced in intensity in the spectrum of the LT-CHI microbeads. The LT peaks at 968.2cm^{-1} and 1241.9cm^{-1} represented stretching vibrations of $^{+}N(CH_3)_3$ and P=O respectively (Wang *et al*., 2013). These researchers noted a reduction in the intensity of the P=O peak and a disappearance of the $^{+}N(CH_3)_3$ peak (Wang *et al*., 2013). The LT-CHI microbeads saw a similar shift in the FTIR band at 1241.9cm^{-1} to a lower frequency of 1225.1cm^{-1} and an $^{+}N(CH_3)_3$ peak that conglomerated with another peak almost disappearing in a similar fashion.

In summary, the FTIR spectra (Figures 4.17 and 4.18) show evidence of complexation by virtue of the fact that the microbead complexes have very different and unique FTIR spectra with the disappearance, transition or change in intensity of characteristic CA, DA or LT bands as discussed.

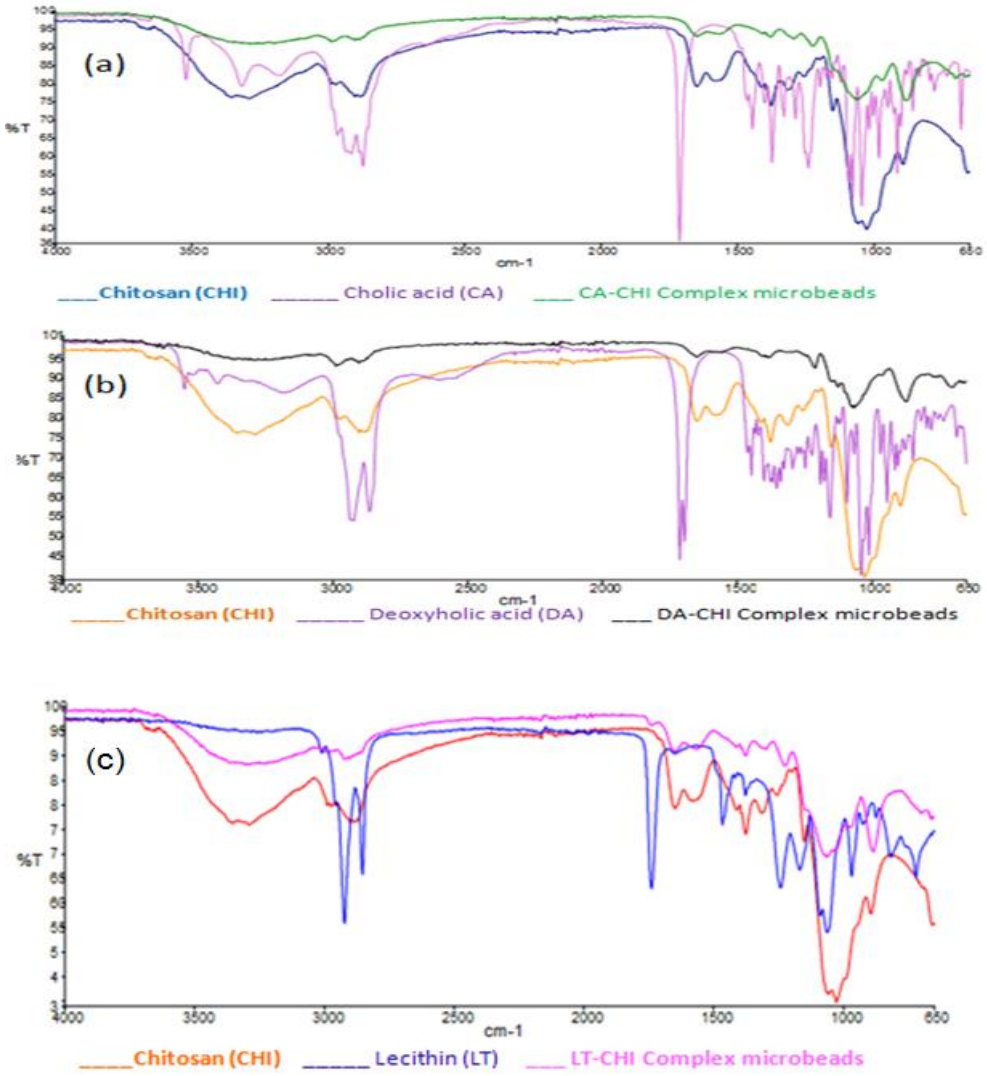


Figure 4.17: FTIR spectra of (a) chitosan (CHI), cholic acid (CA), and CA-CHI complex microbeads; (b) chitosan (CHI), deoxycholic acid (DA), and DA-CHI complex microbeads; (c) chitosan, lecithin, and lecithin-chitosan complex (LT-CHI).

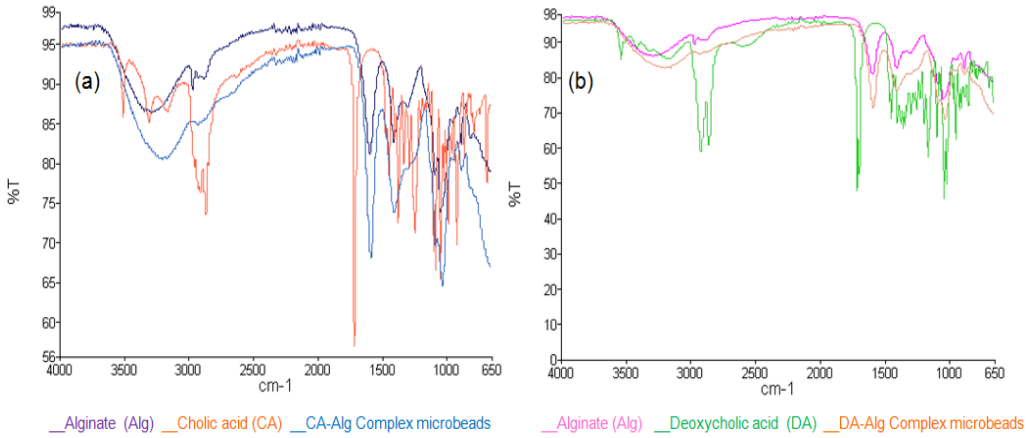


Figure 4.18: FTIR spectra of (a) alginate (Alg), cholic acid (CA), and CA-Alg complex microbeads; (b) alginate (Alg), deoxycholic acid (DA), and DA-Alg complex microbeads.

4.3.11. Thermodynamic analysis of microbead complexes by Differential Scanning Calorimetry (DSC)

Figures 4.19 and 4.20 show the DSC thermograms of the native bioactives (lecithin, deoxycholic acid and cholic acid), chitosan, alginate, and the resultant chitosan and alginate microbeads.

The bile acids (cholic acid and deoxycholic acid) exhibited distinct high melting points indicative of crystalline compounds, yet their complexes revealed intermediate type endothermic peaks between that of the bile acids and the polymers. Bile acid complexes revealed right shifted endotherms compared to their respective polymers (chitosan or alginate) (Figure 4.19d and 4.20c). The microbead complexes of CA, DA and LT revealed flattened, right-shifted endotherms characteristic of amorphous substances (Figure 4.19 and 4.20). CA powder had a defined endothermic melting point at 217°C (Figure 4.19a) during chitosan bead studies and at 204°C in alginate bead studies (Figure 4.20a). DA revealed endothermic melting points at 175^{o}C (Figures 4.19 and 4.20). The CA endotherm was in alignment with the CA peak reported by other researchers who also noted CA's endotherm to be in the region of 201°C-204°C (Caira *et al*., 1994). Recently other groups have reported bile acid endotherms at similar temperatures (CA: 200°C and DA: 178°C) (Mooranian *et al*., 2014).

A high melting point of the bile acids, although beneficial to thermal stability, may be detrimental during dissolution because highly crystalline structures take longer to dissolve than amorphous compounds. Such physical characteristics may result in slow or even incomplete dissolution and therefore inadequate dispersion and release into physiological media for intended surfactant activity of the bile acids. Both cholic acid polymeric beads, CA-CHI and CA-Alg, showed no sign of the CA peak due to a shift in thermal behaviour as a result of interactions with chitosan and alginate. The DA endotherm at 175°C also disappeared in the DA microbead complexes of chitosan and alginate. An endothermic shift and disappearance of the bile acid peaks and the presence of a single unified peak was also noted in two studies conducted by Mooranian and co-workers (2014) who formulated microcapsules containing CA or DA with alginate or chitosan and the antidiabetic agent, gliclazide. The disappearance of bile acid endotherms in the microbead complexes indicates the presence of a compound that is less crystalline with shifted thermal properties indicative of an amorphous compound with improved solubility. Similarly, the chitosan endotherm has been shifted to a higher temperature in the

CA-CHI and DA-CHI microbeads (Figure 4.19a, b, and d). These observations indicate interactions between the polymers and the bile acids. Sodium alginate powder revealed a wide endotherm water loss peak between 90^{o}C and 110^{o}C and a degradation exotherm at 240^{o}C. The disappearance of the alginate degradation exotherm in the DA-Alg and CA-Alg microbeads provided further evidence to indicate complexation between the bile acids and alginate (Figure 4.20) (Takka and Cali, 2012).

Figure 19c depicts a very early endothermic peak for LT that occurred at approximately 20°C which is of concern if one was to include this bioactive in a formulation uncomplexed. LT would be highly susceptible to degradation with such a low melting point. Uncomplexed lecithin would most likely melt and degrade within a delivery vehicle prior to reaching the site of dissolution in the GIT. The LT thermogram also revealed a degradation that occurred from about 145^{o}C (Figure 4.19c). Complexation with chitosan succeeded in increasing lecithin's resilience to heat as observed in the thermogram of the LT-CHI complex that demonstrated a right shifted flattened endotherm without the early LT peak (Figure 4.19c). Similarly the water loss endoderm of chitosan has been right-shifted in the LT-CHI microbead complex (Figure 4.19d). The observed stable thermal properties of the LT complexes without degradation would impart an ability to withstand thermal variations that may otherwise lead to premature degradation and reduced efficacy. Furthermore, the inclusion of a constituent that is vulnerable to thermal degradation may compromise the integrity of other bioactives co-formulated.

Preliminary thermal analysis therefore confirmed complexation/ interaction between CA, DA and LT and the polymers (chitosan and alginate) and an improved robustness to heat, highlighting preference for complexes instead of uncomplexed CA, DA and LT as BAP constituents.

Figure 4.19d and 4.20c shows three markedly different DSC curves for the bioactive-chitosan and bioactive-alginate microbeads when compared to their individual constituents. It was evident that an interaction occurred between the bioactives and polymers due to dissimilar thermograms. Changes in physical behaviour, in response to heat, of the polyelectrolyte complexes evidenced by differences in endothermic and exothermic curves, confirmed complexation.

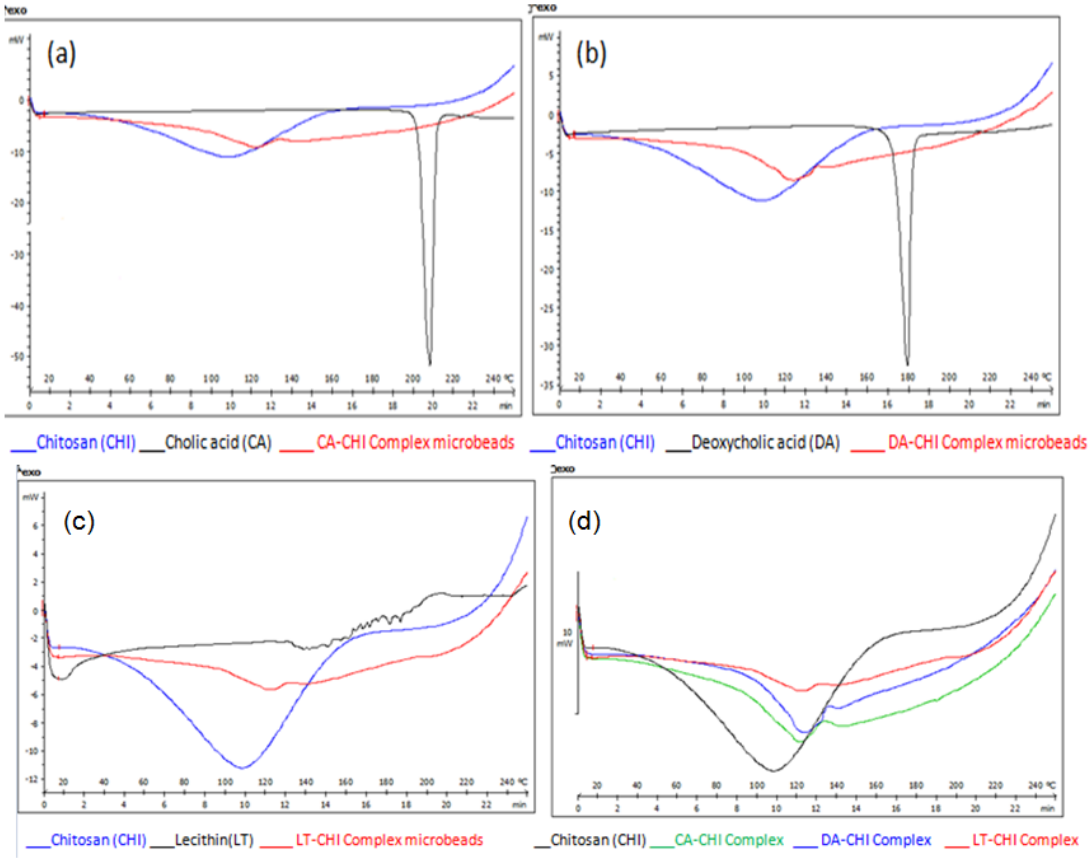


Figure 4.19: DSC profiles of (a) chitosan (CHI), cholic acid (CA) and CA-CHI complex microbeads; (b) chitosan (CHI), deoxycholic acid (DA) and DA-CHI complex microbeads; (c) chitosan (CHI), lecithin (LT) and LT-CHI complex microbeads; (d) chitosan, CA-CHI microbeads, DA-CHI microbeads, LT-CHI microbeads.

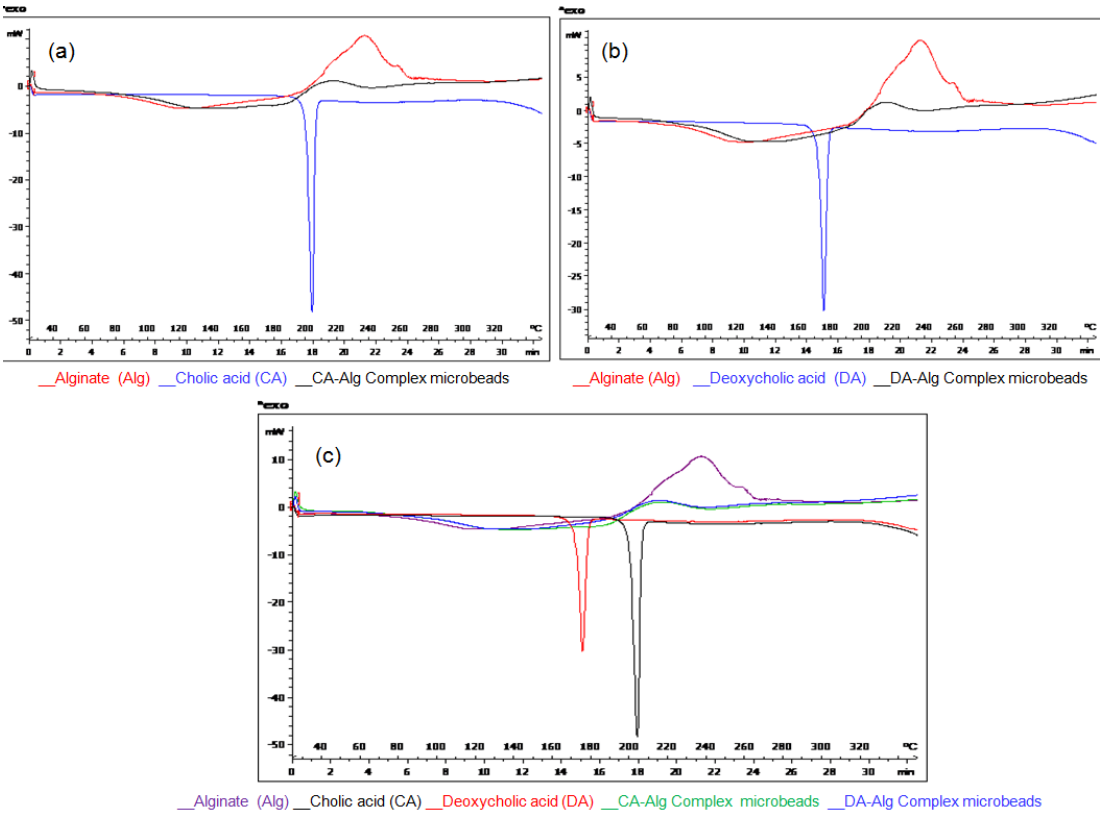


Figure 4.20: DSC profiles of (a) alginate (Alg), cholic acid (CA), CA-Alg complex microbeads; (b) alginate (Alg), deoxycholic acid (DA), DA-Alg complex microbeads; (c) alginate (Alg), cholic acid (CA), deoxycholic acid (DA), CA-Alg complex microbeads, DA-Alg complex microbeads.

4.3.12. Microbeads as suitable BAP candidates

FTIR and DSC analysis confirmed an interaction between the microbead polymers and cholic acid (CA), deoxycholic acid (DA) and lecithin (LT). Due to low initial EE values obtained with LT chitosan beads (which marginally improved with alginate), no characterizations were conducted with LT-Alg microbeads. As observed by other research groups, it is a common phenomenon for drug to leach out of polymeric microbeads during the formulation process (George and Abraham, 2006). Similarly this observation was deemed a noticeable limitation in the current study when chitosan and alginate beads were utilized to entrap CA, DA, and LT. It has been reported that enzyme bioactives suffer leakage from the porous polymeric matrices (Won *et al*., 2005). For this reason no further attempts were made to include other BAP bioactives, such as enzymes or hormones. Despite alginate beads achieving markedly improved EE values for CA and DA compared to chitosan beads, the BAP concept required a more efficient entrapment of bioactives with the assurance of maximal bioactive retention during formulation and no risk of loss during manufacture. Microbeads are known to be problematic carriers unless the leaching

phenomenon is overcome by coating surfaces of polymeric crosslinked beads with other polymers including, silicate, DEAE-dextran, proteins or chitosan, to reduce porosity and drug leaching (Won *et al*., 2005; George and Abraham, 2006). Such an additional formulation step was not considered viable since the BAP concept already involved multiple procedures and carrier constituents. It was also noted that bile acids, CA and DA, may not be the most ideal bile constituents owing to certain physico-chemical limitations. Bile acids are only slightly soluble in aqueous media and thus may not dissolve adequately to allow for accurate quantification or for an efficient diffusion process when released from the formulation. The solubility limitation of bile acids was considered critical when selecting final bile constituents to impart the necessary surfactant effects on the model drug, thus alternative salt forms were considered attractive for further investigation. Bile salts have improved aqueous solubility and would disperse within the aqueous environment in a more efficient manner. When evaluating the future commercial manufacturing processes, microbead synthesis was considered difficult to scale up and therefore this dosage form was discarded from further BAP development studies due to such challenges.

4.3.13. Bile salt-alginate scaffolds release studies

The mechanism of bioactive release from scaffolds follows a documented process: When scaffolds are added to dissolution media, divalent cations are lost to the solution, causing the subsequent degradation of each crosslinked scaffold and the subsequent dissolution of the alginate scaffold and release of entrapped bioactive. The degradation rate of each scaffold may be controlled by the extent of crosslinker included in the device and the concentration of polymer. It has been noted that the "stress-strain response of a hydrogel is dependent upon three factors: (i) the extent of crosslinking, (ii) the porous structure of the matrix, and (iii) the water flow within" (Grondahl *et al*., 2010). Since all scaffolds were synthesized using the same methods and materials and the dissolution study parameters were maintained as identical for each sample, any differences observed in the bioactive-scaffold release profiles were attributed to the extent of crosslinking or to the bioactive-alginate interaction.

4.3.13.1. Preliminary bile salt scaffold release studies

Figure 4.21 shows images of the preliminary release study from synthesized alginate bile scaffolds. The preliminary results showed a more rapid release of sodium dexoycholate from scaffold containing no crosslinker and the slowest release from scaffold containing 1%$^{w}/_{v}$ calcium gluconate crosslinking agent (Figure

4.22). The 0.5%$^{w}/_{v}$ crosslinked scaffold produced a bile salt release profile that was intermediate to the 0%$^{w}/_{v}$ and 1%$^{w}/_{v}$ formulations. These observations were consistent with the amount of crosslinking agent contained within the polymer matrix. Since the degree of crosslinking within alginate scaffolds influences the diffusion efficiency of a bioactive within a hydrogel, these results are in line with other studies (Lin *et al*., 2010). Since bile salt release from alginate scaffolds has never been quantitatively studied and compared, these results add value information to formulation science. The 0.5%$^{w}/_{v}$ cross-linked NaD scaffolds demonstrated an intermediate type release are were selected for further release studies with NaD and NaC bile salts using a modified USP 2 dissolution method.

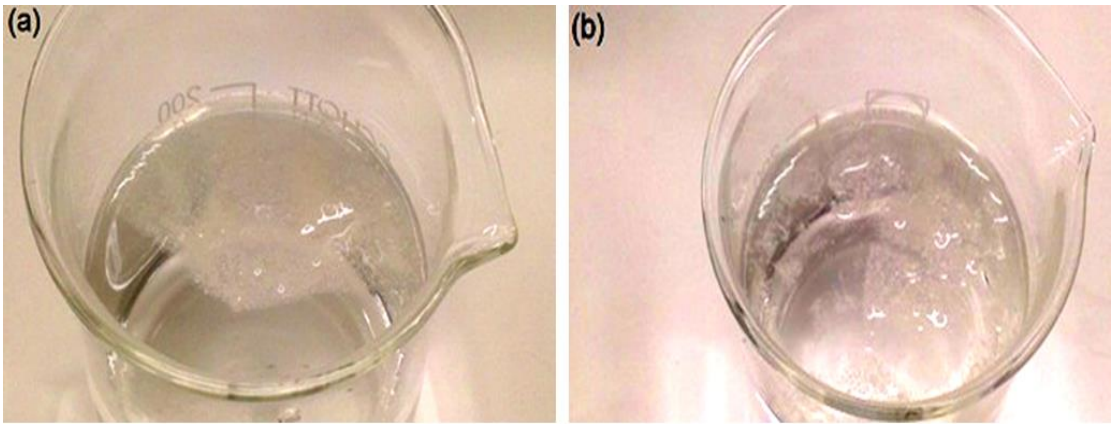


Figure 4.21: Preliminary release testing of Na dexoycholate- 4%$^{w}/_{v}$ alginate scaffold (0.5%$^{w}/_{v}$ CL) at (a) 30 minutes and (b) 3 hour time points. It was evident that at 30 minutes the scaffold had hydrated, expanded and was fully submerged but was still an intact single mass. By 3 hours the scaffold integrity was lost with separation into fragmented parts allowing the majority of the bile salt to be released into solution.

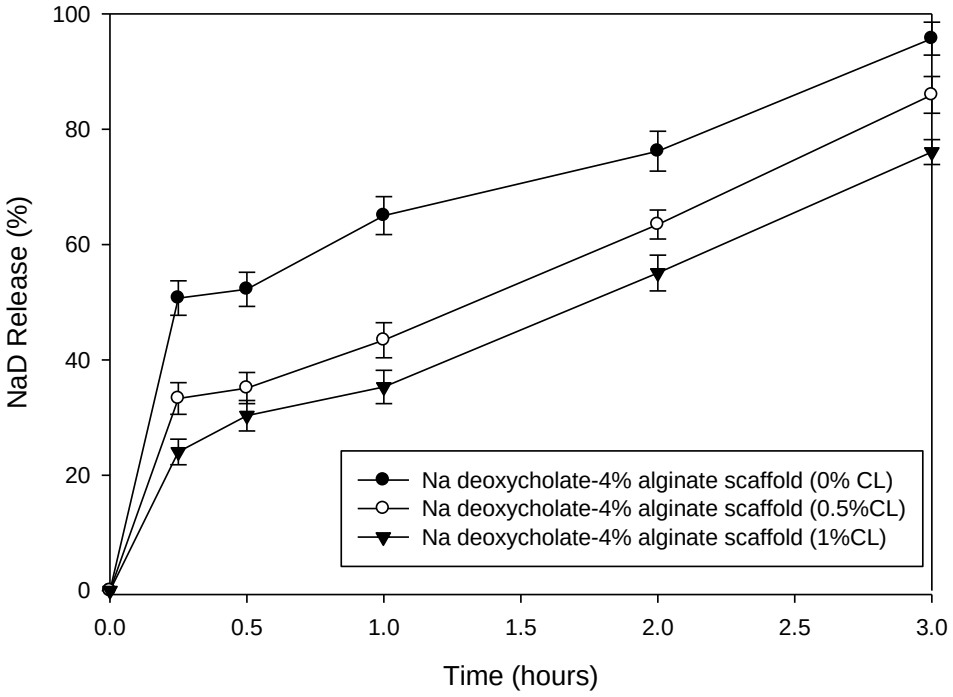


Figure 4.22: Preliminary bile salt release profiles of sodium dexoycholate (4%$^{w}/_{v}$ alginate) scaffolds containing crosslinker at varying concentrations (0%$^{w}/_{v}$, 0.5%$^{w}/_{v}$, 1%$^{w}/_{v}$) in 200mL phosphate buffer (pH 6.8).

4.3.13.2. Final bile salt-alginate scaffold release studies: USP method

The intermediate release profile obtained during preliminary release testing of NaD scaffolds (Figure 4.22) prompted the use of NaD and NaC scaffolds containing 0.5%$^{w}/_{v}$ calcium gluconate crosslinker for a comparative evaluation between the two different bile salts using a USP dissolution method. The subsequent USP dissolution testing of the 0.5%$^{w}/_{v}$ crosslinked bile salt scaffolds resulted in successful controlled release profiles for both bile salts with no evidence of bile salt "dose dumping" (Figure 4.23). Both sodium deoxycholate and sodium cholate scaffolds were compared in a 3 hour USP dissolution study to evaluate the differences in the respective bile salt release profiles from polymeric scaffold of the same composition. As corroborated by other research groups, both scaffolds produced an initial burst release of bile salts with 32-33% of NaD and NaC being released within the first 15 minutes (Lin *et al*., 2010) (Figure 4.23). However, sodium cholate was released at a more rapid rate with nearly 60% of the bile salt being released within 30 minutes. The sodium dexoycholate scaffold released only 36% of bioactive within 30 minutes. Both scaffolds had similar initial burst profiles (T_0-T_{15} mins), however by 1 hour the NaC scaffold had achieved almost twice the quantity of bile salt release compared to

the NaD scaffold (83.95% vs. 43.4%). The quantity of bile salts released by 3 hours was similar between scaffolds with the NaD scaffold reaching 85% vs. 92% for the NaC formulation. In summary, a more gradual release profile was observed for sodium deoxycholate compared to the sodium cholate hydrate when crosslinked with the same crosslinking agent within the same alginate ($4\%^{w}/_{v}$) polymer matrix (Figure 4.23). The more rapid release profile of the NaC scaffold may be explained by a higher aqueous solubility of the sodium cholate hydrate salt compared to sodium deoxycholate salt. NaC is more hydrophilic than NaD which would explain the differences in release rates (Subuddhi and Mishra, 2007). From the results obtained from the bile salt scaffolds, the sodium cholate hydrate scaffold released bile salt at a higher rate, reaching 82% release within 60 minutes and a total of 92% released by 3 hours. The sodium deoxycholate release profile was less rapid with 42% bile salt released within the first 60 minutes up to a maximum of 85% by 3 hours (Figure 4.23). Both profiles were favourable for a controlled release of bile salts within the duodenum.

Other research groups have incorporated bile salts as passively-delivered excipients to enhance the intestinal permeability and bioavailability of lipophilic and hydrophilic drugs (Sharma *et al*., 2005; Samstein *et al*., 2008; Mahajan *et al*., 2012). Instead the current study demonstrated how bile-salt scaffolds may be utilized as controlled release mechanisms for the provision of bile components to the GIT at a pre-defined and modifiable rate. Such a customizable release system may be used to mimic the physiological release of bile constituents in response to food to assist in the absorption of fat-soluble vitamins from the BAP. Other researchers have successfully tested the effect of bile salt systems on increasing the solubility of non-ionisable drugs (Zughaid *et al*., 2012). Zughaid and co-workers (2012) found that as the concentration of bile salts increases so does the solubility of certain lipophilic drugs. The scaffolds formulated in the current research may offer similar advantages albeit in a more controlled manner because of the presence of crosslinker and specific polymer compositions within the release mechanism. The scaffolds were able to release predetermined amounts of bile constituents into solution at appropriate time intervals for improved solubility and permeability of bioactives dosed concomitantly or from the same DDS. Both scaffolds provided distinctly different but rapid release profiles of each bile salt. A rapid release profile is favourable for the provision of bile salts to the intestine to assist in the dissolution of fat-soluble bioactives by providing a type of “surfactant-bile salt reservoir” device.

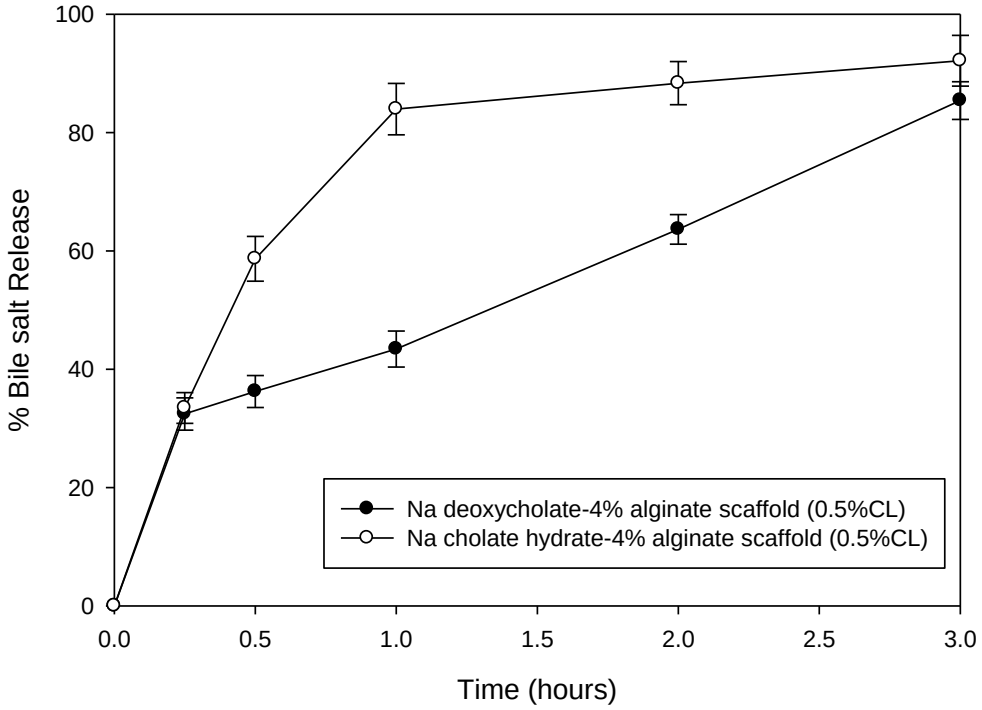


Figure 4.23: Release profile of bile salt alginate (4%$^{w}/_{v}$) scaffolds crosslinked with 0.5%$^{w}/_{v}$ calcium gluconate containing the bile salts: sodium deoxycholate or sodium cholate hydrate in phosphate buffer (SIF pH 6.8) (USP method: USP 2 Apparatus).

4.3.14. Pancreatic lipase-alginate scaffolds dissolution studies

Alginate has long since been used as an immobilization matrix for lipase, however very few studies have evaluated the release profile of this bioactive from alginate carriers (Hertzberg *et al*., 1992; Betigeri and Neau, 2002). It is clear from the dissolution profiles obtained in the current study that formulations with higher amounts of crosslinker impeded the release of pancreatic lipase from the scaffold component (Figure 4.24). The Lip-Alg (0%) scaffold containing no crosslinker was rapidly hydrated and swelled to release lipase at the quickest rate with maximum enzyme release achieved by the 7 hour time point (83%). The Lip-Alg (0.5%$^{w}/_{v}$) scaffold containing more calcium gluconate cosslinker demonstrated a dissolution curve that may be described as intermediate for the release of lipase, with 52% of the enzyme released within 7 hours. The slowest release profile was demonstrated from a scaffold with a crosslinked matrix of 1.25% calcium gluconate, and described as having a slow release rate delivering only 22% pancreatic lipase by the 7 hours.

The release profiles obtained for the lipase-alginate scaffolds demonstrated clearly the impact of varying the concentration of calcium gluconate crosslinker on the

release of pancreatic lipase from each formulation (Figure 4.24). These profiles were considered sufficient to make a decision regarding an appropriate release profile required in the BAP DDS without further formulation modifications as three diverse profiles were obtained. Other methods made be utilized to modify the matrix characteristics and scaffold geometry of alginate scaffolds further to suit the intended applications should this be required (Grondahl *et al*., 2010). Alginate scaffolds degrade in the presence of sodium ions in the physiological milieu and are therefore adept at releasing bioactives in a controlled rate over time. Other researchers have shown a sustained delivery and accelerated uptake of bioactives from specially developed alginate scaffolds (Wu *et al*., 2011), therefore an alginate scaffold was considered especially attractive for controlled delivery of pancreatic lipase as a component of the BAP DDS.

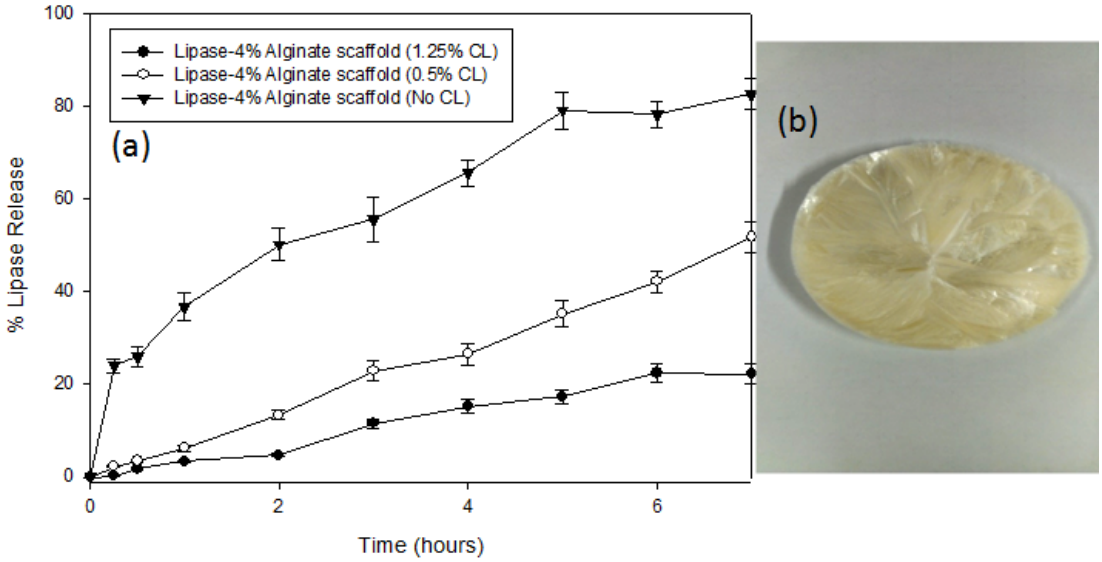


Figure 4.24: (a) *In vitro* release profile of different pancreatic lipase-alginate scaffold formulations in phosphate buffer (SIF pH 6.8) (USP 2 Apparatus); (b) Photographic image of a typical Lipase-4% Alginate scaffold (0.5%CL).

4.3.15. An artificial milieu environment using bile and lipase scaffolds

As discussed the various alginate polymeric scaffolds were optimized to release either bile salts (NaC and NaD) or pancreatic lipase at pre-determined rates based on crosslinker concentration. Patients with exocrine deficiencies or hepatic malfunction would benefit greatly from these polymeric structures that are able to mediate an exogenous supply of deficient enzymes or bile molecules without “dose dumping” for improved and sustained action from the delivery mechanism. A drawback to the use of scaffolds was the size of these devices and inability to bend and compress for successful inclusion in a multi-component capsule or tablet

dosage form. A possible solution that was proposed was the pre-administration of a bioactive-scaffold in discrete dispensed “biscuit portions” prior to dosing the model drug. Cholecalciferol would then be dosed in the BAP in a separate format directly following consumption of the pre-dose scaffold. Each scaffold may be further customized to suit an individual patients needs and would prove useful in enhancing the uptake of cholecalciferol if dosed concomitantly or shortly prior to taking a supplemental dose of the vitamin component of the BAP. The administration of scaffold devices could provide an artificial means to release bile and pancreatic lipase to mimic the normal physiological GIT mechanisms. Figure 4.25 shows the overlaid release profile of bile salts and lipase if both devices were dosed by a patient. Since pancreatic and bile deficiencies are associated with fat-soluble vitamin malabsorption, the customized delivery of these components from scaffolds would enhance the absorption of cholecalciferol. Since alginate is pH responsive and releases most of the embedded actives preferentially at duodenal pH, the scaffold would provide suitable protection from gastric degradation and a targeted intestinal release. Imperative to any successful enzyme therapy is the need to provide consistent dispersion of bioactive throughout the digestion phase. This would ensure maximal exposure of the model drug to the enzyme and bile fractions. Since the bile and lipase profiles depicted in Figure 4.25 illustrate linear time-release curves a consistent 1^{st} order response may be guaranteed by the novel BAP scaffold candidate. Additionally, conventional enzyme and bile replacement therapy are not without adverse effects that are predominantly caused by high dose dumping and mucosal tissue damage. The consistent controlled supply of bile and lipase from the BAP scaffolds would offer clinical advantages by minimizing deleterious effects and improving cholecalciferol bioavailability.

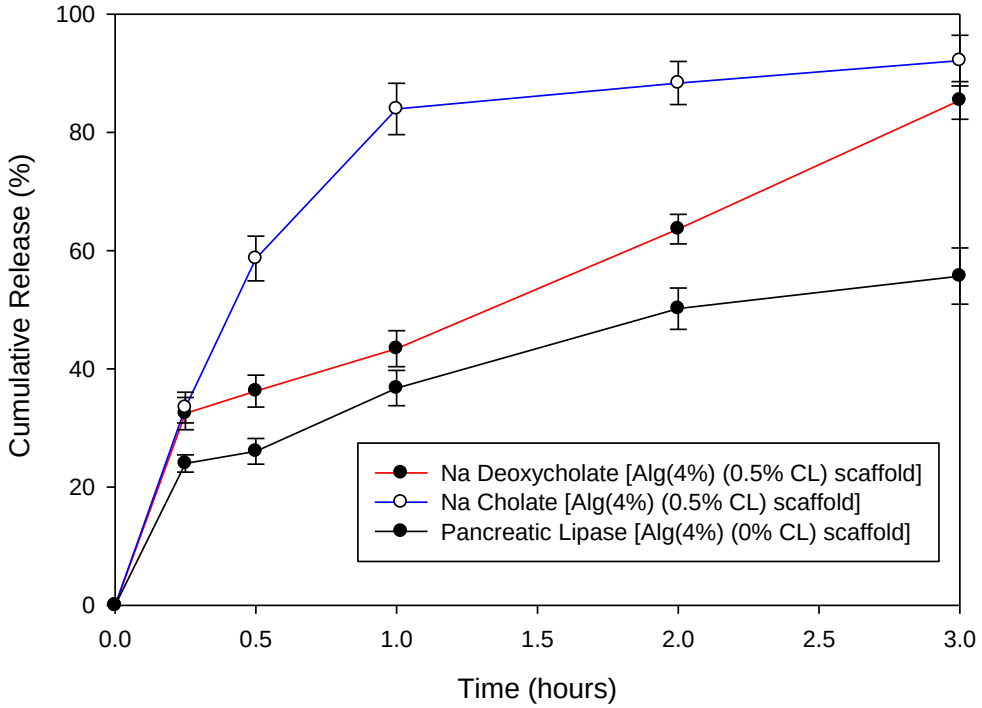


Figure 4.25: Overlaid scaffold release curves showing the release profiles of two bile salts (NaD, NaC) and pancreatic lipase from customizable polymeric scaffolds.

4.3.16. Rheological properties of film forming solutions

Rheological analysis of solutions of alginate-bile salt and alginate-lipase gels and gels containing varied combinations of all three bioactives was performed prior to crosslinker addition and drying to form films. This study was undertaken to determine the elastic (G') and viscous (G") modulus as a function of frequency. Figures 4.26-4.29 illustrate oscillatory frequency sweeps of different alginate film-forming solutions/ pregels containing varying amounts of plasticizer and bioactives (lipase, NaC, NaD). The crosslinker and plasticizer effect on alginate gels has been documented but the effect of lipase and bile salts on rheological characteristics of gels has yet to be elucidated. The mechanical properties of the resultant polymer matrix is said to have a direct effect on drug release properties and was therefore a pertinent parameter to be quantified.

4.3.16.1. Rheology: General observations

In general, the addition of lipase, bile salts or the combination thereof lowered the viscosity (η) of the pregels prior to cross-linking and film formation. However, for all profiles G" (viscous modulus) was greater than G' (elastic modulus) as the

frequency increased, and both moduli were frequency dependent, which is a documented characteristic of pregels (Bonino *et al.*, 2011). Greater G" throughout the studies meant that all solutions were predominantly viscous and less elastic in nature. Since crosslinker was not present both moduli never intersected to reach the same value as would have been expected on gelation post crosslinking (Bonino *et al*., 2011). Other researchers have confirmed that alginic acid gels are considered viscoelastic (Draget *et al*., 2003). It was also observed that at the highest frequencies, all solutions became predominantly viscous losing all elastic properties entirely (Figures 4.26-4.29)

4.3.16.2. Rheology: Bioactive combination pregels (NaD, NaC, and Lip)

The addition of both bile salts and pancreatic lipase in equal combination to a gel solution (lipase, sodium dexoycholate or sodium cholate hydrate) had no effect on the viscosity (G") of the gel samples regardless of quantity of bioactive added, with G" remaining constant throughout the study (Figures 4.26-4.29). However, elasticity (G') varied distinctly according to gel composition. Gel solutions without bioactive (4%A, 4%A2%G and 4%A4%G) lost elasticity at or before a frequency of 10rad/s (Figures 4.26-4.28). Compared to the "bioactive-free" gels, a marked contrast was observed with pregels containing bioactives where the G' (elasticity modulus) continued at higher frequencies (Figure 4.26b; Figure 4.27b and c; and Figure 4.28b). When the same alginate/ plasticizer composition was used ($4\%^{w}/_{v}A$/ $2\%^{v}/_{v}G$) and combination drug was increased progressively from 50mg (low dose) to 200mg (high dose) a dramatic increase in elasticity was noted at higher frequencies (Figure 4.27b vs. Figure 4.27c). The maximum elasticity point in 4%A2%G Comb50 was 17 (G') vs. 70 (G') for 4%A2%G Comb200. Therefore the combination of bile salts and lipase added to pregels caused a large increase in elasticity beyond the point where elasticity was lost in solutions without bioactive. Thus in the combination 4%A/2%G samples, an increasing amount of bioactive led to a greater G'/G" ratio (Figure 4.27). Most combination gel solutions showed characteristic "hockey-stick" curves for G' which have yet to be reported in the literature and were rarely present in "bioactive-free" gels (Figures 4.27-4.28).

An interesting observation was noted in that combination pregels maintained the same physico-mechanical properties when the amount of drug was doubled and the plasticizer was halved. These results illustrated almost identical starting points and end points in G' values (Figure 4.28b vs. Figure 4.27c). This observation lends to a

hypothesis that the combined bile salts and pancreatic lipase mixture acted as a plasticizer substitute, improving the elasticity of the pregels.

Addition of high plasticizer quantities to gels containing the same quantity of the three bioactive combinations resulted in larger depressions/ dips in the elasticity point and a more pronounced “hockey-stick” shaped G’ curve (Figure 4.26b vs. 4.28b).

4.3.16.3. Rheology: Bile salt pregels

Sodium cholate and sodium deoxycholate pregels demonstrated different visco-elastic properties to one another despite the two salts having documented similarity in their molecular structure, physicochemical and biological properties. Oscillatory frequency sweeps produced G’ and G” profiles that were distinctively different for pregels containing NaD and those containing NaC. Sodium cholate gels revealed a similar “hockey-stick” shaped elasticity profile (G’) as noted for the combination gels and a straight G” (Figure 4.29a and b). Similar to the combination gels, the addition of plasticizer resulted in a larger depressions in G’ and a more definitive “hockey-stick” elasticity modulus (Figure 4.29a and b). In contrast, sodium dexoycholate pregels did not show “hockey-stick” shaped G’ moduli, rather two perfectly parallel G’ and G” moduli (Figure 4.29c). Both bile salt solutions were again predominantly viscous and found in characteristic pregel states with G”>G’ throughout the frequency range. Sodium dexoycholate solutions were more viscous than sodium cholate film-forming solutions with yield stresses of 1.198Pa and 0.1335Pa respectively.

4.3.16.4. Pregel rheological parameters and their implications

Some researchers have indicated that the rheological properties of plain alginate solutions may not be indicative of the properties of their resultant gels. (Fu *et al*., 2011). However the current study showed for the first time the influence of bile and enzymatic constituents on the rheology of a polymeric vehicle with noted rheological differences between the plain polymer and bile and enzyme loaded pregels. The current study provides evidence for the influence of bile salts and lipase on pregel rheology which may translate into similar observations following film formation with subsequent effects on the release and activity profiles of the bile and lipase constituents.

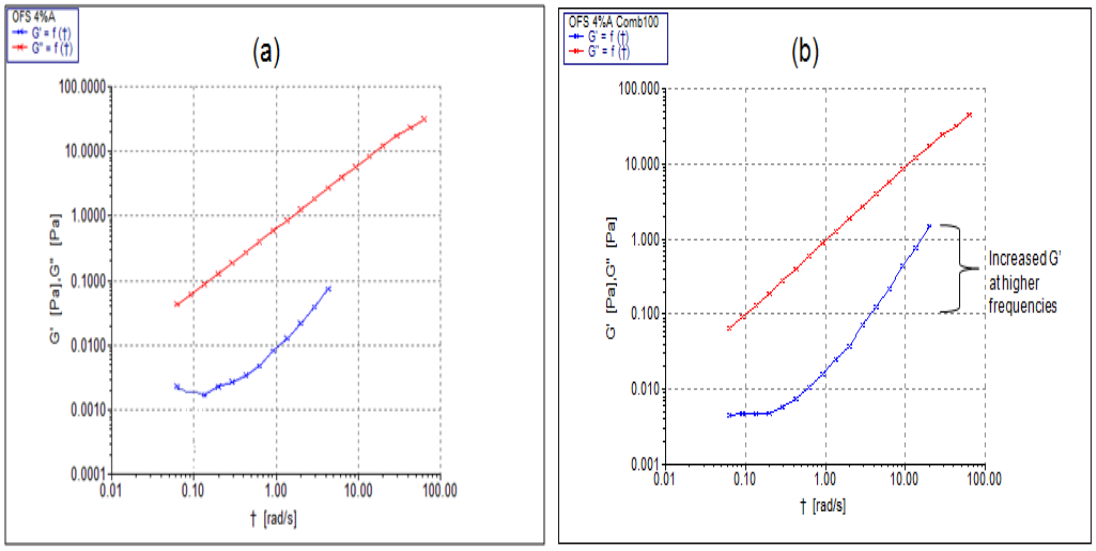


Figure 4.26: Oscillatory frequency sweep showing the viscous (G") moduli (----) and the elastic moduli (G') (-----) of two different alginate pregel solutions as a function of frequency: (a) 4%A vs. (b) 4%A Comb100.

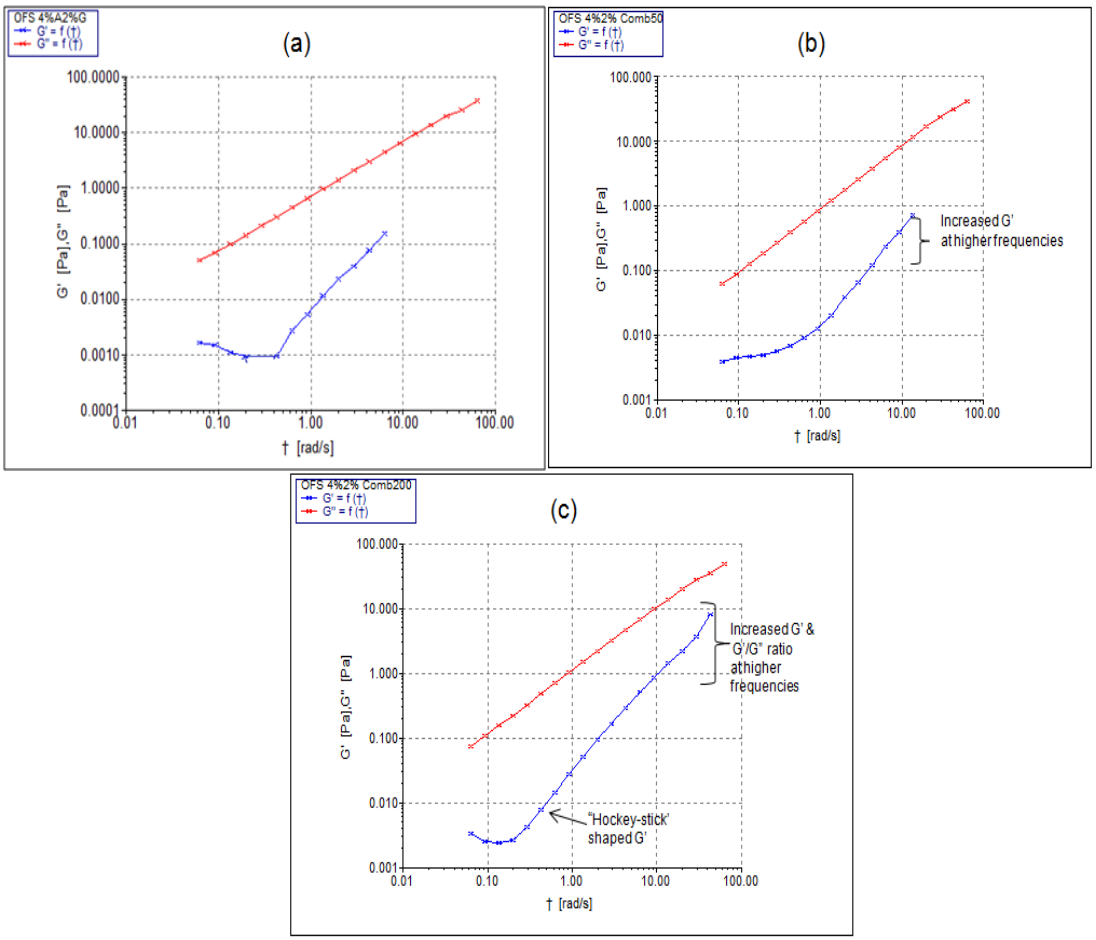


Figure 4.27: Oscillatory frequency sweep showing the viscous (G") moduli (----) and the elastic moduli (G') (-----) of three different alginate pregel solutions as a function of frequency: (a) 4%A2%G vs. (b) 4%A2%G Comb50 vs. (c) 4%A2%G Comb200.

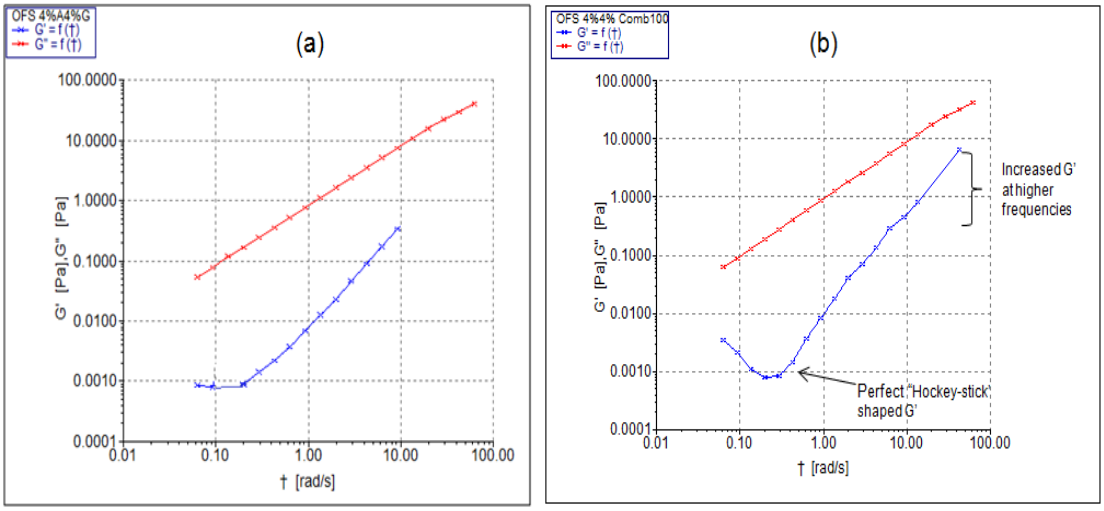


Figure 4.28: Oscillatory frequency sweep showing the viscous (G") moduli (----) and the elastic moduli (G') (-----) of two different alginate pregel solutions as a function of frequency: (a) 4%A4%G vs. (b) 4%A4%G Comb100.

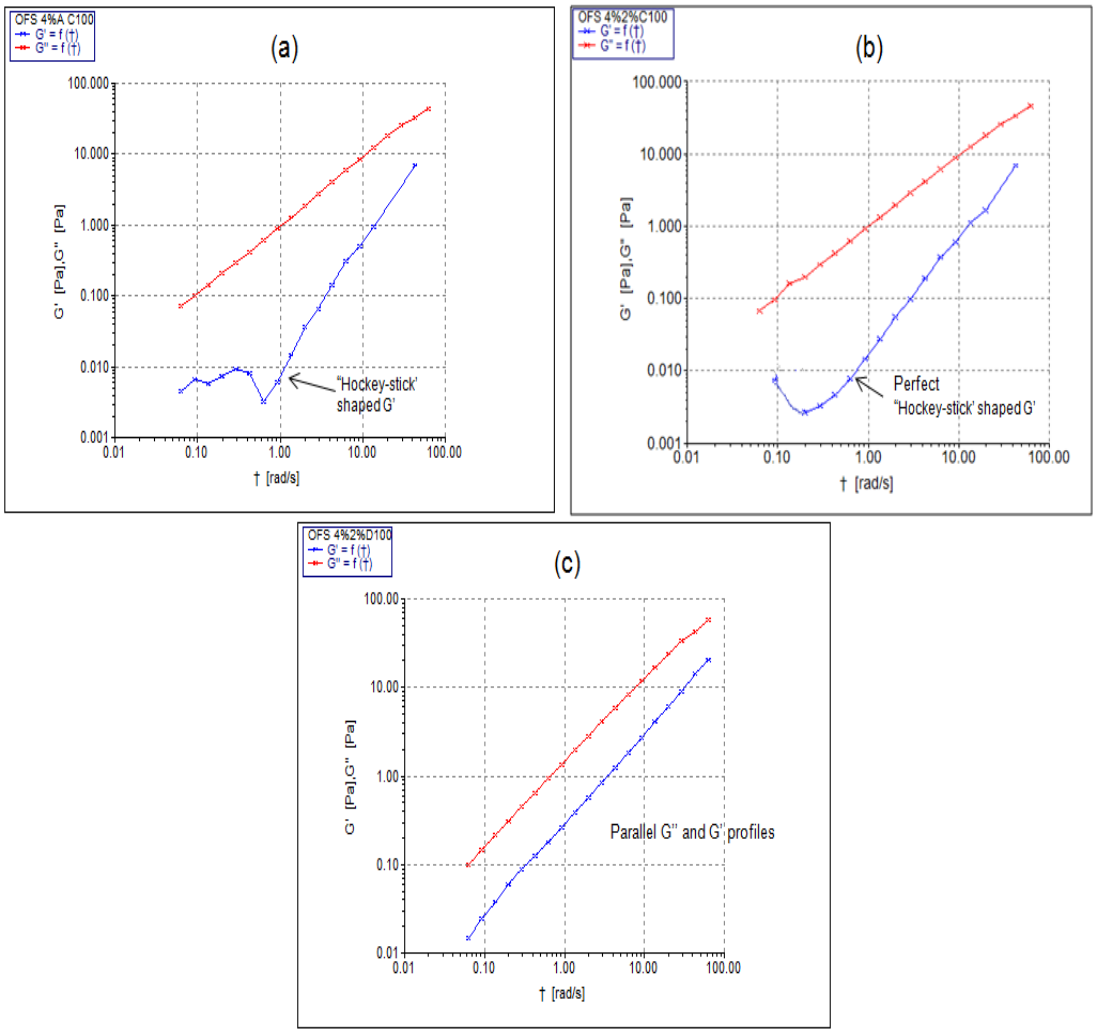


Figure 4.29: Oscillatory frequency sweep showing the viscous (G") moduli (----) and the elastic moduli (G') (-----) of three different bile salt alginate pregel solutions as a function of frequency: (a) 4%AC100 vs. (b) 4%A2%C100 vs. 4%A2%D100.

4.3.17. Karl Fischer moisture content analysis of 66B/33L films

The moisture content of the five different bioactive-alginate films containing 100mg NaD, 100mg NaC and 100mg pancreatic lipase are shown in Table 4.13. The higher the calcium gluconate cross-linker content the lower the water content that was entrapped within each bioactive film (Figure 4.30). Likewise the lower the crosslinker the higher the water content contained within the film. The bioactive film with no calcium gluconate had a noticeably higher percentage moisture content than any other film. Thus the formulation methods including extent of crosslinker addition influenced the moisture content of each bioactive film. Other researchers have noted similar findings whereby film preparation methods have influenced the water content of alginate films (Rhim, 2004). Since moisture content affects the stability of a formulation, it is often preferable to have components of lower moisture content for favourable stability profiles. The 0.7% and the 0.5% cross-linked formulations had the lowest moisture content and were therefore deemed the most suitable formulations due to reduced risk of microbial contamination. Other researchers investigated the use of alginate coatings to act as antimicrobials in food based applications (Sipahi *et al*., 2013). Since alginate films have the ability to impart antimicrobial protection to nutraceutical constituents it would be prudent to incorporate film formulations with the lowest water content to maintain this characteristic. Thus alginate films of low water content would be the most adept at ensuring extended shelf life and efficacy of embedded actives compared to more water dense options. Since water content of formulations determines the release of their active ingredients, as well as their physical, microbial, chemical and shelf-life properties this is an important aspect to be evaluated. Figure 4.30 clearly illustrates the relationship that was demonstrated between crosslinker concentration and water content of the synthesized films containing bile constituents and pancreatic lipase. The data suggested that the moisture content was indirectly proportional to crosslinker quantity. Table 4.13 lists the moisture content contained in each individual film formulation.

Table 4.13: Moisture content of 66B/33L film formulations with different crosslinker concentrations subjected to Karl Fischer hydration testing

Film Formulation	Alginate ($\%^{w}/_{v}$)/ glycerin ($\%^{v}/_{v}$)	Bioactive (mg)	Bile salt: lipase ratio	Calcium gluconate crosslinker ($\%^{w}/_{v}$)	Mean moisture content (%)
66B/33L(0%)	4%/ 2%	NaC: 100 NaD: 100 Lip: 100	2:1	0	**1.147**
66B/33L(0.2%)	4%/ 2%	NaC: 100 NaD: 100 Lip: 100	2:1	0.2	**1.043**
66B/33L(0.3%)	4%/ 2%	NaC: 100 NaD: 100 Lip: 100	2:1	0.3	**0.993**
66B/33L(0.5%)	4%/ 2%	NaC: 100 NaD: 100 Lip: 100	2:1	0.5	**0.357**
66B/33L(0.7%)	4%/ 2%	NaC: 100 NaD: 100 Lip: 100	2:1	0.7	**0.349**

NaD: Sodium deoxycholate; NaC: Sodium cholate hydrate; Lip: Pancreatic lipase

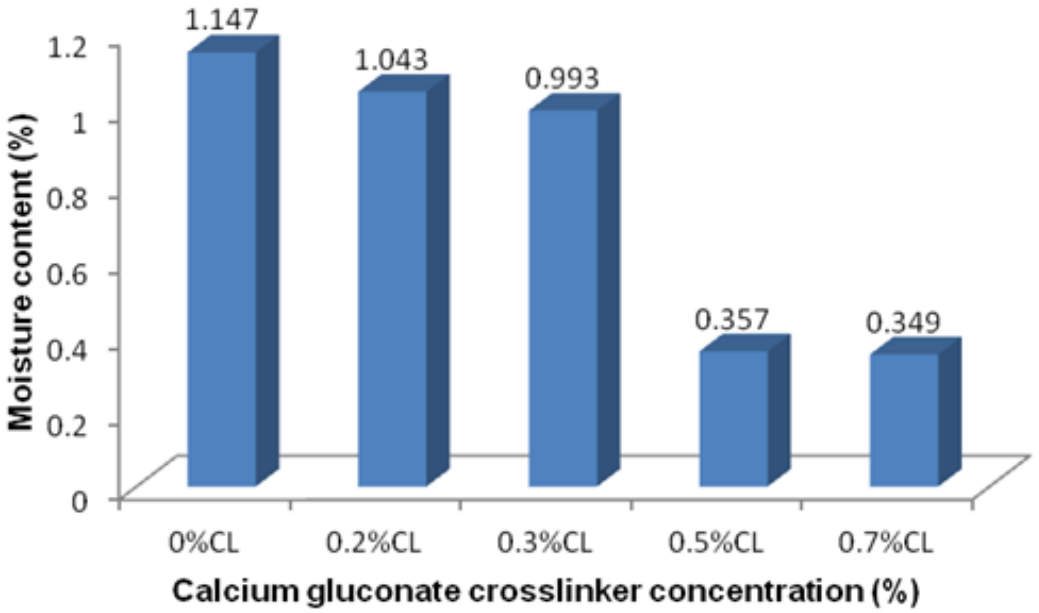


Figure 4.30: Bar-chart illustrating the relationship between crosslinker concentration and moisture content of five different bioactive films: Comparison of five bioactive film formulations: 66B/33L(0%); 66B/33L(0.2%); 66B/33L(0.3%); 66B/33L(0.5%); 66B/33L(0.7%).

4.3.18. Investigation of the physico-mechanical behaviour of films

It has been observed that a change in matrix resilience occurs when the concentration of polymer is varied in alginate cross-linked scaffolds (Pillay *et al*., 2009). Many researchers have researched the physicomechanical properties of dry alginate based films (Rhim, 2004, Wang *et al*., 2007; Olivas and Barbosa-Canovas, 2008). The current study set out to investigate the effect of varied crosslinker concentration on the physico-mechanical properties of combined bile salt and lipase films. The same 5 formulations from the Karl Fischer moisture content studies were subjected to texture profiling: 66B/33L(0%); 66B/33L(0.2%); 66B/33L(0.3%); 66B/33L(0.5%); 66B/33L(0.7%) and their mechanical properties are reported in Table 4.14.

Tensile stress measurements provided important information regarding the films strength and flexibility. Films needed to be flexible enough to be manipulated and rolled without fracturing for easy inclusion as a component of the BAP DDS. As shown in Figure 4.31a the maximum break force required to fracture the films increased as the crosslinker concentration increased up to 0.5% indicating that cross-linking within the matrix of the hydrogel films strengthened their mechanical properties. Figure 4.31c illustrates how the tensile strength of the films increases with an increase in crosslinker. Other researchers have confirmed the same by noting that crosslinked films have a greater tensile strength than non-crossllinked films (Benavides *et al*., 2012). The 0.5% formulation had the highest TS and was thus the most successful formulation with respect to crosslinker content. However, at 0.7%$^{w}/_{v}$ CL, the maximum tensile force prior to fracture dropped possibly due to brittleness imparted on the films when too much CL was added. When examining the tensile strength of each film formulation it was evident that films in general were extremely soft and did not demonstrate high TS values (Figure 4.31c). The softness of the films could be explained by the high water content and glycerin plasticiser content (2%$^{v}/_{v}$). It was interesting to note that an inversely proportional relationship was observed between film water content and the resultant tensile strength. The same was noted by other researchers who reported that water contained within films acts as a plasticizer reducing the tensile strength of a film (Olivas and Barbosa-Canovas, 2008). Since plasticizers are known to decrease the intermolecular forces along polymer chains they are known to increase flexibility. Additionally, the softness of the films may also be explained by the presence of bile and lipase. As already observed during rheological studies of pregels, the elastic modulus of film-forming solutions increased on addition of bile and lipase constituents. Therefore, the

increase in elasticity and decrease in tensile strength of resultant films not only due plasticizer, but could be attributed to the presence of NaC, NaD and lipase and their resultant interactions within the film.

The results obtained during texture analyzer testing correlated well with the water content data in the Karl Fischer moisture analysis. The lower the crosslinker concentration, the higher the moisture content contained in a film and the lower the tensile strength (Figure 4.31b). This is explained by the fact that water in the films acted as a plasticizer thereby lowering the tensile strength of the films as more water was present. Figure 4.31d shows a 3D-Mesh plot correlating tensile strength with crosslinker concentration and moisture content of the film formulations synthesized during the study. Table 4.14 lists the crosslinker maximum break force, tensile strength and moisture content of each cross-linked film.

Based on the results obtained for the combined bile salt-lipase films, the $0.5\%^{w}/_{v}$ CL formulation was deemed the most successful due to highest TS and maximum break force when subjected to elongation pressures. A higher CL composition beyond $0.5\%^{w}/_{v}$ resulted in brittle films that snapped easily and could not be rolled and manipulated for inclusion in a capsular dosage form, thus deemed unsuitable for BAP inclusion. Films with CL content below $0.5\%^{w}/_{v}$ were too soft and bent too easily without maintaining the required matrix integrity for rolling into an appropriate BAP constituent. It was also important to control synthesis conditions to ensure consistency between films, as drying methods are known to influence the mechanical properties of alginate films, an observation noted by other researchers (da Silva *et al*., 2012).

Table 4.14: Mechanical properties of five 66B/33L bioactive films containing different amounts of crosslinker

Film Formulation	Calcium gluconate crosslinker ($\%^{w}/_{v}$)	Water Content	Maximum Break force (N)	Tensile Strength (MPa)
66B/33L(0%)	0	1.147	7.09	0.012890909
66B/33L(0.2%)	0.2	1.043	10.6	0.019272727
66B/33L(0.3%)	0.3	0.993	12.76	0.0232
66B/33L(0.5%)	0.5	0.357	38.84	0.070618182
66B/33L(0.7%)	0.7	0.349	20.31	0.036927273

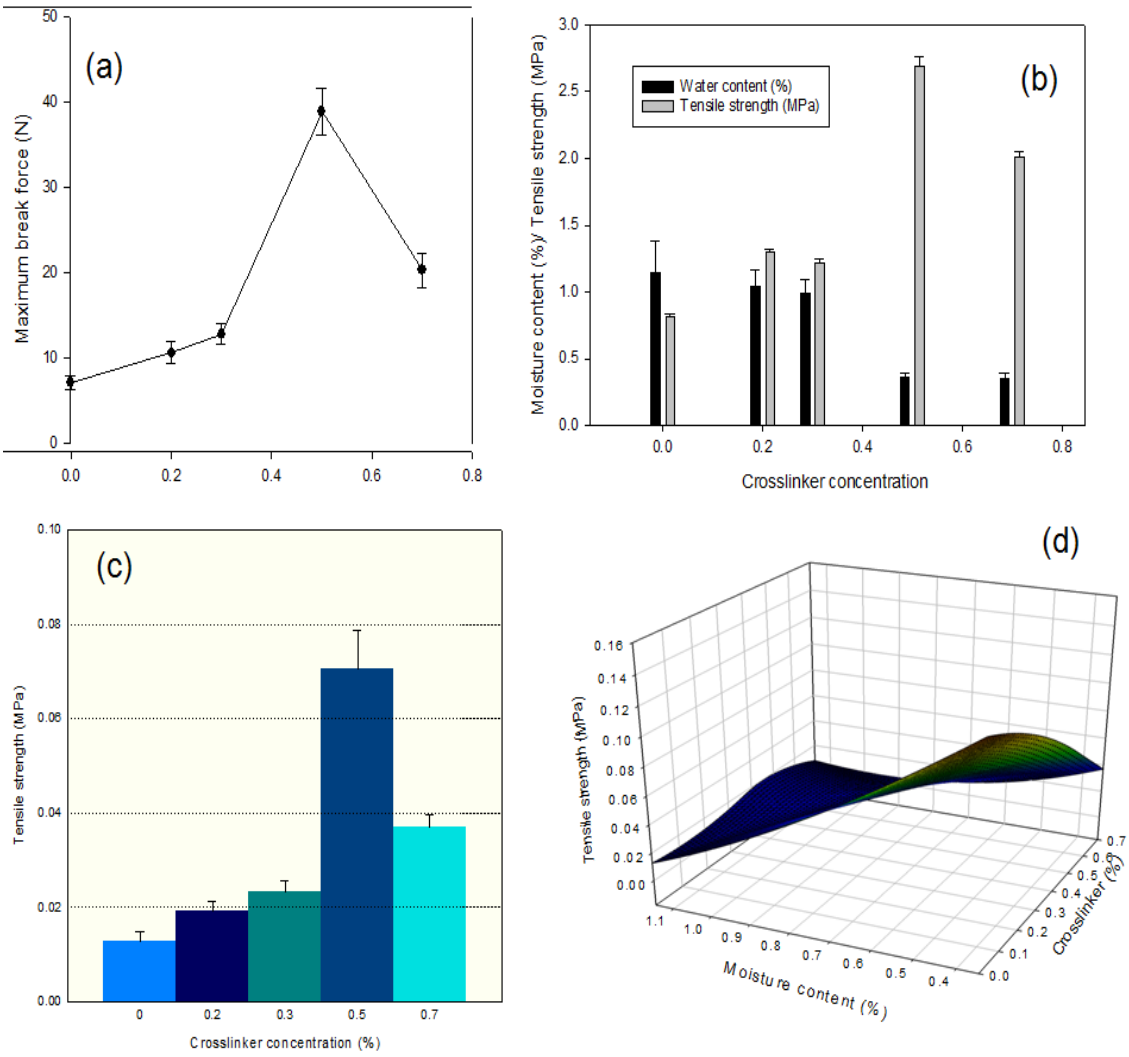


Figure 4.31: Graphical representation of texture analysis results obtained for five bioactive films including: 66B/33L(0%); 66B/33L(0.2%); 66B/33L(0.3%); 66B/33L(0.5%); 66B/33L(0.7%) showing (a) Maximum break force vs. CL %; (b) Water content and Tensile strength vs. CL %; (c) CL % vs. Tensile strength; (d) A 3D-Mesh plot correlating Tensile Strength with Crosslinker concentration and moisture content.

4.3.19. Morphological analysis of 66B/33L films using Scanning Electron Microscopy (SEM)

Scanning electron micrographs of the combined bioactive polymeric films exemplified the surface morphology of the 66B/33L cross-linked films. A homogenous surface was visible which provided evidence for even distribution of all three bioactives within the cross-linked polymeric matrix. Likewise, it was noted recently by other researchers that polyol type plasticisers such as glycerin and sorbitol normally produce alginate films with a “perfectly homogenous surface microstructure” (Santana and Kieckbusch, 2013). Similarly, Thu and Ng (2013)

demonstrated drug content uniformity within novel alginate-based bilayer films and a smooth appearance. Similar observations were made in the present study with the bile salt-lipase-alginate films achieving homogenous distribution of bioactive. Figure 4.32 illustrates SEM images of a cross-linked combined bioactive-polymer film (66B/33L(0.5%)). Figure 4.32a shows what appears to be areas of uneven ridges that have occurred due to contact of the film forming solutions with uneven areas of the plates. In addition figure 4.32b shows white particulate matter in the form of calcium gluconate powder that has been suspended in the gel matrix prior to complete dissolution of the crosslinker. Vigilant mixing and ultrasonication of gel mixtures ensured homogenous dispersion of all three bioactives within films as was confirmed by the SEM images and the formation of smooth films due to optimal inclusion of glycerin plasticiser.

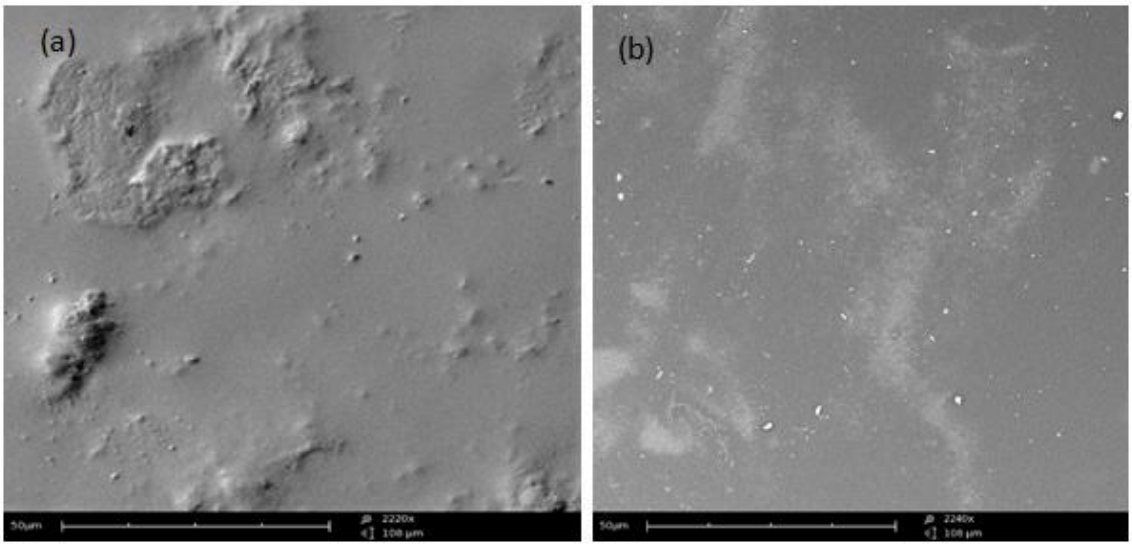


Figure 4.32: Scanning Electron micrographs of the surface morphology of bioactive-alginate film formulation 66B/33L(0.5%) at (a) 2220x magnification and (b) 2240x magnification.

4.4. Concluding Remarks

Extensive synthesis, characterization, IC confirmation and IE determinations proved that the βD_3-8 complex was a favourable BAP candidate for inclusion of the model drug, cholecalciferol. Similarly βC-8 was considered a stable carrier for delivery of ascorbic acid. Solubility improvements and thermal analysis explicated the attractiveness of vitamin-CD complexes as BAP nutraceutical candidates. It was also noted how both alginate and chitosan offered vast flexibility as biocompatible polymeric carriers adept at inclusion and modification of the release of bile (CA, DA,

NaC, NaD) and pancreatic lipase. Polymeric chitosan and alginate microbeads did not achieve sufficiently high IE values, and many other researchers have noted this shortfall with a need to pursue strategies to mitigate drug leakage during synthesis. Microbead synthesis and scale-up may also prove challenging and less efficient and this approach was therefore abandoned. Strategy evolved from problematic microbeads to polymeric alginate scaffolds and films of varied bile, lipase and crosslinker composition. The solubility limits and toxicity concerns of bile acids prompted the formulation design to shift focus to include bile salts instead of bile acids as bile constituents. Alginate scaffolds provided successful and easily modifiable bile salt and lipase release profiles, for the provision of GIT substances at customizable release rates, however their large size limited their usefulness as BAP components. Microbeads, scaffolds and films all offered certain advantages as BAP component candidates, but ultimately the synthesis of films containing NaC, NaD and lipase proved a more attractive conformation for biological co-factor provision. Rheology of alginate/ glycerin pregels, physicomechanical texture profiling, hydration tests, and surface morphology analysis of films provided promising preliminary results. Films were considered attractive BAP candidates, requiring further investigation due to their flexibility and ease of handling and suitability for inclusion in a capsule. Further studies need to be undertaken to elucidate the ideal bile salt/ lipase composition and resultant enzyme activity of bioactive-films for improved cholecalciferol delivery. In summary, Figure 4.33 depicts the four types of BAP BB components synthesized and evaluated in Chapter 4 as BAP formulation candidates. The next chapter will build upon positive preformulation results to further develop the two most successful BB candidates (CD-cholecalciferol IC's and films) into optimized components for inclusion in the final BAP. Chapter 5 will also focus on methods to combine final components into a capsule to form the BAP drug delivery system to undergo decisive *in vitro* comparative analysis.

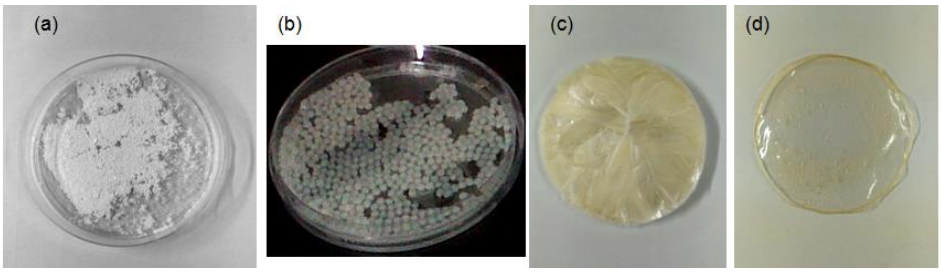


Figure 4.33: Photographic images depicting the four BAP component candidates that were formulated and tested during the preformulation studies: (a) BAP candidate A: CD-vitamin complexes; (b) BAP candidate B: Bioactive microbeads (alginate); (c) BAP candidate C: polymeric-bioactive scaffolds (alginate); (d): BAP candidate D: Bioactive-polymer films.

4.5. References

Alishahi A, Mirvaghefi A, Tehrani MR, Farahmand H, Shojaosadati SA, Dorkoosh FA, Elsabee MZ. 2011. Shelf life and delivery enhancement of vitamin C using chitosan nanoparticles. *Food Chemistry* 126: 935-940.

Al-Rawashdeh NAF, Al-Sadeh KS, AL-Bitar MB. 2013. Inclusion complexes of sunscreen agents with β-cyclodextrin: Spectroscopic and molecular modeling studies. *Journal of Spectroscopy* 2013: 1-11.

Alvarez-Lorenzo C, Blanco-Fernandez B, Puga AM, Concheiro A. 2013. Crosslinked ionic polysaccharides for stimuli-sensitive drug delivery. *Advanced Drug Delivery Reviews* 65: 1148-1171.

Archana D, Upadhyay L, Tewari RP, Dutta J, Huang YB, Dutta PK. 2013. Chitosan-pectin-alginate as a novel scaffold for tissue engineering applications. *Indian Journal of Biotechnology* 12: 475-482.

Betigeri SS, Neau SH. 2002. Immobilization of lipase using hydrophilic polymers in the form of hydrogel beads. *Biomaterials* 23: 3627-3636.

Benavides S, Villalobos-Carvajal R, Reyes JE. 2012. Physical, mechanical and antibacterial properties of alginate film: Effect of the crosslinking degree and oregano essential oil concentration. *Journal of Food Engineering* 110: 232-239.

Bonino CA, Samorezov JE, Jeon O, Alsberg E, Khan SA. 2011. Real-time *in situ* rheology of alginate hydrogel photocrosslinking. *Royal Society of Chemistry (Soft Matter)* 7: 11510-11517.

Caira MR, Nassimbeni LR, Scott JL. 1994. Inclusion compounds of cholic acid with aliphatic esters. *Journal of the Chemical society, Perkin Transactions* 2: 623-628.

Carrier RL, Miller LA, Ahmed I. 2007. The utility of cyclodextrins for enhancing oral bioavailability. *Journal of Controlled Release* 123: 78-99.

Chadha R, Gupta S, Pathak N. 2012. Artesunate-loaded chitosan/lecithin nanoparticles: Preparation characterization and *in vivo* studies. *Drug Development and Industrial Pharmacy* 38(12): 1538-1546.

da Silva MA, Bierhalz ACK, Kieckbusch TG. 2009. Alginate and pectin composite films crosslinked with Ca^{2+} ions: Effect of the plasticizer concentration. *Carbohydrate Polymers* 77: 736-742.

da Silva MA, Bierhalz AC, Kieckbusch TG. 2012. Influence of drying conditions on physical properties of alginate films. *Drying Technology* 30(1): 72-79

Del Valle EMM. 2004. Cyclodextrins and their uses: a review. *Process Biochemistry* 39: 1033–1046.

Draget KI, Stokke BT, Yuguchi Y, Urakawa H, Kajiwara K. 2003. Small-angle x-ray scattering and rheological characterization of alginate gels.3. alginic acid gels. *Biomacromolecules* 4: 1661-1668.

Dua K, Pabreja K, Ramana MV, Lather V. 2011. Dissolution behavior of β-cyclodextrin molecular inclusion complexes of aceclofenac. *Journal of Pharmacy and Bioallied Sciences* 3(3): 417-425.

Fu S, Thacker A, Sperger DM, Boni RL, Buckner IS, Velankar S, Munson E, Block LH. 2011. Relevance of rheological properties of sodium alginate in solution to calcium alginate gel properties. *AAPS PharmSciTech* 12: 453-460.

Garnero C, Chattah AK, Longhi M. 2014. Improving furosemide properties through supramolecular complexes of β-cyclodextrin. *Journal of Pharmaceutical and Biomedical Analysis* 95: 139-145.

George M, Abraham TE. 2006. Polyionic hydrocolloids for the intestinal delivery of protein drugs: Alginate and chitosan- a review. *Journal of Controlled Release* 114: 1-14.

Ghosh A, Biswas S, Ghosh T. 2011. Preparation and evaluation of silymarin β-cyclodextrin molecular IC's. *Journal of Young Pharmacists* 3: 205-210.

Giordano F, Novak C, Moyano JR. 2001. Thermal analysis of cyclodextrins and their inclusion compounds. *Thermochimica Acta* 380: 123-151.

Grondahl L, Lawrie G, Jejurikar A. 2010. Alginate-based drug delivery devices. Woodhead Publishing Limited. 236-266.

Guttoff M, Saberi AH, McClements DJ. 2015. Formation of vitamin D nanoemulsion-based delivery systems by spontaneous emulsification: factors affecting particle size and stability. *Food chemistry* 171: 117-122.

Hashem FM, Mostafa M, Shaker M, Nasr M. 2013. *In vitro* and *in vivo* evaluation of oxatomide β-cyclodextrin inclusion complex. *Journal of Pharmaceutics* 2013: 1-9.

He D, Deng P, Yang L, Tan Q, Liu J, Yang M, Zhang J. 2013. Molecular encapsulation of rifampicin as an IC of hydroxypropyl-β-cyclodextrin: Design, characterization and *in vitro* dissolution. *Colloid Surface B: Biointerfaces* 103: 580-585.

Hertzberg S, Kvittingen L, Anthonsen T, Skjak-Braek S. 1992. Alginate as immobilization matrix and stabilizing agent in a two-phase liquid system: Application in lipase-catalysed reactions. *Enzyme and Microbial Technology* 14: 42-47.

Higuchi T, Connors KA. 1965. Phase solubility techniques. *Advances in Analytical Chemistry and Instrumentation* 4: 117-212.

Ho BT, Joyce DC, Bhandari BR. 2011. Encapsulation of ethylene gas into α-cyclodextrin and characterisation of the inclusion complexes. *Food Chemistry* 127: 572-580.

Hu X, Wei B, Wu C, Bai Y, Xu X, Jin Z, Tian Y. 2012. Preparation of the β-cyclodextrin-vitamin C (β-CD-Vc) inclusion complex under high hydrostatic pressure (HHP). *Carbohydrate Polymers* 90: 1193-1196.

Hua S, Ma H, Li X, Yang H, Wang A. 2010. pH-sensitive sodium alginate/poly(vinyl alcohol)hydrogel beads prepared by combined Ca2+ crosslinking and freeze-thawing cycles for controlled release of diclofenac sodium. *International Journal of Biological Macromolecules* 46: 517-523.

Iacovino R, Caso JV, Rapuano F, Russo A, Isidori M, Lavorgna M, Malgieri G, Isernia C. 2012. Physicochemical characterization and cytotoxic activity evaluation of hydroxymethylferrocene: β-cyclodextrin inclusion complex. *Molecules* 17: 6056-6070.

Ignjatovic N, Uskokovic V, Ajdukovic Z, Uskokovic D. 2013. Multifunctional hydroxyapatite and poly (D,L-lactide-co-glycolide) nanoparticles for the local delivery of cholecalciferol. *Materials Science and Engineering: C* 33: 943-950.

Jansook P, Ritthidej GC, Ueda H, Stefansson E, Loftsson T. 2010. γCD/HPγCD Mixtures as solubilizer: Solid-state characterization and sample dexamethasone eye drop suspension. *Journal of Pharmacy and Pharmaceutical Sciences* 13(3): 336-350.

Kawakami K. 2012. Modification of physicochemical characteristics of active pharmaceutical ingredients and application of supersaturable dosage forms for improving bioavailability of poorly absorbed drugs. *Advanced Drug Delivery Reviews* 64: 480-495.

Kim H, Knowles JC, Kim H. 2005. Porous scaffolds of gelatin-hydroxyapatite nanocomposites obtained by biomimetic approach: characterization and antibiotic release. *Journal of Biomedical Materials Research Part B: Applied Biomaterials* 74B: 686-698.

Kim SH, Youn JJ, Kim KM, Kang KC, Pyo HB, Lee SJ. 2010. Characterization of an inclusion complex of 7-dehydrocholesterol and cyclodextrin. *Journal of Industrial and Engineering Chemistry* 16: 119-121.

Koontz JL, Marcy JE, O'Keefe SF, Duncan SE. 2009. Cyclodextrin IC formation and solid-state characterization of the natural antioxidants α-Tocopherol and quercetin. *Journal of Agricultural and Food Chemistry* 57:1162-1171.

Lin H, Yeh Y. 2004. Porous alginate/hydroxyapatite composite scaffolds for bone tissue engineering: preparation, characterization, and *in vitro* studies. *Journal of Biomedical Materials Research Part B: Applied Biomaterials* 71B: 52-65.

Lin H, Ciou S. 2010. Modifications of alginate-based scaffolds and characterizations of their pentoxifylline release properties. *Carbohydrate Polymers* 80: 574-580.

Liu B, Li W, Zhao J, Liu Y, Zhu X, Liang G. 2013. Physicochemical characterisation of the supramolecular structure of luteolin/cyclodextrin inclusion complex. *Food Chemistry* 141: 900-906.

Loftsson T, Hreinsdottir D, Masson M. 2007. The complexation efficiency. *Journal of Inclusion Phenomenon and Macrocyclic Chemistry* 57: 545-552.

Loveday SM, Singh H. 2008. Recent advances in technologies for vitamin A protection in foods. *Trends in Food Science & Technology* 19: 657-668.

Luo Y, Teng Z, Wang Q. 2012. Development of zein nanoparticles coated with carboxymethyl chitosan for encapsulation and controlled release of vitamin D3. *Journal of Agricultural and Food Chemistry* 60: 836-843.

Mahajan S, Mahajan RK. 2012. Interactions of phenothiazine drugs with bile salts: micellization and binding studies. *Journal of Colloid and Interface Science* 387: 194-204.

Martins Mendes Gomes L, Petito N, Goncalves Costa V, Quintanilha Falcao D, de Lima Araujo KG. 2014. Inclusion complexes of red bell pepper pigments with β-cyclodextrin: Preparation, characterization and application as natural colorant in yogurt. *Food Chemistry* 148: 428-436.

Mercê ALR, Nicolini J, Khan MA, Bouet G. 2009. Qualitative study of supramoleculkar assemblies of β-cyclodextrin and cholecalciferol and the cobalt (II), copper (II) and zinc (II) ions. *Carbohydrate Polymers* 77:402-409.

Misiuk W, Zalewska M. 2009. Investigation of inclusion complex of trazodone hydrochloride with hydroxypropyl-β-cyclodextrin. *Carbohydrate Polymers* 77(3): 482-488.

Mooranian A, Negrulj R, Mathavan S, Martinez J, Sciarretta J, Chen-Tan N, Mukkur TK, Mikov M, Lalic-popovic M, Stojancevic M, Golocorbin-Kon S, Al-Salami H. 2014. An advanced microencapsulated system: a platform for optimized oral delivery of

antidiabetic drug-bile acid formulations. *Pharmaceutical Development and Technology*. Posted early online ahead of print: pages 1-8. Retrieved from URL: http://www.ncbi.nlm.nih.gov/pubmed/24798888. [Accessed online 9 October 2014].

Mooranian A, Negrulj R, Chen-Tan N, Al-Salami HS, Fang Z, Mukkur T, Mikov M, Golocorbin-Kon S, Fakhoury M, Arfuso F, Al-Salami H. 2014. Novel artificial cell microencapsulation of a complex gliclazide-deoxycholic bile acid formulation: a characterization study. *Drug Design Development and Therapy* 8: 1003-1012.

Mura P. 2014. Analytical techniques for characterization of cyclodextrin complexes in aqueous solution: A review. *Journal of Pharmaceutical and Biomedical Analysis* 101: 238-250.

Murakami M, Morita Y, Koide T, Saito H, Tanimoto T. 2003. Cholecalciferol reference standard (control 031) of the national institute of health sciences. *Bulletin of National institute of Health Sciences* 121:65-67.

Murakami M, Morita Y, Koide T, Saito H, Tanimoto T. 2003. Tocopherol acetate reference standard (control 021) of the national institute of health sciences. *Bulletin of National institute of Health Sciences* 121:68-70.

Nagahama H, Maeda T, Kashiki T, Rayakumar R, Furuike T, Tamura H. 2009. Preparation and characterization of novel chitosan/gelatine membranes using chitosan hydrogel. *Carbohydrate Polymers* 76 (2): 255-260.

Nguyen TA, Liu B, Zhao J, Thomas DS, Hook JM. 2013. An investigation into the supramolecular structure, solubility, stability and antioxidant activity of rutin/ cyclodextrin inclusion complex. *Food Chemistry* 136: 186-192.

Norajit K, Kim KM, Ryu GH. 2010. Comparative studies on the characterization and antioxidant properties of biodegradable alginate films containing ginseng extract. *Journal of Food Engineering* 98: 377-384.

Olivas GI and Barbosa-Canovas GV. 2008. Alginate-calcium films: Water vapour permeability and mechanical properties as affected by plasticizer and relative humidity. *LWT- Food Science and Technology* 41: 359-366.

Pillay S, Pillay V, Choonara YE, Naidoo D, Khan RA, du Toit LC, Ndesendo VMK, Modi G, Danckwerts MP, Lyuke SE. 2009. Design, biometric simulation and optimization of a nano-enabled scaffold device for enhanced delivery of dopamine to the brain. *International Journal of Pharmaceutics* 382: 277-290.

Piai JF, Lopes LC, Fajardo AR, Rubira AF, Muniz EC. 2010. Kinetic study of chondroitin sulphate release from chondroitin sulphate/chitosan complex hydrogel. *Journal of Molecular Liquids* 156: 28-32.

Prabaharan M, Rodriguez-Perez MA, de Saja JA, Mano JF. 2007. Preparation and characterization of poly(L-lactic acid)-chitosan hynrid scaffolds with drug release capability. *Journal of Biomedical Materials Research Part B: Applied Biomaterials* 81B: 427-434.

Racz C, Santa S, Tomoaia-Cotisel M, Borodi G, Kacso I, Pirnau A, Bratu I. 2013. Inclusion of α-lipoic acid in β-cyclodextrin. Physical-chemical and structural characterization. *Journal of Inclusion phenomenon and Macrocyclic Chemistry* 76: 193-199.

Rhim J. 2004. Physical and mechanical properties of water resistant sodium alginate films. *LWT- Food Science and Technology* 37: 323-330.

Ruz V, Froeyen M, Busson R, Gonzalez MM, Baudemprez L, Van der Mooter G. 2012. Characterization and molecular modelling of the IC's of 2-(2-nitrovinyl) furan (G-O) with cyclodextrins. *International Journal of Pharmaceutics* 439: 275-285.

Sambasevam KP, Mohamad S, Sarih NM, Ismail NA. 2013. Synthesis and characterization of the inclusion complex of β-cyclodextrin and azomethine. *International Journal of Molecular Sciences* 14: 3671-3682.

Samstein RM, Perica K, Balderrama F, Look M, Fahmy TM. 2008. The use of deoxycholic acid to enhance the oral bioavailability of biodegradable nanoparticles. *Biomaterials* 29: 703-708.

Sangpheak W, Kuntawee W, Wolschann P, Pongsawasdi P, Rungrotmongkol T. 2014. Enhanced stability of a naringenin/2,6-dimethyl β-cyclodextrin inclusion

complex: Molecular dynamics and free energy calculations based on MM- and QM-PBSA/GBSA. *Journal of Molecular Graphics and Modelling* 50: 10-15.

Sankalia MG, Mashru RC, Sankalia JM, Sutariya VB. 2007. Reversed chitosan-alginate polyelectrolyte complex for stability improvement of alpha-amylase: optimization and physicochemical characterization. *European Journal of Pharmaceutics and Biopharmaceutics* 65: 215-232.

Santana AA, Kieckbusch TG. 2013. Physical evaluation of biodegradable films of calcium alginate plasticized with polyols. *Brazilian Journal of Chemical Engineering* 30: 835-845.

Shanmugasundaram N, Sundaraseelan J., Uma S, Selvaraj D, Babu M. 2006. Design and delivery of silver sulfadiazine from alginate microspheres-impregnated collagen scaffold. *Journal of Biomedical and Materials Research Part B: Applied Biomaterials* 77B: 378-388.

Sharma P, Varma MVS, Chawla HPS, Panchagnula R. 2005. Absorption enhancement, mechanistic and toxicity studies of medium chain fatty acids, cyclodextrins and bile salts as peroral absorption enhancers. *IL Farmaco* 60: 884-893.

Sharma R, Majer F, Peta VK, Wang J, Keaveney R, Kelleher D, Long A, Gilmer JF. 2010. Bile acid toxicity structure-activity relationships: Correlations between cell viability and lipophilicity in a panel of new and known bile acids using an oesophageal cell line (HET-1A). *Bioorganic and Medicinal Chemistry* 18: 6886-6895.

Singh R, Bharti N, Madan J, Hiremath SN. 2010. Characterization of cyclodextrin inclusion complexes-A Review. *Journal of Pharmaceutical Sciences and Technology* 2(3): 171-183.

Sipahi RE, Castell-Perez ME, Moreira RG, Gomes C, Castillo A. 2013. Improved multilayered antimicrobial alginate-based edible coating extends the shelf-life of fresh-cut watermelon (Citrullus lanatus). *LWT- Food Science and Technology* 51: 9-15.

Subuddhi U, Mishra AK. 2007. Effect of sodium deoxycholate and sodium cholate on DPPC vesicles: A Flourescence anisotrophy study with diphenylhexatrine. *Journal of Chemical Sciences* 2: 169-174.

Takka S, Cali AG. 2012. Bile salt-reinforced alginate-chitosan beads. *Pharmaceutical Development and Technology* 17(1): 23-29.

Teng Z, Luo Y, Wang Q. 2013. Carboxymethyl chitosan-soy protein complex nanoparticles for the encapsulation and controlled release of vitamin D_3. *Food Chemistry* 141: 524-532.

Thu H, Ng S. 2013. Gelatine enhances drug dispersion in alginate bilayer film via the formation of crystalline microaggregates. *International Journal of Pharmaceutics* 454: 99-106.

Uekaji Y, Jo A, Ohnishi M, Nakata D, Terao K. 2012. A new generation of nutra-ceuticals and cosme-ceuticals complexing lipophilic bioactives with γ-cyclodextrin. *Procedia Engineering* 36: 540-550.

Vaid FHM, Shaikh RH, Ansari IA, Ahmad I. 2005. Spectral study of the photolysis of aqueous thiamine hydrochloride and ascorbic acid solutions in the presence and absence of riboflavin. *Journal of Chemical Society of Pakistan* 27 (3): 227-232.

Wang L, Auty MAE, Kerry JP. 2010. Physical assessment of composite biodegradable films manufactured using whey protein isolate gelatin and sodium alginate. *Journal of Food Engineering* 96: 199-207.

Wang J, Cao Y, Sun B, Wang C. 2011. Physicochemical and release characterization of garlic oil-b-cyclodextrin inclusion complexes. *Food Chemistry* 127: 1680-1685.

Wang D, Li H, Gu J, Guo T, Yang S, Guo Z, Zhang X, Zhu W, Zhang J. 2013. Ternary system of dihydroartemisinin with hydroxypropyl-β-cyclodextrin and lecithin: Simultaneous enhancement of drug solubility and stability in aqueous solutions. *Journal of Pharmaceutical and Biomedical Analysis* 83: 141-148.

Wen J, Liu B, Yuan E, Ma Y, Zhu Y. 2010. Preparation and physicochemical properties of the complex of naringenin with hydroxypropyl-β-cyclodextrin. *Molecules* 15: 4401-4407.

Won K, Kim S, Kim K, Park HW, Moon S. 2005. Optimization of lipase entrapment in Ca-alginate gel beads. *Process Biochemistry* 40: 2149-2154.

Wu SY, Chang H, Burgess M, McMillan NAJ. 2011. Vaginal delivery of SiRNA using a novel PEGylated lipoplex-entrapped alginate scaffold system. *Journal of Controlled Release* 155: 418-426.

Yang L, Xu Y, Su Y, Wu J, Zhao K, Chen J, Wang M. 2005. FT-IR spectroscopic study on the variations of molecular structures of some carboxyl acids induced by free electron laser. *Spectrochimica Acta Part A* 62: 1209-1215.

Yang J, Wiley CJ, Godwin DA, Felton LA. 2008. Influence of hydroxypropyl- β-cyclodextrin on transdermal penetration and photostability of avobenzone. *European Journal of Pharmaceutics and Biopharmaceutics* 69: 605-612.

Yap KL, Liu X, Thenmozhiyal JC, Ho PC. 2005. Characterization of the 13-*cis*-retinoic acid/cyclodextrin inclusion complexes by phase solubility, photostability, physicochemical and computational analysis. *European Journal of Pharmaceutical Sciences* 25: 49-56.

Zaibunnisa AH, Siti Rashima R, Nur Ain AH. 2011. Stabilisation of curcumin with γ-cyclodextrin: phase solubility study and its characterisation. 2011 *2nd International Conference on Biotechnology and Food Science* 7: 9-13.

Zughaid H, Forbes B, Martin GP, Patel N. 2012. Bile salt composition secondary to bile salt concentration in determining hydrocortisone and progesterone solubility in intestinal mimetic fluids. *International Journal of Pharmaceutics* 422: 295-301.

CHAPTER 5

IN VITRO FORMULATION, CHARACTERIZATION, AND TESTING OF THE FINAL BAP DRUG DELIVERY SYSTEM

5.1. Introduction

One of the highlights of the previous chapter was the synthesis of bioactive-scaffold devices capable of delivering bile and lipase constituents to mimic *in vivo* exocrine release. However, the size of these structures was identified as a limitation to further promulgation of this strategy. Since the BAP dosage form was intended to incorporate multiple delivery devices with more than one release mechanism, scaffolds were deemed unsuitable for inclusion in the final system. Synthesis and preliminary testing of films in Chapter 4 provided insights into an alternative formulation approach for delivery of the bile and enzyme bioactives. The next phase of research detailed herein shifted towards the creation of an all-inclusive dosage form and elucidated the influence of the BAP components on the release of model drug and synergistic vitamins. Films were pursued in more depth as practical alternatives to carry lipase and bile salts within the original DDS design. In addition, the evaluation of pancreatic lipase activity post inclusion in films was necessary to validate the efficacy of this DDS constituent. Contrary to the limitation of scaffolds, the small size of vitamin inclusion complexes, did not exclude their use in the final device. However, a strategy to effectively incorporate the optimized vitamin IC's in the final BAP DDS needed to be developed.

The optimization of selected BAP components and building of the final BAP capsule was the focus of this chapter. Highlights of this phase of the research included: synthesis, characterization, *in silico* modeling, and performance testing. Characterization via thermal analysis, infrared spectroscopy, texture profiling, disintegration, and moisture content evaluation was undertaken to understand the nature of each final component. The dissolution profiles of all included synergistic vitamins, the extent of enzyme activity and the impact of biological co-factor release on model drug dissolution kinetics were investigated. Critical to the success of each component was the ultimate *in vitro* release profile of model drug, cholecalciferol, as well as its membrane diffusion behaviour in comparison to a conventional market comparator. The overall objective of this chapter was to build upon previous results

in the creation of the final BAP DDS with superior *in vitro* parameters as a means to improve cholecalciferol release and to solve current formulation challenges.

5.2. Materials and Methods

5.2.1. Materials

Cholecalciferol, ascorbic acid, alginic acid, βCD, calcium carbonate, pancreatic lipase, sodium cholate hydrate, phosphate buffered saline tablets, sodium deoxycholate, lipase activity assay kit, amaranth, Kollicoat® methacrylic acid/ ethyl acrylate (MAE) 100P, and Poly(ethylene glycol) methyl ether were all purchased from Sigma Aldrich® Inc. (St. Louis, MO, USA). Kolliphor® TPGS was kindly donated by BASF (Ludwigshafen, Germany). Methanol, ethanol, and glycerin solution were obtained from Merck Chemicals (Pty) Ltd. (Wadeville, Gauteng, South Africa). Oasis HLB cartridges were also procured for use (Waters Corporation, Milford, MA, USA).

5.2.2. BAP component A: "3-vitamin" minitablets as final vitamin carriers

5.2.2.1. A novel minitablet formulation: A rational approach for multivitamin inclusion in the BAP

The BAP design necessitated the combining of multiple bioactive-boosters into a single capsule with the potential for numerous laborious steps which needed to be minimized. To lessen formulation complexity and reduce industrial preparation steps, only one vitamin, the model drug- cholecalciferol, was complexed with CD's. The other bioactive vitamins, ascorbic acid and α-tocopherol were to be included without complexation with minimized formulation procedures. However, α-tocopherol still posed aqueous solubility challenges if included in its native form in the BAP, thus a novel format was identified in the form of D-α-Tocopheryl polyethylene glycol 1000 succinate (vitamin E TPGS/ Kolliphor TPGS) termed "TPGS". TPGS provided a water-soluble form of α-tocopherol in a versatile matrix material with solubility and absorption enhancer effects and beneficial surfactant-like properties (Mu and Feng, 2003; Gill *et al*., 2012). TPGS was also considered an attractive excipient additive due to its ability to form tablets with multiple bioactives using granulation techniques (Mu and Feng, 2003; Guo *et al*., 2013). For these reasons, TPGS was selected as a waxy 'bioactive booster' excipient to which ascorbic acid powder could be directly added and compressed into a minitablet for the provision of vitamin E and vitamin C. This tablet combination was proposed to provide a more hydrophilic form of vitamin

E and to improve disintegration, solubility and permeation characteristics of all other vitamin constituents. Recently other water-soluble vitamins have been successfully combined with TPGS which supported the rationale of combining ascorbic acid with TPGS in a novel minitablet component of the BAP (Ostacolo *et al*., 2013). Likewise a successful TPGS: ascorbic acid compressible tablet could act as a vehicle to incorporate the optimized βD_3-8 complex for provision of model drug, cholecalciferol.

5.2.2.2. Comprehensive molecular mechanics simulations of cholecalciferol complexes to confirm optimized IC for inclusion in minitablet

Based on the final formulation design, only cholecalciferol was to be complexed with cyclodextrin. Therefore additional molecular mechanics simulations were carried out with cholecalciferol CD complexes to confirm the optimized IC for final inclusion in the "3-vitamin" minitablet. *In silico* simulations were performed for a second time using the model drug and the three parent CD's and one CD derivative. The study investigated three different mechanistic models to explicate the process behind favourable IC conformations and to select the optimal cholecalciferol CD complex. Additional molecular modelling studies would also provide the most reasonable rationale behind the superior IE results reported in Chapter 4 for βD_3 IC's. Molecular simulations provided information pertaining to energetic stabilization, binding/inclusion mode; geometrical orientation, and the 3D space-fit of Vitamin D_3 within the α-CD||VitD, β-CD||VitD, γ-CD||VitD, and HP-β-CD||VitD inclusion complexes. These studies were considered essential to validate the initial pilot molecular simulations and earlier experimental results obtained for cholecalciferol inclusion complexes in Chapter 4.

Molecular Mechanics computations in vacuum, which included the model building of the energy-minimized structures of CD-VitD complexes, were performed using HyperChem™ 8.0.8 Molecular Modeling software (Hypercube Inc., Gainesville, FL, USA) and ChemBio3D Ultra 11.0 (CambridgeSoft Corp., UK). Cyclodextrins - α-CD, β-CD, γ-CD, and HP-β-CD – were modeled by incorporation into a macrocyclic ring of o-glucose projections, each constructed in a chair conformation using standard bond lengths and bond angles (with neutral charge) on the Sugar Builder Module on HyperChem™ 8.0.8. Equal torsional angles at α (1-4) glycosidic linkage between the rings provided a regular torus structure of multi-fold symmetry (Figure 5.1). The structure of vitamin D_3 (VitD) was built with pre-defined natural bond angles and neutral charge. The generation of the overall steric energy associated with the energy-minimized structures was initially executed via energy-minimization using the

MM+ Force Field and the resulting structures were once again energy-minimized using the AMBER 3 (Assisted Model Building and Energy Refinements) Force Field (Figure 5.1). The conformers having the lowest energy were used to create the α-CD||VitD, β-CD||VitD, γ-CD||VitD, and HP-β-CD||VitD complexes. To find the energetically most stable geometrical conformation, all possible modes of guest-host interaction were tested. Full geometrical optimizations were performed in vacuum employing the Polak–Ribiere Conjugate Gradient method and the generation of energy minimized-stabilized structure and complexes were based on the target RMS gradient of 0.001kcal/mol. For computations of energy attributes, the Force Fields were utilized with a distance-dependent dielectric constant scaled by a factor of 1. The 1-4 scale factors followed electrostatic (0.5) and van der Waals (0.5) (Kumar *et al*., 2011; Kumar *et al*., 2013).

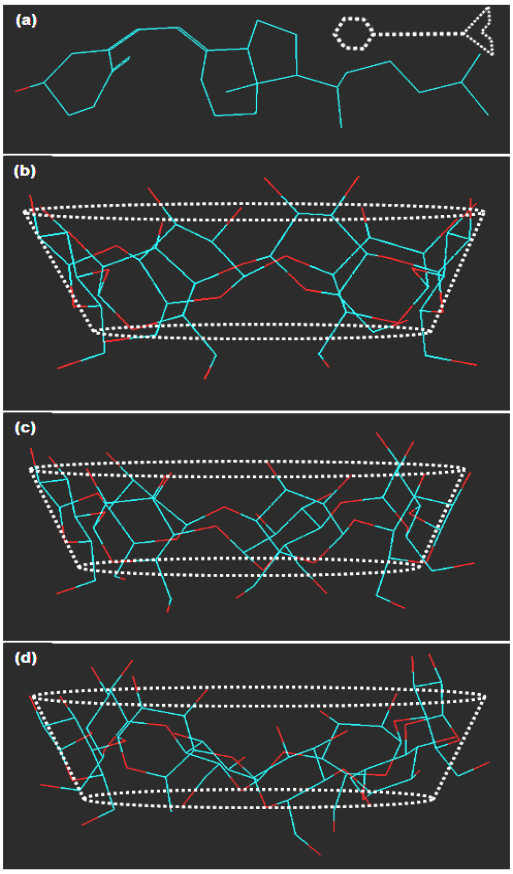


Figure 5.1: Models depicting the molecules used in the study showing (a) chemical structure of vitamin D; (b) stereographic view of the α-cyclodextrin bucket; (c) stereographic view of the β-cyclodextrin bucket; and (d) stereographic view of the γ-cyclodextrin bucket. The upper wider ring in cyclodextrin bucket represents the secondary hydroxyl groups and the lower narrower ring represents the primary hydroxyl groups. Colour codes for elements are: Carbon (cyan), Oxygen (red) and Nitrogen (blue). Hydrogen atoms are not shown for clarity.

5.2.2.3. Formulation of "3-vitamin" minitablets

Cholecalciferol, α-tocopherol and ascorbic acid have well recognized anti-inflammatory and anti-oxidant properties and the three micronutrients are suspected to play a synergistic role in the treatment or prevention of chronic diseases due to their documented cytokine-micronutrient effects (Garcia-Bailo *et al*., 2012). For this reason the three vitamins were considered appropriate for combined inclusion in the BAP minitablet component. Despite numerous enhancing benefits outlined in the literature for TPGS, its low melting point and softness have often limited its usefulness as a formulation excipient unless other excipients were added to the formulation. Combining ascorbic acid powder and cholecalciferol IC not only provided the model drug and synergistic vitamins, but also assisted in increasing the hardness of minitablets for suitable compressibility. Thus an optimal ratio of TPGS: ascorbic acid required investigation to ensure successful formulation development whilst accommodating the most efficacious amounts of each vitamin for clinical effectiveness. Addition of further excipients to the tablet mixture was avoided due to the already complex nature of the BAP system. This strategy also facilitated the synthesis of novel "excipient-free" minitablets.

After preliminary experimentation with various amounts of TPGS wax and ascorbic acid powder, an optimized ratio of TPGS: ascorbic acid (1:3) was reached. A 1:3 ratio of TPGS: vitamin C allowed for the successful compression and formation of 'soft' minitablets without the need for further binders and provided clinically relevant amounts of e

ach vitamin. A 1:4 ratio produced more resilient tablets however this ratio was not ideal as it did not allow for sufficient supplemental amounts of vitamin E as required according to recommended daily allowances (Gibbon *et al*., 2007). Higher amounts of TPGS did not result in an intact tablet due to the softness of the TPGS wax impeding upon direct compressibility of the powder blend. In addition to being a form of α-tocopherol and providing multiple bioactive enhancing affects, TPGS acted as an effective binder without the need for excipients. The optimized TPGS: vitamin C ratio ensured the formation of a soft tablet for rapid release of vitamin constituents. The 1:3 design allowed for the provision of clinically relevant amounts of vitamin C and vitamin E per minitablet. The mean weight of each minitablet was 82mg providing 20.5mg TPGS (equivalent to 5.13mg vitamin E) and 61.5mg vitamin C (Table 5.1). Optimized βD_3-8 IC was synthesized using the same modified co-precipitation method as outlined in Chapter 4 with a molar synthesis ratio of βCD: cholecalciferol of 2.5:1. The βD_3-8 IC powder was included in the TPGS: vitamin C

mixture. The provision of three minitablets delivered 15.39mg vitamin E (α-tocopherol), 184.5mg vitamin C and sufficient βD_3-8 IC to deliver at least 1000IU cholecalciferol (RDA: vitamin E: 15mg; vitamin C: 50-100mg as a dietary supplement and 100-300mg for deficiencies) (Gibbon *et al*., 2007). Table 5.1 shows the composition of the directly compressed "3-vitamin" minitablets. Higher amounts of βD_3-8 IC were also added to increase the dose of cholecalciferol from 1000IU to 4000IU so that low dose and high dose "3-vitamin" minitablet were formulated with respect to model drug, cholecalciferol composition. Table 5.1 illustrates the formulation used to create the "3-vitamin" minitablets.

The punch and die mechanism was manufactured with specialised tooling and is illustrated in Figure 5.2. The specialised punch and die mechanism allowed for a variable compression force to be applied which could be monitored using the hydraulic force gauge on a Carver Hydraulic Press (Carver Industries Inc., Wabash, IN) which was utilised to generate minitablets under a uniform pressure (less than 1 metric ton). The punch and die mechanism was manufactured from stainless steel and contained seven parts that assembled into a complete unit to be used with any table top tableting press (Figure 5.2). The mechanism was placed within a table press, exposed to the desired compression and the minitablet was then collected after disassembling the punch and die. The customized mini-punch and die produced mini-pellets or minitablets with a diameter of 4mm and a variable length (dependant on the amount of powder added) (Figure 5.4). The procedure used to manufacture the novel excipient free "3-vitamin" minitablets is outlined in detail in Figure 5.3.

Table 5.1: Composition of the directly compressed "3-vitamin" minitablets (low dose cholecalciferol minitablets):

Components	**Mean vitamin content (mg) per 82mg minitablet**	**Mean vitamin content (mg) per three minitablets**
1. Kolliphor TPGS	20.5	61.5
containing α- tocopherol:	5.13	15.39
2. Ascorbic acid	61.5	184.5
3. βD_3-8 IC	0.08722 (87,22ug)	0.261 (261.66ug)
containing cholecalciferol:	0.00834 (8.34ug/	0.02502 (25.02ug/

Components	Mean vitamin content (mg) per 82mg minitablet	Mean vitamin content (mg) per three minitablets
	(333IU)	(1000IU)

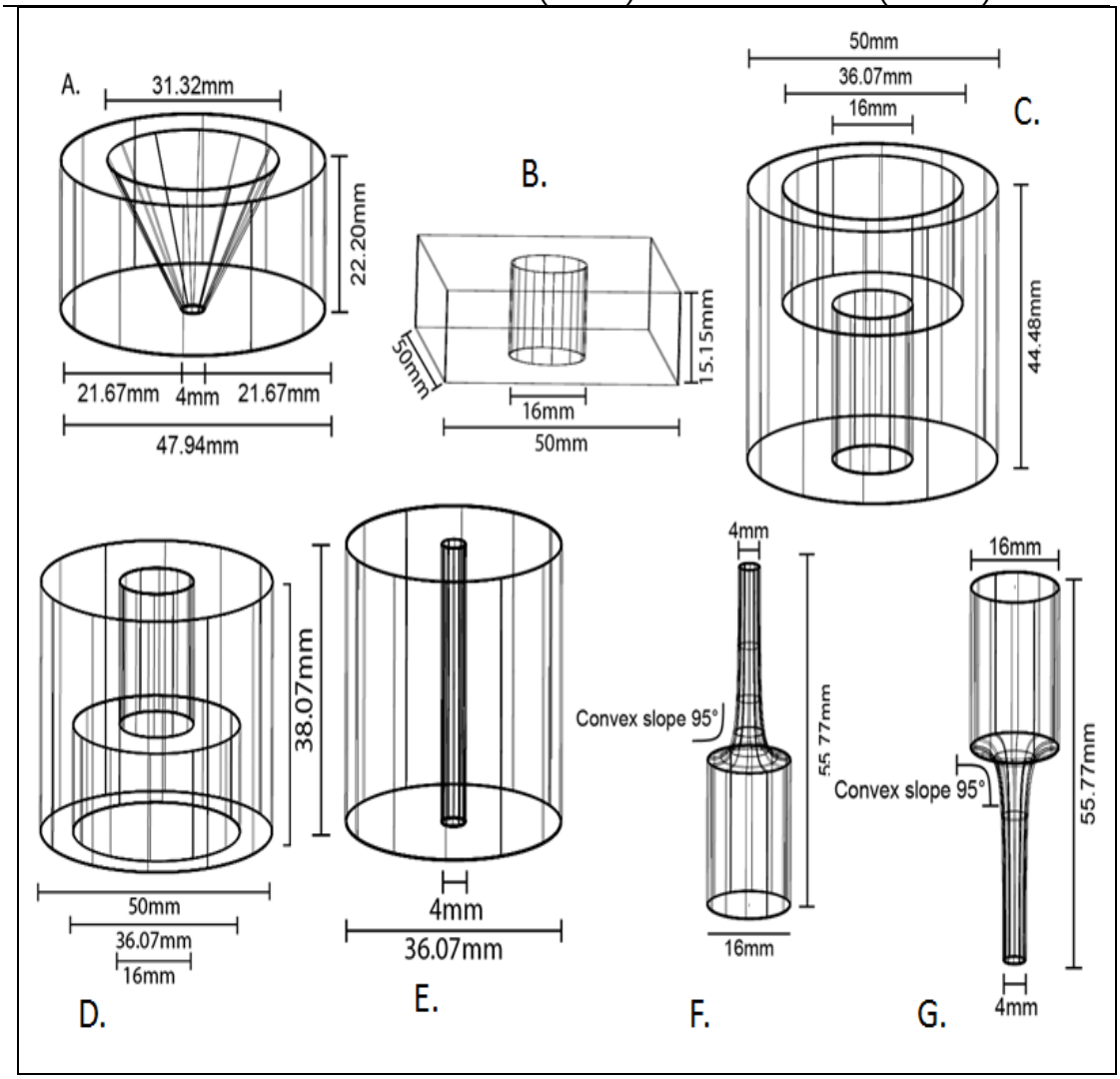


Figure 5.2: Punch and die mechanism: A: Stainless steel funnel; B: Stainless steel base plate; C: Stainless steel bottom sheath; D: Stainless steel top sheath; E: Stainless steel die; F: Stainless steel bottom punch; G: Stainless steel top punch.

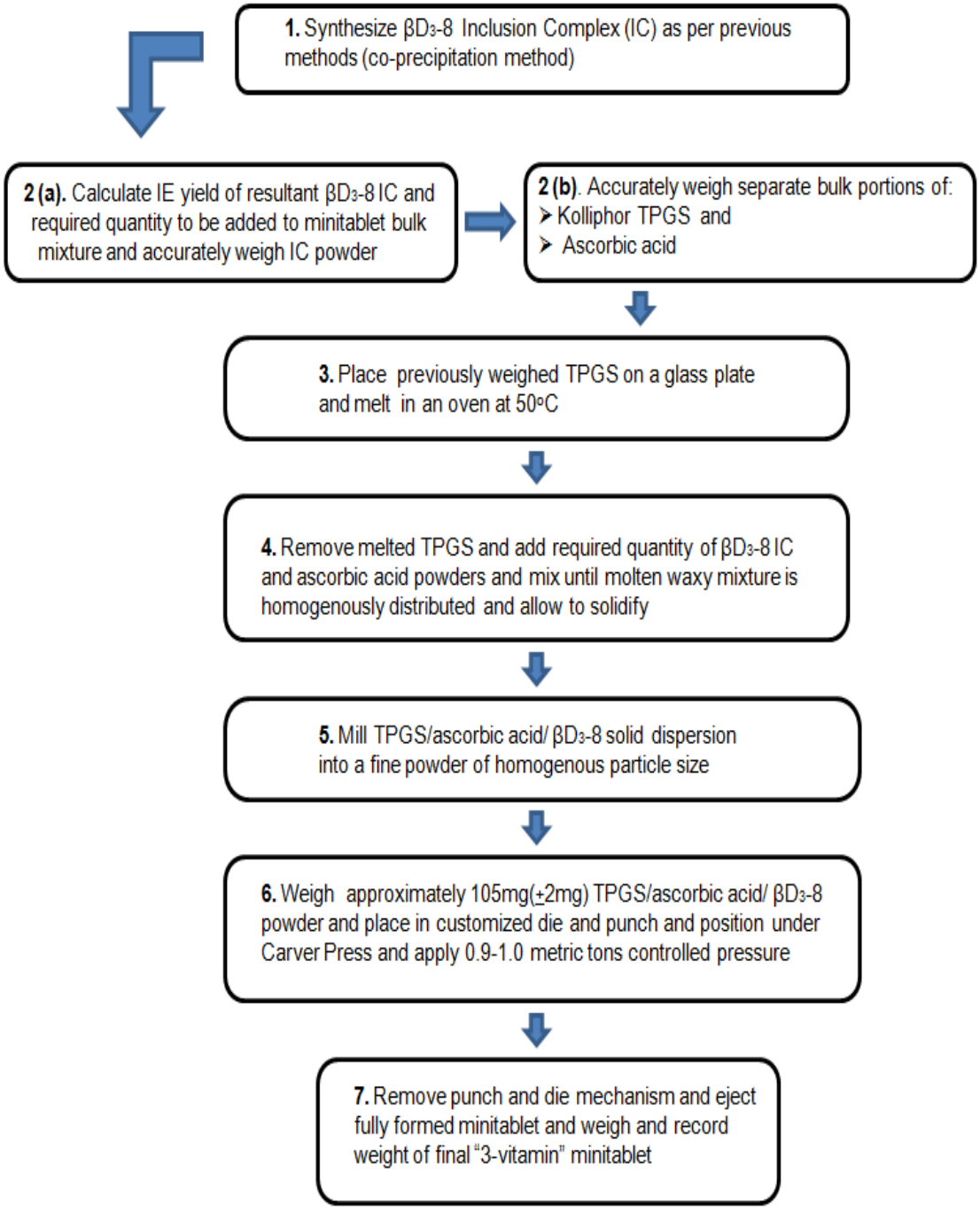


Figure 5.3: Schematic of the stepwise method used to manufacture the "3-vitamin" minitablet component.

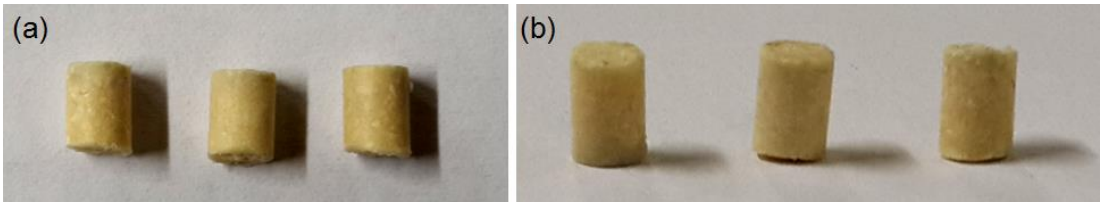


Figure 5.4: "3-vitamin" minitablets formed after compression using a modified die and punch: (a) top-view; (b) side-view.

5.2.2.4. Karl Fischer moisture content analysis of "3-vitamin" minitablets

A Karl Fischer volumetric titrator (C30) (Mettler Toledo) was used to determine the moisture content within the minitablets using a coulometric method. Minitablets (mean wt of 78.6mg) were added to the titration cell containing the reagent and solvent. The quantity of current required to convert the water contained in each minitablet tested was used to determine the quantity of moisture locked within each film formulation. Multiple samples were tested (n=5).

5.2.2.5. Texture Analysis (TA) of minitablets to determine hardness, resilience and compressibility

The "3-vitamin" minitablet formulations were evaluated with regards to matrix resilience (MR) and matrix hardness (MH). A texture analyzer (TA.XT *plus,* Stable Microsystems, Surrey, UK) was used. The texture analyzer was fitted with a cylindrical steel probe and all studies were conducted in triplicate and at 25^{o}C, 1atm pressure. MR (%) was calculated by the percentage of the ratio between the area under the curve (AUC) of the peak to baseline (after the force was removed i.e. $AUC_{2\text{-}3}$) and the baseline to peak (before the force was removed i.e. $AUC^{1\text{-}2}$) from a force-time profile (Hibbins *et al*., 2013). Therefore MR (%) was calculated from a force time profile using Equation 5.1:

$$MR = (AUC_{Anchor\ 2\text{-}3})/ (AUC_{Anchor\ 1\text{-}2}) X100 \quad \text{[Equation 5.1]}$$

Hardness of the minitablets was derived from the force (N) required to produce a given deformation and was obtained from the force-time profile. Compressibility was calculated from the area under the curve of the first positive curve of a force-time plot (Murphy *et al*., 2012). The texture analysis test parameter settings are shown in Table 5.2.

Table 5.2: Textural parameters employed for physicomechanical evaluation of "3-vitamin" minitablet formulations

Parameter	Matrix hardness (MH) (N/mm) settings	Matrix resilience (MR) (%) settings
Pre-test speed	1mm/s	1mm/s
Test speed	1mm/s	1mm/s
Post-test speed	10mm/s	10mm/s
Test mode	Compression	Compression
Target mode	Force (Distance)	Force (Strain)
Trigger type	Auto (Force)	Auto (Force)
Trigger force	0.05N	0.05N
Test distance	0.5mm	0.5mm

5.2.2.6. Magnetic Resonance Imaging (MRI) to illustrate minitablet dissolution

MRI was performed to observe the changes in hydration and erosional behaviour that occurred during the dissolution of the minitablets. A magnetic resonance system with a digital MARAN-i System configured with a DRX2 HF Spectrometer console (Oxford Instruments Magnetic Resonance, Oxon, UK) fitted with a compact 0.5 Tesla permanent magnet stabilized at 37^{o}C and a dissolution flow through cell was utilized for viewing of the erosion behaviour of the minitablets. The lower part of the cell was filled with glass beads to provide laminar flow at 16mL/min and the minitablets were placed inside the cell which was positioned in a magnetic bore and magnetic resonance images were obtained over a 45 minute time frame using MARAN-i software (version 1.0). The images obtained were used to estimate the dissolution time and provide evidence for the rapid dissolution of the "3-vitamin" minitablets upon exposure to buffer medium (pH 6.8) and under mechanical agitation with photographic images captured at set time intervals (0, 5, 10, 15, 20, 25, 30, 35, 40, 45 minutes).

5.2.2.7. Comparative ex vivo permeability of cholecalciferol from "3-vitamin" minitablets vs. a conventional comparator tablet

Membrane permeation studies were performed to assess the extent of cholecalciferol permeation across pig intestinal tissue using a Franz Diffusion Cell (FDC) apparatus (PermeGear Inc. Bethlehem, PA, USA) that consisted of a 2mL donor compartment, a clamp, a 27mL receptor compartment, and a stirrer-bar (Figure 5.5). The Static Franz Diffusion Cell Apparatus: is a well-known model used for human intestinal mucosal drug permeation. Gastro-intestinal duodenum samples were obtained from freshly euthanized Large White pigs at the Central Animal Services, Wits Medical School, University of the Witwatersrand. Samples were snap-frozen and stored at -80°C until the experiment was performed. The experiment was a component of an animal study protocol approved by the Animal Ethics Screening Committee (AESC) of the University of the Witwatersrand (Clearance certificate number 2011/43/05). Prior to the study, frozen tissue samples were allowed to thaw in phosphate buffer (pH 7.4) for 15 minutes and cut into 4mm diameter sections whilst removing excess adipose and connective tissue. Freshly thawed excised pig duodenal mucosa was placed between the donor and receptor compartments of the FDC apparatus. Simulated plasma (pH 7.4; 37°C) was placed in the receptor compartment and continuously agitated with the stirrer (Giannola *et al*., 2007). A 4000IU "3-vitamin" minitablet (High dose) and a 4000IU cholecalciferol market comparator tablet were each dissolved separately in 2mL simulated

intestinal fluid (phosphate buffer, pH 6.8) and placed in an orbital shaker at 37°C for 15 minutes to assist with dissolution prior to placing in respective donor cells. The two sample solutions were then assessed for cholecalciferol transit through the porcine duodenal mucosa by removing samples (300µL) and replacing with an equivalent volume of simulated plasma to maintain sink conditions at the following hourly time intervals 0.5, 1, 2, 4, 5, 6, 19, 24, 28 hours (over a total period of 28 hours). Samples were dried under a fume hood for 48 hours, reconstituted with ethanol and subjected to quantitative analysis using a UV nanophotometer. The experiment was conducted in triplicate. The cumulative cholecalciferol permeation (%) vs. time profiles for the minitablet and the conventional tablet were plotted using SigmaPlot V11.0 (Build 11.0.077, Systat Software Inc, Germany).

In addition, the extent of passive permeation of cholecalciferol across the pig duodenal tissue was determined in terms of drug flux. The flux ($mg.cm^{-2}.hr^{-1}$) across the intestinal tissue was calculated at steady-state per unit area by linear regression analysis of permeation data and using Equation 5.2:

$$J = \frac{Q}{A} \times t \qquad \text{[Equation 5.2]}$$

where, J is the flux ($mg.cm^{-2}.hrs^{-1}$), Q (mg) is the quantity of cholecalciferol that diffused through the pig intestinal tissue into the receptor compartment, A (cm^2) is the cross-sectional area available for drug permeation and t (h) is the time of drug exposure to the duodenal tissue.

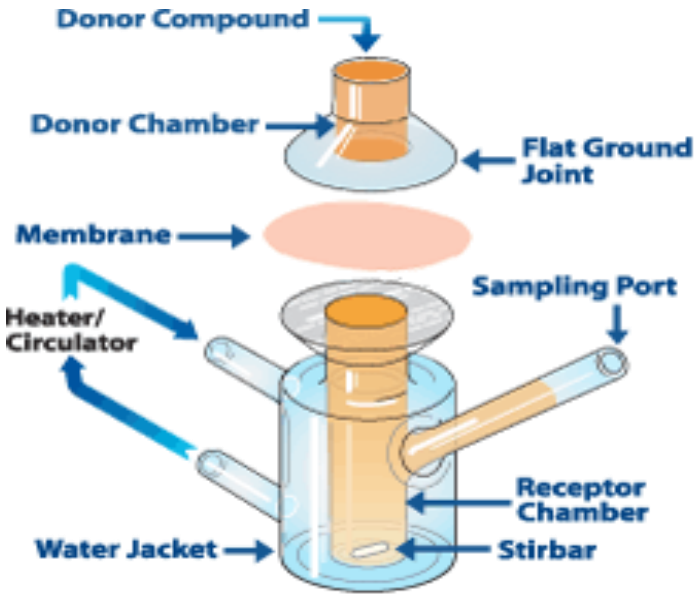


Figure 5.5: Schematic showing the components making up a single Franz Diffusion cell used for the *ex vivo* cholecalciferol permeability studies (Vertical Franz Cell: www.permegear.com).

5.2.2.8. Thermodynamic analysis of minitablets by Differential Scanning Calorimetry (DSC)

DSC analysis was performed on minitablet samples and individual constituents (ascorbic acid, TPGS, vitamin D_3, βD_3-8 complex) using a Differential Scanning Calorimeter (Mettler Toledo) fitted with $Star_e$ software (Mettler Toledo, Switzerland). The scan rate was set at 10°C/min between a temperature range of 10°C and 95°C for the minitablet, TPGS and vitamin D_3. The temperature range for ascorbic acid was set at 10°C-300°C (after an initial water loss run). All samples weighed 10mg and were placed in closed aluminium crucibles covered by a lid with a pinhole. For each DSC run and temperature range, samples were subject to DSC analysis under nitrogen. Reproducibility was assured by examining results obtained from multiple runs in at least triplicate.

5.2.2.9. Chemical structure stability mapping of minitablets by Fourier Transform Infrared Spectroscopy (FTIR)

Fourier Transform Infrared (FTIR) Spectra were recorded between $650cm^{-1}$ and $4000cm^{-1}$ for films, minitablet and individual constituents using a PerkinElmer Spectrum 100 Series FTIR spectrometer coupled with Spectrum FTIR research grade software (Perkin Elmer spectrum 100 Life and Analytical Sciences Inc., Massachusetts, USA). Vibration characteristics of chemical functional groups were detected in response to infrared light interactions. The procedure involved the placement of minitablet samples onto the sampling cup and compressing the sample into the holder using a compression gauge. The samples were placed in the infrared light path and a spectrum was obtained.

5.2.3. BAP component B: Optimized bile salt-lipase film for inclusion in BAP

5.2.3.1. Synthesis of bile salt-lipase alginate films

Films were synthesized following the same methods already described in Chapter 4, section 4.2.5.2. Various compositions of bile salts and pancreatic lipase were loaded to film matrices so as to evaluate film bioactive composition on model drug (cholecalciferol) release from minitablets. Dry bioactive films were collected by peeling off petri dishes and weighed for further testing. Films were also used to assay the lipase enzyme activity levels following exposure and release in simulated intestinal fluid. Table 5.3 lists all bioactive film formulations that were synthesized during the current study.

Table 5.3: Bile salt-lipase alginate film formulations

Film Formulation	Mean weight of film (mg)	Alginate ($\%^{w}/_{v}$)/ glycerin ($\%^{v}/_{v}$)	Bioactive (mg)	Bile salt: lipase ratio	Calcium gluconate crosslinker ($\%^{w}/_{v}$)
1. 66B/33L	201.25	4%/ 2%	NaC: 20 NaD: 20 Lip: 20	2:1	0.5
2. 33B/66L	202.47	4%/ 2%	NaC: 4 NaD: 4 Lip: 16	1:2	0.5
3. 80B/20L	201.04	4%/ 2%	NaC:16 NaD:16 Lip: 8	4:1	0.5
4. 100B High	200.22	4%/ 2%	NaC: 20 NaD: 20	1:0	0.5
5. 100B Low	202.81	4%/ 2%	NaC: 10 NaD: 10	1:0	0.5
6. 100L	200.77	4%/ 2%	Lip: 20	0:1	0.5
7. 66B/33L(0%)	1001.32	4%/ 2%	NaC: 100 NaD: 100 Lip: 100	2:1	0
8. 66B/33L(0.25%)	1011.14	4%/ 2%	NaC: 100 NaD: 100 Lip: 100	2:1	0.25
9. 66B/33L(0.5%)	1005.32	4%/ 2%	NaC: 100 NaD: 100 Lip: 100	2:1	0.5
10. 66B/33L(1%)	1014.36	4%/ 2%	NaC: 100 NaD: 100 Lip: 100	2:1	1

NaD: sodium deoxycholate; NaC: sodium cholate hydrate; Lip: pancreatic lipase

5.2.3.2. Influence of bile salt-lipase films on cholecalciferol release from minitablets: Selection of an optimized film

Scaffold studies in Chapter 4 achieved the controlled release of bile components from scaffold devices, however the release profiles of bio-surfactants holds little relevance to their ability to affect the bioavailability of the model drug. Therefore it was deemed paramount to determine the impact of bile salts on the release parameters of cholecalciferol. In addition, in order to decide on the ideal bile salt-lipase composition within the final bioactive-alginate films, further studies were required to elucidate the effects of bile and lipase on cholecalciferol *in vitro* release. Texture analysis studies in Chapter 4 already proved that $0.5\%^{w}/_{v}$ of crosslinker was an ideal amount to ensure the highest tensile strength but still maintain film flexibility. Therefore various $0.5\%^{w}/_{v}$ crosslinked films containing different bile salt and lipase content were investigated for their influence on cholecalciferol release from minitablets. The bile salt and lipase content in each film was proposed to have

an enhancer effect on *in vivo* bioavailability of cholecalciferol due to the biological surfactant effects of bile salts and the enzymatic activity of lipase. However, prior to *in vivo* evaluation, an exploration into their effect on cholecalciferol *in vitro* dissolution was essential.

The study set out to quantify the affect that various films have on the release profiles of cholecalciferol from a previously formulated (high dose) "3-vitamin" minitablets. Film samples containing bioactive in varying ratios of bile salt to lipase (NaD, NaC, lipase) were selected (Table 5.3 formulations 1-6). Each film contained a standardized polymer/ glycerin composition (4%$^{w}/_{v}$ alginate/ 2%$^{v}/_{v}$ glycerin) and the same crosslinker composition (Ca gluconate 0.5%$^{w}/_{v}$). Each experimental film was wrapped around three previously weighed minitablets each with a mean mass of 84.21mg and collectively containing 4000IU cholecalciferol. The minitablets wrapped in films were placed in separate vessels containing 30mL SIF (pH 6.8) in an orbital shaker (rotating at 30rpm, and maintained at 37^{o}C). Samples (1mL) were withdrawn at appropriate time intervals: 10, 20, 30, 40, 60, 90, 120, 180 minutes and 1mL fresh SIF was replaced in each beaker to maintain sink conditions. Samples were filtered to remove excess alginate and then subjected to solid phase extraction to separate out the fat-soluble vitamin, cholecalciferol, for quantification. A solid phase extraction method was used to extract cholecalciferol from the dissolution samples using an OASIS HLB cartridge according to a similar method employed by Xue and co-workers (2008) prior to HPLC analysis. The amount of cholecalciferol released at each time point was determined using a Waters LC-10A HPLC system (Shimadzu, Kyoto, Japan) using a Waters Atlantis dC18 column and fitted with a Waters 1525 binary HPLC pump. The HPLC mobile phase was methanol-water (98:2, $^{v}/_{v}$) with a flow rate of 1.0mL/min, and an injection volume of 10µL and UV detection with a UV-visible spectroscopy detector at 265nm. Dissolution curves of % release versus time were plotted using SigmaPlot. DDSolver, an add-in program for Excel, was used to generate pharmacokinetic parameters in order to characterize the cholecalciferol drug release curves. DDSolver was utilized to accurately and precisely calculate relevant dissolution profile values for each cholecalciferol release curve to facilitate selection of an optimized film based on bile salt and lipase content (Zhang *et al*., 2010).

Various dissolution values were calculated using DDSolver: The mean dissolution time (MDT), area under the dissolution curve (AUC), dissolution efficiency (DE), relative dispersion of dissolution time (RD), variance of dissolution time (VDT), and

mean residence time of the drug substance molecules in the dosage form (MRT) were calculated using the following equations:

$$MDT = \frac{\sum_{i=1}^{n} \bar{t}_i \cdot \Delta M_i}{\sum_{i=1}^{n} \Delta M_i}$$ [Equation 5.3]

$$\mathrm{AUC} = \sum_{i=1}^{n} \frac{(t_i - t_{i-1})(y_{i-1} + y_i)}{2}$$ [Equation 5.4]

$$\mathrm{DE} = \frac{\int_0^t y \cdot dt}{y_{100} \cdot t} \cdot 100\%$$ [Equation 5.5]

$$\mathrm{RD} = \mathrm{CV}^2 = \frac{\mathrm{VDT}}{\mathrm{MDT}^2}$$ [Equation 5.6]

$$\mathrm{VDT} = \frac{\sum_{i=1}^{n} \left(\bar{t}_i - \mathrm{MDT}\right)^2 \cdot \Delta M_i}{\sum_{i=1}^{n} \Delta M_i}$$ [Equation 5.7]

$$\mathrm{MRT} = \frac{\int_0^t t \cdot (100 - y) \cdot dt}{\int_0^t (100 - y) \cdot dt}$$ [Equation 5.8]

Where ***n*** is the number of sampling points; $\boldsymbol{t_i}$ is the *i*th time point; $\boldsymbol{y_i}$ is percentage of drug dissolved at time t_i; $\boldsymbol{M_{last}}$ *is* accumulative percentage of drug dissolved at the last time point; ***y*** is percentage of drug dissolved at time *t* ; $\overline{t_i}$ is time at the midpoint between *i* and *i*-1; $\triangle \boldsymbol{M_i}$ is additional amount of drug dissolved between *i* and *i*-1; ***k*** is order of the moments of dissolution times; y_{100} is maximum percentage of drug dissolved over the time period 0-*t* (Zhang *et al*., 2010).

5.2.3.3. Enzyme activity profiles of 66B/33L(0%; 0.25%, 0.5%, 1%) films following hydration in SIF: Selection of an optimized film

Following favourable results for the 66B/33L formulation on the release profiles of cholecalciferol, 66B/33L films containing varied quantities of crosslinker (0%$^{w}/_{v}$, 0.25%$^{w}/_{v}$, 0.5%$^{w}/_{v}$, and 1%$^{w}/_{v}$) but same ratio of bile salt to lipase were synthesized and tested for lipase activity (Table 5.3 formulations 7-10). A weighed amount of 200mg of each of the film formulations 7-10 was placed in different cells of a USP 4

apparatus to test the pancreatic enzyme activity of each film (Flow-through cell dissolution tester, Type DFZ60, Erweka). Even though a 0.5%$^{w}/_{v}$ crosslinked film demonstrated the best mechanical properties during TA analysis, it was considered important to ensure that this crosslinker concentration maintained an adequate enzyme activity. The dissolution media consisted of 100mL phosphate buffer solution adjusted to pH 6.8 (simulated intestinal fluid) and maintained at 37°C. The feed rate was maintained at 8mL and 150rpm. Sample aliquots (1mL) were withdrawn at appropriate time intervals (10, 20, 30, 40, 60, 90, 120,180, 240, 360 minutes), and replaced with 1mL of fresh dissolution medium to maintain sink conditions. The lipase activity (milliunits/mL) was determined at each time interval using a lipase activity assay kit (Sigma Aldrich, St. Louise, MO, USA). Dissolution samples, glycerol standards and assay reagents were added to a 96 well flat-bottomed plate and the assay was performed as per the kit protocol. The assay plate results were read on a spectrophotometric multilabel plate reader (Victor X3, PerkinElmer). Lipase activity was determined using a coupled enzyme reaction resulting in a colorimetric product visible at 570nm and quantified via absorbance readings by the multilabel reader. The lipase activity was found to be proportional to the enzyme activity present in each sample solution. Based on the experimental lipase activity data an optimized crosslinker composition was selected for the 66B/33L bile salt-lipase film.

5.2.3.4. Thermodynamic analysis of optimized 66B/33L(0.5%) BAP films by Differential Scanning Calorimetry (DSC)

Optimized film formulations, 66B/33L(0.5%), and individual constituents (alginate, pancreatic lipase, NaD and NaC) were subjected to thermal analysis using a Differential Scanning Calorimeter (Mettler Toledo) fitted with Star$_e$ software (Mettler Toledo, Switzerland). The scan rate was set at 10°C/min between a temperature range of 10°C and 250°C initially. Re-analyses was done by running samples twice consecutively (run 1=10°C-125°C; run 2=10°C-300°C) to reduce water evaporation isotherms. All samples weighed 10mg and were placed in closed aluminium crucibles covered by a lid with a pinhole. For each DSC run and temperature range, samples were subject to DSC analysis under nitrogen. Reproducibility was assured by examining results obtained from multiple runs in at least triplicate.

5.2.3.5. Chemical structure analysis of optimized 66B/33L(0.5%) BAP films by Fourier Transform Infrared Spectroscopy (FTIR)

Fourier Transform Infrared (FTI-R) Spectra were recorded between 650cm^{-1} and 4000cm^{-1} for optimized 66B/33L(0.5%) films and individual constituents (NaC, NaD, Alg) using a PerkinElmer Spectrum 100 Series FTIR spectrometer coupled with Spectrum FTIR research grade software (Perkin Elmer spectrum 100 Life and Analytical Sciences Inc., Massachusetts, USA). Vibration characteristics of chemical functional groups were detected in response to infrared light interactions. Dried films were crushed and ground using a grinder and placed onto the sampling cup of the FTIR. Each sample was compressed into the sample holder using the compression gauge. The samples were placed in the infrared light path and a spectrum was obtained.

5.2.4. Final BAP DDS capsule: Combined technologies for improved release

5.2.4.1. Final BAP: Assembling each BAP DDS capsule

As discussed under section 5.2.2.3 either a high dose or a low dose minitablet was formulated to allow for the inclusion of either 1000IU or 4000IU cholecalciferol per three minitablets (333IU or 1333IU per tablet) in the BAP. The three minitablets were wrapped in 200mg optimized bioactive alginate film (66B/33L) and inserted into two transparent gelatin capsules. The quantity of 66B/33L bioactive film evenly distributed in the two capsules provided a total of 20mg pancreatic lipase, 20mg sodium cholate hydrate and 20mg sodium dexoycholate. The total quantity of model drug in each formulation (consisting of two capsules containing evenly distributed 200mg film, and three “3-vitamin” minitablets) was 1000IU or 4000IU cholecalciferol.

A customized kollicoat® MAE 100P solution (40%$^{w}/_{v}$) was prepared and mixed for 4 hours under magnetic stirring. Controlled, slow mixing was ensured to prevent foam formation. After 4 hours, polyethylene glycol methyl ether (5%$^{w}/_{v}$) was added as a plasticizer and the solution was mixed for a further 20 minutes. Amaranth (30mg) was added to the solution as a colorant and the finished coating was ready to be coated onto each gelatin capsule containing minitablets wrapped in 66B/33L film. Each BAP capsule was carefully rotated whilst ‘dip-coating’ with the Kollicoat® mixture until all surfaces were homogenously covered with a red coloured pH responsive kollicoat® layer. Figure 5.6 shows a schematic illustrating the process used to assemble the final BAP DDS capsules and their resultant composition.

Figure 5.7 shows the actual photographic images of the various optimized components that made up the final BAP capsules (Component A: "3-vitamin" minitablets containing ascorbic acid, TPGS and cholecalciferol IC; and Component B: 66B/33L(0.5%) bile-salt lipase film). Figure 5.8a and b shows images of one BAP DDS at the final stage of synthesis prior to and post the Kollicoat® 'dip-coating' step.

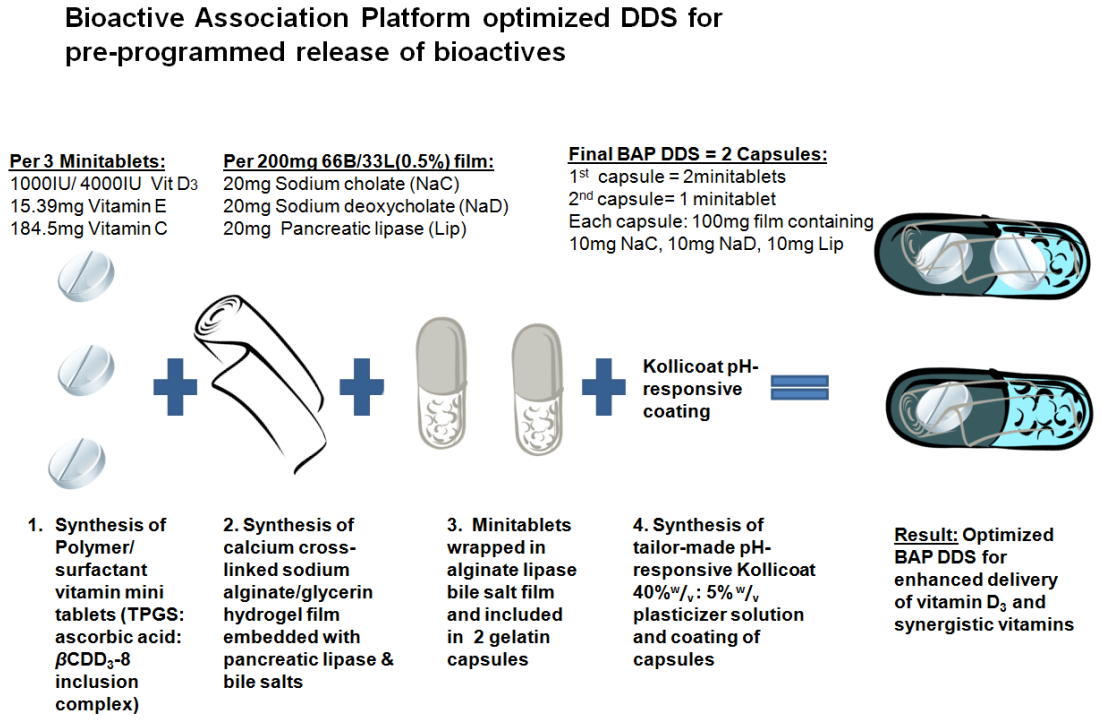


Figure 5.6: Illustrative schematic showing the assembling of the two BAP capsules containing all formulation components.



Figure 5.7: Final BAP components used in the formulation design and to assemble the BAP DDS capsule: Component A: Novel "3-vitamin" minitablets consisting of ascorbic acid, TPGS and βD_3-8 IC; Component B: Bile salt-lipase bioactive film.

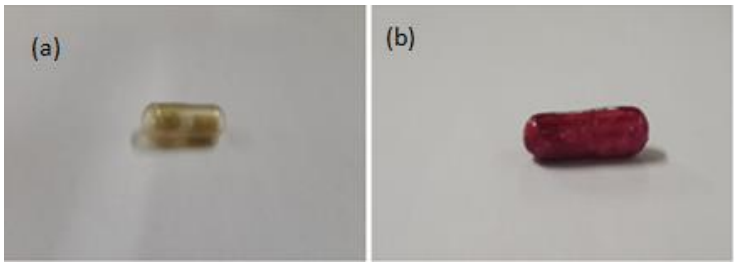


Figure 5.8: BAP DDS capsule: (a) prior to coating; (b) coated with modified Kollicoat® pH responsive coating containing the six bioactives: cholecalciferol (model drug), ascorbic acid, α-tocopherol, pancreatic lipase, sodium deoxycholate, sodium cholate hydrate and various polymers and carrier mechanisms.

5.2.4.2. Comparative in vitro dissolution testing of BAP DDS

The dissolution testing of the BAP DDS capsules containing optimized film and "3-vitamin" minitablets, compared to a commercial comparator vitamin D_3 product was performed using a USP 4 apparatus (Flow-through cell dissolution tester, Type DFZ60, Erweka). Release in gastric medium was not evaluated because preliminary studies confirmed the lack of dissolution of the Kollicoat® coated BAP capsules in USP buffer medium adjusted to pH 1.2 over an 8 hours observation period.

The dissolution media used for the dissolution study consisted of 60mL phosphate buffer solution adjusted to pH 6.8 (simulated intestinal fluid) and maintained at 37°C. A smaller dissolution media volume was used (60mL) due to the small quantity of vitamin D_3 per DDS (1000IU-4000IU cholecalciferol equivalent to 25ug-100ug). The two BAP capsules and a comparator vitamin D_3 tablet were placed separately in specified cells of the dissolution apparatus. The feed rate was maintained at 8mL and 150rpm. A 1mL sample aliquot was withdrawn at appropriate time intervals (10, 20, 30, 40, 60, 120, 180 minutes), and replaced with 1mL of fresh dissolution medium to maintain sink conditions. The amount of vitamin D_3, vitamin C and vitamin E released from the BAP at each time interval was determined using a Waters LC-10A HPLC system (Shimadzu, Kyoto, Japan) using a Waters Atlantis dC18 column and a Waters 1525 binary HPLC pump. A solid phase extraction method was used to extract the fat-soluble vitamins from the dissolution samples using an OASIS HLB cartridge by a similar method used by Xue and co-workers (2008) prior to HPLC analysis. The mobile phase used was methanol-water (98:2, $^{v}/_{v}$) with a flow rate of 1.0mL/min, and an injection volume of 10uL. Detection with a UV-vis detector was at 265nm for vitamin D_3, 230nm for vitamin E and 265nm for vitamin C. The concentration of the samples was evaluated from the area under the curve and calculated using the respective standard curves for each vitamin. The same method was utilized to quantify the cholecalciferol release profile of the

comparator vitamin D_3 product. The cholecalciferol release profile of the BAP was compared to the cholecalciferol release from the commercial comparator.

Vitamin dissolution data was fitted to different kinetic models: First-order, Zero-order, Higuchi, Korsmeyer-peppas, Hixson-Crowell, Weibull and logistic, and Makoid-Banakar. The model determination coefficient (R^2_{adjusted}) and the minimum Akaike information criterion (AIC) were evaluated to select the best fit model. Data analysis was performed using the Excel add-in DDSolver program after the obtained data measurements and standard deviations were plotted within scatter plots using SigmaPlot V11.0 (Build 11.0.077, Systat Software Inc, Germany) (Zang *et al*., 2010). Dissolution curves of cumulative vitamin release % versus time were plotted using SigmaPlot. DDSolver was used to generate pharmacokinetic values for the vitamin release curves for the BAP and the comparator D_3 product. The MDT, AUC, DE, RD and MRT values were calculated using DDSolver and Equations 5.3-5.8 as detailed under section 5.2.3.2 (Zang *et al*., 2010). Additionally the dissolution profiles of the BAP cholecalciferol release and the comparator cholecalciferol release were compared using the difference factor (f1) and the similarity factor (f2) calculated by DDSolver as per Equations 5.9 and 5.10. The dissolution profiles of the three vitamins released from the BAP were also compared using f1 and f2 calculations.

$$f_1 = \left[\sum_{t=1}^{n} |R_t - T_t| / \sum_{t=1}^{n} R_t\right] \times 100$$

f1, difference factor
[Equation 5.9]

$$f_2 = 50 \cdot \log\left\{\left[1 + \frac{1}{n}\sum_{t=1}^{n} (R_t - T_t)^2\right]^{-0.5} \times 100\right\}$$

f2, similarity factor
[Equation 5.10]

Where R_t, T_t are the percentage dissolved of the reference and test profile respectively, at time point *t* ; *n* is the number of sampling points (Zang *et al*., 2010; Medina *et al*., 2014).

5.3. Results and Discussion

5.3.1. Evaluation of comprehensive modeling simulations to confirm β-CD||VitD IC superiority

The molecular mechanics simulations for cyclodextrin/VitD complexes were carried out 1) to determine the most energetically stable and feasible CD||VitD inclusion complex; 2) to ascertain the binding/ inclusion mode of VitD with respective cyclodextrin; and 3) to develop a space-filling model displaying the best-fit geometrical conformation. Briefly; VitD was positioned manually vertically into the cyclodextrin "bucket" through (1) the aliphatic end; and (2) the aromatic end of VitD – inserted from the wider end of cyclodextrin. The structures so generated were then energetically minimized employing AMBER3 force field. The most energetically stable conformations (among all possible insertion and complexation modes) for various CD||VitD inclusion complexes are depicted in Figure 5.9.

5.3.1.1. Energetic stabilization of CD||VitD inclusion complexes

Molecular Mechanics simulations, also known as static lattice atomistic simulations, present a method for analytico-mathematical representation of the potential energy surfaces and provide data related to the contributions of bonding (bond stretching contributions, bond angle contributions, and torsional contribution arising from deviations from optimum dihedral angles) and non-bonding energies (van der Waals interactions, hydrogen-bond energy function, and electrostatic energy) towards the geometrical stabilization of cyclodextrin/vitamin inclusion complexes. In addition, the total potential energy deviation, ΔE_{Total} (Table 5.4), was computed as the difference between the total potential energy of the complex system and the sum of the potential energies of isolated individual molecules using Equation 5.11.

$$\Delta E_{Total(A/B)} = E_{Total(A/B)} - [E_{Total(A)} + E_{Total(B)}] \qquad \text{[Equation 5.11]}$$

The molecular stability was then estimated by comparing the total potential energies of the isolated and complexed systems. If the total potential energy of the complex was smaller than the sum of the potential energies of isolated individual molecules in the same conformation, the complex formed was considered more stable and its formation was favoured (Yu *et al*., 2008).

In accordance with Table 5.4; all CD||VitD inclusion complexes were stabilized as compared to the individual components in the range of ≈-19kcal/mol (HP-β-CD||VitD)

to ≈-28kcal/mol (β-CD||VitD) thereby proving the formation of an inclusion complex in each of the four cases. Additionally; this proves that the "perpendicular-insertion" method provided a perfect fit of the vitamin into the cyclodextrin molecular space. The energy trends for the individual CD||VitD complexes are as follows:

1. α-CD||VitD: The α-CD||VitD inclusion complex was stabilized by the non-bonding energy attributes in terms of van der Waals forces (V_{ij}) and electrostatic interactions (V_{el}). Although the final total steric energy of the optimized α-CD||VitD structure is accompanied by stabilization to the value of 22kcal/mol; all the bonding interactions viz V_b, V_θ, and V_φ destabilized the α-CD||VitD structure which may be attributed to the steric hinderences caused by the inability of the small molecular cavity of α-CD to accommodate the steric volume of VitD, as discussed further in this report (Table 5.4).
2. γ-CD||VitD: The γ-CD||VitD inclusion complex was stabilized partially by the bonding attributes (V_b and V_θ) as well as by the non-bonding attribute (V_{ij}). The γ-CD||VitD, however, was destabilized by the torsional contributions (V_φ) and electrostatic interactions (V_{el}) (Table 5.4). This diverse behaviour and higher energy of stabilization (24kcal/mol) may be attributed to the strain-free movement of the VitD molecule to-and-fro in the CD cavity due to its larger volume allowing the molecules to orientate with respect to surrounding molecular groups.
3. β-CD||VitD: The β-CD||VitD inclusion complex was most stabilized among the basic unmodified cyclodextrin (α-, β-, and γ-CD) complexes. Similar to γ-CD||VitD complex; the β-CD||VitD inclusion complex was stabilized by both bonding (V_b and V_θ) and non-bonding (V_{ij}) attributes while destabilized by the torsional contributions (V_φ) and electrostatic interactions (V_{el}). However; notably almost all the energy stabilization was provided by the non-bonding steric contributor – van der Waals forces – hence highlighting the role of perfect-fit of the molecule inside the cyclodextrin cavity (Table 5.4). With the ΔE_{Total} being higher for β-CD||VitD as compared to α-CD||VitD and γ-CD||VitD with lower and higher cavity volume, respectively, confirms the presence of a region-of-maximum w.r.t. the spatial fit among the individual molecules.
4. HP-β-CD||VitD: With β-CD||VitD inclusion complex showing the best energy stabilization; VitD was further complexed with HP-β-CD in order to observe the effect of hydrophilic hydroxypropyl side chains on the inclusion of the vitamin. However; surprisingly the energy of stabilization was least in this case (19kcal/mol) with stabilization provided only by the van der Waals forces (Table 5.4). As explained earlier; this may be attributed to the additional steric hindrance caused by the presence of large aliphatic side chains.

Table 5.4: Inherent energy attributes representing the molecular assemblies modeled using static lattice atomistic simulations in vacuum

Molecular complex	**ΔE** [a]	V_{Σ} [b]	V_b [c]	V_θ [d]	V_φ [e]	V_{ij} [f]	V_{hb} [g]	V_{el} [h]
Vit. D	-	29.950	1.049	12.328	16.038	0.534	0	0
α-CD	-	10.373	2.708	23.071	23.431	15.805	0	-54.643
β-CD	-	5.998	3.443	25.949	26.834	20.958	0	-71.187
γ-CD	-	-10.943	3.683	25.459	21.953	22.269	0	-84.309
HP-β-CD	-	102.982	4.790	107.576	33.278	15.876	0	-58.538
α-CD-VitD	-22.037	18.286	3.806	37.058	43.709	-9.609	0	-56.678
β-CD-VitD	-27.763	8.185	3.966	36.861	44.993	-7.276	0	-70.359
γ-CD-VitD	-24.379	-5.372	4.368	35.531	40.579	-5.462	0	-80.388
HP-β-CD-VitD	-18.818	114.114	5.884	122.485	52.566	-8.333	0	-58.487

[a] $\Delta E_{(A/B)} = E_{(A/B)} - [E_{(A)} + E_{(B)}]$
[b] total steric energy for an optimized structure
[c] bond stretching contributions
[d] bond angle contributions
[e] torsional contribution arising from deviations from optimum dihedral angles
[f] van der Waals interactions
[g] hydrogen-bond energy function
[h] electrostatic energy

5.3.1.2. The inclusion mode of VitD with respective cyclodextrin

It is evident from Figure 5.9 that VitD acquired significantly different inclusion modes with cyclodextrin and can be differentiated on the basis of the position of aromatic/aliphatic end and depth of insertion. The α-CD||VitD complex was formed with the aliphatic end encapsulated into the α-CD "bucket" and the aromatic end remained outside the α-CD bucket leading to aliphatic end positioned towards primary hydroxyl ring (1°OH) and aromatic end positioned towards secondary hydroxyl ring (2°OH) forming "aliphatic end - 1°OH - 2°OH – aromatic end" inclusion mode (Figure 5.9a). Interestingly, no inclusion complex was formed when aromatic ring was inserted into the α-CD bucket (data not shown). However, in case of final β-CD||VitD (Figure 5.9b), γ-CD||VitD (Figure 5.9c), and HP-β-CD||VitD (Figure 5.8d) inclusion complexes; the aromatic end remained in close vicinity of the 1°OH and the aliphatic end positioned towards 2°OH forming "aromatic end - 1°OH - 2°OH – aliphatic end" inclusion mode. A closer look at the respective inclusion complexes reveal that β-CD||VitD and γ-CD||VitD displayed the well-balanced "button-and-string" inclusion mode while α-CD||VitD and HP-β-CD||VitD displayed the typical

“inverted-umbrella” inclusion mode (Figure 5.9). This corroborates with the energy minimization data where the “button-and-string” morphologies are better stabilized than the “inverted-umbrella” morphologies because of better mass distribution on either side of the cyclodextrin cavity in the former case.

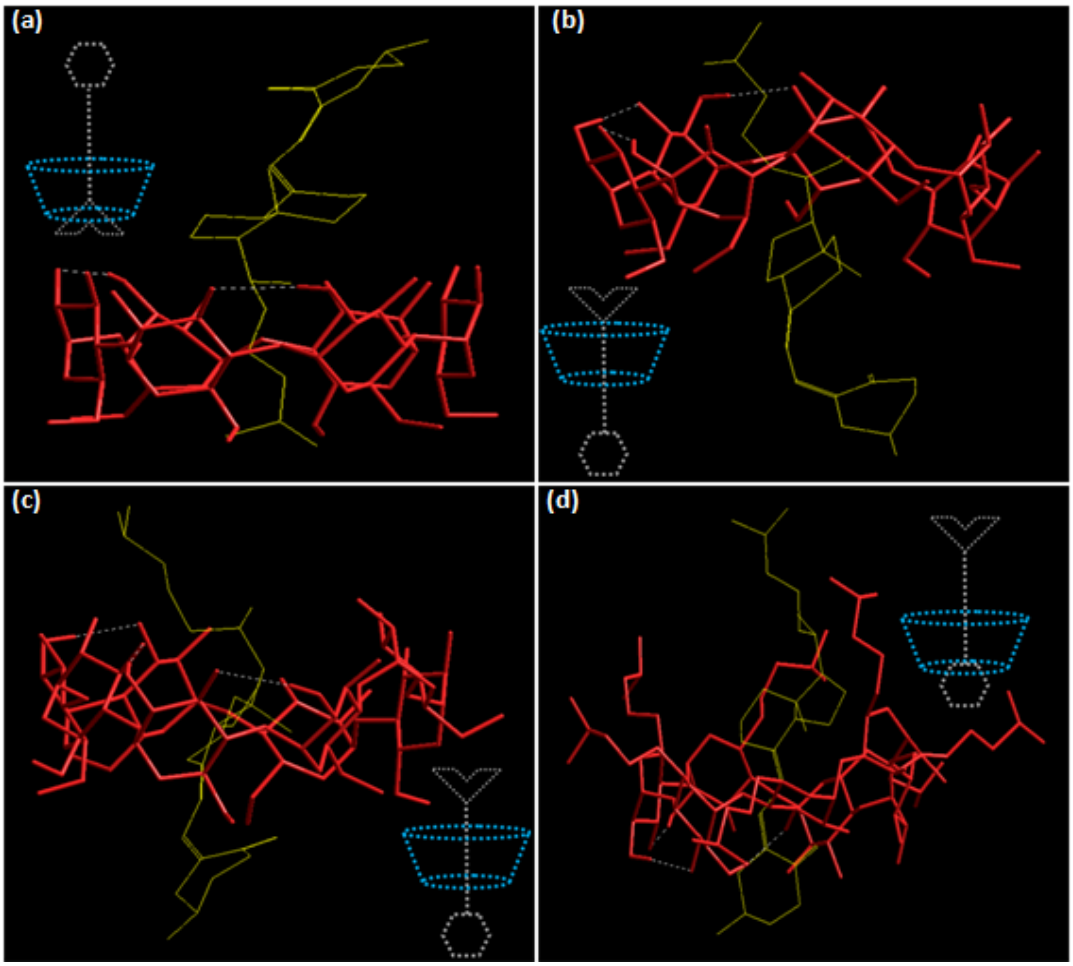


Figure 5.9: Molecular models depicting minimum energy inclusion complexes of VitD with (a) α-CD; (b) β-CD; (c) γ-CD; and (d) HP-β-CD. The 3D models were slightly rotated in order to clearly visualize the H-bonds formed between the molecules. Cyclodextrins are depicted in tube rendering and VitD stick rendering. Template showing the respective configurations are also shown for easy understanding and depiction.

5.3.1.3. Space-filling model for determination of best-fit geometrical conformation

The space-filling model was used to ascertain the best-fit geometrical conformation as shown in Figure 5.10. According to the literature; the cavity size of α-, β- and γ-CD corresponds to 0.47–0.53nm, 0.60–0.65nm and 0.75–0.83nm, respectively (Davis and Brewster, 2004). As evident from Figure 5.10a, that the overlapping spheres of VitD were too large to fit into the α-CD cavity while in Figure 5.10c, there is excessive unfilled space to further provide a perfect-fit. Similarly; the space-filled

structure of HP-β-CD||VitD displayed cluttering and distortion of the original β-CD cavity space (Figure 5.10d). Among the space-filled structures; only β-CD||VitD showed the perfect fit with the vitamin not fully blocking the β-CD cavity - thereby allowing the essential movement of the inclusion molecule. Additionally; no redundant unfilled space was present – thereby preventing undue movement of the vitamin molecule once inclusion complex is formed. This evaluation fits perfectly with the IE data obtained and discussed under section 4.3.7 in Chapter 4, where the superior cholecalciferol complex, *βCDD$_3$-8,* achieved an IE% of 78%. Similarly the quantum of highest to lowest IE correlates well with the space fit model: *βCDD$_3$-8 > γCDD$_3$-4 >2HPβCDD$_3$-4> αCDD$_3$-4*

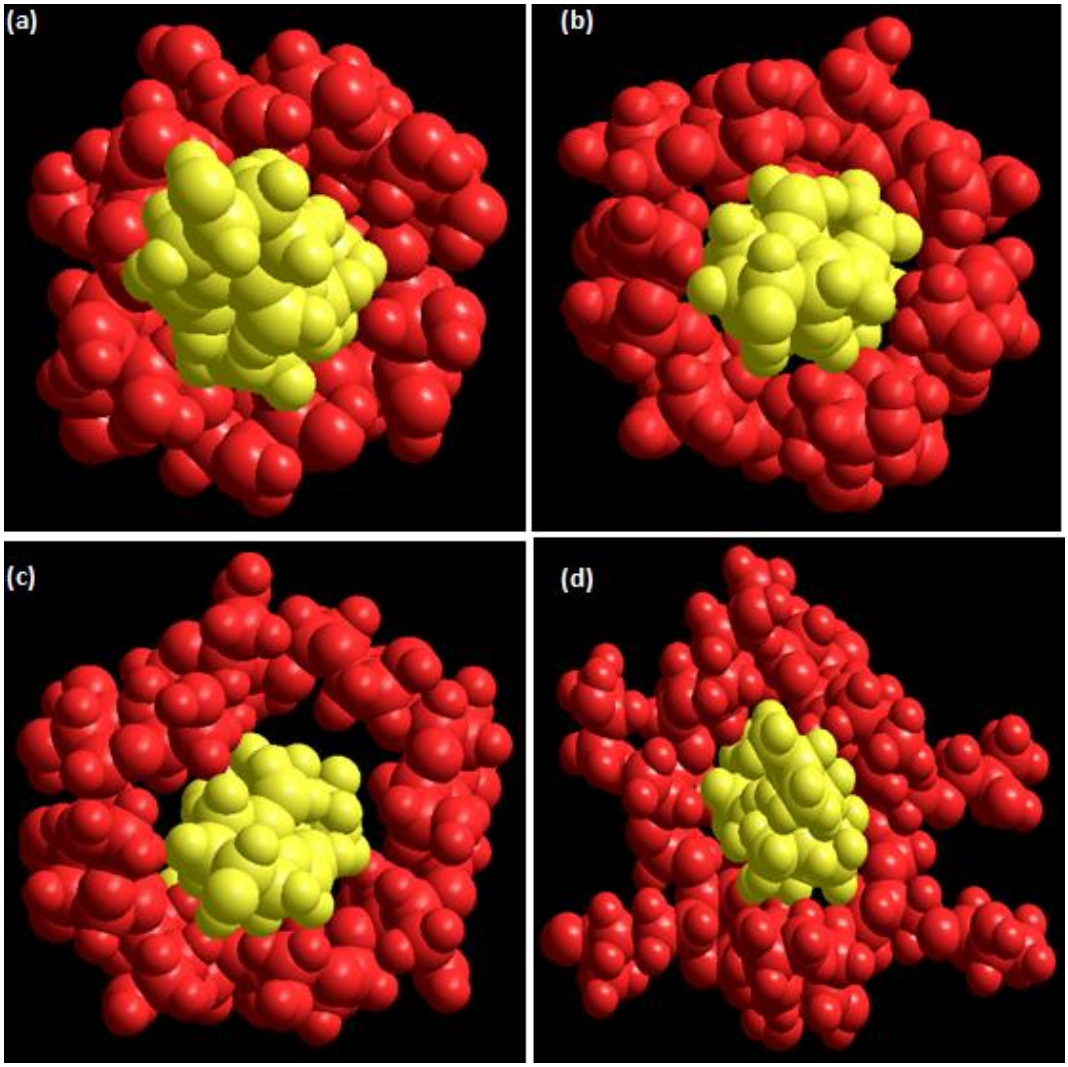


Figure 5.10: 3D overlapping sphere space-filled models for (a) α-CD||VitD; (b) β-CD||VitD; (c) γ-CD||VitD and (d) HP-β-CD||VitD. Colour codes for molecules are: Cyclodextrin (red) and VitD (yellow).

In conclusion, the higher stabilization energy, balanced geometrical orientation, and perfect 3D space-fit is responsible for the higher encapsulation efficiency of VitD in

the β-CD cavity and hence correlates well with the experimental data presented in Chapter 4. The three *in silico* models perfectly explain the higher IE% values of VitD in the βCD cavity of the *βCDD_3-8* complex and lower values observed for α-, HPβ-, and γ- complexes as discussed earlier in Chapter 4 and reported in Table 4.11. Despite other groups investigating docking results with other nutraceuticals and CD's (Bikadi *et al*., 2006), this study elucidated for the first time novel molecular mechanistic phenomena as rationale behind experimentally derived cholecalciferol-CD complexes IE values.

5.3.2. Karl Fischer moisture content of minitablets

The Karl Fischer method is a well-known and established technique for moisture determination of pharmaceutical dosage forms (Pirayavaraporn *et al*., 2012). There are normally no set limits however, moisture values between multiple samples will provide an indication of the consistency between batches and is a common specification tested during release. Following moisture content determinations using the Karl Fischer titrator, the mean moisture content of the novel "3-vitamin" minitablets was found to be 7.922% (SD=0.51). Since the hardness, compressibility, quality and shelf-life of a dosage form is influenced by water content this value becomes an important determinant to be monitored.

5.3.3. Texture analysis profiles of minitablets to determine hardness, resilience and compressibility

Other research groups have evaluated the challenges regarding the tabletability of formulations containing TPGS (Jin and Tatavarti, 2010). Since only one minitablet formulation was assessed due to the optimized formulation already based on clinically relevant ratios of ascorbic acid and TPGS, the rationale behind the TA profiling of minitablets was to assess the tensile strength between multiple synthesized tablets. This would determine whether or not the tableting procedure produced minitablets of consistent quality based on physicomechanical characteristics. The tablet hardness, matrix resilience and compressibility were calculated and reported in Table 5.5. All tablets that were assessed (n=5) achieved similar physicomechanical values attesting to the consistency in formulation and validation of the tableting procedure. Due to the waxy nature and high water content TPGS it is not surprising that the mean hardness of the minitablets was lower than that of minitablets formulated with other polymers by other researchers (Hibbins *et al*., 2013). Other researchers have noted how polyethylene glycol is a plasticizer that lowers the tensile strength of formulations, thus it was not unexpected that the high

TPGS content reduced the hardness of the "3-vitamin" minitablets (Olivas and Barbosa-Canovas, 2008). In addition the moisture content was found to be reasonably high as already reported in section 5.3.2 and would contribute towards the formation of soft tablets with a susceptibility to deformation. Minitablet hardness values ranged from 18.2082N-19.4483N (Mean Hardness=18.84N). Matrix resilience is defined as the ability of a substance to deform elastically but regain its original form on removal of the compressing force, and was also an important physicochemical parameter for evaluation. Mean matrix resilience calculated for the minitablets was 51.26% and mean compressibility was 3.4662N.s. Matrix hardness was represented on a 3-dimensional bar chart that clearly depicted the consistency of MR values between the 5 minitablets tested. Figure 5.11 displays a graphical representation of the MR% for each minitablet illustrating a consistent trend around 50 (Mean MR%=51.26%).

Table 5.5: Mechanical properties of five "3-vitamin" minitablets (1:3 ascorbic acid: TPGS and βCDD_3-8 IC) tested during the TA studies

"3-vitamin" Minitablet Sample	**Hardness (N)**	**Compressibility (N.s)**	**Matrix Resilience (%)**
1	19.4483	3.237	48.72
2	19.0983	3.335	49.93
3	18.2082	3.499	51.40
4	18.905	3.457	55
5	18.5536	3.803	51.26
Mean	**18.84268**	**3.4662**	**51.26**
Std. Deviation	0.4801388	0.214674638	0.02357312

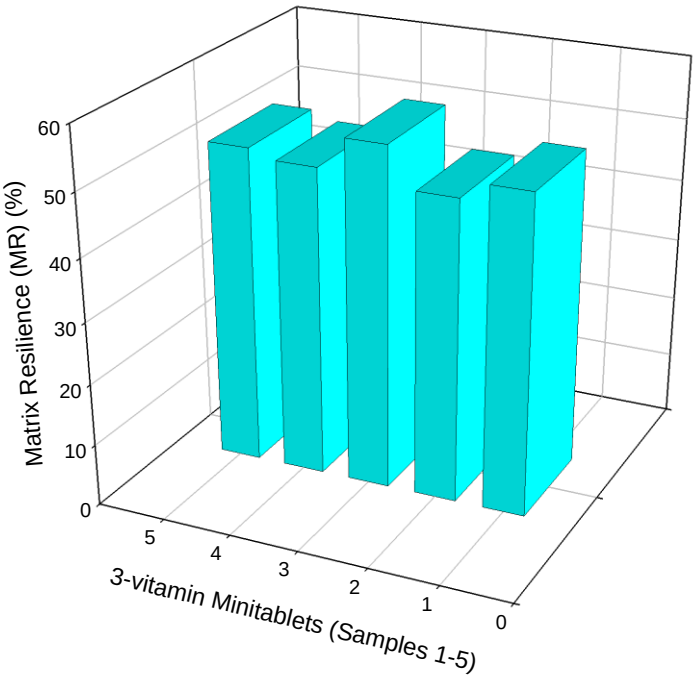


Figure 5.11: Matrix resilience values calculated during TA studies of novel "3-vitamin" minitablets (n=5) represented in a 3-dimensional bar chart format.

5.3.4. Magnetic Resonance Imaging (MRI) depicting minitablet dissolution

Figure 5.12 shows the images of a "3-vitamin" minitablet in phosphate buffer (pH 6.8) at 5 minute intervals. The upper white part is the dissolution buffer medium and the lower part is occupied by the beads onto which the minitablet was resting within the MRI device. It is clear from the images that the minitablet eroded after exposure to buffer solution and gradual agitation. As time passed the minitablet increasingly eroded losing parts of its mass, until the entire minitablet had dissolved into the buffer medium by 30 minutes (image (f)). These findings correlate well with results reported by other research groups who found that solid dispersions containing TPGS attained maximum drug release between 5 and 30 minutes (Goddeeris *et al*., 2008). Rapid disintegration and dissolution is necessary for rapid release of the vitamin constituents, especially in circumstances where vitamins are lipophilic and have inherent physicochemical challenges to dissolution in aqueous media. Cholecalciferol is one such vitamin that requires rapid disintegration and maximal exposure to dissolution media to improve aqueous solubility. MRI provided observations showing that the minitablets were able to achieve such a requirement. Tomographic imaging techniques provide useful tools in the drug release and evaluation process and should be considered as a complimentary approach to comprehensive dosage form evaluation (Li *et al*., 2012).

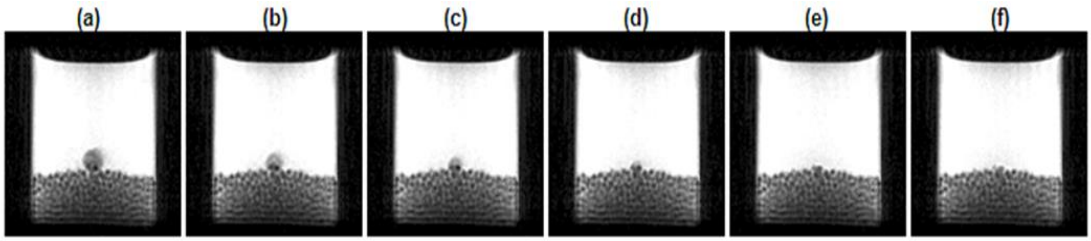


Figure 5.12: Magnetic resonance images of the erosion and dissolution of the "3-vitamin" minitablet in phosphate buffer (pH 6.8) simulating the conditions in the duodenum. Images captured at (a) 5 minutes; (b) 10 minutes; (c) 15 minutes; (d) 20 minutes; (e) 25 minutes; (f) 30 minutes.

5.3.5. *Ex vivo* permeability studies: Franz Diffusion (FD) of minitablets and market comparator

A comparison of the test product (4000IU minitablet) and a 4000IU conventional tablet (control) enabled the evaluation of the effects of the bioactive booster components to accelerate the permeability of cholecalciferol from the minitablet. The FD study was conducted in triplicate for each formulation. Figure 5.13 shows the cumulative cholecalciferol permeation profiles calculated for the "3-vitamin" minitablet and the conventional market comparator tablet following the FD study. It was clear from the results of the diffusion studies that the "3-vitamin" minitablet was superior to the conventional tablet in terms of cholecalciferol passive diffusion through porcine duodenal membrane. By 6 hours 57,59% of cholecalciferol had diffused through the membrane into the acceptor cell compared to only 20.3% from the comparator. This may be due to the influence of the surfactant, solubility and permeation enhancement effects of TPGS, and the phase solubility enhancements afforded by the βCD cholecalciferol complex. Other researchers have found similar biological membrane penetration enhancer effects from formulations containing TPGS and a vitamin (Ostacolo *et al*., 2013). However, the current study results illustrated a marked improvement in cholecalciferol diffusion due to a "dual permeation-solubility" mechanism achieving a higher permeation rate compared to the conventional tablet (Figure 5.13). The dispersion of cholecalciferol IC in TPGS, a self-emulsifying excipient, was postulated to have had an additive effect on the effects of the IC – with a resultant increase in membrane permeation beyond what was expected due to the influence of CD alone. The cholecalciferol permeation from the minitablet continued to exceed that from the conventional tablet until 28 hours when a similar diffusion had been reached by both dosage forms (Figure 5.13).

The extent of passive permeation of cholecalciferol across the pig duodenal tissue was determined using a drug flux calculation. The flux was calculated using

Equation 5.2 (Section 5.2.2.7) and using the linear regression equation of the permeation vs. time curve for both tablets at 6 hours. The calculated flux for the minitablet at 6 hours was 2211.46mg.cm^{-2}.hrs^{-1} compared to 779.52mg.cm^{-2}.hrs^{-1} for the conventional comparator. Therefore the 4000IU minitablet succeeded in improving the permeation of cholecalciferol in a superior fashion to the comparator tablet. By the 28 hour time point the cholecalciferol flux of the minitablet had increased further to 14156.8mg.cm^{-2}.hrs^{-1}. By this time the comparator tablet had reached a similar cumulative level.

TPGS is also known to be a P-glycoprotein inhibitor and thus has the potential to dramatically alter membrane permeability by inhibiting drug efflux mechanisms of intestinal tissues, resulting in increased drug permeation. The contribution of intestinal P-glycoprotein on overall drug absorption is significant only in cases where small oral doses are administered or when the dissolution and diffusion rates of a drug are very slow. Since cholecalciferol is one such drug that is administered in low oral doses (at the microgram level), and aqueous dissolution and diffusion rates are a limiting factor, the permeation enhancer effects of TPGS on P-glycoprotein cannot be underestimated for the minitablet. Despite an acceptance that cholecalciferol intestinal absorption occurs via a passive diffusion process, some researchers have demonstrated that a portion of active transport may also occur via cholesterol transport mechanisms (Reboul *et al*., 2011). Due to the discovery of biological barriers and active membrane protein transporters for cholecalciferol, the enhanced diffusion results reported in the current *ex vivo* study may be an underestimate of the permeation effects, as the results only account for passive mechanisms. There is a strong possibility that during real-time *in vivo* dynamics, which was established in subsequent sections, the BAP minitablet may demonstrate additional improvements in membrane transport as a result of passive and active diffusion phenomena.

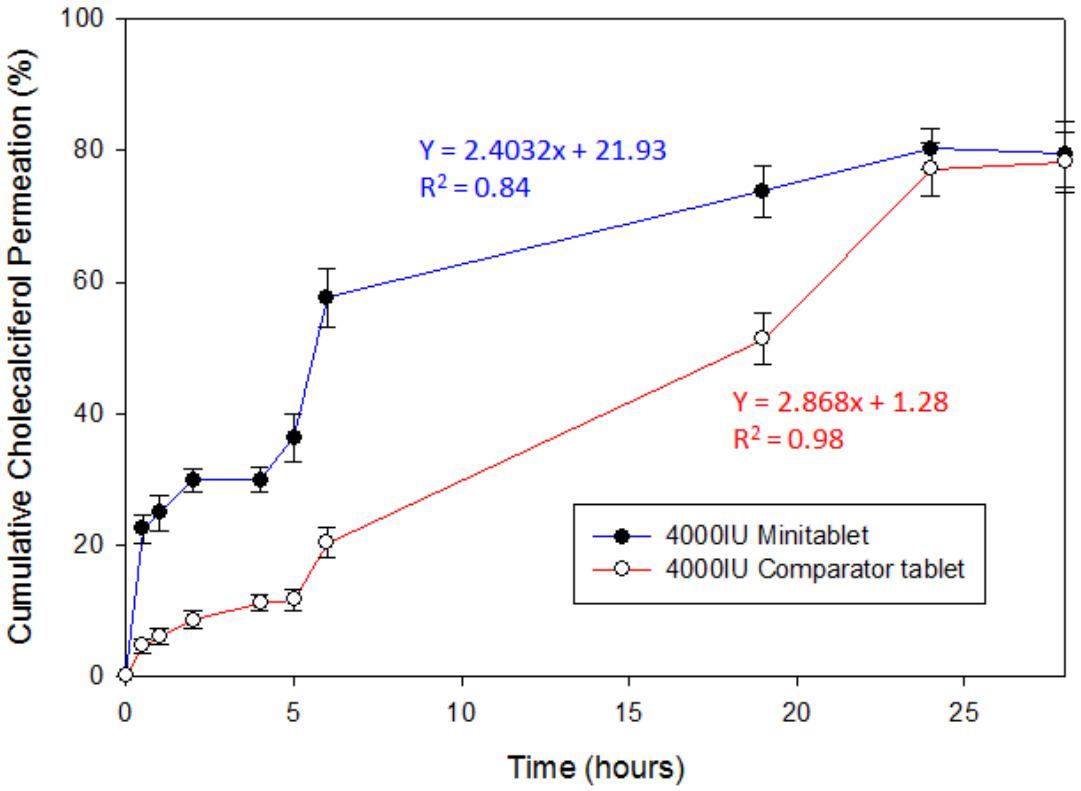


Figure 5.13: Overlaid cumulative cholecalciferol permeation profiles from a novel 4000IU "3-vitamin" minitablet and a conventional 4000IU cholecalciferol comparator tablet.

5.3.6. Thermodynamic analysis of minitablets by Differential Scanning Calorimetry (DSC)

Thermograms for the "3-vitamin" minitablet and individual constituents are shown in Figure 5.14a and b. TPGS exhibited a melting endotherm of 46^{o}C (Figure 5.14a) which is similar, albeit slightly higher than that cited by other researchers who have confirmed a melting point of approximately 37°C-41°C (Mu and Feng, 2003; Shin and Kim, 2003; Guo *et al*., 2013). The marginally higher melting point of the pure TPGS used in the current study may reflect a more crystalline composition than the grade used by other researchers.

Thermal analysis of the minitablet revealed an endothermic melting point for the formulation of 42°C which was below that of TPGS in this study. It is interesting to note how the addition of ascorbic acid and the βD_3-8 IC in the minitablet formulation modified and lowered the melting point of TPGS as was evident in Figure 5.14a. Vitamin D_3 has a characteristic melting endotherm that occurs at approximately 86°C which was not evident in the profile of the minitablet due to inclusion in the βD_3-8 complex. The disappearance of the cholecalciferol oxidation peak in the

minitablet due to inclusion in the complex indicates that the vitamin was protected from oxidation when complexed to βCD and contained within the minitablet mixture. Similar results were observed in a study by other researchers with inclusion complexes (Dua *et al.*, 2011 and Wang *et al.*, 2011). Since TPGS degradation occurs at a high temperature of 199.3°C and the compound has a low melting point, it has been said that it is thermally stable and thus useful as a stabilizer excipient in formulations (Shin and Kim, 2003). The thermal change observed for the minitablet is evidence for a more amorphous compound and indicative of homogenous distribution of the other vitamin actives within the TPGS wax.

As noted in Figure 5.14b ascorbic acid has a high melting point in agreement with other research (Hu *et al.*, 2012). Despite a high melting point for ascorbic acid, the vitamin tends to crystallize and degrade rapidly thereafter and is highly susceptible to other environmental variations besides temperature. Exposure to changes in oxygen and light may dramatically reduce the amount of functional vitamin C that remains in supplements even at ambient temperature (Alishahi *et al*., 2011). Therefore compounding vitamin actives such as vitamin C and vitamin D_3 within TPGS as per the minitablet formulation, in the form of a solid dispersion or physical mixture, may assist in enhancing stability, modifying release and improving activity (Yuan *et al*., 2013). Changes in thermal characteristics of the resultant minitablet formulation when compared to the individual bioactives, is indicative of a formulation with altered thermodynamic properties and more rapid dissolution.

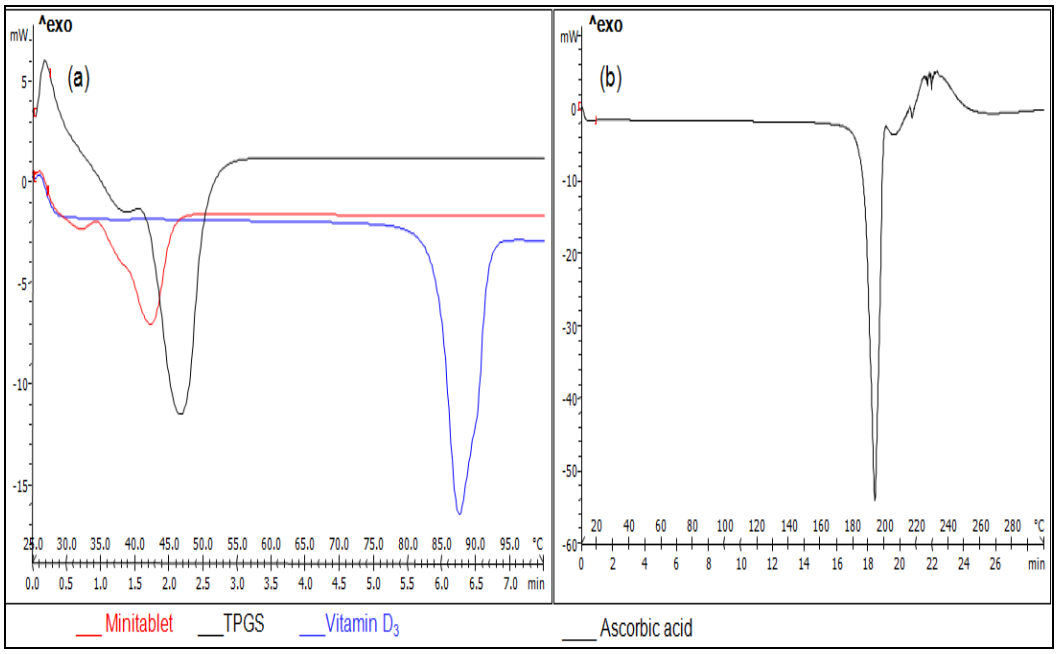


Figure 5.14: DSC thermograms of: (a) overlaid "3-vitamin" minitablet, TPGS and cholecalciferol (vitamin D_3); (b) ascorbic acid.

5.3.7. Chemical structure stability mapping of minitablet and constituents by Fourier Transform Infrared Spectroscopy (FTIR)

FTIR spectra of ascorbic acid showed the prominent absorbance bands consisting of stretching vibrations of O-H groups at 3526.3cm^{-1}, 3409.8cm^{-1}, 3311.2cm^{-1} and 3021.3cm^{-1}. Other characteristic peaks were also visible for ascorbic acid with C-H stretching at 2916.7cm^{-1} and C=O stretching at 1754.2cm^{-1} (Figure 5.15a). Similar observations were noted during FTIR analysis of ascorbic acid by other researchers (Hu *et al*., 2012). The minitablet formulation showed the same first three hydroxyl bands indicative of ascorbic acid (3525.8cm^{-1}, 3409cm^{-1}, 3310.6cm^{-1}) however the fourth O-H stretching band at 3021.3cm^{-1} was no longer evident due to the overlapping presence of the large TPGS band at 2888cm^{-1}. The minitablet spectrum appeared as a superimposition of the profiles of ascorbic acid and TPGS as is common for physical mixtures (Figure 5.15a).

An interesting observation is noted when comparing an intact solid phase minitablet spectrum in Figure 5.15a to the spectrum of the dissolved minitablet spectrum in Figure 5.15b. In comparison to the intact minitablet sample, the dissolved minitablet showed a large O-H stretching band that is characteristic of β-cyclodextrin that normally occurs at an absorption of 3300cm^{-1} (Wang *et al*, 2011). This is due to the solubilization and exposure of the βD_3-8 complex and release of βCD and cholecalciferol into aqueous solution. However, the O-H band o shifted from 3301cm^{-1} in the parent CD to 3367cm^{-1} in the dissolved minitablet spectrum (Figure 5.15b). No characteristic cholecalciferol band was visible in the spectrums of either the intact or the dissolved minitablet due to successful encapsulation within the βCD IC which is evidence for inclusion complex formation (Teng *et al*., 2013). The characteristic peak of cholecalciferol at 2935cm^{-1} was not observed in the spectrum of the minitablet and may also be due to an association between its functional groups and the lipophilic constituents within TPGS and may be evidence for solid dispersion formation (Yuan *et al*., 2013). The greater intensity of the O-H band at 3367cm^{-1} for the dissolved minitablet is due to the overlapping number of hydroxyl groups present in the minitablet mixture due to contributions from ascorbic acid, the βD_3-8 complex and TPGS (Shin and Kim, 2003; Wang *et al.*, 2011; Hu *et al.*, 2012).

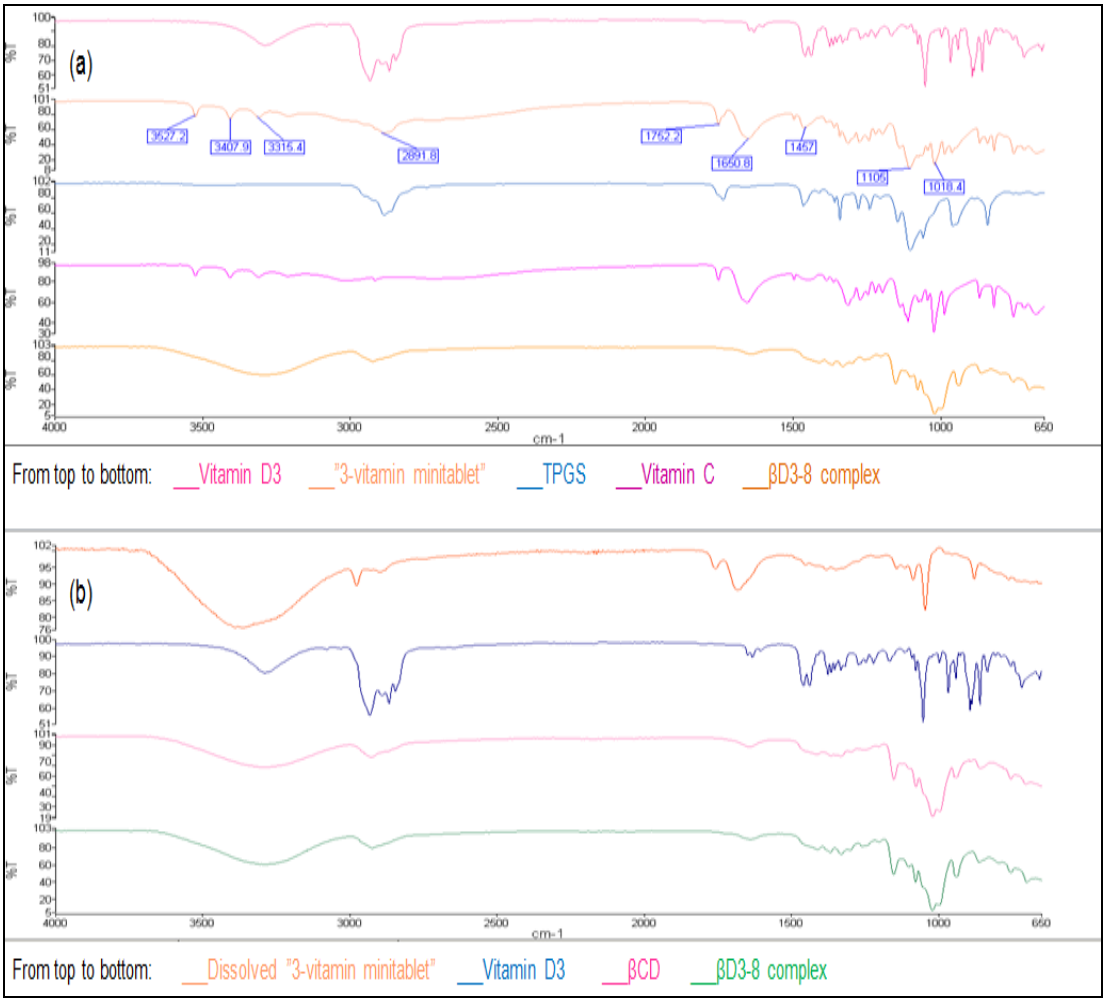


Figure 5.15: FTIR spectra of: (a) minitablet and individual constituents; (b) dissolved minitablet and individual constituents.

5.3.8. Bile salt/lipase influence on cholecalciferol release study: Selection of an optimized film

The use of bile components to improve bioavailability of bioactives is not a new approach (Chen *et al*., 2009; van Hasselt *et al*., 2009; Mahajan, 2012). However, the influence of bile salt and lipase composition of polymeric films, on the dissolution characteristics of cholecalciferol has yet to be investigated. Likewise, the effect of one delivery device (film) on *in vitro* release of drug from another delivery mechanism (minitablet) is a new approach. Following the results from the textural analysis studies in chapter 4 performed on combined lipase-bile salt films, films containing 0.5%$^{w}/_{v}$ cross-linker were deemed mechanically superior and thus utilized in this study. The composition of bile salts and lipase were varied to determine the influence that bioactive composition and ratio of the 0.5%$^{w}/_{v}$ crosslinked films had on D_3 release.

Results of the study revealed that the mean area under the dissolution curve (AUC) for cholecalciferol released from minitablets wrapped with all film formulations was higher than for minitablets without film (Mean $AUC_{(All\ film\ formulations)}$: 10312.69 vs. $AUC_{(no\ film)}$: 9405.37). Four film formulations had superior area under the dissolution curve (AUC) for cholecalciferol release from minitablets namely, 66B/33L, 80B/20L, 100B High, and 100B Low films. The minitablet without bioactive film had a comparably lower AUC for D_3 compared to the minitablets wrapped with the four identified films. Table 5.6 shows the cholecalciferol dissolution data obtained from minitablets wrapped with various films and with no film. On average the cholecalciferol Dissolution Efficiency (DE) for minitablets wrapped with bioactive film was higher than for minitablets without film (Mean $DE_{(with\ film)}$: 0.573 vs. $DE_{(no\ film)}$: 0.522). By the 3 hour time point all minitablets wrapped with "drug-loaded" film formulations achieved a mean cholecalciferol release of 85.67% vs. only 71.36% from minitablets with no film. The mean dissolution time (MDT) for many of the minitablets with bioactive-film was above that of the minitablet without film, as the wrapped film layer slowed the dissolution rate (Table 5.6). The impeded rate did not however effect the overall solubility enhancement with superior AUC values for most bioactive-film wrapped tablets, except 100L and 33B/66L films (Table 5.6).

The film with a $66\%^{w}/_{v}$ bile salt: $33\%^{w}/_{v}$ lipase composition (66B/33L) was identified as the optimized film to include in the BAP DDS due to a high AUC and high DE value. In addition the 66B/33L formulation exhibited the most consistent dissolution profile with mixed-order kinetics. The 66B/33L film illustrated a steep 1^{st} order gradient from 0 to 2 hours followed by a zero order release from 2 to 3 hours as cholecalciferol saturation was reached (Figure 5.16a). This formulation also had the lowest relative dispersion of dissolution time (RD) and variance of dissolution time values which was favourable for more predictable dissolution parameters. Interestingly, the 33B/66L formulation provided similar dissolution efficiency to the minitablet without a film probably due to inadequate bile salt content (Figure 5.16b). Due to low bile content, the 33B/66L film was unable to improve the dissolution of the minitablet beyond the effects of the TPGS and IC contained in the tablet. The 100L film revealed a worse cholecalciferol release profile to the plain minitablets without film which is to be expected during *in vitro* studies (Figure 5.18b). Film without added surfactant in the form of bile salts would merely act as an additional barrier to the exposure of D_3 to the aqueous media. A film containing only lipase would not provide additional surfactant enhancing effects on cholecalciferol and would only impart enzyme effects *in vivo*.

The effect of two films containing only bile salt and no lipase were evaluated (100B High vs. 100B Low). Increasing the concentration of bile salts from 20mg to 40mg per film had no effect on improving the release of D_3 from the minitablets. In fact the 100B High (containing 40mg bile salts) actually resulted in an initial delay in cholecalciferol release (higher MDT) and the 100B Low film (containing 20mg bile salts) formulation resulted in a higher AUC (Figure 5.17 and Table 5.6). The 80B/20L film was evaluated and notably achieved the highest DE, AUC and % cholecalciferol release by the end of the study compared to all film formulations tested (Figure 5.18a). Although a favourable release profile was achieved *in vitro* for the 80B/20L formulation, other researchers have warned of potential interactions that may occur between certain bile components and CD's (Comini *et al*., 1994). Hence excessive bile components may potentially affect the integrity of the CD complex within the DDS. Excess bile salts also have the potential to cause adverse effects *in vivo* (Dahm *et al*., 1988). A film with a more balanced ratio of biological actives was therefore chosen as an ideal formulation: the 66B/33L film contained 20mg NaC, 20mg NaD, and 20mg lipase and was considered preferable. The 66B/33L formulation would also deliver a higher ratio of pancreatic lipase compared to the 80B/20L, ideal for those patients for whom lipase activity requires bolstering for improved digestion.

By 90 minutes the minitablet with no film had released only 58.34% of D_3 whilst D_3 release from the minitablets wrapped with the selected 66B/33L film had achieved 70.76% D_3 release. By the end of the study the minitablet wrapped with 66B/33L film had achieved a cholecalciferol release of 88.36% compared to 71.36% for the minitablet with no film. These results are not surprising since bile salts are amphiphilic molecules known to solubilize non-polar fat-soluble vitamins such as cholecalciferol (Madenci and Egelhaaf, 2010). Other researchers have similarly shown how bile constituents improved the dissolution rate of poorly aqueous soluble drugs (Maestrelli *et al*., 2011). Zughaid and co-workers (2012) also reported how bile salt concentration positively influenced progesterone and hydrocortisone solubility dramatically. Thus the current results tie in with the fact that bile salts may improve dissolution parameters when hydrophobic drugs such as cholecalciferol are added to aqueous media. However, the current research proved that bile salts released from a component of a DDS can still have a positive influence on dissolution. Due to the unique molecular structure of bile salts, these biological surfactants are adept at transporting and solubilizing various hydrophobic compounds (Maldonado-Valderrama *et al*., 2011). As such it would be interesting to

quantify the enhancer effects on the vitamin E constituent also contained in the minitablets as a follow-on investigation.

In addition to the enhanced dissolution characteristics shown in the current study, bile salts play a vital role in lipid digestion and thus would provide an even greater advantage during the *in vivo* digestive process. Bile components function as transport vectors and may improve cholecalciferol *in vivo* permeability through GIT membranes due to their penetration enhancing effects. Therefore the enhancements on bioavailability may be further strengthened when these BAP components are dosed and evaluated *in vivo*. The current study has shown in a novel fashion how a specialized BAP component (bioactive bile salt-lipase film) can be used to improve *in vitro* dissolution of cholecalciferol from unique "3-vitamin" minitablets.

Table 5.6: Dissolution data obtained following cholecalciferol release from a 4000IU minitablet with/ without polymer bioactive films of varied composition

Formulation:	**MDT** (mins)	**AUC** (ug/mL*min)	**DE**	**RD**	**VDT**	**MRT** (mins)
Minitablets & no film	60.15	9405.37	0.522	0.60	1761.37	65.98
Minitablets & 66B/33L Film*	52.35	11278.53	0.627	0.30	826.97	50.88
Minitablets & 33B/66L Film	76.08	9271.95	0.520	0.59	3462.17	65.59
Minitablets & 80B/20L Film	44.28	12604.6	0.700	0.57	1114.72	46.46
Minitablets & 100B High Film	60.16	9405.38	0.52	0.60	2182.29	65.98
Minitablets & 100B Low Film	48.23	10654.50	0.59	1.01	2363.84	66.89
Minitablets & 100L Film	68.67	8661.15	0.48	0.61	3627.56	68.67

Key: MDT, mean dissolution time; AUC, area under the dissolution curve; DE, dissolution efficiency; RD, relative dispersion of dissolution time; VDT, variance of dissolution time; MRT, mean residence time of the drug substance molecules in the dosage form. * Film selected for inclusion in BAP.

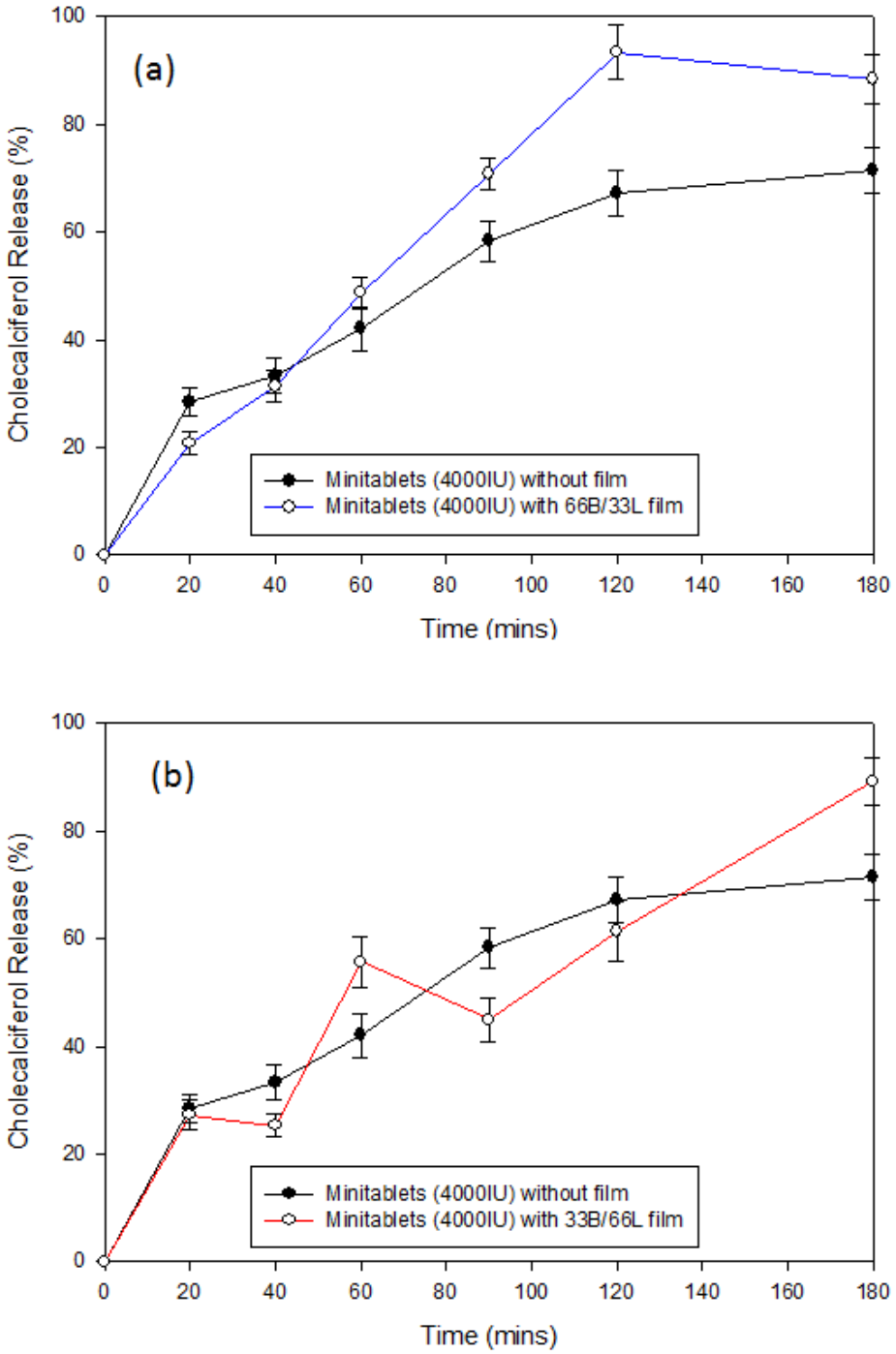


Figure 5.16: *In vitro* dissolution profiles showing comparative cholecalciferol release from (a) "3-vitamin" minitablets vs. "3-vitamin" minitablets wrapped with 66B/33L film; and (b) "3-vitamin" minitablets vs. "3-vitamin" minitablets wrapped with 33B/66L film.

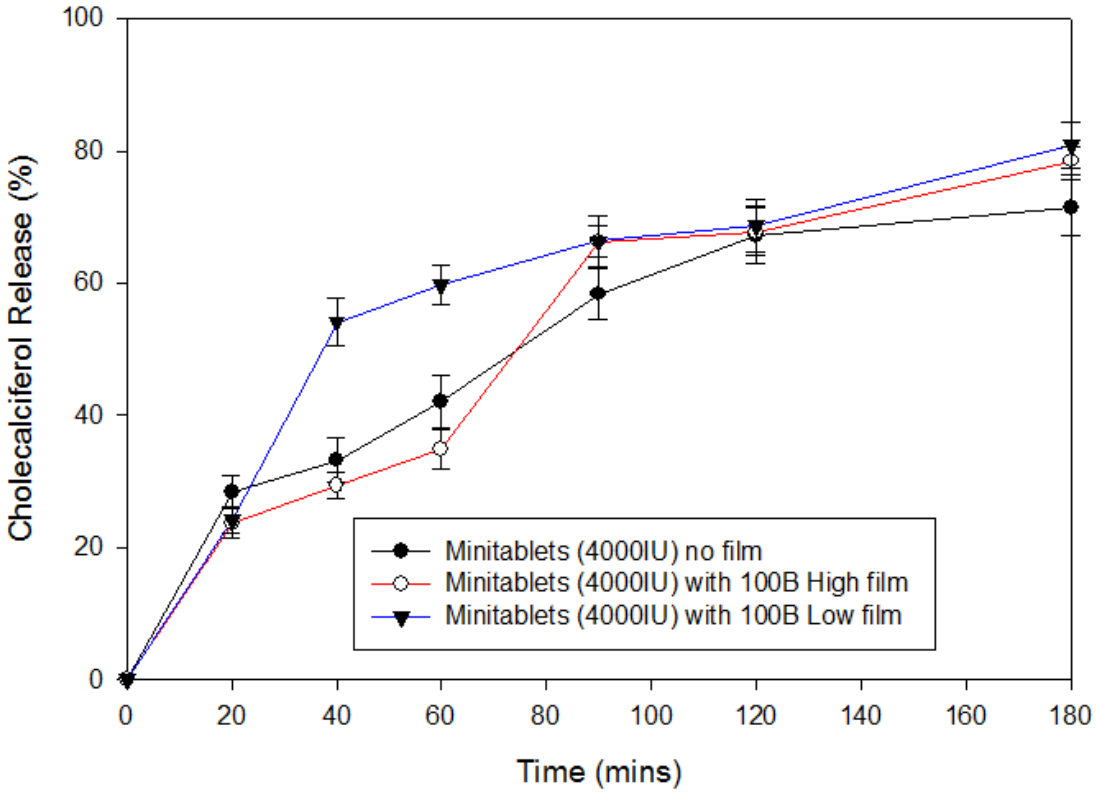


Figure 5.17: *In vitro* dissolution profiles showing comparative cholecalciferol release from “3-vitamin” minitablets vs. “3-vitamin” minitablets wrapped with 100B High film vs. “3-vitamin” minitablets wrapped with 100B Low film.

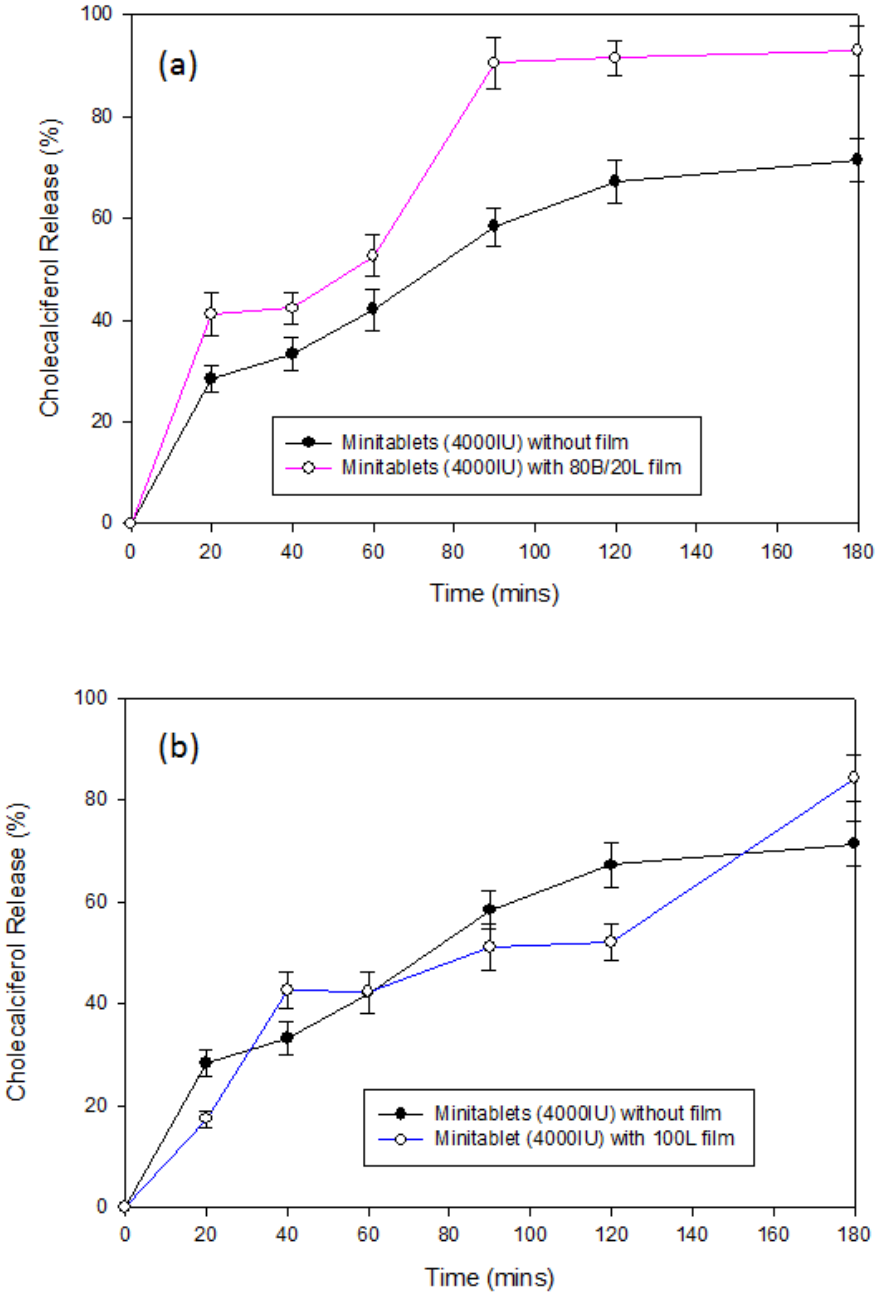


Figure 5.18: *In vitro* dissolution profiles showing comparative cholecalciferol release from (a) "3-vitamin" minitablets vs. "3-vitamin" minitablets wrapped with 80B/20L film; and (b) "3-vitamin" minitablets vs. "3-vitamin" minitablets wrapped with 100L film.

5.3.9. Lipase enzyme activity profiles of combined lipase-bile salt films- Selection of an optimized film based on enzyme activity

Earlier preformulation studies in Chapter 4 succeeded in modifying the release of pancreatic lipase in a controlled manner from alginate hydrogel scaffolds. However the release of a biological active such as an enzyme or hormone does not determine its ultimate physiological activity. In many cases enzymes are denatured or degraded by the physiological environment and rendered inactive prior to entering

the site of action in which they are intended to function. Other researchers have commented on the importance of preserving enzyme activity when lipase is attached to a polymeric vehicle for biochemistry related applications (Knezevic *et al*., 2002). Lipases are extensively utilized in industrial processes as biocatalysts to break down oils and fats, in de-greasing formulations and in the pharmaceutical industry, and are routinely bound to polymers to improve their functional stability to temperature and pH (Bhushan *et al*., 2008). In addition, it has been noted how specific alginates may inhibit pancreatic lipase activity (Wilcox *et al*., 2014). Therefore the design of a delivery system for pancreatic lipase without due consideration for quantifying the enzyme activity or control of such activity would prove fruitless. To advance further with the BAP film design, it was deemed paramount to assess and control the activity level of pancreatic lipase when released from the film instead of performing a 2nd lipase release study as conducted in Chapter 4 for the scaffolds.

It was also necessary to confirm whether variations in crosslinker content would influence enzyme activity in the 66B/33L films that had previously achieved the best D_3 dissolution data. Although 0.5%$^{w}/_{v}$ crosslinker had proven ideal from a physicomechanical standpoint, other crosslinker concentrations warranted investigation to evaluate their effect on enzymatic activity and confirm that 0.5%$^{w}/_{v}$ CL was optimal. Following the lipase activity assay conducted in SIF a number of interesting observations were recorded. For all film formulations, lipase activity differed according to crosslinker composition. Crosslinker had a direct impact on the lipase activity of each film as can be seen in the lipase activity profiles plotted (Figure 5.19). The 66B/33L(0.25%) films had an enzyme activity curve with lower lipase activity for the first 2 hours of the study compared to the 66B/33L(0.5%) and 66B/33L(0%) formulations. Thereafter the 66B/33L(0.25%) film had an increase in lipase activity beyond the 0.5% formulation. The 66B/33L(1%) cross-linked film provided the lowest enzyme activity curve of all formulations (Figure 5.19). The film without crosslinker, 66B/33L(0%), had a steep 1st order release gradient of activity that was superior to all formulations.

The film with the most “efficient” activity to suit the needs of the BAP DDS application was the 66B/33L(0.5%) film. This film was selected as the preferred film component as it demonstrated an initial 1st order lipase activity curve followed by a zero order profile thereafter. A burst activity within the 1st hour (steep 1st order curve) is preferable to accelerate the lipid and fat-soluble vitamins digestive process, and then a constant activity thereafter (zero order) would maintain a consistent lipase

activity in the patient. Despite some researchers noting the ability of alginate to reduce lipase activity, the 66B/33L(0.5%) film produced a constant zero order activity profile ideal to provide a controlled supplemental dose of enzyme for the BAP application (Wilcox *et al*., 2014). This activity level would ensure optimal digestion of the fat-soluble vitamins, including the model drug cholecalciferol, and ultimately enhance bioavailability. An increase in lipase activity from 0 up to 5 hours following dissolution would serve no purpose in the current delivery mechanism. Figure 5.19 depicts the overlaid lipase activity profiles obtained for the four different film formulations that were assessed after dissolution in SIF.

The use of an alginate-based film offers formulation advantages as documented by other researchers in terms of improved thermal stability and modification of activity levels (Charusheela and Arvind, 2002; Matsumoto and Ohashi, 2003). The current results are congruent with other research that has demonstrated the manner in which alginate composition influences lipase enzyme activity (Knezevic *et al*., 2002). These researchers found that an alginate bead immobilized lipase yielded the maximum enzyme activity with an alginate concentration of $2\%^{w}/_{v}$, and any concentrations above this showed an activity reduction (Knezevic *et al*., 2002). In comparison, the current study elucidated the effect of crosslinker concentration, instead of polymer concentration, on lipase activity when the enzyme was bound to an alginate ($4\%^{w}/_{v}$)/ glycerin ($2\%^{v}/_{v}$) film containing co-incorporated bile salts. Instead of attempts to minimize loss of enzyme from a bead matrix, the films in the current study facilitate lipase enzyme retention without the risk of bioactive loss from the delivery matrix. Other researchers have synthesized beads for lipase immobilization that consist of a polymeric blend of sodium alginate ($5\%^{w}/_{v}$)/ gelatin ($3\%^{w}/_{v}$) and have reported no loss in enzyme activity over repeated uses (Fadnavis *et al*., 2003). The film matrix in the current study is anticipated to offer similar retention of the observed enzyme activity seen in Figure 5.19 over a prolonged time in an *in vivo* environment post dosing. The alginate/ glycerin films provided a mean lipase enzyme activity of 30.48milliunits/mL. It was postulated that the other bioactives present in the film (bile salts) and the high alginate concentration ($4\%^{w}/_{v}$) may reduce enzyme activity, nevertheless the results indicate a positive trend in activity. The films may also offer enzyme actives the protection from thermal variations and retain activity. Since the amount of cholecalciferol in the DDS was small: 1000IU (25ug) or 4000IU (100ug), only a moderate lipase activity was deemed necessary to facilitate breakdown of the model drug in the final DDS when it enters the GIT. Thus further studies to enhance enzyme activity beyond that

obtained in the current study were not undertaken. Results of the current study again confirmed the superiority of the 0.5%$^{w}/_{v}$ crosslinked film in terms of an appropriate enzyme activity profile.

Not only does the optimized bile salt-lipase film provide a suitable BAP component with a consistent and controlled lipase activity profile, but it offered a novel delivery vehicle for use in enzyme replacement therapy. As discussed by Fieker and co-workers (2011), effective pancreatic lipase therapy is *"limited by an ability to replicate the physiologic process of enzyme delivery to the appropriate site, at the appropriate time"*. The polymeric films formulated in this study have provided an effective means to protect lipase enzyme, target delivery to the duodenum, and demonstrated a preliminary ability to control enzyme activity. The bioactive-film component may therefore be used to mimic the physiologic process of enzyme delivery and hold merit in pancreatic enzyme treatment modalities. Further studies should be focused on increasing lipase activity in the films for specific applications in enzyme deficient patients. Figure 5.20 shows a photographic image of the 66B/33L(0.5%) film.

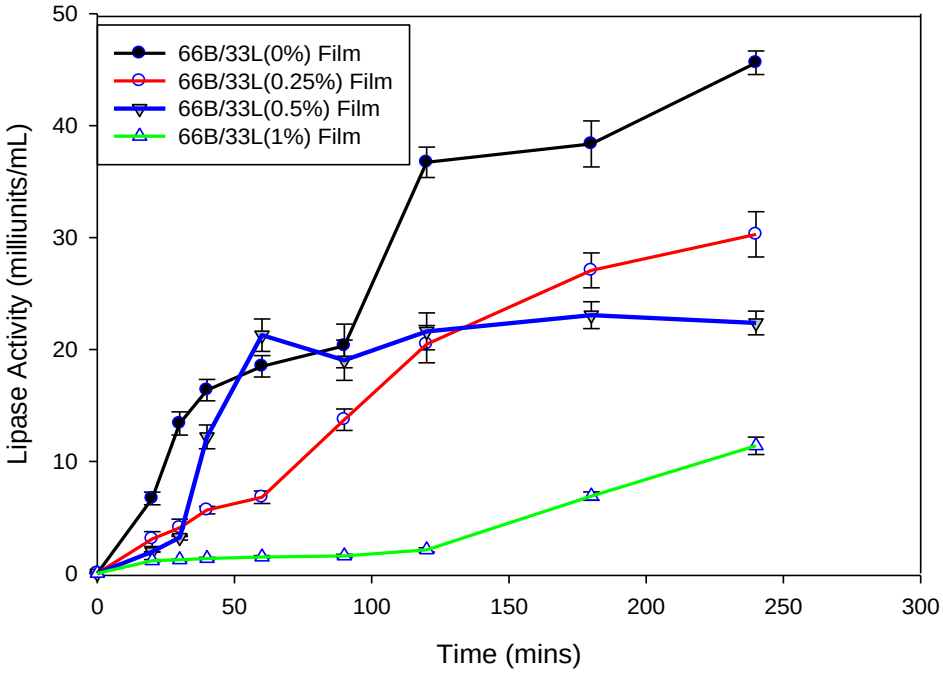


Figure 5.19: Lipase activity profiles of 66B/33L (0%-1%$^{w}/_{v}$ CL) films (200mg) containing: 20mg NaC, 20mg NaD, 20mg lipase.



Figure 5.20: Photographic image of 66B/33L(0.5%) film containing: pancreatic lipase (100mg), sodium deoxycholate (100mg) and sodium cholate (100mg).

5.3.10. Thermodynamic analysis of optimized 66B/33L(0.5%) BAP films by Differential Scanning Calorimetry (DSC)

The DSC thermograms represented for the 66B/33L(0.5%) films in Figure 5.21a and b show distinct thermal differences to the peaks evident for the individual constituents. The film had an exothermic peak followed by an endothermic peak at approximately 210^{o}C-235°C and then a wide decomposition peak starting at approximately 250°C (Figure 5.21b). A similar observation was made in a study by other researchers with films containing alginate and glycerin (Pongjanyakul and Puttipipatkhachorn, 2007). In contrast, pure sodium alginate exhibited decomposition that started at around 208°C with maximal decomposition having occurred by approximately 260°C. Thus the films containing the 3 bioactives had a higher decomposition temperature than plain alginate. Other researchers noted similar observations when additional constituents were added to alginate films resulting in a slowed thermal decomposition and an increase in the thermal stability due to chemical interactions between the bioactives and alginate (Huq *et al*., 2012; Pereira *et al*., 2013). This is evidence for bioactive inclusion in the film formulation. Two characteristic endotherms were evident in the thermogram of pancreatic lipase at 145°C and 205°C that were no longer present in the bioactive film, providing evidence that the film may afford thermal protection to the enzyme. The exothermic peak in the film at 210°C (Figure 5.21) occurred at an intermediate temperature between that of the two characteristic exotherms for the individual bile salt constituents (NaD=195°C; NaC_1=215°C; NaC_2=238°C). The occurrence of a prominent exothermic peak of the bioactive film that occurs between the expected temperatures of each bile salt is evidence for bile salt inclusion.

The difference in the thermogram of the film compared to plain alginate and the individual formulation constituents is due to bioactive-polymer interactions within the films. It is not uncommon to find shifts in thermal peaks due to drug-polymer interactions in films due to the formation of crystalline aggregates of drug and their

dispersion within the polymeric alginate matrix (Thu and Ng 2013). Such interactions indicate dispersion of the bioactives within the alginate/ glycerin matrix and the existence of a film that is less crystalline in nature than the original bile salts yet less amorphous than pure alginate.

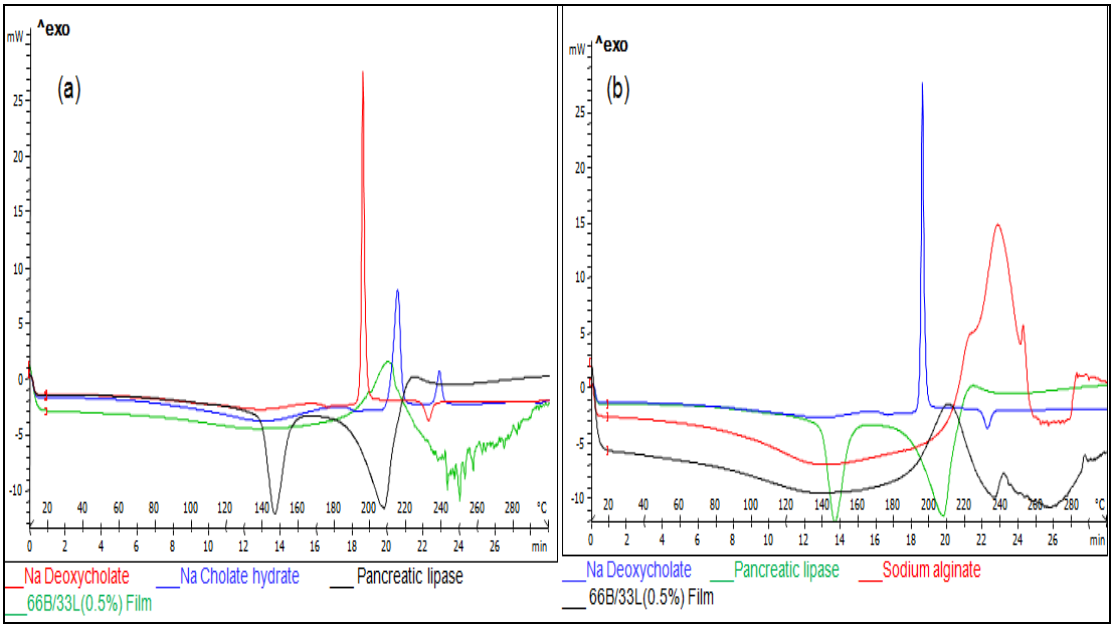


Figure 5.21: DSC thermograms of (a) Overlaid NaD, NaC, pancreatic lipase and 66B/33L(0.5%) film; (b) Overlaid NaD, pancreatic lipase, sodium alginate, 66B/33L(0.5%) film.

5.3.11. Chemical structure analysis of optimized 66B/33L(0.5%) films by Fourier Transform Infrared Spectroscopy (FTIR)

Hydroxyl stretching occurred at 3274cm^{-1} for glycerin, at 3326cm^{-1} for NaC, at 3337cm^{-1} for NaD, and at 3255cm^{-1} for pancreatic lipase in accordance with observations of other research groups (Yang *et al*., 2005, Ahmed *et al*., 2010) (Figure 5.22). Researchers have noted shifts in the wavelength of the O-H band in alginate to a lower wavenumber in the presence of plasticisers such as glycerin (Pongjanyakul and Puttipipatkhachorn 2007). In contrast in the current study, the O-H stretching peak of alginate that occurred at 3195cm^{-1} was shifted to a higher wavelength of 3294cm^{-1} in the 66B/33L(0.5%) bioactive film due to the presence of the plasticizer and the three bioactives' O-H stretching bands that all appeared at higher frequencies than alginate (Figure 5.22). Thus the results observed in the shifting of the O-H band to a higher frequency, instead of a lower frequency, accounted for the presence of the three bioactives (NaC, NaD and lipase) and not due to the glycerin plasticizer.

Two distinct characteristic C-H bands were observed in the spectra of NaC at 2931cm^{-1} and 2864cm^{-1}, and at 2927cm^{-1} and 2862cm^{-1} for NaD (Figure 5.22). The 66B/33L(0.5%) film revealed the same prominent “fork-like” bands at 2932cm^{-1} and 2864cm^{-1} indicating that only minor alterations occurred in this region for the bile salts when included in the films. This indicates only minimal changes and thus less CH chain bond interactions between the bile salts and the polymer compared to the hydroxyl group interactions as noted above.

The characteristic sodium alginate carboxyl group that normally occurred at 1596cm^{-1} in agreement with other researchers (Thu and Ng, 2013), shifted to a lower wavelength of 1555cm^{-1} in the bioactive film in the presence of the bile salts, lipase and plasticizer (Figure 5.22).

These observations confirmed the presence of bioactives in the films and indicated interactions that may affect surfactant and enzyme activity and may illustrate changes in mechanical properties of the resultant films. Larger shifts in bands suggested greater bond interactions between the biological constituents and the polymer matrix which may impact on the activity and malleability of the film formulation. Other groups have highlighted how the type of polymer used as the support matrix for lipase has an effect on the enzymes specificity and activity (Charusheela and Arvind, 2002). FTIR spectra showed the extent of shifts in characteristic peaks of the individual constituents due to interactions which may influence factors including efficacy, specificity and selectivity of bile and enzyme components of the BAP film formulation.

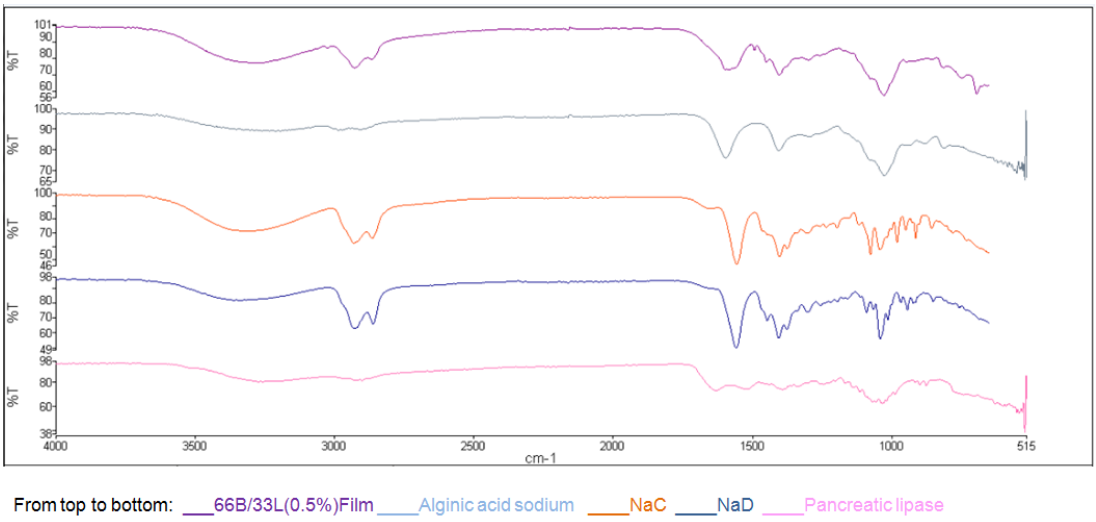


Figure 5.22: FTIR spectra of bioactive alginate/ glycerin film containing bile salts and lipase and individual constituents.

5.3.12. Comparative *in vitro* drug release studies of the final BAP DDS

In vitro dissolution testing was used as a method to predict *in vivo* absorption of cholecalciferol from the BAP DDS in relation to the release of cholecalciferol from a comparator product. Likewise, the release of all three vitamins (cholecalciferol, ascorbic acid and α-tocopherol) from the BAP were evaluated and compared in the current dissolution study. The *In vitro* dissolution study of the final BAP DDS was conducted on the final formulation consisting of a 66B/33L film (200mg) wrapped around three "3-vitamin" minitablets encased in a two coated capsules. The study was performed using a USP 4 apparatus (Flow-through cell dissolution tester) as shown in Figure 5.23a and b. A solid phase extraction method was employed using a manifold, pump and oasis HLB extraction cartridges (Figure 5.23c). Sigma Plot was used to plot mean data point drug concentrations vs. time, resulting in drug release profiles showing standard deviations using multiple error bars for each concentration/ time point following triplicate readings as shown in Figures 5.27-5.29. Modeling and comparison of dissolution data was performed using non-linear optimization techniques to fit drug release data by using the DDSolver add-in program for Excel, which is an accurate, fast and reliable method for dissolution profile analysis and results are shown in Table 5.7 (Zhang *et al*., 2010). HPLC cholecalciferol standards and samples eluted at a retention time of 7.279 minutes (Figure 5.24a). α-tocopherol standards and sample peaks were observed at 9.853 minutes (Figure 5.24b) and an HPLC peak for ascorbic acid was recorded at 3.041 minutes (Figure 5.24c). The relevant vitamin calibration curves are shown in Figures 5.25 and 5.26.

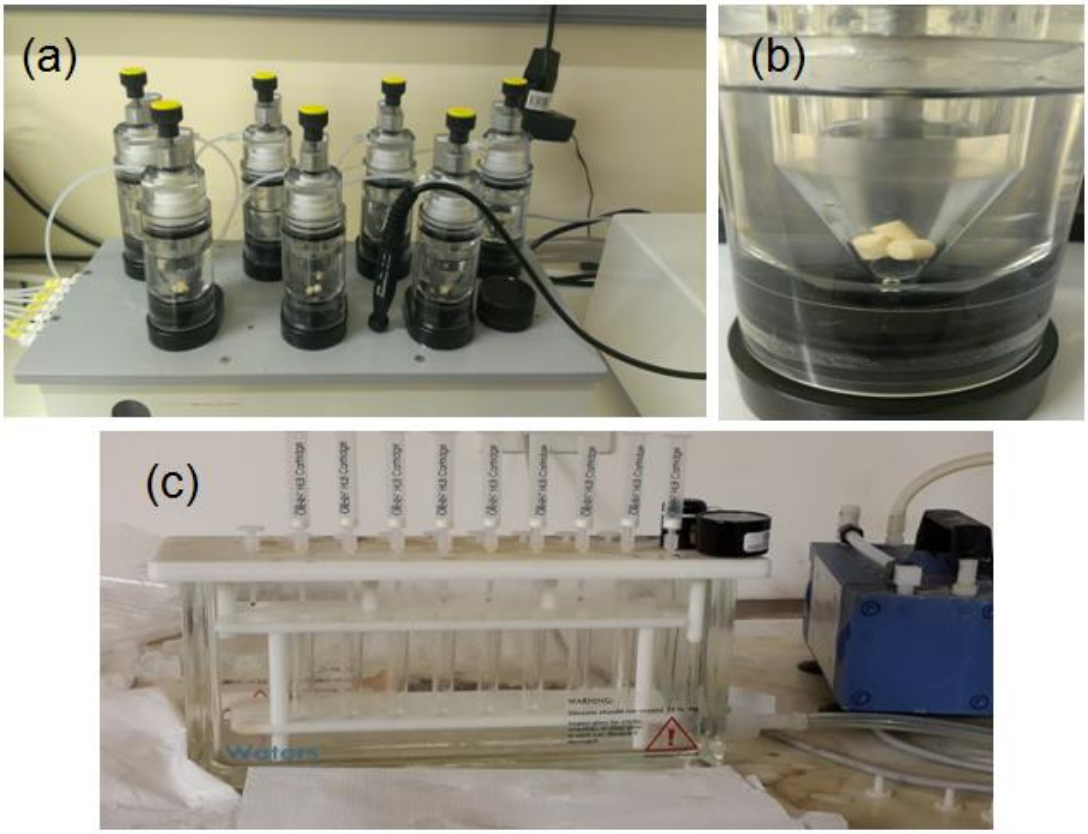


Figure 5.23: *In vitro* dissolution study of BAP DDS using a USP 4 apparatus (Flow-through cell dissolution tester, Type DFZ60, Erweka). (a) Seven cells containing BAP DDS components at different stages of the dissolution study; (b) Exposed minitablets in one cell after dissolution of capsules; (c) Manifold, pump and HLB Oasis cartridges used for the solid phase extraction of fat-soluble vitamins from dissolution samples prior to HPLC analysis.

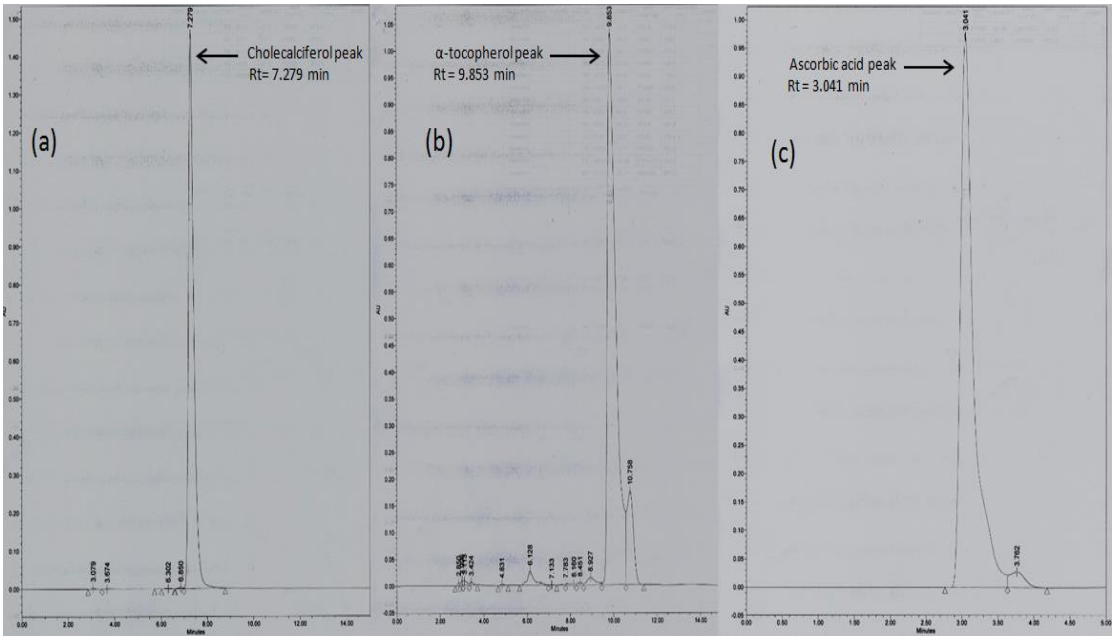


Figure 5.24: HPLC chromatograms of standard vitamin peaks: (a) Cholecalciferol peak at 7.279 minutes; (b) α-tocopherol peak at 9.853 minutes; (c) Ascorbic acid peak at 3.041 minutes.

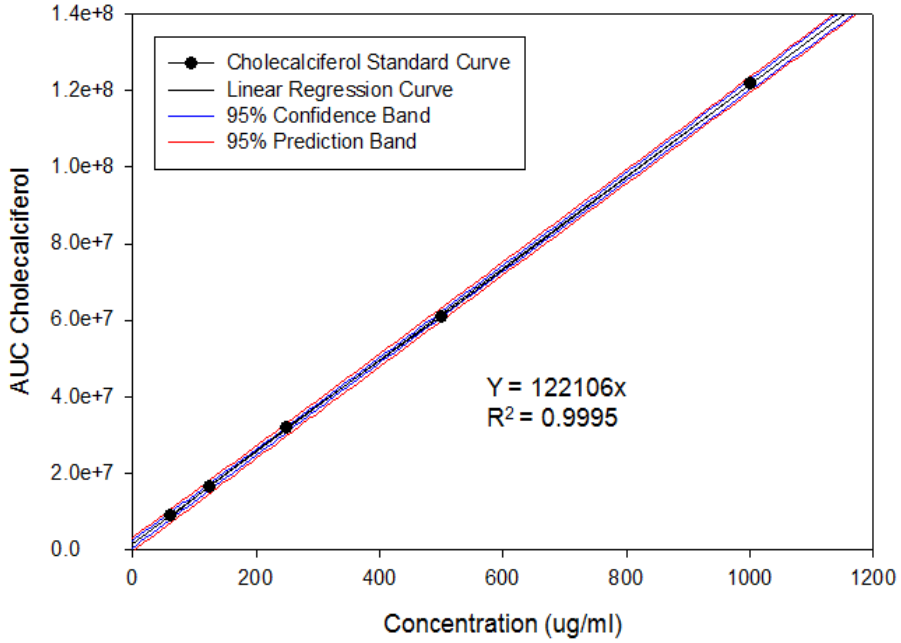


Figure 5.25: Calibration curve generated for cholecalciferol standards (UV detection at 265nm) for HPLC quantification of dissolution samples during vitamin release studies.

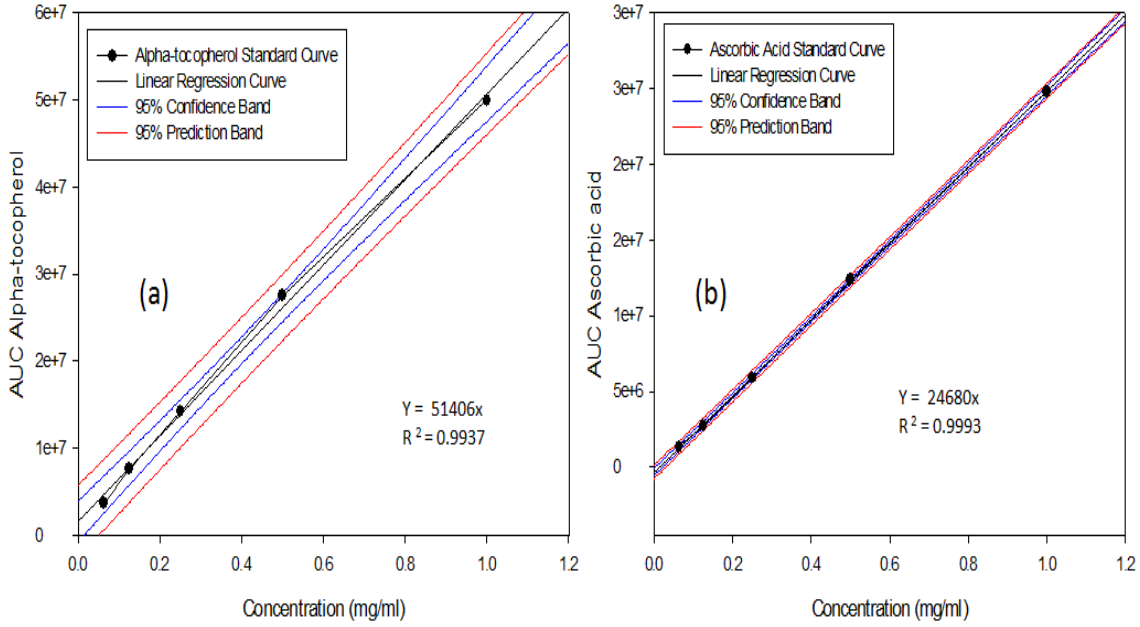


Figure 5.26: Calibration curve generated for: (a) α-tocopherol standards (UV detection at 295nm) and (b) ascorbic acid standards (UV detection at 265nm) for HPLC quantification of dissolution samples during vitamin release studies.

5.3.12.1. A superior BAP cholecalciferol dissolution profile

Figure 5.27 shows the dissolution profiles obtained for cholecalciferol released from the 1000IU and 4000IU BAP in comparison to the respective conventional D_3 products. There was an initial burst release of D_3 during the first 20 minutes from both BAP systems showing a linear profile. The initial burst was due to the diffusion release of cholecalciferol IC's found at the surface and outer portion of the minitablet

matrix. When comparing D_3 release from the BAP to the release from the conventional comparator tablet the difference factor (f1) is greater than 15 and the similarity factor (f2) is less than 50 (1000IU: f1=29.97 and f2=33.03; 4000IU: f1=36.74 and f2=35.48). This indicates that the dissolution profiles are considered different. After the initial linear burst phase, cholecalciferol release from the BAP slowed, possibly due to the 66B/33L bile-salt lipase film acting as a diffusion barrier. This second phase of release may have been controlled by: (i) the alginate crosslinked film taking time to swell and unravel from each minitablet; (ii) the time required for the minitablet matrix to erode in aqueous media; and (iii) the time taken for the surfactants, bile salts and TPGS, to dissolve and traverse the media to reach model drug for action. An interaction between cholecalciferol and the βCD carrier and the TPGS matrix may have also influenced the unique biphasic release pattern observed in Figure 5.27a and b. The initial burst phase was followed by a plateau and a zero-order release phase for the BAP after 60 minutes.

No binder or specific excipients were used to delay the release, however the BAP demonstrated an initial delay in release, compared to the comparator that "dose dumped" within the first 10 minutes (Figure 5.27a and b). TPGS, ascorbic acid, and βCDD_3-8 IC are all soluble to different extents in water compared to plain cholecalciferol in the conventional tablets. The *in situ* forming control mechanism exhibited by the BAP succeeded in reducing the risk of dose dumping that occurs with conventional tablets. This control was assured due to TPGS and βCD's affinity for cholecalciferol and their ability to modify the solubility and release rate of the vitamin in an efficient manner. It is also known that cyclodextrins and their complexes form aggregates that solubilise bioactives using micellar-type mechanisms (Loftsson *et al*., 2007). It was postulated that the formation of micelles took place due to the presence of 3 suspending agents (NaC, NaD, TPGS) and the βCDD_3-8 IC which enabled a secondary release of the vitamin actives into aqueous solution.

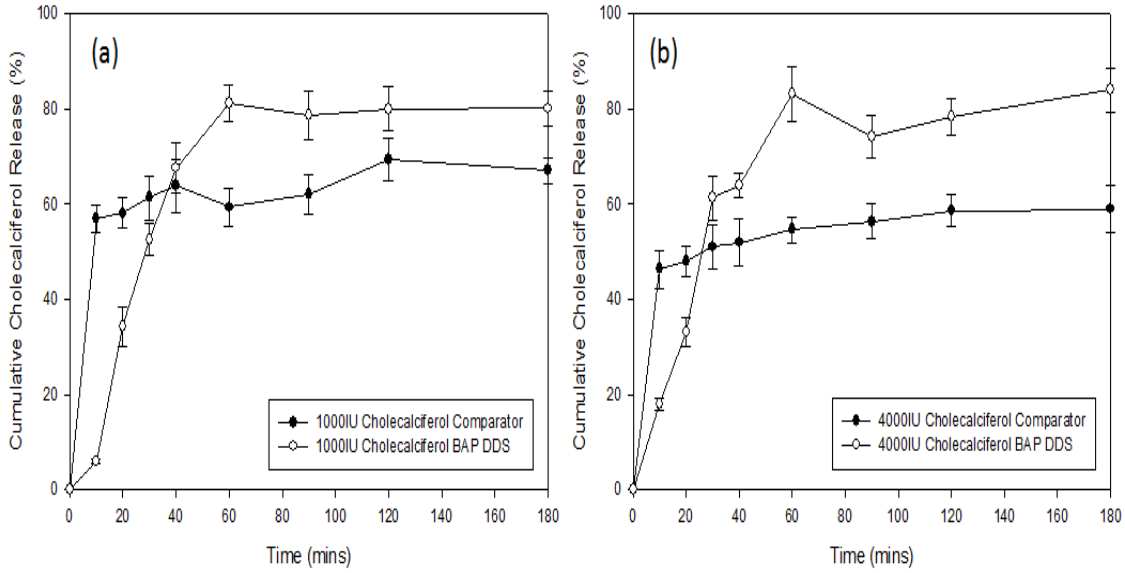


Figure 5.27: Dissolution profiles of (a) Cholecalciferol release from 1000IU BAP DDS and 1000IU comparator product; (b) Cholecalciferol release from 4000IU BAP DDS and 4000IU comparator product in SIF (USP4 apparatus).

5.3.12.2. Dissolution calculations and cholecalciferol model selection

It was noticeable from Tables 5.7 and 5.8 that the area under the dissolution curve (AUC) for D_3 released from the 1000IU and the 4000IU BAP was higher than their respective comparator D_3 products. For the 1000IU BAP the AUC was 10% higher than the comparator (12334.55 vs. 11206.55) (Table 5.7). The 4000IU BAP demonstrated an even greater AUC compared to its comparator with an AUC 28% higher than that of the conventional product (12436.41 vs. 9700.76) (Table 5.8). Therefore the total amount of cholecalciferol released from both BAP DDS's was higher than the conventional counterparts (1000IU: D_{AUC}=1128 and 4000IU: D_{AUC}=2735.65). A greater fraction of cholecalciferol was therefore released over the 3 hour dissolution study from each BAP compared to their respective comparators. A total of 80.15% of cholecalciferol was released from the 1000IU BAP compared to 67.12% from the conventional 1000IU comparator. Similarly 84.01% of D_3 was released from the 4000IU BAP vs. only 59% from the 4000IU comparator.

Based on the AUC results it was not surprising that the Dissolution Efficiency (DE) was also noted to be higher for D_3 released from the BAP vs. the comparator products (4000IU: 0.69 vs. 0.54 and 1000IU: 0.69 vs. 0.62). An 11%-28% increase in dissolution efficiency is attributable to the solubility improvement afforded by the unique BAP delivery system. The Mean Dissolution Time (MDT) for all three vitamins released from the BAP was however noted to be longer than the MDT for D_3 from each comparator (Table 5.7 and 5.8). This is logical as the BAP system

consisted of numerous BB formulation components and layers that controlled and delayed dissolution. In contrast, a low MDT of the comparator is evidence again for dose dumping compared to the more controlled release pattern noted for the BAP. Dose dumping of the comparator was evident in Figure 5.27 with 46%-56% of cholecalciferol released from both comparators vs. 6%-18% from the BAP systems within the first 10 minutes of the study.

Dissolution data for vitamin D_3 release from the BAP DDS' best fitted Weibull's model with a co-efficient of determination (R^2) of 0.96 and the lowest Akaike Information Criterion (AIC) value of 57.93 when fitting to multiple dissolution models.

Weibull 1 Model equation:

F=100{1-Exp[-((t-Ti)^β)/α]}* Weibull's model equation [Equation 5.12]

-Where *F* is the fraction (%) of drug released in time *t* ; *α* is the scale parameter which defines the time scale for the process; *β* is the shape parameter which characterizes the curve ; *Ti* is the location parameter which represents the lag time before onset of dissolution or release process (Costa and Lobo, 2001; Zhang *et al*., 2010).

Other researchers have reported release kinetics described by Weibull's equation for dissolution profiles of other immediate release products including those containing β-cyclodextrin as was included in the BAP (Koester *et al*., 2004; Medina *et al*., 2014). Cholecalciferol release data fitted to Weibulls model showed the smallest Mean Square Error (MSE) and the largest Model Selection Criterion (MSC).

In comparison, the dissolution data for the comparator D_3 products best fitted the Logistic model with an R^2 of 0.99 and the smallest AIC of 14.13. The Logistic model showed the smallest Mean Square Error (MSE) and the largest Model Selection Criterion (MSC) for this model using the dissolution data derived from the comparator products release.

The Logistic Model equation:

*F=100*Exp[α+β*log(t)]/{1+Exp[α+β*log(t)]}* Logistic model equation [Equation 5.13]

-Where *F* is the fraction (%) of drug released in time *t* ; *α* is the scale factor; *β* is the shape factor (Zhang *et al*., 2010).

The superior AUC and DE values for the BAP DDS's provided confirmation of a successful release mechanism that was able to produce an efficient and improved aqueous dissolution phenomenon for cholecalciferol.

5.3.12.3. A unified vitamin release phenomenon

The release profiles of the three vitamins included in the BAP were also compared and found to be similar to one another (f1<15 and f2>50) proving that the novel DDS was able to impart rapid dissolution to the two fat soluble vitamins similar to that of the hydrophilic ascorbic acid constituent (Figure 5.28). It is interesting to note the similarity of dissolution data obtained for cholecalciferol and α-tocopherol, with TPGS releasing D_3 and vitamin E at similar dissolution rates (Table 5.7). The phenomenon observed during earlier phase-solubility studies of IC's of D_3 and ascorbic acid in chapter 4, highlighted a potential to harmonize the release of vitamins of different solubilities from one formulation. Despite the incorporation of only a cholecalciferol IC and ascorbic acid as an uncomplexed physical mixture with TPGS, the BAP dissolution profiles demonstrated a successful unified release profile of all three vitamins (Figure 5.28d and 5.29d). It is hypothesized that TPGS slowed ascorbic acid dissolution and simultaneously enhanced α-tocopherol and cholecalciferol solubility and dissolution, whilst the presence of soluble inclusion complexes and bile salts aided this process. This "in concert" vitamin release phenomena" was confirmed by the dissolution results illustrated in Figures 5.28d and 5.29d showing the successful unified release of the three vitamin bioactives from the BAP irrespective of BCS class of each agent.

Table 5.7: 1000IU BAP Dissolution parameters calculated for the *in vitro* dissolution study using DDSolver add-in software

	Ascorbic acid from BAP	**α-tocopherol from BAP**	**Cholecalciferol from BAP**	**Cholecalciferol from comparator**
MDT (min)	25.56	26.52	26.11	13.03
AUC (ug/mL*min)	12106.65	11995.7	12334.55	11206.55
MRT (min)	64.72	65.64	63.07	81.22
DE	0.67	0.67	0.69	0.62
RD	0.273	0.52	0.362	2.46

Key: MDT: Mean dissolution time;
AUC: Area under the dissolution curve;
MRT: Mean residence time of the drug molecules in the dosage form;
DE: Dissolution Efficiency;
RD: Relative dispersion of dissolution time

Table 5.8: 4000IU BAP vitamin dissolution parameters calculated for the *in vitro* dissolution study using DDSolver add-in software

	Ascorbic acid from BAP	α-tocopherol from BAP	Cholecalciferol from BAP	Cholecalciferol from comparator
MDT (min)	24.71	28.13	31.96	15.58
AUC (ug/mL*min)	11957	11724	12436.41	9700.76
MRT (min)	65.57	67.99	63.38	83.11
DE	0.66	0.65	0.69	0.54
RD	0.038	0.94	1.27	2.75

Key: MDT: Mean dissolution time;
AUC: Area under the dissolution curve;
MRT: Mean residence time of the drug molecules in the dosage form;
DE: Dissolution Efficiency;
RD: Relative dispersion of dissolution time

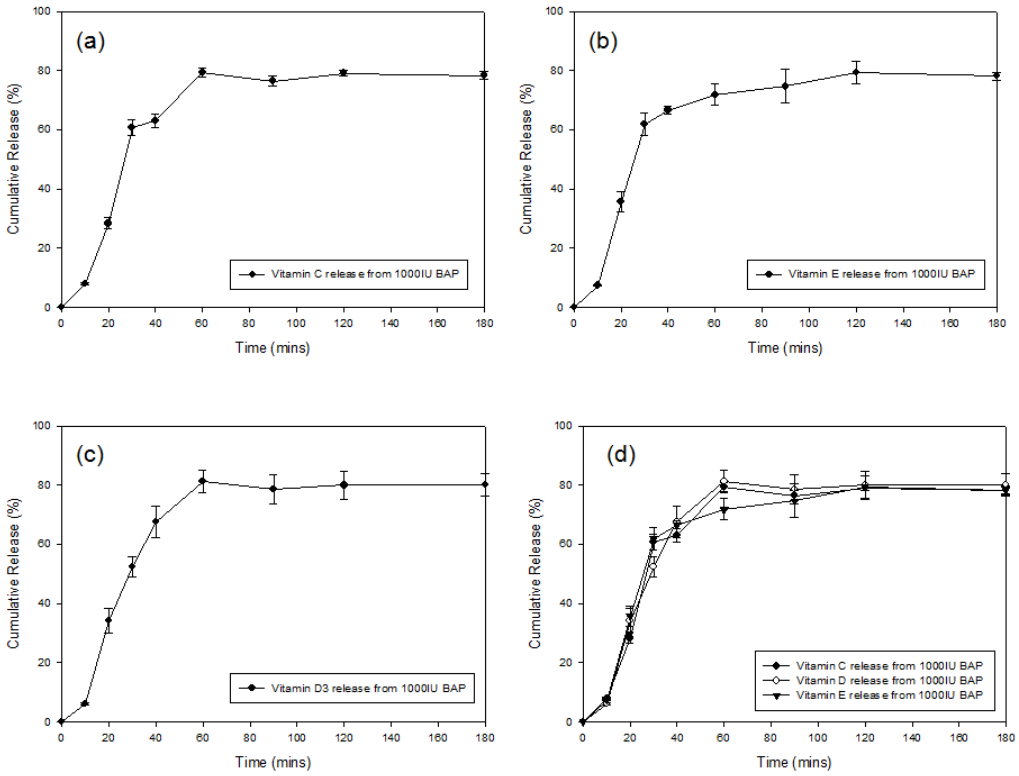


Figure 5.28: Dissolution profiles of vitamin release from 1000IU BAP DDS (a) Vitamin C release; (b) Vitamin E release; (c) Vitamin D_3 release; (d) Profiles of all vitamins released from 1000IU BAP (vitamin D_3, ascorbic acid and α-tocopherol) in SIF (USP4 apparatus).

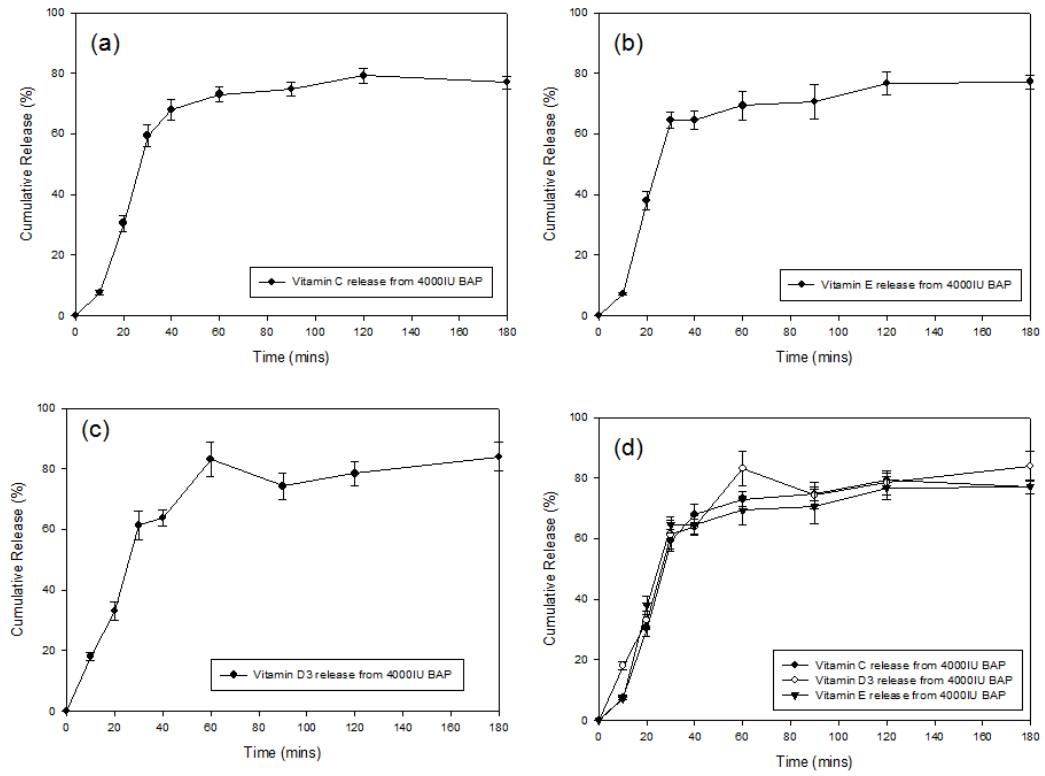


Figure 5.29: Dissolution profiles of vitamin release from 4000IU BAP DDS (a) Vitamin C release; (b) Vitamin E release; (c) Vitamin D_3; (d) Profiles of all vitamins released from 4000IU BAP (vitamin D_3, ascorbic acid and α-tocopherol) in SIF (USP4 apparatus).

5.3.12.4. A unique BAP vitamin delivery mechanism

The matrix composition of the minitablets containing three diversely soluble non-swelling components displayed a unique disintegration profile which contributed towards the delayed, biphasic release profile. Overall, the vitamin release behaviour was postulated to be a result of a dynamic interaction that occurred between the various BAP constituents. The profiles provided evidence for a more efficient as well as a more effective release mechanism that was able to delay vitamin release and simultaneously achieve a higher concentration of vitamin D_3 available for absorption. The amount of cholecalciferol that dissolved from the BAP in the release study exceeded the dissolution of cholecalciferol from the standard comparator tablet due to a number of factors, including: (i) TPGS functioning as a rapid emulsifier to the lipophillic vitamins; (ii) cyclodextrin increasing phase solubility of lipophillic vitamins and reducing phase-solubility of the hydrophilic vitamin; and (iii) the surfactant effects of the bile salts released from the films that enhanced wettability and aqueous dispersion of the model drug (a unique triple phenomenon). The large differences in the dissolution results, including superiority in the cumulative release % and AUC for the BAP compared to the comparators is evidence for efficient vitamin dispersion within the TPGS matrix that may be likened to enhancements

observed in other studies that used TPGS (Yuan *et al*., 2013). Synergistically, the existence of the βCDD$_3$-8 complex was expected to improve solubility parameters of the TPGS matrix of each minitablet with an overall improvement in disintegration and solubility (Goddeeris *et al.*, 2008; Jin and Tatavarti, 2010). The unique BAP formulation provided further synergisms to ultimately result in superiority in D_3 dissolution and aligned release profiles of all three vitamins that have not been reported in previous studies. The triple mechanism of cholecalciferol solubility and disintegration enhancements afforded by the BAP, were conclusively verified in the results of the comparative dissolution study and as depicted in Figures 5.27-5.29.

In addition to the successful unified vitamin release observations, the BAP's unique film formulation was functionalized not only to enhance D_3 dissolution due to bile salt delivery, but also to deliver pancreatic lipase for *in vivo* action. The film provided a controlled and customizable enzyme pattern as detailed under section 5.3.9. The film therefore presented another distinct advantage to the BAP dosage form by delivering pancreatic lipase with a consistent level of enzyme activity that was intended to assist further in the digestive process for improved *in vivo* bioavailability of vitamin D_3. The combined vitamin release profiles and lipase enzyme activity levels provided by the BAP mechanism are illustrated in Figure 5.30.

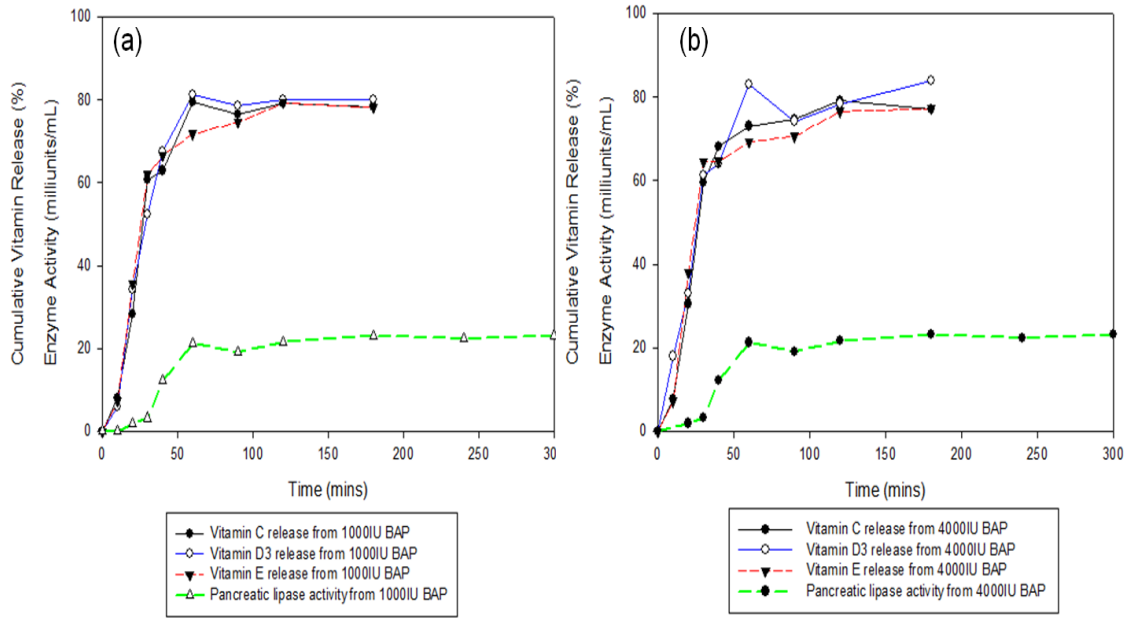


Figure 5.30: Dissolution profiles showing the release/ activity level of all bioactives from the BAP including (a) all vitamins released and lipase enzyme activity provided by the 1000IU BAP; (b) all vitamins released and lipase enzyme activity provided by the 4000IU BAP.

5.4. Concluding Remarks

Comprehensive static atomistic simulations confirmed the superiority of the βD_3 IC as the complex of choice for inclusion in the BAP and successfully validated the experimentally derived IE phenomena reported previously in Chapter 4. Three mechanistic models highlighted the underlying processes behind the preferential formation of βCD complexes. An optimal "3-vitamin" minitablet was formulated to include customizable and clinically relevant amounts of each synergistic vitamin (ascorbic acid and α-tocopherol) and also was functionalized as a vehicle to incorporate the βD_3-8 complex containing model drug, cholecalciferol. *Ex vivo* permeation studies demonstrated the superiority of the novel minitablet to increase solubility and permeation of cholecalciferol through biological membranes. The 66B/33L film was selected as the optimized film candidate for inclusion in the BAP due to favourable influences on cholecalciferol dissolution from the minitablet component and due to a consistent lipase enzyme activity with $0.5\%^{w}/_{v}$ crosslinker. Ultimately, the Final BAP DDS produced a superior biphasic *in vitro* dissolution profile and membrane diffusion compared to same dose market comparators for both the high and low dose cholecalciferol products. Interestingly, the BAP DDS was successful at improving the aqueous dissolution characteristics of cholecalciferol in such a way that the release profile was similar to that of the water soluble vitamin constituent, ascorbic acid, demonstrating a harmonized vitamin release phenomena. All three vitamins were released in a rapid unified and controlled manner reaching maximal dissolution within 60-90 minutes regardless of their inherent solubilities. The BAP prevented dose dumping, which occurred with the respective market comparators, illustrating the achievement of a controlled release mechanism for cholecalciferol. Improved *in vitro* dissolution was evidenced by a higher fraction of cholecalciferol released from the BAP (superior AUC) and higher DE values compared to the comparators. The improved *in vitro* dissolution, provision of a synergistic enzyme bioactive, and the enhanced membrane permeability characteristics of the BAP, need to be assessed for applicability to improved *in vivo* performance as a next stage of this research.

5.5. References

Alishahi A, Mirvaghefi A, Tehrani M.R, Farahmand H, Shojaosadati S.A, Dorkoosh FA, Elsabee MZ. 2011. Shelf life and delivery enhancement of vitamin C using chitosan nanoparticles. *Food Chemistry* 126: 935-940.

Ahmed MK, McLeod MP, Nezivar J, Giuliani AW. 2010. Fourier transform infrared and near-infrared spectroscopic methods for the detection of toxic diethylene glycol contaminant in glycerin based cough syrup. *Spectroscopy* 24: 601-608.

Bikadi Z, Kurdi R, Balogh S, Szeman J, Hazai E. 2006. Aggregation of CD's as an important factor to determine their complexation behaviour. *Chemistry & Biodiversity* 3: 1266-1278.

Bhushan I, Parshad R, Qazi GN, Gupta VK. 2008. Immobilization of lipase by entrapment in ca-alginate beads. *Journal of Bioactive and Compatible Polymers* 23: 552-562.

Charusheela A, Arvind L. 2002. Enzyme hydrolysis of esters using reversibly soluble polymer conjugated lipases. *Enzyme and Microbial Technology* 30: 19-25.

Chen Y, Lu Yi, Chen J, Lai J, Sun J, Hu F, Wu W. 2009. Enhanced bioavailability of the poorly water-soluble drug fenofibrate by using liposomes containing bile salt. *International Journal of Pharmaceutics* 376: 153-160.

Comini S, Olivier P, Riottot M, Duhamel D. 1994. Interaction of β-cyclodextrin with bile acids and their competition with vitamins A and D_3 as determined by H-NMR spectrometry. *Clinica Chimica Acta* 228: 181-194.

Costa P, Lobo JMS. 2001. Modeling and comparison of dissolution profiles. *European Journal of Pharmaceutical Sciences* 13: 123-133.

Dahm L, Hewett JA, Roth RA. 1988. Bile and bile salt potentiate superoxide anion release from activated rat peritoneal neutrophils. *Toxicology and Applied Pharmacology* 95: 82-92.

Dua K, Pabreja K, Ramana MV, Lather V. 2011. Dissolution behavior of β-cyclodextrin molecular inclusion complexes of aceclofenac. *Journal of Pharmacy and Bioallied Sciences* 3(3): 417-425.

Fadnavis NW, Sheelu G, Kumar BM, Bhalerao MU, Deshpande AA. 2003. Gelatin blends with alginate: Gels for lipase immobilization and purification. *Biotechnology Progress* 19: 557-564.

Fieker A, Philpott J, Armand M. 2011. Enzyme replacement therapy for pancreatic insufficiency: present and future. Journal of *Clinical and Experimental Gastroenterology* 4: 55-73.

Garcia-Bailo B, Roke K, Mucth DM, El-Sohemy A, Badawi A. 2012. Association between circulating ascorbic acid, αotocopherol, 25-hydroxyvitamin D, and plasma cytokine concentrations in young adults: a cross-sectional study. *Nutrition and Metabolism* 9 (102): 1-10.

Giannola LI, De Caro V, Giandalia G, Siragusa MG, Tripodo C , Florena, AM, Campisi, G. 2007. Release of naltrexone on bucal mucosa: Permeation studies, histological aspects and matrix system design. *European Journal of Pharmaceutics and Biopharmaceutics* 67: 425-433.

Gibbon CJ. South African Medicine Formulary (SAMF) 7th Edition. 2005. Health and Medical Publishing Group of the South African Medical Association, Cape Town. 78.

Gill KK, Kaddoumi A, Nazzal S. 2012. Mixed micelles of PEG2000-DSPE and vitamin-E TPGS for concurrent delivery of paclitaxel and parthenolide: enhanced chemosensitization and antitumor efficacy against non-small cell lung cancer (NSCLC) cell lines. *European Journal of Pharmaceutical Sciences* 46: 64-71.

Goddeeris C, Willems T, Van den Mooter G. 2008. Formulation of fast disintegrating tablets of ternary solid dispersions consisting of TPGS 1000 and HPMC 2910 or PVPVA 64 to improve the dissolution of the anti-HIV drug UC 781. *European Journal of Pharmaceutical Sciences* 34: 293-302.

Guo Y, Luo J, Tan S, Otieno BO, Zhang Z. 2013. The applications of Vitamin E TPGS in drug delivery. *European Journal of Pharmaceutical Sciences* 49: 175-186.

Hibbins AR, Choonara YE, Kumar P, du Toit L, Pillay V. 2013. Physicomechanical characterization and optimization of EDTA-mPEG and Avicel-EDTA-mPEG *in situ* melt dispersion mini-pellets. *AAPS PharmSciTech* 14 (3): 935-949.

Hu X, Wei B, Wu C, Bai Y, Xu X, Jin Z, Tian Y. 2012. Preparation of the β-cyclodextrin-vitamin C (β-CD-Vc) inclusion complex under high hydrostatic pressure (HHP). *Carbohydrate Polymers* 90: 1193-1196.

Huq T, Salmieri S, Khan A, Khan RA, Le Tien C, Riedl B, Fraschini C, Bouchard J, Uribe-Calderon J, Kamal MR, Lacroix M. 2012. Nanocrystalline cellulose (NCC) reinforced alginate based biodegradable nanocomposite film. *Carbohydrate Polymers* 90: 1757-1763.

Jin F, Tatavarti A. 2010. Tabletability assessment of conventional formulations containing vitamin E tocopheryl polyethylene glycol succinate. *International Journal of Pharmaceutics* 389: 58-65.

Knezevic Z, Bobic S, Milutinovic A, Obradovic B, Mojovic L, Burgarski B. 2002. Alginate-immobilized lipase by electrostatic extrusion for the purpose of palm oil hydrolysis in lecithin/isooctane system. *Process Biochemistry* 38: 313-318.

Koester LS, Ortega GG, Mayorga P, Bassani VL. 2004. Matehmatical evaluation of *in vitro* profiles of hydroxypropylmethylcellulose matrix tablets containing carbamazepine associated to β-cyclodextrin. *European Journal of Pharmaceutics and Biopharmaceutics* 48: 13-19.

Kumar P, Pillay V, Choonara YE, Modi G, Naidoo D, du Toit LC. 2011. *In silico* theoretical molecular modeling for Alzheimer's disease: The nicotine-curcumin paradigm in neuroprotection and neurotherapy. *International Journal of Molecular Sciences* 12: 694-724.

Kumar P, Choonara YE, du Toit LC, Pillay V. 2013. In silico elucidation of the inclusion phenomenon and permeation behavior of a zidovudine–cyclodextrin complex via static lattice atomistic simulation. *Journal of Inclusion Phenomenon and Macrocyclic Chemistry* 78: 445-455.

Li H, Yin X, Ji J, Sun L, Shao Q, York P, Xiao T, He Y, Zhang J. 2012. Microstructural investigation to the controlled release kinetics of monolith osmotic pump tablets via synchrotron radiation X-ray microtomography. *International Journal of Pharmaceutics* 427: 270-275.

Loftsson T, Hreinsdottir D, Masson M. 2007. The complexation efficiency. *Journal of Inclusion Phenomenon and Macrocyclic Chemistry* 57: 545-552.

Madenci D, Egelhaaf SU. 2010. Self-assembly in aqueous bile salt solutions. *Current Opinion in Colloid and Interface Science* 15: 109-115.

Maestrelli F, Cirri M, Mennini N, Zerrouk N, Mura P. 2011. Improvement in oxaprozin solubility and permeability by the combined use of cyclodextrin, chitosan, and bile components. *European Journal of Pharmaceutical Sciences* 78: 385-393.

Mahajan S, Mahajan RK. 2012. Interactions of phenothiazine drugs with bile salts: micellization and binding studies. *Journal of Colloid and Interface Science* 387: 194-204.

Maldonado-Valderrama J, Wilde P, Macierzanka A, Mackie A. 2011. The role of bile salts in digestion. *Advances in Colloid and Interface Science* 165: 36-46.

Matsumoto M, Ohashi K. 2003. Effect of immobilization on thermostability of lipase from *candida rugosa*. *Biochemical Engineering Journal* 14: 75-77.

Medina JR, Salazar DK, Hurtado M, Cortes AR, Dominguez-Ramirez AM. 2014. Comparative *in vitro* dissolution study of carbamazepine immediate-release products using the USP paddles method and the flow-through cell system. *Saudi Pharmaceutical Journal* 22 (2): 141-147.

Mu L, Feng SS. 2003. A novel controlled release formulation for the anticancer drug paclitaxel (Taxol): PLGA nanoparticles containing vitamin E. *Journal of Controlled Release* 86: 33-48.

Murphy DJ, Sankalia MG, Loughlin RG, Donelly RF, Jenkins MG, McCarron PA. 2012. Physical characterisation and component release of poly (vinyl alcohol)-

tetrahydroxyborate hydrogels and their applicability as potential topical delivery systems. *International Journal of Pharmaceutics* 423: 326-334.

Olivas GI, Barbosa-Canovas GV. 2008. Alginate-calcium films: Water vapour permeability and mechanical properties as affected by plasticizer and relative humidity. *LWT-Food Science and Technology* 41: 359-366.

Ostacolo C, Caruso C, Tronino D, Troisi S, Laneri S, Pacente L, Del Prete A, Sacchi A. 2013. Enhancement of corneal permeation of riboflavin-5-phosphate through vitamin E TPGS: A promising approach in corneal trans-epithelial cross linking treatment. *International Journal of Pharmaceutics* 440: 148-153.

Pereira R, Carvalho A, Vaz DC, Gil MH, Mendes A, Bartolo P. 2013. Development of novel alginate based hydrogel films for wound healing. *International Journal of Biological Macromolecules* 52: 221-230.

PermeGear Inc. Equipment that measures permeation through membranes. Retrieved from URL: http://www.permegear.com/franz.htm. [Accessed 20 September 2014].

Pirayavaraporn C, Rades T, Tucker IG. 2012. Determination of moisture content in relation to thermal behaviour and plasticization of Eudragit RLPO. *International Journal of Pharmaceutics* 422: 68-74.

Pongjanyakul T, Puttipipatkhorn S. 2007. Alginate-magnesium aluminium silicate films: Effect of plasticizers on film properties, drug permeation and drug release from coated tablets. *International Journal of Pharmaceutics* 333: 34-44.

Reboul E, Goncalves A, Comera C, Bott R, Nowicki M, Landrier J, Jourdheuil-Rahmani D, Dufour C, Collet X, Borel P. 2011. Vitamin D intestinal absorption is not a simple passive diffusion: Evidence for involvement of cholesterol transporters. *Molecular Nutrition and Food Research* 55: 691-702.

Shin S, Kim J. 2003. Physicochemical characterization of solid dispersion of furosemide with TPGS. *International Journal of Pharmaceutics* 251: 79-84.

Teng Z, Luo Y, Wang Q. 2013. Carboxymethyl chitosan-soy protein complex nanoparticles for the encapsulation and controlled release of vitamin D_3. *Food Chemistry* 141: 524-532.

Thu H, Ng S. 2013. Gelatine enhances drug dispersion in alginate bilayer film via the formation of crystalline microaggregates. *International Journal of Pharmaceutics* 454: 99-106.

Van Hasselt PM, Janssens GEPJ, Slot TK, van der Ham M, Minderhoud TC, Talelli M, Akkermans LM, Rijcken CJF, van Nostrum CF. 2009. The influence of bile acids on the oral bioavailability of vitamin K encapsulated in polymeric micelles. *Journal of Controlled Release* 133: 161–168.

Wang J, Cao Y, Sun B, Wang C. 2011. Physicochemical and release characterization of garlic oil-b-cyclodextrin inclusion complexes. *Food Chemistry* 127: 1680-1685.

Wilcox MD, Brownlee IA, Richardson JC, Dettmar PW, Pearson JP. 2014. The modulation of pancreatic lipase activity by alginates. *Food Chemistry* 146: 479-484.

Yang L, Xu Y, Su Y, Wu J, Zhao K, Chen J, Wang M. 2005. FT-IR spectroscopic study on the variations of molecular structures of some carboxyl acids induced by free electron laser. *Spectrochimica Acta Part A* 62: 1209-1215.

Yuan T, Qin L, Wang Z, Nie J, Guo Z, Li G, Wu C. 2013. Solid dispersion of calcitriol with enhanced dissolution and stability. *Asian Journal of Pharmaceutical Sciences* 8: 39-47.

Yu BY, Chung JW, Kwak SY. 2008. Reduced migration from flexible poly(vinyl chloride) of a plasticizer containing β-cyclodextrin derivative. *Environmental Science and Technol*ogy 42: 7522–7527.

Zhang Y, Huo M, Zhou J, Zou A, Li W, Yao C, Xie S. 2010. DDSolver: An add-in program for modelling and comparison of drug dissolution profiles. *AAPS Journal* 12: 263-271.

Zughaid H, Forbes B, Martin GP, Patel N. 2012. Bile salt composition secondary to bile salt concentration in determining hydrocortisone and progesterone solubility in intestinal mimetic fluids. *International Journal of Pharmaceutics* 422: 295-301.

CHAPTER 6

COMPARATIVE IN VIVO PRECLINICAL EVALUATION OF THE BAP DRUG DELIVERY SYSTEM IN THE LARGE WHITE PIG MODEL

6.1. Introduction

In order to assess the *in vivo* efficacy of the BAP Drug Delivery System (DDS) at improving cholecalciferol bioavailability, a preclinical assessment of the formulation needed to be undertaken. Ethics clearance for the *in vivo* assessment was obtained from the Animal Ethics Committee of the University of the Witwatersrand, Ethics Clearance no. 2011/43/05 (kindly refer to Appendix (i)).

6.1.1. The pertinence of *in vivo* analysis of novel drug delivery systems and applicability of the pig model

Although *in vitro* evaluations of the novel drug delivery system may provide valid information regarding the drug release characteristics under simulated conditions, they cannot entirely represent *in vivo* conditions. Therefore, *in vivo* studies still need to be conducted to obtain relevant pharmacokinetic data (Miller and Ullrey, 1986; Ndesendo *et al*., 2011). The pig model was specifically selected for this project to assess the novel DDS as this model animal has a gastrointestinal tract similar to that of human and was thus identified as a suitable surrogate (Kolawole *et al*., 2010; Metges, 2010) and the costs of maintaining pigs are minimal. The pig model is an ideal model to use for the investigation of drug disposition as porcine physiology is very similar to that of human physiology particularly in terms of cytochrome enzymes and transporters and thus preclinical studies will provide invaluable pharmacokinetic data in this respect (Thörn *et al*., 2011). It is known that the pig gastrointestinal physiology resembles human gastrointestinal physiology in terms of intestinal transit, drug absorption and mucin structure (Varum *et al*., 2010). Thus the gastrointestinal system of the pig offers some anatomical advantages in terms of similarity to humans (Bode *et al*., 2010) and functional advantages for *in vivo* testing in terms of absorption and enzyme metabolism. Various studies have used the porcine model to extrapolate experimental results to humans due to the similarities of GIT physiology (Cordova *et al*., 2012; Bawa *et al*., 2013, Ngwuluka *et al*., 2013). Similarly pig studies have investigated the effects of vitamin D supplementation on health status and the course of serum 25-hydroxyvitamin D levels in these animals (Witschi *et al*., 2011; Tousignant *et al*., 2013). For the above mentioned reasons the

Pig Model is ideally suited for *in vivo* preclinical evaluations of BAP efficacy and safety.

6.1.2. Study objectives*: In vivo* parameters under evaluation

The main outcome measure of the preclinical study was the determination of the drug molecule concentration in the blood plasma or serum with respect to time for the test, comparator and placebo. The primary objective was therefore to determine the *in vivo* drug release kinetics of the model drug, cholecalciferol from the BAP DDS. Since the cholecalciferol metabolite, 25-hydroxyvitamin D_3, is considered the universal indicator of vitamin D status, it was important to also evaluate the ability of the system to deliver sufficient cholecalciferol to facilitate an increase in serum 25-hydroxyvitamin D_3 levels through the course of treatment (Diarrassouba *et al*., 2015). Therefore serum concentrations of 25-hydroxyvitamin D_3 following dosing and throughout the study were assayed.

The pharmacokinetics of the novel DDS were compared to the pharmacokinetics of a conventional cholecalciferol product on the market. Two test dose formulations were assessed: (i) 1000IU dose and (ii) 4000IU dose. Ultimately it was decided whether or not the *in vivo* results following BAP oral dosing translated into superior therapeutic efficacy and improved bioavailability of cholecalciferol with a subsequent rise in 25-hydroxyvitamin D_3 compared to the respective control products.

A secondary objective involved the gross tissue toxicity testing of the BAP device on the GIT tissues. Local cellular damage or evidence of immunological abnormalities was evaluated via histopathology of excised sections of the GIT. Histopathotoxicity effects are critical to evaluating the benefit risk ratio of any novel or existing drug or delivery device that comes into contact with biological tissue as part of the safety assessment of a product.

This chapter therefore discusses the *in vivo* studies conducted on the BAP and comparator products through the determination of plasma and serum drug and principle metabolite concentrations generated by the device or comparator in healthy large white pigs via: histopathological examination and pharmacokinetic analysis. These factors will assist in the measurement of the overall clinical efficacy and safety of the device.

6.1.3. Safety evaluation of the cholecalciferol study dose and delivery mechanism

6.1.3.1. Safety assessment in humans

It has been documented that vitamin D_3 may cause hypercalcaemia due to excessive intake. Symptoms may include anorexia, nausea, vomiting, muscle weakness, headache, and fatigue. More serious manifestations of excessive vitamin D activity may include impairment of renal function (Gibbon, 2007). However, vitamin D toxicity is extremely rare and some studies have shown that only cumulative daily doses of more than 50000IU will result in a rise of 25-hydroxyvitamin D_3 to levels above 150ng/mL that may lead to hypercalcemia and hyperphosphatemia (Zhang and Naughton, 2010). Some studies have shown that the upper limit of safety may be a dose as high as 10000IU/day for many consecutive months (Schwalfenberg *et al*., 2010).

6.1.3.2. Safety assessment in pigs

Excessive intake of vitamin D may result in adverse effects in pigs due to deposits of calcium in soft tissues. However, the recommended dietary additions of vitamins from concentrates, base mixes or premixes for growing-finishing pigs suggests a daily intake of vitamin D_3 to be 70IU/pound. Thus for a 40kg animal the recommended daily intake would be approximately 6300IU/day (Reese and Hill, 2007). Researchers have even used much higher doses of supplements containing 40000IU–80000IU cholecalciferol daily in pre-weanling and nursery pigs over a 52 day period without safety concerns (Flohr *et al*., 2014). A daily intake of up to 15000IU of vitamin D_3 over a 12-18 day period had no negative effect on weanling pigs in a study by Li and co-workers (2000). Only 150000IU/day was found to be toxic after a 12-18 day period (Li *et al*., 2000).

The enhancing bioactives used (bile salts, pancreatic, vitamin E, ascorbic acid, calcium gluconate) are either micronutrients found in the diet or functional substances that are present or secreted within the GIT and some major organs. Therefore these substances were unlikely to have adverse effects on the study animals.

Despite the apparent innocuous nature of the test and placebo formulations all animals were carefully monitored throughout the study. All pigs utilized in the study were weighed at least once a week. The base weight measurements that were

originally obtained were used to determine whether the pigs remained in good health as the study progressed by comparing updated weight measurements with the initial weight measurements (i.e. current weight measurements were compared with initial weight measurement and the second last weight measurement). The behaviour of the pigs was carefully observed by the CAS staff, the researcher and co-workers to ensure that all animals were well adjusted and behaved in a healthy manner. CAS staff and researchers decided whether any animal should continue with the study if a loss of more than 10% body weight was observed. If any animal behaved in a manner that was anti-social towards other animals (i.e. aggressive behaviour) or was under extreme stress, the animal would be removed from the study. Additionally, all study animals were monitored regularly for any infection or inflammatory reactions and treatment was initiated if necessary.

6.2. Materials and Methods

6.2.1. Materials and preparative work

All medication and surgical equipment for administration to the pigs was supplied by the Central Animal Services of the University of the Witwatersrand, Johannesburg, South Africa, and is listed in Table 6.1. The following was also procured for use during the *in vivo* study: Heparin (1000IU/5mL) (Fresenius Kabi, Halfway House, South Africa), Normal saline (1L) bags (Sabax, sodium chloride 0.9%, Adcock Ingram Critical Care (Pty) Ltd, Johannesburg, South Africa) and indwelling intrajugular catheters.

Blood collection tubes: Heparinised plasma collection tubes (4mL) (quantification of plasma cholecalciferol) and serum separator tubes (SST) (4mL) (quantification of 25-hydroxyvitamin D_3) were purchased from BD (Becton Dickinson Pty. Ltd, Woodmead, Gauteng, South Africa).

ELISA: A porcine vitamin D_3 (VD3) solid-phase ELISA assay kit (BlueGene, China) was purchased from Biocombiotech (Lyttleton, Centurion, South Africa) for quantitative determination of cholecalciferol in plasma samples. A porcine 25-hydroxyvitamin D_3 ELISA assay kit (Cusabio, China) was purchased from Biocombiotech (Lyttleton, Centurion, South Africa) for quantitative determination of 25-hydroxyvitamin D_3 in serum samples.

Table 6.1: Medication and recommended dosages administered to pigs during the *in vivo* study

Trade name & Active Drug	Manufacturer	Route (e.g., I.V., I.M.)	Dose	Frequency
Test & Comparators (Cholecalciferol)	-	Oral	1000IU or 4000IU	Once off (Oral)/ day
Anaket (ketamine)	Bayer (Pty) Ltd, Animal health division Isando, South Africa	I.M./ I.V.	40mg/kg	Once off (I.M. / I.V.)/ dosing day
Dormicum (Midazolam)	Roche Products (Pty) Ltd, Isando, South Africa	I.M./ I.V.	0.3mg/kg	Once off (I.M. / I.V.)/ dosing day
Medical Oxygen	Afrox Healthcare, South Africa	Inhalation	12%	Once off (Inhalation)/ dosing day
Temgesic (Buprenorphine)	Shering-Plough, Johannesburg, South Africa	I.M.	0.05mg/kg	Once off (I.M.)/ dosing day
Rimadyl (Carpofen)	Pfizer laboratories, Johannesburg, South Africa	I.M.	4mg/kg	Once off (I.M.)/ dosing day
Lignocaine	Bayer (Pty) Ltd, Animal health division Isando, South Africa	Topical	-	Once off (topical)/ dosing day
Isofor (Isoflurane)	Safe Line Pharmaceuticals (Pty) Ltd, Roodepoort, South Africa	Inhalation	2%	Once off (inhalation)/ dosing day
Euthapent (Sodium pentobarbitone)	Kyron Laboratories (Pty) Ltd, Benrose, South Africa	I.V.	> 50mg/kg	On euthanasia
Baytril (Enrofloxacin)	Bayer (Pty) Ltd, Animal health division Isando, South Africa	SC or I.M.	0.5mL/kg	For infection
Finadyne (Flunixin)	Intervet (Pty) Ltd, MSD Animal Health, Spartan, South Africa	I.M.	2.2mg/kg	For pain and fever (analgesic/ antipyretic)

6.2.2. Surgical and invasive procedures and *in vivo* animal study design

All surgical procedures described below were undertaken by Associate Professor Kennedy Erlwanger of the School of Physiology, Faculty of Health Sciences, University of the Witwatersrand (Johannesburg, South Africa). Professor Erlwanger possesses the following qualifications: BVSc (Hons), MSc, DPhil and is a registered veterinarian with the South African Veterinary Council. Qualified Central Animal Services (CAS) staff of the University of the Witwatersrand (Johannesburg, South Africa) assisted in all surgical procedures throughout the study. All animals were housed at the Central Animals Services (CAS) of the University of the Witwatersrand and the housing conditions were maintained as recommended by CAS Standard Operating Procedures. The pigs were initially housed together prior to the initial intrajugular catheter procedure but were then housed separately after the surgery to ensure that the catheter were not damaged by additional animals within the enclosure.

6.2.2.1. Preparative procedures: Insertion of jugular catheter

An initial procedure was performed prior to the administration of the test, comparator and placebo drugs. Surgery was undertaken to insert a jugular catheter into the study animals. The implantation of the catheter into the jugular vein was done under general anaesthetic in order to minimize stress to the pig. The pig was anaesthetised using ketamine HCl 11mg/kg, midazolam 0.3mg/kg, topical lignocaine, and maintained under medical oxygen and isoflurane gas (2%) for 30 to 60 minutes (Hodgson, 2007; Linkenhoker *et al*., 2010) during the insertion of the catheter into the jugular vein. Carpofen (4mg/kg I.M.) and Buprenorphine (0.05mg/kg I.M.) was administered for inflammation and analgesia. A 7 gauge double lumen 35cm catheter (CS-28702) (Arrow Deutschland GmdH, Erding, Germany) was surgically inserted into the left jugular vein under aseptic conditions by a veterinarian authorized by the Wits animal ethics committee and registered with the SAVC. The jugular vein was exposed by an incision made dorsal to the jugular groove on the left lateral aspect of the neck. The jugular vein was isolated by blunt dissection and 10 cm of the catheter was inserted into the lumen of the vein. The portion of the catheter that was inserted into the lumen of the jugular vein was then fastened to the wall of the vein by purse suture technique. The remaining 25cm of catheter was tunnelled subcutaneously to an exit point cranial at the dorsal aspect of the scapula with the use of a trocar. The external injection ports of the catheter were neatly sutured to the skin of the pig to prevent excessive bending. The function of the catheter was then tested by the removal of blood and flushing with heparinised

saline (1000IU heparin in 1L of 0.9% saline) from both ports. The pig was allowed to recover for at least 10 days after the procedure to enable the animal to make a full recovery prior to continuing with the study (Pento, 1974; Forauer *et al*., 2006; Kolawole *et al*., 2010).

The intrajugular catheter was maintained on a bi-daily basis whereby the catheter was flushed out with heparinised saline (5000IU heparin in 1L of 0.9% saline) twice in the morning (between 7:30am & 9:00am) and in the afternoon (between 3:30pm & 5:30pm). A timetable was created by the researcher and co-workers so that the catheters' were flushed at least twice per day. Before and after the catheter was flushed with heparinised saline, it was inspected to ensure that it was in a good condition and functioning correctly. The location in which each catheter was implanted in each animal was inspected before and after each heparin flush so that any pathology such as an infection could be addressed immediately. The intrajugular catheter was maintained throughout the study by the respective researcher and co-workers.

6.2.2.2. In vivo design: Dosing study – A comparative in vivo relative bioavailability study

Three intake groups consisting of six Large White pigs (±30kg) in each group were used to assess the *in vivo* efficacy of the DDS in comparison with a commercial comparator product and placebo. Blood sampling was performed via a surgically inserted indwelling jugular catheter. Prior to the product administration each pig was sedated using ketamine (11mg/kg) and midazolam (0.3mg/kg) directly into a previously inserted intrajugular catheter, and maintained under medical oxygen and isoflurane gas (1.82%) for 30 minutes. All products (DDS, comparator and placebo) were administered via an intragastric tube to fasted pigs. Dosing was performed on each study animal once daily for 5 consecutive days at time: 0, 24, 48, 72 and 96 hours. Thus the 6 pigs housed in the CAS facility at each time were randomized into groups of 2 pigs. Each group of 2 pigs received a different treatment (i.e. Test, Control or Comparator) to eliminate intergroup variability. Test animals were administered the BAP DDS containing 1000IU cholecalciferol or a commercial comparator containing 1000IU cholecalciferol. Similarly, two other test animals were administered either a BAP DDS containing 4000IU cholecalciferol or a 4000IU cholecalciferol comparator product. Another 2 pigs were administered a placebo product. Pigs were randomly allocated to each study group within an intake group.

Blood samples (4mL) were taken at times: 0, 1, 2, 4, 6, 8, 12, 18, 24 hours after a single dose to determine the time course of plasma cholecalciferol concentrations. Plasma was collected using lithium- heparin tubes and centrifuged for 15 minutes (3000rpm) within 30 minutes of collection. Samples were aliquoted and stored at -80^{o}C prior to assaying. A commercial porcine vitamin D_3 solid-phase ELISA assay kit (BlueGene Biotech, China) was used for quantitative determination of cholecalciferol concentration in each blood sample over 24 hours.

Blood samples (4mL) were also collected at 24, 48, 72, 96 and 120 hours to quantify the change in the 25-hydroxyvitamin D_3 [25(OH)D_3] metabolite over the five day dosing period. Serum was collected using serum separator tube. Samples were allowed to clot at room temperature and then overnight at 2^{o}C-8^{o}C prior to centrifuging for 15 minutes (3000rpm). Serum was removed and stored at -80^{o}C until assay analysis. A commercial porcine 25-hydroxyvitamin D_3 ELISA assay kit (Cusabio, China) was used for quantitative determination of the time course of the major metabolite, 25-hydroxyvitamin D_3, over a 6 day period during and after dosing. The schematic depicting the *in vivo* study design is shown in Figure 6.1.

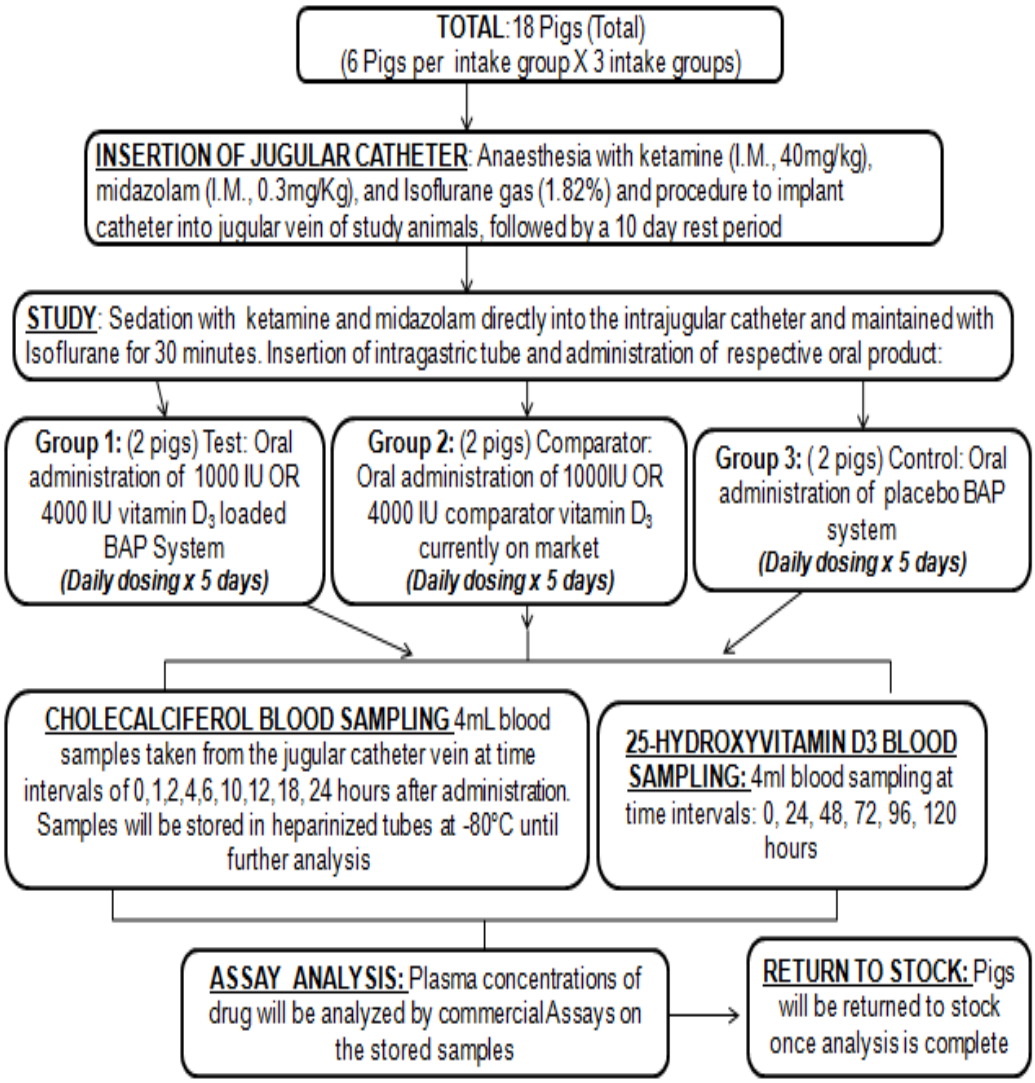


Figure 6.1: Schematic of the experimental design and *in vivo* testing employed in animal species (Pigs underwent surgical insertion of jugular catheter 10 days after arrival at CAS followed by a 10 day recovery period; The dosing study occurred 10 days following jugular catheter surgery with daily dosing from day 0 to day 5).

6.2.3. X-ray studies for gastrointestinal tracking of the BAP

X-ray studies were conducted using barium sulphate as the contrast agent within the DDS. Images were captured as the BAP delivery system moved through the gastrointestinal tract of one of the pigs and X-ray images were taken. Only one of the pigs included in the experimental group were subjected to X-ray studies. This procedure was conducted on a pig administered the vitamin D_3 loaded BAP system that also contained barium sulphate ($15\%^{w}/_{w}$) as the radio contrast agent. X-ray procedures were conducted in such a manner that anaesthesia was minimized and performed not more than twice per day separated by a minimum of a 7 hour interval. The study animal was first anaesthetized for 30-60 minutes to allow the DDS capsule to be administrated via an intragastric tube and an X-ray image was then

captured shortly thereafter. On the same day, after a 7 hour time interval, the pig was anaesthetized once again for an X-ray image to be captured for a second time. The animal was monitored each time before and after the procedure to ensure that the pig maintained good health throughout the study. X-ray photography of the vitamin D_3 loaded BAP was conducted by Central Animal Services nursing staff.

6.2.4. Histological analysis of intestinal tissue samples

Literature reports regarding the safety of the test actives and excipients is insufficient to provide conclusive evidence of safety of the novel system. Therefore it was pertinent to perform histopathological analysis of tissue samples of the GIT after exposure to the test product.

Following humane euthanasia, GIT tissue samples were harvested from two study animals: one pig administered a placebo product and one pig administered a 4000IU test product over the 5 day study period. Multiple samples were removed from each study animal (10 samples each) so that a representative analysis may be obtained for the effect of each product on the GIT tissues. Samples were removed from three areas of the small intestine (duodenum, jejenum and ileum), and from various locations of the colon (proximal, transverse and sigmoid colon). The tissue samples were transferred immediately into laboratory container and immersed in formalin to preserve the integrity of the samples prior to histological analysis. A transverse section was cut from each of the samples and placed in histological tissue cassettes for automated histological tissue processing. Following processing, tissue blocks were prepared and sections of 5-6µm were cut on a microtome from each of the blocks. The sections were stained in an automated haematoxylin and eosin stainer and mounted for histological evaluation.

Histopathological tests were done to assess the level of inflammation and toxicity that might have been caused by the presence of the drug releasing polymeric drug delivery system and the active drug in the GIT. Tests included evaluation for: Cell proliferation; Exudate presence; Stromal reaction; Fibrosis; and Signs of inflammation.

The time-line of a single pig through the *in vivo* study from arrival at the Central Animal Unit until the end of the study, includes the following essential procedures: catheter implantation, dosing study, x-rays, and histology (Figure 6.2).

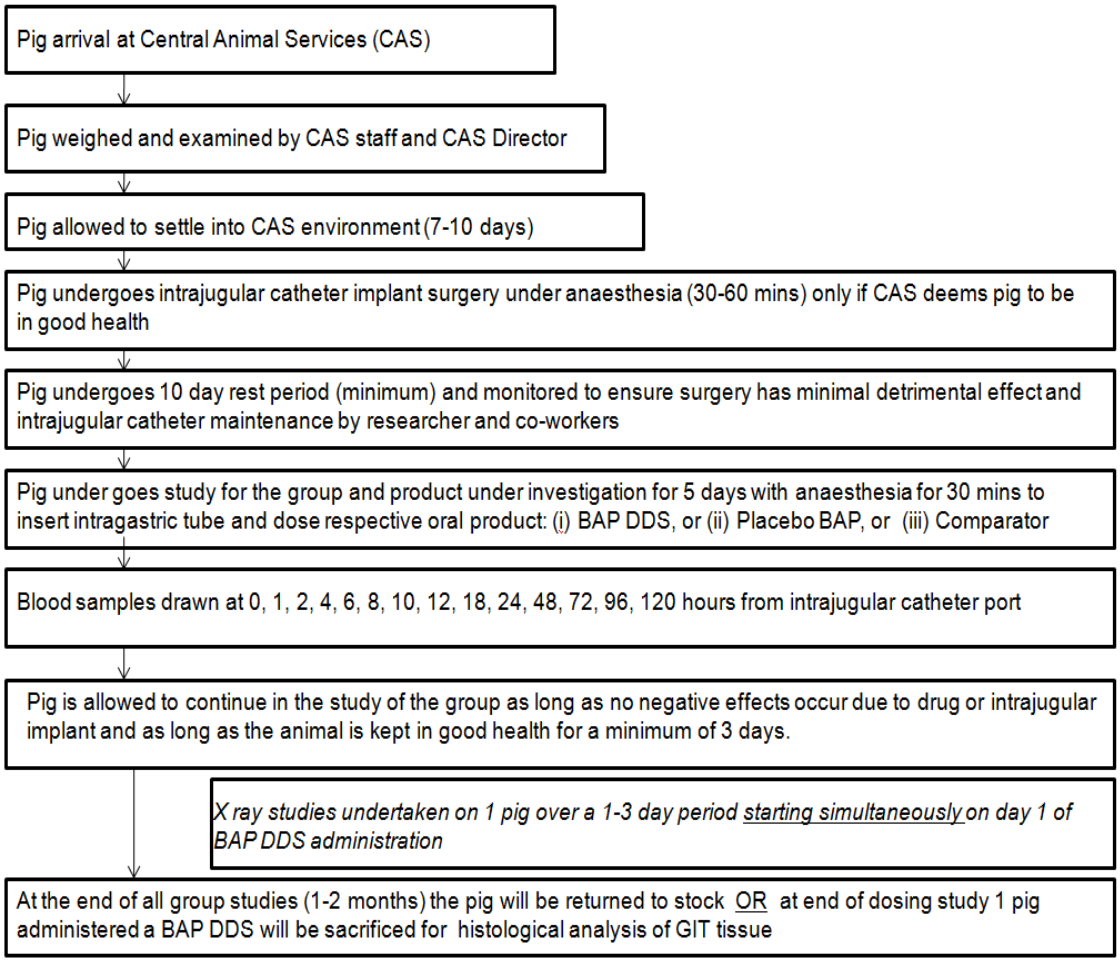


Figure 6.2: Time-line of a single pig throughout the entire study where two phases of anaesthesia will occur, during implantation of the intrajugular catheter (once off) and once daily for a period of 5 continuous days during the dosing study. X-ray studies were performed additionally on 1 pig and histopathology on 1 pig following humane euthanasia.

6.2.5. Quantification of *in vivo* cholecalciferol and 25-hydroxyvitamin D_3 concentrations released from the BAP and comparator products

6.2.5.1. Quantification of in vivo cholecalciferol concentrations in plasma

After collection in 4mL heparinised plasma collection tubes, blood samples were centrifuged for 15 minutes at 3000rpm to separate plasma from cells. Plasma was removed using new syringes and needles for each tube and aliquoted into 2mL epindorphs and stored at -80^{o}C to avoid loss of bioactivity and contamination. Prior to assay, frozen samples were brought to room temperature slowly and mixed gently. A commercial porcine vitamin D_3 (VD3) solid-phase ELISA assay kit (BlueGene Biotech, China) was used for quantitative determination of cholecalciferol concentration in each blood. The VD3 ELISA kit was based on the competitive enzyme immunoassay technique using a monoclonal anti-VD3-HRP conjugate in a

pre-coated plate. Appropriate micropipettes and disposable tips were used for the assay procedure. Reagent preparation involved bringing the kit to room temperature, and preparing 1L of wash solution by diluting 10mL wash solution concentrate with 990mL deionized water. A key was prepared to guide which samples and standards were to be placed in each assay plate well. 100µL of kit standards and the plasma samples were added to the appropriate wells of the antibody pre-coated microtiter plate and 50µL of conjugate was then added to each well (except the blank) and mixed. The plate was then covered with foil and incubated for 1 hour at 37^{o}C. After the hour had passed the plate was removed and manually washed by aspirating incubation mixture from all wells, and then filling each well with wash solution and removing the solution for five repeated cycles. 50µL of kit Substrate A and 50µL of kit Substrate B was then added to each well and the plate was covered and incubated for a second time at 37^{o}C for 15 minutes. Stop Solution (50µL) was then added to each well and mixed thoroughly using a micropipette. The optical density of each well was then determined at 450nm using a spectrophotometric multilabel plate reader (Victor X3, PerkinElmer). A Standard curve was plotted for the average optical density/ absorbance of each standard vs. concentration and used to calculate the concentration of cholecalciferol for each recorded absorbance reading.

6.2.5.2. Quantification of in vivo 25-hydroxyvitamin D_3 concentrations in serum

After collection in 4mL serum separator tubes (SST) blood samples were allowed to clot overnight at 4^{o}C prior to centrifugation for 15 minutes at 3000rpm to separate serum from cells. Serum was removed using new syringes and needles for each sample tube and aliquoted into 2mL epindorphs for storage at -80^{o}C. A commercial porcine 25-hydroxyvitamin D_3 ELISA assay kit (Cusabio, China) was used for quantification of 25-hydroxyvitamin D_3 in serum samples. The assay employed a competitive inhibition enzyme immunoassay technique. The kit provided high sensitivity and specificity for the detection of porcine 25-hydroxyvitamin D_3. Prior to assay frozen samples were brought to room temperature and fresh standards were prepared by serial dilution. Wash buffer, standards, reagents and samples were prepared according to the kit protocol. A key was prepared to guide which samples and standards were to be placed in each assay plate well. 50µL of sample, standard and control were added to each well followed by 50µL of HRP-conjugate . Each well was mixed with a micropipette and then covered and incubated for 60 minutes at 37^{o}C. Following incubation, each well was aspirated and washed five times with wash buffer (300µL) using a multi-channel pipette. At the last wash all remaining

liquid was removed by inverting the plate and blotting against a paper towel. 50µL of Substrate A and 50µL of Substrate B was added to each well and the plate was incubated for a second time at 307^{o}C for 15 minutes. After the second incubation the plate was removed and 50µL of stop solution was added to each well. The optical density/ absorbance of each well was determined by visualizing the plate at 450nm using a spectrophotometric multilabel plate reader (Victor X3, PerkinElmer). A standard curve was constructed by plotting the mean absorbance for each standard vs. concentration. The concentration of 25-hydroxyvitamin D_3 in each sample was calculated from the standard curve equation.

6.2.6. Pharmacokinetic modelling of drug release data employing noncompartmental and compartmental algorithms

Quantitative evaluation of the drug transport process occurring in the GIT necessitates selection of a suitable PK model for fitting concentration-time data. Appropriate model selection required the use of diagnostics such as the correlation coefficient, sum of squares of residuals (SS), standard error of weighted residuals (SE), Akaike's Information Criterion (AIC) and Schwarz's Bayesian Criterion (SBC). AIC and SBC hold the most significance (Zhang *et al*., 2010). The AIC and SBC values are a measure of goodness of fit based on maximum likelihood. When comparing several models for a given set of data, the model associated with the smallest value of AIC or SBC is regarded as giving the best fit. Lower values of the index indicate the preferred model, that is, the one with the fewest parameters that still provides an adequate fit to the data; although it is not the actual value but rather the difference between the values in a set. The value that is the lowest in the set represents the best fit. In this case each set is the different kinetic model. Pharmacokinetic data analysis was done using PKSolver, a menu-driven add-in program for Microsoft Excel. Subsequently the above-mentioned "goodness of fit" criteria were utilized to assess which pharmacokinetic model best described the kinetics of cholecalciferol release from the BAP and the market comparators.

6.2.7. Establishment of an *in vitro-in vivo* correlation for cholecalciferol release from the BAP DDS

In vitro-in vivo correlations (IVIVC) are one of the greatest challenges in pharmaceutical research, nevertheless they are an essential criteria that need to be elucidated during the formulation development process (Choudhury *et al*., 2013). An IVIVC is generated by describing the strength of the correlation between an *in vitro* result (such as drug dissolution), and an *in vivo* result (such as drug plasma

concentrations following drug absorption). IVIVC tools that accurately correlate *in vitro* data with *in vivo* effects hold high value in the pharmaceutical industry due to an ability to shorten lengthy drug development timelines (Emami, 2006). As pointed out by other researchers, continual advancements and improvements in methods to design *in vitro* methods to model *in vivo* performance of dosage forms, will ultimately lead to more accurate IVIVC's and thus improve patient outcomes (Kostewicz *et al*., 2014).

WinNonLin software (V5.3 with IVIVC Toolkit Build 20091211139, Pharsight Software, Statistical Consultants Inc., Apex, NC, USA) was used for generating a Level A IVIVC in the current study. For testing a level A IVIVC, the percentage of drug absorbed up to time *t* was plotted versus the amount of drug released *in vitro*. Input data consisted of *in vitro* cholecalciferol release data, and the relevant *in vivo* pharmacokinetic data derived from the preclinical pig-model study.

6.3. Results and Discussion

6.3.1. Surgical procedures and post-surgical assessment of the pig model following catheter surgery and dosing study

The BAP was well-tolerated with no animals demonstrating any signs of hypervitaminosis or adverse effects from the study products. Prior to the start of one of the dosing studies, one animal became noticeably ill with pyrexia and anorexia and was prescribed antibiotic treatment (enrofloxacin) and analgesic/ antipyretics (flunixin) by CAS veterinarian. Despite treatment the pig did not recover and was excluded from the dosing study and subsequently euthanized after a decision by CAS staff. Two of the pigs suffered mortality at various stages of the dosing study, however sufficient prior blood sampling had taken place to extrapolate results to the end of the study. The quantity of study animals reaching study completion was sufficient to allow for statistical significance. Post-mortem of these animals revealed pre-existing respiratory conditions (pneumonia, pleuritis, and haemorrhagic bowel syndrome) that pre-disposed to anaesthetic risk and subsequent mortality. Mortalities were unrelated to the study product or procedures. No animals demonstrated any abnormal changes in behaviour or eating habits. Figure 6.3a-e portrays the jugular catheter procedure and the position of the catheter port on the dorsal aspect of the spine of one pig following surgery.

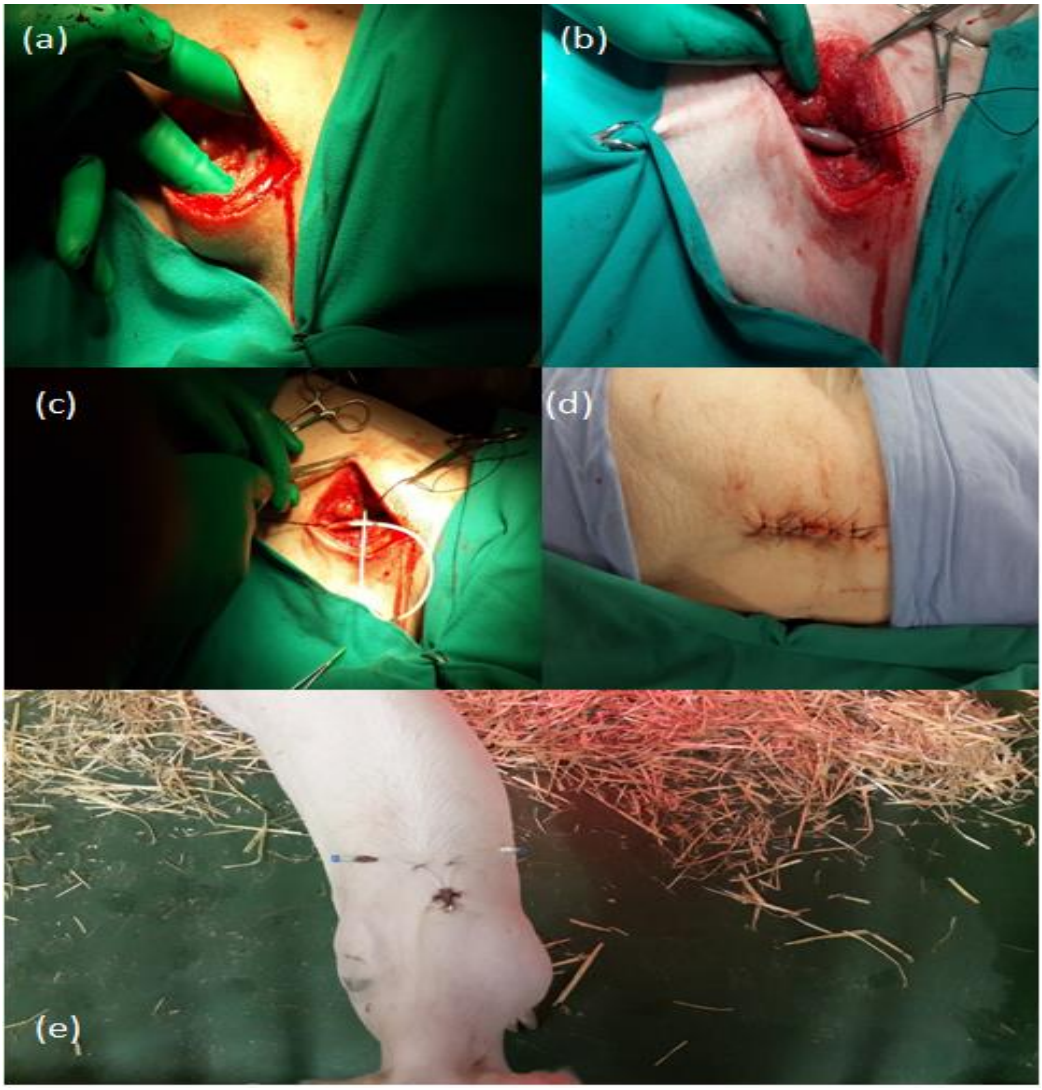


Figure 6.3: Sequential images depicting the intrajugular catheter surgery in one study animal during the *in vivo* evaluation of the BAP DDS: (a) and (b) Surgical incision to expose the jugular vein; (c) Insertion of the jugular catheter into the lumen of the jugular vein and fastening to the wall of the vein; (d) Sutured left lateral aspect of the neck of a pig after completion of jugular catheter surgery; (e) External injection ports of the catheter positioned on the dorsal aspect of the scapula.

The animals were subjected to short anaesthesia on a daily basis for 5 days in order to dose each product by gastric lavage via an intragastric tube. In order to limit risk to each animal and reduce excessive trauma to the oesophagus, only two attempts were made at “tubing” and flushing the DDS or comparator capsule into the stomach of each animal. Only one animal failed a dosing procedure on day 3 of the dosing study. Emesis of one pig an hour after a dosing procedure with a test DDS (4000IU) was noted on day 3 of the study. The provision of sufficient medical oxygen and careful monitoring ensured that each animal recovered completely after each procedure. Figure 6.4 shows images of the housing of pigs, one animal under general anaesthetic during the dosing study and blood sampling from jugular ports.



Figure 6.4: Photographic evidence of (a) Housing of the pigs at CAS; (b) Pig under general anaesthetic during dosing study; (c) Sterile blood sampling from jugular catheter ports during dosing study.

6.3.2. X-ray studies for gastrointestinal tracking of the BAP

X-ray studies were conducted to provide evidence of the intact BAP within the GIT prior to dissolution. The contrast agent (barium, 15%$^{w}/_{w}$) contained within the DDS revealed a clearly visible image of the capsule after lateral and medial images were taken at the CAS facility. Figure 6.5 shows the images obtained 30 minutes after dosing one pig with a BAP 4000IU DDS. Similarly, other researchers found X-ray imaging a useful technique for visualization and tracking of capsules in other animal model studies (Saphier *et al*., 2010). Since the median gastric emptying time in adult pigs was estimated to range between 31 to 52 minutes, one was still able to visualize the DDS at 30 minutes after dosing in the current study (Cordova *et al*., 2012). Other researchers have noted that complete gastric emptying time may range from 31-141 minutes and is likely to be delayed by anaesthesia (Anderson, 2002). It was therefore estimated that the BAP DDS would reach the intestine within a maximum of 1-2 hours with maximal dissolution having occurred by 2-3 hours. This correlates well with the peak plasma concentration achieved by the 2 hour time point during the *in vivo* study and reported later in the pharmacokinetic data evaluation (section 6.3.5.). Due to the release mechanism, the majority of the drug release occurred in the alkaline pH of the small intestine. No study animals were harmed during the X-ray procedure.

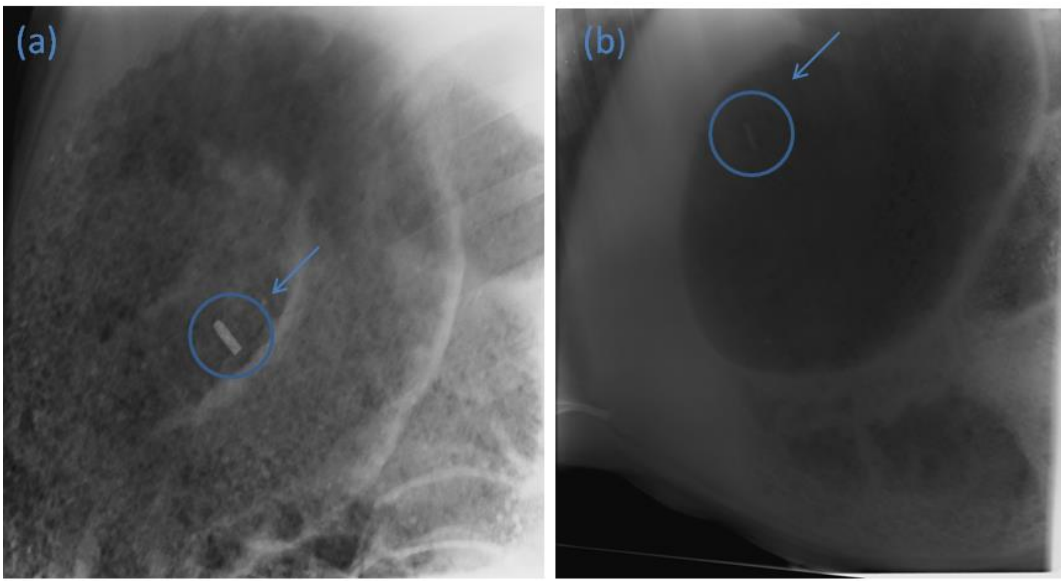


Figure 6.5: X-ray images of one study animal dosed a test product containing barium showing the outline of the capsule at 30 minutes post dosing: (a) lateral X-ray image of stomach; (b) medial X-ray image of stomach.

6.3.3. Histological analysis of intestinal tissue following 5 day dosing study

Two pigs were humanly euthanized using sodium pentobarbitone and tissues were immediately harvested from various areas of the small intestine and large intestine for histopathological analyses. Intestinal samples were excised from multiple regions of the intestine (duodenum, ileum, jejenum, colon, caecum) in duplicate. Histopathological examination was performed by IDEXX (Pretoria, South Africa) Laboratories on 10 samples removed from various areas of the intestine of a pig administered a placebo product and on 10 samples removed from another pig administered the BAP DDS. It was reported that there was no observable difference between the GIT tissue samples derived from either animal, with no pathology evident in any of the samples.

6.3.3.1. Placebo tissue samples

Six different sections of the duodenum and jejenum were examined with no pathological lesions found (Figure 6.6Ia). Four different sections of the ileum were examined with no pathological lesions present (Figure 6.6Ib). Four different sections of the colonic mucosa and wall of the colon were examined and appeared normal (Figure 6.6Ic).

6.3.3.2. BAP DDS tissue samples

Evaluation of five sections from the duodenum revealed normal duodenal anatomy with glands of Lieberkuhn in the intestinal mucosa and no pathological changes

present (Figure 6.6IId). Evaluation of four different sections of the ileum showed normal gut-associated lymphoid tissue which appeared active without any evidence of pathological changes (Figure 6.6IIe). Three sections from the large intestine, including colon and caecum, were examined and appeared normal with no pathology within the mucosa, submucosa, muscle layers of the wall and large intestine serosa. A normal population of lymphoplasma cells was observed in the lamina propria (Figure 6.6IIf).

Microscopic slide images that were captured clearly demonstrated the condition of each tissue sample in support of the final pathological assessments as outlined above (Figure 6.6).

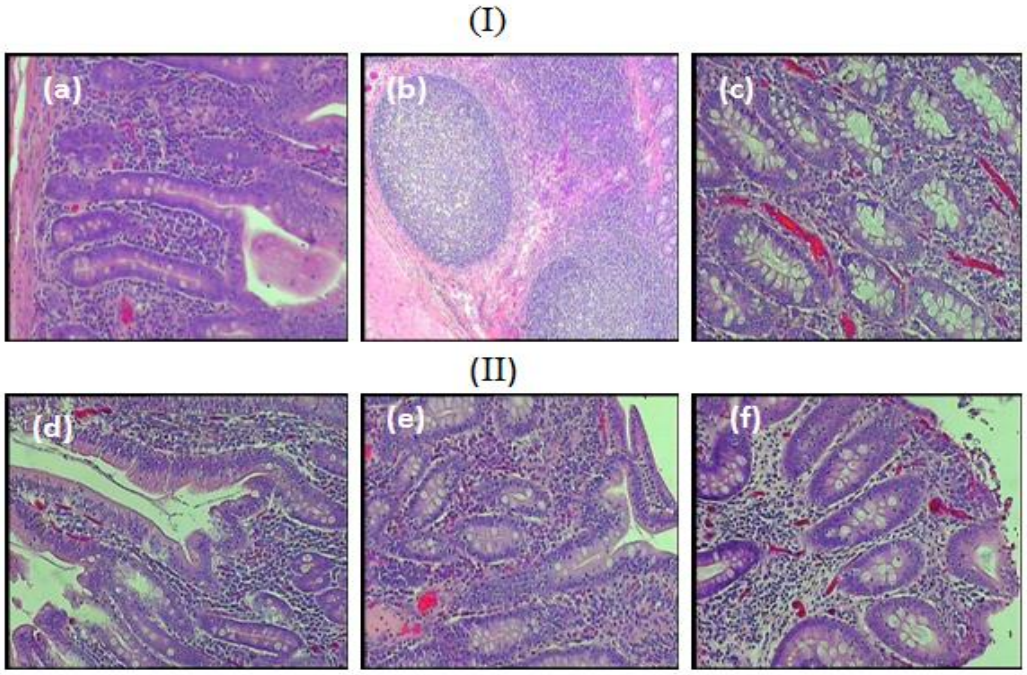


Figure 6.6: Microscopic slide images demonstrating the condition of each tissue sample harvested from two study animals: **(I)** Pig dosed Placebo product: (a) duodenum & jejenum; (b) ileum; (c) colon & **(II)** Pig dosed 4000IU BAP DDS test product: (d) duodenum; (e) ileum; (f) colon and caecum.

In summary, histopathological examination revealed that neither the BAP DDS nor the placebo DDS caused any observable tissue damage during the study. No specific pathology, including evaluation for cell proliferation, exudation, sub-epithelial stromal reactions, fibrosis or inflammation was found in any of the sections analyzed. There were no histological differences observed between the tissue sections derived from different parts of the intestine of the animal administered the placebo and the animal administered the test BAP DDS product.

6.3.4. Quantification of *in vivo* cholecalciferol and 25-hydroxyvitamin D_3 concentrations released from the BAP DDS and comparator products

The accuracy of vitamin D testing is becoming even more critical at a time where research has outlined the correlation between vitamin D and various chronic diseases. A reliable method for quantification of vitamin D and its metabolites is paramount to understanding the clinical picture and making the best decision for the patient. A number of methods have been developed to determine vitamin D levels in humans including: direct UV detection after HPLC, competitive protein-binding assays, and radioiodine based RIA kits (Hollis, 2000). Commercial immunoassays, such as those used in the current study, are more frequently used in clinical laboratories as they produce quicker results than the traditional chromatographic methods (Ong *et al*., 2012). Researchers have demonstrated good correlations between commercial assays and LC-MS/MS based on the Passing Bablok regression equation (Ong *et al*., 2012). Therefore the assays procured for use in the current study were considered of acceptable accuracy and standard and proved suitable due to the rapidly of the assay procedure and the quantity of samples to be tested.

Figure 6.7 shows the cholecalciferol and 25(OH)D_3 standard curves plotted for the ELISA assays that were performed to determine the plasma and serum concentrations in the pig-model studies. The sensitivity of the Porcine VD3 ELISA Kit (BlueGene Biotech, China) was 1.0ng/mL, and an excellent specificity for detection of vitamin D_3 with no cross-reactivity or interference between VD3 and other analogues was assured. The sensitivity of the Pig 25-hydroxyvitamin D_3 ELISA Kit (Cusabio, China) was stated to be less than 5µg/L and was determined by the manufacturer from 20 replicates of the zero standard added by their standard deviations. Specificity of the Cusabio 25-hydroxyvitamin D_3 assay was stated to be high with no cross-reactivity or interference between pig 25(OH)D_3 and other vitamin D metabolites. The results of the assays of the samples for all test and reference products are discussed in detail in the pharmacokinetic analysis section of this chapter.

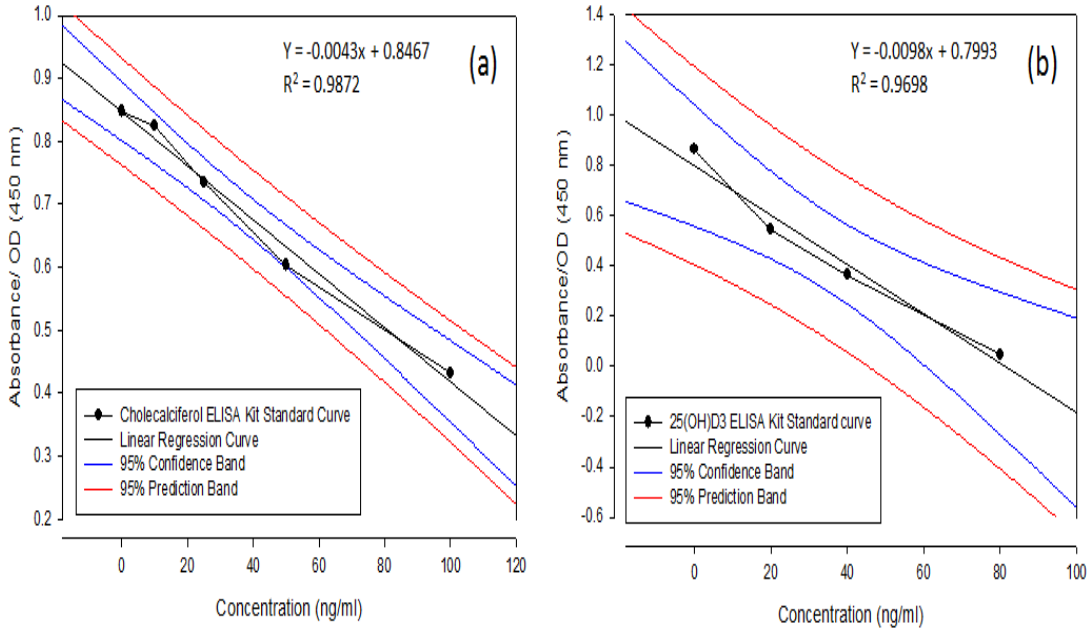


Figure 6.7: Calibration curves generated for (a) cholecalciferol and (b) 25-hydroxyvitamin D_3 from the ELISA Kits used to quantify the levels of actives in plasma and serum respectively.

6.3.5. Pharmacokinetic analysis: Comparative *in vivo* evaluation of the BAP DDS and comparator products

6.3.5.1. BAP DDS and comparator 4000IU *cholecalciferol noncompartmental and compartmental analyses*

Noncompartmental methods estimate the exposure to a drug by estimating the area under the curve of a concentration-time graph. Compartmental methods estimate the concentration-time graph using kinetic models. The DDS and Market comparators were subjected to noncompartmental analysis and four compartmental models (i.e. one compartment without time lag, one compartment with lag, two compartment without lag, and two compartment with lag). All systems failed to be described via two compartment models. In accordance with the smaller AIC and SBC, and higher correlation between observed and predicted values, the release of cholecalciferol from the 4000IU DDS is best described by a one compartment model with no lag. The corresponding Market Comparator (4000IU) was also best described by the one compartment without lag kinetic model.

The results of the noncompartmental and compartmental analysis of the 4000IU BAP are shown in Table 6.2 and Table 6.4 below and Figure 6.8. Likewise, the

noncompartmental and compartmental analysis of the 4000IU comparator product is presented in Table 6.3 and Table 6.5 and Figure 6.9.

For both the test and comparator products, PK analysis revealed that the cholecalciferol release was best described by a one compartment model without lag due to favourable R^2, Akaike Information Criterion (AIC) and Schwarz Criterion (SC) values. R^2 values were similar between compartmental models, however the AIC and SC values were lowest for one compartmental models without lag for both products. The 1st order rate constant (K_a) value for BAP release was 6.58586.

When comparing time to maximum peak plasma concentration (T_{max}) the BAP took longer to reach maximum drug concentration with a T_{max} of 0.83587 hours vs. 0.2981. This is evidence for a delayed mechanism of release imposed by the various components of the delivery system. However, despite the delay to reach peak cholecalciferol concentration, the BAP achieved a substantially greater exposure of drug during the 24 hour time frame. The 4000IU BAP had an $AUC_{0\text{-}t}$ of 1808.02 vs. 1053.638 for the comparator product (Tables 6.4 and 6.5). The BAP $AUC_{o\text{-}inf}$ was remarkably higher at 3768.50 compared to 1179.585 for the comparator product. The increased extent of cholecalciferol absorption is evidence for improvement in bioavailability of cholecalciferol from the BAP due to the delivery system's enhancer properties imparted by the TPGS, alginate, CD and biological excipients (bile salts and lipase). The $AUC_{o\text{-}inf}$ was 3.2x higher for the BAP compared to the commercial comparator. Similar sustained release and AUC magnification was demonstrated by other researchers with the addition of TPGS to other delivery systems (Saadati and Dadashzadeh *et al*., 2014). It has been noted that TPGS is adept at increasing the systemic exposure of various drugs including, colchicine, cyclosporine, and the nutraceuticals curcumin and co-enzyme Q10 (Guo *et al*., 2013). TPGS and alginate are known to enhance permeation through biological membranes and the AUC increase may be attributable to both enhancement in dissolution and greater GIT mucosal permeation (Zhang *et al*., 2012). Enhancement in the passive diffusion processes of cholecalciferol through the duodenum as was demonstrated in earlier permeation studies (Chapter 5) would also contribute to the observed improvement *in vivo* bioavailability.

The current study revealed that the BAP DDS enhancing components increased not only AUC but also the Mean Residence Time (MRT): 36.64 hours vs. 10.75 hours (comparator). The BAP also induced a significantly increased cholecalciferol half-life

($t_{1/2k10}$=25,29 hours) compared to the literature value of approximately 4-6 hours (Jones, 2008). Figure 6.10 shows the overlaid cholecalciferol plasma versus time curves for the 4000IU BAP and 4000IU comparator. The BAP had a prolonged release profile and delayed elimination with a different plasma-time profile to the comparator. The comparator exhibited an initial increase in plasma cholecalciferol followed by a sharper drop in cholecalciferol levels. The BAP, in contrast, maintained significantly higher plasma levels at later time points from 4 hours until 24 hours post dose (Figure 6.10).

Cholecalciferol enters the body from external sources including exposure to sunlight and food sources, therefore all pigs had initial baseline cholecalciferol levels above 0. No dietary restrictions were imposed on the study animals thus the difference between the mean cholecalciferol baseline levels and the maximum achieved plasma cholecalciferol (C_{max}) were compared to illustrate the ability of each product to increase plasma levels. The mean difference from baseline to C_{max} was 55ng/mL for the BAP vs. 46ng/mL for the comparator from time 0 to 2 hours post dosing (Figure 6.10). Therefore the BAP was deemed superior at achieving a greater mean peak difference between baseline and peak cholecalciferol concentration.

Most researchers have investigated the time course in the rise of the cholecalciferol metabolite, 25-hydroxyvitamin D_3 and not cholecalciferol (Vieth, 1999; van Groningen *et al*., 2010; Wagner *et al*., 2011). One research group that did follow the plasma time course of cholecalciferol over 3 days post a single oral dose compared the efficacy of two calciferols: D_2 vs. D_3 (Armas *et al*., 2004). This research group compared the relative potencies of vitamin D_2 and vitamin D_3 after a single dose but measured calciferol concentrations only at three time points: day 0, day 1 and day 3. The current research is novel in its design as it explicates the rise and fall in cholecalciferol over a 24 hour time frame after a single oral dose following multiple plasma sampling points.

In summary the BAP 4000IU demonstrated the highest absorption *in vivo* with a greater change from baseline to C_{max} (better dose response) and higher AUC values (Figure 6.10). Similar *in vivo* bioavailability enhancements were attributed to other drugs when bile salts were included in formulations by other research groups (Chen *et al*., 2009; Niu *et al*., 2012). Chen and co-workers (2009) demonstrated the utility that the bile salt NaD offers in terms of increasing the bioavailability of fenofibrate 1.57 fold relative to conventional liposomes without bile salt. It is not surprising that

cholecalciferol *in vivo* bioavailability was improved from the BAP, especially considering research has demonstrated bile components have a positive influence on oral bioavailability of other fat soluble vitamins (van Hasselt *et al*., 2009). However, the current improvements in pharmacokinetic parameters of the 4000IU BAP may be attributable to not only the effects of the bile salt release but also the synergistic effect of TPGS, lipase, alginate hydrogel, βCD, and the bile components. A higher exposure to cholecalciferol in terms of greater AUC and AUMC will enhance the clinical benefits of cholecalciferol in both the deficient and supplemental patient.

Table 6.2: Results of noncompartmental analysis of BAP 4000IU cholecalciferol release

Parameter	Unit	Value
λ_z	1/h	0.014187966
$t_{1/2}$	h	48.85458402
T_{max}	h	2
C_{max}	ng/mL	101.4094741
T_{lag}	h	0
$C_{last\ obs}/C_{max}$		0.572379131
AUC $_{0\text{-}t}$	µg/mL*h	1781.150771
AUC $_{0\text{-}inf_obs}$	µg/mL*h	5872.270412
AUC $_{0\text{-}t/0\text{-}inf_obs}$		0.303315523
AUMC $_{0\text{-}inf_obs}$	µg/mL*h^2	405808.0721
MRT $_{0\text{-}inf_obs}$	h	69.1058217
Vz/F$_{_obs}$	(µg)/(µg/mL)	1.200255798
Cl/F$_{_obs}$	(µg)/(µg/mL)/h	0.017029189

Table 6.3: Results of noncompartmental analysis of comparator 4000IU cholecalciferol release

Parameter	Unit	Value
λ_z	1/h	0.047912076
$t_{1/2}$	h	14.46706628
T_{max}	h	2
C_{max}	µg/mL	106.8096528
T_{lag}	h	0
C_{last_obs}/C_{max}		0.291589875
AUC $_{0\text{-}t}$	µg/mL*h	1119.3018
AUC $_{0\text{-}inf_obs}$	µg/mL*h	1769.338614
AUC $_{0\text{-}t/0\text{-}inf_obs}$		0.632610282
AUMC $_{0\text{-}inf_obs}$	µg/mL*h^2	39568.89911
MRT $_{0\text{-}inf_obs}$	H	22.36366674
Vz/F$_{_obs}$	(µg)/(µg/mL)	1.179625234
Cl/F$_{_obs}$	(µg)/(µg/mL)/h	0.056518294

Table 6.4: Results of compartmental analysis of BAP 4000IU cholecalciferol release

Parameter	Unit	Value	Diagnostics	Value
One compartment model without T_{lag}				
A	ng/mL	103.6978729	r obs-pre	0.895023954
K_a	1/h	6.585861227	SS	2297.960017
k_{10}	1/h	0.027402519	WSS	2297.960017
$t_{1/2ka}$	h	0.105247766	R^2	0.964139756
$t_{1/2k10}$	h	25.29501644	WR^2	0.964139756
V/F	(µg)/(ng/mL)	0.968369135	SE	18.1184989
CL/F	(µg)/(ng/mL)/h	0.026535754	AIC	83.39777059
T_{max}	h	0.835874048	SC	84.30552587
C_{max}	ng/mL	100.9279663		
AUC $_{0-t}$	ng/mL*h	1808.026613		
AUC $_{0-inf}$	ng/mL*h	3768.500406		
AUMC	ng/mL*h^2	138096.0764		
MRT	H	36.64483521		
One compartment model with T_{lag}				
A	ng/mL	103.7111137	r obs-pre	0.895028688
K_a	1/h	6.361556442	SS	2298.021069
k_{10}	1/h	0.027412532	WSS	2298.021069
T_{lag}	h	1E-06	R^2	0.964138803
$t_{1/2ka}$	h	0.108958741	WR^2	0.964138803
$t_{1/2k10}$	h	25.28577753	SE	19.57047551
V/F	(µg)/(ng/mL)	0.968389698	AIC	85.39803627
CL/F	(µg)/(ng/mL)/h	0.026546013	SC	86.60837664
T_{max}	h	0.859948004		
C_{max}	ng/mL	100.8584001		
AUC $_{0-t}$	ng/mL*h	1807.506937		
AUC $_{0-inf}$	ng/mL*h	3767.043983		
AUMC	ng/mL*h^2	138012.6633		
MRT	h	36.63686008		

Table 6.5: Results of compartmental analysis of comparator 4000IU cholecalciferol release

Parameter	Unit	Value	Diagnostics	Value
One compartment model without T_{lag}				
A	ng/mL	110.7961078	r obs-pre	0.759029639
K_a	1/h	17.67815894	SS	4986.944653
k_{10}	1/h	0.093431608	WSS	4986.944653
$t_{1/2ka}$	h	0.03920924	R^2	0.875161581
$t_{1/2k10}$	h	7.418765425	WR^2	0.875161581
V/F	(µg)/(ng/mL)	0.907354279	SE	26.6912095
CL/F	(µg)/(ng/mL)/h	0.084775569	AIC	91.14578707
T_{max}	H	0.29814824	SC	92.05354235
C_{max}	ng/mL	107.1828245		
AUC $_{0-t}$	ng/mL*h	1053.638444		
AUC $_{0-inf}$	ng/mL*h	1179.585124		
AUMC	ng/mL*h^2	12691.84412		
MRT	h	10.75958307		
One compartment model with T_{lag}				
A	ng/mL	110.8002159	r obs-pre	0.759030108
K_a	1/h	9.806357429	SS	4987.088852
k_{10}	1/h	0.0934367	WSS	4987.088852
T_{lag}	h	1E-06	R^2	0.875157971
$t_{1/2ka}$	h	0.070683451	WR^2	0.875157971
$t_{1/2k10}$	h	7.418361084	SE	28.83021809
V/F	(µg)/(ng/mL)	0.911207463	AIC	93.14607622
CL/F	(µg)/(ng/mL)/h	0.085140218	SC	94.35641659
T_{max}	h	0.479105288		
C_{max}	ng/mL	104.940019		
AUC $_{0-t}$	ng/mL*h	1048.603951		
AUC $_{0-inf}$	ng/mL*h	1174.533044		
AUMC	ng/mL*h^2	12690.13353		
MRT	h	10.80440741		

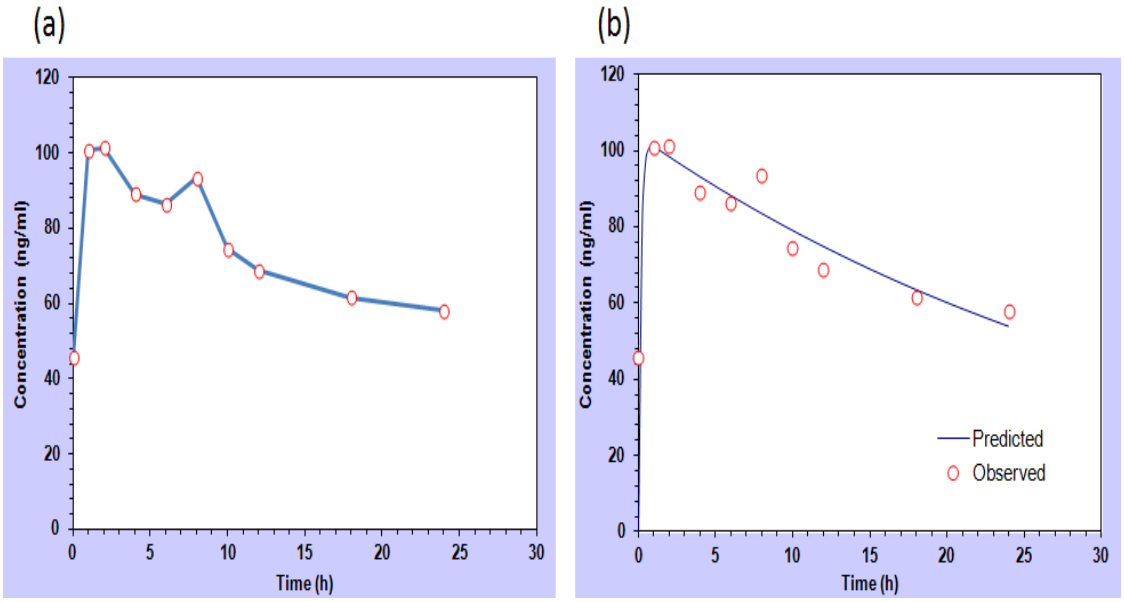


Figure 6.8: Graphical results for (a) noncompartmental and (b) compartmental PK analysis of cholecalciferol release from BAP DDS 4000IU.

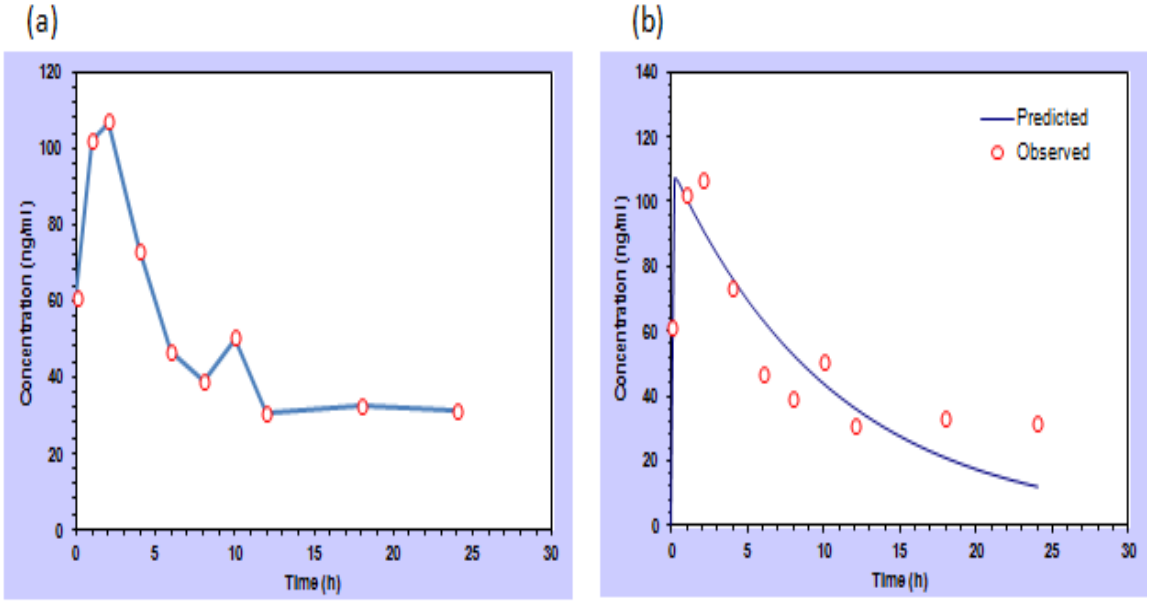


Figure 6.9: Graphical results for (a) noncompartmental and (b) compartmental PK analysis of cholecalciferol release from Comparator 4000IU.

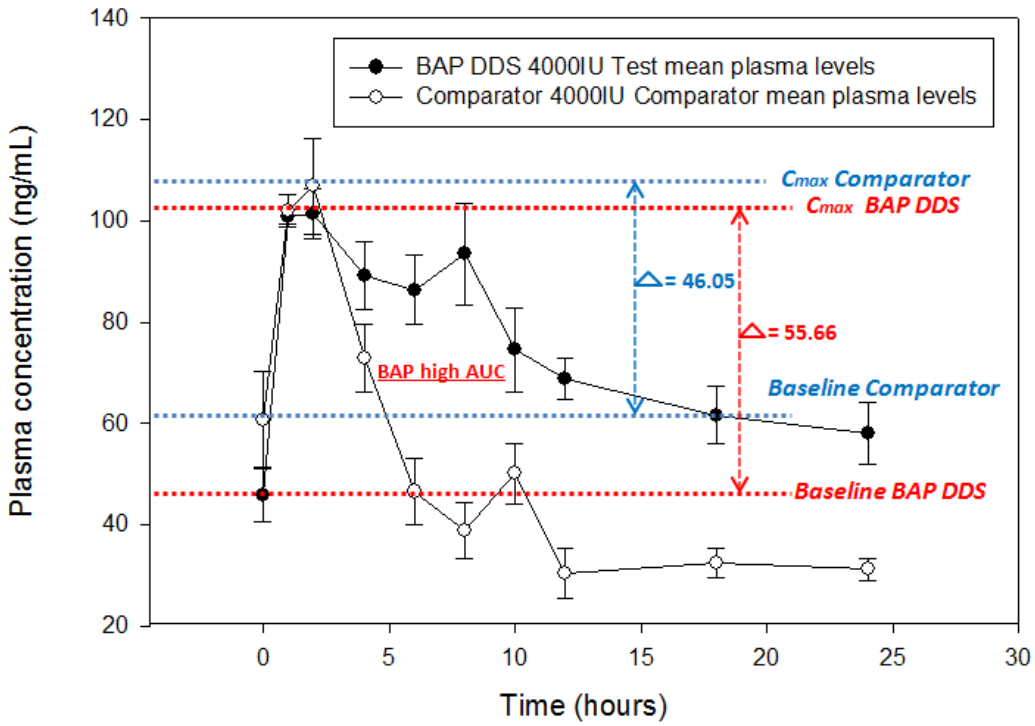


Figure 6.10: Overlaid mean plasma concentration-time profiles of cholecalciferol following single oral administration of BAP DDS 4000IU and comparator 4000IU.

6.3.5.2. BAP DDS and comparator 1000IU *cholecalciferol noncompartmental and compartmental analyses*

In terms of model fitting criteria, the 1000IU BAP and corresponding market comparator were also subject to the same NCA and compartmental analyses as the 4000IU products. As expected, pharmacokinetic modeling trends were likened to the 4000IU products with the AIC and SC/SBC values also confirming a compartmental kinetic model without lag for both 1000IU products. The results of the noncompartmental and compartmental analysis of the 1000IU BAP are shown in Table 6.6 and Table 6.8 below and Figure 6.11. Likewise, the noncompartmental and compartmental analysis of the 1000IU comparator product is presented in Table 6.7 and Table 6.9 and Figure 6.12.

The 1000IU DDS was less successful than the 4000IU delivery system at improving the extent of cholecalciferol absorption versus a same dose comparator. The $AUC_{0\text{-}t}$ was lower than the market 1000IU product (1518.97ng/mL/hr vs. 1733.82ng/mL/hr) (Table 6.8 and Table 6.9). This may be due to the fact that at lower drug dose the BAP constituents had less of an impact on influencing the extent of exposure. However, the 1000IU DDS reached a C_{max} of 118.10ng/mL compared to a lower C_{max} of 113.48ng/mL for the reference product. In addition, the mean difference from baseline to peak plasma concentration was 38.24ng/mL for the DDS vs. 26.18ng/mL

for the comparator from time 0 to 2 hours post dosing (Figure 6.13). Thus, like the 4000IU DDS, the 1000IU DDS achieved a greater mean peak difference between baseline and peak plasma concentration, indicative of a better initial response to dose. In comparison to the 4000IU DDS the 1000IU DDS had a shortened T_{max} compared to the market comparator, reaching peak plasma concentration by 1.8 hours. The reference comparator reached peak levels only later, at 2.14 hours. Thus the 1000IU DDS achieved a more rapid increase in plasma levels reaching peak concentration sooner. The higher peak plasma concentration and shorter time to peak but lower AUC of the 1000IU DDS may reflect an accelerated metabolism and conversion of cholecalciferol to vitamin D metabolites.

Table 6.6: Results of noncompartmental analysis of BAP 1000IU cholecalciferol release

Parameter	Unit	Value
λ_z	1/h	0.060046811
$t_{1/2}$	h	11.54344702
T_{max}	h	2
C_{max}	ng/mL	131.5467233
T_{lag}	h	0
C_{last_obs}/C_{max}		0.212176796
AUC $_{0\text{-}t}$	µg/mL*h	1644.459389
AUC $_{0\text{-}inf_obs}$	µg/mL*h	2109.28278
AUC $_{0\text{-}t/0\text{-}inf_obs}$		0.779629647
AUMC $_{0\text{-}inf_obs}$	µg/mL*h^2	34591.5239
MRT $_{0\text{-}inf_obs}$	H	16.39966164
$Vz/F_{_obs}$	(µg)/(µg/mL)	0.197385504
$Cl/F_{_obs}$	(µg)/(µg/mL)/h	0.01185237

Table 6.7: Results of noncompartmental analysis of comparator 1000IU cholecalciferol release

Parameter	Unit	Value
λ_z	1/h	0.016347777
$t_{1/2}$	h	42.400088
T_{max}	h	2
C_{max}	µg/mL	117.5016801
T_{lag}	h	0
Cl_{ast_obs}/C_{max}		0.418974406
AUC $_{0\text{-}t}$	µg/mL*h	1773.785951
AUC $_{0\text{-}inf_obs}$	µg/mL*h	4785.216611
AUC $_{0\text{-}t/0\text{-}inf_obs}$		0.370680388
AUMC $_{0\text{-}inf_obs}$	µg/mL*h^2	274257.9641
MRT $_{0\text{-}inf_obs}$	h	57.31359444
$Vz/F_{_obs}$	(µg)/(µg/mL)	0.319580082
$Cl/F_{_obs}$	(µg)/(µg/mL)/h	0.005224424

Table 6.8: Results of compartmental analysis of BAP 1000IU cholecalciferol release

Parameter	Unit	Value	Diagnostics	Value
One compartment model without T_{lag}				
A	ng/mL	140.5131765	r obs-pre	0.616191322
K_a	1/h	1.83283979	SS	9926.632575
k_{10}	1/h	0.072666152	WSS	9926.632575
$t_{1/2ka}$	h	0.378182089	R^2	0.860380056
$t_{1/2k10}$	h	9.538790197	WR^2	0.860380056
V/F	(µg)/(ng/mL)	0.185264389	SE	37.65754065
CL/F	(µg)/(ng/mL)/h	0.01346245	AIC	98.02976583
T_{max}	h	1.833765758	SC	98.93752111
C_{max}	ng/mL	118.1074101		
AUC $_{0-t}$	ng/mL*h	1518.967275		
AUC $_{0-inf}$	ng/mL*h	1857.017067		
AUMC	ng/mL*h^2	26568.65281		
MRT	h	14.30716674		
One compartment model with T_{lag}				
A	ng/mL	140.5143435	r obs-pre	0.616189284
ka	1/h	1.832744954	SS	9926.67856
k_{10}	1/h	0.072666589	WSS	9926.67856
T_{lag}	h	1E-06	R^2	0.860379409
$t_{1/2ka}$	h	0.378201658	WR^2	0.860379409
$t_{1/2k10}$	h	9.538732911	SE	40.67488693
V/F	(µg)/(ng/mL)	0.185263292	AIC	100.0298122
CL/F	(µg)/(ng/mL)/h	0.013462451	SC	101.2401525
T_{max}	h	1.833833209		
C_{max}	ng/mL	118.1074447		
AUC $_{0-t}$	ng/mL*h	1518.969881		
AUC $_{0-inf}$	ng/mL*h	1857.01691		
AUMC	ng/mL*h^2	26568.54952		
MRT	h	14.30711232		

Table 6.9: Results of compartmental analysis of comparator 1000IU cholecalciferol release

Parameter	Unit	Value	Diagnostics	Value
One compartment model without Tl_{ag}				
A	ng/mL	130.4492743	r obs-pre	0.541633183
K_a	1/h	1.683609928	SS	9010.008172
k_{10}	1/h	0.050677206	WSS	9010.008172
$t_{1/2ka}$	h	0.411702954	R^2	0.880530798
$t_{1/2k10}$	h	13.67769144	WR^2	0.880530798
V/F	(µg)/(ng/mL)	0.197592987	SE	35.8767895
CL/F	(µg)/(ng/mL)/h	0.01001346	AIC	97.06091258
T_{max}	h	2.145354349	SC	97.96866786
C_{max}	ng/mL	113.4884699		
AUC_{0-t}	ng/mL*h	1733.828196		
AUC_{0-inf}	ng/mL*h	2496.639413		
AUMC	ng/mL*h^2	50748.4389		
MRT	h	20.32669941		
One compartment model with T_{lag}				
A	ng/mL	130.4487319	r obs-pre	0.541628504
K_a	1/h	1.683612744	SS	9010.047016
k_{10}	1/h	0.050676683	WSS	9010.047016
T_{lag}	h	1E-06	R^2	0.880530283
$t_{1/2ka}$	h	0.411702265	WR^2	0.880530283
$t_{1/2k10}$	h	13.67783235	SE	38.75144517
V/F	(µg)/(ng/mL)	0.197593736	AIC	99.06095569
CL/F	(µg)/(ng/mL)/h	0.010013395	SC	100.2712961
T_{max}	h	2.145358298		
C_{max}	ng/mL	113.4881503		
AUC_{0-t}	ng/mL*h	1733.830219		
AUC_{0-inf}	ng/mL*h	2496.655681		
AUMC	ng/mL*h^2	50749.27465		
MRT	h	20.32690172		

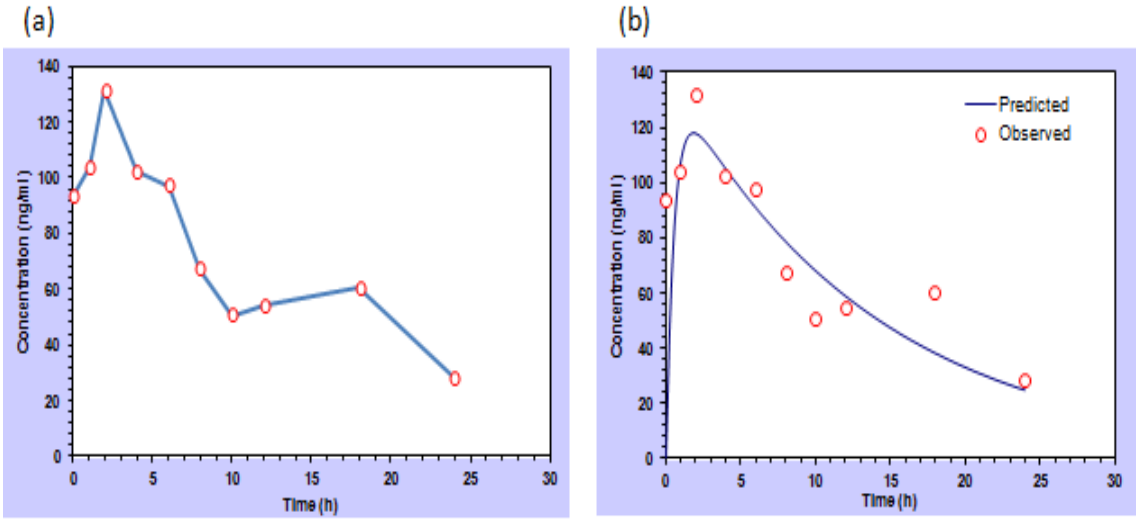


Figure 6.11: Graphical results for (a) noncompartmental and (b) compartmental PK analysis of cholecalciferol release from BAP DDS 1000IU.

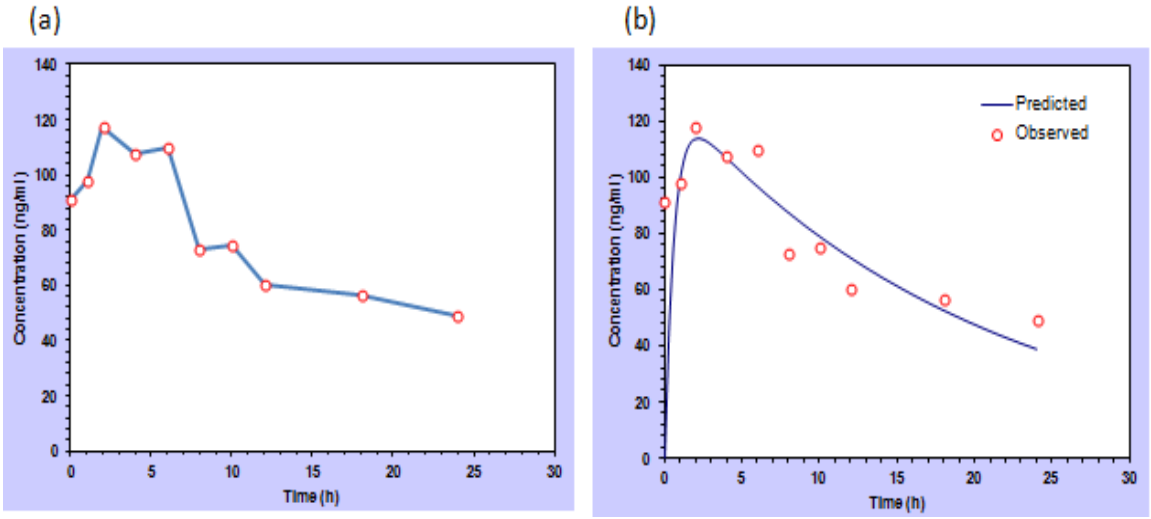


Figure 6.12: Graphical results for (a) noncompartmental and (b) compartmental PK analysis of cholecalciferol release from Comparator 1000IU.

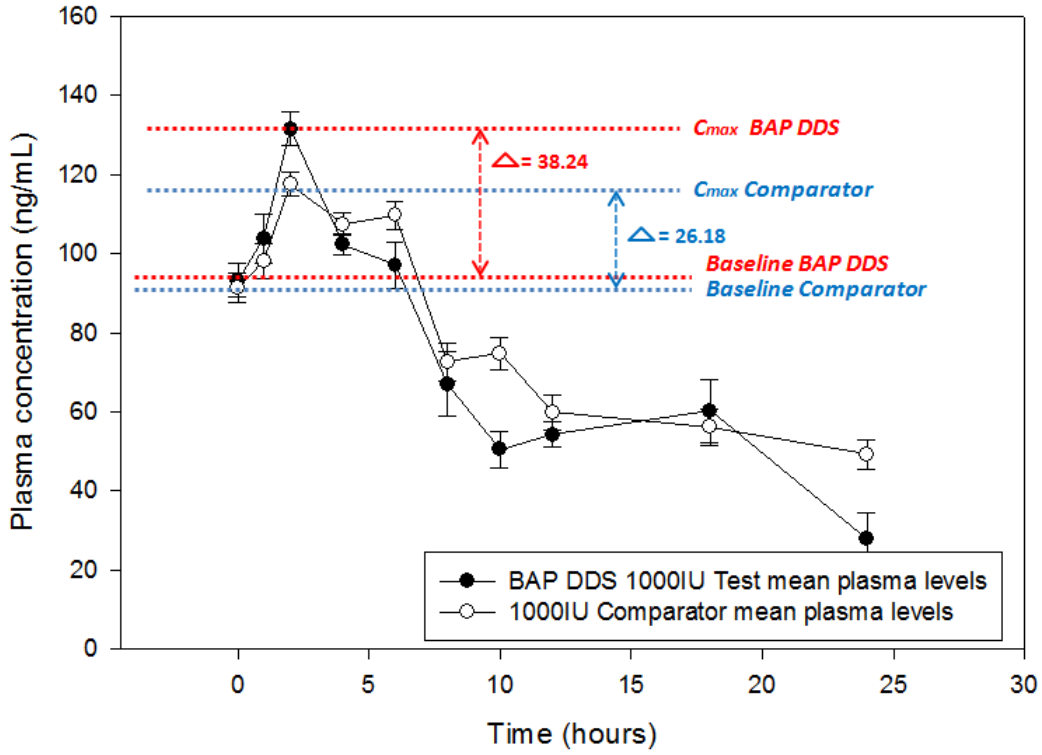


Figure 6.13: Overlaid mean plasma concentration-time profiles of cholecalciferol following single oral administration of BAP DDS 1000IU and Comparator 1000IU.

6.3.6. Comparative *in vivo* evaluation of 25-hydroxyvitamin D_3 serum levels in response to BAP DDS and comparator product dosing

6.3.6.1. Rise in 25-hydroxyvitamin D metabolite as an essential biomarker of an effective cholecalciferol formulation

When assessing the impact of supplemental vitamin D_2 or D_3 it is vital to assess the effect of product dosing on the rise in 25-hydroxyvitamin D_3 serum levels. Since levels of this metabolite correlate well with clinical disease, 25-hydroxyvitamin D_3, has become the universally accepted indicator of vitamin D status (Wolpowitz, 2006). Most studies have assessed the serum response to various vitamin D doses and forms by evaluating the rise in the 25-hydroxyvitamin D (25(OH)) metabolite (Haddad and Rojanasathit, 1975; Heaney *et al*., 2003; Stephenson *et al*., 2007). 25-hydroxyvitamin D has the longest half-life of the vitamin D metabolites in circulation and is thus a clinically useful indicator of vitamin D sufficiency of deficiency.

6.3.6.2. Evaluation of 25-hydroxyvitamin D_3 response to BAP and comparator products

Table 6.10 lists the 25-hydroxyvitamin D_3 levels obtained for the various cholecalciferol formulations dosed in the *in vivo* study. The mean 25(OH)D_3 baseline

between treatment groups ranged from 62.08ng/mL to 74.39ng/mL (mean baseline=68.24ng/mL). Thus the baseline serum level was slightly below the normal expected serum concentration in healthy adult pigs which is documented in the literature to be 76ng/mL (Horst *et al*., 1997). This is understandable since the study animals had minimal exposure to sunlight due to housing in-doors at the CAS unit. Both the DDS products achieved greater peak plasma concentrations than their respective comparators. C_{max} was reached within 2-3 days for all treatment groups. Serum $25(OH)D_3$ levels remained above baseline by day 5 for all treatment groups except the 1000IU comparator that failed to maintain the metabolite above baseline by the end of the study. Both high and low dose DDS's were superior in $25(OH)D_3$ response with respect to their market comparators with mean change from baseline to C_{max} superior for the BAP systems in both cases (Table 6.10). In addition, the 4000IU DDS achieved $T_{max,}$ more rapidly than the 4000IU comparator, reaching a peak serum concentration of 91.58ng/mL within 52 hours in comparison to the comparator C_{max} of 86.53ng/mL by 72 hours. Similarly, other researchers found that the greatest incremental increase in $25(OH)D_3$ was observed in the early stages of treatment, within the first 4 days of supplementation in vitamin-D deficient pigs (Pointellart *et al*., 1986). An earlier C_{max} achieved by the BAP formulations within a 2-3 day timeframe reflects a more efficient metabolic response and rapid conversion to the metabolite. Considering that the normal serum level is approximately 76ng/mL and the mean baseline levels fell below this due to reduced sun exposure of the animals in captivity, it is probable that a deficient animal may respond to cholecalciferol supplementation more efficiently. Other researchers have similarly shown how cholecalciferol is able to significantly increase $25(OH)D_3$ levels after supplementation (Stephenson *et al*., 2007, Flohr *et al*., 2014). It is also important to note that a greater disease pressure may lead to a more pronounced effect to supplementation and thus a sooner C_{max} for all formulations (Tousignant *et al*., 2013).

Figure 6.14 and Figure 6.15 demonstrate the time course of the rise in serum $25(OH)D_3$ levels after daily dosing of the high dose BAP and comparator, low dose BAP and comparator, and placebo over the five day *in vivo* dosing study. It is evident that the 4000IU DDS resulted in an almost immediate rise to a high C_{max} (91.58ng/mL) within 48 hours, whereas the 4000IU comparator exhibited a more gradual response. Both the 4000IU and 1000IU BAP formulations proved superior in maintaining $25(OH)D_3$ levels above the respective data points of their comparators in most cases proving that the novel system was adept at increasing levels of the

major circulating metabolite. The general trend of the BAP 25(OH)D_3 profiles showed curves above that of their respective conventional comparators. The superior bioavailability of the BAP formulations compared to the conventional D_3 products may be ascribed to the success of the DDS mechanism at increasing solubility, protection and emulsification of cholecalciferol. Recent *in vivo* studies with other novel vitamin D_3 formulations also showed oral bioavailability improvements when tested in a rat-model (Diarrassouba *et al*., 2015). In contrast, the current research showed improved cholecalciferol bioavailability in the pig-model using a novel multivitamin containing BAP DDS. The improved oral absorption of the BAP is important in light of recent research by other groups who have shown suboptimal responses to other conventional D_3 products (Shab-Bidar *et al*., 2013). The greater the serum level of 25(OH)D_3, the greater the propensity for conversion to the active metabolite, 1,25 dihydroxyvitamin D which is available for biologic action. It is noticeable how the placebo product BAP showed a level of 25(OH)D_3 that remained relatively static ending with a gradual decline by the end of the study due to a lack of supplementation.

It is also important to note that the erratic nature of the 25(OH)D_3 as demonstrated in Figures 6.14 and 6.15, is evident of differences in metabolism and negative feedback mechanisms that are at play within each study animal. Circulating 25(OH)D_3 levels reflect a number of inter-related factors, including; exposure to dietary sources, supplementation, metabolic conversion, mobilization from lipid stores, conversion to inactive or degradation products, and differences in hepatic and renal capacity (Brannon *et al*., 2008).

Table 6.10: 25-hydroxyvitamin D_3 levels over a 6 day period

Serum 25(OH)D_3 (ng/mL)	**4000IU DDS**	**4000IU Comparator**	**1000IU DDS**	**1000IU Comparator**
Mean Baseline(Day 0):	62.08	64.79	74.39	66.92
C_{max}	91.58	86.73	99.59	85.66
Mean Change from baseline to C_{max}:	**29.50**	21.73	**25.19**	18.74
Mean Final (Day 5):	78.99	70.30	81.00	53.23

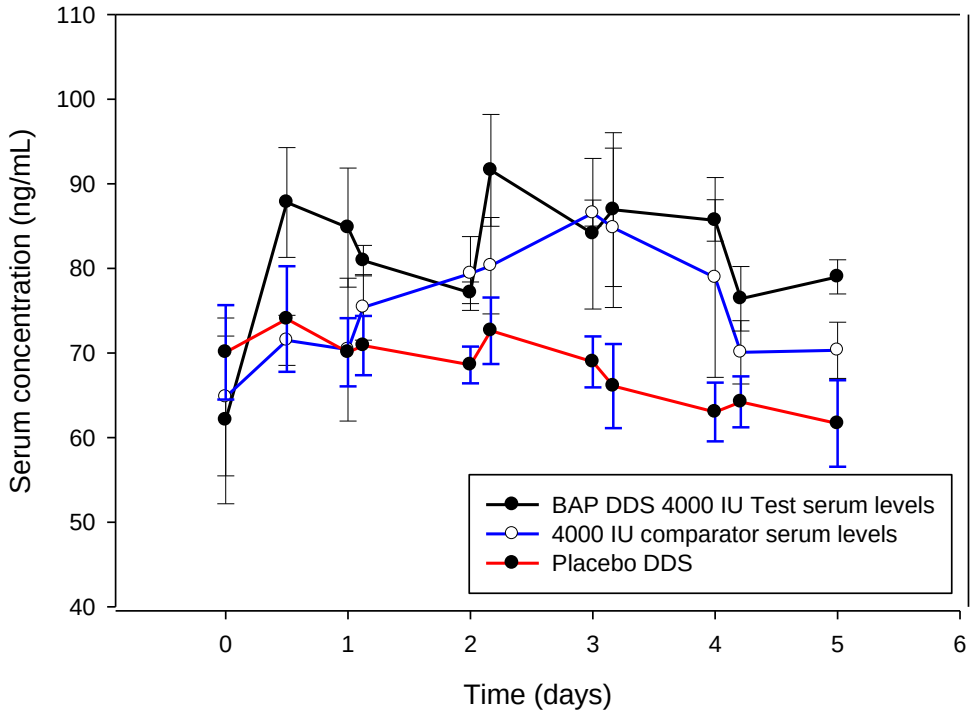


Figure 6.14: Time course of the rise in serum 25(OH)D_3 levels following daily doses of BAP DDS (4000IU cholecalciferol), the comparator (4000IU cholecalciferol), and a placebo DDS.

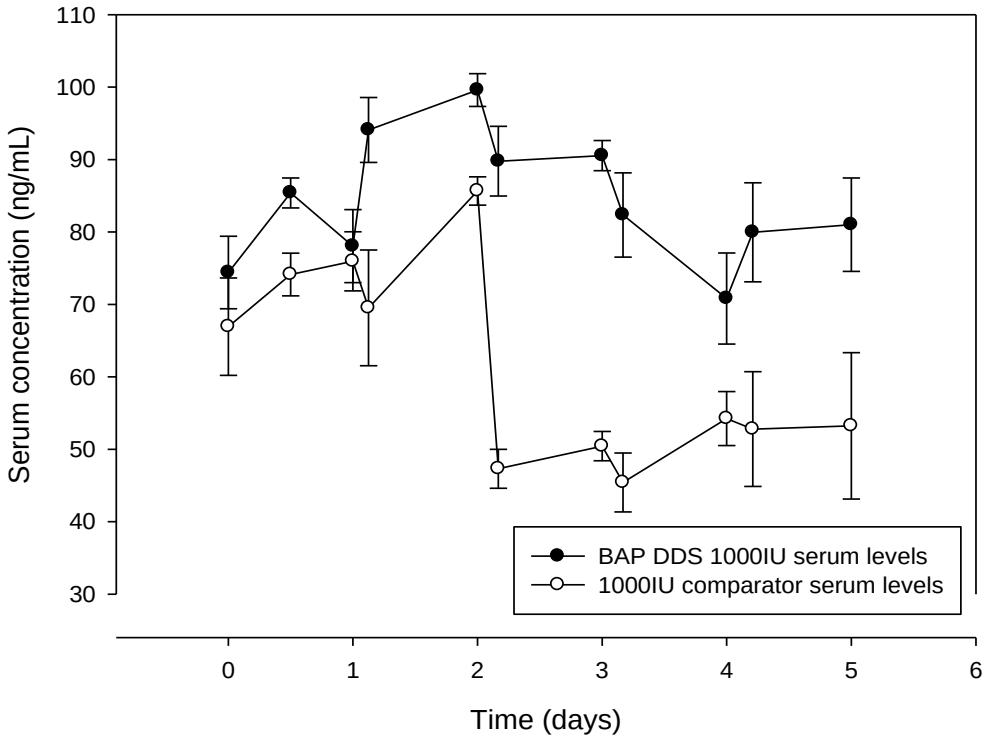


Figure 6.15: Time course of the rise in serum 25(OH)D_3 levels following daily doses of BAP DDS (1000IU cholecalciferol), and Comparator (1000IU cholecalciferol).

6.3.7. Establishment of an *in vitro-in vivo* correlation for cholecalciferol release from the BAP DDS

The importance of a valid IVIVC is that it will allow for dissolution testing of subsequent formulations (due to optimization or changes in required dissolution kinetics) without the need for additional bioavailability/ bioequivalence studies. It is for this reason that a sound IVIVC is key to "fast-tracking" the drug development process by mitigating the need for repetitive and extensive *in vivo* studies for every formulation candidate. Since formulation development is an ongoing process and because manufacturing and equipment changes may impact on product performance, it is important that an IVIVC has been established to ensure that *in vitro* behaviour can be correlated to *in vivo* performance. An established IVIVC thus allows for the dissolution tests of further batches to substitute for further *in vivo* studies. The US Pharmacopoeia (USP) defines an IVIVC as "the establishment of a relationship between a biological property, or a parameter derived from a biological property produced from a dosage form, and a physicochemical property of the same dosage form" (Emami, 2006). The FDA defines IVIVC as "a predictive mathematical model describing the relationship between an *in vitro* property of an extended dosage form and a relevant *in vivo* response" (CDER, 1997).

In general the successfulness of an IVIVC requires that dissolution be the rate-limiting step during the bioactive dosing and absorption process (Lu *et al.,* 2011). Therefore the correlation of *in vivo* results using dissolution data is best for Biopharmaceutics Classification System (BCS) Class II drugs that have dissolution as the rate-limiting parameter (Nandy *et al*., 2011). Cholecalciferol is classified as a Class II drug with extensive metabolism and high permeability, but low solubility (Chang *et al*., 2006). Therefore a Level A correlation was developed as the most suitable type of IVIVC, which used all the information of the dissolution and absorption curves, in contrast to levels B or C, and was based directly upon each of the assayed time points (Amann *et al*., 2010). In simplistic terms the IVIVC in this study related the amount of drug dissolved *in vitro* to the amount of drug absorbed *in vivo* using mathematical parameters. Level A analysis is therefore able to account for both qualitative patterns of release in addition to time-based positioning. The amount of drug absorbed following oral administration of the DDS or comparator was calculated by the Wagner Nelson method using the linear trapezoidal rule. For testing a level A IVIVC, the percentage of drug absorbed up to time *t* was plotted versus the amount of drug released *in vitro*.

The PK conditions derived from this investigation conforms to the requirements of deconvolution through convolution as the drug release from the DDS into the vascular compartment was aptly described via simple one-compartmental pK models. Deconvolution of the observed cholecalciferol concentration-time data against the *in vitro* release profile provided the cumulative *in vivo* release-time profile.

Level A analysis of the 4000IU DDS yielded a Levy Plot with an R^2 value of 0.8729, indicative of a good level of correlation between *in vitro* and *in vivo* data (Figure 6.16). The corresponding market comparator possessed a lower correlation with an R^2 of 0.7846 observed for the Levy Plot. Level A analysis of the 1000IU DDS yielded a Levy Plot with an R^2 value of 0.8552, indicative of a good level of correlation between *in vitro* and *in vivo* data (Figure 6.17). The corresponding market comparator also achieved a level A correlation with a high R^2 value of 0.9053 observed for the Levy Plot. A Level A correlation is considered the highest level of correlation achievable because it is a point to point comparison between *in vitro* dissolution data and *in vivo* absorption rate (Nandy *et al*., 2011). The relationship achieved in the current study was a linear one and the curves of dissolution and *in vivo* absorption were superimposable with acceptable degrees of correlation as indicated by the correlation co-efficient values described already (Figure 6.16 and Figure 6.17).

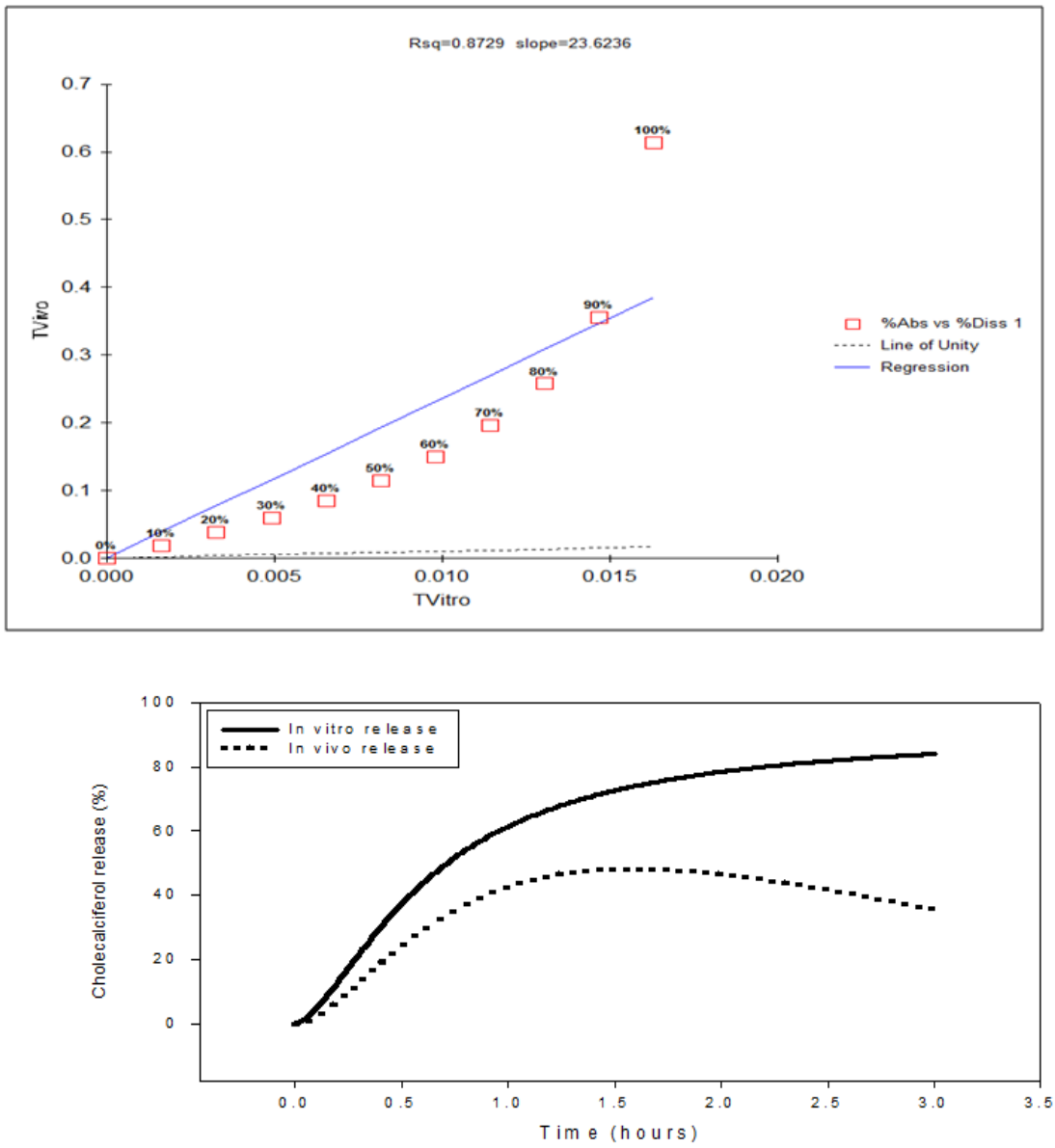


Figure 6.16: (a) Levy Regression Plot showing the relationship between the % of cholecalciferol absorbed *in vivo* and the % released *in vitro* from the 4000IU DDS; and (b) Drug release profiles of the *in vitro* cholecalciferol release and the observed mean *in vivo* release profile extracted using deconvolution analysis for a single dose cholecalciferol released from the 4000IU BAP.

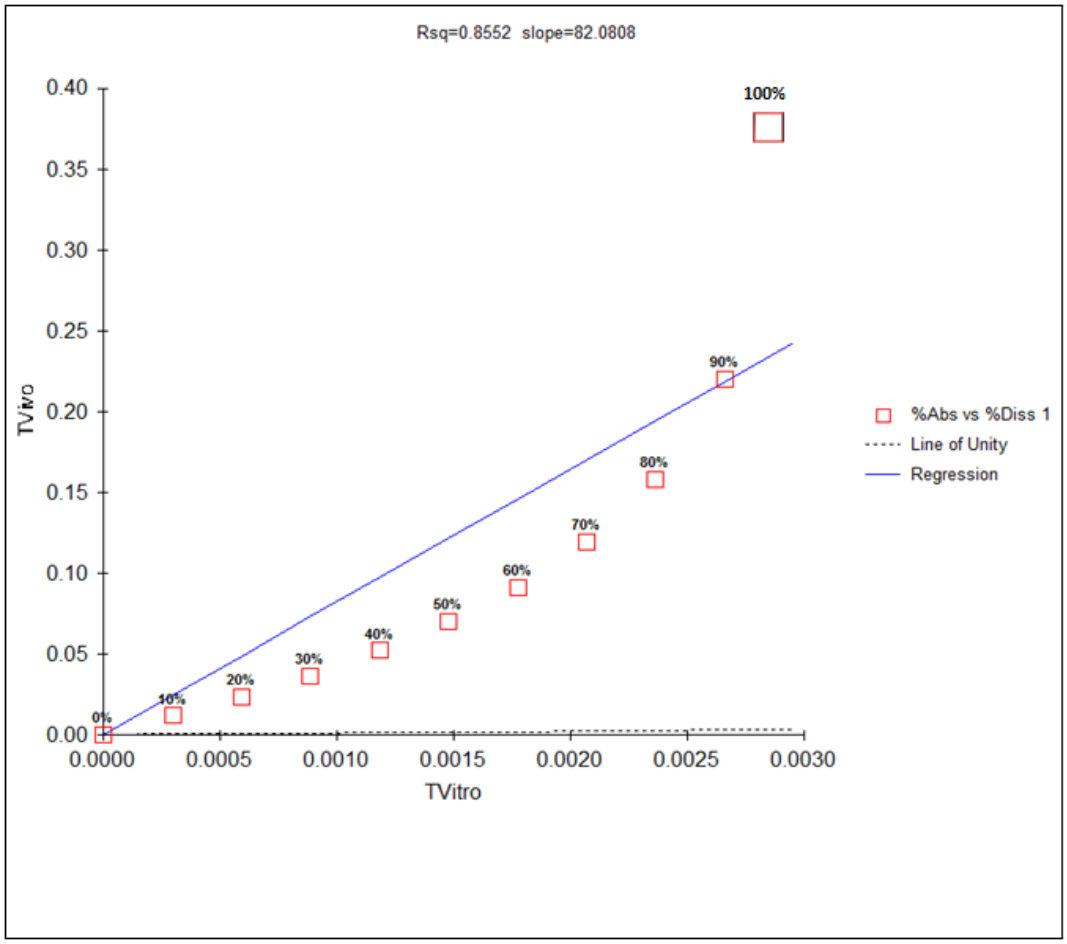


Figure 6.17: Levy Regression Plot showing the relationship between the % of cholecalciferol absorbed *in vivo* and the % released *in vitro* from the 1000IU DDS.

6.4. Concluding Remarks

The BAP DDS was well-tolerated after ingestion with histopathology results reporting an absence of any visible tissue damage or induced pathology in all GIT samples. X-ray studies clearly demonstrated evidence of the passage of the DDS through the GIT of the study animal. Pharmacokinetic results noted a superior change from baseline cholecalciferol to C_{max} for both the high dose and the low dose DDS' in comparison to their respective conventional comparators. The mean change from baseline cholecalciferol to C_{max} for the 1000IU DDS was 38.24ng/mL vs. 26.18ng/mL for the reference product. The mean change from baseline cholecalciferol to C_{max} for the 4000IU DDS was 55.66ng/mL vs. 46.05ng/mL for the market comparator. The cholecalciferol bioavailability was enhanced for the 4000IU DDS with an $AUC_{0\text{-}inf}$ 3.2x greater than that of the conventional product. Both BAP products successfully enhanced and maintained *in vivo* serum levels of the vitamin D_3 storage metabolite $25(OH)D_3$. Even though the 1000IU DDS did not achieve a

higher cholecalciferol AUC compared to the reference, the novel DDS was still superior to the reference at increasing 25(OH)D_3 levels during the 6 day study period. A level A IVIVC analysis provided convincing correlations between the *in vitro* release data and *in vivo* absorption data. Ultimately the BAP improvements demonstrated during *in vitro* studies translated into enhancements in *in vivo* performance due to the unique BAP formulation. Since many studies comparing the increase in 25-hydroxyvitamin D following vitamin D intake have yielded inconsistent results and suboptimal responses, a DDS that is more reliable and efficacious at enhancing serum levels, in the absence of cutaneous production, would add significant value. Improvements in circulating 25(OH)D_3 as provided in this preliminary preclinical evaluation, position the BAP system as a potential candidate to advance vitamin D-related outcomes in the clinical setting.

6.5. References

Amann LC, Gandal MJ, Lin R, Liang Y, Siegel SJ. 2010. *In vitro-in vivo* correlations of scalable PLGA-risperidone implants for the treatment of schizophrenia. *Pharmaceutical Research* 27: 1730-1737.

Anderson DL, Bartholomeusz D, Kirkwood ID, Chatterton BE, Summersides G, Penglis S, Kuchel T, Sansom L. 2002. Liquid gastric emptying in the pig: effect of concentration of inhaled Isoflurane. *Journal of Nuclear Medicine* 43 (7): 968-971.

Armas LAG, Hollis BW, Heaney R. 2004. Vitamin D_2 is much less effective than vitamin D_3 in humans. *The Journal of Clinical Endocrinology and Metabolism* 89: 5387-5391.

Bawa P, Choonara YE, Du Toit LC, Kumar P, Ndesendo MK, Meyer LCR, Pillay V. 2013. A novel stimuli-responsive alloy-treated matrix for space-defined gastrointestinal delivery of mesalamine in the large white pig model. *Journal of Controlled Release* 166: 234-245.

Bode G, Clausing P, Gervais F, Loegsted J, Luft J, Nogues V, Sims J. 2010. The utility of the minipig as an animal model in regulatory toxicology. *Journal of Pharmacological and Toxicological Methods* 62: 196–220.

Brannon PM, Yetley AE, Bailey RL, Picciano MF. 2008. Summary of roundtable discussion on vitamin D research needs. *American Journal of Clinical Nutrition* 88 (suppl): 5875S-5892S.

Chang C, Nahadduri PM, Polli JE, Swaan PW, Ekins S. 2006. Rapid identification of p-glycoprotein substrates and inhibitors. *Drug Metabolism and Disposition* 34: 1976-1984

Chen Y, Lu Yi, Chen J, Lai J, Sun J, Hu F, Wu W. 2009. Enhanced bioavailability of the poorly water-soluble drug fenofibrate by using liposomes containing bile salt. *International Journal of Pharmaceutics* 376: 153-160.

Choudhury SR, Basu A, Nag T, Sengupta K, Bhowmik M, Goswami A. 2013. Expedition of *in vitro* dissolution and *in vivo* pharmacokinetic profiling of sulfur

nanoparticles based antimicrobials. *Environmental Toxicology and Pharmacology* 36: 675-679.

Cordova H, Guarner-Argente C, Martinez-Palli G, Navarro R, Rodriguez-D Jesus A, Rodriguez de Miguel C, Beltran M, Martinez-Zamora M, Comas J, Lacy AM, Thompson CC, Fernandez-Esparrach G. 2012. Gastric emptying is delayed in transgastric notes: A randomized study in swine. *Journal of Surgical Research* 174: e61-e67.

Diarrassouba F, Garrait G, Remondetto G, Alvarez P, Beyssac E, Subirade M. 2015. Improved bioavailability of vitamin D_3 using a β-lactoglobulin-based coagulum. *Food Chemistry* 172: 361-367.

Emami J. 2006 *In vitro-in vivo* correlation: From theory to applications. *Journal of Pharmacy and Pharmaceutical Sciences: A Publication of the Canadian Journal of Pharmaceutical Sciences* 9: 169-189.

Varum FJO, Veiga F, Sousa JS, Basit AW. 2010. An investigation into the role of mucous thickness on mucoadhesion in the gastrointestional tract of pig. *European Journal of Pharmaceutical Sciences* 40(4): 335-341.

Flohr JR, Tokach MD, Dritz SS, Henry SC, Potter ML, Tokach LM, Goff JP, Horst RL, Nietfeld JC, Madson DM, Ensley SM, Goodband RD, Nelssen JL, Bergstrom JR, DeRouchey JM. 2014. Effects of supplemental vitamin D_3 on serum 25-hydroxycholecalciferol and growth of preweaning and nursery pigs. *Journal of Animal Science* 92(1): 152-163.

Forauer AR, Theoharis CGA, Dasika NL. 2006. Jugular vein catheter placement: Histological features and development of catheter-related (Fibrin) sheaths in a swine model. *Radiology* 240: 427-434.

Gibbon CJ. Division of Pharmacology Faculty of Health Sciences University of Cape Town. 2007. South African Medicine Formulary (SAMF). South African Medical Association Health and Medical Publishing Group. Cape Town. 83-84.

Guo Y, Luo J, Tan S, Otieno BO, Zhang Z. 2013. The applications of vitamin E TPGS in drug delivery. *European of Pharmaceutical Sciences* 49: 175-186.

Haddad JG, Rojanasathit S. 1976. Acute administration of 25-hydroxycholecalciferol in man. *Journal of Clinical Endocrinology and Metabolism* 42: 284-290.

Heaney RP, Davies MK, Chen TC, Holick MF, Barger-Lux MJ. 2003. Human serum 25-hydroxycholecalciferol response to extended oral dosing with cholecalciferol. *American Journal of Clinical Nutrition* 77(1) 204-210.

Hodgson DS. 2007. Comparison of isoflurane and servoflurane for short-term anesthesia in piglets. *Journal of Veterinary Anaesthesia* 2: 117-124.

Hollis BW. 2000. Comparison of commercially available I25I-based RIA methods for the determination of circulating 25-hydroxyvitamin D. *Clinical Chemistry* 46 (10): 1657-1661.

Horst RL & Reinhardt TA. 1997. Chapter 2. Vitamin D metabolism. In: Vitamin D. 2nd Edition. (Feldman D, Glorieux FH, Pike WJ eds.). Academic Press San Diego: 13-32.

In vitro Release Testing and *In vivo* Bioequivalence Documentation. Guidance for industry. U.S Department of Health and Human Services, Food and Drug Administration, Centre for Drug Evaluation and Research (CDER). 1997. U.S government printing office. Washington DC.

Jones G. 2008. Pharmacokinetics of vitamin D toxicity. *American Journal of Clinical Nutrition* 88: 582S-586S.

Kolawole OA, Pillay V, Choonara YE, du Toit LC, Ndesendo VMK. 2010. The influence of polyamide 6,10 synthesis variables on the physiochemical characteristics and drug release kinetics from a monolithic tablet matrix. *Pharmaceutical Development and Technology* 15: 595-612.

Kostewicz ES, Abrahamsson B, Brewster M, Brouwers J, Butler J, Carlert S, Dickinson PA, Dressman J, Holm R, Klein S, Mann J, McAllister M, Minekus M, Muenster U, Mullertz A, Verwei M, Vertzoni M, Weitschies W, Augustijns P. 2014. *In vitro* models for the prediction of *in vivo* performance of oral dosage forms. *European Journal of Pharmaceutical Sciences* 57: 342-366.

Li D, Liu H, Xi P, Chen Y, Li Y. 2000. Effects of Vitamin D_3 on Immunity and Performance of Weanling Pigs. *Asian-Australasian Journal of Animal Sciences* 13 Supplement C: 103-106.

Likenhoker JR, Burkholder TH, Linton CGG, Walden A, Abusakran-Monday KA, Rosero AP, Foltz CJ. 2010. Effective and Safe Anesthesia for Yorkshire and Yucatan Swine with and without Cardiovascular Injury and Intervention. *Journal of American Association for Laboratory Animal Science* 49: 344-351.

Lu Y, Kim S, Park K. 2011. *In vitro-in vivo* correlation: perspectives on model development. *International Journal of Pharmaceutics* 418: 142-148.

Metges CC. 2010. Classical and post-genomic methods to study GIT function with emphasis on the pig. *Livestock Science* 133:10–19.

Miller ER, Ullrey DE.1987. The pig as a model for human nutrition. *Annual Review of Nutrition* 7: 361–387.

Nandy BC, Roy Sandipan R, Mazumder B, Meena KC, Ahuja D, Makhija M, Jain S, Sharma S, Shrivastava A, Saxena P. 2011. *In vitro-in vivo* correlation: application in pharmaceutical development of various dosage forms. *Journal of Chemical and Pharmaceutical Research* 3 (5): 550-564.

Ndesendo VM, Pillay V, Choonara YE, Du Toit LC, Buchmann E, Kumar P, Khan RA. 2011. *In vivo* evaluation of the release of zidovudine and polystyrene sulfonate from a dual intravaginal bioadhesive polymeric device in the pig model. *Journal of Pharmaceutical Sciences* 100(4): 1416-1435.

Ngwuluka NC, Choonara YE, Modi G, Du Toit LC, Kumar P, Ndesendo MK, Pillay V. 2013. Design of an interpolyeletrolyte gastroretentive matrix for the site-specific zero-order delivery of levodopa in parkinson's disease. *AAPS PharmSciTech* 14(2): 605-619.

Niu M, Lu Y, Hovgaard L, Guan P, Tan Y, Lian R, Qi J. 2012. Hypoglycemic activity and oral bioavailability of insulin-loaded liposomes containing bile salts in rats: The effect of cholate type, particle size and administered dose. *European Journal of*

Pharmaceutics and Biopharmaceutics 81: 265-272.

Ong L, Saw S, Sahabdeen NB, Tey KT, Ho CS, Sethi SK. 2012. Current 25-hydroxyvitamin D assays: Do they pass the test? *Clinica Chimica Acta* 413: 1127-1134.

Pento JT. 1974. Measurement of Plasma Calcitonin *In vivo* in the pig using a chronically-implanted catheter for infusion and blood sampling. *Journal of Animal Science* 39: 885-888.

Pointillart A, Fontaine N. 1986. Effects of vitamin D on calcium regulation in vitamin-D-deficient pigs given a phytate-phosphorous diet. *British Journal of Nutrition* 56: 661-669.

Reese DE, Hill GM. 2007. Trace Minerals and Vitamins for Swine Diets. *National Swine Nutrition Guide* 1-16.

Saadati R, Dadashzadeh S. 2014. Marked effects of combined TPGS and PVA emulsifiers in the fabrication of etoposide-loaded PLGA-PEG nanoparticles: *In vitro* and *in vivo* evaluation. *International Journal of Pharmaceutics* 464: 135-144.

Saphier S, Rosner A, Brandeis R, Karton Y. 2010. Gastro intestinal tracking and gastric emptying of solid dosage forms in rats using X-ray imaging. *International Journal of Pharmaceutics* 388: 190-195.

Schwalfenberg GK, Genuis SJ, Hiltz MN. 2010. Addressing vitamin D deficiency in Canada: A public health innovation whose time has come. *Public Health* 24: 350–359.

Shab-Bidar S, Bours SPG, Geusens PPMM, van der Velde RY, Janssen MJW, van den Bergh JPW. 2013. Suboptimal effect of different vitamin D_3 supplementations and doses adapted to baseline serum 25(OH)D on achieved 25(OH)D levels in patients with a recent fracture: a prospective observational study*. European Journal of Endocrinology* 169: 597-604.

Stephenson A, Brotherwood M, Rober R, Atenafu E, Corey M, Tullis E. 2007. Cholecalciferol significantly increases 25-hydroxyvitamin D concentrations in adults

with cystic fibrosis. *American Journal of Clinical Nutrition* 85: 1307-1311.

Thörn HA, Lundahl A, Schrickx JA, Dickinson PA, Lennernäs H. 2011. Drug metabolism of CYP3A4, CYP2C9 and CYP2D6 substrates in pigs and humans. *European Journal of Pharmaceutical Sciences* 43:89–98.

Tousignant SJP, Henry SC, Rovia A, Morrison RB. 2013. Effect of oral Vitamin D_3 supplementation on growth and serum 25-hydroxyvitamin D levels of pigs up to seven weeks of age. *Journal of Swine Health and Production* 21(2): 94-98.

van Groningen L, Opdenoordt S, van Sorge A, Telting D, Giesen A, de Boer H. 2010. Cholecalciferol loading dose guideline for vitamin D-deficient adults. *European Journal of Endocrinology* 162: 805-811.

Van Hasselt PM, Janssens GEPJ, Slot TK, van der Ham M, Minderhoud TC, Talelli M, Akkermans LM, Rijcken CJF, van Nostrum CF. 2009. The influence of bile acids on the oral bioavailability of vitamin K encapsulated in polymeric micelles. *Journal of Controlled Release* 133: 161–168.

Vieth R. 1999. Vitamin D supplementation, 25-hydroxyvitamin D concentrations, and safety. *American Society for Clinical Nutrition* 69: 842-856.

Wagner D, Hanwell HE, Schnabl K, Yazdanpanah M, Kimball S, Fu L, Sidhom G, Rousseau D, Cole DEC, Vieth R. 2011. The ratio of serum 24,25-dihydroxyvitamin D3 to 25-hydroxyvitamin D_3 is predictive of 25-hydroxyvitamin D_3 response to vitamin D_3 supplementation. *Journal of Steroid Biochemistry and Molecular Biology* 126: 72-77.

Witschi AKM, Liesegang L, Gebert S, Weber GM, Wenk C. 2011. Effect of source and quantity of dietary vitamin D in maternal and creep diets on bone metabolism and growth in piglets. *Journal of Animal Science* 89: 1844-1852.

Wolpowitz D, Gilchrest BA. 2006. The vitamin D questions: How much do you need and how should you get it? *Journal of the American Academy of Dermatology* 54: 301-317.

Zhang R, Naughton DP. 2010. Vitamin D in health and disease: Current perspectives. *Nutrition Journal* 9: 65. Retrieved from URL: http://www.nutritionj.com/content/9/1/65. [Accessed 12 March 2012].

Zhang Z, Tan S, Feng S. 2012. Vitamin E TPGS as a molecular biomaterial for drug delivery. *Biomaterials* 33: 4889-4906.

CHAPTER 7

CONCLUSION AND RECOMMENDATIONS

7.1. Conclusion

As discussed already the oral delivery route is considered the most acceptable means for administering pharmaceuticals. Despite the convenience of the oral route many promising therapeutic agents fail to meet intended therapeutic end-points, due to the bioactives' physicochemical limitations to oral bioavailability. Successful efforts to remedy these challenges warrant the use of creative formulation strategies. Such approaches need to draw upon not one but many innovative formulation approaches to generate inventive solutions in the quest for truly novel and collaborative drug delivery enhancements. To this point the BAP Drug Delivery System (DDS) achieved a coming together of various technologies to reach the goal of superior dissolution and *in vivo* pharmacokinetic characteristics compared to conventional reference products. It is crucial in closing this investigation to consider whether the research questions and objectives discussed in Chapter 1 have been adequately addressed. The discussion that follows elaborates on specific key milestones achieved by the BAP components in the evolution of the final BAP DDS in support of the achievement of the studies research aim.

7.1.1. BAP component achievements

- Polymeric scaffolds for modifiable delivery of bile salts at a controlled rate to assist in GIT emulsification, dissolution and transport of lipids and fat-soluble vitamins including cholecalciferol.
- Customizable delivery of pancreatic lipase from polymeric scaffolds to aid the GIT process of enzymatic breakdown of cholecalciferol.
- Improved solubility, dissolution and thermal stability parameters of cholecalciferol through inclusion in an optimized βCD inclusion complex.
- A novel "3-vitamin" minitablet formulation demonstrating superior cholecalciferol passive diffusion through biological membranes.
- Individually packaged bioactives for a lower potential for inter-component interactions or drug-drug interactions: enhanced integrity and predictability of DDS performance.

7.1.2. Final BAP DDS capsule(s) achievements

- Successful combining of different formulation strategies: Films, IC's, minitablets into a single DDS with sound rationale for model drug bioavailability improvements.
- The provision of an optimized ratio of bile salts and lipase (biological co-factors) within a customized film matrix with maximal improvements on model drug (cholecalciferol) dissolution kinetics and for improved GIT milieu absorption.
- The provision of pancreatic lipase released from a film component of the DDS with a controlled level of enzyme activity to promote GIT function for enhanced milieu effects on cholecalciferol absorption.
- Superior cholecalciferol *in vitro* dissolution kinetics and aqueous solubility in comparison to conventional market products through a "Triple phenomenon" of (i) Rapid emulsification and surfactant effects on lipophilic vitamins imparted by TPGS; (ii) Phase solubility effects on vitamin bioactives; and (iii) bio-surfactant effects of two bile salts released from films to enhance wettability and dissolution of model agent.
- Provision of 3 synergistic vitamins from the DDS, including ascorbic acid, α-tocopherol and model drug-cholecalciferol, released at similar *in vitro* release rates despite differing physicochemical characteristics: Unified "in-concert" vitamin release.
- Provision of clinically relevant amounts of cholecalciferol to meet latest supplemental recommendations in line with identified global insufficiency (1000IU and 4000IU formulations).
- Targeted release of all DDS constituents including model drug at an alkaline pH in the duodenum for improved absorption and protection from gastric degradation. Achieved through a dual pH responsive mechanism: alginate and Kollicoat action.
- Ability to deliver multiple bioactives in a controlled manner from a single framework with enhanced *in vivo* bioavailability of cholecalciferol through synergistic mechanisms. Evidenced by superior pharmacokinetics following comparative preclinical evaluation.
- Rapid incremental serum response to cholecalciferol doses, clearly observable during *in vivo* studies: Improved cholecalciferol pharmacokinetic parameters and 25-hydroxyvitamin D_3 serum levels compared to reference market comparators. Indicating improved bioavailability and efficacy of the BAP compared to conventional oral formulations.
- Flexibility in formulation design with an ability to tailor-make a BAP DDS for patients with exocrine deficiencies or an inability to absorb fat-soluble micronutrients.

- Ability to customize the BAP for inclusion of allopathic bioactives or other nutraceutical model agents. This will allow formulation of fixed dose combination (FDC) products with multiple clinical benefits and serve as a generic platform to deliver other hydrophobic Class II bioactives.

It has long since been recognized that current vitamin D products provide insufficient elevations in 25(OH)D to achieve an optimal target plasma concentration (Vieth, 2004). Current vitamin D formulations tend to either under deliver in remedying the requirements for vitamin D sufficiency or provide inconsistent and substantial between-individual variability in response (Binkley *et al*., 2006). This may in part be due to a lack of consensus regarding optimal amounts and dosing, and also due to poorly validated formulations. Until such time as a consistent dosing recommendation is reached one may need to look to smart delivery mechanisms to improve the physiological response to supplemental doses. The current study reported successful improvements in 25(OH)D_3 levels in response to the BAP DDS. The novelty of the BAP designed and validated in this research lies in the use of synergistic vitamins, synthetic enhancers and biological enhancers to increase cholecalciferol bioavailability. Other research groups have also recently designed cholecalciferol DDS's with improved bioavailability of the vitamin, however these formulations contained only vitamin D_3 and did not include additional synergistic vitamins nor biological co-factors as achieved in the current BAP research (Diarrassouba *et al*., 2015; Guttoff *et al*., 2015).

Most nutraceutical products contain multiple agents in a combined multivitamin product hence formulations consisting of two or more vitamins are more applicable to the current market needs and clinical requirements. The presence of biological co-factors (enzyme and bile) as contained in the BAP may also provide a more predictable and improved response in patients with exocrine deficiencies and reduce inter-patient variability. Encouraging to note was the fact that improvements in the *in vitro* dissolution parameters and *ex vivo* diffusion behaviour translated into similar positive efficacy results in the preliminary preclinical *in vivo* assessment. It is accepted that the constituents of biliary lipids and the presence of GIT enzymes have positive influences on the solubility of poorly water-soluble drugs (Nandy *et al*., 2011). The current investigation showed how a novel multicomponent system can deliver biological and synthetic co-factors in a controlled manner to synergistically augment the *in vitro* and *in vivo* exposure to cholecalciferol. Since altered GIT topology has a greater impact on modified dosage forms than conventional

formulations, it is paramount that intelligent systems evolve to mitigate this effect through the customizable delivery of model drug and biological enhancer molecules.

7.2. Recommendations

Future outlook must involve greater collaboration between scientists from multidisciplinary backgrounds to facilitate knowledge sharing of individual breakthroughs and the combining of these technologies into one DDS with multiple benefits. The current study took preliminary steps in the combinatorial approach to creating elegant and practical solutions to nutraceutical multivitamin enhancement within a single combined vehicle for enhanced efficacy of cholecalciferol. Future developments should build further towards the creation of "smart" nutraceutical multivitamin FDC's instead of single vitamin products. Likewise an approach to fully understand the mechanisms underpinning bioavailability and bioefficacy enhancements imparted by all categories of enhancers whether, biological, micronutrient or herbal in origin needs to be explored (Dudhatra *et al*., 2012). Future research should focus on testing the efficacy of the BAP in patients with pathological states that require seamless GIT delivery despite the lack of essential metabolic enzymes/ exocrine factors. This will provide evidence towards the robustness of the BAP's performance in both normal and pathological states. Such an avenue will also quantify the success of enzyme delivery and assess the need to adjust enzyme activity to achieve optimal effects. Furthermore it would be appropriate to investigate the use of the BAP concept for the delivery of allopathic agents for improved treatment of life-threatening diseases including cancer, HIV, and cardiovascular disease where organ function is already compromised. *In vivo* studies undertaken in the current investigation were limited to a 6 day period and provided a mere "snap-shot" into the success of the BAP. In future studies, a prolonged *in vivo* study should be designed to investigate the long-term benefits of the BAP and the serum rise of 25(OH)D_3 over a 3-6 month period. This will provide essential safety and efficacy data to assess the long-term utility of the BAP as an innovative drug delivery platform for nutraceutical and chronic therapy applications.

7.3. References

Binkley N, Gemar D, Engelke J, Gangnon R, Ramamurthy R, Krueger D, Drezner MK. 2011. Evaluation of ergocalciferol or cholecalciferol dosing, 1600IU daily or 50 000IU monthly in older adults. *Journal of Clinical Endocrinology and Metabolism* 96(4): 981-988.

Diarrassouba F, Garrait G, Remondetto G, Alvarez P, Beyssac E, Subirade M. 2015. Improved bioavailability of vitamin D_3 using a β-lactoglobulin-based coagulum. *Food Chemistry* 172: 361-367.

Dudhatra GB, Mody SK, Awale MM, Patel HB, Modi CM, Kumar A, Kamani DR, Chauhan BN. 2012. A comprehensive review on pharmacotherapeutics of herbal bioenhancers. *The Scientific World Journal* 2012, article ID 637953: 1-33.

Guttoff M, Saberi AH, McClements DJ. 2015. Formation of vitamin D nanoemulsion-based delivery systems by spontaneous emulsification: factors affecting particle size and stability. *Food chemistry* 171: 117-122.

Nandy BC, Roy Sandipan R, Mazumder B, Meena KC, Ahuja D, Makhija M, Jain S, Sharma S, Shrivastava A, Saxena P. 2011. *In vitro-in vivo* correlation: application in pharmaceutical development of various dosage forms. *Journal of Chemical and Pharmaceutical Research* 3 (5): 550-564.

Vieth R. 2004. Why the optimal requirement for vitamin D_3 is probably much higher than what is officially recommended for adults. *Journal of Steroid Biochemistry and Molecular Biology* 89-90: 575-579.

8. APPENDICES

8.1. Animal Ethics Clearance Certificate

AESC3

STRICTLY CONFIDENTIAL

ANIMAL ETHICS SCREENING COMMITTEE (AESC)

CLEARANCE CERTIFICATE NO. 2011/43/05

APPLICANT: **Mr M Braithwaite**

DEPARTMENT: **Pharmacy and Pharmachology**

PROJECT TITLE: ***In Vivo Assessment of a Novel 'Bioactive Association Platform' (BAP) Delivery System in Pigs***

Number and Species

16 Pigs

Approval was given for to the use of animals for the project described above at an AESC meeting held on **27 September 2011**. This approval remains valid until **30 September 2013**.

The use of these animals is subject to AESC guidelines for the use and care of animals, is limited to the procedures described in the application form and to the following additional conditions:

Approved with the following conditions and recommendations:

Conditions that must be met as follows:

1. The study includes a 16th pig which is included in the experimental group (so that n = 6 for this group).

   This additional pig should be used for X-ray measures, but otherwise treated in the same way as other pigs in this group.
2. The period over which this pig is X-rayed does not exceed 5 days.
3. Catheters are flushed 3 times per day (not 'at least twice').
4. Pigs are housed at the CAS under control of the CAS staff. Each group of pigs should be housed together.
5. Transport of pigs follows CAS's SOPs.
6. All logistics are discussed and agree upon with Dr Leith Meyer prior to commencement of the study.

1/2

Recommendations for consideration

1. Sex should be standardized to remove any possible gender-based effects.
2. The experimental design should be randomized.

Note: The PI is advised that he should follow the instructions on the application form carefully and refrain from removing parts or the form. Failure to do so in future will result in rejection of the application.

Signed: _____ (Chairperson, AESC) Date: 10/10/2011

I am satisfied that the persons listed in this application are competent to perform the procedures therein, in terms of Section 23 (1) (c) of the Veterinary and Para-Veterinary Professions Act (19 of 1982)

Signed: _____ (Registered Veterinarian) Date: 25/10/2011

cc: Supervisor:
Director: CAS

8.2. Modifications & Extension Approvals to Animal Study

AESC 2009

ANIMAL ETHICS SCREENING COMMITTEE

MODIFICATIONS AND EXTENSIONS TO EXPERIMENTS

a. Name: Miles Braithwaite

b. Department: Pharmacy and Pharmacology

c. Experiment to be modified / extended **AESC NO:**

Original AESC number	2011	43	05
Other M&E's :			

d. Project Title: *In Vivo* Assessment of a Novel 'Bioactive Association Platform' (BAP) Delivery System in Pigs

e.	Number and species of animals **originally approved**:		16
f.	Number of additional animals **previously allocated on M&Es**:		n/a
g.	Total number of animals **allocated** to the experiment to date:		16
h.	Number of animals **used** to date:		0

i. Specific modification / extension requested:

A request for an additional 2 pigs to be allocated to the study. Thus the total number of pigs would be 18 instead of 16 animals.

j. Motivation for modification / extension:

An 18 pig design would assist with the randomization of animals between test, comparator and control groups. A maximum of 18 pigs will be used, where the pigs will be divided into 3 intake groups consisting each of 6 pigs. Only one intake group of 6 pigs will be maintained at the CAS at a particular time and will be further divided into 3 sub-groups of 2 pigs. Within an intake group 2 pigs will be used to dose the test, 2 to dose the comparator and 2 pigs will be used to dose the placebo formulation. The stratification within an intake group will assist in reducing intergroup variability and allow for randomization with minimal increase in the sample size. This change in the protocol has been done to accommodate the conditions of the AESC in order to facilitate randomization and an improved overall study design.

Date: 4/11/2011 Signature: .....

RECOMMENDATIONS:

Approved.

Date: 8/11/2011 Signature: .....

Chairman, AESC

AESC 2013

Please note that only typewritten applications will be accepted. Should additional space be required for section "i"and/or "j", please use the back of this form.

ANIMAL ETHICS SCREENING COMMITTEE

MODIFICATIONS AND EXTENSIONS TO EXPERIMENTS

a. Name: Miles Braithwaite.....

b. Department: Pharmacy and Pharmacology.....

c. Experiment to be modified / extended AESCNO:

Original AESC number	2011/ 43/ 05
Other M&E's : 1	

d. Project Title: In Vivo Assessment of a Novel "Bioactive Association Platform" (BAP) Delivery System in Pigs

e.	Number and species of animals originally approved:	16	
f.	Number of additional animals previously allocated on M&Es:	2	
g.	Total number of animals allocated to the experiment to date:	18	
h.	Number of animals used to date:	0	

i. Specific modification / extension requested:

1) Change in dosing schedule for the 3 intake groups of pigs and additional blood sampling.
2) Provision of a higher dose test product (containing 4000IU D_3) to 2 of the test animals and a higher dose comparator product (containing 4000 IU D_3) to 2 of the comparator animals.
3) Updating of co-workers to assist with study.
4) Request to sacrifice 2 pigs from study for histological studies
5) Request to take pictures of pigs for inclusion in thesis and papers

j. Motivation for modification / extension:

1) Change in dosing schedule from a single dose 24 hour study to dosing at time 0, 24 hours, 48 hours, 72 hours and 96 hours is requested for all 18 pigs. The current "once-off" dosing of the Drug Delivery System (DDS) containing only 1000IU Vitamin D_3 on day 0 will not obtain a measurable rise in the 25-hydroxyvitamin D3 metabolite. Therefore a *5* day dosing schedule is requested (Days 0- 4). The 25-hydroxyvitaminD3 metabolite is considered the universal indicator of vitamin D status and needs to be measured in addition to the model drug, vitamin D_3. Blood sampling will still be done at 0, 1, 2, 4, 6, 8, 12, 18, 24 hours after the initial dose on day 0 as originally approved for the study to determine the rise in vitamin D_3. Additional blood sampling is however also requested at the following time points per animal: 24 hours, 48 hours, 72 hours, 96 hours and 120 hours to quantify the change in the 25-hydroxyvitamin D3 metabolite over the five day dosing period. Kindly note that *5* day consecutive doses will not result in toxicity of vitamin D in the test and comparator animals. As indicated in the original approved ethics application, a daily intake of up to 15 000IU of vitamin D_3 over a 12-18 day period had no negative effect on weanling pigs in a study by Li *etal* (2000). Only 150 *000IU* / day was found to be toxic after a 12-18 day period (Li *et al.*, 2000). Thus a *5* day dose of 1000IU would fall considerably under the daily recommendation and pose no harm to the test animals.

2) It is proposed to dose two of the test animals with a higher dose test product containing 4000 IU vitamin D_3 daily from days 0-4. Likewise it is proposed to dose two of the comparator animals with a conventional product containing 4000 IU vitamin D_3 daily from days 0-4. Other studies have dosed higher dose vitamin D_3 products over longer periods and measured baseline and final 25-hydroxyvitamin D_3 levels over a minimum of 4 weeks (Vieth, 1999). A study by Barger-Lux *et al* (1998) concluded that a dose of 10 ug/day (400 IU/day) for 8 weeks would raise 25-hydroxyvitamin D by 11 nnmoll l. Hence a higher dose of 4000 IU is requested to be dosed in 2 of the test and 2 of the comparator animals to ensure a measurable rise is obtained over a five day period. As explained in 1) above a 4000 IU dose will not lead to toxicity. The same sampling points as explained under 1) above are requested.

References:

- Armes LAG, Hollis BW, Heaney R. Vitamin D_2 is much less effective than vitamin D_3 in humans. Clin Endocrinol Metab 2004; 89: 5387-91.
- Barger-Lux MJ, Heaney RP, Dowell S, Chen TC, Holick MF; Vitamin D and its major metabolites: Serum levels after graded oral dosing in healthy mean; Osteoporosis International; 1998; 8: 222-230.
- Vieth R; Vitamin D supplementation, 25-hydroixyvitamin D concentrations, and safety; Am J Clin Nutr; 1999; 69 842-56.
- Wolpowitz D, Gilchrest BA. The vitamin D questions: How much do you need and how should you get it?; Journal of the American Academy of Dermatology 2006; 54: 301-17.
- LiD, Liu H, Xi P, Chen Y, Li Y; Effects of Vitamin D_3 on Immunity and Performance of Weanling Pigs; Asian-Australasian Journal of Animal Sciences; 2000; 13 Supplement C: 103-106.

3) Additional co-workers to assist with animals: Felix Mashingaidze (B.Pharm, SAPC); Karen Mochaba (B.Pharm, SAPC)

Addition of Prof. Kennedy Erlwanger (SAVC) to replace Dr. Leith Meyer as registered veterinarian to undertake procedures and administration of drugs to animals.

4) Request to sacrifice 1 pig dosed a placebo DDS and 1 pig dosed the test DDS so that GIT (duodenum) tissues may be obtained for histological examination to ensure that the test product does not cause damage to the duodenum.

5) A request to take pictures of experimental procedures and animals for inclusion in thesis and publications.

Date: 30/07/2013 Signature: .....

RECOMMENDATIONS:

Approved

Date: 19 August 2013 Signature:

Chairman, AESC

AESC 2013

Please note that only typewritten applications will be accepted. Should additional space be required for section "I" and/or "j", please use the back of this form.

ANIMAL ETHICS SCREENING COMMITTEE

MODIFICATIONS AND EXTENSIONS TO EXPERIMENTS

a. Name: Miles Braithwaite.....

b. Department: Pharmacy and Pharmacology.....

c. Experiment to be modified / extended **AESC NO:**

Original AESC number	2011	43	05
Other M&E's : 2 x modifications only			

d. Project Title:

In Vivo Assessment of a Novel "Bioactive Association Platform" (BAP) Delivery System in Pigs

e.	Number and species of animals **originally approved**:	16	
f.	Number of additional animals **previously allocated on M&Es**:	2	
g.	Total number of animals **allocated** to the experiment to date:	18	
h.	Number of animals **used** to date:	12	

i. Specific modification / extension requested:

Request for an extension of AESC clearance to use animals to test the *in vivo* efficacy of the study product.

j. Motivation for modification / extension:

AESC approval expires on 30 September 2013. However the study is still in progress and due to logistical constraints an intake group of six animals still needs to be dosed to evaluate the *in vivo* efficacy of the developed drug delivery system. A request is made to extend ethics clearance beyond 30th September 2013 so that the research may conclude.

Date: 17/09/2013 Signature:

RECOMMENDATIONS:

Approved: Extension of time to June 2014.

Date: 19 September 2013 Signature:

Chairman, AESC

8.3. Doctoral Research Publications (2011-2014)

8.3.1. Paper 1: Medical hypothesis

Medical Hypotheses 81 (2013) 656–663

Contents lists available at SciVerse ScienceDirect

Medical Hypotheses

journal homepage: www.elsevier.com/locate/mehy

Vitamin D therapy and related metabolomics: Is the calciferol dose and form the only requirements for successful clinical therapeutics?

M.C. Braithwaite, P. Kumar, C. Tyagi, L.K. Tomar, Y.E. Choonara, V. Pillay *

University of the Witwatersrand, Faculty of Health Sciences, Department of Pharmacy and Pharmacology, 7 York Road, Parktown, 2193 Johannesburg, South Africa

ARTICLE INFO

Article history:
Received 4 June 2013
Accepted 12 July 2013

ABSTRACT

A nutraceutical that has exploded onto the prescription pad in recent years is the fat soluble vitamin, vitamin D. This is due to an increasing medical interest in the utility of the vitamin in the treatment and prevention of an array of diseases and ailments. Despite the continued debate over the correct dose, form and serum levels, many clinicians fail to achieve intended therapeutic responses with their patients and deficiencies still exist. This may be due to medical professionals being less aware of the multitude of factors that can influence treatment when dosing a product. In this paper we explore the magnitude of interactions that exist between the host physiology and the vitamin and cite such points as a reason for confounding treatment end points. Aspects that are proposed to influence treatment success more critically than dose and molecular form prescribed are: organ pathology, intracellular states, the endocrine system, concomitant products, genetics, lifestyle, quality of product, and modern delivery systems.
© 2013 Elsevier Ltd. All rights reserved.

Introduction

Many researchers have investigated the use of vitamin D in the treatment and prevention of multiple diseases [1,2]. Despite much interest in this field, many clinical plans often fail to achieve the intended therapeutic outcomes and deficiency remains in the global population [3,4]. In addition, there is little consensus over the ideal dose or formulation required to successfully achieve treatment goals in all patients and all indications. Controversy exists regarding the optimal prescribed dose, the most effective vitamin form and regimen, ideal daily amount, and the safest serum levels to be monitored [5]. Many researchers have made claims and recommendations regarding safe upper limits, toxicity levels and optimal doses, but few are fully cognoscente of the power that physiological factors and interactions have on the ultimate fate and activity of the vitamin as a determinant of treatment success.

Early researchers questioned the efficacy and usefulness of oral vitamin D supplements in patients with disorders in underlying intestinal malabsorption syndromes, making a case for considering the physiological state rather than just the dose [6]. Some studies have recommended the use of vitamin D in conjunction with vitamin A and vitamin K as a means to achieve a greater treatment impact than relying solely on a single prescribed dose or molecular form of vitamin D [5]. Some researchers have confirmed that the potency of the two main supplemental forms of vitamin D namely vitamin D_3 (cholecalciferol) and vitamin D_2 (ergocalciferol) is not equivalent. Studies have noted that cholecalciferol may be twice to three times more potent than ergocalciferol at increasing plasma levels of vitamin D [7,8]. However, other compounds in the immediate microenvironment need to be considered in conjunction with the form prescribed. For example, a strong relationship exists between vitamin D_2 and magnesium in terms of bone health; however the exact mechanism that occurs when the two interact within the biological system has yet to be fully elucidated [9]. Such a large number of variables that exist unnoticed at a biological level make it very challenging to predict an elicited biochemical response in each and every patient and with every dose. Without comprehensively evaluating the biological processes, underlying host factors, or pharmacodynamic and kinetic effects, the reasons for under- or over-shooting sought after treatment goals will continue to elude physician and patient alike.

Although vitamin D is generated within the body from sun exposure, recent research has sparked debate over the risk between too little and too much sun exposure and the best approach to achieve healthy serum levels [3]. Focus has thus shifted to adequate use of supplements and the diet instead of sun-exposure to achieve ideal levels. Therefore it is important to know how such products will perform in an ever changing environment. Many patients are prescribed various molecular forms, metabolites and doses of vitamin D but still show slower than expected rise in levels and poor clinical improvements in the targeted disease. Titrating up dosages or varying the form prescribed to a more active molecule in the vitamin D pathway may still fail to result in an associated improvement in a patient within the required time frame. It has been estimated that for every 100 IU of vitamin D taken daily, its blood level increases by only a fraction (1 ng/mL over

* Corresponding author. Tel.: +27 11 717 2274; fax: +27 11 642 4355/86 553 4733.
E-mail address: viness.pillay@wits.ac.za (V. Pillay).

0306-9877/$ - see front matter © 2013 Elsevier Ltd. All rights reserved.
http://dx.doi.org/10.1016/j.mehy.2013.07.022

8.3.2. Paper 2: Review

JOURNAL OF FUNCTIONAL FOODS 6 (2014) 82–99

Available at www.sciencedirect.com

ScienceDirect

journal homepage: www.elsevier.com/locate/jff



Nutraceutical-based therapeutics and formulation strategies augmenting their efficiency to complement modern medicine: An overview

*Miles C. Braithwaite, Charu Tyagi, Lomas K. Tomar, Pradeep Kumar, Yahya E. Choonara, Viness Pillay**

University of the Witwatersrand, Faculty of Health Sciences, Department of Pharmacy and Pharmacology, 7 York Road, Parktown, 2193 Johannesburg, South Africa

ARTICLE INFO

Article history:
Received 7 August 2013
Received in revised form
9 September 2013
Accepted 25 September 2013
Available online 19 October 2013

Keywords:
Nutraceutical formulations
Nutrient-based treatment
Polymer
Nanotechnology
Multicomponent formulation

ABSTRACT

Awareness of the role that nutraceuticals play in the treatment and prevention of disease has led to an explosion of research in this exciting arena that seems to overflow into the food, cosmetic, nutraceutical, and pharmaceutical industries. Nutrients, supplements and herbal compounds have shown promise as either alternatives to modern medicine or complementary tools in the treatment and prevention of disease. This review provides a brief outlay of the advantages and challenges of nutraceutical delivery via dermatological, oral and ophthalmic routes. Emphasis is directed towards nutraceutical formulation strategies adopted to overcome physicochemical challenges and instability of natural bioactives in order to improve their delivery and bioavailability to the body. This paper highlights how novel techniques have achieved products with greater commercial viability and efficacy than their conventional counterparts. Importance of multicomponent products where individual bioactives potency is not subdued by each other has been marked. Ultimately it is the adoption and merging of the different formulation technologies and prudent scientific validation that will dictate the future success of nutraceuticals. This is especially pertinent in a market where an informed consumer demands an innovative all-in-one product that does not compromise in its results.

© 2014 Published by Elsevier Ltd.

Contents

1. Introduction . . . 83
2. Routes of nutraceutical delivery . . . 84
   2.1. Oral delivery . . . 84
   2.2. Dermal delivery . . . 84
   2.3. Ophthalmic delivery . . . 85
3. Nutraceutical formulation strategies . . . 85
   3.1. Liposomal carrier systems . . . 85
   3.2. Electrospun fiber mats . . . 85
   3.3. Microsponges and nanosponges . . . 86

* *Corresponding author.* Tel.: +27 11 717 2274; fax: +27 11 642 4355, +27 86 553 4733.
E-mail address: viness.pillay@wits.ac.za (V. Pillay).

1756-4646/$ - see front matter © 2014 Published by Elsevier Ltd.
http://dx.doi.org/10.1016/j.jff.2013.09.022

8.3.3. Additional papers to be submitted (2014)

8.3.3.1. Paper 3: Research paper I

A Novel Multi-Tiered Experimental Approach Unfolding the Mechanisms behind Cyclodextrin-Vitamin Inclusion Complexes for Enhanced Vitamin Solubility and Stability

Miles C. Braithwaite, Yahya E. Choonara, Pradeep Kumar, Charu Tyagi, Lomas K. Tomar and Viness Pillay

Wits Advanced Drug Delivery Platform Research Unit, Department of Pharmacy and Pharmacology, School of Therapeutic Sciences, Faculty of Health Sciences, University of the Witwatersrand, Johannesburg, 7 York Road, Parktown, 2193, South Africa.

***Corresponding Author:**
Professor Viness Pillay
Tel: +27-11-717-2274
Fax: +27-11-642-4355
Fax2Email: +27-86-553-4733
Email: viness.pillay@wits.ac.za

ABSTRACT – **Purpose.** To investigate the efficiency of complexing various vitamins with multiple cyclodextrins (CD) to form complexes for enhanced solubility and stability. The study was conducted to provide a mechanistic account for understanding synthesis, characterization and solubility phenomena of vitamin complexes using experimental and novel *in silico* molecular modeling strategies. New geometric, molecular and energetic analyses were pursued to explicate experimentally derived cholecalciferol complexes. **Methods.** CD molecules (α-, β- , hydroxypropyl β-, and γ-) were complexed with three vitamins, cholecalciferol, ascorbic acid and α-tocopherol. DSC, FT-IR and XRD analysis confirmed inclusion within stable complexes. Novel *In silico* molecular modeling (MM+) was used to reinforce the thermodynamic stability of cholecalciferol CD-vitamin Inclusion Complexes (IC). **Results.** The Inclusion Efficiency (IE%) was computed for each CD-vitamin complex with 'βCDD$_3$-8' proving the most successful cholecalciferol complex (highest IE%). Molecular simulations highlighted new mechanistic information pertaining to preferential binding modes, bond energy stabilizations and 3D space-fitting criteria of cholecalciferol in association with each cyclodextrin. Highest IE% values were reported with βCD-ascorbic acid (82%), βCD-cholecalciferol (78%) and γCD-cholecalciferol (72%) IC's. The highest IE% achieved for a cholecalciferol complex was for 'βCDD$_3$-8', after utilizing a unique CD: cholecalciferol molar synthesis ratio of 2.5:1, never before reported as successful. 2HPβCD-cholecalciferol, γCD-cholecalciferol and α-tocopherol IC's reached maximal IE% with a CD:vitamin molar ratio of 5:1. **Conclusion.** The results demonstrate that IE%, thermal stability, concentration, carrier solubility, molecular dynamics and intended release profile are key factors to consider when synthesizing vitamin-CD complexes. Static lattice atomistic simulations were able to validate experimentally derived cholecalciferol IE phenomena and are invaluable parameters when formulating strategies using CD's for improved solubility and efficacy of vitamins. Phase-solubility data provided insights into the design of formulations with IC's that may provide analogous oral vitamin release profiles even when hydrophobic and hydrophilic vitamins are co-incorporated.

8.3.3.2. Paper 4: Research paper II

A Bioactive Association Platform Oral Drug Delivery System for Enhanced Efficacy of Cholecalciferol: Synthesis, Characterization, and *In Vitro* and *In Vivo* Analysis

Miles C. Braithwaite[a], Pradeep Kumar[a], Lomas K. Tomar[a], Lisa C Du Toit[a], Yahya E. Choonara[a] and Viness Pillay[a*]

[a]University of the Witwatersrand, Faculty of Health Sciences, Department of Pharmacy and Pharmacology, 7 York Road, Parktown, 2193, Johannesburg, South Africa

***Corresponding Author:**
Professor Viness Pillay
Tel: +27-11-717-2274
Fax: +27-11-642-4355
Fax2Email: +27-86-553-4733
Email: viness.pillay@wits.ac.za

ABSTRACT
An intuitive problem with many drug delivery systems (DDS's) is the reliance on a specific physiological climate within a patient for intended performance. Despite the advent of intelligent stimuli responsive drug delivery mechanisms, many patients reflect abnormal physiology during disease which impedes such devices. Few researchers have investigated the use of multiple physiological enhancers combined with synthetic carriers to augment delivery of nutraceuticals. The current work explicates the development of an oral DDS termed a "Bioactive Association Platform" (BAP) capable of delivering multiple nutraceutical actives and biological constituents from a formulation framework for enhanced *in vitro* and *in vivo* performance of model drug, cholecalciferol (D_3). Synthesis of a novel "3-vitamin" minitablet and an optimized bile salt/lipase alginate-glycerin film provided unique components for inclusion in a BAP capsule for oral delivery. Component optimization studies and physicochemical characterization included, lipase activity dissolution assays, chemical structure mapping by Fourier Transform Infrared Spectroscopy (FTIR), thermodynamic analysis by Differential Scanning Calorimetry (DSC), and Magnetic Resonance Imaging (MRI). *In vitro* dissolution studies of the BAP produced an Area Under the dissolution Curve (AUC) for cholecalciferol release that was 28% greater than a conventional comparator. A total of 84.01% of D_3 was released from the BAP vs. only 59% from a 4000IU comparator. A unified release of all 3 vitamins was demonstrated from the BAP evident in the similarity of vitamin dissolution profiles. *Ex vivo* permeation studies revealed superior cholecalciferol membrane diffusion from the "3-vitamin" minitablet BAP component compared to a conventional D_3 tablet. *In vivo* performance results showed that the BAP achieved a greater mean change from baseline D_3 to peak plasma levels (C_{max}) compared to the comparator (55,66ng/mL vs 46.05ng/mL). Cholecalciferol bioavailability was improved with an $AUC_{0\text{-}inf}$ for the BAP 3.2x greater than the conventional product. The BAP was also superior at improving and maintaining serum levels of 25-hydroxyvitamin D_3 compared to the conventional comparator. *In vitro* and *in vivo* results confirmed improvements in D_3 disintegration, dissolution, membrane permeability and plasma drug levels, and improved levels of 25-hydroxyvitamin D_3 *in vivo*. The study results position the BAP as an ideal oral delivery vehicle for enhanced efficacy of cholecalciferol with harmonized multi-component release capability.